AD-753 243

THE USE OF THE LASER DOPPLER VELOCIMETER FOR FLOW MEASUREMENTS

W. H. Stevenson, et al

Purdue University

Prepared for:

Office of Naval Research

November 1972

PROJECT SQUID

AN OFFICE OF NAVAL RESEARCH PROGRAM

THE USE OF THE LASER DOPPLER VELOCIMETER FOR FLOW MEASUREMENTS

PROCEEDINGS OF A WORKSHOP
CO-SPONSORED BY THE U.S. ARMY MISSILE COMMAND
HELD AT PURDUE UNIVERSITY
ON MARCH 9-10, 1972

CHAIRMEN and EDITORS:

W. H. STEVENSON and H. D. THOMPSON

Project SQUID is a cooperative research program in the field of Jet Propulsion. It is administered at Purdue University under contract N00014-67-0226-0005. This document has been approved for public release and sale; distribution is unlimited.

PROJECT SQUID HEADQUARTERS
JET PROPULSION CENTER
SCHOOL OF MECHANICAL ENGINEERING
PURDUE UNIVERSITY
LAFAYETTE, INDIANA 47907

Unclassified

Security Classification

DOCUMENT CONTROL DATA - R&D

(Security classification of title, body of abstract and indexing annotation must be entered when the overall report is classified)

1. ORIGINATING ACTIVITY *(Corporate author)*
Project SQUID, Jet Propulsion Center, Purdue University, West Lafayette, Indiana 47907

2a. REPORT SECURITY CLASSIFICATION
Unclassified

2b GROUP
N/A

3 REPORT TITLE

THE USE OF THE LASER DOPPLER VELOCIMETER FOR FLOW MEASUREMENTS

4. DESCRIPTIVE NOTES *(Type of report and inclusive dates)*
Project SQUID/Army Missile Command Workshop held March 9-10, 1972

5 AUTHOR(S) *(Last name, first name, initial)*

Thompson, H.D. and Stevenson, W.H.

6. REPORT DATE	7a. TOTAL NO. OF PAGES	7b. NO. OF REFS
November 1972	~~564~~ 554	

8a. CONTRACT OR GRANT NO.	9a. ORIGINATOR'S REPORT NUMBER(S)
N00014-67-A-0226-0005	N/A
b. PROJECT NO. NR-098-038	
c.	9b. OTHER REPORT NO(S) *(Any other numbers that may be assigned this report)*
d	N/A

10. AVAILABILITY/LIMITATION NOTICES
This document has been approved for public release and sale; its distribution is unlimited.

11 SUPPLEMENTARY NOTES	12. SPONSORING MILITARY ACTIVITY
N/A Details of illustrations in this document may be better studied on microfiche	Office of Naval Research Power Program, Code 473 Dept. of the Navy, Arlington, Va. 22217

13 ABSTRACT

This report contains the proceedings of the Workshop on The Use of The Laser Doppler Velocimeter For Flow Measurements held on March 9-10, 1972 at Purdue University. This workshop was co-sponsored by Project SQUID and the U.S. Army Missile Command, Huntsville, Alabama. The workshop participants included representatives from universities, industry, government and abroad.

ig

DD FORM 1 JAN 64 1473

Unclassified

Security Classification

14 KEY WORDS	LINK A		LINK B		LINK C	
	ROLE	WT	ROLE	WT	ROLE	WT
Laser Doppler Velocimeter						
Flow Measurement						
Laser Instrumentation						
Laser Velocimeter						
Laser Doppler Anemometer						
Optical Methods for Flow Measurements						

Project SQUID

An Office of Naval Research Program

U. S. Army Missile Command

Huntsville, Alabama

THE USE OF THE LASER DOPPLER VELOCIMETER FOR FLOW MEASUREMENTS

Proceedings of a Workshop

held at

Purdue University

on March 9-10, 1972

Editors and Co-chairmen:

W. H. Stevenson and H. D. Thompson

Project SQUID Headquarters
Jet Propulsion Center
Purdue University
West Lafayette, Indiana 47907

Project SQUID is a cooperative research program in the field of jet propulsion. It is administered at Purdue University under Contract N00014-67-A-0226-0005. This document has been approved for public release and sale; its distribution is unlimited.

IC

TABLE OF CONTENTS

TECHNICAL SESSION VI - APPLICATIONS B.
SESSION CHAIRMAN: B.Z. JENKENS

Page

WILD CARD SESSION
SESSION CHAIRMAN: R. GOULARD

FOREWORD

Over its short history since 1960 when the first laser was successfully operated by T. H. Maiman, it has found many and varied applications. One of the most interesting of these is its use in an instrument for making virtually intereference free measurements of the velocity of flowing fluids. Operation of this instrument, which has become known as a laser doppler velocimeter or LDV, is based on the frequency shift (doppler shift) produced when coherent laser radiation is scattered from small (micron size) particles moving in a fluid stream. The principle is easy to grasp; the instrument becomes practical, however, only when the variety of challenging problems posed by requirements on the optical system and the electronic signal processing equipment are fully understood and overcome.

In order to evaluate the current state of development in LDV systems and to highlight areas requiring further research and study a Workshop on "The Use of the Laser Doppler Velocimeter for Flow Measurements" was held at Purdue University on March 11 and 12, 1972. This report represents the proceedings of this Workshop.

The Workshop was organized at the suggestion of Professor Robert Goulard, Director of Project SQUID. The U. S. Army Missile Command, Huntsville, Alabama, cosponsored the event since they had a contract involving LDV research with Purdue University on which the editors were the principal investigators. Most of the Workshop participants were actively engaged in both development and use of LDV systems. The participation of researchers from Western Europe (France, England and Germany were represented) gave the Workshop an international flavor and added significantly to the discussion.

The Workshop was run on an informal basis, although both "formal" and "informal" presentations were given. All of the presentations and the discussion were recorded on tape for later transcription with the exception of the welcoming address by Purdue President Arthur G. Hansen. (Those present will long remember his hilarious stories of smoke generation for flow visualization in the good old days at NACA). The material is arranged essentially in the order in which it was presented. Some editing has been done both by the authors and the participants. In many cases authors chose to submit prepared papers in lieu of editing the tape transcriptions. To save ourselves work (and to retain our friendships) we encouraged these substitutions and have even allowed some editing of the informal presentations. Even though this has detracted some from the informal and lively spirit of the Workshop it

does provide a clearer explanation of many important details that were discussed.

For some reason the recordings of our own words do not fit our mental image of what we really said, although they are quite accurate in regard to what others said. In our preliminary editing of the tapes we therefore tried to produce a transcript which conveyed the intent of the speaker as we perceived it. This often required rather heavy editing to make the report read smoothly. However, we believe the important material has been retained with as much of the informal flavor and spirit as was practical.

W. H. Stevenson

H. D. Thompson

ACKNOWLEDGMENTS

A number of people participated in the organization of the Workshop and the preparation of these proceedings. Their contributions are gratefully acknowledged.

We very much appreciated the words of welcome from Purdue's President Authur G. Hansen. He set the tone for the Workshop.

The Graduate Research Assistants working behind the scenes made the Workshop run smoothly and helped record the audio tapes from which the proceedings were transcribed. Our thanks to Ron Flack, Mike Pedigo, John Cowan and Ron Zammit.

Mrs. Suzanne Clavelli performed the difficult task of transcribing the audio tapes and did much of the typing of the final manuscript.

Mrs. Persis Newman assisted in uncountable ways with flawless attention to detail.

Mr. Mark Ocker and the staff at the Purdue Union and at the Stewart Center were very helpful in arranging the Workshop and providing facilities.

About Miss Nancy Cox - she is a gem without whose dedicated efforts the Workshop would still be in the planning stages and the proceedings would not have made it to the printer. Thanks, Nancy.

Finally, our sincere thanks to the session chairman and the participants. They made the Workshop work.

The Editors

PARTICIPANTS

1972 LASER ROCKET WORKSHOP

MARCH 9-10

Dr. John C. Angus
Dept. of Chemical Engineering
Case Western Reserve University
Cleveland, Ohio 44106

Dr. Jeffrey A. Asher
General Electric Company
Corp. R & D, K-1
Combustion Building
Schenectady, New York 12301

Dr. Charles Benham
Naval Weapons Center
Research Aerospace Engineer
Code 45701
China Lake, California 93555

Dr. John C. Bennett
Applied Gas Dynamics Group
United Aircraft Research Labs
East Hartford, Connecticut 06108

Dr. Neil S. Berman
Chemical Engineering Dept.
Arizona State University
Tempe, Arizona 85281

Mr. M. A. Boutier
Division de la Physique
ONERA
29 Avenue de la Division Leclerc
92 - Chatillon sous Bagneux
France

Mr. Donald B. Brayton
OMD-TS-ER
ARO, Inc.
Arnold Air force Station
Tennessee 37389

Mr. John D. Cowan
Graduate Research Assistant
Jet Propulsion Center
Purdue University
West Lafayette, Indiana 47907

Mr. Les Crosswy
OMT-TS-ER
ARO, Inc.
Arnold Air force Station
Tennessee 37389

Professor William Dunnill
University of Tennessee
Space Institute
Tullahoma, Tennessee 37388

Dr. John W. Dunning, Jr.
NASA Lewis Research Center
21000 Brookpark Road
Cleveland, Ohio 44135

Professor Robert V. Edwards
Chemical Engineering Science Div.
Case Western Reserve University
Cleveland, Ohio 44106

Mr. Bertram K. Ellis
Aviation & Surface Effects Dept.
Code 165, Bldg. 13
Naval Ship Research & Dev. Center
Bethesda, Maryland 20034

Mr. William J. Feller
NASA Langley Research Center
Mail Stop 164
Hampton, Virginia 23365

Dr. L. M. Fingerson
Thermo-Systems Inc.
2500 Cleveland Avenue
St. Paul, Minnesota 55113

Mr. Ronald D. Flack
Graduate Research Assistant
Jet Propulsion Center
Purdue University
West Lafayette, Indiana 47907

Captain David Francis
DYR
Arnold Engineering Dev. Center
Arnold Air Force Base
Tennessee 37389

Dr. William K. George
Dept. of Aerospace Engineering
Pennsylvania State University
University Park, Pennsylvania 16802

Dr. Victor W. Goldschmidt
School of Mechanical Engineering
Purdue University
West Lafayette, Indiana 47907

Dr. Robert Goulard
Jet Propulsion Center
Purdue University
West Lafayette, Indiana 47907

Mr. George Grant
NASA Ames Research Center
Moffett Field
Sunnyvale, California 94040

Mr. Allan Hauer
Pratt & Whitney Aircraft
East Hartford, Connecticut 06108

Captain Robert V. Hayes
Assistant Chief of Research
Code 400
800 North Quincy Street
Arlington, Virginia 22217

Mr. Milton Huffaker
NASA Marshall Space Flight Center
S&E-AERO-AF Bldg. 4610
Huntsville, Alabama 35812

Mr. Ron Humphrey
DISA-SB, Inc.
779 Susquehanna Avenue
Franklin Lakes, New Jersey 06417

Dr. David A. Jackson*
University of Kent
Canterbury, Kent,
England

Dr. Billy Z. Jenkins
Research Aerospace Engineer
AMSMI-RDK
U.S. Army Missile Command
Redstone Arsenal, Alabama 35809

Dr. Martin C. Jischke
Dept. of Aerospace, Mechanical
and Nuclear Engineering
University of Oklahoma
Norman, Oklahoma 73069

Mr. Dennis A. Johnson
NRC Associate
NASA Ames Research Center
Moffett Field
Sunnyvale, California 94040

Dr. T. R. Lawrence
P. O. Box 1103, West Station
Lockheed Missile and Space Co.
Huntsville, Alabama 35803

Mr. Andrew E. Lennert
OMD-TS-ER
ARO, Inc.
Arnold Air Force Station
Tennessee 37389

Prof. Malay K. Mazumder
University of Arkansas
P. O. Box 3017
Little Rock, Arkansas 72203

Mr. James F. Meyers
Mail Stop 234
NASA Langley Research Center
Hampton, Virginia 23365

Captain C. M. Miller
Aerospace Research Labs/LV
Bldg. 450, Area B
Wright-Patterson AFB, Ohio 45433

Mr. David H. Murray
Fluid Dynamic Facilities
Research Laboratory
Aerospace Research Laboratory/LB
Wright-Patterson AFB, Ohio 45433

Dr. Richard Munt
Naval Weapons Center
Research Aerospace Engineer
Code 45701
China Lake, California 93350

Dr. Kenneth Orloff
NRC Associate
NASA Ames Research Center
Moffett Field
Sunnyvale, California 94040

*Dr. Jackson was scheduled to attend the workshop and present a paper in Technical Session VI, but was unable to complete travel arrangements. The manuscript by D. A. Jackson and D. M. Paul was forwarded by Dr. Jackson after the workshop and is included in the proceedings.

Mr. Bharatan R. Patel
Engineer
Westinghouse Electric Co.
A2W, Lester Box 9175
Philadephia, Pennsylvania 19113

Mr. James R. Patton, Jr.
Office of Naval Research
Power Branch, Code 473
Department of the Navy
Arlington, Virginia 22217

Mr. Mike Pedigo
Graduate Research Assistant
School of Mechanical Engineering
Purdue University
West Lafayette, Indiana 47907

Dr. Hans-Joachin Pfeifer
Institute Franco-Allemand
de Recherches de St. Louis
68 - St Louis, France

Dr. Felix Pierce
Department of Mechanical Engineering
Virginia Polytechnic Institute
and State University
Blacksburg, Virginia 24061

Dr. E. R. Pike
Physics Group
Royal Radar Establishment
Malvern, Worcestershire
England

Dr. Bruce A. Reese
Jet Propulsion Center
Purdue University
West Lafayette, Indiana 47907

Dr. Harold Reynolds
Pratt & Whitney Aircraft
Florida R & D Center
Mail Stop D-30
West Palm Beach, Florida 33456

Mr. John D. Roberts
Graduate Student
Case Western Reserve University
10900 Euclid Avenue
Cleveland, Ohio 44106

Mr. Chuck Roehrig
Eustis Directorate
USAAMRDL
Fort Eustis, Virginia 23604

Dr. Anshel Schiff
Department of Aeronautical
and Astronautical Engineering
Purdue University
West Lafayette, Indiana 47907

Mr. Wayne M. Shaffernocker
Mail Drop H 6
General Electric Company
Cincinnati, Ohio 45214

Mr. Henry Shenker
Naval Research Laboratory
Head, Applied Optics Branch
Code 6530
Washington, D. C. 20390

Prof. Cornelius C. Shih
Department of Fluid and
Thermal Engineering
The University of Alabama
P. O. Box 1247
Huntsville, Alabama 35807

Prof. Roger L. Simpson
Institute of Technology
Thermal and Fluid Science Center
Southern Methodist University
Dallas, Texas 75222

Mr. Robert Smid
Staff Engineer
DISA S & B, Incorporated
779 Susquehanna Avenue
Franklin Lakes, New Jersey 07417

Mr. John Steinke
Graduate Student
University of Houston
Department of Chemical Engineering
Houston, Texas 77004

Professor Warren H. Stevenson
School of Mechanical Engineering
Purdue University
West Lafayette, Indiana 47907

Mr. Robert Suhoke
Staff Engineer
DISA S&B, Incorporated
779 Susquehanna Avenue
Franklin Lakes, New Jersey 07417

Professor H. Doyle Thompson
Jet Propulsion Center
Purdue University
West Lafayette, Indiana 47907

Dr. Raymond Viskanta
School of Mechanical Engineering
Purdue University
West Lafayette, Indiana 47907

Dr. H. D. Von Stein
Institute Franco-Allemand
de Recherches de St. Louis
68 - St. Louis, France

Professor C. P. Wang
Department of Aerospace and
Mechanical Engineering Sciences
University of California - San Diego
La Jolla, California 92037

Mr. Nathan E. Welch, President
Electronetics Incorporated
305 Crestwood Drive S.E.
Tullahoma, Tennessee 37388

Dr. James H. Whitelaw
Department of Mechanical Engineering
Imperial College of Science
and Technology
London, S.W. 7, England

Dr. Sigmar Wittig
School of Mechanical Engineering
Purdue University
West Lafayette, Indiana 47907

Mr. Henry S. Woodard
Senior Research Engineer
Detroit Diesel Allison
General Motors
Plant 8, Tibbs and Minnesota
Indianapolis, Indiana

Mr. William J. Yanta
Division 313
Naval Ordnance Laboratory
Silver Spring, Maryland 20910

Mr. Ronald Zammit
Graduate Research Assistant
Department of Mechanical Engineering
Purdue University
West Lafayette, Indiana 47907

TECHNICAL SESSION I - SYSTEM DESIGN A

Session Chairman: H.D. Thompson

1-A

A REVIEW OF LDV DESIGN CONSIDERATIONS

Warren H. Stevenson

Purdue University

For the benefit of those who are new to laser doppler research -- and to generate some discussion topics for those active in the field for some time -- I would like to give a brief review of the important characteristics of laser doppler systems.

The first step in designing a laser doppler instrument is deciding what to call it. Many names have been suggested including laser flowmeter, laser anemometer, and laser doppler velocimeter. I have no strong preferences but will use the latter designation, abbreviated as LDV, in this discussion.

Several types of LDV systems have been utilized with the differences being primarily in the optical configuration and the signal processing scheme used. A basic distinction which affects the signal processing approach is whether one or many particles, on the average, occupy the "probe volume". Figure 1 shows the configuration of the original LDV developed by Yeh and Cummins. A single beam from the laser was focused in the flow. The unscattered light goes directly through and is combined with scattered light collected by a lens on a photomultiplier. Since the two beams are coherent we can obtain interference. Also, since the scattered light is scattered by moving particles it undergoes a doppler shift and we are thus combining light of two different frequencies. Due to the characteristics of the phototube a beat signal at the difference frequency is obtained.

The next development in the optical configuration is sometimes referred to as input aligned optics. A system of this type is shown in Figure 2. In this case we somehow focus two beams at a common point in the flow. The unscattered light from one beam goes directly through serving as the reference beam while the scattered light from the other beam is doppler shifted and the two are mixed on the photomultiplier.

Finally the most recent configuration is the dual scatter system shown in Figure 3. Here we no longer use a reference beam as such but collect only scattered light. In this type of system the region of interest is limited by an aperture and the light then passes on to the detector.

To illustrate the nature of these systems and point out some of the limitations and the problems I want to spend a few minutes talking about the work we did about two years ago.

We were interested in studying oscillating and pulsating laminar flows of liquids in tubes [1,2]. These are flows in which it is difficult to get good measurements with conventional instruments. We used the input aligned system originated by Goldstein and Kreid as shown in Figure 4. Figure 5 shows the electronics used to process the signal. At any instant the signal would appear as in the upper right. Ideally, of course, we would like to have a signal of zero bandwidth, but there are fundamental limitations involved due to the nature of the doppler velocimeter itself. With a reference beam system the signal broadening results first from the fact that the particles move through the focal volume in a finite time. This is often referred to as transit time broadening. The next effect is that if the velocity is not constant throughout the focal volume a frequency spread will be generated due to the varying doppler shift. Finally in the reference beam system the scattered light is collected over a range of angles. This would seem to produce an additional spread in the doppler frequency. Many workers, including the author, have suffered from this misconception. It has been shown, however, that this so-called aperture broadening is, in fact, equivalent to the transit time broadening and not a separate additive effect [3]*.

To process the signal we clip some of the noise outside the frequency range of interest. In the flows we were studying the center frequency of the desired signal varied considerably due to the varying velocity. To allow accurate measurements we therefore found it necessary to go through a tracking filter which reduced the signal bandwidth. The tracking filter output was then fed to a frequency discriminator which produced an output voltage proportional to the input frequency. This voltage was then recorded on a strip chart recorder.

In the particular flow we were studying this gave typical results as shown in Figure 6. These data are for the oscillating flow case which was simply a laminar back and forth movement in the pipe. The figure shows the velocity profile at four different times during an oscillation cycle. There are some interesting flow reversals near the wall. Note that the curves shown are computed and the data was not adjusted in any fashion, so the results are in very good agreement with theory.

In flows of this type the velocity vector direction reverses and, for example, +1 cm/sec gives the same doppler frequency as -1 cm/sec. If we require both the direction and magnitude of the velocity, we must contrive some means of eliminating this symmetry. One approach employed is to frequency shift the reference beam. An added motivation for such frequency shifting is that it permits the output signal to be placed in a range compatible with the electronics.

---

*See also the remarks by J.C. Angus in his informal presentation.

The dashed box labeled SSBSC in Figure 4 represents a single sideband suppressed carrier modulator which is just a frequency shifter placed in the reference beam. This can be one of various types of electroptical devices. Normally these are best suited for use above 20 MHz. Water filled cells utilizing Bragg diffraction from acoustic waves can be employed at lower frequencies, but these tend to be rather bulky. Since we were working with rather low velocities and thus low doppler shifts we chose to use a rotating radial diffraction grating for the frequency shifting [4]. When the grating was rotated in the beam the various orders underwent a frequency shift. One of these orders was then chosen as a reference beam. Figure 7 shows the characteristics of the device.

One of the other important questions in LDV systems is the extent of the region from which a signal is received. In our case we were not particularly concerned with obtaining the smallest probe volume possible, but we did have some concern due to the fact that we were coming into a circular glass tube filled with water from an air environment. We therefore expected that optical aberrations might cause a great deal of trouble. To minimize these effects we put a compensator box filled with water around the tube as shown in Figure 8. More recently we have investigated this problem further and found that the aberration effects are actually of negligible importance in most cases, as far as probe volume size is concerned. However, the compensator box did minimize the loss of signal experienced due to slight vertical motions of the focal spot observed when the tube was traversed.

In general, definition of the probe volume requires consideration of possible aberation effects as noted above plus fundamental considerations of what parameters actually limit the region from which a doppler signal can be received. Obviously some basic limitations are imposed by the physical size of the focal spot. In addition, however, the directional characterstics of the heterodyne detection process impose a limitation which actually dominates in most cases. At the photocathode we are combining a well defined spherical wavefront from the reference beam with other essentially spherical wavefronts scattered from particles in the flow. Over the photocathode aperture the phase difference between the reference and scattered wavefronts will be small -- say less than $\pi/2$ -- for all scattering particles located within a certain angular field as observed from the aperture. Thus only particles located within this angular field contribute to the heterodyne signal. An alternate way of explaining this effect is to think of the reference beam and the wavefront scattered from a single particle located slightly off the reference beam axis as producing a fringe pattern as shown in Figure 9. Due to the doppler frequency difference this pattern will actually be moving perpendicular to the fringes. If the fringe spacing is small compared to the receiver aperture (corresponding to a large angle between the reference and scattered wavefronts) very little signal modulation will be produced. Thus in reference beam systems both the optics and the directional characteristics of the heterodyne process limit the probe volume.

In dual-scatter systems the probe volume is limited by the focal spot size at the beam crossover and by the aperture (pinhole) placed where the crossover region is focused by the receiving optics. When the pinhole is larger than the image of the focal spot the probe volume is ellipsoidal as shown. Rudd has presented a model which is based on the existence of a set of parallel fringe "planes" in the crossover region. Using the known gaussian beam intensity profile the intensity distribution in this "fringe pattern" can be calculated from the beam intersection angle and the light wavelength. One can then predict the output signal which should be produced when a particle moves across the focal region. Obviously when the particle is small compared to the fringe spacing the scattered light received at the detector will exhibit essentially 100 percent modulation, while a particle equal in diameter to the fringe separation will produce negligible modulation.

It should be emphasized that the Rudd model is physically incorrect and can lead to erroneous conclusions unless used carefully. There are, in fact, no fringes in the probe volume. Rather there is a standing electromagnetic wave field which is "seen" by particles as they move through the focal region. This field determines the nature of the scattered light.

To summarize we show in Figure 10 a comparison between the characteristics of reference beam and dual scatter systems. In reference beam systems the doppler shift f_D varies with angle, since the reference beam direction is fixed and scattered light is collected over some finite angle. This broadening in the frequency spectrum is equivalent to the transit time broadening as mentioned earlier. The photomultiplier current I in a reference beam LDV is indicated by the equation in Figure 10. Below the equation is a sketch showing the photocurrent for the case of a single particle traversing the probe volume. Note that the A.C. component of the photocurrent is proportional to the amplitudes of both the reference beam, E_2, and the scattered light, E_3, at the photocathode. The optimum signal-to-noise ratio for a reference beam system is obtained when the reference beam amplitude is much larger than the scattered light amplitude at the detector.

Comparable features of dual-scatter systems are also indicated in Figure 10. Most of these are self-explanatory with the possible exception of the latter two items. Multiple particles are undesirable in dual-scatter systems since a distorted signal will be generated unless they happen to pass through the probe volume with the proper spacing to generate signals which are in phase. This is not likely, so dual-scatter systems perform best when the particle density is low enough to insure that particles pass through the probe volume sequentially.

One final comment is in regard to frequency shifting. In reference beam systems this is a relatively straightforward problem as discussed earlier. In dual-scatter systems this may not be the case, since down-shifting the frequency means reducing the effective number of fringes a particle sees as it passes through the probe volume. This may cause difficulties with the data processing.

We have glossed over many details in this brief discussion. Many of these will, I'm sure, be brought out by other speakers. Thank you for your attention.

References

1. Denison, E. B. and Stevenson, W. H., "Oscillatory Flow Measurements with a Directionally Sensitive Laser Velocimeter," Rev. Sci. Instr. 41, 1475 (1970).

2. Denison, E. B., Stevenson, W. H., and Fox, R. W., "Pulsating Laminar Flow Measurements with a Directionally Sensitive Laser Velocimeter," A.I.Ch.E. Journal, 17, 781 (1971).

3. Edwards, R. V., Angus, J. C., French, M. J. and Dunning, J. W., Jr., "Spectral Analysis of the Signal from the Laser Doppler Flowmeter: Time Independent Systems," Jour. App. Physics 42, 837 (1971).

4. Stevenson, W. H., "Optical Frequency Shifting by Means of a Rotating Diffraction Grating," Applied Optics 9, 649 (1970).

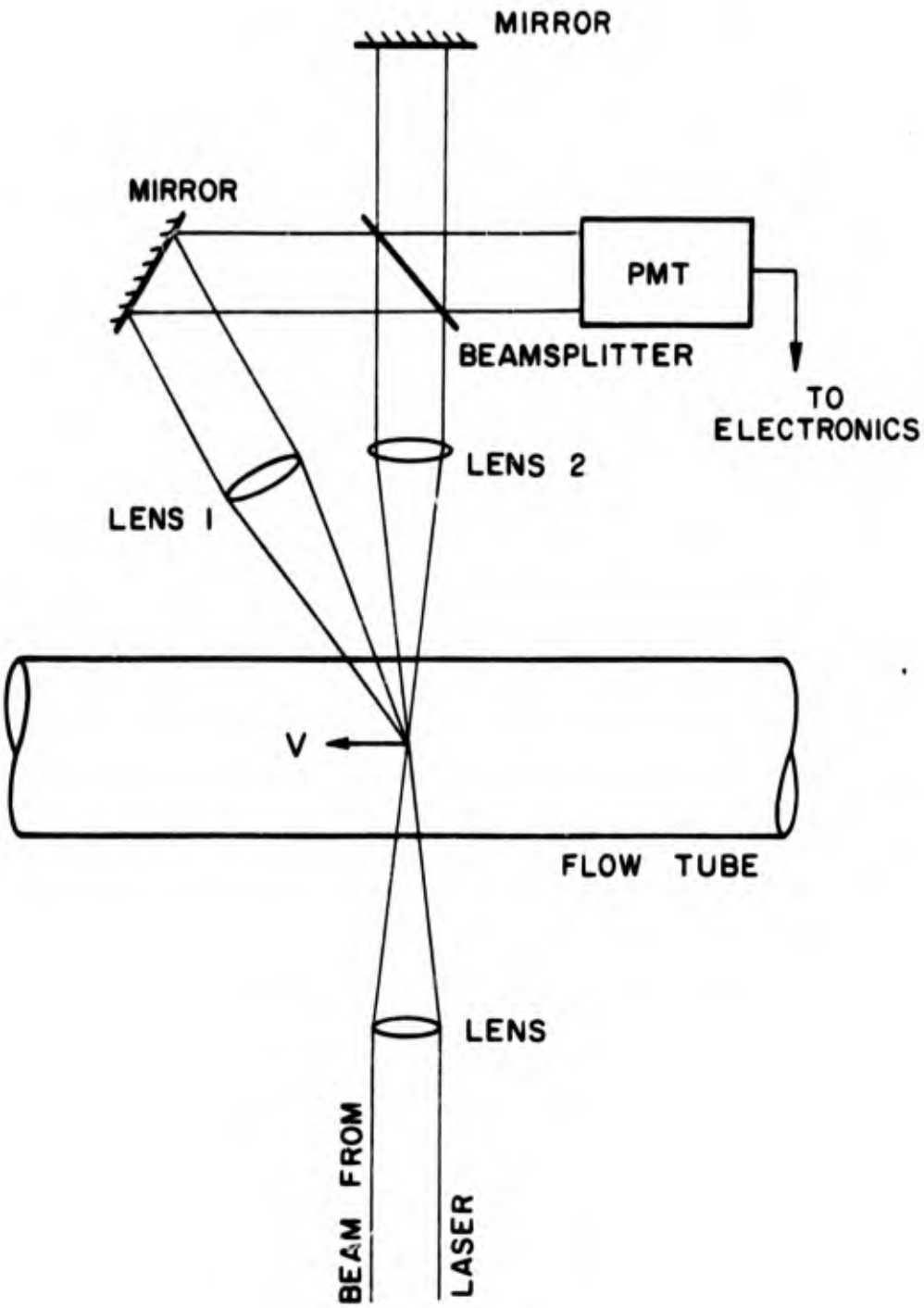

Figure 1 Original Yeh and Cummins LDV System

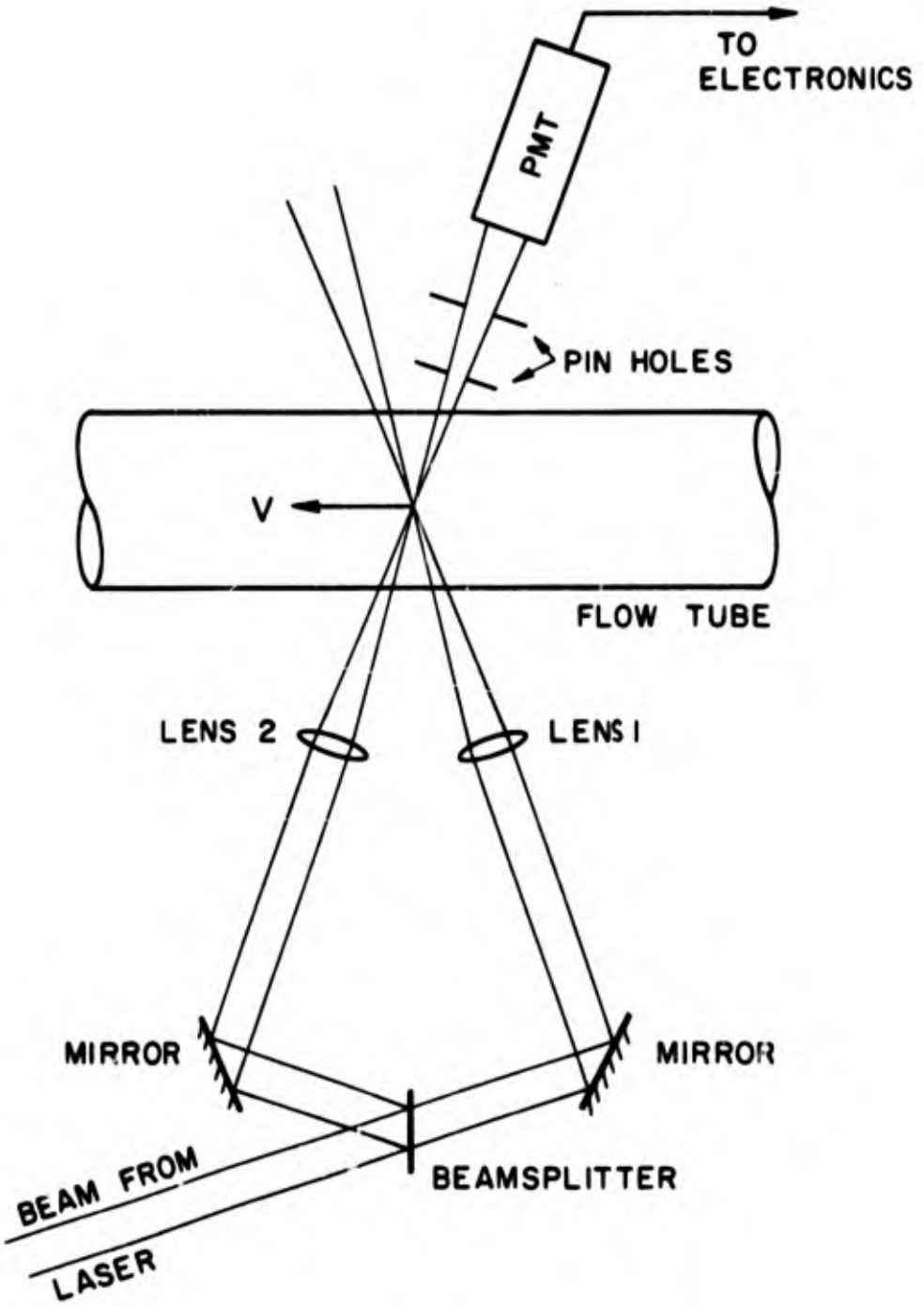

Figure 2 Input Aligned Optics (Goldstein and Kried)

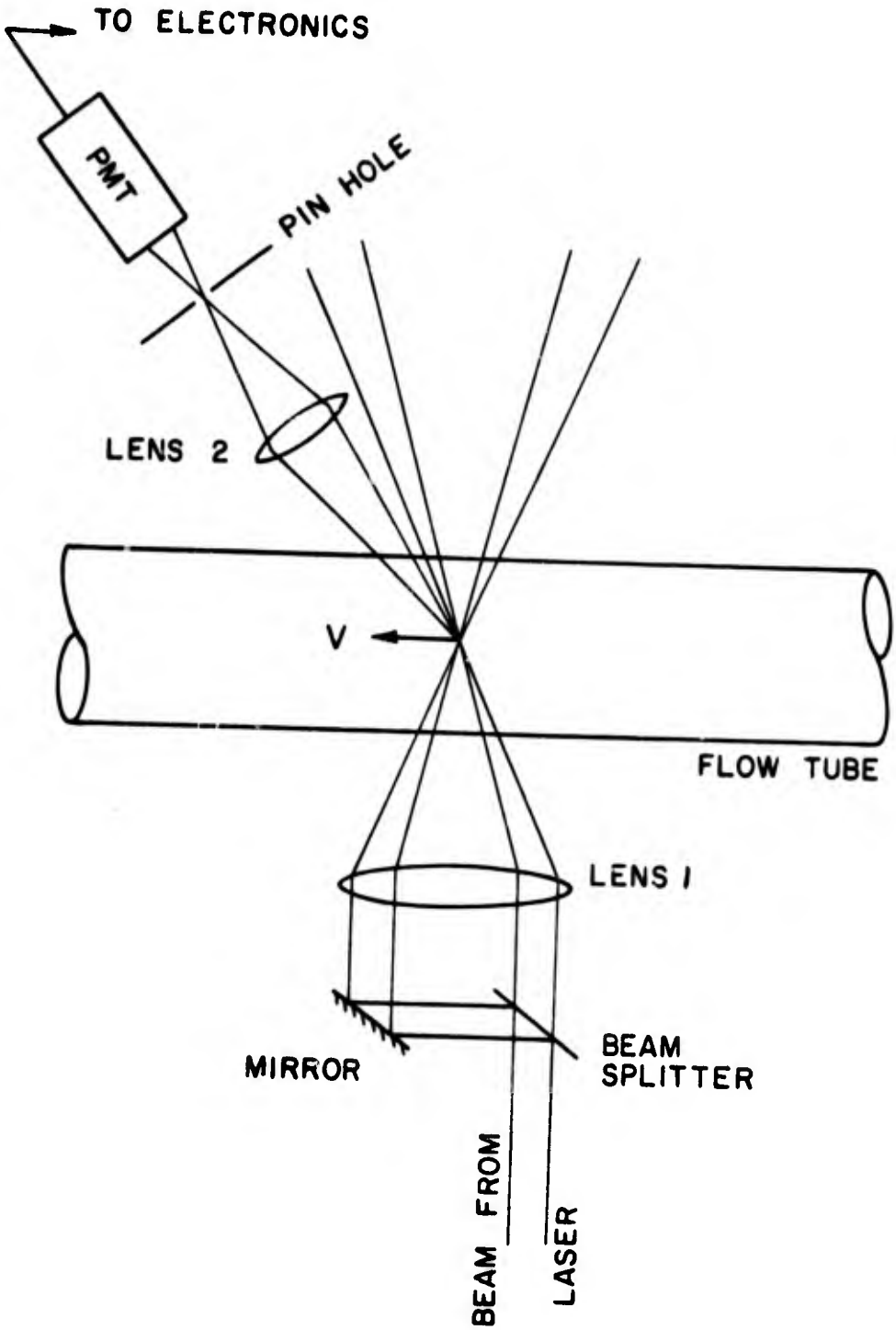

Figure 3 Dual Scatter Beam LDV

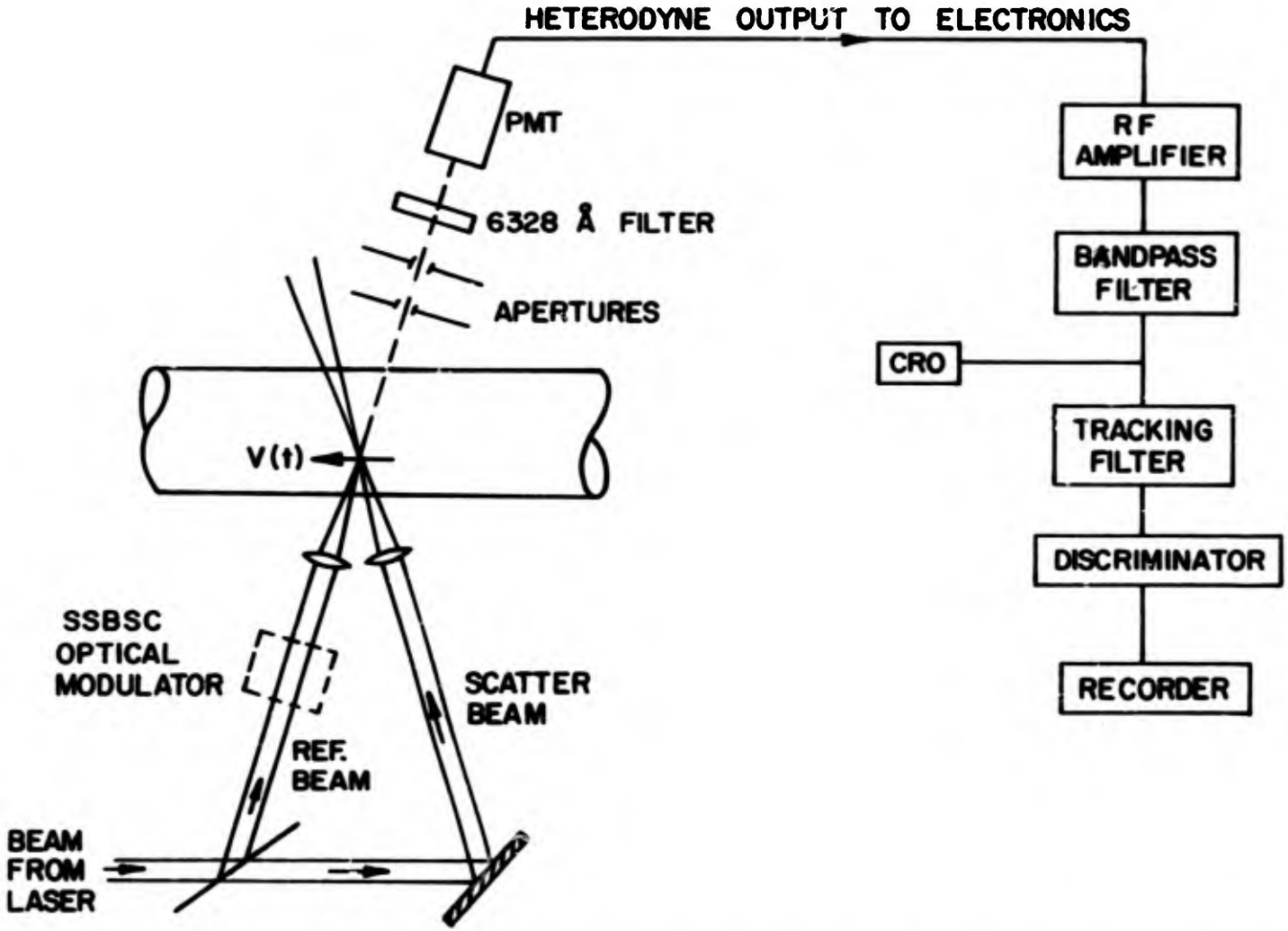

Figure 4 Directionally Sensitive LDV for Oscillating and Pulsating Flow Studies

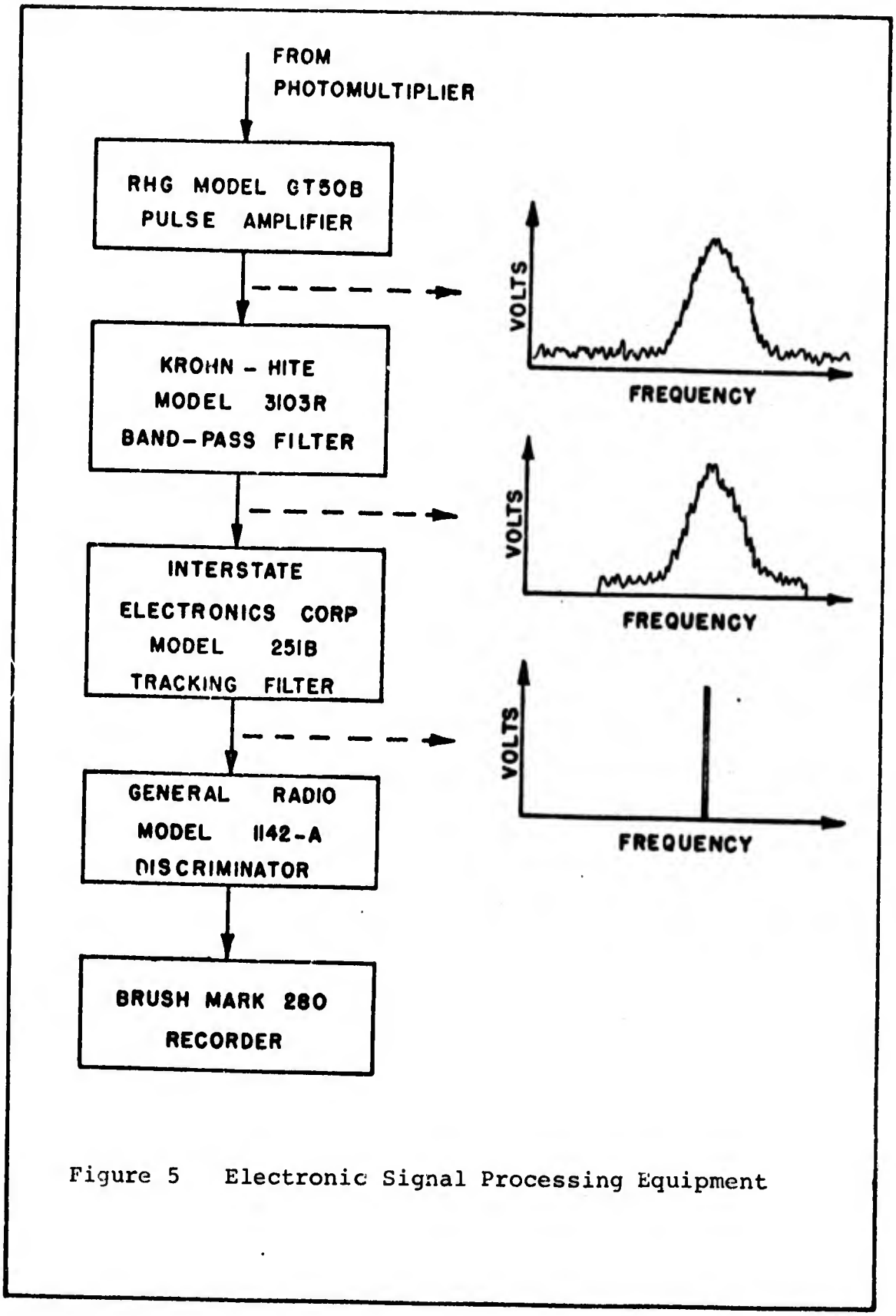

Figure 5 Electronic Signal Processing Equipment

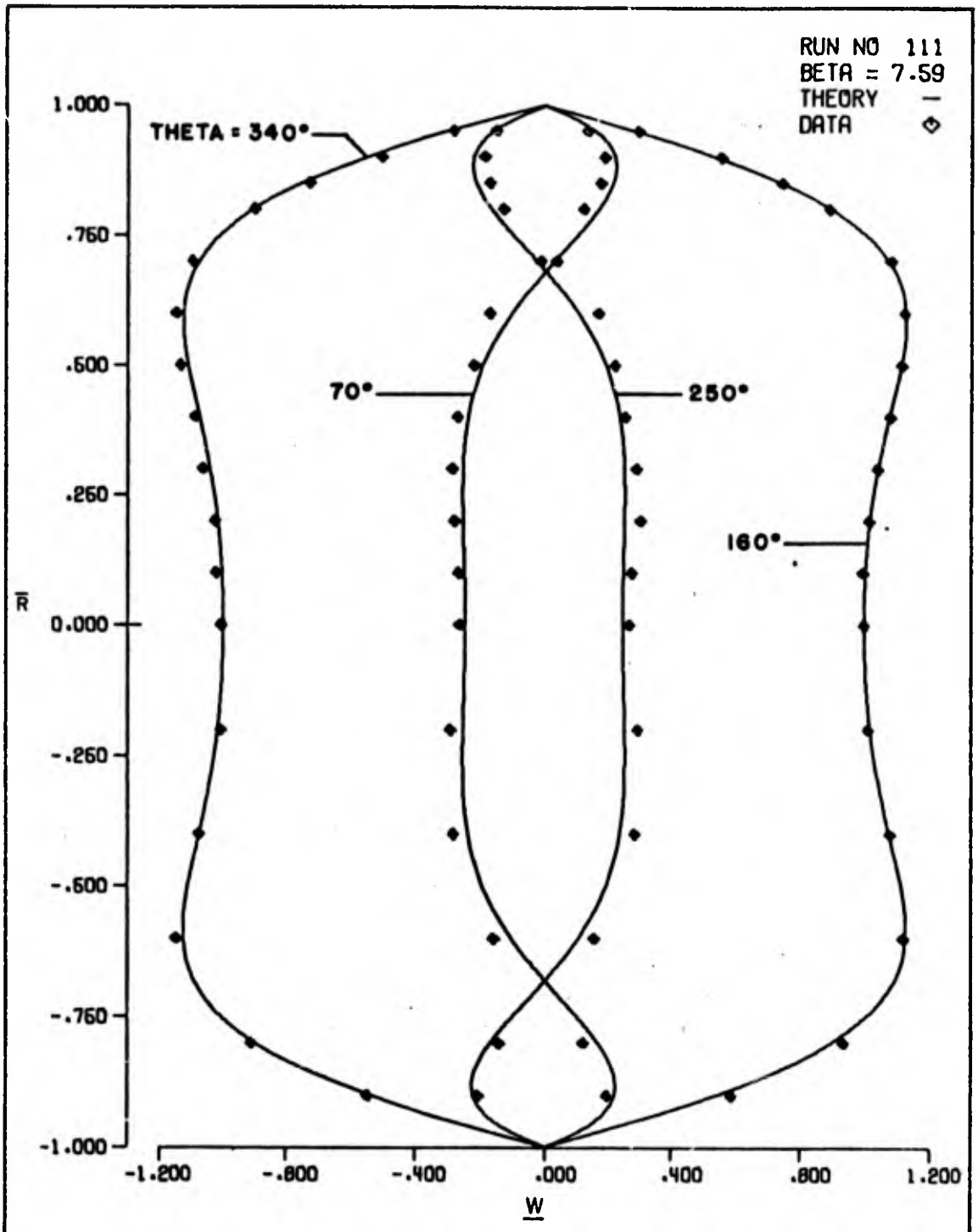

Figure 6 Typical Velocity Profiles in Oscillating Laminar Flow

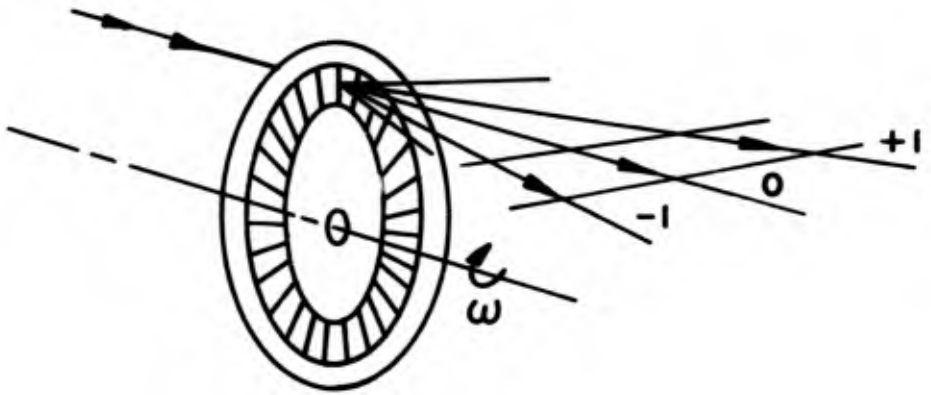

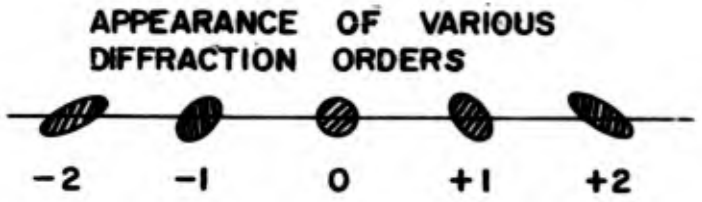

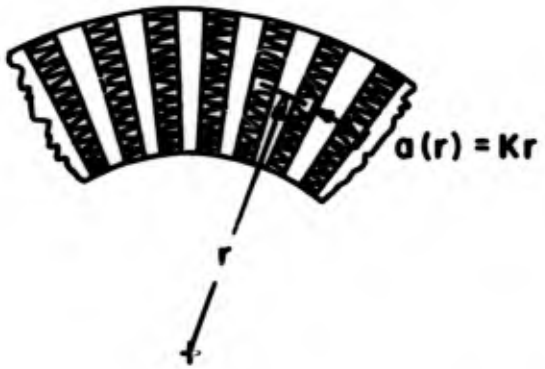

$$\nu = \nu_0 + \frac{v}{a}$$

$$= \nu_0 + \frac{r\omega}{Kr}$$

$$= \nu_0 + \frac{\omega}{K}$$

Figure 7 Diffraction Grating Frequency Modulator

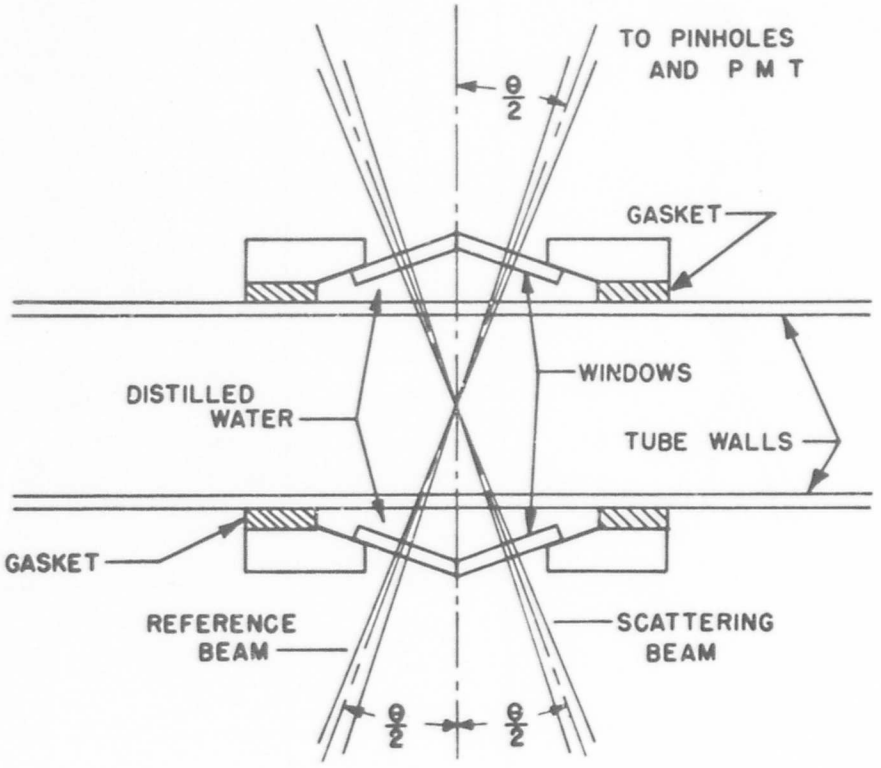

Figure 8 Optical Compensator Box

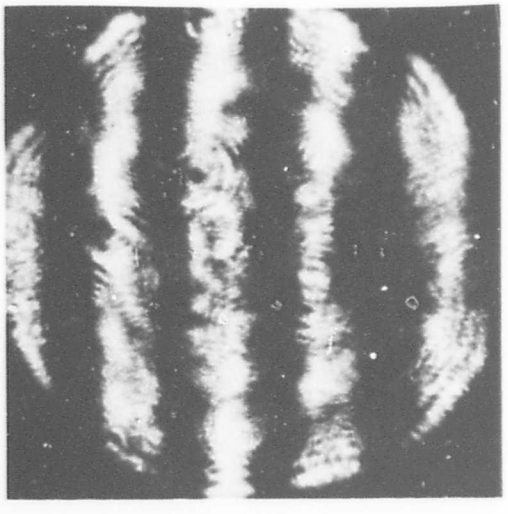

Figure 9 Fringe Pattern Formed at the Photocathode by Interference Between Reference and Scattered Wavefronts

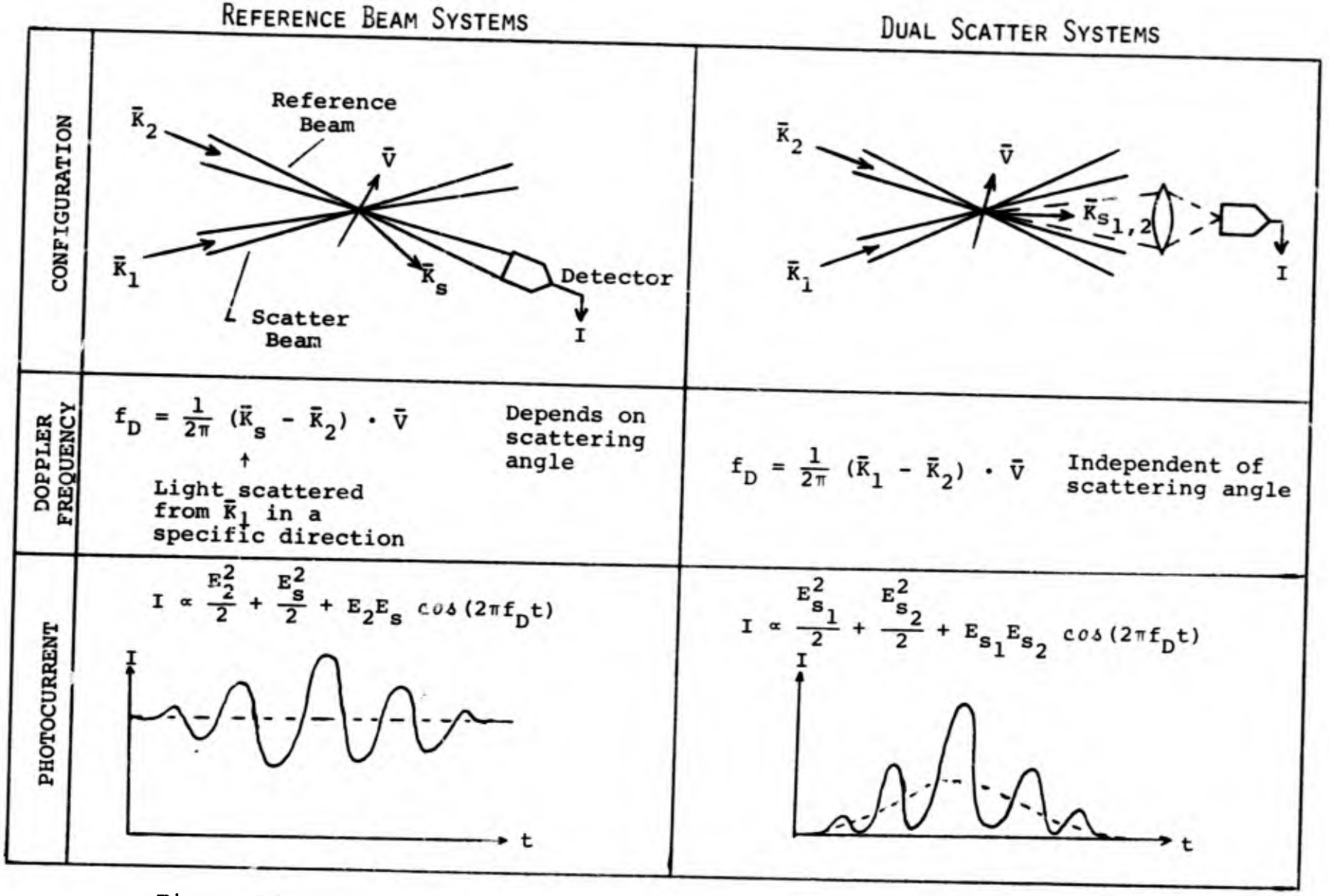

Figure 13 Characteristics of LDV Systems

	Reference Beam Systems	Dual Scatter Systems
PROBE VOLUME	Probe volume controlled by incident beam focusing and heterodyne considerations	Probe volume controlled by incident beam focusing and aperture in collecting optics
S/N	$E_2 >> E_s$ for optimum S/N	$E_{s_1} = E_{s_2}$ for optimum S/N
PARTICLE DENSITY	Multiple particles required in probe volume	Multiple particles in probe volume are undesirable

Figure 10 (CONTINUED) Characteristics of LDV Systems

DISCUSSION

PIKE: There are two points that I might raise after your introduction. The first is a really trivial one. That is the use of the word self-aligning. You showed the laser beam focus as being where the beams cross. This is not really ever true because most lasers have divergent outputs. You really want two lenses rather than one. With one lens it's not really self-aligning. The second point is that you said on several occasions the reference beam system was one in which the finite receiver aperture affected the frequency broadening.

STEVENSON: Right.

PIKE: I don't believe it. I'm sure this point will be brought out later in the program.

LENNERT: The statement made with regard to the use of moving fringes was wrong. When you use a modulator you get a net effective increase in the number of fringes you have in the focal volume. I'm talking about dual scattering because we've given up the academic exercise of reference beams a long time ago. Our doppler processor system is designed to accept a certain number of frequency counts. The accuracy of this system is of course dependent upon the design criteria. You get four cycles, stop counting, print out, and get four more. Or you could use 8, 16, or 32. It's mostly dependent upon the design criteria and on the accuracy you want.

STEVENSON: My concern was for the case where you are downshifting the frequency.

WHITELAW: I wanted to take exception to one of the last comments. Reference beams systems are not necessarily an academic exercise. It may be true if you are concerned with space or any situation where there are few particles around, but when you have particles around like you have in blood or in mist flows then you are going to use the reference beam system.

LENNERT: In dual scatter with a multiplicity of particles in the focal volume you have the phase behavior to consider, I think you'll find that the signal/noise ratio under certain circumstances goes as the square root of the number of particles in the field so you get an increase of signal/noise ratio as opposed to losing it.

EDWARDS: On the last point, Wednesday I ran a dual doppler system. I poured particles in. I watched the signal as the particle

density increased and the signal to noise rises, reaches a peak, and then drops.

LENNERT: How large a particle?

EDWARDS: I think 4,310 angstroms. (Laughter)

VOM STEIN: I think the signal/noise ratio is independent of the number of particles for the noise is proportional the number of particles and the signal is to the square root of the number of particles and thus the signal to noise ratio is practically independent of the number of particles with regard to order of magnitude. That's not the problem. People always suggest a big difference between the reference beam system and the dual scattering system. I think in both cases you have a system of fringes and it's independent of the way you use this system. If you have the photo multiplier or your detector in the reference beam, it is nearly the same as if you go out of the reference beam. I think it is nearly independent.

GEORGE: I think Mayo showed that most of the heterodyning taking place in reference beam systems is the forward scattered light or equivalently the light that is coming from the location of the particles. That would tend to substantiate that there is very little difference between the two systems.

VOM STEIN: That's right. The main advantage of the dual scattering system is that your spacial resolution will be improved, since it is possible to use a 90° observation. In this case we have the highest spacial resolution (the smallest probe volume).

DESIGN CRITERIA FOR THE OPTIMIZATION OF OPTICAL SYSTEMS

Dr. James Whitelaw

Imperial College of Science and Technology
London, S.W.7, England

I want to talk about optical systems because, although I suspect that most of our discussions will relate to signal processing, we can't signal process unless we have the signal to process. Many signals I have seen in other laboratories are of poor quality, and this stems from not recognizing that the various constituent components of any optical anemometer have to be matched, first to one another and then to the flow situation in question.

Signal quality can be measured in terms of a signal-to-noise ratio but the term has many meanings. When we talk about discrete particles, signal-to-noise is easy to define because you can observe the signal from one particle and measure the noise as a proportion of the modulated rf signal. In our laboratory we ensure that we have signal-to-noise ratios, according to this definition, which are in excess of 40 db. I want to identify components first, very quickly, so that you will know what my terminology is. Then I will present some results. The words I want to use are laser, which we all know; then optical unit, then something I would like to call the light collecting system; then the photomultiplier and finally the signal processing system. I will start by saying a few words about lasers. Laser sources are necessary for this kind of work because they provide a collimated, coherent light beam of the required power. A simple amalysis indicates that the number of photons reaching the photomultiplier cathode is a function of the variables shown on Figure 1. I want to draw attention to two specific dependences: the number of photons which reach the cathode is proportional to the power of your laser (also to its wavelength, of course), and also to the reciprocal velocity. You cannot achieve a large number of photons on the cathode with a very small laser at a very high speed.

As a rule of thumb, assuming a helium-neon laser, particles which are one micron in diameter, a focal length of the optical system of 300 millimeters at an angle of 10 degrees and 2000 photons per wave cycle, we find that the laser power required is equivalent to about .4 milli-watt per meter per second of velocity. This is based on several criteria which are arguable and I want to emphasize that it is a rule of thumb; but I would emphasize that you do have to match your laser power to

$$N_p = \frac{P_\ell \lambda}{8(h\nu) F^2 U \sin\phi} \frac{\sin (2q \sin \phi)}{2q \sin \phi}$$

$$\sqrt{(\eta_{sp})_1 (\eta_{sp})_2} \int_\Omega \sqrt{\Gamma_1 \Gamma_2} \, d\Omega$$

where F = F-number of lens

h = Planck's constant

N_p = number of photons per wave cycle

q = $2\pi r_p/\lambda$

r_p = radius of scattering particle

U = instantaneous velocity

η_{sp} = spatial distribution of light intensity

λ = wave length of incident light

ϕ = half angle between two incident light waves

Γ = Mie scattering function

Ω = space angle over which light is collected

FIGURE 1

your flow system and also to the rest of your anemometer configuration.

The second point I want to make is that the signal-to-noise will vary depending upon the ratio of the particle size to the fringe distance. We have done some simplified analysis with square particles and if you have some square particles, we would be happy to provide you with the analysis. In reality, you have to guess meaningful size and then adjust your fringe system so that you get the maximum signal-to-noise. You can of course, arrange particle sizes which will deplete your signal altogether and therefore you can, if you wish, arrange to preferentially view some particles.

The last point I wanted to make in regard to optimization is that for spectrum analysis, you need 100 fringes because $\Delta f/f$ (change in frequency divided by the frequency) is proportional to one over the number of fringes. Thus, if you want one percent accuracy in your result you need 100 fringes to be seen by the photomultiplier. We always operate with more than 100 fringes but arrange a light collecting system to see only 100 of these; in this way we cut out the small particles or the big particles going through the edge and help to ensure that we only have good signals to work with.

One last point on light collecting systems before I go on. If you use a fringe system then your signal-to-noise ratio will drop off if you have too many particles; we all know this. If you have a reference beam system and arrange it so that you have coherent reception, as Les Drain from Harwell has shown, then you will find that the signal-to-noise will increase because the light waves coming off the particles in the control volume will be in phase. It is true that most of us are concerned with fringe systems because we have less than one particle in the control volume at all times.

These are the brief points that I wanted to make in connection with what one can do to optimize a system. One would conclude, I think, that you choose the laser depending upon the velocity, you decide the angle depending upon the particle size, and then you ensure that this arrangement is compatible with 100 fringes seen by the photomultiplier. The length and diameter of your control volume can then be calculated and this, together with a knowledge of the particle concentration allows you to decide whether to operate with a fringe system or with a reference beam system.

Now we come to the hardware. We recommend flexibility in the optical unit because we are concerned with a very wide range of flow situations. We measure in blood flows and in mist flows, as well as operating in those situations where you get very few particles like flames. So our optical systems are contrived to allow us to have any of these three arrangements here. The top arrangement on Figure 2 is a simple fringe system, the one below it is the fringe system in reverse, and really the properties of the first one and the second one are the same in terms of signal-to-noise. The third one down becomes a reference beam system just by changing the ratio of the beam splitter in the integrated optical unit. These units also operate in backscatter; we have a hole through the middle so that if we want to use backscatter with any of these systems we can. We have second channels which we can bolt on to the end, so that we can get the orthogonal component of velocity. They are vibration free as far as we know. We can kick them around, and even graduate students don't appear to be able to break them. Also they are easy to align. Alignment of one of these can give you a very good signal from scratch in perhaps

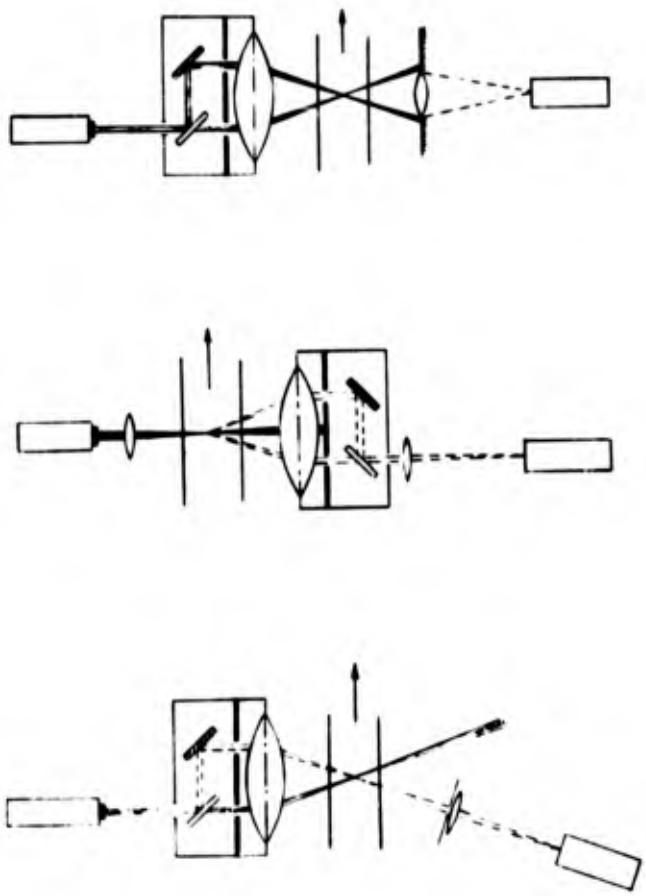

FIGURE 2

an hour. If you have it half set it takes about 5 minutes.

The hardware is shown in Figure 3. This is a one channel optical unit and photomultiplier housing. We have two channel ones as well. I think it is important to point out that the entire unit has two degrees of rotation and three degrees of translation, so that alignment of the whole system (both of the optical unit and of the photomultiplier) is easy. I would, in contrast to Roy Pike, plug for single lenses. If you don't have them, it is very difficult to attain optimum alignment.

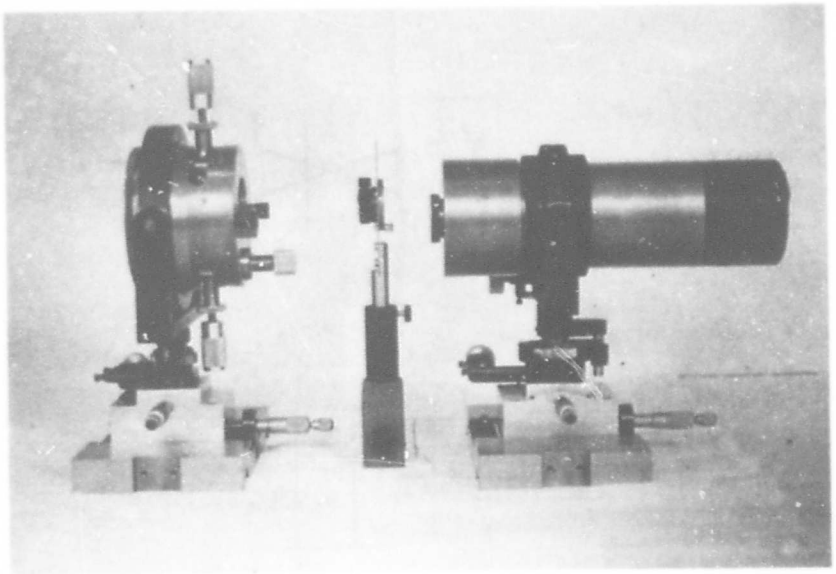

FIGURE 3

Figure 4 shows a measuring system with a two channel optical unit arranged on a traversing table. All the components of the optical system can be moved and aligned very rapidly. That is all I want to say on optimization. I suspect there are some points of contention there.

I want to run through some results to acquaint you with some of the things that we are doing, and to do that I have to say just one word about signal analysis. We have a variety of forms of signal analysis, some of them sophisticated, some of them not. We use spectrum analyzers of various kinds including a Nelson-Ross PSA205 which I cannot recommend. We tend to use a Hewlett-Packard analyzer although it is, unfortunately American. We have been fortunate enough to have for the past nine months the DISA tracking facility or at least the prototype tracker which was built by our colleagues at the AERE, Harwell. This works very well. We have our own phaselocked tracker which is easy to operate. Like many people here, we like counting systems and use the Hewlett-Packard computing counter system.

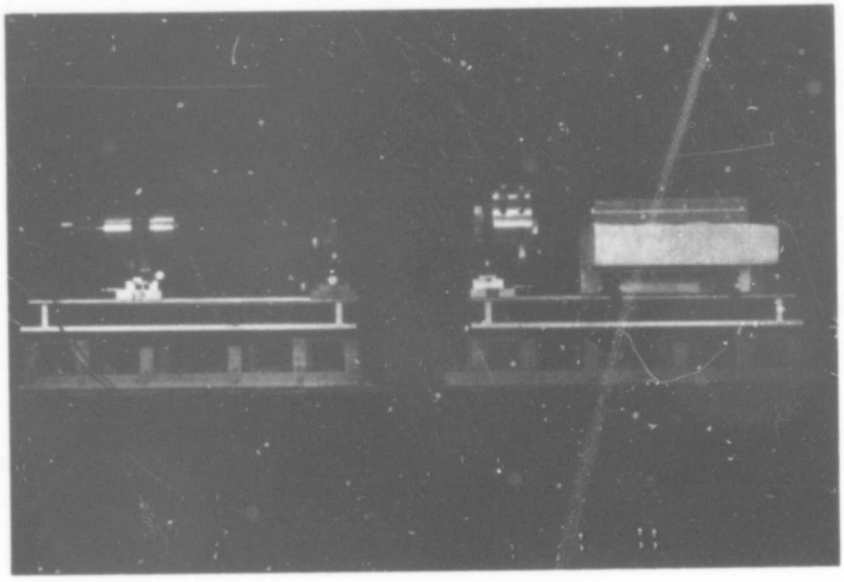

FIGURE 4

Some results. We have made measurements, for example in the vicinity of a sudden contraction and a sudden expansion, in particular, in the separated region (see Figure 5); so far we have worked with laminar flow as a preliminary to our intended efforts in turbulent, separated flows. We will have to frequency shift to measure throughout the turbulent flows, but this was not necessary for the laminar results.

We also believe, because our major interest is in fluid mechanics that our turbulent flow measurements should agree with previous measurements made by people who are recognized to be competent with hot wires, so we check the use of our optical anemometer against low turbulence flows like this one (Figure 6) and also against highly turbulent flows. This low turbulence flow is a two-dimensional channel flow. Two-dimensional channel flow has been investigated very well indeed by Comte-Bellot and Laufer. Our mean velocity results, are in very good agreement using either mode of operation with the anemometer. These measurements are in water and the particle concentration gives almost a continuous signal. That is without adding anything, just London water. The turbulence intensity, one component of which is shown here, is really remarkably good. We subtracted from these results about .8% broadening uniformly

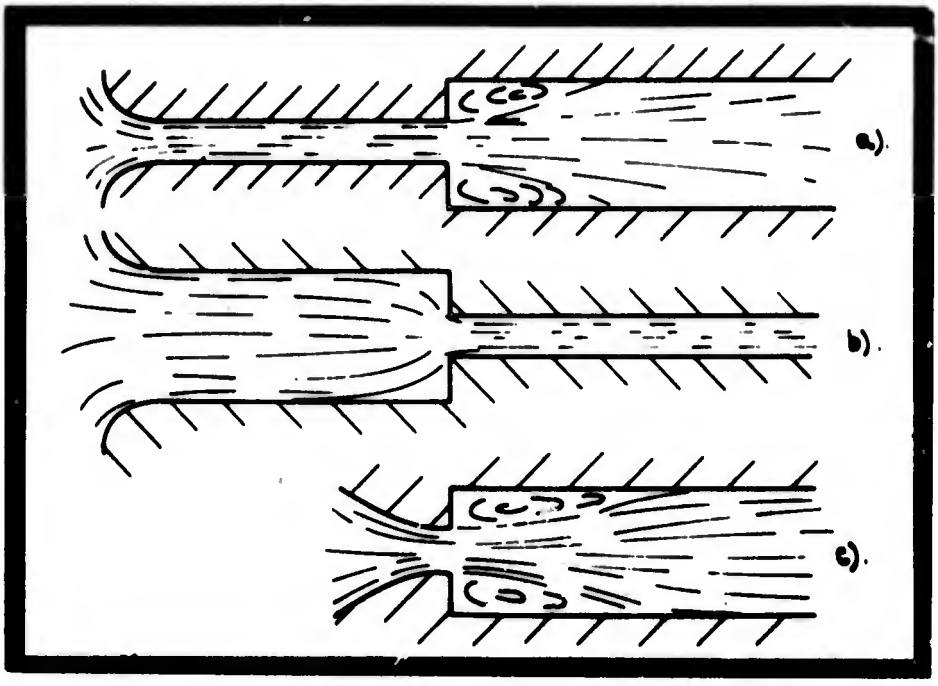

FIGURE 5

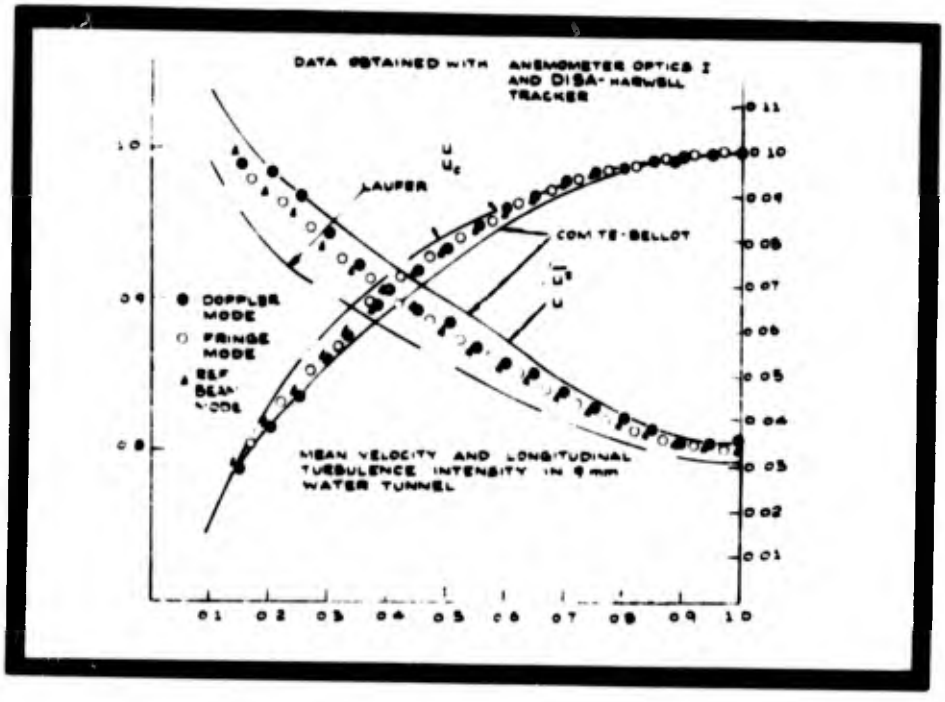

FIGURE 6

all the way along and obtained results which compare very favorably indeed with the hot wire results.

A word on jet flows. A jet constitutes a high turbulence flow. One of the main reasons for using laser anemometry when the turbulence intensity is high is because the laser has a linear response whereas the hot wire does not. Figure 7 shows some measurements in jets. The mean centerline velocity is as it should be and the three

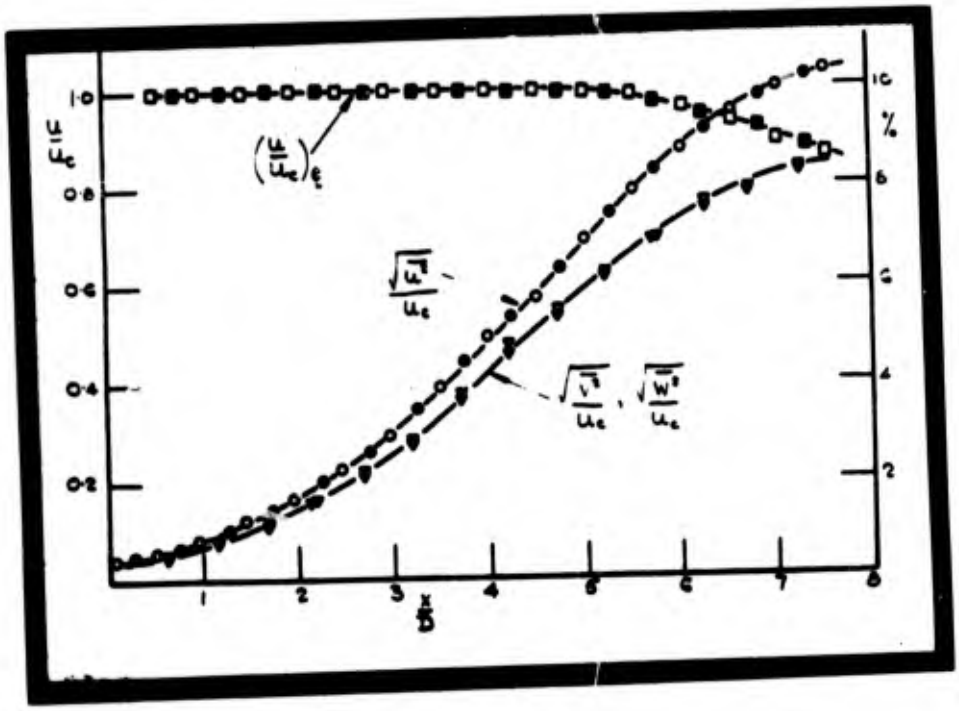

FIGURE 7

components of turbulence intensity also agree exactly with the measurement of Bradshaw. The one defect on the slide, of course, is that we only go about eight diameters downstream. The furthest we have been able to go in a jet flow is about 40 diameters because the particle concentration becomes too low, and we can't afford to wait for the results. We can also measure the cross stream profiles. Here are some cross stream profiles of two of the components of the turbulence intensity, the u' component and the v' component on the top of Figure 8, the mean velocity and the Reynolds shear stress measured across the flow with a single channel unit in the same way you would operate with a sloping hot wire. We are quite happy that we are getting the right kind of results on these test flows.

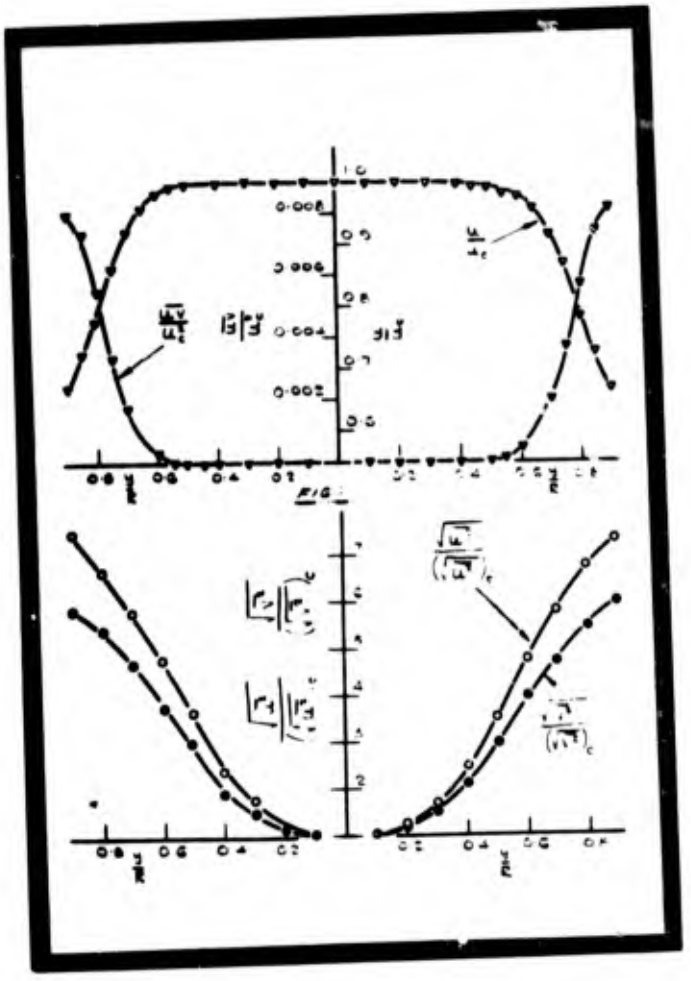

FIGURE 8

Having been satisfied that we can measure in test flows, we went back to our kind of thing that we like to do, which is to try to measure in combustion systems. Here is a flow situation where a laser anemometer can measure and other techniques cannot measure. I do not believe that the optical anemometer is the answer to any maiden's prayers or even to my prayers, but there are flows where it's use is very considerable or where you can't use anything else. On that little flame we can measure, for instance, the centerline velocity down in the flame. This is something that hasn't been done before. This is a regular bunsen flame; we can measure right through the flame front, and we find that we get a rapid acceleration through the flame front followed by a deceleration and you pick up your acceleration again as you go downstream. This is a combustion effect that you can find with a laser anemometer and you cannot get from any other instrumentation.

This is my last figure, Figure 9. These are some of the

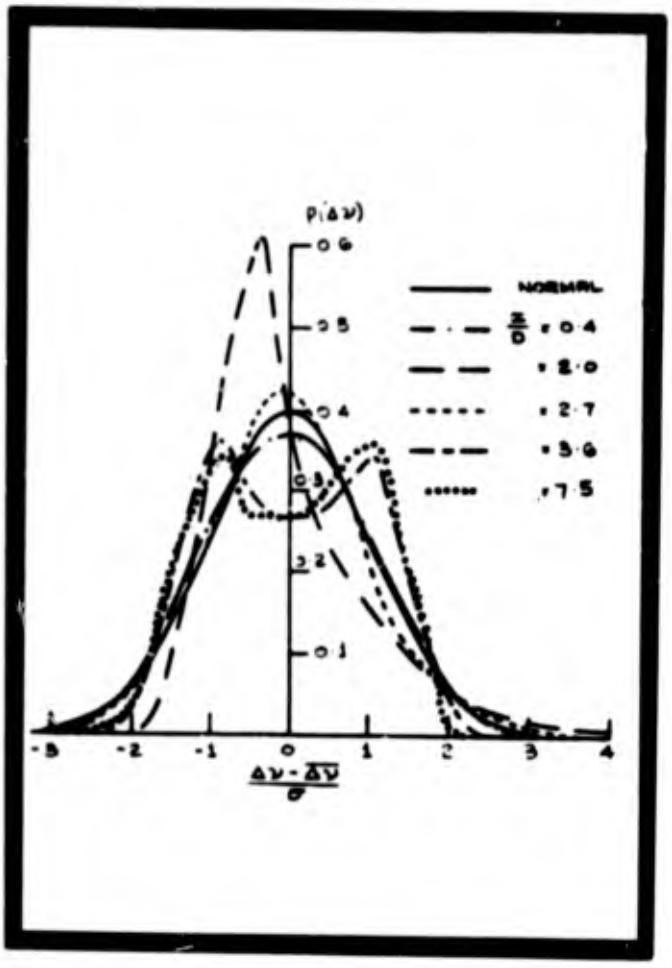

FIGURE 9

probability density distributions measured in the flame. We can, of course, get from these the turbulence intensity, we can get the skewness factor, the flatness factor or any correlation of the one point velocity that you care to mention. But perhaps the useful thing about this picture is that it demonstrates that in and around the flame front there is a probability density distribution with a hole in the middle and if you do a Fourier transform and find out what that means; you find that, instead of having a turbulent signal in the vicinity of the flame front, you have a regular periodic signal. I have other slides which I could show which would demonstrate the real-time signal which is distinctly periodic. What

is happening is that in the flame front you are getting extinction and then combustion and then extinction in a periodic manner. This is something that you cannot find with any other technique that I know.

Finally, my thanks to my colleagues, in particular F. Durst and A. Melling, for their major contributions to the work described in this presentation and to you for listening.

DISCUSSION

ASHER: I am quite interested in the flame work that you did. Like yourself I did some propane work. I found that using our counter technique we were able to get traverses. There was one thing that I did notice though. If we went to a very low excess air we would get a much lower temperature and this played havoc with the laser focus due to refraction effects. This generated noise in our signal and we really gave up those measurements, at least temporarily.

WHITELAW: We didn't find any specific problems of this type with our methane and hydrogen flames. We did not use propane. We may have not been quite where we thought we were in the flame, but the sums we did indicate that the distance from where we thought we were was very small indeed and insignificant in terms of the fluid mechanic measurements we were making. Experimental checks have confirmed this.

ASHER: I think that if you had used a highly turbulent propane torch you would have had real problems.

WHITELAW: If we had used a highly turbulent propane torch there wouldn't have been any particles.

ASHER: We introduced the excess air ourselves and that's how we were able to cut back on it very easily. But when you allowed it to go turbulent, you would find that the focal spot would actually jiggle.

WHITELAW: Yes this is so. If you put a light beam through and just watch it on the wall you see it move.

ASHER: That's exactly the point. Now in your collector optics you have a slit and you are focused at a particular spot to improve your spacial resolution. You would probably have your signal go out and this can happen periodically.

WHITELAW: That's true.

ASHER: Now the probability distributions that you showed are independent of time. That's the statistical analysis that you do to the turbulence level. That hole in the middle of your spectrum I don't believe is true because of these effects.

WHITELAW: I can answer that. We've been through this. We got these results about 9 months ago. We were puzzled. We didn't know what we had. We've gone back and measured in premixed flames, diffusion flames, and pulsating flames, all types of flames, and we find the same effect. If we look at the instantaneous signal we have a regular sinewave coming through. On some occasions its a slightly

modulated sinewave, but its not a turbulence effect. The old concept of combustion generated turbulence is something I don't believe. It depends on how you define turbulence. What we have here is a combustion generated sinewave which, if you look at it as an rms signal, will look like turbulence, but if you look at the instantaneous signal it's not.

ASHER: The point that you are bringing out of course is that all along people have been using rms meters such as hot wires not knowing what they have as far as signal content. My point is that I have been able to generate those kinds of probability distributions and have shown them to be errors. I have been able to repeat them at different doppler frequencies with better signal/noise and have just thrown them to the basket.

WHITELAW: I do believe we've covered this point. We did go back and set up pulsating flows, regular flows, and looked at them and checked that we got against what we should get. We knew what the pulsation was. We made sure that the tracking system got the same result. A big pulsation which drowned out the little one. Then we went back and got the little one again. We've done it with many particles. We've done it with few particles. It's there. Its a real effect. I do believe that we have checked that very thoroughly indeed. We were worried as you are.

VOM STEIN: The second question. You distinguish between coherent and incoherent scattering. Do you think it is possible to use really coherent scattering? That is when your signal is proportional to the number not just the square root of the number of particles.

WHITELAW: I think that the comments I made on coherent scattering were not original. They come from contacts with Les Drain of Harwell. He's written a paper in the Journal of Physics D (5, 481, 1972). He has plots of signal to noise ratio for different optical modes. He points out, I thought quite clearly, that if you take the reference beam mode then you can augment your signal to noise ratio with many particles by looking at it coherently. That is by making sure that when your light collecting system sees a lot of particles in the control volume, all of these particles scatter light waves which are in phase. Then the sum of all of these light waves adds up and you get an augmented signal to noise. I don't believe it applies to the fringe system. The fringe system is incoherent.

PIKE: You stated that you need 100 fringes to get 1% accuracy. That's not exactly true. In fact you can get an accuracy with any number of fringes. It just depends on what noise you've got as well. Secondly, you stated that you would like to have 2000 photons per doppler cycle. This is a question of processing and I shall be talking this afternoon about a system in which we have 10^4 times less.

WHITELAW: The 1% with 100 fringes relates to spectrum analysis. I think that most people do not signal process in the manner you are talking about. The required number of photons is arguable; the number I quoted was just a demonstration and a reminder that one should take them into account.

PIKE: I was very interested to see a number in any case. It's very rare that one sees such a number quoted. Regarding my first point I'm saying that if you know the ambiguity broadening then you can fit to infinite accuracy.

WHITELAW: Yes, but in a turbulent flow you don't know anything a priori. Are you talking about counting systems?

PIKE: Its a general point. If you know the broadening you can find the mean velocity.

WHITELAW: There is no difficulty with the mean velocity.

BRAYTON: I'd like to amplify one point concerning whether you use the reference beam or dual scatter. The cut off point is really not that well defined. I would say in liquid flows certainly the reference beam is dominating. Certainly where you have a lot of scatter centers the reference beam system is more easily used. The reference beam is much easier to use if you get rid of these apertures near the detector. Just let the open beam go in -- it doesn't hurt the spacial resolution at all. If you do have a lot of scatter centers and they are very small in size (like submicron atmospheric aerosal impurities) and laser power isn't sufficient to get a good signal with the reference beam then you have to take advantage of the increased sensitivity of the dual scatter where you can collect a much larger solid angle from the particle without any increased frequency broadening effects.

WHITELAW: I would agree with the first statement you made -- that the number at which you change from reference beam to fringe system is not well defined. My students and I were discussing this before I left home and were suggesting numbers which varied from one in the control volume to five in the control volume. They guessed that if they had five particles in the control volume at any one time, they would prefer to use a reference beam.

BRAYTON: But certainly if you had a large number, say 20, but they were very small (undetectable by the use of a reference beam) you can see the advantage of going to dual scattering to detect the velocity of the small particles.

WHITELAW: I don't think we're saying anything that's significantly different. I would say one other thing. In water in fact we prefer to use not the reference beam, but the fringe system. Perhaps London water is cleaner than Tennessee water I don't know.

MAZUMDER: With submicron particles at high temperature we've had Brownian motions which are significant. Did this effect cause any problem in flame measurements?

WHITELAW: No. The Brownian motion is not important in these flames. The particles we are using are 0.7235 microns in diameter.

MILLER: I was wondering if you had any problems with dark current in the EMI 9558 B causing spectral broadening? I had an EMI 9558 B and switched to the RCA 4526 and the signal became much narrower.

WHITELAW: That's American prejudice. The only trouble we've had with any EMI tube was when one student rolled one off the bench.

EDWARDS: What size were the photocathodes?

MILLER: The 4526 has a smaller photocathode, but the spot size was the same.

THOMPSON: Maybe you just had a faulty tube.

MILLER: This is from three different tubes.

TECHNICAL SESSION II - SYSTEM DESIGN B

Session Chairman: J.W. Dunning, Jr.

32-B

VELOCITY MEASUREMENTS IN GAS AND LIQUID FLOWS WITH AN INTERFERENTIAL VELOCIMETER

by ALAIN BOUTIER and MICHEL PHILBERT

OFFICE NATIONAL D'ETUDES ET DE RECHERCHES AEROSPATIALES
29, Avenue de la Division Leclerc, 92 CHATILLON (FRANCE)

Summary

An interferential velocimeter using forward scattering is described and the results obtained in a wind-tunnel, into which were injected twenty micron glass balls and one micron marble particles, are presented. For comparison a method using black-background photography and two pulsed ruby laser was experimented in the same wind-tunnel : typical results are shown.

Another interferential velocimeter, using back-scattering, has been experimented on plain tap water flows; results obtained are briefly summarized.

The principle of a two-component interferential velocimeter using two wavelengths is presented. It has been built, but not yet experimented.

I. INTRODUCTION

O.N.F.R.A., the French National Institute for Aerospace Research, is operating a number of wind-tunnels for which its Optics division has been developing visualization techniques such as Schlieren, interferometric or holographic displays, recently supplemented by work on laser velocimeters.

This paper is divided into four parts.

- The first part is concerned with a velocimeter using forward light scattering, which has been used to measure velocities of twenty micron glass balls and one micron marble particles; velocities ranged from 3 m/s to 160 m/s.
- In the second part there is a description of the wind-tunnel facility and of the particle injectors, and the photographic methods with which the interferential velocimeter has been compared. Some typical results will be given.
- The third part will describe a velocimeter using back-scattering, and results obtained in plain tap water flows will be briefly summarized.
- The fourth part will present the principle of a two-component velocimeter using a couple of wavelengths.

II. INTERFERENTIAL VELOCIMETER USING FORWARD SCATTERING

The first device built in our laboratories was a 'crossed-beam' velocimeter using forward scattering (*fig. 1*).

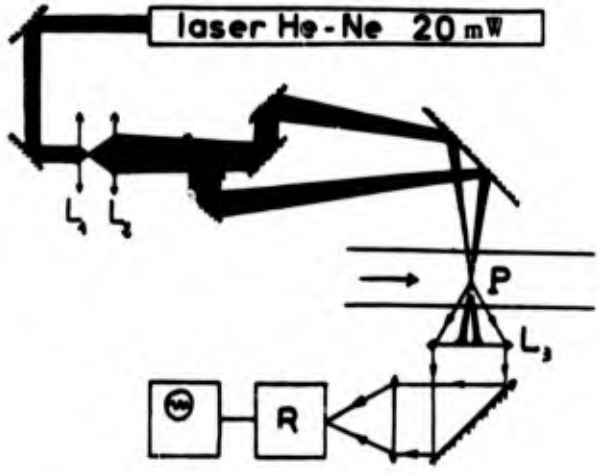

Fig. 1 a - Interferential velocimeter using forward scattering.
L_1 and L_2 : telescope
P : probe volume
L_3 : lens collecting scattered light
R : receiver.

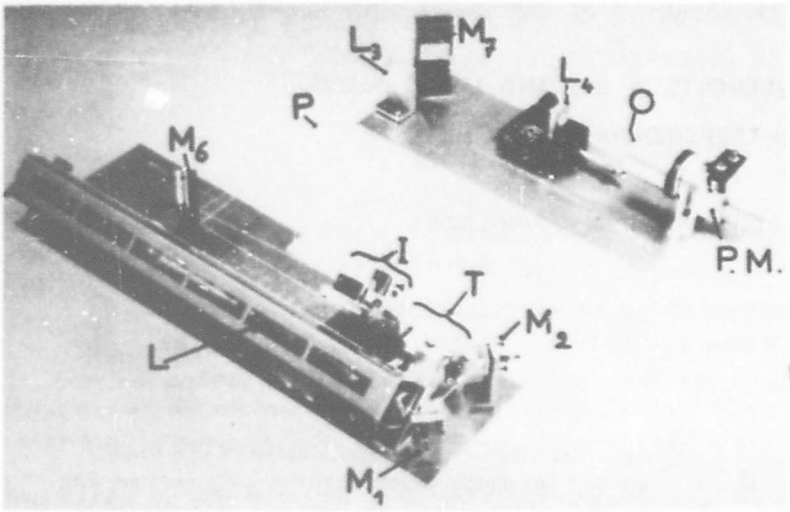

L : laser He-Ne (20 mW)
M_1, M_2, M_6, M_7 : mirrors
T : telescope
I : beam-dividing system
P : probe volume
L_3 : lens collecting scattered light
L_4 : lens to focus scattered light on the P.M.
O : small hole before the P.M.
P.M. : photomultiplier tube with an S-20 photocathode.

Fig. 1 b - Interferential velocimeter using forward scattering.

Two beams running from a twenty milliwatt helium-neon c.w. laser are focussed at point P into the flow by means of a telescope made up of lenses L_1 and L_2. The beam-dividing system provides two beams of equal intensity joining up at point P with the same path length and the same polarization. These beams create a fringe pattern about point P. These two beams are intercepted by two small screens on lens L_3. The receiver is a photomultiplier tube with an S-20 photocathode. The signals are displayed on an oscilloscope; the scope trace is photographed with a Polaroïd camera.

Either of two perpendicular velocity components of the scattering particles could be measured with the apparatus. Figure 2 gives a close-up view of the beam-dividing system. This system splits the incident beam into two beams with the same state of polarization, the same path length, the same intensity, in order to get a better fringe contrast. Depending upon the position of prism C, the beams are contained either in a vertical or in a horizontal plane.

Fig. 2 -

Close-up view of the beam-dividing system.

L : laser He-Ne
M_1 and M_2 : mirrors
S : partial mirror
M_3, M_4, M_5 : mirrors of the beam-dividing system
C : translatable reflecting prism.

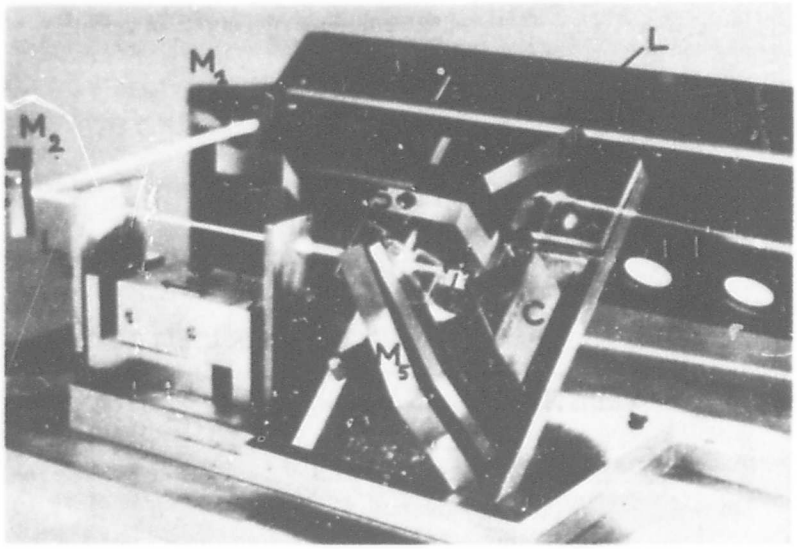

III. WIND-TUNNEL FACILITY – PARTICLES INJECTION – PHOTOGRAPHIC METHOD

III,1. Wind-tunnel – Particles injection

The general outline of the facility with the particles injectors is given on figure 3. Two methods to measure velocities have been developed : the interferential velocimeter and a photographic method which provided a calibration for the former. Besides the two windows on either side of the wind-tunnel for the interferential velocimeter and for taking pictures with the photographic method, a third window was added on top to let through the laser beams necessary, in the photographic method, to illuminate the particles.

There were two flows : the main flow and a secondary flow through the porous wall; particles were injected either into the main flow or through the wall. The measurements were performed in the main flow and near the throat.

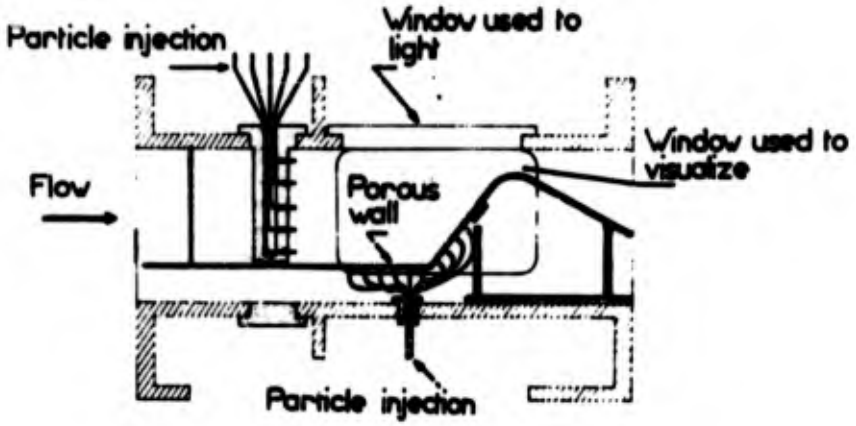

Fig. 3 - Outline of the wind-tunnel.

III,2. Photographic method

The principle of the photographic method using black-background photography is described figure 4. It uses either a He-Ne laser or two pulsed ruby lasers : one of them Q-switched and the other one free-running.

With the c.w. laser illuminating the flowing particles one could take pictures of their trajectories with a standard still camera; the trajectories are recorded against a frame.

The Q-switched ruby laser is triggered and generates a train of two or three pulses by proper adjustment of the dye concentration; the free-running ruby laser is then triggered with a tunable delay. The two laser beam paths are made to coincide on the partial mirror 1. After a reflection on a prism, the mixed beams illuminate the particles contained in a portion of a vertical plane, which is obtained through a cylindrical lens. The laser pulses are monitored on an oscilloscope, giving the time delay between them.

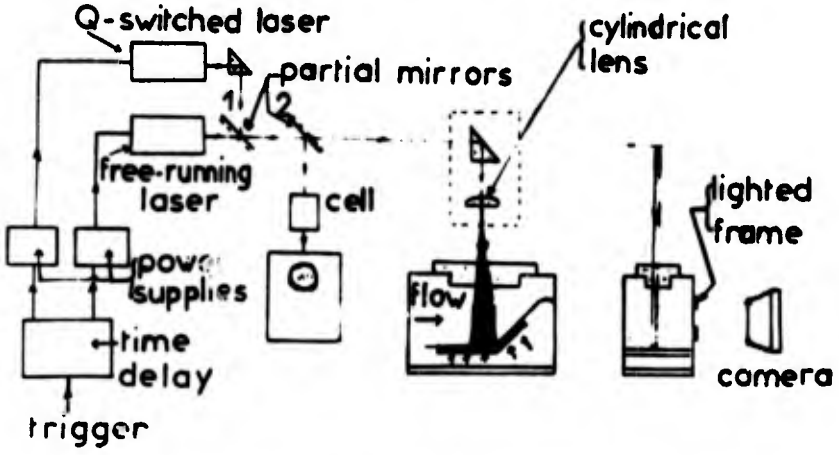

Fig. 4 - Velocity recording with a photographic device.

III,3. Results

Some typical results obtained with the photographic method and the interferential velocimeter are presented below.

Figure 5 shows the flow of one micron particles emitted by one of the injectors as photographed with the He-Ne laser with a thirty second exposure time. These photographs showed where to measure the velocities in the flow.

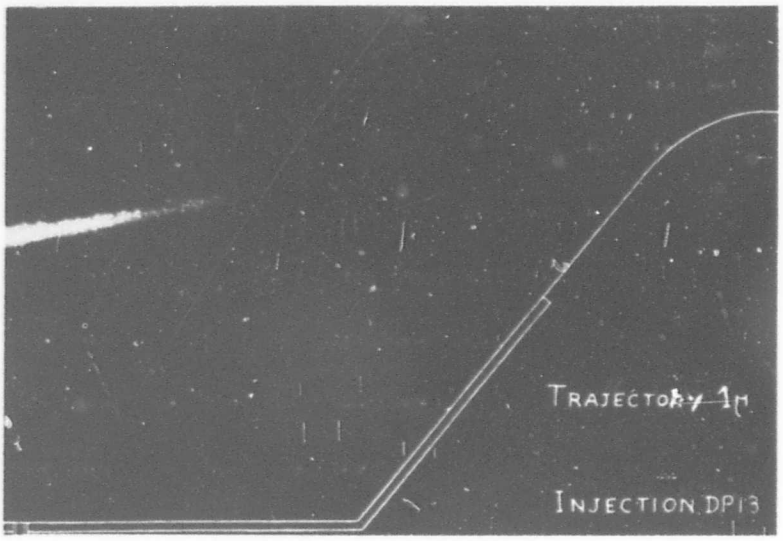

Fig. 5 - Mean trajectories obtained by the photographic method (30 sec. exposure).

Figure 6 shows a typical picture obtained with the photographic method for velocity measurements. Each particle was illuminated by the pulses from the Q-switched ruby laser, producing on the picture two or three bright spots; then the free-running ruly laser produced a train of spots in line with the previous ones; this made easier to find the first dots. In the corner of figure 6 a typical oscillogram is shown, giving the time between the various positions of the pulses from which the average momentum vector between points A and B can be calculated.

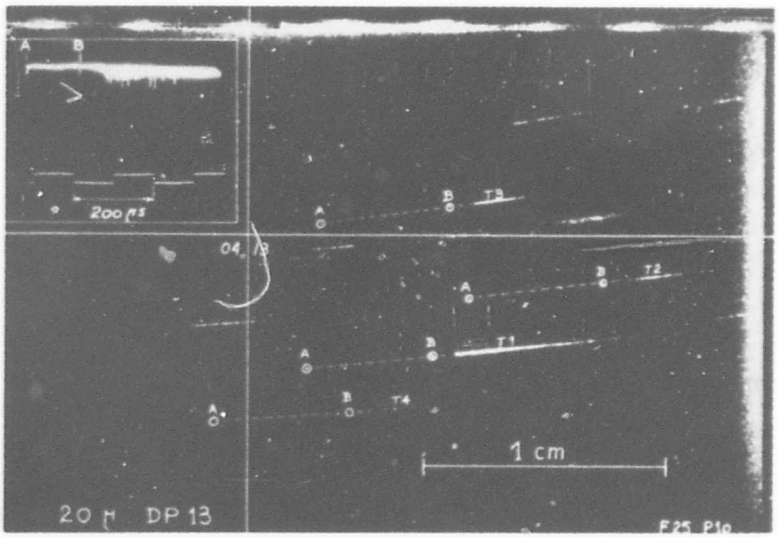

Fig. 6 - Typical picture of velocity recording by photographic method.

The results obtained (*fig.* 7) showed a great dispersion because of turbulent phenomena in the flow and a dispersion in the size of particles.

Figure 8 shows typical signals obtained in the wind-tunnel with the interferential velocimeter. From pictures of these sine signals, histograms were built (*fig.* 9) in order to find the mean value of each component and its root mean square. The measured velocities ranged from 3 m/s to 160 m/s. There were obviously important differences of velocity between twenty micron and one micron particles. For instance it was found close to the throat (*fig.* 10) 160 m/s for one micron particles instead of 100 m/s for twenty micron particles. It was

intended to measure the velocity of the 1 micron particles and not that of the flow itself. The precision of the measures was about 2 %, but the dispersion was more important, due to the same phenomena as those mentioned for the photographic method.

Details about this experiment will be published very shortly in the journal 'La Recherche Aérospatiale'.

Some experiments have been worked out in hydrodynamic tunnels with the same velocimeter using forward scattering; with plain tap water good signals were obtained.

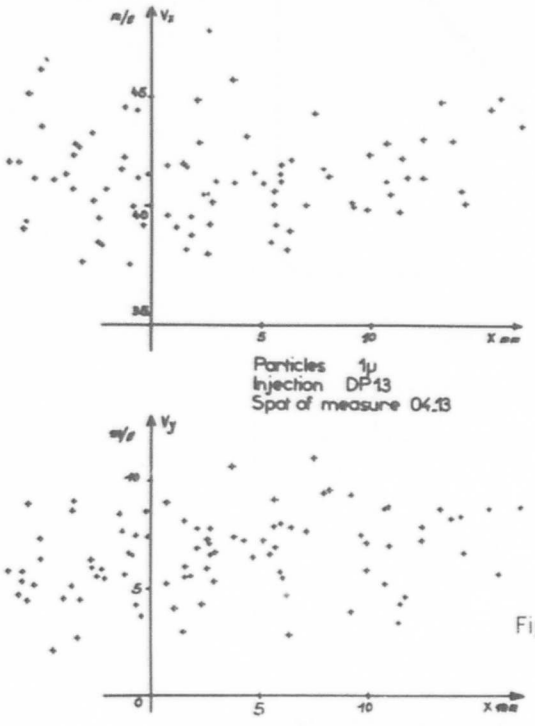

Fig. 7 - Velocities measured with the photographic method in the main flow.

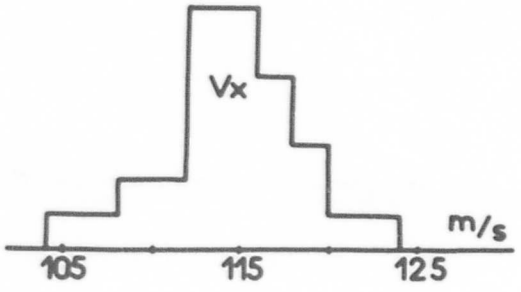

Fig. 9 - Histogram - 20 μm particles near the throat.

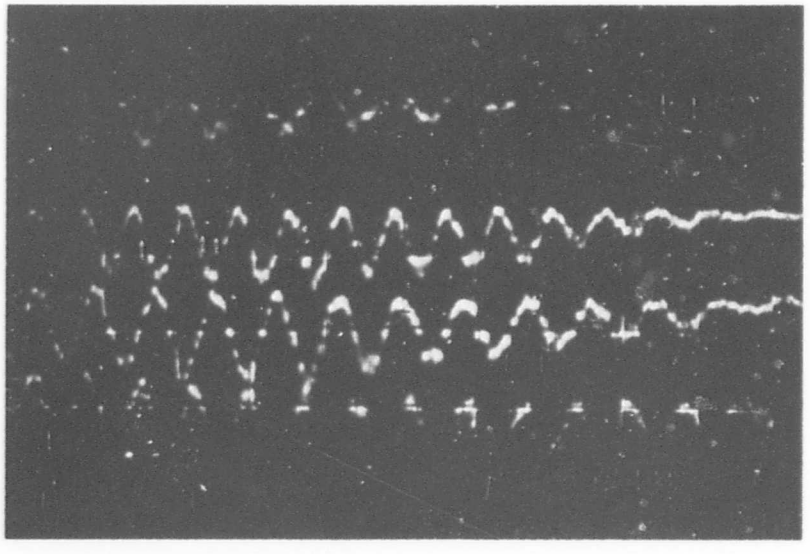

Fig. 8 - Typical sine signals from the velocimeter.

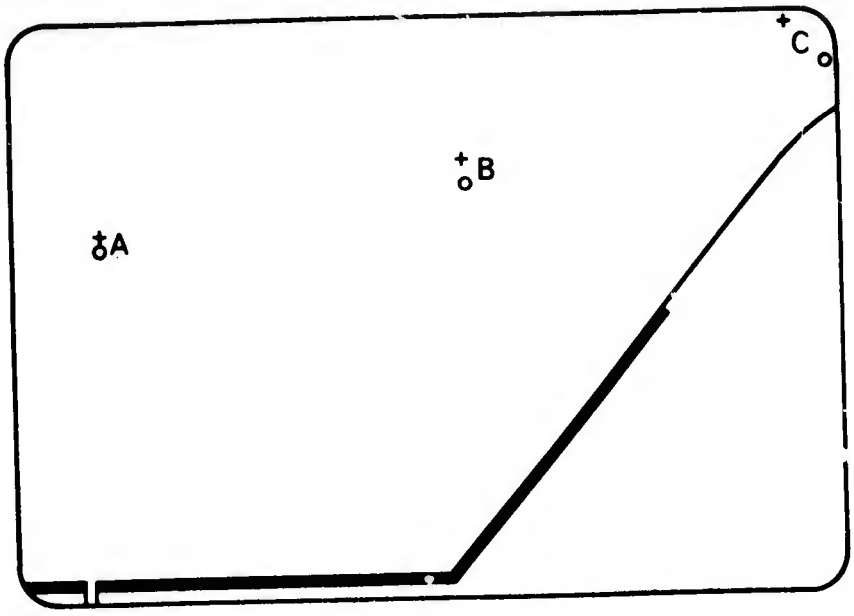

Fig. 10 - Map of the results obtained with the velocimeter.

Positions		A	B	C
Mean velocities (m/s) $\bar{V}_x$	1 μ particle (o)	40 ±1	59 ±3	158 ±8
	20 μ particle (+)	40 ±1	49 ±2	108 ±6
Mean velocities (m/s) $\bar{V}_y$	1 μ particle (o)	9 ±1	25 ±2	42 ±2
	20 μ particle (+)	4.6 ±0.4	19 ±2	56 ±5

IV. INTERFERENTIAL VELOCIMETER USING BACK-SCATTERING

The main purpose of the research was to design a more compact device, in order to make easier the exploration of flows; to this end it was found necessary to build an apparatus based on back-scattering (*fig. 11*).

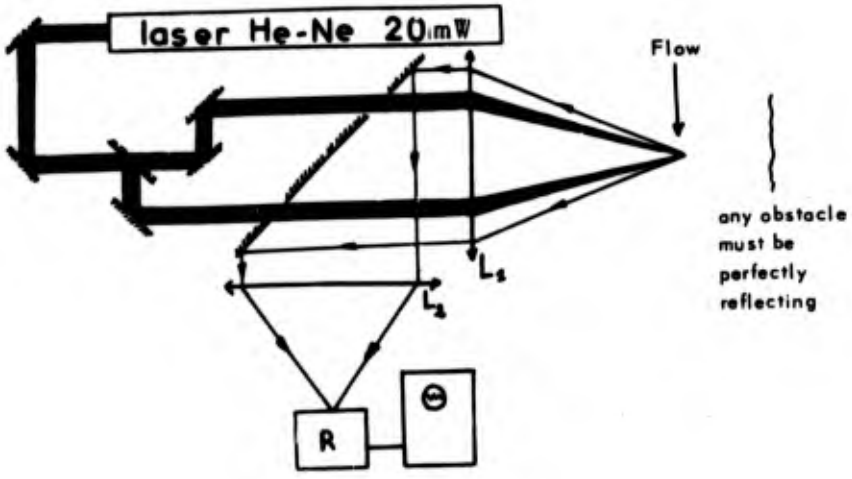

Fig. 11 a - General diagram.

The same beam-dividing system was used, but the two beams issued from it are paralliel. They cross in the probe volume at the focus of lens L_1. The light scattered by the particles passing through the probe volume is collected by the same lens L_1 and is focussed by lens L_2 on the receiver (which is still the photomultiplier tube with an S-20 photocathode), after reflection on a mirror in which two holes are bored in order to allow the two incident beams to go through.

The apparatus shown figure 11-b measured the horizontal velocity component of tap-water running in a glass tube. With a similar device velocities were measured in hydrodynamic tunnels, from a few cm/s to 11 m/s. The same technique was used of taking pictures of scope traces to build histograms.

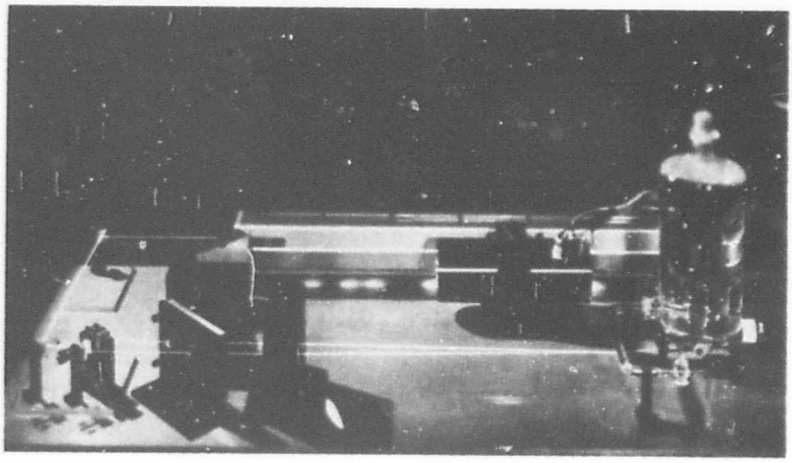

Fig. 11 b - The apparatus as presented at the Paris ' Exposition de Physique'.

Figure 12 sums up results obtained in a water flow with a velocimeter using back-scattering; an obstacle, or pier, had been introduced into the flow in order to detect turbulence behind it. Without the pier the velocity is greater and the turbulence less important. The precision of the measures was estimated to be 1,5%.

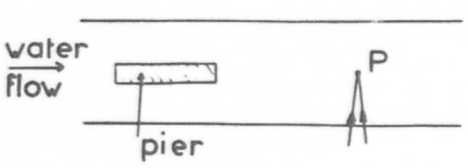

with pier : $\bar{V} = 39,2$ cm/s, $\Delta\bar{V} = 5,4$ cm/s

without pier : $\bar{V} = 44,2$ cm/s, $\Delta\bar{V} = 3,5$ cm/s

Fig. 12 - Results in a water flow.

V. TWO-COMPONENT VELOCIMETER

In this part will be described the principle of a two-component interferential velocimeter, at present under development at O.N.E.R.A.

Two fringe patterns are created, at two different wavelengths (*fig. 13*). An argon laser is used which delivers several wavelengths simultaneously. The beam-dividing system provides for instance three beams; the beam with wavelength λ_1 previously isolated, and the global beam $\Sigma\lambda$ create a fringe pattern with wavelength λ_1 in one axis; it is the same with λ_2 and $\Sigma\lambda$ which create a fringe pattern with wavelength λ_2 in another axis. In this manner two velocity components U and V can be measured simultaneously; two photomultiplier tubes are necessary, one having an interferential filter for λ_1 and the other for λ_2. The two components so obtained can be transformed into rectangular components u and v by appropriate computation.

Of course, with the same principle and a third wavelength λ_3, a three-component velocimeter could be designed.

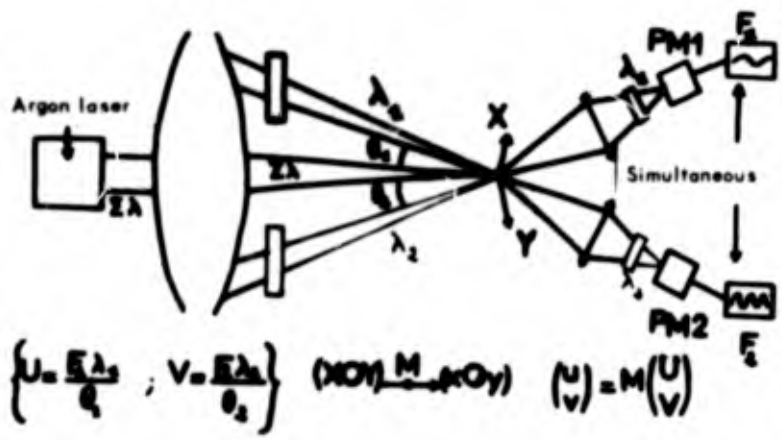

Fig. 13 - Two-component interferential velocimeter.

VI. CONCLUSION

Till now we have worked mainly on optics and mechanics of three types of velocimeters : the first one using forward scattering, the second one using back-scattering and the third one which is a two-component velocimeter. The corresponding automatic processing has not yet been developed.

We hope to experiment in the near future a one-component velocimeter on a flow, the velocity map of which will be perfectly known by aerodynamic calculations; so we shall be able to validate the measurements performed by laser anemometry. Our purpose is to use counting techniques, because the particles arrive randomly and signals last a finite time. So the interesting quantity seems to be the period of the phenomenon; moreover, as the signals are not continuous we plan to make statistics with histograms and to calculate the mean value of the local velocity and its root mean square. Yet it is interesting to record instantaneous velocities for further processing if needed.

The authors express their thanks to Dr. J.P. TARAN who built the first interferential velocimeter in our laboratory and who contributed to the first experiments.

DISCUSSION

FELLER: Regarding your direct measurement by the photographic method of particle trajectory, you found a difference in the trajectory between one micron and twenty micron particles. There is some analytical and experimental work by someone (I don't remember his name) on the fact that in a shear flow there will be a net lift force, lifting the particle away from the wall. Did you try to get trajectories of particles near the wall to see if there was in fact a reduction in the particle density closer to the wall?

BOUTIER: We injected particles through the wall, but they were very quickly dispersed in a cloud. It was not easy to find the trajectory of these particles. We measured velocities with a great dispersion of 10 or 14 percent.

HAUER: Was there any significant component out of the plane? In other words, a component perpendicular to the plane in your photograph?

BOUTIER: It was a two dimensional flow. The tunnel was designed to be two dimensional.

ASHER: Could you tell about the cylindrical lens you used in this velocimeter?

BOUTIER: After the cylindrical lens, the light was dispersed into a plane. We used two kinds of cylindrical lens: the first one for the trajectories, the second one for the velocity measurements. In the direction parallel to the axis of the cylindrical lens we had a plane of one millimeter thick. In the other direction we had a diverging beam the size of which was about 10 or 15 centimeters for the first kind of lens and 2 or 3 centimeters for the second one; these sizes were measured in the field of the photograph. Nevertheless, we used an additional spherical lens in order to avoid a divergence of the thickness of the plane of light.

ASHER: Is the position where you were actually making your measurements where the focus of this lens system was?

BOUTIER: No, it is not. The measurements were made where the thickness was about 1 millimeter; the foucs of the cylindrical lens was close to the lens and the focus of the spherical lens was close to the porous wall.

SPECTRUM OF LIGHT FROM LASER DOPPLER VELOCIMETERS: STATIONARY FLOWS

R. V. Edwards,* J. C. Angus* and J. W. Dunning, Jr.**

*Case Western Reserve University and **NASA-Lewis, Cleveland

Most of the people here will be representing the electronics and optics in the system, and I will start my talk by saying that I am here to represent the particles, which after all, do the dirty work in the system. Briefly, here are the basic ideas. We will assume that we have a nice, plane incoming wave. Over some finite region of the world we have particles that we can see and they scatter light down to the photomultiplier tube. We would like to examine exactly what happens because of this, so the name of the game is to write down the E field due to the scattered light in terms of the particle position (the time dependent particle position). I should point out here that, for heterodyne signals at least, it suffices to only examine the spectrum, or the statistics of the light. It is a fairly easy matter once you have those statistics to arrive at statistics for the photomultiplier current.

$$\varepsilon(K,t) = \text{const.} \sum \exp\left[i\ K \cdot (r_n(t) + vt + L)\right] \times \exp\left(-i\omega_o t\right) P(r_n(t) + vt + L) \tag{1}$$

We have essentially two basic terms here. This is a term due to the time dependent positions of the particles, which represents the phase of the signal (where it is in the fringe pattern) and this term P represents the intensity of the light that is received and heterodyned. The thing we would like to do is calculate the autocorrelation of the E field with itself. That is represented formally by this expression,

$$R_{ii}(K, \tau) = \text{const. Re} \exp(i\omega_o\tau) \ll \exp(-iK\cdot v\tau) \sum_m \sum_n \left(\exp\left\{ iK \cdot [r_n(0) - r_m(\tau)]\right\} P(r_n(0))\ P(r_m(\tau) + v\tau)\right) \gg \tag{2}$$

which is simply the expression for the ε-field at time zero (we

assume a stationary system) times its complex conjugate at time τ. The dual brackets here represent a double average. The reasons for the double average become obvious a little later. You will notice that we really have two terms here. We have the m not equal to n terms, which is to say the interaction between the nth particle and the mth particle in a system. Unless you have an incredibly dense system of particles, or you are scattering from multiple sites on the same polymer, this term will be a random variable and you won't get a contribution from the nth particle interacting with mth particle, so we drop that term coming down to here. I think that is the major change coming from Equation 2 to Equation 3.

$$R_{ii}(K,\tau) = \text{const. Re } \exp(i\omega_o\tau) \ll \exp(-iK\cdot v\tau)\Sigma_n \exp[-iK\cdot\Delta r_n(\tau)]\ P(r_n(o))\ P(r_n(o) + \Delta r_n(\tau) + v\tau) \gg \quad (3)$$

We rewrite things slightly since we now are talking only about the position of the nth particle as a function of time, and this term $r_n(o)-r_n(\tau)$ is rewritten as just Δr_n. It is the change in position of the nth particle in time τ. This expression can be formally evaluated if we have two probability density functions. The first one is the probability of the particle being at some position r. We need that, since we need to know the initial position of the particle. In these systems that is just proportional to the size of the volume that you are looking at. There is a fudge factor to make sure that the integral of the probability density function turns out to be one-integrated over all space.

The second part is a little trickier. That is the probability that the particle will move a distance Δr at time t. In this presentation, we have divided that movement into two parts. There is a Kvt term which essentially the mean flow term and a Δr. This Δr is defined as Δr with respect to the mean motion of the system. What you formally need is the probability density function that describes the probability that a particle will move distance Δr in time τ, and here it appears. $G(\Delta r,\tau)$ is the probability that a particle will move a distance Δr in time τ. By evaluating this integral, at least in principle, you have the autocorrelation of the light. Equation 4 is a result of applying these operations.

$$R_{ii}(K,\tau) = \text{const. } \rho \text{ Re } \exp(i\omega_o\tau) \int_{-\infty}^{\infty} G(\Delta r,\tau) \exp[-iK\Delta r] \times \int_{-\infty}^{\infty} \exp(-iK\cdot v\tau)\ P(r(o))\ P(r(o) + \Delta r + v\tau)\ dr(o)\ d\Delta r \quad (4)$$

$$Q_c = \int_{-\infty}^{\infty} P(r)\, P(r + \Delta r + v\tau)dr \qquad (4a)$$

We call it the master equation because we calculated many things from it. For instance, you could consider that you are doing a Brownian motion study, trying to measure particle sizes for instance. Well $G(\Delta r,\tau)$ in that case, would be the probability density for a Brownian walk problem, something like $\left|\frac{e^{-\frac{\Delta r^2}{4Dt}}}{\sqrt{4\pi Dt}}\right|$. The inner integral represents the effect of the optics of the system--the fact that we do have a finite volume that we look at.

We have solved these equations in gory detail for laminar flows, where $G(\Delta r,t)$ is a very simple form, i.e., the Dirac delta function $\delta(\Delta r)$ in which you say that the particles do not diffuse with respect to the mean flow at least in terms of your measurement. If you plug that in, you can grind through and get the spectrum you do observe for laminar flow.

Figure 1 illustrates typical behavior of the $G(\Delta r,t)$ function. Typically, these probability density functions are such that at time zero this is a Dirac delta function which is to say that the particle doesn't go anywhere in zero time. As time increases, it gets a little fuzzier, in other words, it becomes more and more probable that the particle is somewhere other than where it started and as time increases, the function gets fatter and fatter. This phenomena is rather important to the analysis of the system for turbulent flows. We give you a heuristic argument in the next slide for why that is. The first thing one does, is to rewrite the equation for R_{ii}.

$$R_{ii}\ (K,\tau) = \text{const. Re} \int \hat{G}(K',\tau)\ \hat{Q}_o(K-K')\ e^{-iK'v\tau}\ dK' \qquad (5)$$

You remember there was a term that was $e^{-ik\Delta r}$ times two functions of Δr. Essentially that was a Fourier transform, so we represented it as a convolution of Fourier transforms of the two separate parts of the integral. This term $\hat{G}$ is a Fourier transform of your probability density function and this function $\hat{Q}_o$ is the weighting function for the K vector. This term (Q_c) you can call the finite angle broadening term. You will notice that this is simply the Fourier transform of $[P(r)]^2$. What we would like to do is examine the decay of this function R_{ii}. I guess everyone here is familiar with the first decay mechanism. That is the fact that Q_o represents a finite volume, so as particles come in and leave the volume we have the finite transit time effect. That would cause this R_{ii}, which is the autocorrelation of the signal with itself, to decay. The decay time is the time it takes the particle to go all the way through the volume.

But $G(\Delta r,t)$ gets fatter with time and that implies that the $\hat{G}(K,\tau)$ function, its Fourier transform, gets narrower with time. To make that a little more explicit, if we take some measure of the width of $G(\Delta r,t)$, for instance its rms width (σ_R), and take the same kind of measurement for $\hat{G}(K,\tau)$, σ_K, then from Fourier transform theory we know that product is on the order of one. We define the decay time for the function G as the time when K divided by σ_K is equal to 1. In other words, G(K) is getting narrower and as its width gets down to be the size of K, we define that to be the decay time. We find that $\frac{K}{\sigma_K(\tau_o)} \approx K\sigma_R(\tau_o) = O(1)$. This means that $\sigma_R(t_o)$, which is the width of $G(\Delta r,t)$ (or roughly the mean distance the particle diffuses with respect to the mean flow in time t_o), is on the order of 1/K.

Typical flow meters run with K's around 10^4 or 10^5 inverse centimeters. This roughly means that $\sigma_R(t_o)$, is less than or equal to about 10^{-4} centimeters. In other words, by the time your particles diffuses about 10^{-4} centimeters, the function R_{ii} has started to decay significantly. What we decided to do was to compare the decay time for a particle diffusing distance $\sigma_R(t_o)$ to a typical time scale in the turbulence. We made a very crude approximation here, but I think it works pretty well. We said

$$\sigma_R(\tau) = \sqrt{v'^2}\ \tau \tag{6}$$

That is a very good approximation for very short times compared to Lagrangian integral time scale and is very conservative for large ones, but nevertheless, it gives you the ball park.

$$\Lambda_L = \sqrt{v'^2}\ \tau_L$$
$$\tau_\ell = \int_0^\infty R_L\ (\tau)\ d\tau \tag{7}$$

Equation 7 relates the integral length scale to the time scale. The best we could tell, these length scales are on the order of the shear dimensions in the system. In other words, for pipe flow this number will be somehwere on the order of magnitude of the radius. If we shove this relation back into the previous relation we find t_o (the decay time for R_{ii}) divided by the Lagrangian time scale is on the order of $1/K\ell$. You recall K is about 10^4 cm^{-1} and ℓ's are typically around a centimeter at the smallest, but let us assume it is a millimeter or so. You can still see this number ($1/K\ell$) is on the order of 10^{-2} or 10^{-3}, so the decay time for R_{ii} (the autocorrelation of the light signal) is very small compared

to τ_ℓ. Essentially all we have said is that this term contributes to a decay in the autocorrelation of the signal that is essentially independent of finite transit time term, and that the decay on this term can indeed be very fast. It turns out, for instance, if you are working with a very large sample volume, Q_o would turn out to be a very narrow function so the decay rate for finite transit time effects would be very slow. You can get situations where τ_o would then completely dominate. I will show you that in a little more detail. What we did was assume a situation where the time when we can observe the particles was very short compared to τ_ℓ. Now using a Batchelor type model for $G(\Delta r,\tau)$, basically whatever a particle's doing when we start to observe it, it will continue to do as long as we continue to observe it. In other words, it won't change its velocity significantly over the time that we observe it.

$$G(\Delta r,\tau) \cong \int_{-\infty}^{\infty} F(v')\ \delta\ (\Delta r - v'\tau)\ dv'$$

$$G(\Delta r,\tau) \cong \frac{1}{\tau}\ F\ \left(\frac{\Delta r}{\tau}\right) \tag{8}$$

Using that approximation, we get this form for $G(\Delta r,\tau)$, i.e., $G(\Delta r,\tau)$ is essentially $1/\tau$ times the probability density function for a turbulent fluctuation. $F(v')$ is probability density function for a turbulent fluctuation with respect to the mean flow. Plugging that in, you get an approximation for $G(\Delta r,\tau)$ that appeared in the earlier equations.

Having done that, and plugging that result into the expression for R_{ii}, we get

$$R_{ii} = \int \frac{\hat{F}(K'\tau)}{\tau} \exp\ [-iK' \cdot v\tau]\ Q_o\ (K-K')\ dK' \tag{9}$$

From R_{ii}, since R_{ii} is the time Fourier transform of the spectrum, we can just take the time transform formally and get the spectrum of the signal.

$$I(K,\omega) = \int \frac{F(x)}{x+\bar{v}}\ \hat{Q}_o\ \left(\frac{K\bar{v} - -\omega+Kx}{x+\bar{v}}\right)\ dx \tag{10}$$

$$I(K,\omega) = \frac{1}{|K|}\ F\ \left[\frac{\omega-K\cdot\bar{v}}{K}\right] \tag{10a}$$

This term is the spectrum you would get from a system that was running at a velocity $\bar{V}+x$. The term Q_o, is just the spectrum you could get from laminar flow for a particle moving at velocity $\bar{V}+x$. That spectrum you see is weighted by the probability density function for a turbulent fluctuation. If you consider a very large sample volume, simply make Q_o

a δ function, and you get Equation 10a for a spectrum: the spectrum is for all intents and purposes the probability density function for the turbulent fluctuation. Numbers of these plots have appeared in the literature where people have rather large sample volumes. I think the most striking one is one that appeared in the DISA technical bulletin (No. 12). Essentially it shows the spectrum you would derive from an oscillating flow. Indeed, you do get the probability density function for a sine wave, which you will remember as a two horn beast. It works rather nicely. They did have rather large sample volumes, so we are pretty confident that this result is correct. Inadvertently we have run the system at the opposite extreme where we have incredibly small sample volumes where this term can actually be dominant and you cannot even see the effect of that term. I think you will see how this happens in this slide where we calculate the various statistics of the signal.

The first thing we calculate is the mean doppler shift.

$$\text{MEAN} = K \cdot \bar{v} \tag{11}$$

I would like to echo Dr. Pike here in that at no time have we said that you have a problem in finding the mean frequency. It is just a matter of patience. If you sit and average long enough, you get a nice smooth plot and even a graduate student could find the peak of it. So, you can measure mean velocity with a great deal of accuracy.

$$\text{VAR} = \frac{\overline{V^2}}{4\sigma^2} + \frac{\overline{v'^2}}{4\sigma^2} + \overline{(K \cdot v')^2} \tag{12}$$

Equation 12 represents the variance (the central second moment) of the spectrum. You see we have three components. This $\left(\frac{\overline{V^2}}{4\sigma^2}\right)$ is the finite transit time component, this $(\overline{K \cdot v'^2})$ is essentially the straight turbulent broadening which is due to fluctuations in the direction of the K vector, and this strange term $\left(\frac{\overline{v'^2}}{4\sigma^2}\right)$, which really bothered us for a while, is essentially due to the fact that if the particles leave the volume due to a turbulence fluctuation then you also lose correlation of the signal. In real life, it is very small, so do not worry about it too much, but nevertheless, it does come out of the analysis.

We were also able to calculate an excess term for the spectrum.

$$\text{EXCESS} = \frac{3\overline{v'^2}}{\sigma^2 \left[\frac{\overline{v^2}}{4\sigma^2} + \frac{\overline{v'^2}}{4\sigma^2} + \overline{(K \cdot v')^2}\right]} \tag{13}$$

These are all rather formal expressions, but it turns out now, that if you have the data, you can calculate these things. For instance, it is rather easy to get a precise turbulence intensity from it, if you get a nice smooth spectrum.

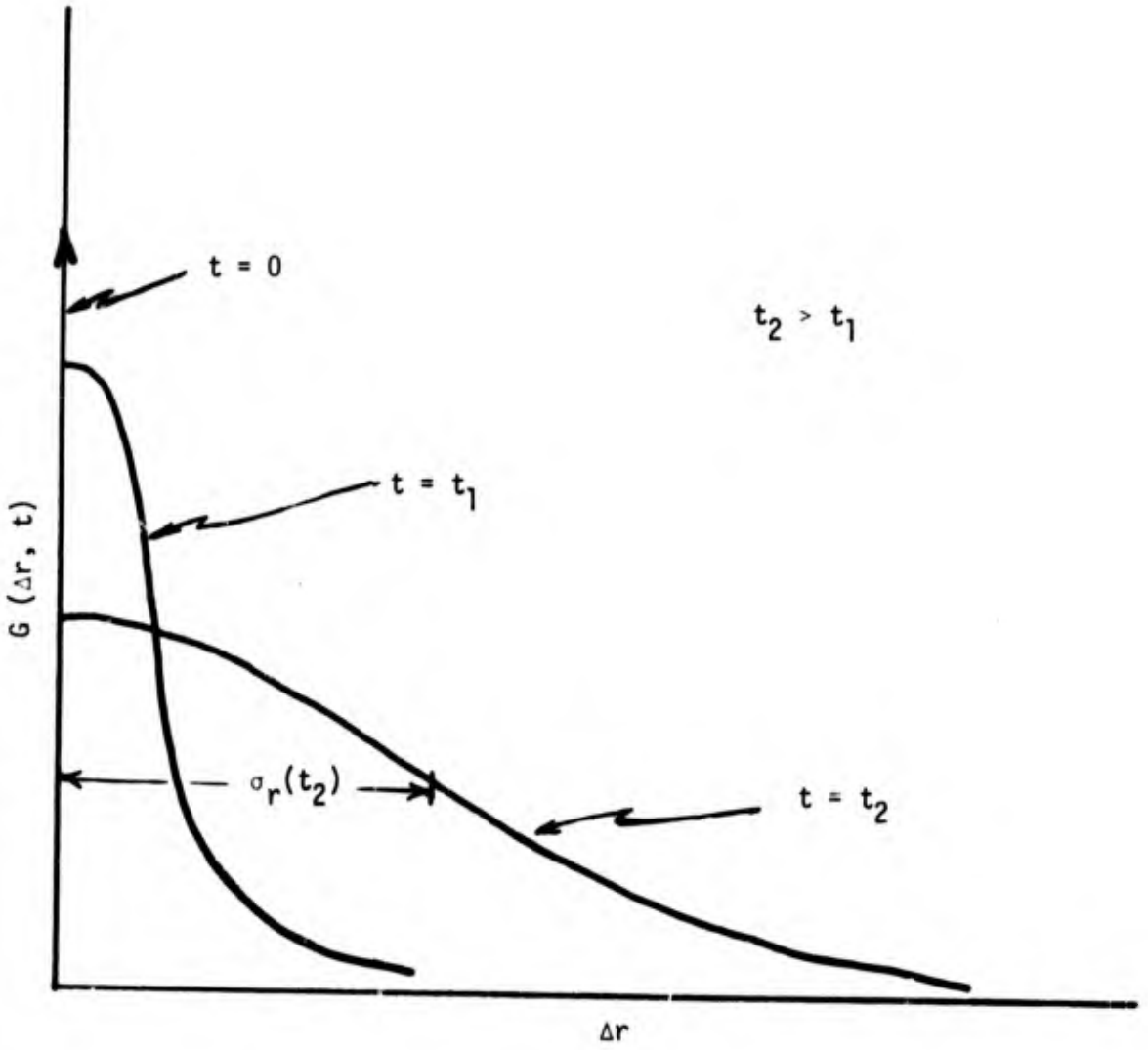

Figure 1

DISCUSSION

GEORGE: I like this presentation. I think it's well done. I think this is the way to look at this problem. My first comment is a minor one. When you talked about the double summation you made the same comment that I've seen in the literature a number of times, that is, that you never have to worry about this double summation unless you have a large number of particles. That's exactly opposite of the true case. If you have a large number of particles the phases, being random because of their random locations, tend to cancel out. In fact you can show that if you have more than ten particles its a 1% contribution. The problem comes in when you have very few particles (one or two) because then that double summation makes a contribution right in the doppler band and can be very significant.

EDWARDS: That depends on the following. Notice I never say anything about the number of particles. That is because there is an implicit assumption in the whole analysis that you do the averaging procedure, whatever it is, well enough to believe the statistics. If you believe that the ergodic assumption applies to this system, then essentially what we're saying is either you have to average for a long time (so that effectively you're looking at many particles even if there are only a few in the system). Or you are looking at a large enough chunk of the system with many particles in it. So that term is not zero, but over a long time average the ratio of the mn term (the pair term) is small in comparison to the contribution of the other term. It's never exactly zero I agree.

GEORGE: My point is, if you have a standard LDV where you sit there and look at the frequency track signal you can very well have a sizable contribution when you have only one or two particles in the system. Now my other comment relates to the last slide. There is a term missing.

EDWARDS: We realize there's a term missing but it's small.

GEORGE: No it isn't small. When I give my presentation tomorrow I'll show you where it comes from. You remember you treated the inner particle correlation. This is what you called $P(\Delta r)$. You showed that that gave rise to this term. But there's another term. Let me show you. You have a scattering volume and suppose you're in uniform turbulence and have a flow coming in like this. This particle is going to contribute. Any doppler velocimeter averages the velocities.

EDWARDS: Right.

GEORGE: It defines what we call the average velocity persistency.

EDWARDS: Right.

GEORGE: Each of these particles deviates. And they deviate from each other. That gives rise to another term, another broadening term which is not related to that one. This is really, as you pointed out, a transit time term which is small. But you get another term something like $(\varepsilon/\upsilon)^{\frac{1}{2}}$ which is related to the inverse time scale of turbulence, the microscale. This term can be dominant for large scattering volumes.

EDWARDS: I hate to disagree. Basically the idea is this. At any one time I agree that you have to know the position of all the particles to know the signal and that they do interact at any one time. The point is that each of these particles is statistically independent. At any one time I agree you're exactly correct, but over a long period these terms don't matter because the particles are statistically independent.

GEORGE: The particle's velocity is evolving in time.

EDWARDS: Right.

GEORGE: The changes in particle velocities in terms of the volume contribute a significant broadening effect. I have data to back it up.

EDWARDS: Let me just point out the following. We say essentially that the measurement length scale for the LDV measurements (looking at the light spectrum) is essentially the fringe spacing. Once a particle wanders more than say three fringes then we have lost correlation with that particle and for all intents and purposes it's a new particle. So we predict that above a given size in the sample volume which is say 100 fringes long, you will see absolutely no change in effect if you don't have a gradient in the mean flow or a gradient in the turbulence intensity.

PIKE: There is an experiment that we published some time ago in which we showed some of the things that Dr. Edwards is talking about, where the width of the spectrum is a function of the spacial volume you look at. This is an experiment in a tube of about one centimeter diameter. You have size of the observation volume as a ratio with diameter of the tube. You see that the doppler spectrum is a function of volume in the way you expect it to be. The turbulence that appears in the middle has recently been of interest and was discussed in a Physical Review letter in the last week or two by Bruce Barriden. They are in fact specifically interested in just this term. It's small in laser doppler circles but large in other circles. The analysis that goes with this paper looks very similar to yours.

EDWARDS: I have not looked at the other paper in detail. We got at this in a very funny way. We were worried about distortion that turns up in the spectrum when you're looking at Brownian motion. That's now this all started. When we hit this G(r,t) function it finally occurred to us that this thing had to be general in the sense that given a correlation it has to exist.

DUNNING. I might point out that we got into the analysis of this from a neutron scattering point of view which gave us this G(r,t) type function rather than a velocity point of view which sometimes leads to trouble. I guess we've introduced a new term, a particle sequence position meter, which is really what it is.

PIKE: Perhaps I could make this last comment on the general question of the theoretical basis of this subject. There is of course a tremendous amount of theory in X-ray scattering on how the form of a scattered beam (even though of higher frequencies) depends on the actual density of the scattering centers. I think it's only a fairly trivial extension to apply that theory here.

A TWO-COMPONENT, DUAL-SCATTER LASER DOPPLER VELOCIMETER WITH FREQUENCY BURST SIGNAL READOUT*

D. B. Brayton, H. T. Kalb and F. L. Crosswy

Experimental Research/Technical Staff
Office of the Managing Director
ARO, Inc.
Arnold Air Force Station, Tennessee 37389

ABSTRACT

A dual scatter laser Doppler velocimeter (LDV) system, designed for measuring wind tunnel flow velocity is described. the system simultaneously measures two orthogonal velocity components of a flowing fluid at a common point in the flow. Essential single velocity component dual-scatter concepts are presented to simplify the description of the more sophisticated two component system. To implement the two component system three laser beams with a 0°, 45° and 90° polarization plane relationship are focused to a common point in the flow by the system transmitting optics. The beams interfere to form two perpendicular sets of interference fringe planes which are orthogonally polarized. The system receiving optics collect and separate the orthogonally polarized components of laser radiation scattered from micron size particles moving with the flowing fluid through the fringes. The system requires no artificial seeding since intrinsic test section aerosols are utilized for radiation scattering. The passage of each scatter particle through the interference fringes simultaneously produces two frequency burst type photo-detected signals, the frequencies of which are directly proportional to two perpendicular components of particle velocity. The system photodetection, signal conditioning and data acquisition instrumentation is specifically designed to process the frequency burst information in the time domain as opposed to spectrum analysis or frequency domain processing. The system was initially evaluated in an AEDC wind tunnel operating over a Mach number range from 0.6 to 1.5. The LDV and calculated wind tunnel mean velocity data agreed to within 1.25 percent; flow direction deviations of a few milliradians were resolved.

---

* The research reported in this paper was sponsored by Arnold Engineering Development Center, Air Force Systems Command, Arnold Air Force Station, Tennessee, under Contract No. F40600-72-C-0003 with ARO, Inc. Further reproduction is authorized to satisfy the needs of the U. S. Government.

I. INTRODUCTION

The merits of laser Doppler shift instrumentation for fluid flow velocity measurements as compared to material probe techniques are well documented.[1-5] The more outstanding features are (1) the velocity is measured directly rather than by measuring a function of velocity, (2) the optical probe, laser radiation, is practically perturbationless as compared to material probes, (3) the detection volume can be as small as 10^{-9} cc, (4) the frequency response can readily reach the 100 MHz range and, (5) measurements can be made in areas inaccessible to and/or not practical for material probes. The laser Doppler velocimeter, hereafter referred to as laser velocimeter, velocimeter or LDV, is being applied at AEDC to obtain velocity data previously unattainable by other techniques.

The first velocimeters,[1-5] reference beam types, measured velocity by detecting the Doppler frequency shift of laser radiation scattered from contaminant particles moving with a flowing fluid. This type velocimeter has been extensively applied[4-5] and has been simplified optically[6-8] so that it is (1) an operational instrument, (2) insensitive to vibrational disturbance, and (3) requires only trivial setup and alignment procedures. However, the signal-to-noise ratio of the reference beam velocimeter is inferior to the dual-scatter type under low scatter particle density conditions.[9] These conditions are encountered when

utilizing intrinsic test section aerosols for radiation scattering. The inpetus to develop LDV systems utilizing intrinsic aerosols is to obviate contamination of wind tunnel instrumentation and the test environment by the commonly used seeding materials (smoke, kerosene vapor, polystyrene spheres, etc.). For these reasons the dual-scatter LDV has been extensively developed at AEDC over the past several years.

The remainder of this paper discusses the fundamentals of one and two-velocity-component, dual-scatter, velocimetry, the operational characteristics of a time domain, electronic, signal processor and the initial transonic wind tunnel evaluation of a two-velocity-component, dual-scatter, velocimeter, signal processor and data acquisition system.

II. SINGLE-VELOCITY-COMPONENT, DUAL-SCATTER, LASER VELOCIMETER

This section presents single velocity component dual scatter velocimeter fundamentals. Some of the material presented in subsections II.A and II.C has been previously published[5,7,8,10,11] and is recapitulated here for completeness. The remainder of the material is derived from recent wind tunnel applications experience and analyses. This section also provides a basis for the subsequent description of the more sophisticated two-velocity component dual scatter velocimeter system.

A. Dual Scatter Fundamentals

Conventional single velocity component dual scatter concepts are presented in Refs. 7, 8, 10 and 11 whereas the self aligning optical design concepts are presented in Refs. 6, 7 and 10 and will be briefly reviewed.

In the optics system diagrammed in Figs. 1a and 1b, the input laser beam 1 is assumed to be collimated, plane polarized, of Gaussian intensity distribution (i.e., TEM_{oo} spacial mode), and to contain, within a few gigahertz bandwidth, many axial or longitudinal modes of a single laser color. Other spacial modes (e.g., TEM_{ol}) can also be effectively employed; however, for analytical convenience the TEM_{oo} mode will be assumed. Beam 1 impinges on the beam splitting glass blocks 2a and 2b with its polarization

plane either parallel or perpendicular to the plane of incidence. The plane parallel working surfaces of the blocks automatically split the input beam into two equal power, parallel path, output beams 3 and 4 which have traveled similar total optical pathlengths. Pathlength matching becomes critical when a short coherence length laser is employed. Lens 5 causes the parallel path beams 3 and 4 to simultaneously focus and intercept at a common point F. Near F each beam focuses to a diffraction limited "spot" or "beam waist" containing planar radiation wavefronts[12]. The minimum beam diameter, D, is[12]

$$D = \frac{4}{\pi} \frac{\lambda}{\Delta\theta} \quad . \tag{1}$$

where λ, the radiation wavelength, and $\Delta\theta$, the beam convergence angle are indicated in Figs. 1b and 1a, respectively. Near F the two plane-wave radiations interfere constructively and destructively to produce parallel planes of adjacently bright and dim illumination or interference fringes. Because the two beams are (1) spacially and temporally coherent, (2) of similar power, and (3) identically plane polarized, the fringe system generated will be of high contrast ratio.

By inspection of Fig. 1b, noting that a bright fringe plane is defined by two wave crests which propagate

in phase with one another, it is seen that adjacent planes of maximum illumination are separated by a distance

$$D_F = \frac{\lambda}{2 \sin \theta/2} \tag{2}$$

where λ and θ are known typically to within .001% and 1%, respectively. When a small light scattering particle of maximum dimension

$$D_{S.C.} \lesssim D_F$$

(particles much larger than a fringe spacing cannot be used to accurately locate a particular fringe position) passes through the beam cross region, it will intercept the fringes at a rate

$$f = \frac{V_o}{D_F} = \frac{2V_o \sin (\theta/2)}{\lambda} \tag{3}$$

where V_o is the velocity component normal to the fringes and Eq. (2) has been substituted. The velocity component V_o is measured by electro-optically collecting and detecting the intensity of light scattered from the fringe region by moving scatter particles. The detected signal frequency is then proportional to the particle velocity component V_o as given by Eq. (3).

Photomultiplier tubes are usually employed for scattered light detection. To eliminate extraneous signals, scattered light is collected only from the beam crossover

region by imaging the crossover region onto a pinhole aperture as indicated in Fig. 1a.

Typical photodetector output signals (current vs. position or time) due to the passage of a single scatter particle through the detection region are shown in Fig. 2. The signal amplitude is proportional to the intensity illuminating the particle and therefore also represents the spacial intensity distribution existing within the detection volume.

An important characteristic peculiar to only the one-component dual-scatter LV is that provided the angle between the illuminating beams is small, any scattered light direction or range of scattering directions can be effectively employed to detect the signal, regardless of the fact that the scattered light is generally elliptically polarized. For spherical particles, the scattered light will remain linearly polarized only for either (1) small angle (paraxial) front or back scattering, or for (2) the electric vector either parallel or perpendicular to the plane of observation.[13] The plane of observation is defined as the plane containing both the illuminating ray and the scattered ray.[13] For nonspherical particles there is generally a polarization change on scattering even in directions making small angles with the incident beam axis.[14] Two colinear elliptically polarized rays scattered from the two illuminating beams in a particular direction add in phase (reinforce one another when the scatter center is

on a bright fringe and add out of phase (cancel one another) when on a dark fringe. Such a polarization situation, however, would introduce cross talk into the two-component dual-scatter LDV of Section III as that system employs selection of linear polarization orientation to eliminate cross talk. The system of Section III will perform most effectively with spherical particles and for either (1) small angle front or small angle back scattered radiation collection, or (2) the polarization plane of each set of fringes oriented either orthogonal or parallel to plane of observation.

The laser power level must be sufficient to scatter at least in the order of one photon into the photodetector as a scatter center moves a distance equal to one fringe spacing, or otherwise the oscillatory signal could not be well defined. Note that this defines a threshold laser power level that is directly proportional to velocity and inversely proportional to the solid angle of radiation collection. Experience has shown that if only residual aerosol contaminant particles are used as a signal source and if the velocity is subsonic, then a few milliwatts of laser power in the visible spectrum is sufficient for detection using front scattered collection, while a few hundred milliwatts is sufficient for similar back scattered collection.

B. Alignment

Proper positioning of the pinhole aperture and the scattered radiation collection lens (Fig. 1a) are the only critical optical alignments required, as the focused, crossed beam condition of the illuminating beams is achieved automatically via the self-aligning optical components. The pinhole aperture and photodetector are usually mounted on a precision adjustable, three-dimensional traverse to facilitate positioning.

A typical surface parallelism specification for the beam splitting blocks (2) of Fig. 1 is one arc second. This is necessary to insure that the illuminating beams will overlap at the beam crossover. It is easily shown that the beam centerline separation distance will not exceed 10% of the focal diameter if the illuminating beams are initially directed parallel to within $\pm 0.127\ \lambda/D_o$ radians, where λ is the wavelength and D_o (Fig. 1) is the initial laser beam diameter.

Ordinary plate glass and plexiglas windows generally deviate the direction of one illuminating beam with respect to the other in a random manner which can cause the beams to intersect poorly. However, such windows can be used efficiently provided the illuminating beams are located approximately normal to the window surfaces

(within a few degrees for most applications) and provided the distance separating the illuminating beams at the window, D_w, satisfies the relationship[15]

$$D_w \ll 0.5\, N_F \text{ cm} \tag{4}$$

where N_F is the number of fringes contained within the detection volume (Eq. 9). Because $N_F \approx 20$, typically, the beam splitting glass blocks (component 4 of Fig. 3) are designed to provide a nominal output beam separation distance of 2.5 cm, thereby satisfying Eq. (4) and insuring a satisfactory beam intersection even though ordinary, nonflat windows are employed.

C. Probe Volume Size

The laser velocimeter probe volume is that region in space from which the Doppler signal information originates. Analyses and measurements of probe volume size are obviously important since these dimensions specify the spacial resolution characteristics of a particular velocimeter system.

The probe volume can be formally defined to be that region of space within which the A.C. Doppler signal amplitude is at least exp (-2) = 0.135 of its peak value.[6,10,16] The peak signal amplitude occurs as a scatter particle passes through the geometrical center of the beam crossover region (0,0,0) as discussed previously. Two effects contribute to the spacial variation of signal amplitude: (1) the gaussian spacial intensity variation of the illuminating beams, and (2) a variation in the scatter collection efficiency of the receiving optics for different points in space.

When a scatter center is located on the ellipsoid

$$z^2 + y^2 \cos^2 (\theta/2) + x^2 \sin^2 (\theta/2) = 2a \left(\frac{\lambda}{\Delta\pi\theta}\right)^2 \qquad (5)$$

it can be shown[16] that the signal current is reduced in amplitude to exp (-a) of its peak value due to effect (1). Therefore, if a very large pinhole aperture is employed (see Fig. 1a) so that the radiation collection efficiency (effect (2) above) is spacially constant, Eq. (5), together

with the previous definition of the "probe volume," dictates that the maximum dimensions of the probe volume are:

$$\Delta z = \frac{4\lambda}{\pi\Delta\theta} , \tag{6}$$

$$\Delta y = \frac{4\lambda}{\pi\Delta\theta \cos(\theta/2)} , \tag{7}$$

and

$$\Delta x = \frac{4\lambda}{\pi\Delta\theta \sin(\theta/2)} ; \tag{8}$$

Note that by inspection of Fig. 1b these x-y-z dimensions of the unapertured probe volume are equal to the x, y, z dimensions of the beam crossover region formed by the intersection of the two cylindrical e^{-2} relative beam intensity contours.

The number of fringes, N_F, contained within the unapertured probe volume (or alternatively within the beam crossover region) is obtained by dividing the width of this region (Eq. (7)) by the fringe spacing (Eq. (2)).

$$N_F = \frac{8 \tan(\theta/2)}{\pi\Delta\theta} \tag{9}$$

Assuming $\lambda = 5\times10^{-5}$ cm, $N_F = 10$, $\theta = 30^{\circ}$, Eqs. (6), (7), (8) and (9) then yield

$$\Delta y \cong \Delta z \cong .001 \text{ cm}$$

$$\Delta x \cong .004 \text{ cm}$$

as minimum dimensions of the beam crossover region attainable with self-aligning optics.

Reference 16 describes radiation collection techniques which effectively reduce the maximum or x-dimension of the probe volume without altering the electrical characteristics of the signal (number of oscillations, amplitude, and frequency). This is accomplished by collecting light from only the centermost or x = 0 portion of the probe volume. This can be done either coaxially ($\theta_s = 0, 180^o$, Fig. 1a) by collecting large amounts of light ($\Delta\theta_s \gg \theta$, Fig. 1a) or by employing off-axis collection ($\theta_s > \theta$ and $180^o - \theta_s > \theta$). For coaxial collection assuming ($\Delta\theta_s \gg \theta$)[16]

$$\frac{\Delta x'}{\Delta x} = \frac{\text{effective probe volume x-dim.}}{\text{unapertured or maximum probe volume x-dim.}} = \frac{e\theta}{\Delta\theta_s} \quad (10)$$

while for off-axis collection[16]

$$\frac{\Delta x'}{\Delta x} = \frac{2 \tan (\theta/2)}{\tan \theta_s},$$

where e = 2.71828 is the natural logarithm base.

D. Accuracy. Flow Direction Dead Zones

Figure 2 illustrates that the angle β between the particle trajectory and the normal to the fringe plane influences the number of signal oscillations above a specified amplitude. For an arbitrary particle trajectory path through any point in the yz plane, the number of fringes intercepted with intensity at lease 13.5% ($1/e^2 = 0.135$) of the peak fringe intensity experienced (near $\sqrt{y^2 + z^2}$ = minimum) is

$$N_F' = N_F \cos \beta \tag{11}$$

where N_F is given by Eq. (7) and β (Fig. 2) is the angle of the particle trajectory with respect to the y-axis. As indicated by Eq. (11) and as illustrated in Fig. 2, as the particle trajectory angle β increases from 0^o to 90^o the number of signal oscillations above a certain relative level continually decreases.

A signal processor of the type described in Section IV.B samples a fixed number of cycles, N_e, of signal information to determine frequency, and thus to detect the velocity of a scatter particle the following condition must be satisfied:

$$N_F' = N_F \cos \beta \geq N_e \tag{12}$$

As discussed in Section IV, this fixed cycle sampler will measure the period of a Doppler burst within an error specification typically $df/f = \pm 0.2\%$ provided the Doppler burst contains a large number of oscillations and is of high signal to noise ratio. The net relative velocity component measurement error,

$$\frac{d\,V_o}{V_o} = \frac{df}{f} - \frac{d\theta}{2\tan(\theta/2)}, \qquad (13)$$

obtained by differentiating Eq. (3), is dependent upon the relative measurement errors of both frequency and angle. Both df/f and $d\theta/\theta$ can be made as small as $\pm 0.2\%$.

To obtain velocity component information for trajectories nearly parallel to the fringe planes (i.e., as β approaches 90^{o}), N_F must be increased and/or the electronic readout must be designed to accommodate very few signal oscillations. For this purpose an electronic signal processor is being designed which will accommodate four cycles of Doppler information. As previously discussed this can be accomplished only with a loss of accuracy. However, when used with an optical system that generates twenty (or forty) usable fringes, so that $N_F = 20$ (or $N_F = 40$), Eq. (12) predicts that velocity component information can be obtained for all particle trajectories except those that make an angle with the fringe planes

less than 14.5^{o} (or 5.7^{o}). Thus a single-component dual-scatter LV contains "dead zones" of flow direction for which velocity component information cannot be extracted. The dead zones appear only when the detected velocity component amplitude comprises only a small portion of the total velocity amplitude. The dead zones can be minimized by sacrificing velocity component measurement accuracy.

III. TWO-COMPONENT DUAL-SCATTER LASER VELOCIMETER

A two-component, dual-scatter, LV detection system will now be described which instantaneously and simultaneously measures two orthogonal components of fluid velocity within a small region of space. The system consists basically of two one-component LV systems identical to the type previously described, with two sets of fringe planes spacially superimposed and located orthogonal to one another. Selective light polarization is employed to discriminate between the two sets of fringes and separately measure two orthogonal velocity components.

An alternate fringe set discrimination technique is to employ two laser colors, one color for each set of fringes.

A. Description

In Fig. 3, the plane polarized laser beam 3 emitted by the laser 1 intercepts the beam expanding and collimating lenses 2 to render it approximately collimated and of suitable diameter. The beam then intercepts three parallel working surface, beam splitting glass blocks 4, which produce three identically plane polarized, parallel

path, optical pathlength compensated, output beams 5, 6' and 7' propagating parallel to the x-axis. As indicated in Fig. 4 these beams are polarized parallel to the z-axis, form a right triangle beam pattern with the most intense beam (beam 6' containing 50% of the laser power) located on the vertex of the right triangle pattern, and with the other two beams each containing 25% of the laser power. After the beams reflect off mirrors 8 and 9, beams 6' and 7' then intercept the polarization rotators 10a and 10b respectively, which rotate the plane of polarization of linearly polarized light around the transmission axis without changing either the degree of polarization, the intensity, or the transmission direction of the light. The polarization rotators (also called polarization rotation plates and circular retarders) are specially designed plates of crystal quartz, cut with their faces normal to the optic axis and of thickness required to produce a specified rotation at a specified wavelength; their faces are polished plane-parallel so as not to deviate the transmission direction. Rotators 10a and 10b rotate the polarization planes by 45° and 90°

respectively, and thereby generate (as shown in Fig. 4) three parallel path beams 5, 6 and 7 with a 0°, 45°, and 90° polarization plane relationship, respectively. Collimating type lens 11 is

positioned such that its axis or geometrical centerline is both parallel to the input beams and intercepts the bisector of the hypotenuse of the right triangle beam pattern as shown in Fig. 4. Lens 11 causes the three beams to cross and focus at point 13. Relatively flat surfaced windows 12 may be present. Collimating type lenses 15 and 16 focus and sharply image the radiation 14 scattered from the crosspoint 13 onto the pinhole aperture 18, while an opaque light stop 17 is employed to block the transmitted illuminating beams 5, 6 and 7. Lens 19 collimates the scattered radiation into a small bundle which intercepts the (Glan-Foucault, air spaced type) polarization separation prism 20. The polarization-separation prism is assumed to be properly positioned via rotation about its transmission axis or the x-axis of the figure such that it will transmit only the y-axis polarization component of the input radiation and will internally reflect only the z-axis component.

The y and z polarized components of scattered radiation thusly separated are directed onto the photomultiplier tube photodetectors 24 and 25, respectively. It is a well-known fact [13] that radiation scattered either forward or backward (approximately parallel or

paraxial to the illumination direction) from a plane polarized illuminating beam is also plane polarized with its polarization plane oriented parallel to that of the illuminating beam. Thus all of the (y-axis polarized) radiation scattered from beam 7 (which is derived from 25% of the total laser power) and the y-axis polarized component of the radiation scattered from beam 6 (which is derived from 50% of the power of beam 6 and thusly from 25% of the total laser power) are directed onto phototube 24. Both of these scattered radiations of course originate only from scatter centers located within the beam crossover region due to the presence of pinhole aperture 18. Similarly, the z-axis polarized radiations scattered from beams 5 and 6 and by scatter centers located within the beam crossover region are collected by lenses 15 and 16 and directed onto phototube 25.

A review of the previous discussion concerning the one component dual scatter LV system together with the preceding discussion regarding polarization separation will reveal that two separate one component velocimeter systems are simultaneously in operation. Beam pairs 5-6 and 6-7 each form plane polarized sets of interference fringes at the crossover point. The two sets of fringe planes are generated by

orthogonally polarized radiations and the planes of one set of fringes are located orthogonal to those of the other. Beams 5 and 7, which are orthogonally polarized, cannot interfere to form a third set of fringe planes. For either front scatter or back scatter (paraxial) radiation collection, the radiation scattered from one set of fringes is cross polarized with that scattered from the other set. The two scattered radiations can thus be easily discriminated using the described polarization separation techniques.

For the two component system described in Fig. 3 and 4, beams 5 and 6 interfere at the crossover point 15 to generate fringe planes orthogonal to the z′ axis (Figs. 4 and 5), and beams 6 and 7 generate fringes orthogonal to the y′ axis. The two velocity components detected are thus parallel to the z′ and y′ axes.

B. Preliminary Proof-of-Principle Measurements

Figure 6 shows simultaneous recordings of the two signals generated by a single low velocity scatter particle passing through the two orthogonal sets of fringe planes of the two component, dual scatter, LDV system previously described and shown in Fig. 3. The signals were simultaneously recorded on a dual trace oscilloscope employing a single electron beam alternating between the two signal channels at a 1 MHz

rate. The 1 MHz signal switching rate is evident in the photographs.

The slight evidences of cross talk indicated in the photographs of Fig. 6 could not be experimentally reduced below the level shown (-20 db typically). As discussed in Section IIA, such cross talk is attributable to the non-linearity or ellipticity of the polarization state of the scattered radiation. Such non-linearity is caused in part by the existence of each of the following conditions: (1) non-spherical scatter centers, (2) relatively large off-axis (non-paraxial) collection of scattered radiation with the plane of observation not being restricted to an orientation approximately either parallel or perpendicular to the polarization plane of either set of fringes.

C. Two Component, Vibration Insensitive, Back Scatter Detection

To obtain two component velocity information by collecting back scattered radiation, scattered radiation 14' of Fig. 3 is collimated by lens 11, reflected by mirror 9 and focused by lens 16' onto pinhole aperture 18'. The remaining optical components 19' through 29' (not shown) are assumed to be present (similar to components 19 through 29 for the front scatter) to process the two components of back scattered signal information. The advantage of having all the optical components except the beam positioning mirror 10 and the focusing lens 11 located near the laser source is that they can be mounted to a common mechanical frame

to virtually eliminate misalignment and resulting signal deterioration due to vibrational disturbances.

Note that additional large mirrors 9 could be used to translate the position of the probe volume 13 throughout a three dimensional space. It is assumed, of course, that such positioning mirrors would be properly oriented with illuminating radiation polarization of beams 5 and 7 either parallel or perpendicular to the plane of incidence) in order to perserve the linear polarization state of firstly the illuminating beams 5 and 7 and secondly of the detected radiations 14' individually scattered from beams 5 and 7. Mirrors 10, lens 11, and windows 12 could then be vibrated through relatively large amplitudes and the backscattered detection system would continue to detect signal, but now with the position of the probe volume oscillating or moving in space.

D. A Comparison of Front and Back Scatter Detection

The front scatter design consists of two spacially separated optical systems individually concentrating on two different small regions of space. It is only when these two regions coincide that signal information can be processed. Vibrational disturbances can cause an intermittent loss of signal and reduce the rate of data acquisition (generally the illuminated region and the collection region will overlap during some portion of the vibrational cycle).

Generally it has been found that the front scatter system is very easy to set up on small wind tunnels, simple to align, and relatively inexpensive. Furthermore, a non-rigidly mounted front scatter system will perform excellently on medium size tunnels with moderate vibrational levels. For example, for the front scatter LDV application of Sec. V, vibrational disturbances caused the system to be misaligned approximately 50% of the time, causing a 50% reduction in the data rate.

The basic advantages of the backscatter system are derived from the fact that its optical components can be constructed into a single integral unit. Such a design is potentially more versatile, potentially provides improved performance in a vibrational environment, and may be more economically applicable to large wind tunnels (the cost of two traverse systems may be greater than the cost of one traverse system and a higher power laser). Extraneously

reflected and scattered laser radiations can create substantial problems with backscatter units, however. Because the scattered intensity is approximately two orders of magnitude reduced for back scattering in comparison to front scattering, higher power lasers must be employed. This increases the level of extraneously scattered and reflected laser radiations reaching the photodetector. Such radiations cannot be optically bandpass filtered because they are essentially the same frequency as the signal. To reduce such extraneous radiations, two types of backscatter system design are being investigated: (1) an off-axis backscatter system employing separate optical units for illumination and collection purposes, and (2) a co-axial backscatter system with light baffles. The off-axis design provides much better rejection of extraneous laser radiation, while the co-axial design lends itself to simplified techniques of alignment and of traversing the probe volume.

E. Non-Simultaneous Detection

If simultaneous time detection of the two velocity components is not required, the flow direction dead zones (Section ID) can be virtually eliminated. This is accomplished by allowing three similarly polarized laser beams to illuminate the probe volume and using one photodetector. Data is taken for a particular velocity component with one of the three beams blocked, such that two illuminating beams remain. By alternately

blocking each of the three beams, one can obtain three non-orthogonal components of velocity all parallel to a common plane. If the total velocity vector is approximately parallel to this plane and is allowed to rotate 360° within this plane, at least two of the three velocity components will remain active at all times. That is, only one component at a time will be in a "dead zone." The two active components can be used to calculate two orthogonal components of velocity.

IV. PHOTODETECTION, SIGNAL CONDITIONING AND DATA ACQUISITION SYSTEMS

The electronic components discussed in this section were designed primarily to accommodate the short time duration, frequency burst type signals commonly encountered with the dual scatter type LDV. However, they have been routinely used with continuous wave signals produced by either the reference beam or dual scatter type LDV systems.

A. Photodetection Electronics

The photodetector assembly consists of a photomultiplier (PM) tube with magnetic, electrostatic and electromagnetic shielding and a wideband amplifier-transmission line driver. An S-20 photocathode was selected to provide a radiant sensitivity range which accommodates either the helium-neon or argon laser. The PM tube pulse rise time specification is 2 (10^{-9}) seconds. The PM tube anode is terminated by the 100 ohm input resistance of the wideband amplifier.

The wideband amplifier-transmission line driver 3 db bandwidth is 10 KHz-220 MHz. The gain is set at a modest 10 db level. Electronic system bulk gain is then provided by bandpass amplifiers in the signal conditioning instrument.

B. Frequency Burst Signal Processing and Data Acquisition Electronics

The frequency burst signal processing electronics system shown in Fig. 7 is a hybrid analog-digital signal conditioning and processing instrument termed a Doppler Data Processor (DDP). The functions of the DDP are (1) to filter out extraneous noise, (2) to determine the average period of eight cycles of the Doppler shift signal, (3) to negate a data recording cycle when the period of eight cycles is not equal to twice the period of the first four cycles, and (4) to provide a visual display and a binary coded decimal output of the period of the Doppler signal. The data acquisition system employs a paper tape digital printer for immediate access to the data and an incremental magnetic tape system for mass data recording and compatibility with subsequent digital computer computations.

The photodetector signal for a small scatter particle passing near the geometric center of the probe volume is indicated in Fig. 2. Ideally, the D.C. shift of the signal (see Fig. 2) is comparable in magnitude to the A.C. or Doppler signal portion; however, this is not the case for unequal illuminating beam intensities, for particles larger than the fringe spacing or for particles passing through the z-axis (Fig. 1) peripheries of the

probe volume. Photodetector shot noise generated by the D.C. shift as well as background radiation tends to obscure the Doppler signal information. A bandpass amplifier is used to remove much of this D.C. shift and to minimize the associated shot noise.

A representative signal introduced at the input to the DDP is shown in Fig. 8a. The bandpass amplifier (Fig. 7) output signal is shown in Fig. 8b. The Schmitt trigger (Fig. 7) output signal is shown in Fig. 8c. An oscilloscope triggered gate (Fig. 7) at the output of the Schmitt trigger prevents passage of pulses to the A-B-C-D ripple counter when the signal level at the oscilloscope is below a certain selectable trigger point. This technique has proven to be a valuable means of signal level selection and noise rejection.

The gated signal applied to the A-B-C-D binary ripple counter produces a single rectangular wave signal or "pulse" at the D Binary output (Fig. 8f) with a time duration equal to the total period of the first eight pulses in the gated pulse train. At this point binary D is inhibited from further toggling by Binary I until a recycle control pulse is received. The D Binary pulse becomes the gating signal for the main gate pulse stretcher (Fig. 8g) which produces a resultant pulse precisely stretched in time by 125 times the D Binary

pulse. Precision current sources contained within the pulse stretcher permit very precise time duration extention of the D Binary pulse width. The stretched pulse controls the main gate of a conventional frequency counter. During the stretched pulse interval, precisely timed clock pulses from a crystal controlled oscillator pass through the main gate and accumulate in the counter decimal counting units (Fig. 7). The resultant counter visual display reads the average period of the Doppler signal information in nanosecond units. The pulse stretching technique is useful for short burst signal period determination at frequencies extending from 100 KHz to 100 MHz. At lower frequencies the main gate pulse stretcher is not required.

The circuits described thus far measure the average period of both periodic and non-periodic signals. When the signal pulse train becomes non-periodic during this time period due to included noise spikes, peak fringe intensity irregularities, or large fluctuations in peak signal amplitude, it becomes necessary to detect this condition and prevent the recording of a data point. A digital pulse rate filter consisting of pulse stretchers and error logic circuitry functions as such a detector.

The operation of the digital pulse rate filter can be explained by referring to Fig. 7. The first four pulses of the sampled pulse train are applied to the Δ binary. This binary is inhibited after the fourth sampled pulse and produces a gating pulse (Fig. 8j) to dual pulse stretchers designated as $\Delta 1$ and $\Delta 2$. The time stretch ratio of these pulse stretchers, nominally 250/1, is adjusted to produce output pulses (Figs. 8h and 8i) that bracket the main gate pulse stretcher output pulse (Fig. 8g) when sampling a pulse train of uniform period. The three pulse stretcher waveforms are initiated at the same instant in time. The $\Delta 1$ and $\Delta 2$ pulse time durations are set greater than and less than, respectively, the main gate pulse duration. This produces a "window" at the trailing edge of the $\Delta 1$ and $\Delta 2$ pulses (Figs. 8g-i). The window width is the time difference between the $\Delta 1$ and $\Delta 2$ pulses and can be as narrow as the stability of the two pulse stretchers permit, typically $\pm$ 0.5% of the main gate pulse duration. AND and NOR logic blocks (Fig. 7) are employed to monitor this window. If the main gate pulse trailing edge occurs within the window time span, no corrective action is initiated and a data point is recorded. Termination of the main gate pulse outside the window, indicating a non-periodic pulse train, produces a reset pulse which negates this data point and resets the entire instrument.

The pulse stretchers function through the medium of constant current sources charging and discharging timing capacitors. The resultant ramp voltage waveform excursions possess optimum minimum and maximum limit values that should not be exceeded for linear operation. Overrange detectors in the form of digital comparators sense the presence of input pulse data that would cause pulse stretcher limiting.

The DDP main gate pulse stretcher will measure the period of a standard oscillator signal source with a long term accuracy of $\pm$ 0.2%. If the Doppler signal is of large signal to noise ratio, is highly periodic, and contains a large number of oscillations (e.g., 15 or more), the DDP should also record its period to $\pm$ 0.2%. At worst, i.e., with poor signal conditions, the accuracy of the DDP should approximately equal the pulse stretcher window width, which is usually set at $\pm$ 2%.

A $\pm$ 2% window width will increase the data acquisition rate substantially over a $\pm$ ½% window width, with the possibility of a slight loss in accuracy. Included noise in the signal will cause the Schmitt trigger (which is essentially a level crossing detector) output period to be nonuniform. Also very few cycles or large D.C. shift will cause substantial D.C. shift to pass through the bandpass amplifier with the Doppler signal; these conditions will

also, in general, cause the Schmitt trigger output pulse train period to be nonuniform. The period nonuniformities caused by included noise and/or D.C. shift are largely rejected with a $\pm$ ½% window and largely passed with a $\pm$ 2% window.

The Doppler Data Processor sampling rate is dependent upon the Doppler frequency, the repetition rate of the incoming burst data, and the counter recycle time. The counter recycle time (present minimum 2 milliseconds) limits the DDP sample rate to a maximum of 500 samples per second.

Further processing of the information stored in the counter is accomplished by standard digital equipment as shown in Fig. 7. For a two velocity component system, burst data at two different Doppler frequencies must be processed together with position and time information. A digital scanner is employed to sequentially direct the data from each source to a digital line printer and to an incremental digital tape recorder. The tape system offers the significant advantage of direct compatibility with a digital computer whereby rapid data reduction may be accomplished.

The sampling circuits in the DDP make extensive use of emitter coupled logic integrated circuits.

V. APPLICATION TO A TRANSONIC WIND TUNNEL

A. General

Reference 17 describes in detail the successful utilization of a two-component dual-scatter LDV to measure velocity in a transonic wind tunnel located at the Arnold Engineering Development Center. In this evaluation test, 6,729 individual data points were recorded in approximately 8 hours run time, at various test section positions, and over a Mach number range of 0.6 to 1.5. No artificial seeding of flor was employed. Flow angularities as a function of tunnel position were detected to within a few milliradians. The magnitude of the LDV velocities that were measured at the tunnel centerline averaged 1.25% higher than predicted by aerodynamic calculations.[17] This discrepancy can be attributed to systematic errors of either or both the LDV and the aerodynamic velocity measurement instrumentation used.

During the test, individual particle Doppler burst signals were simultaneously recorded on both a CRT storage oscilloscope and by the Doppler Data Processor. Examples of real time CRT oscilloscope signal photographs and the corresponding period recorded by the Doppler signal processor are shown in Fig. 9. The trigger gate output of the oscilloscope was used to trigger the Doppler Data Processor. In

this way, two independent period measurements of the signal generated by the same scatter center were compared. It was found that the discrepancy between the signal processor data and signal period calculations from the oscilloscope photographs was within ± 2% for each frequency burst type Doppler signal from 4.0 to 20.0 MHz.

B. System Design Considerations

This section discusses the general considerations which led to the particular system design employed for the LDV instrument evaluation test in the transonic wind tunnel.

Figure 3 is a scale drawing of the system used, with different scale factors for the x and y axes. Figures 4 and 5 are expanded cross-sectional views of certain features of Fig. 3. Figures 3, 4 and 5 completely describe the final LDV optical system design. All important dimensions such as beam diameter and spacing, lens focal length and diameter, pinhole aperture diameter, etc., are either drawn to scale or specified in the figure descriptions.

Referring to Figs. 3, 4 and 5, the two sets of fringe planes were each located at 45° with respect to the -y directed flow. This permitted two velocity components to be simultaneously monitored such that the amplitude and direction of the total velocity vector could be calculated. It was decided to use front scattered radiation collection to maximize the signal and signal to noise ratio. The size of the tunnel and tunnel obstructions dictated that the

illuminating and receiving optics could not be mechanically connected and simultaneously traversed. On-axis rather than off-axis radiation collection was chosen to facilitate realignment of the two optical units as the test section was traversed.

The probe volume position was changed by first moving the illuminating optics (component 11 for an x-traverse and components 9, 10 and 11 simultaneously for a y-traverse). Optical realignment was then accomplished with the opaque stop 17 removed; components 18, 19 and 20 were simultaneously x-y traversed until the transmitted illuminating beams focused on the pinhole aperture 18. The opaque stop 17 was then reinserted. Final alignment adjustments were accomplished by observing and maximizing signal amplitude on the oscilloscope while simultaneously y-z traversing components 18, 19 and 20.

The information contained in Figs. 3, 4 and 5 along with Eqs. 4-10 can be used to show that (within the measurement precision of the scaled quantities):

(1) For each velocity component approximately 21 fringes (Eq. 7) were contained within the probe volume.

(2) For each velocity component approximately 15 of these fringes (Eq. 8) were crossed by a y-directed particle. This number is sufficiently large (Eq. 9) to permit operation of the Doppler signal processor.

(3) The nominal calibration constants for each velocity component were (Eq. 4)

$$Vo/f \cong 16.7 \quad \text{meter} \cdot \text{sec}^{-1} \cdot \text{MHz}^{-1}$$

(4) The diameter and length of each beam crossover region were (Eq. 5, 6 and 7)

$$\Delta y \cong \Delta z \cong 0.35 \text{ mm}$$

$$\Delta x \cong 70 \text{ mm}$$

(5) The effective length of each probe volume was reduced because the radiation collecting lens subtends a larger angle than the angle between the illuminating beams. This limits the x dimension of each probe volume to (Eq. 10)

$$\Delta x' = 32 \text{ mm}$$

REFERENCES

1. Foreman, J. W., Jr., Appl Optics 6, 821 (1967).

2. Goldstein, R. J., and Kried, D. K., Trans. A.S.M.E., Ser. E, J. Appl. Mech., 34, 813 (1967).

3. Davis, D. T., I.S.A. Trans. 7, 43 (1968).

4. Angus, J. G., Morrow, D. L., Dunning, J. W., and French, M. J., Industr. Engr. Chem. 61, 8 (1969).

5. Lennert, A. E., Brayton, D. B., Crosswy, F. L., AEDC-TR-70-101, (1970).

6. Brayton, D. B., 1969 Proceedings Electro-Optical Systems Design Conf. (Industrial and Scientific Conference Management, Inc., 222 W. Adams St., Chicago, Ill., 1970), pp. 168-177.

7. Mayo, W. T., J. Sci. Inst. (J. Phys. E) 3, 235 (1970).

8. Rudd, M. J., J. Sci. Inst. (J. Phys. E) 2, 55 (1969).

9. The concept of "threshold laser power level" as discussed in the latter part of Section II A for the dual scatter LDV is also applicable to the reference beam LDV. For all reference beam configurations except for that of backscattered radiation collection, the scattering direction must be severely restricted in range due to frequency broadening considerations[1-6]. Thus, except for back scattering, the reference beam LDV requires a higher threshold laser power level.

10. Brayton, D. B. and Goethert, W. H., Trans. Inst. Soc. Am. 10, 40 (1971).

11. Penny, C. M., I.E.E.E. J. Quantum Mech. QE5, 318 (1968).

12. Kogelnik, H., Bell Sys. Tech. J., March 1965, pp. 467-470.

13. Born, M., and Wolf, E., "Principles of Optics" (3rd revised ed., Pergamon Press, New York, N. Y., 1965), pp. 652.

14.

15. Let it be assumed that wedge refraction caused by the poor surface flatness of an ordinary window will cause the direction of each illuminating beam to be deviated by an average angular amount, α_W, in a random direction. One can then show that the beam separation distance at the window, D_W, must satisfy $D_W \ll N_F \lambda/\alpha_W$ if substantial beam overlap at the beam crossover point is to be maintained. The quantity, α_W, has been experimentally determined to be about 1×10^4 radian by examining the crossover point after inserting many ordinary plate glass and plexiglass windows.

16. Brayton, D. B., and Farmer, W. M., "An Analysis of the Probe Volume of a Dual-Scatter Laser Doppler Velocimeter," to be published.

17. Smith, F. H., Lennert, A. E., and Hornkohl, J. O., AEDC-TR-71-185 (1971).

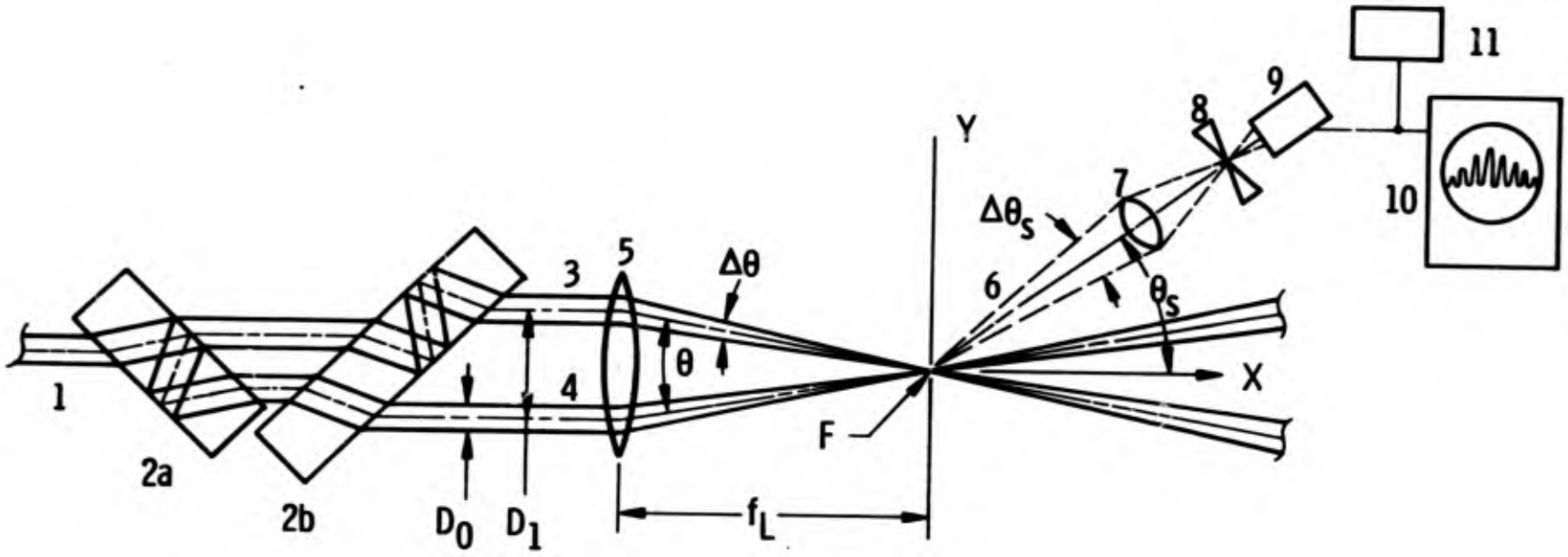

Fig. 1a Single Velocity Component, Dual-Scatter, LV Detection Scheme. The parallel surface, coated optical flats 2a and 2b cause the laser beam 1 to be split into two equal intensity, parallel path beams, 3 and 4. Lens 5 causes these beams to both cross and focus at a common point F. Light 6, scattered from particles moving through the adjacently bright and dark interference fringe planes established near F, is first selectively collected by the lens-pinhole aperture combination 7 and 8, and then detected by the photodetector system 9. Light intensity versus time is displayed on the CRT oscilloscope 10 and the signal period is simultaneously determined by the Doppler burst signal processor 11.

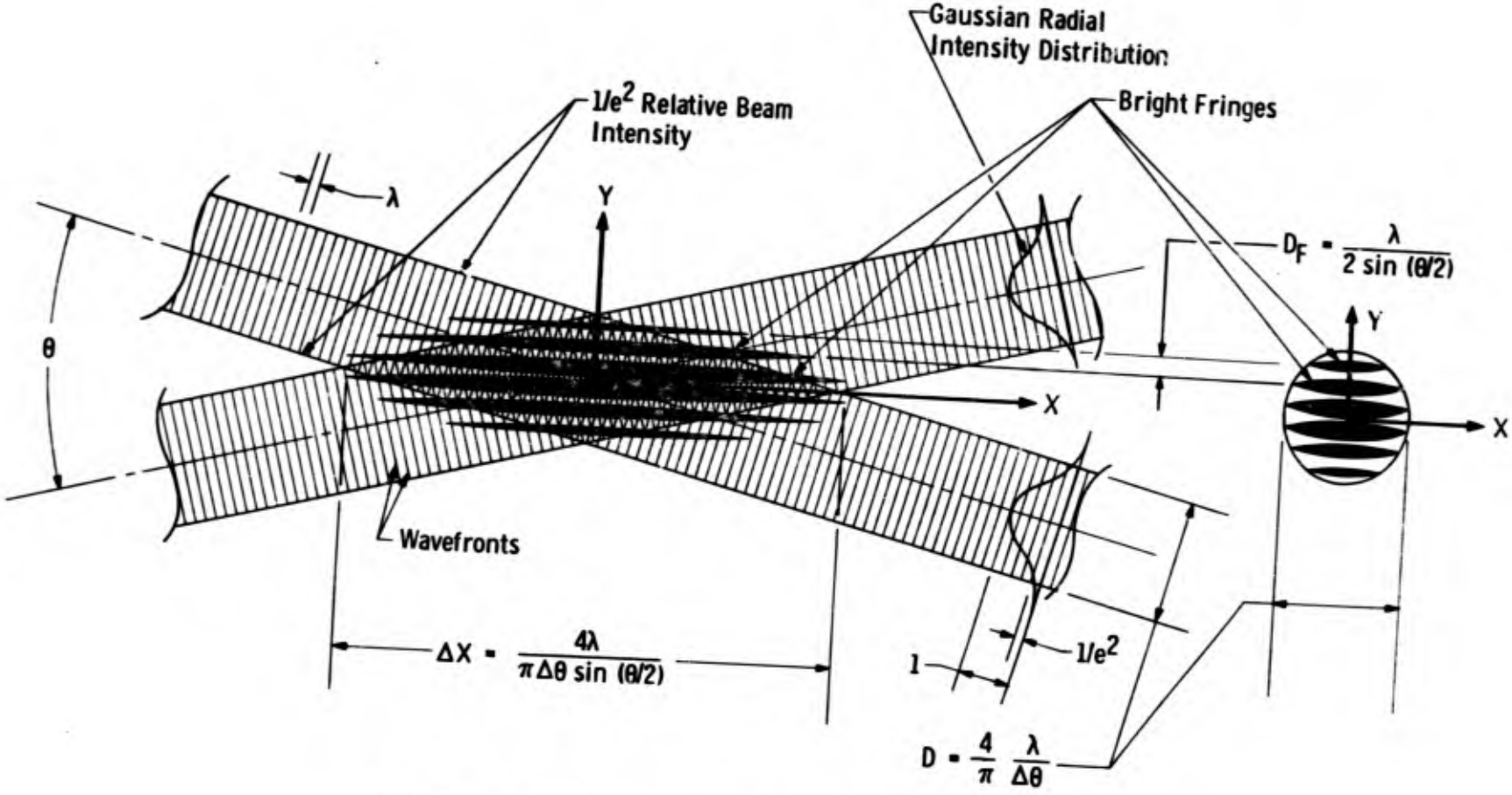

Fig. 1b Enlarged cross-sectional views of the beam crossover region F of Figure 1a. The indicated fringe width is proportional to the local peak fringe intensity.

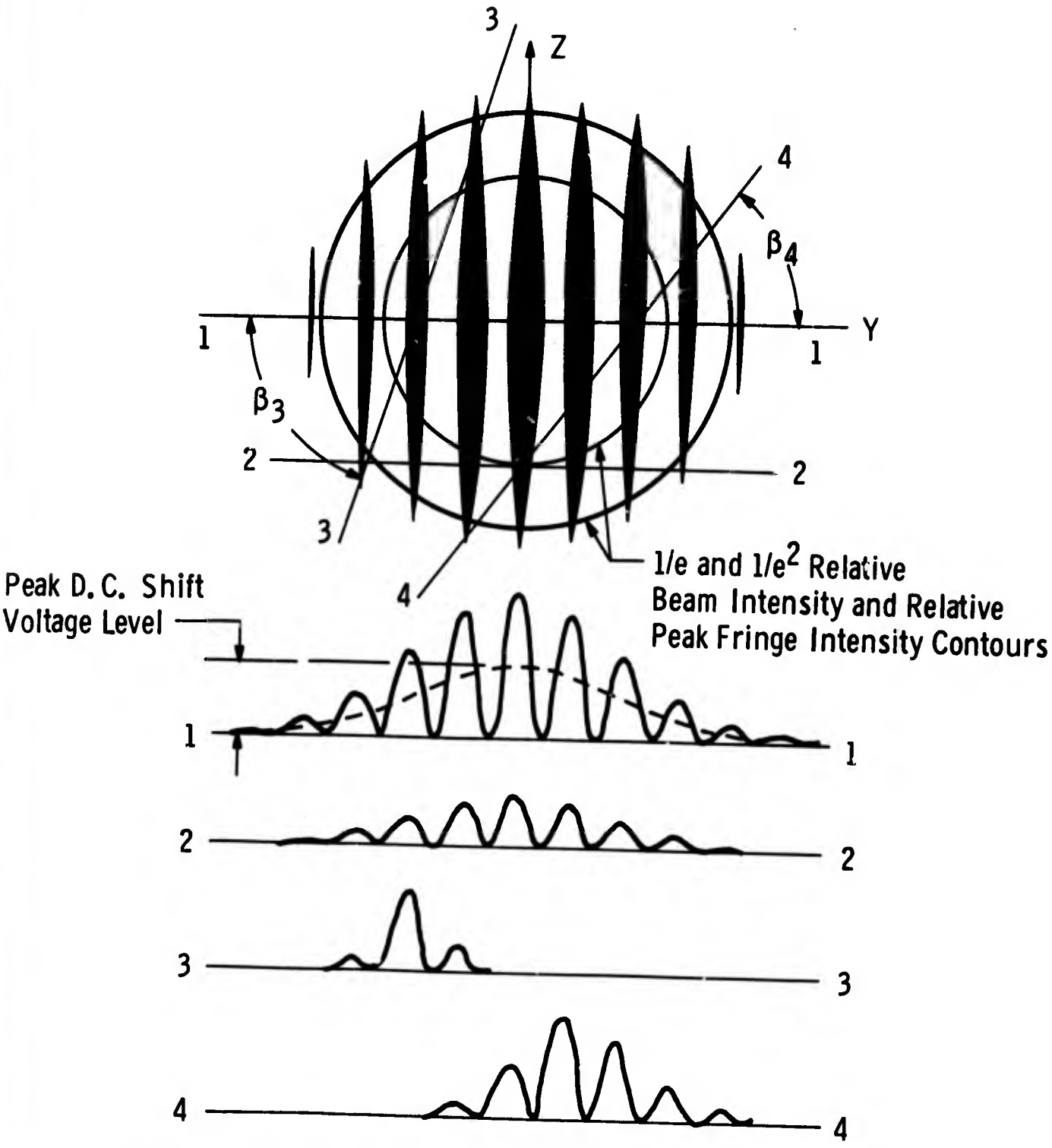

Fig. 2 Signal Amplitude versus Particle Position near X = 0 for a Number of Particle Trajectories. The indicated fringe width is proportional to the local peak fringe intensity.

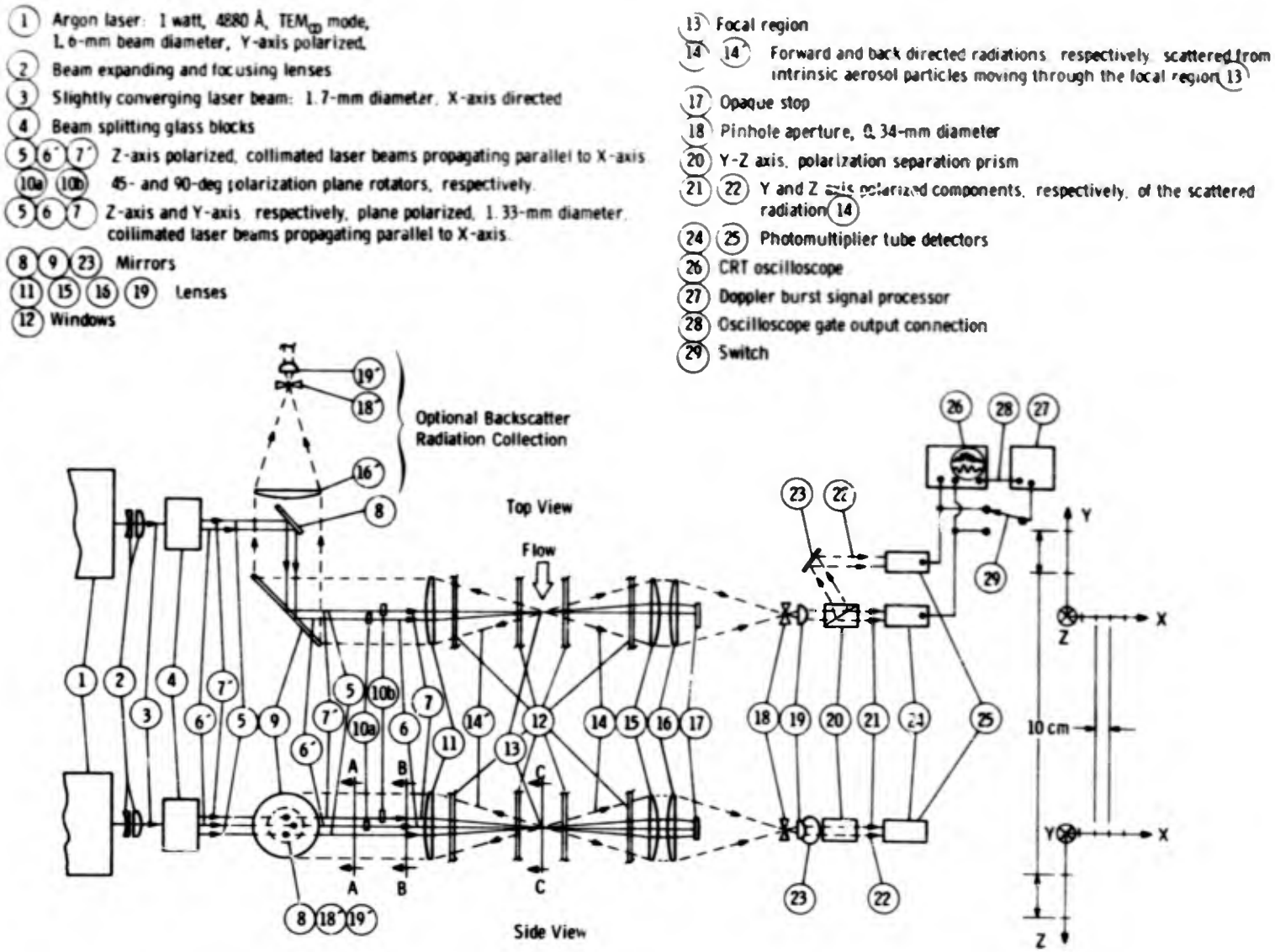

Fig. 3 Two orthogonal views of the two-component velocity detection system as applied to the transonic wind tunnel PWT-1T located at the AEDC. The scale factors indicated are accurate for all component dimensions and relative component positions except for components 19-29 inclusively.

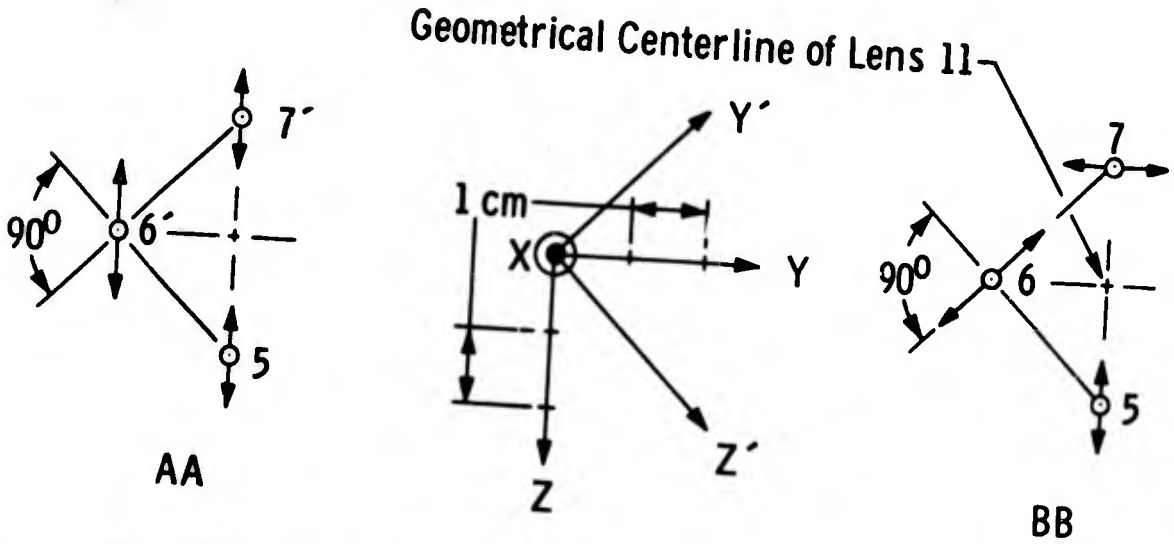

Fig. 4 Enlarged cross-sectional views of the three illuminating beams of Fig. 3 before (AA) and after (BB) polarization plane rotation. Electric field vector amplitude and direction is indicated.

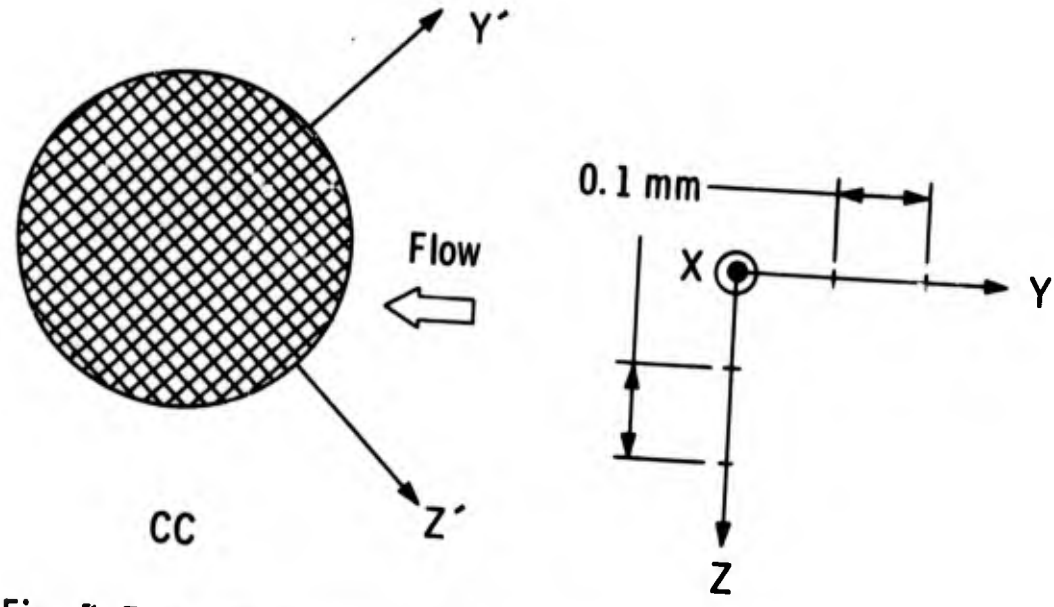

Fig. 5 Enlarged cross-sectional view (CC) of the focal region 13 of Fig. 3 showing the fringe planes established by beams 5, 6, and 7.

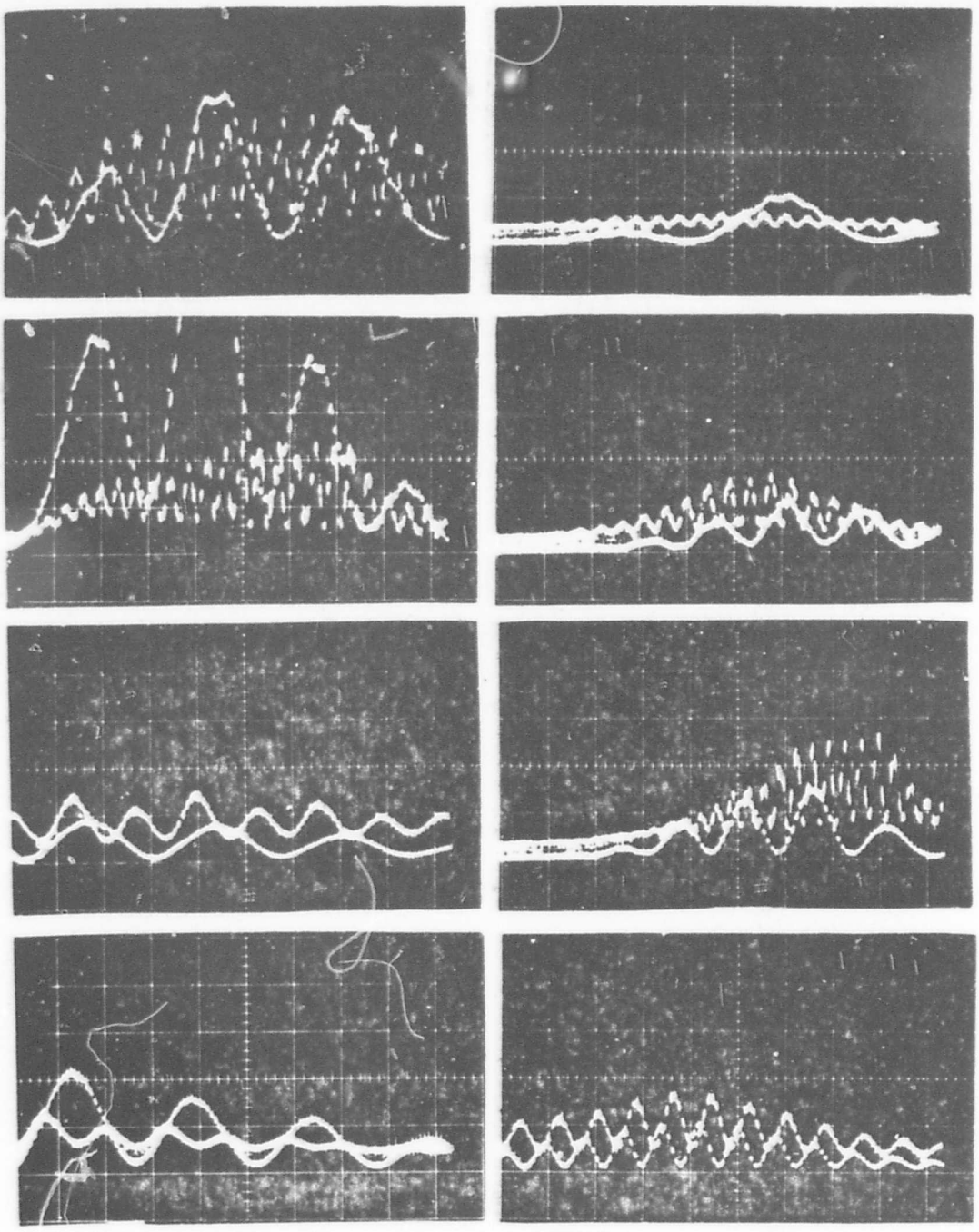

Fig. 6 Examples of two simultaneously recorded signals due to the passage of a single, submicron size scatter particle through two crossed-polarized, orthogonally located sets of interference fringes; polarization separation was used to discriminate between the two signals and the LV system of Fig. 3 was employed. Signal channel alternating rate: 1 MHz; sweep rate 10 μsec/div.

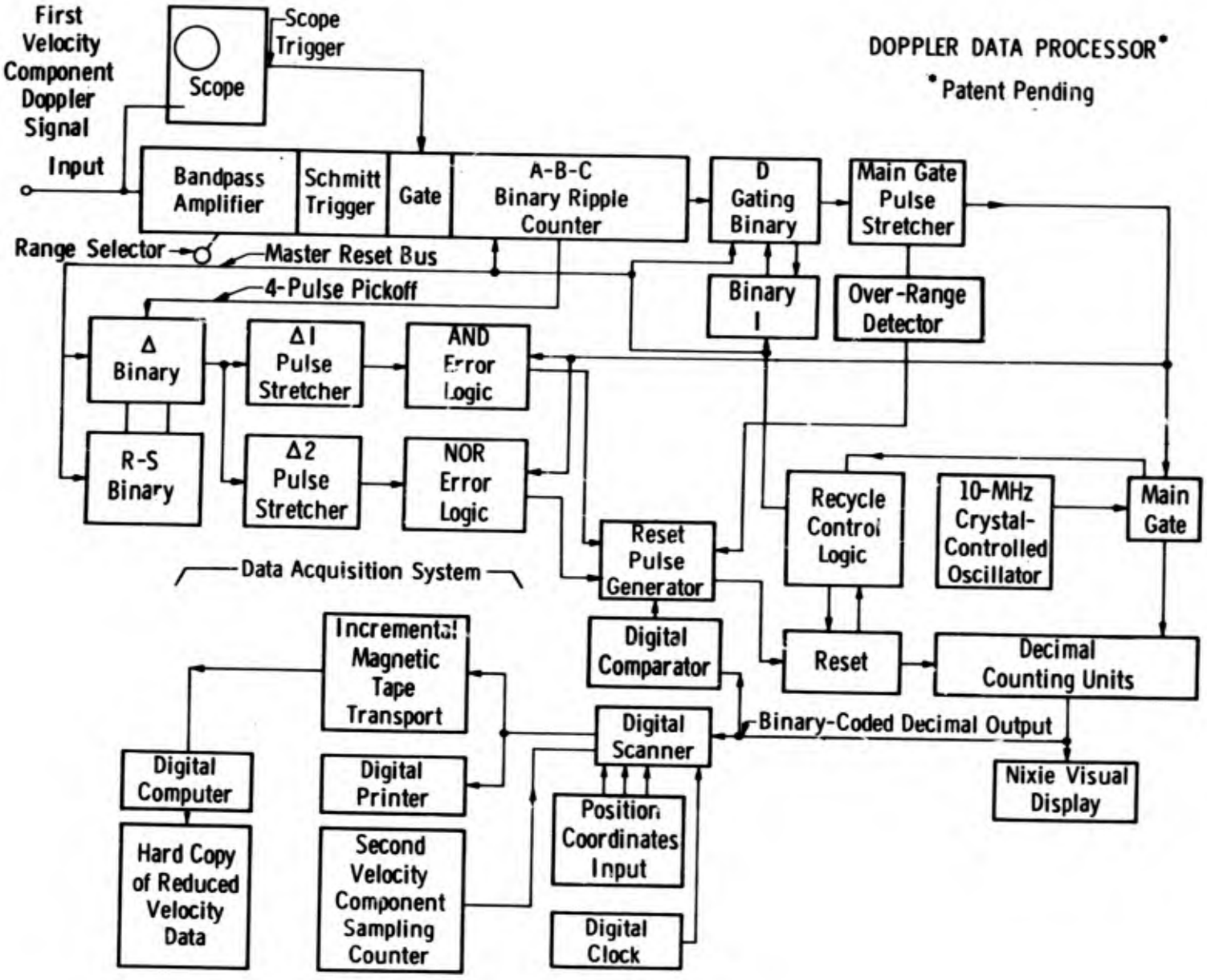

Fig. 7 Doppler Data Processor

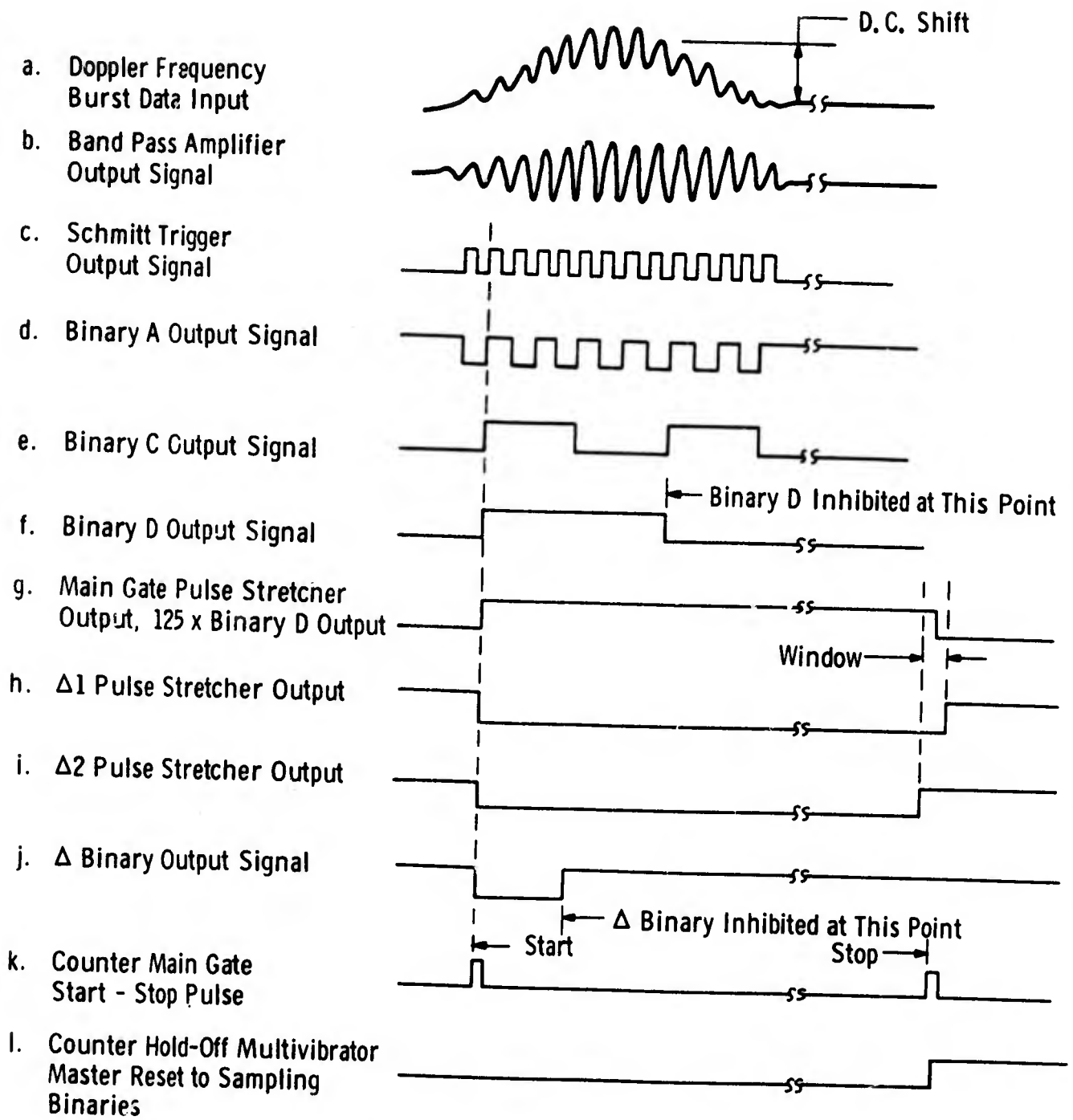

Fig. 8 Doppler Data Processor Signal Waveforms

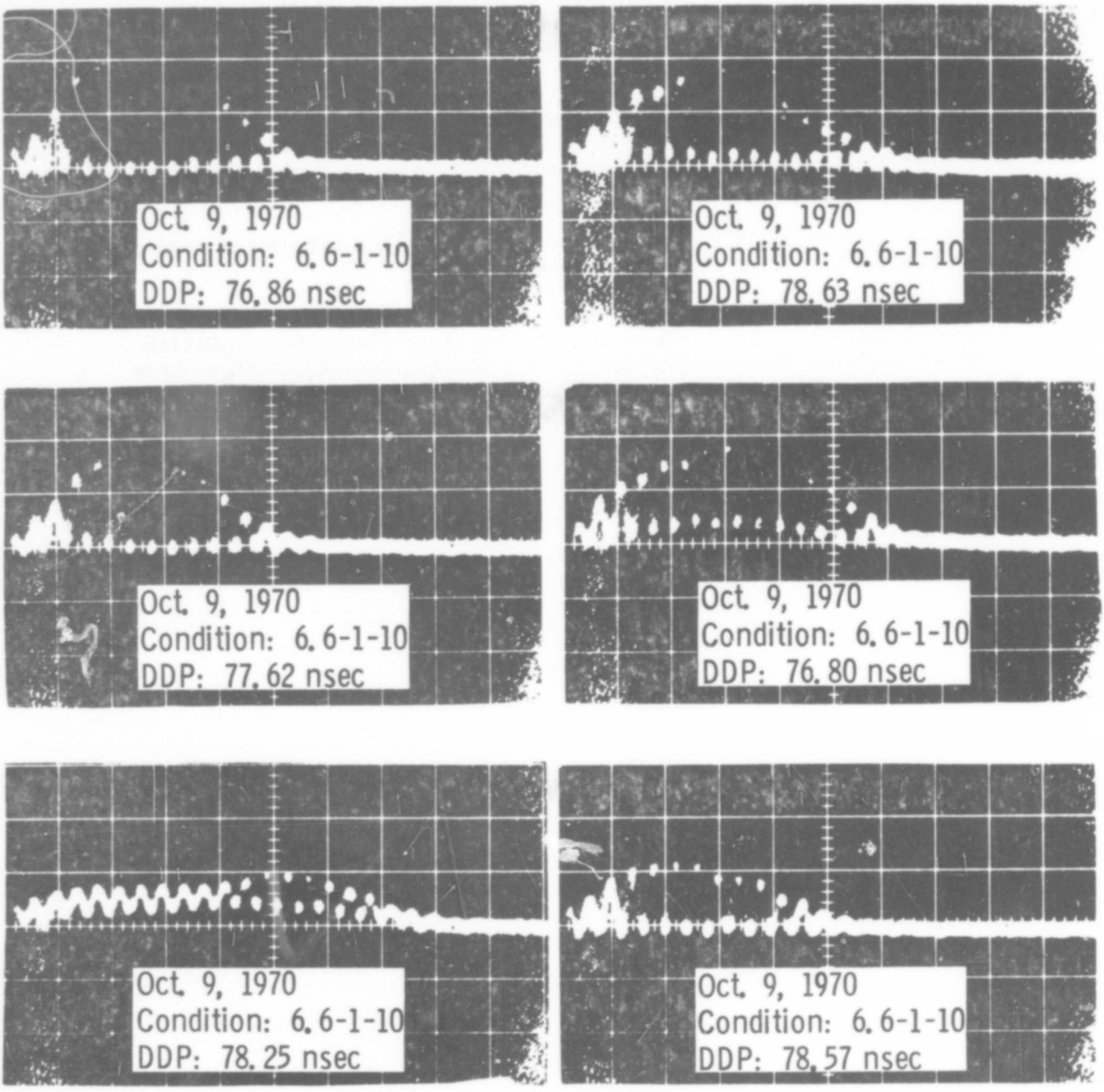

Fig. 9 Six CRT photographed signal bursts at Mach No. 1.0 with the corresponding period recorded by the Doppler Data Processor (DDP). Vertical sensitivity: 2.3×10^{-9} cathode amp/cm. (S-20 response). Horizontal: 0.2 μ sec/cm.

DISCUSSION

ASHER: How do you compare the separation of polarization directions with, for instance, using a total reflecting mirror and a multi-color laser output and then using spike filters in front of your detector?

BRAYTON: We are using both now. The two color system is more efficient. It's also better with regard to cross talk. But this scheme is very easily implemented and cross talk isn't really that much of a problem.

BOUTIER: Don't you think you will have a problem of depolarization by particles that are very small?

BRAYTON: For a spherical particle at least, there is no depolarization on axis. Born and Wolf define a plane of observation which contains the illuminating ray and the scatter ray. If you have your polarization either parallel to this plane or perpendicular to it such that your scattered rays lie in the plane of observation, then the scattered light is polarized identically parallel to the illuminating light. The data typically shows no cross talk.

TECHNICAL SESSION III - SIGNAL PROCESSING

Session Chairman: H. Reynolds

100-B

LASER DOPPLER ANEMOMETRY: A SIGNAL PROCESSING PROBLEM

By: Robert W. Smid, Staff Engineer
Disa-S&B, Inc., Franklin Lakes, New Jersey

ABSTRACT

This paper will cover the problem of continuous detection of the Doppler frequency. This is done to obtain in an analog presentation of the velocity of very small suspended particles, and thusly of the fluid. The design of a frequency tracker will be described.

The frequency tracker makes it possible to measure turbulent velocity fluctuations and this will be demonstrated by the measurement of oscillatory flow generated from vortex shedding. On a basis of practical experience with laser anemometry applied to the studies of water and air flow, it is shown that future applications of this new measuring technique extend to many of those that have either been very difficult or impossible when using hot wire and hot film anemometers.

The signal we obtain from the photodetector of a Laser Doppler Anemometer contains the desired information in the form of a center frequency corresponding to the mean flow and frequency modulation about this center frequency which contains the turbulence information. Detection of this signal in the best possible way is necessary to optimize the usefulness of the entire system. At present, there are basically four methods of processing the Doppler signal. These systems all have their own relative merits and short comings. Disa has just introduced a new frequency tracker as part of a total system of Laser Doppler Anemometry. The usefulness of this system can be more clearly seen when this method of detection is contrasted with other existing methods of detection.

The first, and perhaps the most common, method is to employ a commercially available spectrum analyzer. This system presents, usually on an oscilloscope type instrument, the response to the Doppler signal of a tuned narrow band filter whose center frequency is swept slowly through the spectral region of interest. This system, while offering simplicity, does not efficiently use the available information since the filter can resolve only a small portion of the total signal spectrum at any instant. Turbulence is difficult to process as the analyzer can only indicate the magnitude of frequency fluctuations (modulation) due to turbulence but not their modulation frequency or frequency distribution. A great deal of difficulty and controversy is also encountered when such a system is used when the experiment requires flow correlation.

A possible alternative system is to use a frequency-sensitive discriminator which is band-pass tuned for the frequency range of interest. This provides an analog voltage of the Doppler frequency only if the signal is somewhat idealized. The Doppler signal will, unfortunately, disappear as a result of some random event in the flow stream which is usually referred to as "drop-out". Additional difficulties arise in the selection of an appropriate setting of the bandpass filter and discriminator range. An increase in the dynamic range will result in an increase of noise and a loss of frequency-voltage resolution.

The best solution to date for the demodulation of the Doppler signal is the frequency tracker. In this system the incoming frequency is compared with a local oscillator. The resulting difference in frequency is then used as an error voltage in a servo loop which keeps the frequency of the voltage-controlled local oscillator very close to the incoming Doppler frequency. This system allows accurate

measurement of the Doppler frequency in spite of high signal-to-noise ratios and total loss of signal, both common to the Doppler signal. For these reasons, Disa has used this type of detection in its Laser system.

A far more complex system is possible using an arrangement of frequency counters, digital logic and a digital computer. This system in detail in other papers presented later in this conference. This technique seems justifiable in experiments where the scattering density must be extremely low and data reguarding the phenomena can be taken for extended periods of time.

Figure 1 is a block diagram of Disa 55L20 Frequency Tracker. The Doppler signal from the photodetector is amplified and band-pass filtered in the preamplifier stage. The filter is automatically adjusted by the frequency range switch. The signal is then combined with the output of a voltage-controlled local oscillator in a mixer stage. The difference frequency appearing at the mixer output is narrow-band pass filtered and amplified by the I.F. stage to remove as much noise as possible, then passed through the Limiter in order to remove the amplitude fluctuations in the signal, and thence to a sensitive frequency discriminator. This provides a D.C. output voltage proportional to I.F. frequency deviation from a fixed center value f_o; after suitable smoothing, with a long time constant, this voltage is fed back to the control input of the VCO. The result of the feedback is that, provided a suitable value of loop gain is chosen, the oscillator frequency tracks that of the Doppler signal maintaining a nearly constant difference equal to I.F. frequency. Thus, the VCO control voltage provides an electrical analogue of instantaneous Doppler frequency, and hence of flow velocity.

The frequency discriminator consists of a second I.F. stage also tuned to f_o together with the Limiter and a Phase Comparator. (See Figure 2.) This second I.F. stage selects only the fundamental component of the rectangular waveforms delivered by the first Limiter. The circuit is arranged so that its output lags its input by 90° at resonance and by more at higher frequencies or less at lower frequencies, the phase lag approaching zero at low frequencies and 180° at high frequencies. The Limiter in the discriminator generates a rectangular wave form of defined amplitude, similar to that from the first Limiter, and the Phase Comparator performs a simple analogue multiplication of the discriminator input and the second Limiter; its output is therefore a rectangular wave, fundamentally at twice the I.F. frequency, whose mark/space ratio varies with the phase difference of the inputs. The mean D.C. level of the output voltage is positive for I.F. frequencies below resonance, negative for frequencies above resonance and zero at resonance.

If the oscillator operates at a frequency higher than the Doppler signal, the amplified (non-inverted) VCO control voltage is then in the correct sense to give overall feedback, at least for slow modulation of the Doppler frequency.

Range switching is accomplished by switching the oscillator frequency range simultaneously with the resonant frequency of the two I.F. filters and also, (for reasons which will appear), the capacitor value in the R-C integrator. (Table 1 gives the frequency ranges of f_D, f_{osc} and also the value of f_o, for each of the seven ranges.) A voltage derived from the oscillator control voltage is applied to the Meter Unit, which has an output meter graduated directly in terms of Doppler frequency, and the same voltage is available at two parallel output sockets for oscillographic display and/or further processing.

In use it is convenient to be able to vary the acceptance bandwidth of the tracker, defined by the Q of the first I.F. stage, to suit different signal/noise conditions. The twin I.F.'s allow this to be done without altering the D.C. loop gain; it is, however, necessary to vary the resistance value in the R-C integrator simultaneously with the damping resistor in the first I.F. stage in order to maintain optimum transient loop characteristics. The total effect of all this is that, not surprisingly, narrow bandwidth settings of the first I.F.'s Q inevitably restrict the rate at which the tracker can follow a changing input frequency, and consequently the optimum adjustment of the tracker in a practical situation is always a compromise between speed of response and satisfactory rejection of noise.

There are two different types of bandwidth limitations, i.e. the small signal bandwidth and the large signal bandwidth.

The small signal bandwidth arises because the tracker acts as a low-pass filter. By measurements with simulated Doppler signals, it is found that the measured values are about 1/3 below the theoretical ones. It is, therefore, possible to state a conservative value of the small signal bandwidth, 10% of the first I.F.'s bandwidth. (In Table 2 is given the value of f_{co} for all the tracker ranges, and for two different bandwidth settings.)

For the large signal response of the tracker, we consider the input Doppler frequency with a large sinusoidal modulation. This can be written as:

$$f = f_d \ (1 + k \sin \omega t)$$

where

f_d = mean Doppler frequency

k = modulation index

ω = modulation frequency (signal frequency)

When the modulation is increased, one gets to a point where the phase comparator in Fig. 2 saturates. The signal from the phase comparator will have its maximum positive or negative value, depending on in what direction the Doppler frequency is changing. The control voltage to the VCO, and thereby the frequency analog output, will be a positive or negative going ramp, the slope of which we will designate the Slew-Rate.

If we assume the above mentioned sinusoidal modulation, the maximum rate of change of the Doppler signal is the product of the mean Doppler frequency, the modulation constant and the modulation frequency. That is:

$$\left.\frac{dr}{dt}\right|_{max.} = f_d \omega \ (k)$$

This rate of change shall be less than the one that can be obtained from the VCO when a ramp voltage of maximum Slew-Rate is imposed. If the modulation frequency is made bigger than the maximum, the demodulated output will first become triangular in shape; and if it is still increased, the tracker will go out of lock. (See Note #1 for details.)

When there is noise in the input signal, and it is heavily amplitude modulated, as is the case for genuine Doppler signals, the performance is derated. This has been tested with artificial Doppler signals. Derating factor as function of the signal-to-noise ratio is shown in Fig. 3.

The amplitude modulation is 95% normal amplitude modulation, and the noise added is white, gaussian noise.

It is seen that decreasing the signal-to-noise ratio increases the derating factor, and that an increase in the modulation constant also increases the derating factor. The quantitative values on the above figure are specific only for this one type of amplitude modulation.

Normally any Doppler signal will contain drop-outs or short intervals when the signal level is insufficient. In general, there will be related periods when the I.F. signal also falls to

low levels and fails to trigger Limiter 1. When this happens, the product output of the Phase Comparator is always large and positive, giving a positive-going ramp of voltage on the capacitor of the T_o-integrator, which may cause loss of lock by the time the Doppler signal amplitude recovers. To minimize the likelihood of this happening, a special drop-out circuit is incorporated which detects when the I.F. signal disappears and immediately isolates the integrating capacitor, by switching off a normally-conducting field effect transistor connected in series. The capacitor thus retains a voltage, equivalent to the last known value of Doppler frequency, until the signal reappears. A rectangular logic waveform, generated simultaneously, is fed to an output socket, for gating external signal processing equipment.

The circuit has been designed in such a way that the detector activates upon a loss of signal. It is not reactivated until a signal, with the appropriate period for the expected Doppler, appears. By detecting of the signal period, we have reduced the possibility of noise triggering the drop-out detector.

Operation of the Tracker requires selecting the appropriate frequency range, preliminary manual tuning, using a panel control with the feedback loop opened by means of a panel switch. (See Figure 4.) When the Doppler frequency has been found, as indicated by the presence of an I.F. signal, the loop is closed and the tracker should then remain locked to the Doppler signal. If it does not, this may be because of inability to track a rapidly varying Doppler frequency, in which case a wider bandwidth setting should be used; on the other hand, it may be due to insufficient signal/noise ratio, in which case a narrower bandwidth should improve matters, unless the Doppler signal itself has excessive (ambiguity) bandwidth.

The Disa tracker covers a total Doppler frequency range of 2.5 KHz to 15 MHz. This total range is divided into 7 overlapping ranges within which the Doppler frequency is tracked automatically. Figure 5 shows the flow range as a function of scattering angle for a Helium-Neon laser (6328Å). The standard optical unit 55L01 in the Disa system permits the selection of beam angles from 24° to 1.7° corresponding to a flow range of 3mm per sec. to 320 meters per second with the He-Ne Laser. A practical experiment with oscillating water flow was designed as a means of testing the performance of the total Laser Anemometer System.

Normal tap water without any addition of scattering particles was pumped through a 13mm diameter glass tube in which a wedge-shaped body with a flat front was set up across the flow to generate an oscillating flow by vortex shedding. (See Figure 6c).

From previous measurements with hot film sensors we knew that the vortex shedding at the edge of the body creates an almost sinusoidal velocity variation in the boundary layer on the front of the body even at high Reynolds numbers.

The reference beam method was used with a scattering angle of 12.6° and the beam was focused to a diameter of about 100 μm in their point of intersection.

The velocity fluctuations were first measured in the axial direction of the tube between the wall and the vortex generating body. The D.C. coupled output directly from the Tracker is shown in Fig. 6 together with the corresponding spectrum of the Doppler frequency. The vortex frequency appears as a 55 Hz oscillation with higher frequency turbulence and noise superimposed.

Measurements were then taken in the oscillating boundary layer in front of the body. The radial velocity was measured in a point 0.3 mm from the surface of the body and 1 mm from the edge. The body itself was 3.1 mm wide. The measuring point was chosen outside the oscillation zone of the stagnation line in order to avoid reverse flow since the present Laser Anemometer is unable to indicate flow direction.

The spectrum of the Doppler signal, which covers a frequency band of 50-220 KHz, is shown in Figure 7(a), and the time variations of the Doppler frequency represented by the 100 Hz low-pass filtered output from the Frequency Tracker is shown in Figure 7(b). The 75-500 KHz range of the Tracker was used in both cases, and in this particular boundary layer experiment, the Tracker was, therefore, operating close to the lower limit of the range. Figure 7(c) shows an example of the distortion of the velocity measurement when the Doppler frequency sweeps below the range. In order to make use of the full capability of the Tracker to track frequency variations of $\pm$ 70% about the mean, one may shift the Doppler frequency by beating it with a local oscillator or by changing the scattering angle, thereby shifting the center of the Doppler frequency in one of the operating ranges of the Tracker.

To check the function of the drop-out detection facility, a series of measurements were taken in an oscillating air flow. The oscillations were generated as edge tone vortices and the flow was seeded with an Ammonium Chloride fume (particle diameter 0.1 - 3 μ m), (3). The optical unit was operated in the fringe differential mode with a conversion factor of 0.50 MHz per m/sec. and the scattering volume was measured to be approximately 100 μm.

Figure 8 presents the output signal from the frequency tracker for different sensitivity settings of the Limiter. In (a), the sensitivity is so high that the tracker will track an electronic noise during short periods of low signal to noise ratio and in (d), the sensitivity is so low that only the large amplitude Doppler signal bursts are detected. (b) and (c) correspond to intermediate sensitivity settings.

The Tracker thus provides the user with a comparatively simple system which will permit measurements in various applications in research and industry. The entire system permits the researcher to cope with various measuring problems and adds to his arsenal of measuring equipment.

BIBLIOGRAPHY

1. "Instruction Manual for Disa 55L Laser Anemometer", October 1971.

2. Deighton, M.O., "An Electronic Tracker for the Continuous Measurement of Doppler Frequency from a Laser Anemometer", Disa Information No. 12, October 1971.

3. Buchhave, P., "Edge-tone Oscillations in Air Measured with Laser Anemometer", Disa Information No. 12, October 1971.

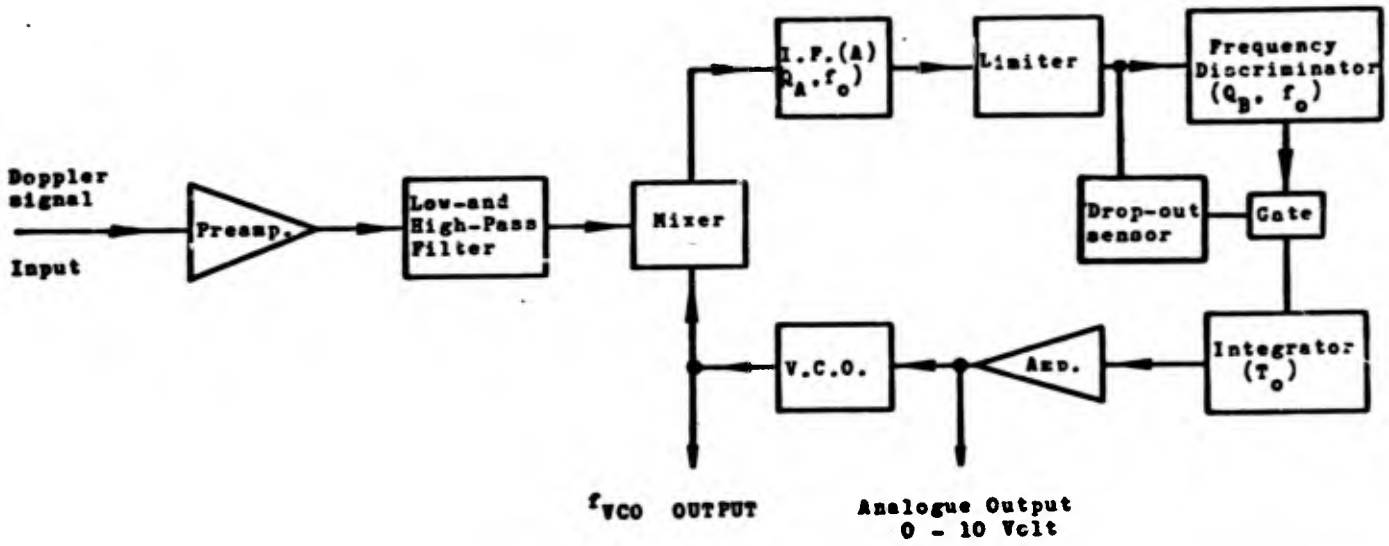

Figure 1. Disa Frequency Tracker, Type 55L20

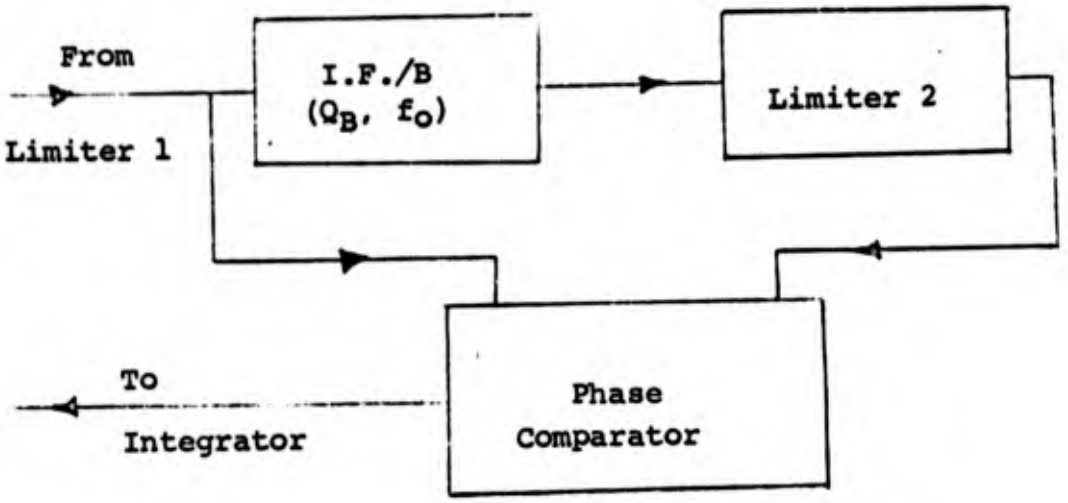

Fig.2 Block Diagram of The Frequency Discriminator of 55L20 Doppler Signal Processor

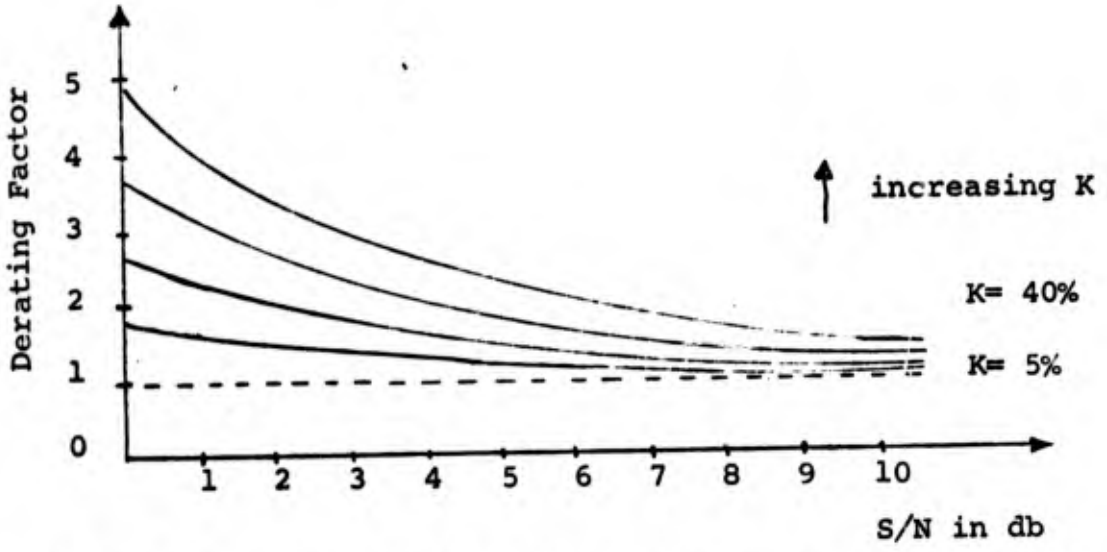

Fig.3 The Derating Factor for various S/N. The Amplitude is 95% and the noise added is white, gaussian noise

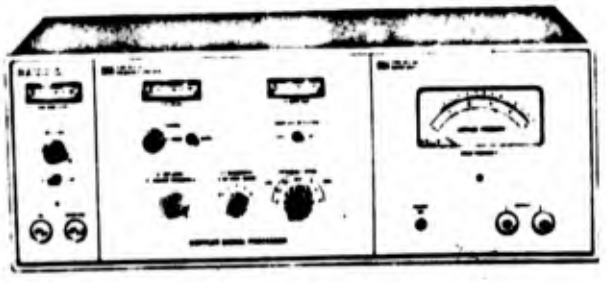

55L20 Doopler Signal Processor

Fig.4

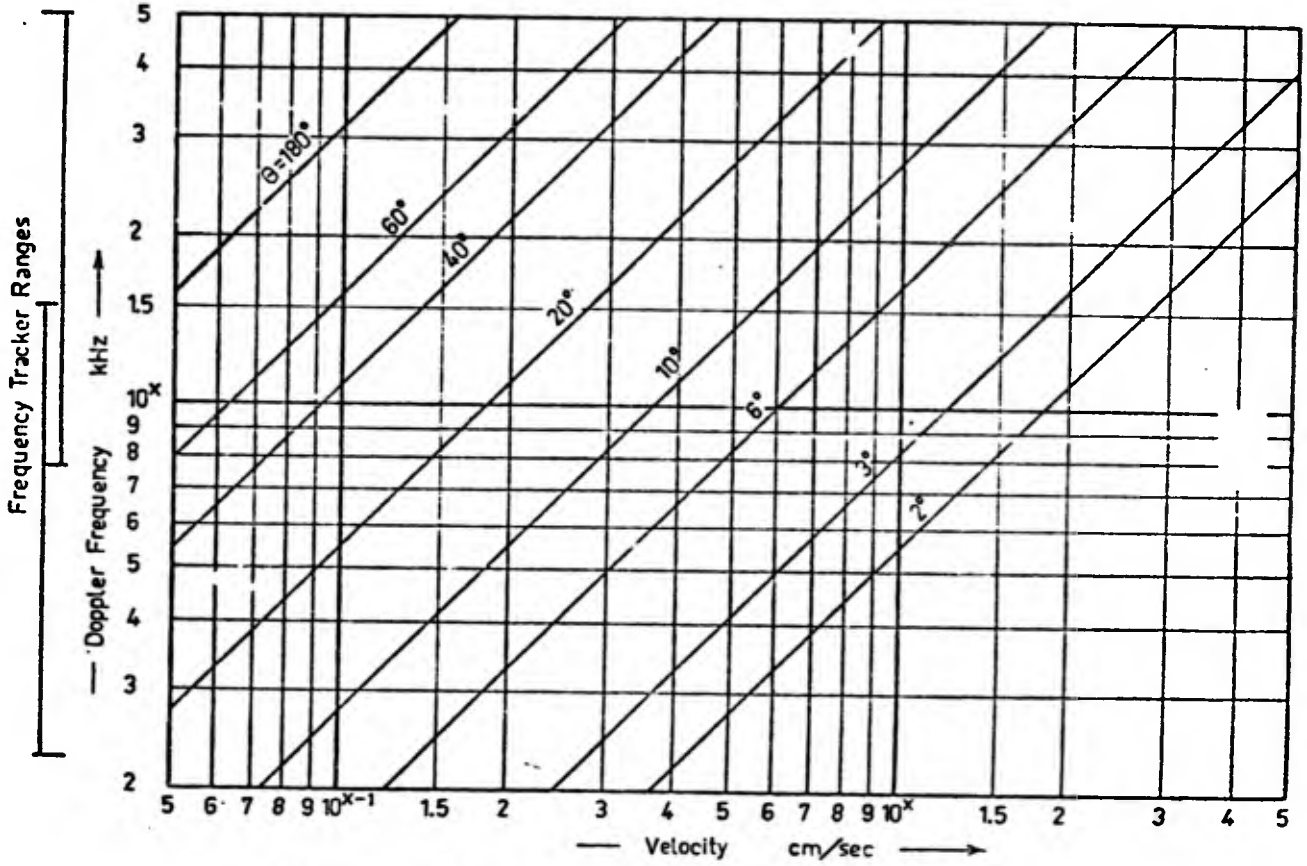

Figure 5. Doppler frequency as a function of scattering angle θ and flow velocity. The total range of the Frequency Tracker is 2.2 KHz - 15 MHz (λ = 6328 Å)

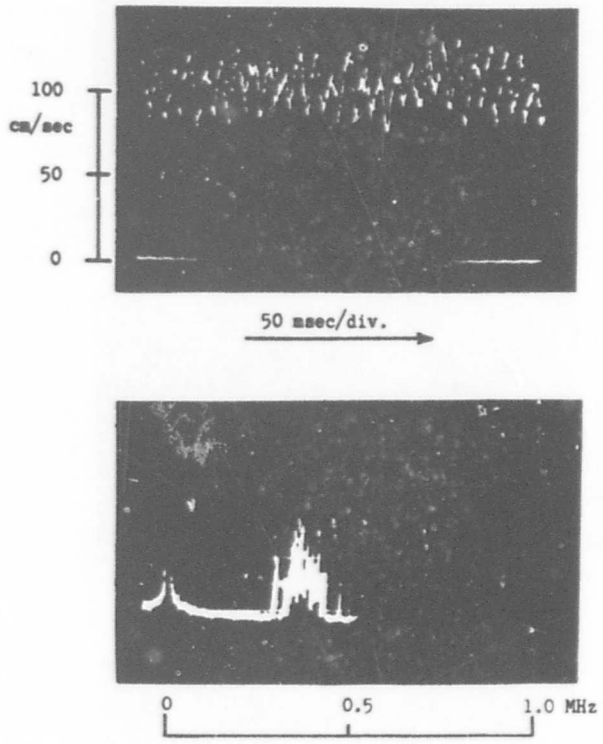

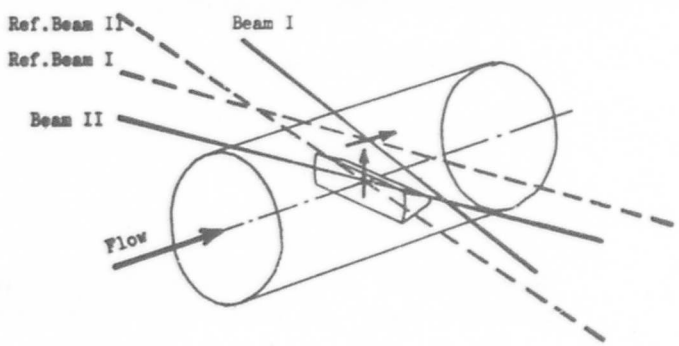

Figure 6. Measurement of vortex shedding

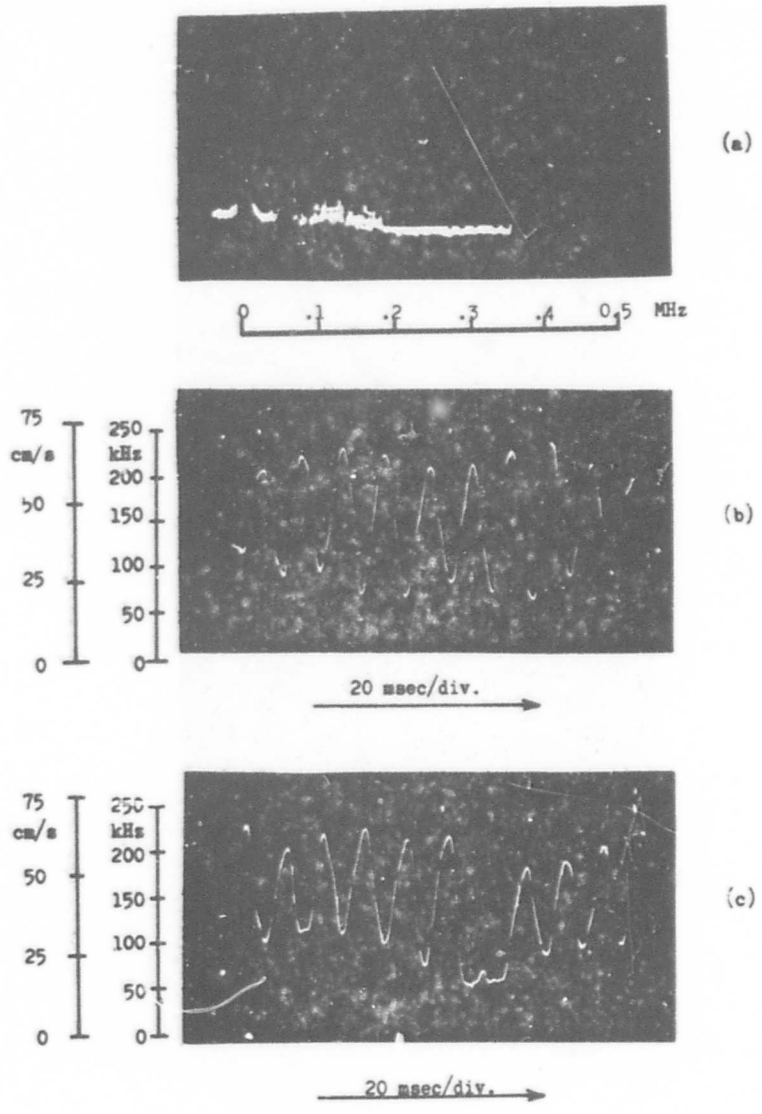

Figure 7. Measurements of oscillatory flow in the boundary layer in front of a blunt body.

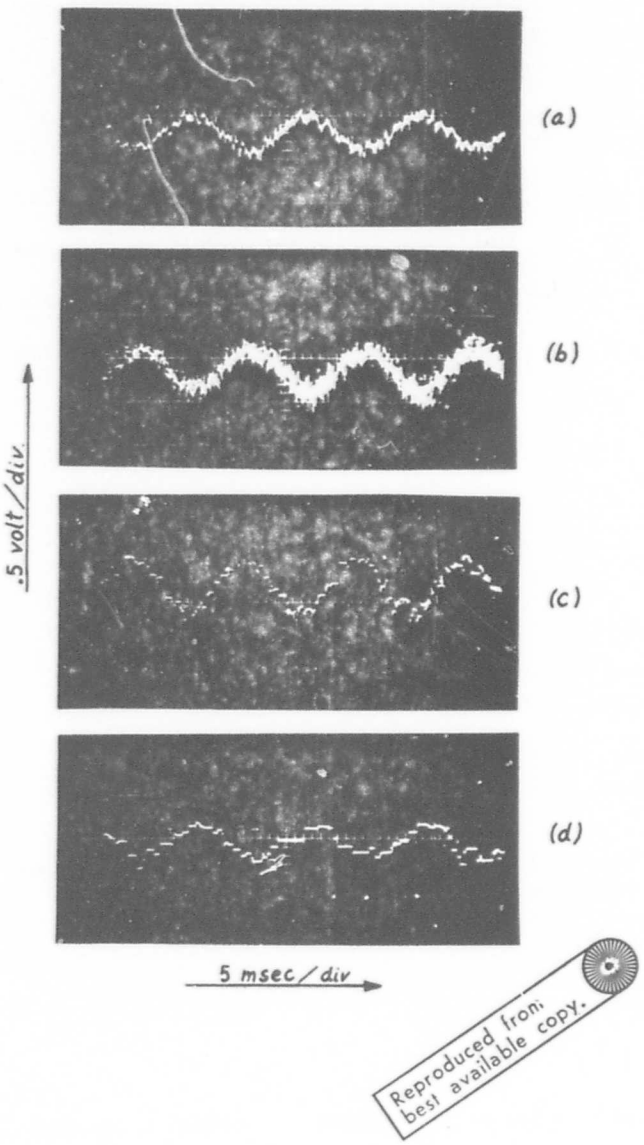

Fig. 8 55L20 Doppler Signal Processor output at various setting.. of the Threshold control

TABLE 1.

Range	f_d	f_o	f_{osc}
1	2.25 - 15 KHz	1.5 KHz	4 - 16.5 KHz
2	8 - 50 KHz	5 KHz	13 - 55 KHz
3	2.5 - 150 KHz	15 KHz	40 - 165 KHz
4	80 - 500 KHz	50 KHz	130 - 550 KHz
5	0.225- 1.5 KHz	150 KHz	0.4 - 1.65 MHz
6	0.8 - 5 MHz	500 KHz	1.3 - 5.5 MHz
7	2.25 - 15 MHz	1.5 KHz	4 - 16.5 MHz

TABLE 2.

Range %BW	15KHz	50KHz	150KHz	500KHz	1.5MHz	5MHz	15MHz
8	0.133 V/msec	0.445 V/msec	1.33 V/msec	4.45 V/msec	13.3 V/msec	44.5 V/msec	133 V/msec
0.5	6.65 V/msec	0.022 V/msec	0.066 V/msec	0.22 V/msec	0.665 V/msec	2.32 V/msec	6.65 V/msec

F_{co}, the small signal bandwidth at different ranges and bandwidth settings.

TABLE 3.

Range %BW	15KHz	50KHz	150KHz	500KHz	1.5MHz	5MHz	15MHz
8	116Hz	388Hz	1.16KHz	3.88KHz	11.6KHz	38.8KHz	116KHz
0.5	5.8Hz	19Hz	58 Hz	193 Hz	580 Hz	1.93KHz	5.8KHz

NOTE #1

The following is a derivation of the values shown in Table 3:

If we assume the above mentioned sinusoidal modulation, the maximum rate of change of the Doppler signal is:

$$\left(\frac{df}{dt}\right)_{max} = f_d \quad k$$

This rate of change shall be less than the one there can be obtained from the VCO when a ramp voltage of maximum Slew-Rate is imposed. I.e.:

$$f_d \quad k < k_{vco} \qquad \text{(Slew-Rate)}$$

$$F_{max} = \frac{k_{vco} \qquad \text{(Slew-Rate)}}{f_d \quad k}$$

where k_{vco} = V.C.O. control constant in Hz/Volt. If the modulation frequency is made bigger than F_{max}, the demodulated output will first become triangular in shape; and if it is still increased, the tracker will go out of lock.

The theoretical value of the Slew-Rate is given by:

$$\text{Slew-Rate} = \frac{0.6 \quad f_a \quad f_b}{k_{vco}}$$

By measurements on simulated Doppler signals, it is found that the Slew-Rate is better than 2/3 the theoretical value. On the nomogram is given the maximum modulation frequency f_{max} for a modulation $k = 0.1$. For another value of k, say k , f_{max} is given by $f_{max} = \frac{f_{max}}{k}$ (0.1).

In table 3 is given the Slew-Rate for all the tracker ranges, and for two different bandwidths.

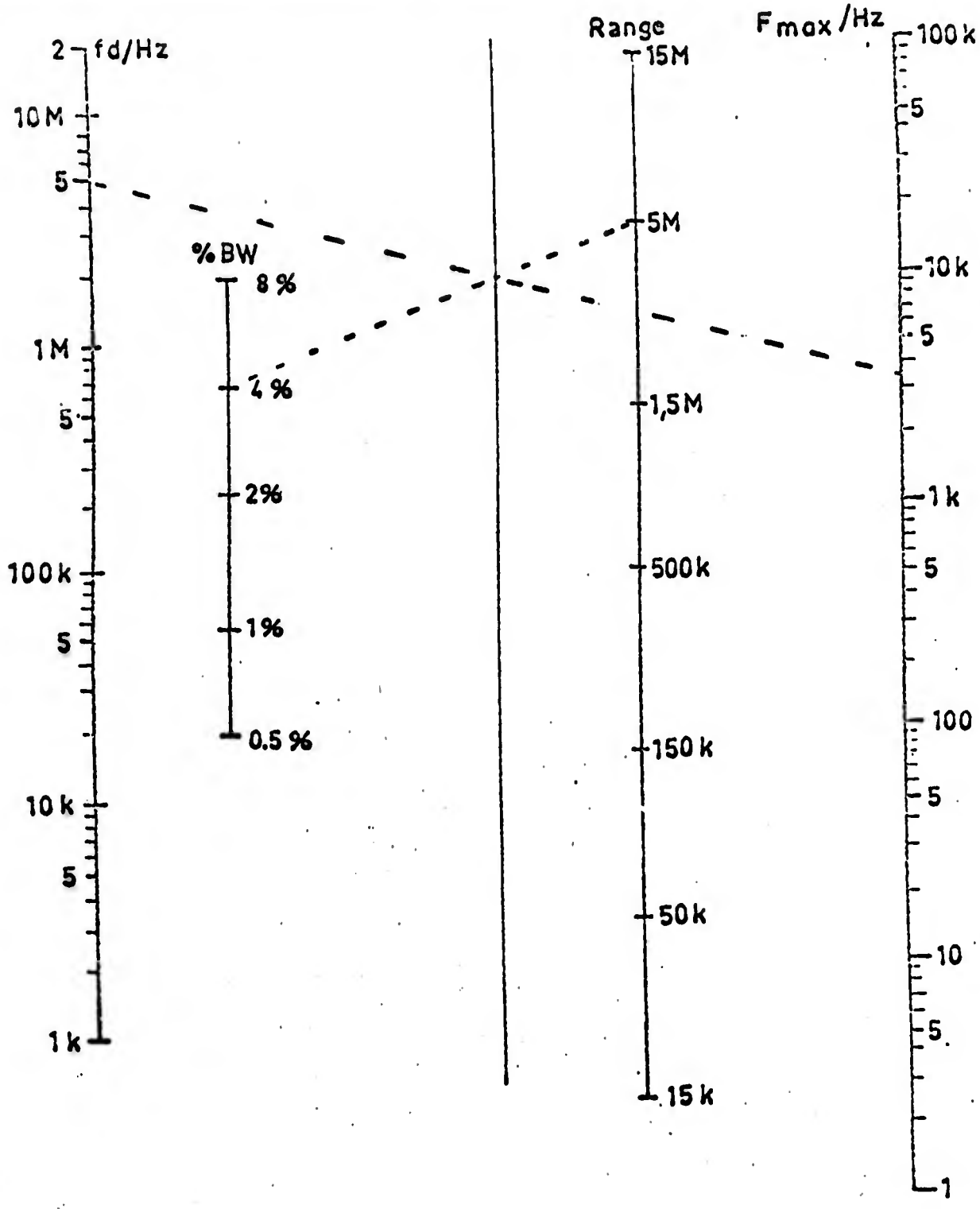

Fig. 9 Nomogram for determination of maximum tracking frequency

DISCUSSION

MEYERS: What is the signal-to-noise requirement for tracking?

SMID: We've successfully tracked signals with just a little over zero db signal/noise ratio.

MEYERS: What was the bandwidth?

SMID: You mean the IF bandwidth on the tracker or what was the spectra of the noise?

MEYERS: The IF bandwidth of your discriminator controls the noise bandwidth.

SMID: We set that on the minimum. That would be 1/2% bandwidth.

MEYERS: What was the measurable deviation of doppler frequency?

SMID: It's plus or minus 70% if you are in the center of the range.

MEYERS: What is the modulation rate possible?

SMID: I tried to point out that for small signal turbulence you can go up to well in excess of 100 KHZ. Your large signal response is determined by the slew rate of the tracker. This is described in detail in DISA 12.

MEYERS: What is the duty cycle required?

SMID: You mean the time of the burst?

MEYERS: Duty cycle, the way I define it, is the percentage of time that you have a doppler signal versus the time that you do not.

SMID: If you define it that way, it will track the small bursts that you get if you had, let's say, 99% dropout. We have a dropout meter on the front panel which indicates the relative time of dropout in per cent.

MEYERS: In other words, you're saying that if you got a data burst that is one microsecond long, you can be off ninety-nine microseconds and still hold lock?

SMID: It will detect the doppler signal in that one microsecond or millisecond and hold it for the next ninety-nine until the signal reappears. If it's not too far away from the last value, it will pick that up.

MEYERS: So you're saying that if your duty cycle goes down your tracker will hold the last known value and not drift off to a noise spike.

SMID: Right.

DUNNING: Jim forgot to ask the most important and obvious question - what is the price?

SMID: Well the tracker costs just a little under $7,000.

CROSSWY: Could you comment on the relationship between the dropout percentage and the resultant accuracy in frequency range of a power spectrum measurements which you track. I realize this is sort of involved.

SMID: I wouldn't care to comment on that. We haven't checked that.

CROSSWY: Would your literature answer this question?

SMID: It will start to. It won't give you the total answer.

GEORGE: You make a comment that the frequency tracker will respond to turbulent fluctuations up to 100 KHz. I would correct that. It will respond to fluctuations in the doppler frequencies up to 100 kilocycles. I don't think anyone would contend that there is measurable turbulence at that frequency. Certainly it is well obscured in doppler ambiguity.

SMID: The reason I say it's in excess of 100 KHz is because we have developed a doppler signal simulator in which we have noise and then we can amplitude modulate some signal with the noise on it.

WELCH: I'd like to risk a question. As I understand you said when a burst comes through on the tracker, you have a gated system. When the burst comes through it tracks during the burst and then retains the value. Essentially you have a track and hold. Does it merely retain the voltage or does your voltage controlled oscillator remember the last frequency?

SMID: What happens is when the dropout sensor detects dropout, we have a gate (in reality a FET) which opens the circuit to this capacitor integrator which then holds the control voltage to the VCO. What happens is that the VCO stays at the same frequency it was, because the controlling voltage is still the same.

WELCH: It appears to me that, if you hold the prior voltage, the VCO is set up in such a way that it would drive the input to zero error condition. By holding this prior voltage rather than remembering the prior frequency, what you might be doing is driving it off to some other frequency.

SMID: We are opening the loop, so there is no net change.

WELCH: OK, so you're letting it free run at its last frequency.

SMID: Right. The error voltage is not then fed through the loop.

WELCH: OK, so you take it out, there is no voltage going in and it's free running at its prior frequency. This system will therefore apparently hold information in a burst situation. I've seen quite a few publications in DISA 12. Has this system been used for actual turbulence measurements with dropout?

SMID: Yes it has. There have been quite a few experiments in turbulence measurements. Some of the experiments that Dr. Whitelaw mentioned this morning used the tracker.

WHITELAW: I'd like to make several points. The bandwidth, which you can track, is no good anyway once the probability of negative velocity comes up unless you've got some kind of frequency shifting on the light beam. So the maximum turbulence intensity you can measure is something like 30%. The second point is on dropout. This is a personal view. I'm very unhappy tracking with dropout with this tracker or any other tracker. That's partly prejudice. My unhappiness doesn't stem from getting out mean velocity, but rather these rms quantities. There is a finite time to pick up a signal and a finite time to lose the signal. If I look at what happens with the tracker we made ourselves we find spikes when you stop to pick up the signal. These contribute to the rms signal, so when the dropout becomes significant I'm dubious about the results. The third point I would make is one that applies to all trackers and this one too. There aren't any idiots here, but if you think you can get one to use a tracker successfully, you're wrong. One of my good Ph.D. students used this instrument to measure the turbulence intensity down the centerline of a jet and got ridiculous results. The point is it's possible to track a noise signal unless you know what you're doing. But that apart, this is a very convenient instrument to use and we have been very happy with it.

CROSSWY: Could you tell me what your IF frequency is and what were the criteria for the selection?

SMID: The IF frequency is a function of the range. It varies from 1.5 KHz on the lowest range to 1.5 MHz on the highest range. The criteria we used in the selection was that you wanted a frequency which would allow you to operate your VCO in a suitable range - also the electronics. Of course, the time lag or the frequency response of the tracker as

a whole would be changed by these. The response of the tracker is far better at the higher frequency ranges. The slew rate is higher.

EDWARDS: I just have a general comment about dropout. As far as I can tell if you run your system and just let the signal go to zero, or just hold with an RC filter and let it decay toward the free running frequency of the VCO, then when you measure mean velocity you should always be off due to the fact that you have dropout. When you have a system with a clipper, for example, it will always go only one direction. For instance, if your mean signal is below the free running frequency, when it drops out the system will try to move back to the free running frequency and your average measured frequency will always be high. I was curious. With your system do you really hold it rock steady when it drops out or do you have an RC filter?

SMID: Yes. We hold the last known value steady.

ASHER: Concerning the type of track and hold which in your case is an integrator. If I'm not mistaken that capacitor can be changed depending on what kind of frequency response you desire. Normally track and hold does have a droop in it. The answer you gave Dr. Edwards indicated that it did not have droop. I'm sure that's not the case.

SMID: Yes, it has a droop, but with a very long decay time.

ASHER: If it becomes a long decay time, you also require a long time to make a change of value depending on where you are setting.

SMID: I've opened the FET on the capacitor. So now I have equivalently a very high resistance on that capacitor and a very low drain.

ASHER: In other words, leakage off that capacitor is very small.

SMID: Very small. So in the time scale you're talking about with normal dropout, you are not going to see anything of the decay. As soon as that FET conducts, you have the driving power of the discriminator.

AN AUTOMATIC DATA PROCESSING SYSTEM FOR LASER ANEMOMETERS

H. D. vom Stein
and
H. J. Pfeifer

Institut Franco-Allemand
de Recherches de St. Louis
St. Louis, France

A new data evaluation procedure will be described. It is based on the usage of two counters and a data processor and it allows to determine the mean velocity value and its fluctuations. Beside the higher accuracy compared with the data acquisition procedures known so far it is well suited for small particle densities and extremely small turbulence degrees.

During recent years laser velocimeters have been used extensively for turbulence studies in gas and liquid flows (1, 2, 3). The reasons are the complete absence of flow disturbances, the high temporal and spatial resolution as well as the possibility of applying these methods at high temperatures and at velocites of hundreds of meters per second. At low particle density and extremely small turbulence degrees, all the different kinds of laser anemometry suffured from the disadvantage that data acquisition and evaluation was too time consuming or inaccurate. In this paper an automatic data processing system will be described which enables us to overcome these difficulties. One of the advantages of this technique is that the natural impurities present in many flow fields serve as scattering particles. Thus the selection of an artifical tracer material and a method of entrainment in the flow field can be avoided.

In order to demonstrate the ranges of application of this automatic data processing system the so called doppler difference or dual scattering method was used which, for better understanding, will briefly be reviewed (4, 5). This procedure is based on the frequency shift of two coherent electromagnetic waves scattered or reflected by a moving object as you may see in Figure 1. The essential parts of this Figure are: the powerful laser, the focussing lens system, the beam divider, the scattering particles, the image forming system, the pinhole, the photomultipliers and the oscilloscope. Due to the different angles with respect to the velocity vector, the frequency shifts of the two beams differ and, as a matter of fact, the difference frequency of the scattered beams picked up by the detector will be a very accurate measure of velocity. Regarding the velocity measurement in flow fields, the CW laser serves as a radiation source and small particles imbedded in the flow field as scattering centers.

With the aid of an optical interferometer, a completely equivalent and even more simple explanation of this measuring procedure can be given. The beam emanating from a high power laser is split up by means of a Köster prism into two parts intersecting each other in the measuring volume. Due to the mutual coherence they form parallel fringes. The relation between the separation of the fringes D and the angle of intersection 2β and the laser wavelength λ is given by the simple formula $D = \lambda/2 \sin \beta$. The particle passing through the fringe system becomes bright and dark according to its position. In consequence, a photodetector picks up a burst from each tracer involving a frequency $f_D = V/D$, V being the velocity component perpendicular to the fringes. The useful number of cycles in each burst is determined by the number of fringes of intensity high enough to guarantee sufficient signal-to-noise ratio.

Many efforts have been made to define an optimum evaluation procedure for these bursts. In this connection the following points are to be noted. As the accuracy of the electronic data processing increases with the number of fringes, it is necessary to produce as many fringes as possible. Moreover, in order to avoid too high values of the doppler frequency (and thus expensive electronic equipment) the fringe distance should be adapted to the interesting velocity range according to the equation $f_D = V/D$. On the other hand the observation volume should be so small that even for high turbulence degrees, no perceptible velocity variation within this volume occurs. Under the condition that the time of flight in the fringe system for each particle is short enough the frequency within each burst is constant, and the velocity fluctuation can only be determined by a great number of particles. Up to now, many different data processing methods have been used in the doppler difference method which, without going into detail, may be divided in the following way. First, the frequency of the signal is picked up by the photodetector and the signal is directly sent to a frequency tracker (6) or frequency analyzer (1). In spite of the long time constants, these methods are well suited for the acquisition of the mean velocity value and its fluctuation. They require, however, a very high particle concentration in order to get a continuous signal and therefore the seeding of the flow field with tracers is necessary.

Additionally, due to the possible destructive interference when several particles are simultaneously present in the measurement volume, the signal-to-noise ratio can be diminished.

The second method, mainly developed for low particle density, primarily determines not the frequency of the signal, but the time interval between equal phase points. This can be done by examining an evaluating the doppler difference signal by means of an image retaining oscilloscope. This procedure has the advantage that the signal as a function of time can be controlled. By this method it is guaranteed that, on the one hand, only particles producing a good signal-to-noise ratio are included in the result and, on the other hand, that all signals showing visible phase discontinuities due to destructive interferences of several particles may be excluded. To improve the sophisticated and extensive evaluation method, a semi-automatic data procedure was proposed. Here the time interval for a given number of cycles is measured. This can be done with all counters offering the possibility of period measurement. To obtain maximum accuracy, the number of cycles must be as high as possible. In order to minimize the acquisition of low signal-to-noise ratio data a certain trigger level can be adjusted. However the automatic decision is carried out if the signal is disturbed by destructive interference. In addition, under certain circumstances, the time element between successive bursts from adjacent particles will be included in the indicated value. Thus it is necessary to monitor the doppler difference signal on an image retaining oscilloscope together with the start and stop pulse of the counter.

A similar but analog-digital device is described by Iten and Mastner (7). Here the probability of false data is diminished because only the time interval of one cycle with a good signal-to-noise ratio is determined. But, nevertheless, all of these methods suffer from the disadvantages that either they are time consuming or the accuracy is not sufficient for extremely small turbulence degrees. The method I will present now overcomes these difficulties. It is based on the second above mentioned method - the period measurement of a great number of cycles in the burst of a single particle. To avoid false data, two counters are used which are triggered successively or at the same instant. The first method is illustrated in Figure 2.

In this case the two counters determine consecutively the periods T_1 for n_1 and T_2 for n_2 cycles respectively. The criteria, whether the signal is to be processed or not, is the validity of the relation written here $n_1/T_1 = n_2/T_2$. In the upper part of this the calculated signal of a single particle is sketched. In this case, this formula is strictly fulfilled. For the signal in the lower part, it has been assumed that two particles are moving at the same velocity only separated from each other by approximately half the fringe system diameter. Due to the resulting time difference Δt, this value may be eliminated, for in this case, this condition is not fulfilled.

The same condition as indicated here holds also when both counters are triggered at the same instant, and are stopped after n_1 and n_2 cycles respectively. As a result of this logic decision it is possible, in contrast to most of the other methods of evaluation, to make use of all the cycles of one burst for the determination of one velocity value. Due to the slightly different properties of the two counters, concerning the count ambiguity, the time base stability, and the trigger error, a rigorous application of this equation is not possible. That means a certain deviation equal to $n_1/n_2 - T_1/T_2$ the absolute value of which is termed ε must be admitted which, in any case, would be smaller than the expected velocity variation. A possible flow diagram of our data acquisition and processing system is shown in Figure 3. The signal from the photodetector is fed into a filter and into an internally triggered gate. This assures that only bursts with a high signal amplitude and thus good signal-to-noise ratio pass to the two identical counters. These measure the time intervals T_1 ans T_2 respectively.

In the next set, the digital sorter decides if the modulus of the different $n_1/n_2 - T_1/T_2$ for given n_1 and n_2 is smaller than the chosen value of ε. If this is true, the value of T_1 is accepted by the data processor and independently, if the condition $n_1/n_2 - T_1/T_2$ is fulfilled or not, the digital sorter resets both counters to start a new cycle.

With the aid of the fringe separation (the value D) and the values of n_1 and T_1 the data processor finally calculates the velocity values of each particle, the mean velocity of a number of particles, the standard deviation, the histogram and so on.

In the following example, the just discussed method has been applied for demonstration purposes, especially in view of its precision. Unfortunately, the interface between the two counters and the digital sorter was not yet available to us, so that the data from the digital display of the counter were fed into the digital sorter by hand. A small nozzle (diameter of 35 mm) produced an air jet with a mean velocity to 16 meters per second. Just at the exit of the nozzle, the value of the velocity fluctuation measured with the hot wire anemometer was .34%. The frequency spectrum of the turbulence was below 1 kilohertz. The velocity of a great number of micron sized dust particles, imbedded in the air jet (natural impurities) was measured at the same point with the laser anemometer. As a light source a CW argon laser with a power of 1.4 watt at 488 nanometers was used. The diameter of the two laser beams was about 1 mm, the fringe distance about 50 micrometers, and the observation volume was limited to about 1 mm cubed by means of the image forming system of the detector. Due to the low frequency characteristics of the flow, it is safe to conclude that no perceptable variation of the velocity occurs during the time of flight of the particles in the fringe system. According to the mean velocity of 16 m/s and the size of the fringe system, the mean time of flight of the particles was about 62 microseconds. The two counters have a time accuracy of about .02 microseconds. Corresponding to these values the precision is mainly influenced by the

signal-to-noise ratio and the quality of the optical fringe system.

In order to improve the signal-to-noise ratio, and to minimize the trigger errors of the counter, the scheme of Figure 4 is used. The signal at the output of the photodetector consists of amplitude modulated bursts according to the Gaussian intensity distribution of the two laser beams.

After the filter, the dc component is rejected resulting in a signal symmetrical to the zero line. By means of the trigger level (of the gate) only signals with amplitudes at least 25 db above noise level entered the counters.

The influence of the low frequency amplitude modulation can be reduced by measuring the time interval between 10 and 20 zero axis crossings respectively. As a result of the error in trigger level caused by the signal-to-noise ratio, the corresponding time error is less than .1% for signals free of destructive interferences.

An accurate measurement of the error arising from a possible distortion of the fringe system is very difficult. To get an idea of the upper limit of distortion the fringe system was enlarged by means of an objective to a diameter of about 20 centimeters. Even with this additional optical component, the error in reading maximum variation of the fringe separation is less than .2%. As stated, for a data acquisition and processing example, the second method I described was used. That means both counters were triggered at the same instant. The first one measures the time period for 10 cycles of the doppler difference signal and the second one for 20 cycles. From a total number of 135 values, first of all, only those were selected for which n_1/n_2 and T_1/T_2 differ by an amount of less than .1%. The velocity variation calculated from the forty-six values fulfilling this condition was .34% and in good agreement with the above mentioned hot wire results. Now allowing a maximum deviation of the value ε of .35% between the difference of the two coefficients, the velocity fluctuation calculated on the basis of 103 values was .38%.

In order to illustrate this procedure, the doppler difference signal together with the stop pulse of the second counter is shown in Figure 5. In the upper part of this figure, the deviation of both quotients with respect to each other was .2%, whereas it was for the disturbed signal in the lower part 5.4%. That means this signal has to be neglected and the first signal can be used with a certain value ε of let's say .3%.

With the same wind tunnel, turbulence degrees up to 10% have been measured with the same good agreement between the laser and the hot wire anemometer. You will see some values in Figure 6. In this case the double counting method has been used at different points of the flow field indicated here as x and y. An extension of this data processing system to higher velocity values than reported with this example can be carried out without difficulty by the proper choice of

counters with higher resolution and by adapting the fringe distance and observation volume to the interesting velocity range. Provided that the interface between counters and digital sorters are available, complete automatic data processing will be possible. To get an idea of the time necessary to measure, in this case, the mean velocity and the standard deviation, a particle density of about 1 per millimeter cubed may be assumed. If the measuring volume is a cube of 1 millimeter on a side and the flow velocity is 10 meters per second, then 10^4 doppler bursts are available per second. Even with a drop out rate of 90% of the values, 10^3 doppler bursts will be picked up per second. Thus all the substantial conditions will be fulfilled in order to improve the doppler difference method as an operational instrument for turbulence measurement.

While other instrumentation systems have been employed for the same purpose, the system described here offers a particular advantage of eliminating false data by using a direct comparison of two independent time intervals in a single burst. Because very low values can be selected for ε, even in the case of turbulent flow, the accuracy of the system described here is very high.

REFERENCES

1. Yeh, Y. and Cummins, H.Z., Appl. Phys. Lett., Vol. 4, No. 10, 1964, p. 176.

2. Goldstein, R. J. and Hagen, W. F., Physics of Fluids, Vol. 10, No. 6, June 1967, p. 1349.

3. vom Stein, H. D., Pfeifer, J. J. and Koch, B., Opt. Comm., Vol. 1, No. 5, 1969, p. 207.

4. Pfeifer, H. J. and vom Stein, H. D., ISL, T 12/67.

5. vom Stein, H. D. and Pfeifer, H. J., Metrologia, Vol. 5, No. 2, 1969, p. 69.

6. Huffaker, R. M., Appl. Opt., Vol. 9, No. 5, 1970, p. 1026.

7. Iten, P. D. and Mastner, J., KLR-71-07 Brown Boveri Research Report.

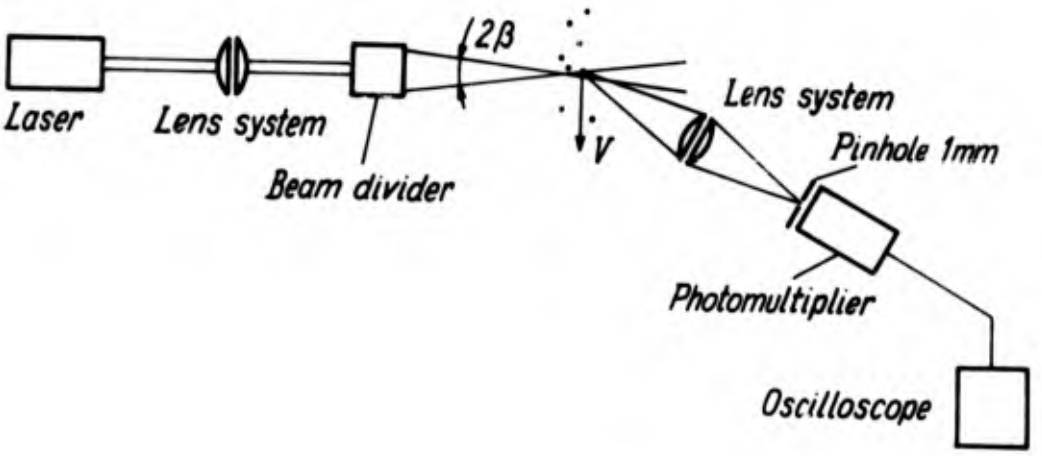

Fig.1 The Doppler-Difference-Method.

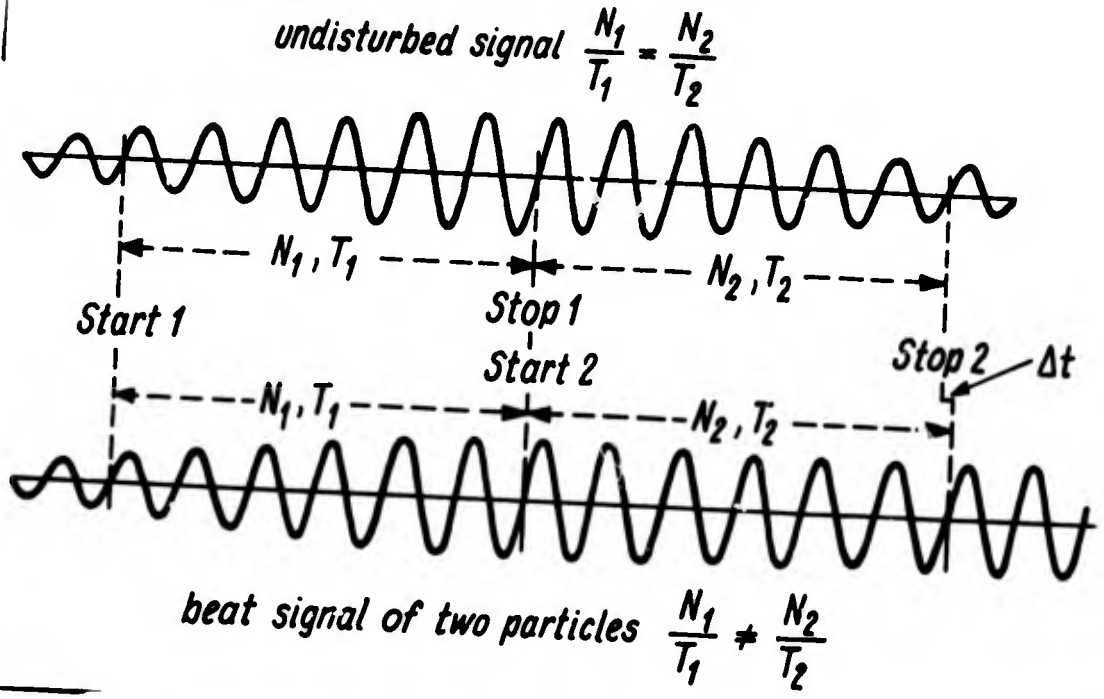

Fig.2 Calculated Doppler signal.

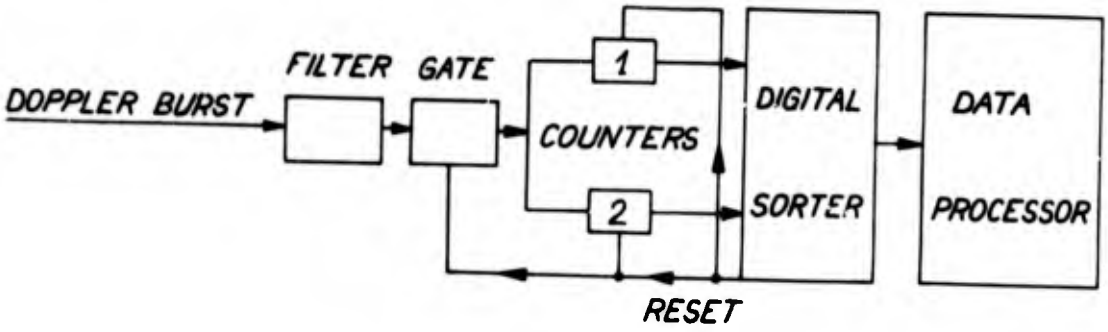

Fig.3 Flow diagramm

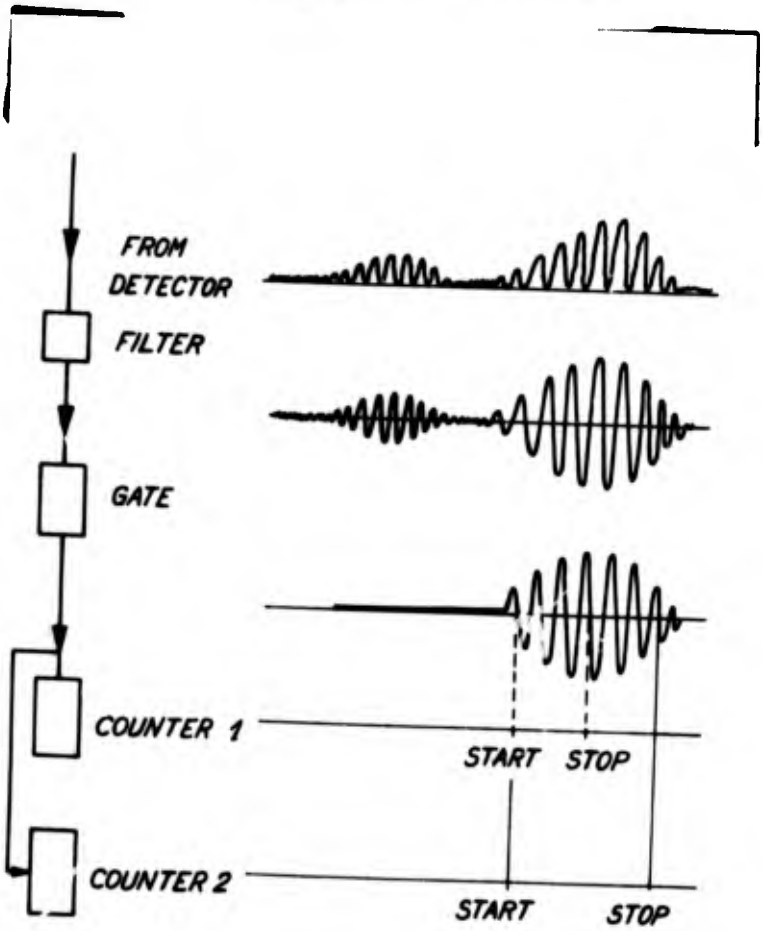

Fig.4 Signal processing.

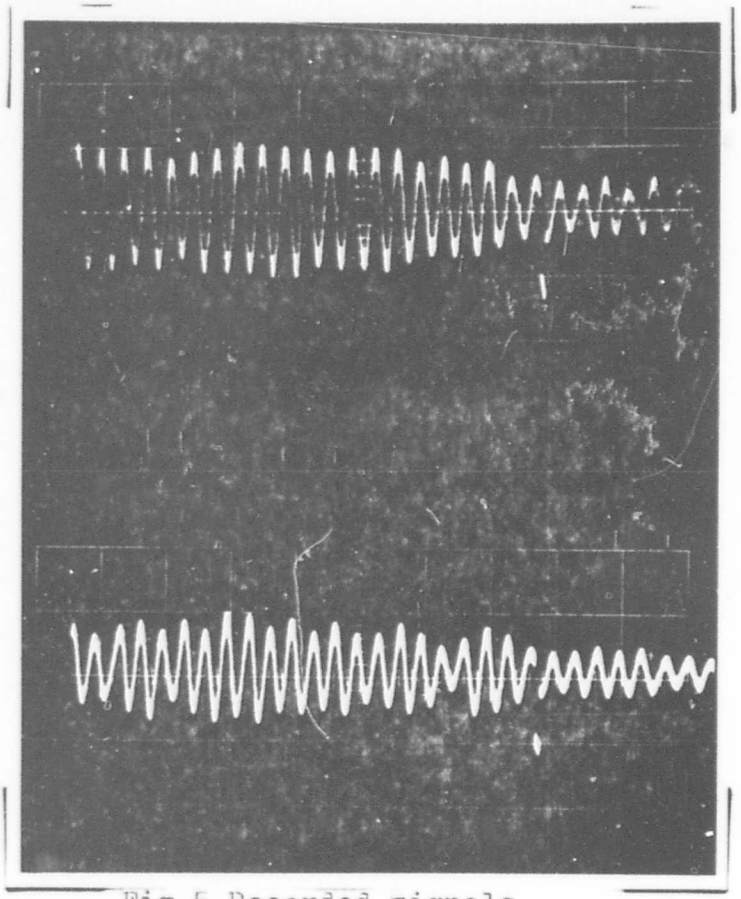

Fig.5 Recorded signals.

No.	POSITION X/cm	POSITION Y/cm	HOT FILM ANEMOMETER ΔV/V / %	HOT WIRE ANEMOMETER ΔV/V / %	LASER ANEMOMETER ΔV/V / %	
1	3.0	0.	0.4	0.78	0.85	SINGLE COUNTER WITH MONITOR
2	3.0	0.5	0.4	0.84	1.18	
3	3.0	1.	0.85	1.58	1.90	
4	3.0	1.5	3.0	9.57	10.0	
5	3.4	0.		1.12	1.13	DOUBLE COUNTING METHOD
6	12.8	0.		7.06	7.12	
7	0.	0.		0.34	0.34	

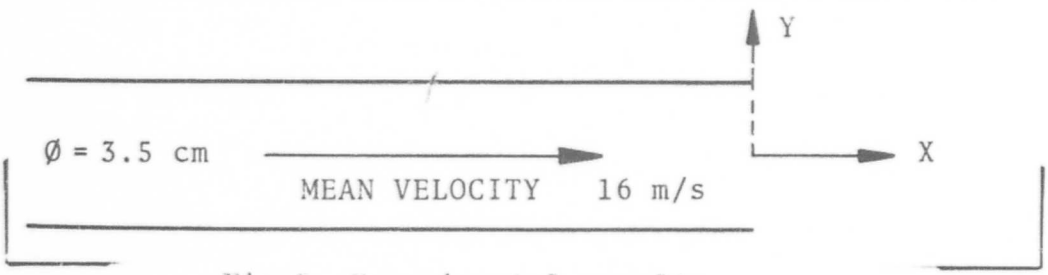

Fig.6 Experimental results.

DISCUSSION

LAWRENCE: With regard to your statement that the laser flowmeter does not effect the flow, I'd like to point out a recent Scientific American article on the pressure of laser light on a small particle. I'm just wondering about the amount of time that particle can stay in that beam without getting some impulse.

VOM STEIN: Yes, we have done some estimations. I think our observation volume is larger than the one quoted here. We have about one millimeter cube and a 1.4 watt laser. From our estimations, there is no influence due to the laser light on the small particles.

MEYERS: Our measurement volume is about 0.6 x 2 millimeters. We calculate that due to radiation pressure you get a 0.003 percent velocity change and the change is not in the direction that you are measuring.

VOM STEIN: Yes. Its perpendicular to the direction where you measure the flow velocity.

THE APPLICATION OF PHOTON-CORRELATION SPECTROSCOPY TO LASER DOPPLER VELOCIMETRY

E. R. Pike

RRE Malvern, England

The Royal Radar Establishment has kept a very active watch on the laser as a potential radar device since its invention more than a decade ago. In very early studies we came to grips with the problems of atmospheric propagation, returned signal power, heterodyne performance and photon noise effects. It was clear that real applications in the atmosphere awaited more powerful and more frequency stable lasers than were available at that time and work was therefore confined to the laboratory for some years. A fundamental programme was started in 1964 to characterise and investigate the noise properties of laser and other light sources, particularly the most perfect, coherent, gas lasers which, of course, come closest to an ideal radar transmitter.

The first fruits of this work, reported in Puerto Rico in 1965[1] represented the beginning of an era in which fast modern electronics was applied to the processing of light signals in the form of statistical analysis of photon counting distributions.

In this early work the quantity of interest was the so called single photon-counting distribution, that is the frequency histogram of the number of photons detected in a fixed time at a point in the radiation field. The output of an optical detector is illustrated in Figure 1. The second moment or the related relative variance of the photon counting distributior is a commonly used measure of the noise on a steady radiation beam.

For a perfect laser the theoretical distribution is Poissonian but we had to wait until the development of small, single-mode, stable lasers around this time before this theoretical performance was approximated satisfactorily in practice with a real laser (Spectra Physics 119). On the other hand, an ideally incoherent or "Gaussian" source gives rise to a geometric, rather than Poisson, distribution with correspondingly higher noise. The theory was developed for arbitrary light fields also at this time, mainly by Glauber at Harvard, and we reported satisfactory experimental agreement with the theory up to the sixth moments for laser and Gaussian light (produced by randomly scattering laser light) in

Paris in 1966[2]. With the situation with regard to the single probability distributions of fluctuations in good shape, we moved on to the problem of the spectral analysis of general optical signals, which is one concerned with the correlation of photon-counting fluctuations at different times. This is illustrated in Figure 2. The statistical and spectral properties of scattered laser light were of dominating interest and our theoretical and practical knowledge of Gaussian light in particular led us to look forward to a whole new field of photon-correlation spectroscopy in which optical studies of phenomena in the frequency range below 10^8Hz would provide a means of analysis quite unavailable previously. An idea of the scope of the new techniques and the relationship to other techniques is given in Figure 3.

Of course, we were not alone in realizing the potential applications of laser scattering spectroscopy and, among others well-known groups at Johns Hopkins, M.I.T., and Columbia were making rapid progress. With our background in statistical processing, however, our own approach was somewhat different from that of these other groups in its emphasis on the digital nature of the optical signal or photon flux and the consequences of this for signal processing arrangements.

If one considers the general problem of signal processing one may identify four distinct major methods of spectral analysis. These are the combinations of single channel or parallel channel processing in the frequency or time domains. See Table 1 (Frequency tracking would fall somewhere between single and parallel channel processing in the frequency domain.)

Domain / Type	Time	Frequency
Single channel	Delayed coincidence	Wave Analyser
Parallel Channels	Autocorrelator	Bank of filters

TABLE 1 Different spectral analysis techniques which can be applied to the photodetector output signal.

The full parallel channel methods are clearly superior in information usage. The bank of filters is not as flexible or convenient as one would like although it can be effective for single purpose instruments on occasion. The parallel correlation is, therefore, of particular interest.

To implement parallel correlation of the train of photon pulses constituting an optical signal in principle requires multiplying integers in real time and storing. We require to construct the function

$$G^{(2)}(\tau) = \langle n(\tau)\, n(0) \rangle$$

where n(t) is the number of photons detected in a fixed time T, small compared with the inverse bandwidths of interest. Such a real-time computer would be limited in its highest frequency performance and would be expensive. Fortunately, we have been able to overcome these practical problems by making use of known results of radar theory and transposing them into optics. It was shown, in fact, by Van Vleck and Middleton in 1943[3] that a Gaussian radar signal may be processed by hard limiting or "clipping" and autocorrelating the remaining zero-crossing positions. The multiplications now involve only single bits and may be performed with simple gate circuits. In radar this is known as one-bit correlation. The corresponding theorums in optical signal processing have been developed by Dr. Jakeman and myself at RRE[4], taking advantage also of the digital nature of the photons. We find that, for instance, if the signal n(t) is represented by a clipped signal $n_c(t)$ which is one zero accordingly as n is above or below its mean value, then the cross correlation of this clipped signal with the original gives a true representation of the spectrum. Such "single-clipped" correlation is illustrated in Fig. 4[4]. The formula for the single-clipped autocorrelation function is

$$g^{(2)}(\tau) = 1 + \frac{1 + k}{1+\langle n \rangle} \left| g^{(1)}(\tau) \right|^2$$

where $\langle n \rangle$ is the mean count rate, k the clipping level, $g^{(2)}(\tau)$ the normalised intensity or photon correlation function and $g^{(1)}(\tau)$ the optical correlation function or field spectrum.

The hardware necessary for such processing is very simple in concept, although still expensive if very fast real time operation is required. A block diagram is shown in Figure 5. Our method has been widely adopted and correlators for this type have been constructed, working at various speeds, for instance at the Ecole Normale, NYU, Johns Hopkins, Harvard, MIT, and Columbia. A commercial version is now available and has been installed in various laboratories, including several British Universities and also two laboratories in Israel.

This optimum method of optical signal processing has had most impact to date in the fields of Rayleigh scattering from stationary fluids and from solutions of macromolecules undergoing Brownian motion. It is perfectly applicable, however, to the study of the optical signals which arise in the LDV field. Our original interest in LDV dates back to our collaboration with AERE Harwell in 1967 which has led to the commercial development for DISA which has been described at this meeting. We have recently turned our attention to the use of photon-correlation measurements in LDV.

To determine the power of photon-correlation techniques in this field we have made an experimental study, performed in collaboration with the Royal Aircraft Establishment at Farnborough, in which a Malvern Type K7023 Correlator was compared with three other methods of signal processing, namely, frequency-tracking filter, Hewlett Packard computing counter and simple wave analyser. The signal was derived from an unseeded air flow, in a rectangular duct.

In an initial experiment with 10mW of He-Cd laser power using f 2.8 optics in backscatter at one meter the signal consisted of individual photons arriving at a rate of one every five Doppler cycles. An oscillogram is shown in Figure 6. The Doppler frequency was 0.5MHz corresponding to a flow of $10ms^{-1}$ and a good record could be obtained in one second. The correlation function is shown in Figure 7.

This signal level was insufficient for the other three methods to operate and so the same system was set up in forward scatter. The f 2.8 lens was stopped down until each method failed to give satisfactory performance and the photon rates for this condition were recorded. The exact evaluation of the experiment was not straightforward and we are still studying the results. The main conclusions, however, can be stated roughly that the computing counter is only suitable for very high signal strengths if accurate results are required, the wave analyser requires either high signal strengths or a long analysis time and the frequency tracker was very good compared to these but still required signal strengths some one or two orders of magnitude larger than the photon correlator. None of the commercially available analogue signal correlators available (e.g. HP, Saicor) were tried in this experiment but these are real time instruments only at low audio frequencies and would give results similar to the much cheaper wave analyser; in other experiments on macromolecular diffusion they are some two orders of magnitude slower than the Malvern instrument in the higher frequency region.

A description of our own frequency tracker will be given in my discussion of our CO_2 laser anemometry work later in this conference.

To conclude, photon correlation spectroscopy offers an optimum signal processing method for LDV systems where the frequencies are within its range. With the fastest modern electronics this should be sufficient

for all flows encountered in practice save perhaps for the high supersonic regime. The Fabry-Perot interferometer will then be the best instrument to use. A Special Projects Division at RAE Farnborough is conducting research into LDV instrumentation of their wind tunnels with our collaboration and a major objective in the near future will be to decide at what velocities unseeded backscatter LDV should be performed by Fabry-Perot rather than by photon correlation, given existing laser beam powers.

REFERENCES

(1) F. A. Johnson, T. P. McLean and E. R. Pike, Physics of Quantum Electronics Eds. P. L. Kelley, B. Lax and P. E. Tannenwald, p. 706 (New York 1966).

(2) E. Jakeman, C. J. Oliver and E. R. Pike, J. Phys. A 1 497 (1968).

(3) J. H. Van Vleck and D. Middleton, Proc. IEEE, 54 2 (1966).

(4) E. Jakeman and E. R. Pike, J. Phys. A 2 411 (1969).

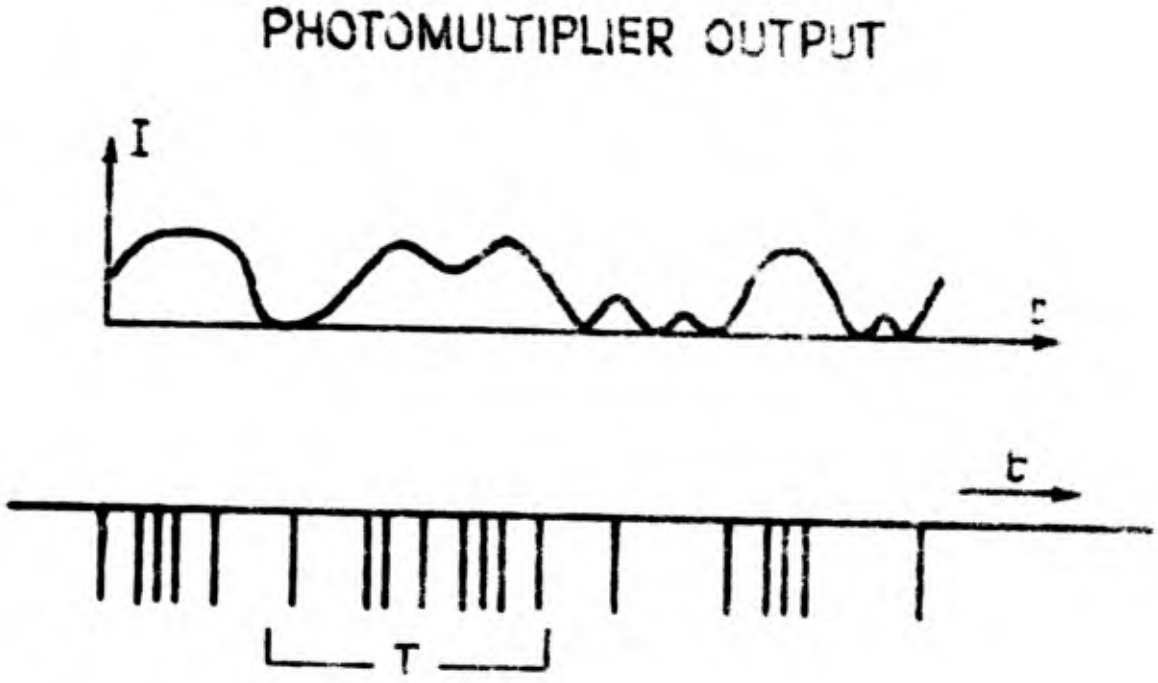

Figure 1 Photomultiplier output, each current pulse results from a photon absorption at the photocathode

CORRELATION OF PHOTODETECTIONS

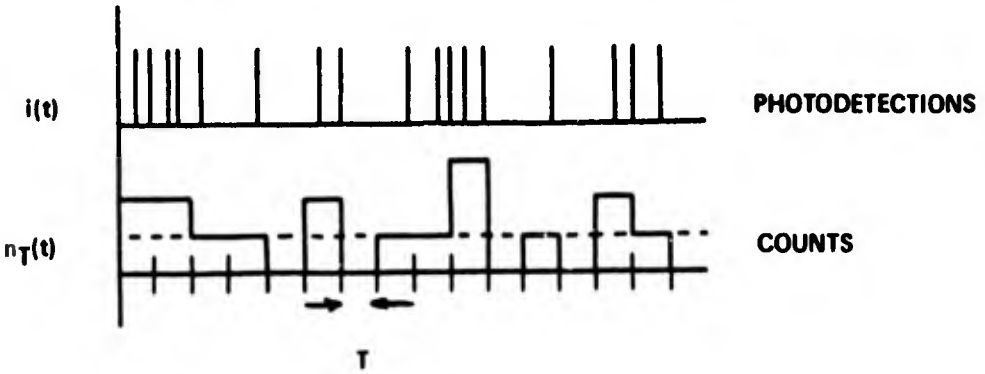

Autocorrelation function of $n_T(t)$ is

$$g^{(2)}(t,t') = \frac{\langle n_T(t)\, n_T(t') \rangle}{\langle n_T(t) \rangle^2}$$

For Gaussian statistics

$$g^{(2)}(t,t') = 1 + \left| g^{(1)}(t,t') \right|^2$$

(Siegert)

Figure 2 Correlation of photon counting fluctuations

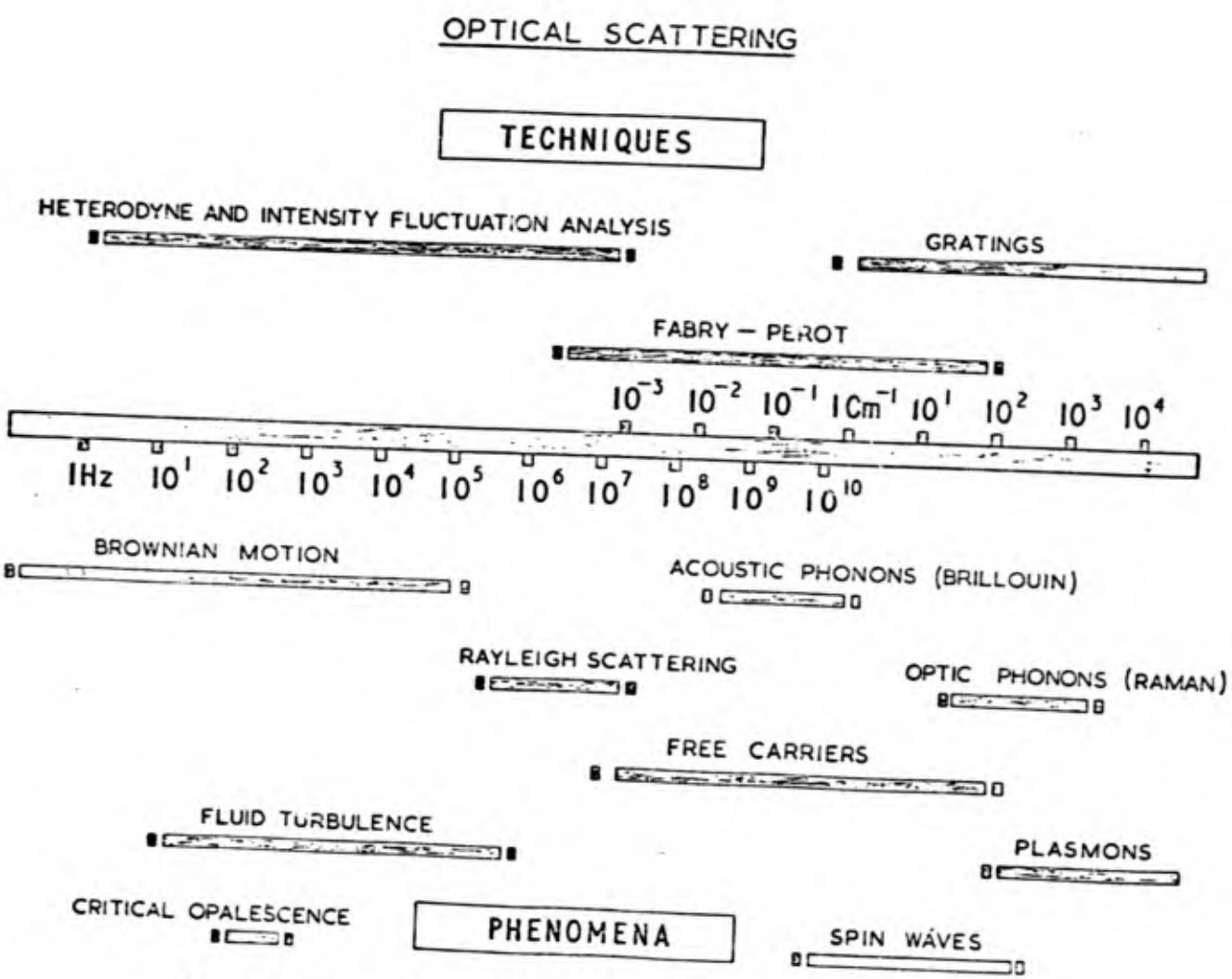

Figure 3. Optical scattering techniques and phenomena

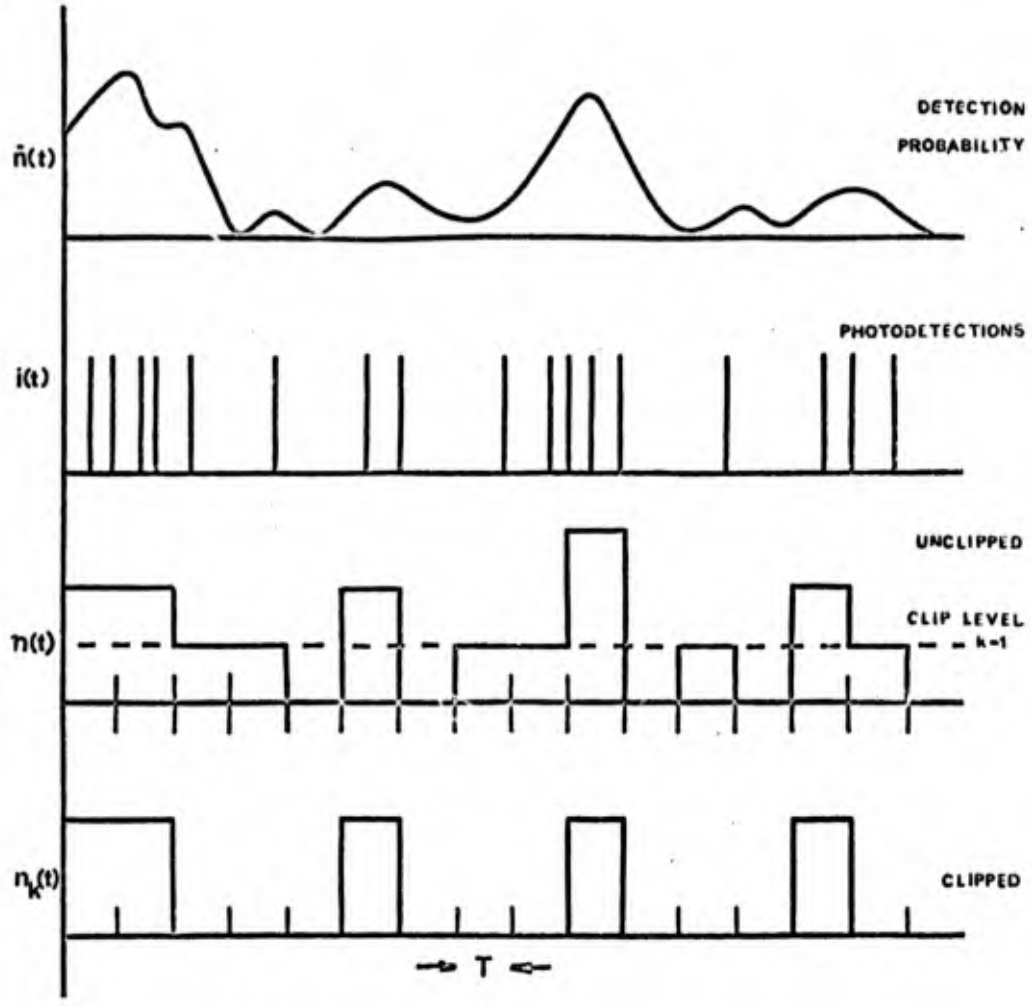

For Gaussian statistics

$$\frac{\langle n_k(\tau)\, n(0)\rangle}{\langle n_k\rangle \langle n\rangle} = 1 + \frac{1+k}{1+\langle n\rangle} |g^{(1)}(\tau)|^2$$

Figure 4. Single clipped photon correlation

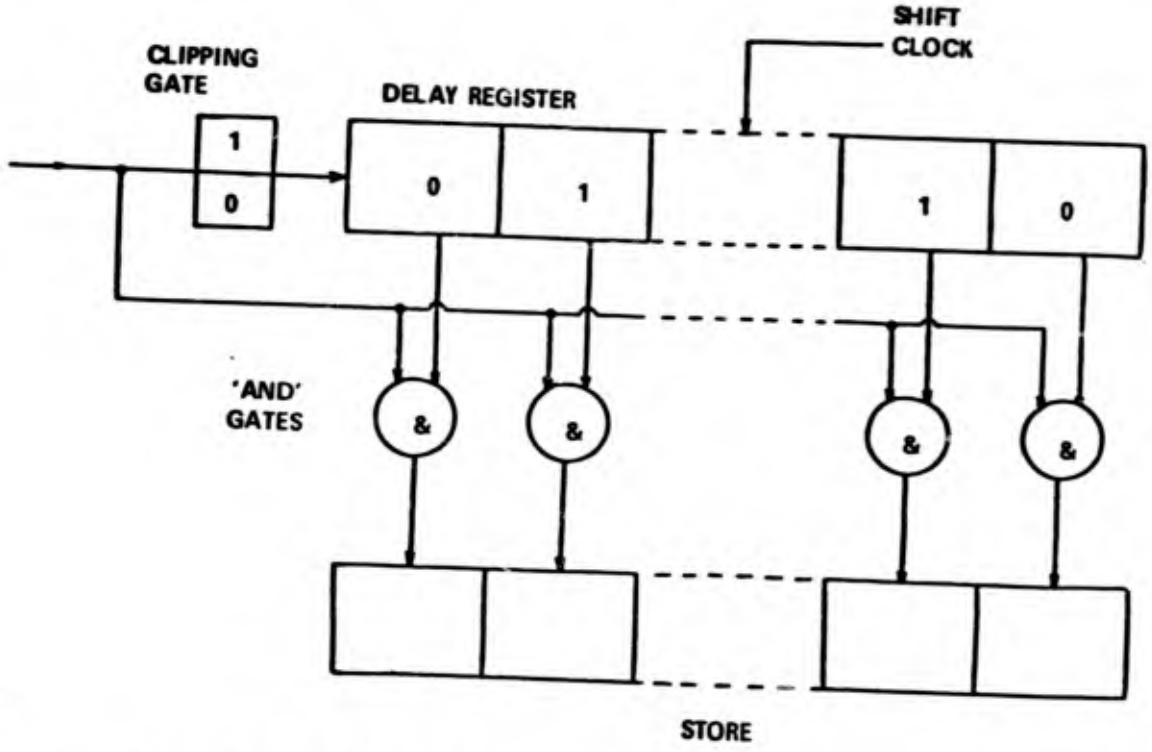

Figure 5 BLOCK DIAGRAM OF SINGLE CLIPPING CORRELATOR

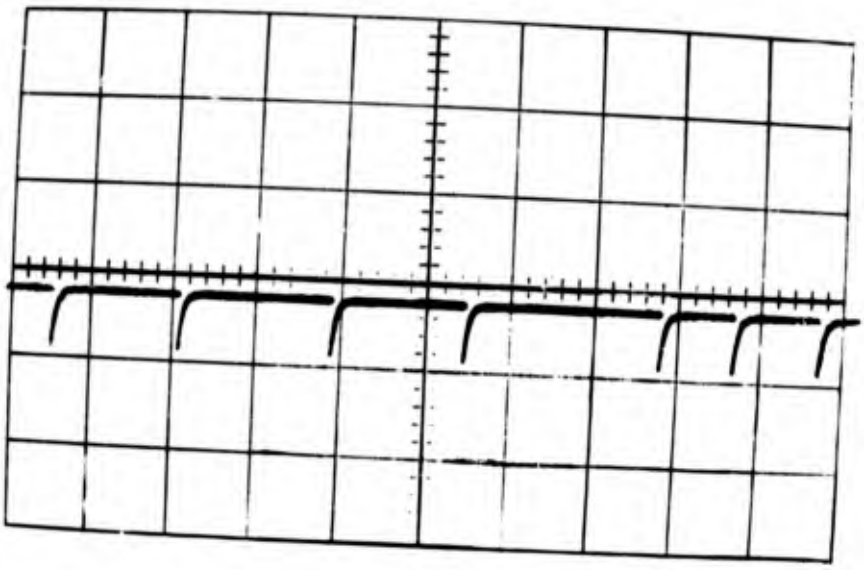

Figure 6 Oscillogram of Doppler signal (10 μs/cm) showing individual photon pulses

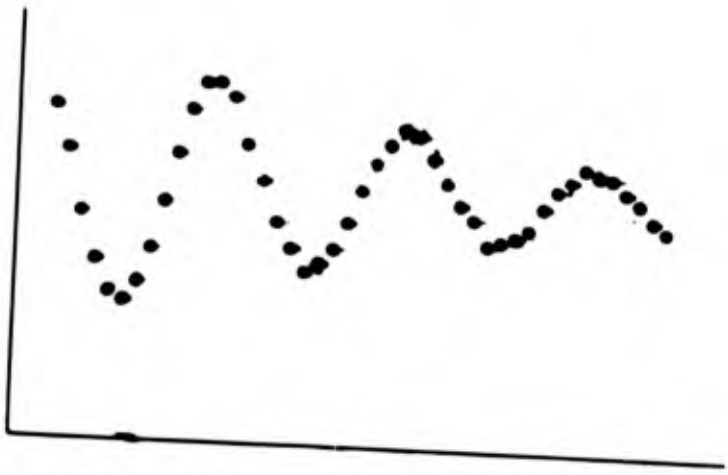

Figure 7 Digital photon correlation function (200 ns/channel) showing Doppler frequency and damping

EDWARDS: This is a question in terminology. You refer to the Hewlett-Packard as being an analog device and I assume you mean that it takes an analog input. One still believes that the current is proportional to the number of photons per second. Couldn't you really say it was a digital device with a very high Q-level? Q I think was the term used for the decision level in your one bit correlator.

PIKE: The whole principle is different. One would have to take the analog signal and digitize it.

EDWARDS: The SAICOR for instance digitizes.

PIKE: Yes, they digitize it in the back end. In fact you need to go from the input signal. The beauty of the optical signal is that it is digital. It's not advantageous to put it into a device which accepts volts and then turn it into pulses.

EDWARDS: I discussed that with the designer and in fact one that they have is designed to do exactly what you are talking about. They don't bother to go from volts and back into digital form.

PIKE: I hope they look after our patent rights.

EDWARDS: We run ours such that one channel is essentially a one bit correlator.

PIKE: I suggest that you're really concentrating on the least important facet. You can perhaps get over the fact that you need to change the signal into pulses or the other way around. The most important thing is that the real time cycling speed corresponds to an audio decay rate. Whereas ours goes at 50 nano seconds. There is a vast difference.

EDWARDS: The new SAICOR is about 100 nanoseconds.

PIKE: No it is not. That's the sampling time not the cycle rate. The cycle rate is audio. We are talking about signal utiliza-tion.

WANG: As I understand it the correlation function corresponds to the Fourier transform of the spectrum. How do you get the signal itself?

PIKE: I didn't go into tremendous detail on the form of the correlation function from different types of input signal. The logarithmic decrement of the signal is basically the equivalent of the frequency width due to the mean square turbulence in the signal. You

don't have to transform it. All the data can be taken from the time record. Basically you can set up an experiment, for instance in a windstream, and if there is no turbulence present the correlation function will be just a continuous sine wave without decay. If you then blow another fan across to cause a mixup, you immediately see the correlation function damp out and the decay time is then proportional to the mean square turbulence. I didn't mention anything about tracking with this type of signal processing. We haven't got on to that yet, but in principle one is accepting photons from the signal and they are going into usable places. One should be able to dig them out again. In fact, the machine that I illustrated there (the commercial machine) has computer interfacing and Farnborough will hook it directly onto the computer. They probably won't bother with doing any interpretation on the side. I'm sure that if necessary boxes could be put on top to present the signal frequency.

LAWRENCE: Who manufactures the machine you showed?

PIKE: This is manufactured by a firm called Precision Devicies and Systems Malvern Link, England. I have a number of their brochures in back. Unfortunately, I have no financial stake in this, it is sponsored by our National Research & Development Corporation.

VOM STEIN: I'm astonished at the precision of your one bit correlator.

PIKE: This is well known in radar. You lose very little with one bit correlation. In fact its $2/\pi$ or something like that.

MAZUMDER: What is the maximum doppler frequency you can count?

PIKE: This particular instrument, as it is sold, has a 50 nano second time -- sampling time. So the answer to your question depends on how many "spots" you want on the sine wave. It would be typically five or ten magacycles. This is not the fastest possible. You can go faster than that in fact with more expensive electronics.

MAZUMDER: Often we have problems where there are few particles available and the frequency is high. You would think that photon counting would be a good choice, but the number of photons that are available per cycle becomes very low.

PIKE: The beauty of this method is that you just sit back and wait. It doesn't matter how many photons per doppler cycle you have. You just wait until the picture is smooth enough and then you take the data. There are no knobs, you just plug it in. It's not like driving a frequency tracker. By the way, frequency tracking can be made very simple. Our frequency tracker which I'll discuss tomorrow has only one knob on the front. Of course that's a question of how much money you want to spend.

CROSSWY: In a typical application would you consider that your data sampling rate would be sufficient to plot out eventually a power spectral density curve?

PIKE: This is basically the power spectral density curve that comes out except that it's the Fourier transform.

CROSSWY: I see. That is the time domain autocorrelation function that is plotted out on your scope.

PIKE: Yes.

EDWARDS: On one slide, you have a term that I assume was the autocorrelation of the number of counts with itself and there is a 1/n term in front.

PIKE: No there was a $(1+q/1+\bar{n})$ which is unity for all $\bar{n}$ if $q = \bar{n}$.

EDWARDS: I was just wondering if there is any advantage in taking all of our lasers, putting more stops in front of them, and just going around the analog input.

PIKE: You buy a cheaper laser for simple applications that's the point. However, if you go to Farnborough they say we don't want seeding, we want back scattering and we want to get a mile away from it. You then use the most powerful laser you have and the most powerful signal processing you have.

WILD CARD SESSION

Session Chairman: W.H. Stevenson

146.B

ODDS-AND-ENDS RELATING TO APPLICATION OF LASER VELOCIMETER

by Jeff Asher

General Electric Corporation

To begin with I want to go over the type of particle seed we use at General Electric. There are a few ambiguities that I'd like to go into as well, and then open it up for the general discussion.

We've had great success in the recent past using a fluidized bed of particles that were "boiled" by air rushing through, and then having those particles injected into our main flow. We've used alumina of various diameters and taken some photomicrographs of them. For alumina powder (specific gravity of 3.5) of various sizes the deduced relaxation time in microseconds is given in Fig. 1. This gives an idea of how well this type of particle will follow the fluid. From this work and studies by J. Meyers (NASA Langley) and W. Yanta (NOL) which are going to be presented here it is felt that it is necessary to use 0.1 to 0.3 microns size alumina powder with such a large specific gravity. We have some data which I'll present tomorrow substantiating this.

This slide (Fig. 2) will give you an idea of other types of substances. Water, which has a specific gravity of one, and for a diameter of about 0.5 micron has about three quarters of a microsecond relaxation time. Titanium Dioxide has a very high specific gravity and if anyone has used it, they know that it balls up very easily. I added it to the list just to indicate that it was a rather poor choice.

There are several interesting points I would like to bring up at this time. Let's begin with a very interesting phenomena that might happen to your laser output (Fig. 3). This is what is called a TEM_{01}^{*} mode or a doughnut shape. People talk about doppler dropout occurring for various reasons. This is one of those reasons. And you can imagine how much havoc this would play if a particle happened to pass through this doughnut or missing fringe pattern. It's this kind of problem that I'm referring to when I say to people that you should be very cautious when you use your laser. Normally the TEM_{01}^{*} happens at high power, but I've been able to reproduce it very nicely at low power just by having the laser beam misaligned with respect to the center of the bore. So due caution should be used.

FIGURE 1. DEDUCED RELAXATION TIME FOR VARIOUS TYPES OF SPHERICAL PARTICLES/TRAVERSING A SHOCK FRONT IN AIR AT STP

PARTICLE NAME	DIAMETER (MICRON)	SPECIFIC GRAVITY	DEDUCED RELAXATION TIME (MICRON SECOND)	ASSOCIATED LENGTH AT 1000 f/s (mm)
Alumina (Al_2O_3)	0.10	3.50	0.13	0.040
	0.25		0.65	0.200
	0.50		2.65	0.810
	1.00		10.10	3.100
Water	0.50	1.00	0.75	0.230
Titanium Dioxide (TiO_2)	0.25	4.9	2.65	0.810

FIGURE 2

CHARACTERISTICS OF CANDIDATE SEEDING

Substance	Specific Gravity	Refractive Index	Melting Point (°C)	Color	Texture	Remarks Concerning High Temperature Environment	Aggregation		Sizing (microns)			
							Tendency	Number in Clump	High	Low	Average	Variability
Talc		1.59	88	White	Jagged flakes	Doubtful	None	Single	20.0	0.5	4.0	Large
Arizona fine dust				Tan	Irregular flake or ellipsoid		None	Single	6.0	0.1	0.5	Moderate
Colloidal alumina	3.7			White	Smooth ellipsoid	Sinters at high temperature	None	Single	22.0	0.5	6.0	Small
TiO	4.9		1750	White	Smooth ellipsoid	Should decrease in size	High	Moderate	0.5	0.1	0.3	Very small
MgO (light)	3.7	2.16	2700	White	Jagged flakes		None	Single	4.0	0.1	1.5	Moderate
Alumina:												
0.3μ	3.7	1.672	2060	White	Irregular flake or ellipsoid		Very high	High	3.0	0.1	0.3	Moderate
1.0μ	3.7	1.672	2050	White	Irregular ellipsoid		Small	Small	1.0	0.3	0.7	Small
3.0μ	3.7	1.672	2050	White	Irregular ellipsoid		Small	Small	4.0	0.2	2.0	Moderate
1.0μ (pure)	3.7	1.672	2050	White	Irregular ellipsoid		High	Large	1.0	0.1	0.7	Small

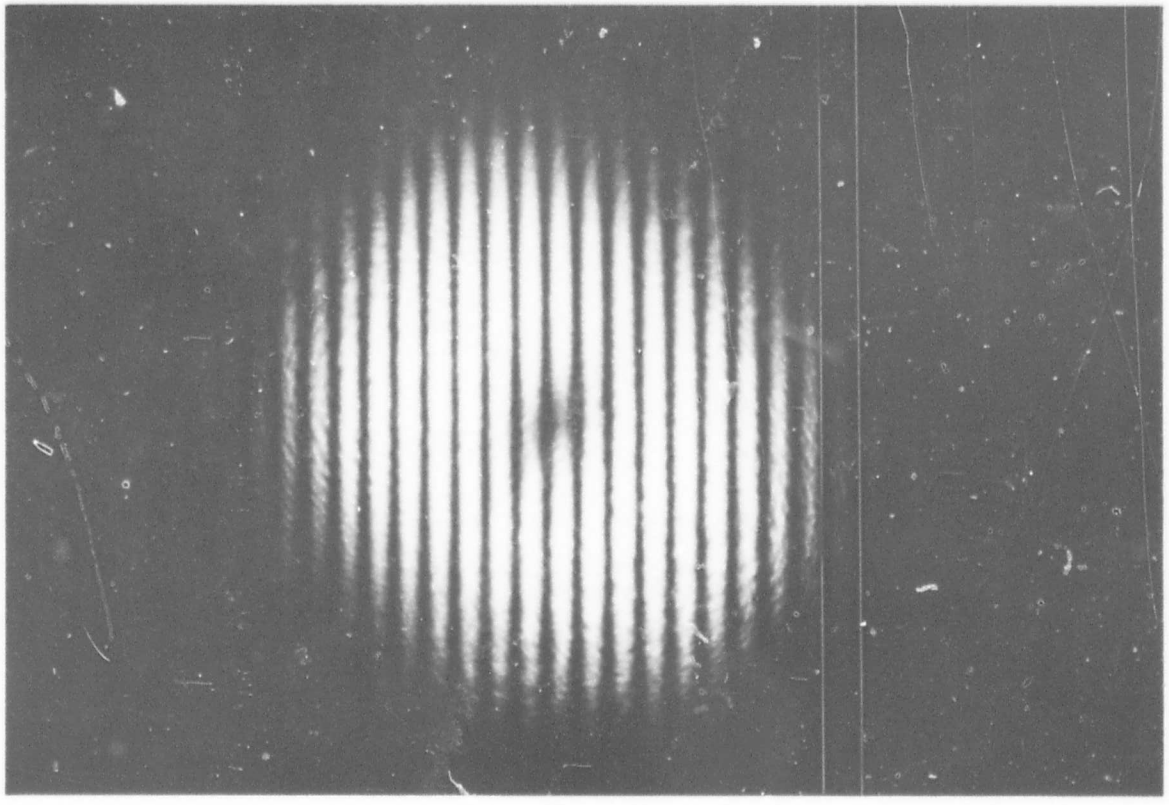

FIG. 3. Enlargement of Interference Pattern in Scattering Volume with TEM_{01*} Laser Output Present (note center). Actual Fringe Spacing Equal to 100 Microfoot.

For those of you that have used the laser velocimeter a bit and you may have realized that the statistical sample that you are generating may be biased in several ways. One of those ways was recently brought to my attention (P. Mossey, General Electric, Evendale, Ohio). The typical histograms (shown as Figures 3 to 5 in the last paper in Technical Session V) were sampled for a long enough time and thus we can say that the statistical sample is time independent. So we now have particle velocities versus probability of occurrence. As an example, for a potential flow inside a jet core we find the velocity distribution is quite peaked while in the turbulent region we have a very large distribution. Statistically, you find that the standard deviation defines the turbulence levels in both of these cases. The question that I would raise is, should we weightour distributions so that slow particles are weighted upward in establishing their population in the histogram, since their slower speed requires them to pass less frequently through the scattering volume.

That's one bias that I would like to mention. There are others. For instance, let's take the case where we have an air jet. Outside the jet boundary we entrain air. When one probes within the jet flow you have total isolation from the entrained air, but when you are in the region near the boundary, you may have, in the entrained air, a different population density of seed particles. You begin to wonder if you are biasing your data towards the higher speed particles by looking at the boundary and seeing entrained air without particulates versus looking at the jet boundary where you have a large amount of particulates from within the jet flow. So the mixing phenomena perhaps is not being seen as it should. An equal seeding of the jet and entrained flows is therefore required.

One other point concerns the fringe patterns. Normally to reduce our probe volume length as much as possible the collector optics have aperture slits. Let's say you have a slit length that has been reduced. If you have a particle (and this is especially true in the counter) going through at a large angle with respect to the fringes it's possible, for a count of four or eight, that the particle would go through and this particle's velocity would be completely omitted from further analysis because it would not satisfy the counter. So we are omitting a subset of data, of particles that may be highly skewed with respect to the fringes. That data depends on the length of the slit you are using. In other words, the smaller the slit, the more you are restricting your data to the particles that are coming perpendicular to the fringes. So it's possible that you will be losing low velocity data and again your distribution would be biased.

I would like to see in the future refraction effects understood as it applies to the laser velocimeter. We've found it a little bit perplexing. I know there are rules of thumb but I don't think we

understand enough of how to utilize the LDV in heated flows where refraction effects should be present in a steady and unsteady manner. There may be beam movement. I've observed that. I found that for a propane torch and with oxygen supplement there was hardly any movement of my scattering volume. As we reduced the oxygen supplement (and the temperature decreases) the scattering volume did move as it started to follow the large scale convection patterns. Velocity data in this latter circumstance, if obtainable, would yield incorrect results to be sure.

DISCUSSION

LENNERT: We have run across the particular condition in making our flow measurements; Don (Brayton) brought that out in his paper this morning. What we have done in trying to overcome this particular dead spot problem is to (of course depending on the angle and the aperture size as you pointed out) modulate using a Bragg cell. We get directionality from this, but it also enhances the number of fringes. I think by properly designing the system, you can cut the dead spot down to a very small angle. I think one of the exercises he mentioned was about 7 degrees or 5 degrees for the dead spot angle.

BRAYTON: This is if you upconvert the frequency.

ASHER: That I'm saying is we both demand a certain number of counts. In our case 4 and 8, I don't know exactly what you are using. The point is if your particle becomes sufficiently skewed for instance if it came parallel to the fringes it would not cross any fringes at all so you'd get no count. So if there is a situation which certainly will exist where you've cut off most of the scattering volume there is a good possibility that those particles that are going slow and slanted to the fringe pattern won't be counted at all. In other words they will start but not complete a count.

LENNERT: Yes but you minimize that by upconverting so you put moving fringes in there.

BRAYTON: If you frequency offset one beam where you normally get two or three cycles (not enough to process) you can get as many as you like.

LENNERT: Say you had a doppler frequency of a megahertz and you put a carrier on at 30 megahertz so you wind up with 39 net effective fringes in your system.

BRAYTON: Then you can fix up what would initially be an inaccurate measurement due to too few cycles even if you were initially measuring only one or two cycles.

LENNERT: We have found that to be true. In fact as I've said we have quite a bit of success with it. This is one of the things we are incorporating into our system.

YANTA: With respect to your beam fluctuation. We have noticed this with the LDV in water also, particularly salt water. I am not sure the problem is one of movement of the probe volume itself but rather the fluctuation of the fringes within the volume. These fringes really wander.

ASHER: That's true. I was only being attentive to the spot wandering away from the slit. You can also change the fringe spacing as well.

YANTA: In comparison I think it's a really serious problem.

ASHER: We should be cautious and I would hope that someone would do that kind of work.

CROSSWY: I just have one comment regarding the problem you mentioned about the bias due to seeding. In some of our experiments we used the intrinsic aerosols of the air for our scattering so that if your flow setup was derived from laboratory air, you would have the same density of natural aerosols in your core region as you would in entrained air. So this is a solution.

ASHER: This is true. Our problem is that we are developing a system here that is for turbulence spectrum measurements so we are boosting up our acquisition rate and it's no longer possible to rely on what's available in our air. (We have real clean air in Schenectady.)

HUMPHREY: We have done some calculations in reference to the refractive index business on a 2,000 degree centigrade flame study using a differential doppler system. With a 20 degree crossing angle you only have a one percent error due to the refraction effects. However if you go down in angle typically it increases, let's say use 3 degrees and you get a 3 percent error.

ASHER: These results I think would be the opposite for a highly turbulent flame. At a larger intersection angle the beam passes through a larger portion of the flame. There's also another thing. I think you'll find if you had reduced the temperature you would then start getting into more problems. The changes of the index of refraction changes with density are greatest at lower temperatures. What is the percent error Mr. Humphrey referred to in terms of?

HUMPHREY: It's a percentage of the flame diameter.

STEVENSON: I had a question regarding Bill Yanta's comment. Did you make some measurements with a specific angle between the beams? If so, what was it?

YANTA: I don't recall - something like 5 degrees.

STEVENSON: Did you try reducing the beam angle to see if that improved the situation?

YANTA: No.

ASHER: Could I ask one other question or make a statement. The influence on using the back-scatter versus forward-scatter to minimize the refractive effect could be of interest also. If anyone has done anything on that I would like very much to know about it.

PIKE: The idea of using a moving fringe system to increase the number of zero crossings is very interesting, but it isn't immediately obvious that you don't lose out because the number of photons per doppler cycle goes down and therefore the size of the particles you need for a given signal goes up.

BRAYTON. I don't think that's a limitation.

ASHER: This may be accentuated since very small particles are required if one is to do turbulent spectra work with 5 KHz frequency response.

PIKE: But this specific application is to atmospheric work.

LENNERT: Our application is mainly in tunnels and what we've done is try to ascertain whether or not we can extend the range and we've had success. What we have tried to do is clean out the seed. With supersonic flow we had problems. We tried to tell the tunnel people to please clean up their tunnels. They are getting large particles and they discriminate against the small particles.

SIGNAL PROCESSING WITH A FREQUENCY TRACKER

James F. Meyers

NASA Langley Research Center

Hampton, Virginia

Work on the Laser Doppler Velocimeter at NASA Langley began with the goal of measuring the turbulence power spectrum in the boundary layer of the Mach 6 high Reynolds number facility. This entailed, 2 years ago, finding a readout system that would work and give us power spectrum measurements. At the time there was only one instrument so designed, the wide-band frequency tracker made by Raytheon.

The main part of this informal talk is to indicate that trackers work. They work well, but they lie just as well. You have to be very careful with what you use for output data. Case in point: You have a Doppler signal which is not continuous (which you have most of the time in wind tunnels) riding on the 200 MHz noise you get from a photomultiplier tube that is shot noise limited. This noise is essentially white until it goes to the first stage amplifier where it may be subject to possible change. If it changes and gives you a noise spike, you have something that is a good Doppler signal plus a little noise spike. This is no problem. You put it into your tracker. You lock on the Doppler signal. You get good results. Fine, then you look at the edge of the flow. Duty cycle drops - then what? The tracker will take an average between the Doppler signal and that noise spike. Since the instrument locks onto the signal with the highest time average signal-to-noise, it will shift from the Doppler signal to the noise spike as the Doppler duty cycle drops. You have to be very careful since this does show up in the data.

Let me show you on Figure 1, two power spectra taken directly from the photomultiplier tube in a subsonic pipe flow jet that exited into the room. The flat noise level looks nice and clean from the photomultiplier tube, but again the amplifier isn't in the circuit. We have the Gaussian-shaped signal, which is a histogram of the frequencies, on the noise level. The left spectrum was made at the centerline of the pipe. Each of the little spikes is one particle that comes through just when the scanning filter is at the right frequency. This gives you a certain signal-to-noise ratio. Since the vertical scale is logarithmic, the Doppler signal has about a 30 dB signal-to-noise ratio. This is very high, but the tracker doesn't depend on instantaneous signal-to-noise ratio as the counter does. It depends on the average signal-to-noise ratio, which is much less. Signals like this are still very good. You can obtain mean velocity, turbulent intensity, turbulence power spectra, auto correlations, or whatever you desire. This makes a tracker more valuable than a counter for these measurements because the counter, unless it is an extremely fast counter, will not give you power spectrum measurements. Also you must seed your flow, because according to statistics, in order to detect a sine wave you must have two points per cycle. If you don't seed your tunnel you have a long time between data points which means that you can't describe frequencies which are very high. This tracker will work down to approximately a 10% duty cycle which, at the velocity we are talking about here, is about a 1 microsecond signal with 9 microseconds "off" time. This data rate yields, through statistics, a frequency spectrum to 50 kHz. If you have a fast enough counter, it can also do this. I believe Jeff Asher has one, but for other counters that I know about,

this is not the case. This is the reason we bought the tracker, which works quite well if this condition* is satisfied. This is the point to be careful of.

The spectrum on the right of Figure 1 was made at the edge of the flow. You can see the mean velocity has shifted down and the spectrum spread out. It indicates high turbulence intensity, but notice the duty cycle and therefore the average signal-to-noise ratio is down also. In some of the things I will present tomorrow you will see where the tracker continues on its way on a noise spike. These are just a few words of caution on a tracker. I think it is a good instrument. I think it can give you valuable information that you cannot obtain other ways, but be careful with it.

---

*Average signal-to-noise ratio greater than 15 dB.

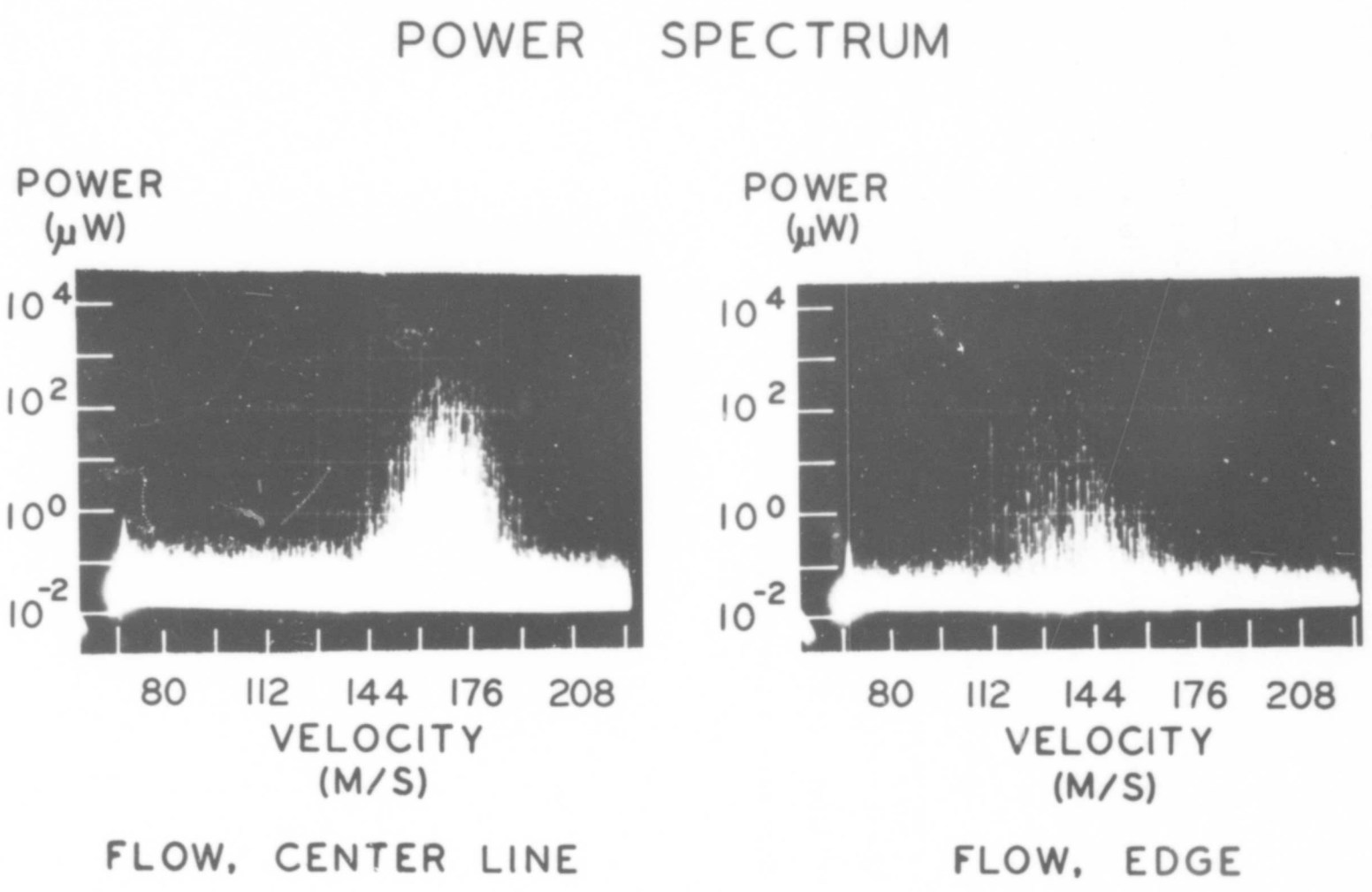

Figure 1. Spectrum analyzer display of the Doppler signal from a 2-inch subsonic pipe flow.

DISCUSSION

BERMAN: I was wondering, in your spectrum near the edge, can you comment on how long an averaging time you think you need in order to get something which is reasonable.

MEYERS: Define averaging time.

BERMAN: Were you just showing one sweep?

MEYERS: No it wasn't one sweep, but several sweeps. I think the exposure time on the film was a hundredth of a second. It is an integration, a long-time integration. It is not one sweep.

BERMAN: With a high turbulence intensity, you need quite a long time to get a reasonable average don't you? It doesn't look to me that you had enough on that particular slide to draw any conclusions.

MEYERS: Do you mean that the turbulence intensity is wide?

BERMAN: Right, you couldn't see it all.

MEYERS: Both exposures were made at the same exposure rate. What I'm saying is that the duty cycle at the edge of the flow was down. From the high spike over on one side to the high spike on the other side was a lot wider than at the centerline. All I'm saying is that the turbulence intensity at that point was higher than it was at the center. This can be correlated with hot wires or whatever instrumentation you want.

BERMAN: Wouldn't you need more data though and more time for your averages to determine anything from the spectrum?

MEYERS: This is just for illustration. We can't use measurements from the Doppler spectrum at all.

BERMAN: OK. I just wanted to make sure. From what you said earlier, I thought you were taking your information right from plots like that.

MEYERS No. This is just to let us know what the duty cycle is and what the signal-to-noise ratio looks like. It's purely diagnostic.

WELCH: I'd like to make a comment on the comparison of different types of electronic systems. What you're saying about trackers of course is true. You can also say the same thing about a counter system or any other system. If the tracker goes astray, then you get a reading out that is ambiguous, whereas in the other systems, sometimes this is not the case. But suppose we use a counter system for example, or if we use phase lock loop or a frequency lock loop, one of these three type tracking systems. Anything like this that we use, it seems to me first of all what we have to do is decide when you have "a good signal condition" and "a not good signal condition." You have to be able to use some logic so that you can decide this. When you have a good signal condition you have to obtain some voltage conversion or some signal with a comparable frequency which you can count or make some other measurements from like running through a correlator. It appears to me that the two basic things that are required, regardless of what you have for an electronics system, is a "good signal condition" with a logic circuit to decide this and then a track and hold. With these two ingredients, I think you can make any of these electronic systems get out reasonably good data. Now of course some have advantages over others. With a phase lock loop, for example, in the case where you only have one particle at a time floating through the sampling volume you have a tremendous problem of acquisition. You have too few cycles to acquire. But if you use a frequency lock using a frequency band to get your discrimination to control or use a track and hold then you can use the same type of precision circuitry that

you use in all the other systems. I think this doctoring, if you want to call it that, is required in any electronic system that you use. Apparently, the way I look at it, when you have these problems in an electronic system, it means you don't have proper doctoring.

MEYERS: My question here is, in a counter system you have comparison circuitry so that random noise does not enter the system. In a frequency domain instrument, a Doppler signal looks just like a noise signal to the instrument. It's a fact of life. You can't say that a Doppler burst comes in, a system hooks on to that and if it goes away for long periods of time, its going to sit there. We have locking systems on ours, but the thing does wander off.

WELCH: Yes, but let us suppose you do this. Forget about the locking system. Suppose you use a discriminator and you use the same decision circuitry in front of it and track and hold the voltage output. Now you are only looking at voltage output during the time that the signal is good enough to give you the proper result and you hold it through the remainder of the time until another burst comes through. Actually the counter itself is a track and hold system.

MEYERS: I'd like to know your definition of a good signal.

WELCH: Well that's true. This is the problem.

MEYERS: I think a narrow band section of noise looks just as good as a Doppler signal.

WELCH: Well it does. You can't do that of course. You can't narrow band a system because you get into bad trouble.

MEYERS: Well what I am saying is that some amplifiers will do this to you. For example, the particular noise spike we have to be careful of is only 2 MHz wide.

WELCH: Well then you're in trouble. I'll agree with you there.

MEYERS: All I'm saying is be careful.

PIKE: There are two points that very much simplify this problem. There can't really be that much difference particularly if the narrow band in the tracker is sufficiently narrow, the noise you get through is white and it will wander around in the low pass filter. The other point is, why does it wander off anywhere - there is no need for it to? Secondly, why does it have to integrate?

MEYERS: Why do you put AFC circuitry in home stero receivers?

PIKE: No, now that's ridiculous. You can certainly make a tracker which sits for a second within a kHz. That's not long. We aren't worried about that sort of thing. We have a tracker that sits perfectly until the next signal comes along - not much different from a frequency counter.

MEYERS: Well then I don't quite understand your tracker, I don't have an answer to that.

CROSSWY: As I understand the DISA tracker, you have a variable threshold.

PIKE: I'm not talking about the DISA tracker.

CROSSWY: OK, any tracker. The one I observed out here in the hall, the gentleman demonstrated, has a variable threshold adjustment which I think might solve the problem you are talking about, in that it will not indicate a lock unless the IF signal is about a certain level. If you have a signal-to-noise ratio that is poor enough so that you are looking at the band-pass filtered white noise, you know it will appear as a signal of varying frequency and amplitude (slightly varying frequency) about the center frequency of the band-pass amplifier. So if you have this variable threshold feature it appears that you might be able to use that to solve the problem you're talking about.

MEYERS: This variable threshold feature is on the tracker. It does do the job - that is one of the answers, but if your seeding density happens to change, it also effects your signal-to-noise ratio, so you could defeat yourself on the threshold.

PIKE: That's not right because you can have broad-band AVC. You can put 50 dB of AVC on.

MEYERS: Define AVC please.

PIKE: Automatic voltage control. You have the discrimination threshold controlled by the actual broad-band signal strength and not the narrow band signal strength. This is how we make an automatic acquisition system. You couldn't do it any other way. It all boils down to the same point. You aren't very different from a frequency counter. In fact you've got a very sophisticated frequency counter.

MEYERS: I guess I'm not understanding what you are saying. When I talk about a threshold I'm saying that if we put a threshold at a voltage level then we would not lock on any signals below that noise. We'll only see something above it. But if your seeding density does happen to change as you move from point to point, this noise could conceivably come above it.

PIKE: No, because the threshold is tied to the broad-band level.

MEYERS: But with more particles scattering light more often, your shot noise is going to go up in proportion.

PIKE: But if you are tied to the actual shot noise level over the broad-band then you are alright.

WHITLAW: I would just like to comment that all Jim says is true and I would agree with him on the basis of the trackers we've played with.

PIKE: They are not a very sophisticated tracker. What I'm saying is that you can make a tracker which is more or less a very sophisticated frequency counter.

WHITLAW: That's right, but what Jim's saying is true. I think it is largely right on the basis of the instrument we've used. As far as the gentleman back here is concerned, I think he is right too. You must make sure you get a good signal-to-noise coming through by adjusting the optics. Then you start with the problem of the particular tracker.

PIKE: You are never interested in a case where you've got lots of signal to monitor - that's kid stuff.

MAZUMDER: From your experience, have you found an average signal-to-noise ratio with which you could work successfully with the tracker?

MEYERS: About 15 dB.

COMMENTS ON WAVE BROADENING

J. C. Angus

Case Western Reserve University

Cleveland, Ohio

I would like to only spend two minutes to try to bury an old chestnut. This is the matter of two kinds of broadening - finite transit time broadening and the uncertainty in wave vector broadening. It's been known that those two types of broadening are equivalent for some time. All I want to do is present a simple physical argument which I think will be convincing to the doubters. This argument should hold true for every kind of laser doppler system - dual beam, reference beam, or what have you - if you have a radiation field which is determined by the transmitting optics and another radiation field which is determined by the collecting optics. One way of handling this problem is to model the fields by a linear superposition of plane waves. In fact that's the classic way of handling radiation problems. What one does is model the input radiation field by linear superposition of plane waves. One does exactly the same thing in the receiving optics. Then the calculation proceeds trivally. One calculates the doppler shift that one gets from each possible pair of plane waves, adds them all together and one obviously gets a distribution of doppler frequencies out of this calculation. This, by the way, is what you would call the uncertainty in wave vector broadening. Now some people would like to add on to this the finite transit time broadening. One could try to do that; however, notice the following. We are doing this all from the linear superposition of plane waves, each one of which has a well defined wave vector. Therefore it is of infinite lateral extent and can contribute no finite transit time broadening. Therefore there is no finite transit time broadening when one is using this model to calculate the broadening. One can do exactly the equivalent calculation if instead of thinking in K space one likes to think in real space. One can model the radiation field directly in real space and do the calculations on that basis. In that case you would speak of the effect as finite transit time broadening and there is no uncertainty in wave vector broadening. It simply doesn't enter into the calculation.

GEORGE: I think the key point is if you define the sample volume in terms of the doppler current that you receive there is only one kind of broadening.

ANGUS: I tried to make this general so that it applies to every kind of a velocimeter; differential velocimeter, reference beam, kinds that are going to be invented in the future. It applies to all.

GEORGE: The problem comes in when people try to define the sample volume in terms of the input optics and they look at the spectrum and say gee whiz it's broader than it should be. That's because their output optics are not looking at the whole sample volume.

ANGUS: I also find plenty of data in the literature to support my point. Data on the broadening from a rotating disc, for example. Also the theory has been presented in different ways and quite awhile ago by a number of people. Yeh, who invented the first flow meter, has done equivalent calculations for the case of Brillion scattering where the photons are moving through a finite sample volume. He did the calculation in K space.

PIKE: I just want to make a comment that I think part of the origin of this misconception is the paper of Goldstein and Hagen where they forgot that the laser beam has a plane wave front at the waist. They drew a picture like geometric optics.

ANGUS: My argument also holds true for the case of very small f/number optics where you actually have curved wavefronts in the sample volume. You're simply in the region analogous to Fresnel diffraction where you can still use linear superposition.

ANALYSIS OF TURBULENT FLOW MEASUREMENTS FROM LDV DATA

W. K. George

Pennsylvania State University

I'd rather give this talk in the turbulence session, but unfortunately it's basic to understanding the Doppler ambiguity. So I'll give essentially what amounts to the first half of what I am going to say tomorrow morning. What I'm interested in is the classical problem in turbulence measurement: What is your probe measuring? How does it relate to the fluid flow? It's the problem that hot-wire anemometry people have been looking at for a long time. The analysis that I'm about to show you is in some way reminiscent of that done many years ago on the spacial resolution of a hot wire--and more recently by Wyngaard[1] when he looked at the effect on the measurement of turbulent spectra. I will talk about instantaneous velocities primarily. In the course of this development, I'll have to also talk about Doppler ambiguity, but I'll try to reserve most of that until tomorrow morning, if I can.

The optical system to which I will confine my discussion is what is known as the Goldstein[2] system (Figure 1). Notice there are no output optics aside from the photomultiplier tube which is large compared to say any diffraction pattern of interest. We can treat this as a scattering problem which is determined by the input optics. The analysis to follow also applies to the so-called dual scatter system.

In Figure (2) is the coordinate system I used--exactly that coordinate system used by Mayo[3],[4] in his analysis of 1969-70. You can see there's a coordinate system defined with a reference beam, a coordinate system defined by the scattering beam, and then what I will call the flow coordinate system with the U component of velocity aligned in the X-direction. The reference beam can be represented by

$$E_r(x'',y'',z'',t) = \hat{E}_r(x'',y'',z'')e^{j2\pi ft} \qquad (1)$$

and the scattering beam by

$$E_i(x',y',z',t) = \hat{E}_i(x',y',z')e^{j2\pi ft} \qquad (2)$$

where $\hat{E}_r$ and $\hat{E}_i$ represent the complex amplitudes, and f represents the frequency.

The total current is given by the integral of the intensity over the surface of the photomultiplier tube.

$$i_{total} \propto \iint_S \left| E_r + \sum_i E_{s_i} \right|^2 dA$$

$$= \iint_S \left\{ E_r E_r^* + E_r \sum_i E_{s_i}^* + E_r^* \sum_i E_{s_i} + \sum\sum_{ij} E_{s_i} E_{s_j} \right\} dA \quad (3)$$

These terms may be recognized as the interaction of the reference beam with itself, the interaction of the reference beam with the scattering particles, and the multiple interaction term.

Following Mayo[3] 1969, we can define a complex current as just that part that contributes to Doppler signal current

$$i = C \iint_S \sum_i E_r^* E_{si} \, dA \quad (4)$$

This is just the amplitude of the scattering particle multiplied by the complex amplitude of the reference beam and then summed over all scattering particles and these amplitudes are integrated over the surface of the photomultiplier tube. It immediately follows that

$$i = \sum_i i_{sp_i} \quad (5)$$

where

$$i_{sp} = C \iint_S E_r^* E_{s_i} \, dA \quad (6)$$

Thus the signal current is just the sum of the currents generated by the individual particles.

The calculation of Mayo assumes the following things: the particle radiation is spherical and all apertures block negligible intensity. Mayo showed that the current can be represented as just a product of the amplitude of the laser light near the focal point (at the center of the flow) and the equivalent reference beam at that location.

The equivalent reference beam at the center of the flow is most easily determined by simply focussing it there to start with. By assuming the beams are Gaussian, a relation for the Doppler current for a single scattering particle as a function of the location of the particle is easily obtained.

$$i \propto E_{o_r} E_{o_i} e^{-\left[\frac{x^2}{2\sigma_1^2} + \frac{y^2}{2\sigma_2^2} + \frac{z^2}{2\sigma_3^2}\right]} \cos \underline{K} x \qquad (7)$$

An ellipsoidal scattering volume is defined and the Doppler shift is contained in the cos $\underline{K}$ x.

Now let's assume that the particle perfectly track the flow. I will pick $\underline{a}$ to be the initial position of the particle and $\underline{U}$ will be the particle velocity. The particle position at any time t is obviously a function of where it started and its velocity history. Thus

$$\underline{x}(\underline{a},t) = \underline{a} + \int_0^t \underline{U}(\underline{a},t_1)\, dt_1 \qquad (8)$$

We are talking about a single particle. Plugging this relation into the cosine term above, a constant phase is obtained which I'll call γ which depends on where the particle started. We also obtain a fluctuating phase which depends on the history of the velocity. Obviously the derivative of this time-dependent phase just gives us back the particle velocity multiplied by the scattering wave number.

$$\theta(t) = \underline{K} \int_0^t \underline{U}(\underline{a},t_1)dt_1 \qquad (9)$$

$$\frac{d\theta}{dt} = \underline{K}\, \underline{U}(\underline{a},t) \qquad (10)$$

This is precisely the operation performed by a zero-counting device.

The important question is: What velocity does the velocimeter see? The answer: a weighted average of velocities of the particles which are in the volume at any instant, i.e.

$$u_o(t) = \int_{\text{volume of initial position s}} \underline{U}(\underline{a},t)\, g(\underline{a})\, d\underline{a} \qquad (11)$$

The function $g(\underline{a})$ is a random function which contributes every place there is a scattering particle and is zero elsewhere. We can define an effective displacement X by looking at the history of this effective velocity.

$$\underline{\bar{X}}(t) = \int_0^t u_0(t_1)\, dt_1 \qquad (12)$$

Now the position of an individual particle may be represented in terms of the initial position of the particle, the effective velocity averaged over all the particles in the beam at any instant, plus the local deviation of that particular particle, say $\Delta(\underset{\sim}{a},t)$.

$$x(\underset{\sim}{a},t) = a + \underline{\bar{X}}(t) + \Delta(\underset{\sim}{a},t) \qquad (13)$$

where

$$\Delta(\underset{\sim}{a},t) = \int_0^t \left[\bar{U}(\underset{\sim}{a},t_1) - u_0(t_1)\right] dt_1 \qquad (14)$$

I'll have more to say about $\Delta(\underset{\sim}{a},t)$ tomorrow; for now we will concentrate on $u_0(t)$, the effective velocity or the particle-averaged velocity.

Recall that the Doppler signal current is the sum of the currents due to the individual scattering particles. Using the expression for the current generated by a single particle it is easy to show that the current may be reduced to

$$\begin{aligned} i(t) &= F(t) \cos \underline{K}\,\underline{\bar{X}} + G(t) \sin \underline{K}\,\underline{\bar{X}} \\ &= [F^2 + G^2]^{\frac{1}{2}} \cos\left[\underline{K}\,\underline{\bar{X}} - \bar{\phi}\right] \end{aligned} \qquad (15)$$

where

$$\phi = \tan^{-1} \frac{G}{F} \qquad (16)$$

Recall that $\underline{\bar{X}}$ is the particle averaged position.

A typical detector differentiates the phase and gives an output proportional to frequency, say ω_1, where

$$\omega_1 = \underline{K} \frac{d\bar{X}}{dt} - \frac{d\phi}{dt} = \underline{K}\, u_0 - \phi' \qquad (17)$$

The term ϕ' is of no interest to us at this point, but clearly will contribute to random velocity-like fluctuations since it includes all the random phase effects--the particle initial positions, gradients of mean velocity, and fluctuating velocities across the scattering point. I'll talk about this in the morning.

Note the appearance of u_o. This is the whole point of this. The LDV responds to a particle averaged velocity, not the Eulerian velocity that might be measured by a fixed probe like a hot wire. If the scale of turbulence inhomogeniety is much larger than the largest dimension of the scattering volume, u_o, the average particle averaged velocity, may be identified as the average Eulerian velocity averaged over the scattering volume. I suggested a criterion that's well known, that is

$$\nabla\bar{u}/\bar{u} \quad >> d \tag{18}$$

where d is a typical scattering volume dimension. $\nabla\bar{u}/\bar{u}$ is a length scale characteristic of the inhomogeneity. Note that $u_o(t)$ still may not be the velocity of the center of the scattering particle as Edwards[5] pointed out very nicely, for example, if there is curvature in the mean velocity profile.

A similar criterion exists for fluctuating velocities since the fluctuating velocities are not Eulerian either. Using the analysis of Lumley[6] that was presented in the Marsailles conference on turbulence in 1963 and assuming incompressibility, homogeneity, stationarity, and isotropy, it can be shown that the fluctuating velocities are Eulerian. Obviously these things are never satisfied in practice, so what one ends up with is a length criterion that the time a particle spends in the scattering volume has to be short compared with the evolution time of the turbulence. In any case under appropriate conditions we can call the measured velocities Eulerian velocities which is what we are usually after.

What is the spatial resolution of the LDV?

The three dimensional turbulence spectrum $\phi_{11}(k_1, k_2, k_3)$ is defined by

$$\overline{u'^2} = \iiint \Phi_{11}\,(k_1,k_2,k_3)\, dk_1\, dk_2\, dk_3 \tag{19}$$

where $\overline{u'^2}$ is the turbulent energy. The one dimensional spectrum is given by

$$F_{11}'(k_1) = \iint \Phi_{11}\,(k_1,k_2,k_3)\, dk_2\, dk_3 \tag{20}$$

The part of the turbulent energy measured from the instantaneous LDV signal is $\overline{u_o'^2}$ and is given by

$$\overline{u_o^{\prime 2}} = \iiint \Phi_{11}(k_1,k_2,k_3)\, W(k_1,k_2,k_3)\, dk_1 dk_2 dk_3 \qquad (21)$$

where $W(k_1,k_2,k_3)$ is the Fourier transform of the scattering volume. The one dimensional measured spectrum $F_o(k_1)$ is defined in an analogous fashion by

$$F_o(k_1) = \iint \Phi_{11}(k_1,k_2,k_3)\, W(k_1,k_2,k_3)\, dk_2\, dk_3 \qquad (22)$$

For a Gaussian scattering volume (which is often the case) is given by

$$W(\underset{\sim}{k}) = \frac{1}{(2\pi)^{3/2}\sigma_1\sigma_2\sigma_3}\, e^{-\left[\frac{k_1^2}{2\sigma_1^2} + \frac{k_2^2}{2\sigma_2^2} + \frac{k_3^2}{2\sigma_3^2}\right]} \qquad (23)$$

where

$$\begin{aligned} k_* &= 1/\sqrt{2}\,\sigma_1 \\ m_* &= 1/\sqrt{2}\,\sigma_2 \\ n_* &= 1/\sqrt{2}\,\sigma_3 \end{aligned} \qquad (24)$$

where $\sigma_1,\sigma_2,\sigma_3$ are the standard deviations of the scattering volume intensities.

By assuming an isotropic form for the three dimensional spectrum and using Pao's[7] spectrum for the turbulence, we may compute the attenuation of the spectrum for the turbulence due to the averaging of turbulent components smaller than the scattering volume. The results are shown in Figure (3) for several values of $m_*\eta$ where η is the Kolmogorov microscale. Recalling that $m_*\eta$ larger corresponds to a smaller scattering volume, it is clear that the scattering volume must be smaller than the Kolmogorov scale if the entire spectrum is to be measured.

By plotting the ratio of the measured spectral value to actual value (Figure 4), we may define a scattering volume transfer function and this is shown for several values of $\tilde{m}_*=m_*\eta$. It is assumed that σ_2 is the largest dimension of the scattering volume as is always the case for small scattering volumes. From Figure (5) it can be seen that the dependence of the half power attenuation point on scattering angle is very weak.

Figure (6) is a spectrum measured in laminar flow. The roll off is due to the filter. You'll notice it's flat. Figure (7) represents a turbulence spectrum measured in a grid turbulence The points actually measured are seen to flatten out as they should according to our theory for the Doppler ambiguity, the results of which will appear tomorrow.

If the Doppler ambiguity is subtracted out (Figure 8), the spectra are seen to lie close to Pao's. There's about a 10% calibration error so in fact they lie right on Pao's values which is surprising considering the low Reynolds number. The attenuated spectrum is an example of what happens when the scattering volume gets too big. In this particular case, the scattering volume was smaller than the Kolmogorov microscale and you can see that indeed the turbulence was significantly attenuated. Because of the low Reynolds number I couldn't really verify the transfer function I showed you earlier.

DISCUSSION

BENNETT: Just one question. If your measuring volume is larger than or of the same size as the scale of turbulence, it seems obvious that you would have this effect.

GEORGE: It is obvious--yes. However, it turns out that the part of the turbulence that is attenuated contributes to velocity gradients within the scattering volume and they can cause a significant contribution to the ambiguity--that is not obvious.

BENNETT: With what precision did you measure the Kolmogorov microscale?

GEORGE: Very close, because I'm working in a well-known turbulent flow. I'm working in homogeneous grid turbulence. I've measured the decay rate downstream. In fact, the measurements of decay rate were made with a hot-film probe. In other words, the flow is very well known.

PIKE: I was just wondering whether ambiguity is really a very good word for this effect. I believe that I invented it.

GEORGE: I think you did, yes.

PIKE: I had in mind the radar case where there is a spread of frequency. In fact, as you've shown, and as I've said earlier today, one can actually take this ambiguity out.

GEORGE: No, I disagree. I didn't show that--quite the contrary.

PIKE: You subtracted it out, so it's not ambiguous anymore.

GEORGE: True. It does turn out that in most turbulent flows in spite of the fact that the ambiguity is dependent on the turbulence, it's uncorrelated with it. If you work in a turbulent flow which is significantly nonGaussian that may not be ture. I'll say more about this tomorrow.

REFERENCES

(1) Wyngaard, J. C. (1968). "Measurement of Small-Scale Turbulence Structure with Hot Wires". Journal of Scientific Instruments (Journal of Physics E), Series 2, Vol. 1.

(2) Goldstein, R. J. and D. K. Kreid (1967). "Turbulent Flow Measurements Utilizing the Doppler Shift of Scattered Laser Radiation". Physics of Fluids, Vol. 10, No. 6, 1349.

(3) Mayo, W. T. (1969). "Laser-Doppler Flowmeter - A Spectral Analysis". Ph.D. Thesis, Dept. of Electrical Engineering, Georgia Institute of Technology, May 1969.

(4) Mayo, W. T. (1970). "Spatial Filtering Properties of the Reference Beam in an Optical Heterodyne Receiver". Applied Optics, Vol. 9, No. 5, pp. 1159-1162.

(5) Edwards, R. V., Angus, J.C., French. M. J., and Dunning, Jr., J. W. (1970). "Spectral Analysis of the Signal from the Laser-Doppler Velocimeter: Time-Independent Systems." Journal Applied Physics, 42, 2, pp. 837-850.

(6) Lumley, J. L. (1961). "The Mathematical Nature of the Problem of Relating Lagrangian and Eulerian Statistical Functions in Turbulence". Mecanique de la Turbulence. Colloques Internationaux du Centre National de la Recherche Scientifique, No. 108. Editions du C.M.R.S., Paris.

(7) Pao, Y. H. (1965). "Structure of Turbulent Velocity and Scalar Fields at Large Wavenumbers". Physics of Fluids, 8, 6, 1063.

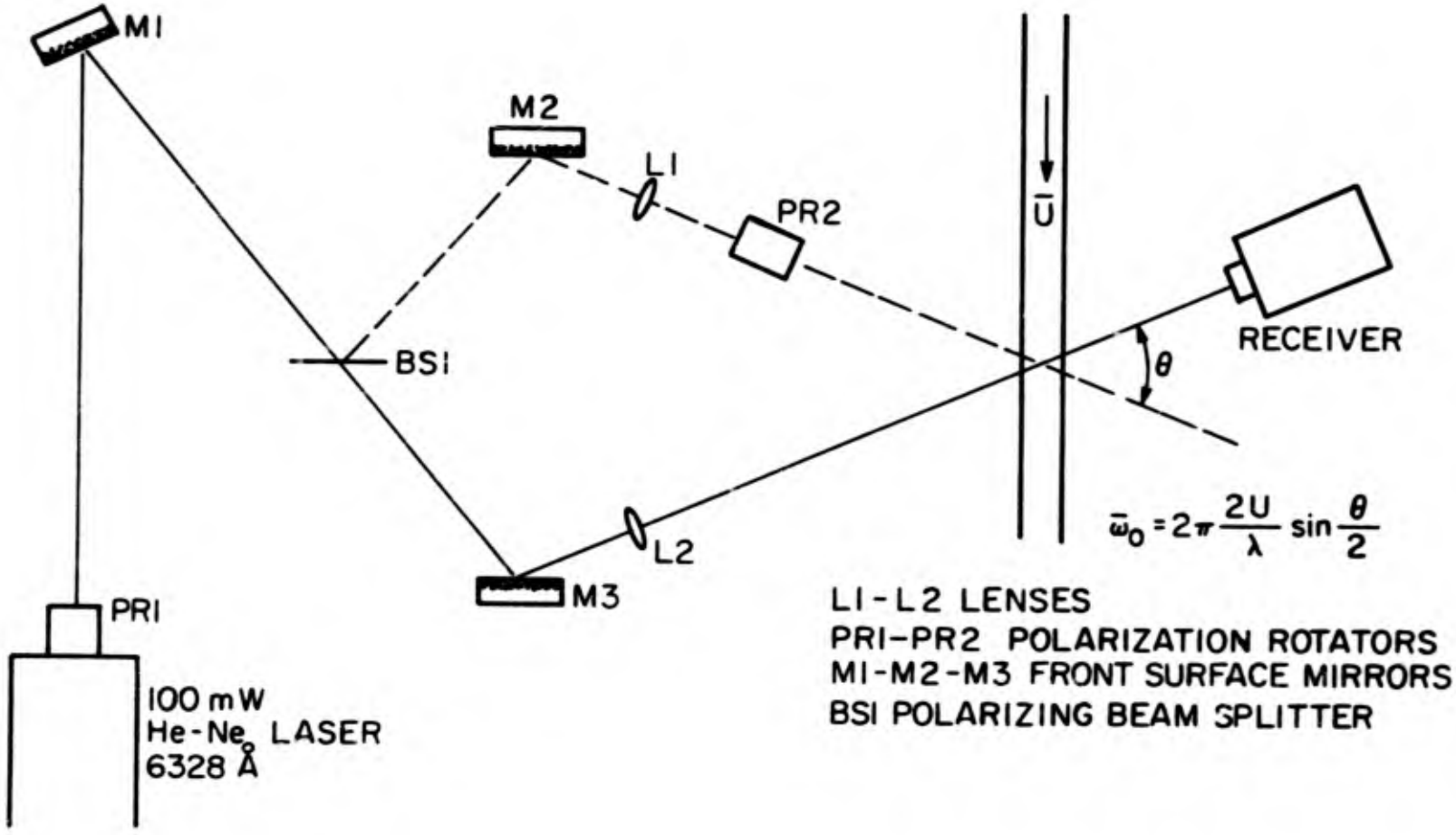

Figure 1. Optical Layout

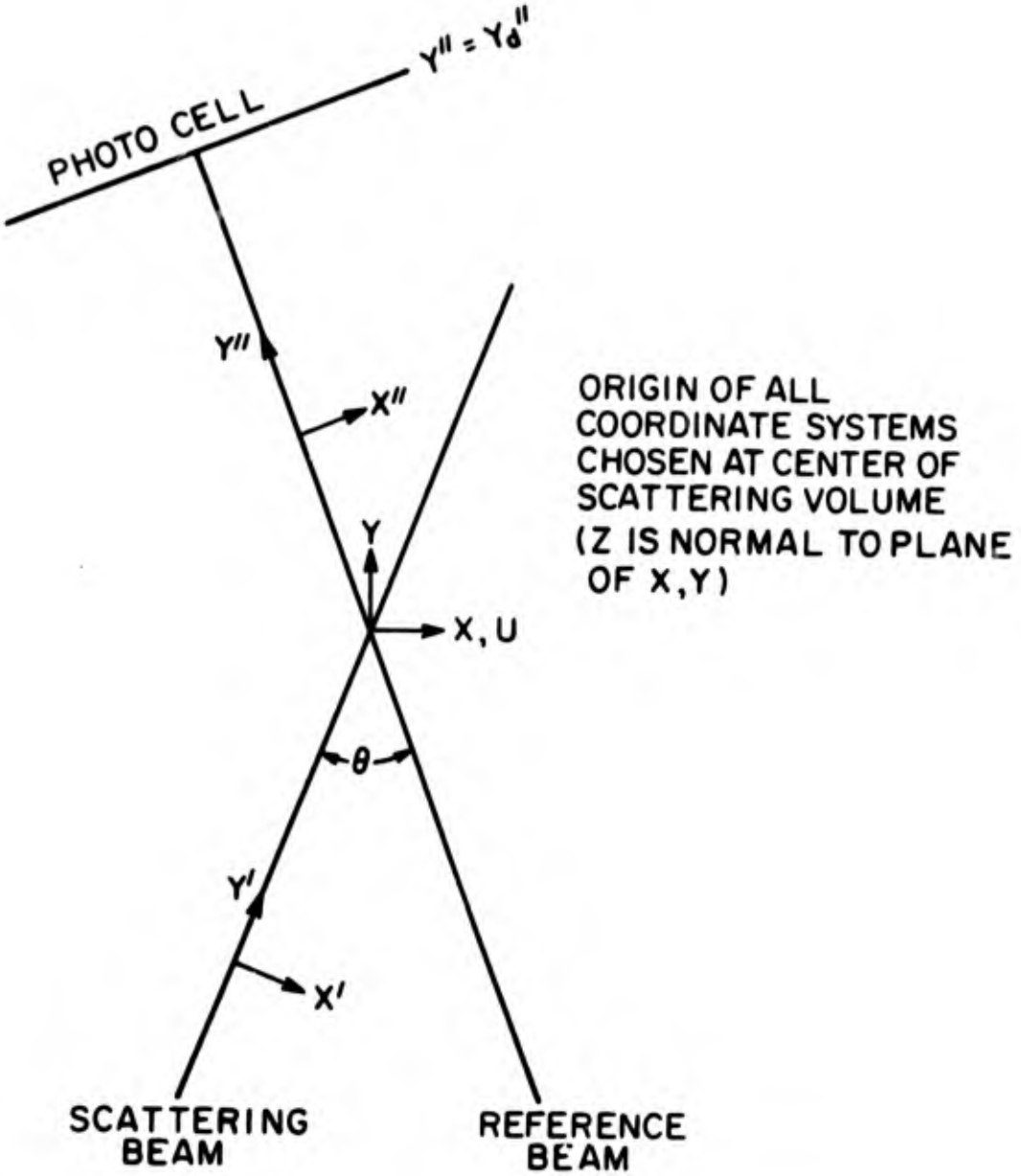

Figure 2. Scattering Volume Coordinates

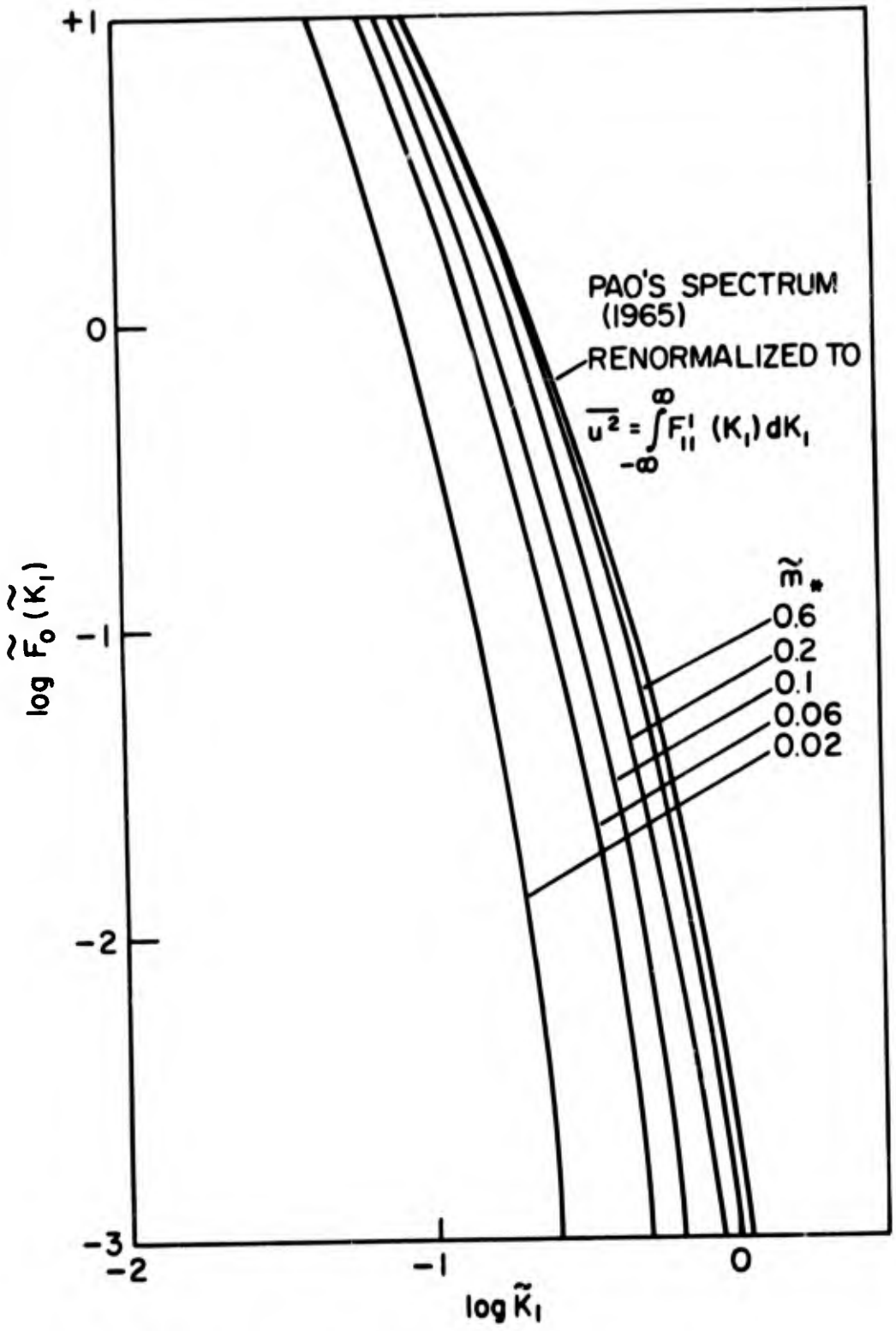

Figure 3. Apparent Turbulent Spectrum

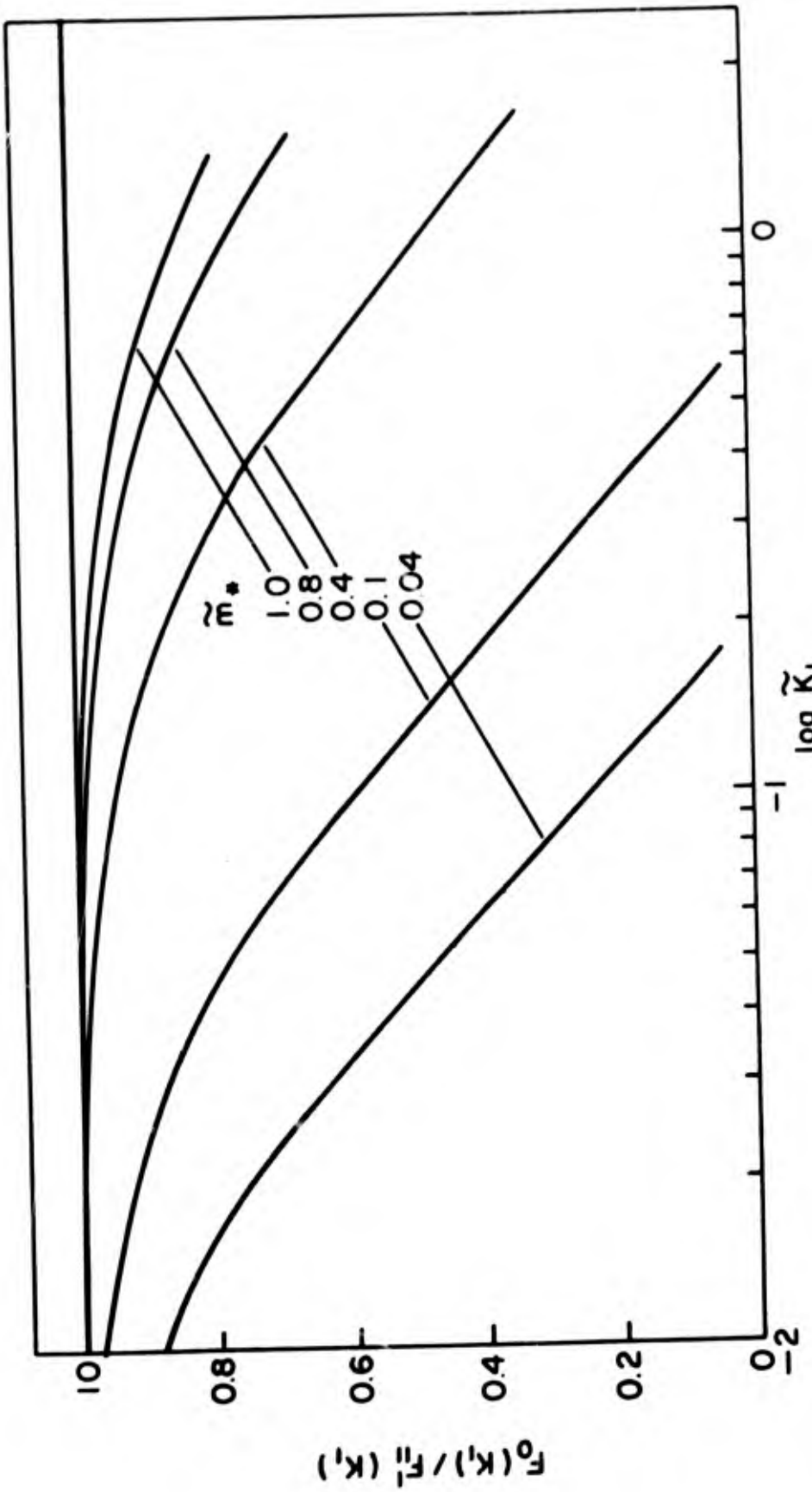

Figure 4. The Velocimeter Transfer Function

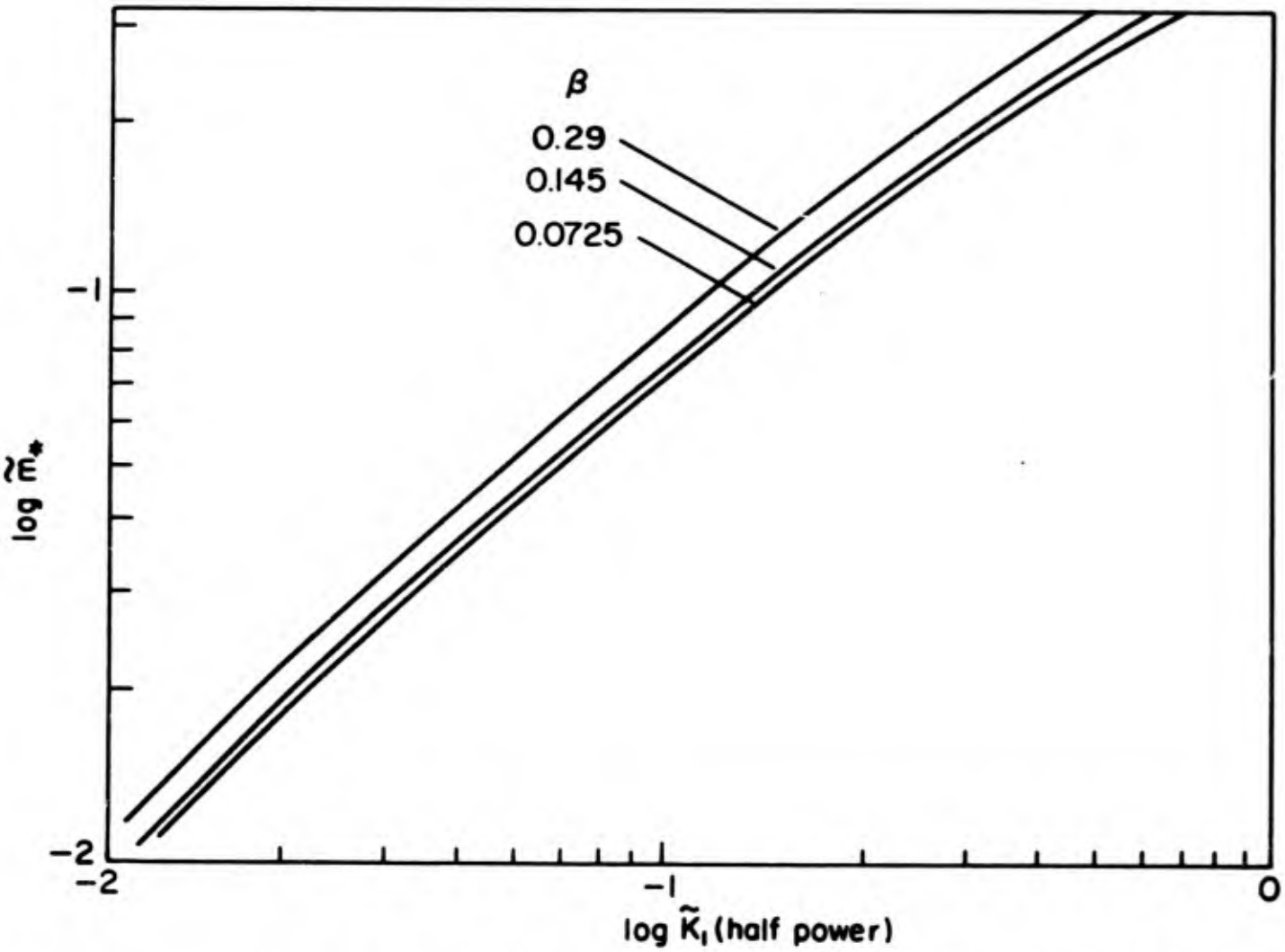

Figure 5. Wavenumber of Half-Power Attenuation as a Function of $m_* = 1/\sqrt{2}\sigma_2$; $\beta = \sin \theta/2$.

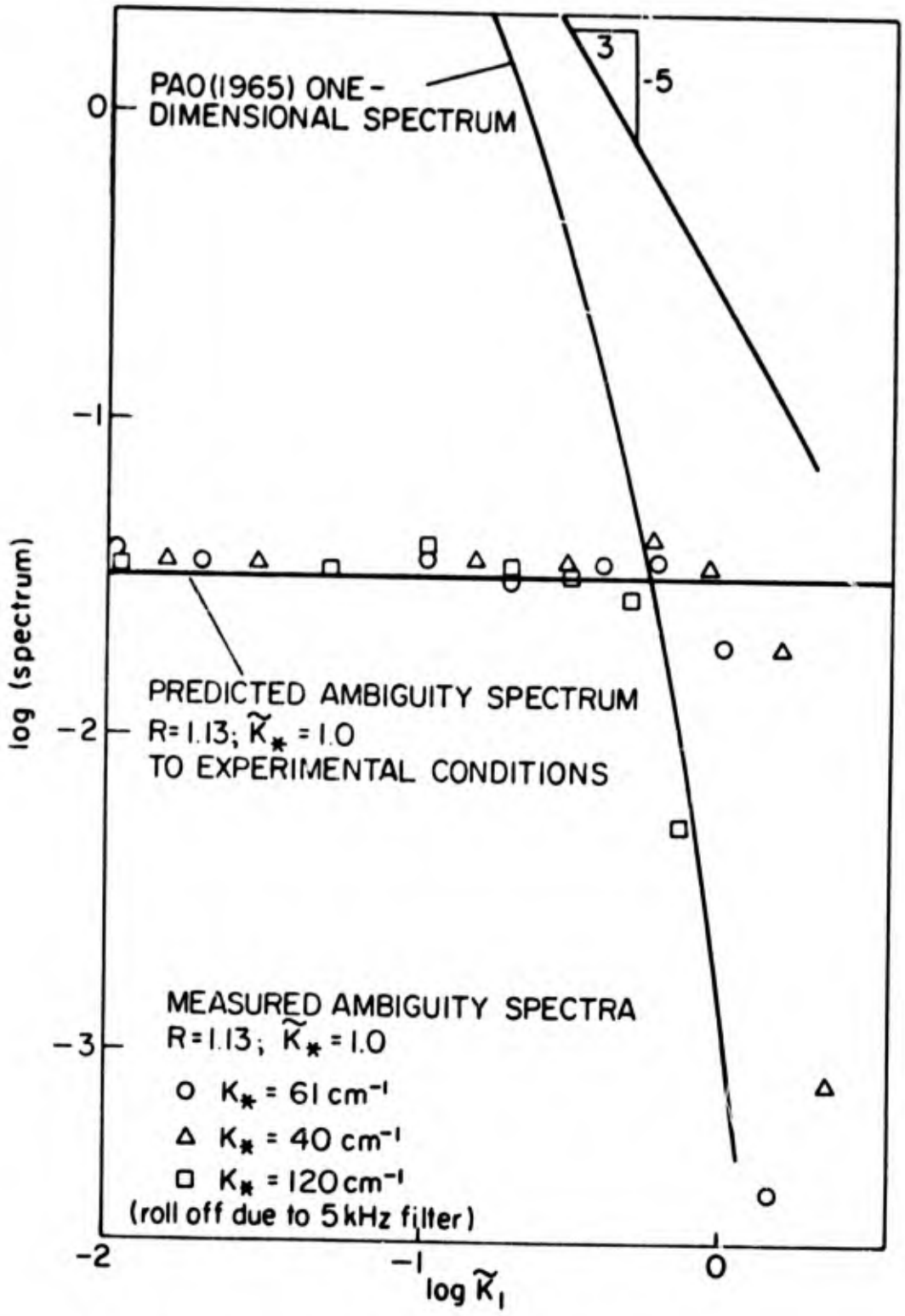

Figure 6. Measured Spectrum in Laminar Flow

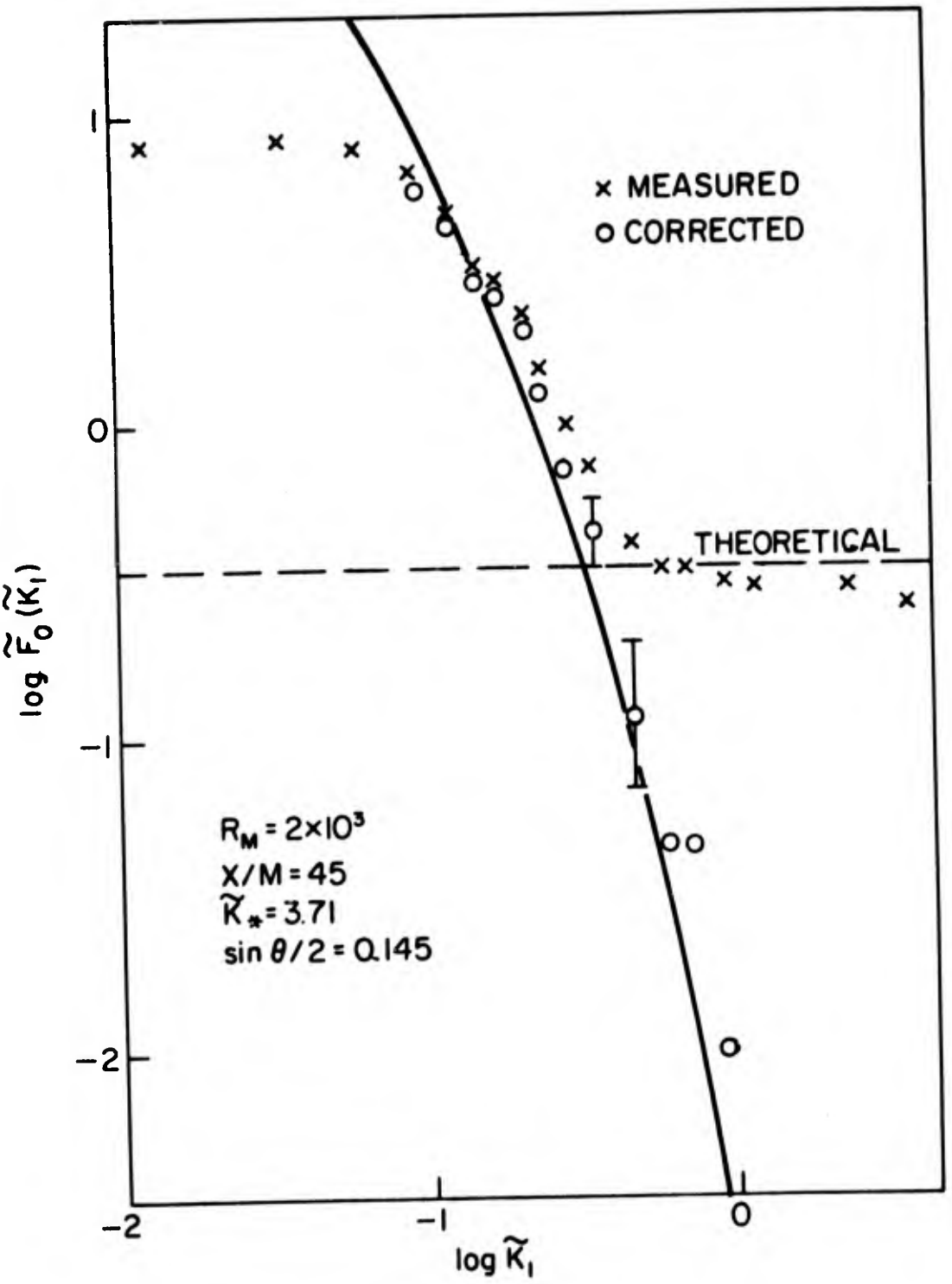

Figure 7. Measured Spectrum in Turbulent Flow

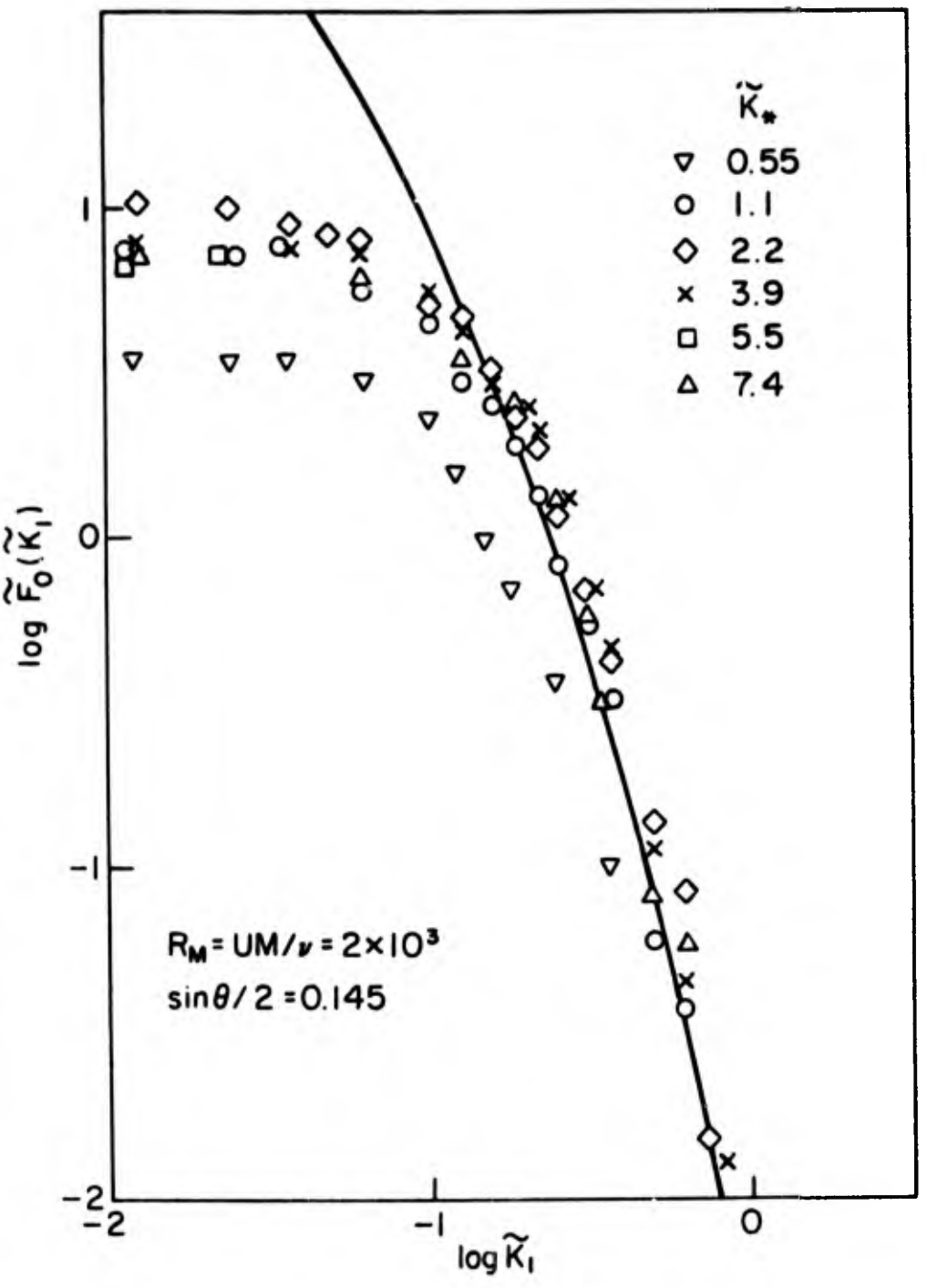

Figure 8. Corrected Turbulence Spectra

DESCRIPTION OF THE DISA SYSTEM

R. L. Humphrey

DISA-SB, Inc.

Franklin Lane, New Jersey

I will give a brief explanation of how we set up the DISA system for the different modes. To set up a crossbeam system, we start out with the optical bench laid out, put our laser on, and mount the optics unit. After that we focus the beam crossing on the microscope objective and thus provide a simple means of aligning the optics at the measuring point that we are interested in. If the optics are out of alignment, we have an adjustment screw to bring them in. You get two circles and bring them to overlapping. If you've done it properly, you see the fringe pattern which tells you that you have things properly adjusted. We then replace the microscope objective with our measuring section. Then we use one of these two pieces with the pin hole aperture in front of the photomultiplier. In this particular case we are using a 0.2 millimeter pin hole. We focus (using the eye piece) on the photomultiplier tube to actually focus the beam crossing that I previously showed you onto the pin hole aperture. We have fine adjustment points in the back of the photomultiplier tube to adjust the beam crossing at the pin hole. Then, open the shutter. (We have a shutter inside to prevent the photomultiplier from getting an overdose of light before it's ready.) When the power supply has been adjusted properly for approximately 500 volts input, the photomultiplier will draw from 40-50 micro amps. We will then be able to set our preamplifier level and begin to process the signal. This is usually what we will have - a frequency-amplitude modulated signal from the photomultiplier tube. We can see this signal from the monitor output of our doppler signal processor. The tracker should be manually turned on as previously discussed by Mr. Smid, and the frequency read off the meter. As part of the system we have included a D. C. voltmeter and true RMS voltmeter with 100 second averaging. This allows us to read the mean and turbulent flow velocity. In addition to these items a signal conditioner offers variable gain and band-pass filtering. We go through a similar technique with the reference beam system.

However, in this particular case we'd use a neutral density filter to bring the reference beam down to near the power level of the scattered beam light. This is an attachment that fits right onto our lens system.

For employment of two scattered beams when we want to do two-dimensional work, we have another attachment where we use a variety of pin holes for the beams to pass through at 90^{o} with respect to one another. We have a facility for a beam splitter to mount to the rear of our optical unit so that we can simultaneously look at the u and the v components.

Finally we can use the back scattering in the system. We've used the system that is set up outside the room with tap water to do back scattering work under very marginal conditions with a five milliwatt laser. However, the adjustments are quite delicate. What we've done for back scattering is provide a path through the optical unit to the detector. Then we get the scattered light back through the optical unit to the photomultiplier tube.

LDV MEASUREMENTS IN ROTATING MACHINERY

W. M. Shafferncker
General Electric Company
Cincinnati, Ohio

Jeff Asher will talk about out data processing system tomorrow. I'm going to present a few slides today to show some of the hardware we have developed in two different areas. We are impatient to use the laser velocimeter. We have two fairly significant problems that will utilize the Laser Velocimeter. One of them is flow field investigation in rotating blade rows, particularly in highspeed fans and compressors. The other area is high temperature nozzle turbulence measurements. Our particular problem right now is to environmentally condition the hardware to find out what our problems are when we take this delicate instrumentation into the real world (150 to 160 db noise levels and various temperatures depending on the local) and try to design out its sensitivity to temperature gradients and noise levels. I think we've had some success along that line. The first program was to look at the velocities within a rotating blade row on a low-speed research compressor (see Figure 1). In order to do this we used a one per revolution pulse from the rotor itself with a time delay generator to pulse the laser. The time delay was introduced so that we could pulse it at various positions in the flow passage. Ours is a back scatter two beam system and we process the signal based on individual particles in the sensitive volume one at a time.

Figure 2 shows the physical layout. The laser itself was incapsulated in a support. The beam came forward, was bent at two right angles and then projected into the blade row. The collection optics collected the light from the individual particles back into the photomultiplier tube mounted in the same physical configuration. We had provided for two-direction mechanical actuation so we could move the beam in and out of the compressor radius. (This compressor is a vertical low speed compressor). We also had provision so that we could mechanically turn the laser system so that we could orient the fringes in two different directions to give us a mechanical adjustment on the velocity component. This shows the compressor approximately 36 inches in diameter. This is the laser beam optical system with its power supply. This is the projection optics and the receiving photomultiplier tube.

Now a closer view (Figure 3) six inch collecting optics, the window in the compressor casing, the photomultiplier tube, and the electronics. This picture shows the blade passages that we were actually projecting the beam into. The data we got from this test were the local velocity direction magnitudes. We did make some measurements ahead and behind the rotating blade row and compared it with hot film to give us some confidence in the correlation of the two types of data. As I said before we could make the velocity measurements at the hub and the tip. We still have some problems with reflection from

surfaces that we need to lick when we go into high speed machinery, but we think we know how to do that.

When we went to the nozzle, we had to repackage the laser system because the noise levels were going to be a lot higher. We used basically the same type of construction though - the laser mounted below and then the collection optics above (see Figure 4). We did some vibration isolation and soundproofing in the initial construction. Again we provided ourselves with two-direction actuation so we could look in the nozzle exit. Figure 5 shows some more soundproofing. We put a lot of attention on soundproofing and I think it really did pay off for us in the final test demonstration. Temperature gradients were also a bit of a problem. Figure 5 shows the laser on site, mounted in the dog house. You see the beam projected out into the stream - a gas stream about 2 feet away from the front surface of the dog house. Plastic was put on because it rained during the week of testing on site. We had to provide some humidity protection for the system. Figure 6 shows an overall view of the outdoor facility. This is the nozzle and the combustion section ahead of it, sound silencer downstream, and then the dog house that housed the laser system.

Figure 7 is a view from a different direction. The laser again was projected out into the stream. Now we did our surveying along the axis of the nozzle by changing transition pieces. We actually moved the nozzle back and forth and kept the laser system in position except for a very slight axial adjustment that the actuator would allow both axially and radially in the jet stream itself.

Figure 8 shows the seeder that was used. As Jeff pointed out we used alumina powder in a fluidized bed and this worked out very well. We were able to get good, uniform density of the alumina particles. They were injected ahead of the burner, passed through the burner and then on out through the exhaust. The number of counts we got depended on the velocity and flow conditions but ranged from a thousand per second to ten thousand and we think we know how we can increase that number with some changes in the seeding density and the location of seeding.

Figure 9 shows the electronics. Currently our equipment is packaged in small consoles. We hope to eventually get it into one five foot rack. This slide I think is injected into here to show that we had to make the electronics immune also to some of the environmental changes. We put a lot of attention in circuitry that didn't require extreme temperature, humidity or line voltage stabilization. When you are working in a real world, it's very important that you address yourself to that problem.

Figure 10 is a night shot showing the nozzle in operation, the shock pattern itself, and then the laser beam being projected from the dog house.

FIGURES 1 THRU 10 (PAGES 187-196) NOT AVAILABLE

DISCUSSION

BRAYTON: What was the power of the laser?

SHAFFERNOCKER: There were two lasers involved. The work that was done in the rotating flow field was the Hughes 30-30-H pulsed Argon laser. The work done in the nozzle was the Spectra-Physics Argon. I think it's about one watt.

BOUTIER: What kind of particles did you use in the compressor?

SHAFFERNOCKER: That was polystyrene particles in a water emulsion. The waterparticle mixture was sprayed into the air and the water was allowed to evaporate away from the small particles.

BOUTIER: How did you eliminate reflections from the walls of the compressor?

SHAFFERNOCKER: We stayed away from them.

BOUTIER: Did you polish them?

SHAFFERNOCKER: No, they were painted black. We always looked in one blade passage so we only had to paint one side of two blades in the passage.

BOUTIER: We had the same problem. We solved it by polishing them.

SHAFFERNOCKER: In other words by polishing you attempt to keep the beam from diffusing and just reflect it out of the area. I guess you could do it either way. We were attempting to absorb the beam.

DUNNING: Have you considered sampling at a rapid enough rate so that you can get a time history from your counter technique other than just mean velocity?

SHAFFERNOCKER: We do real time.

DUNNING: You get a time history?

SHAFFERNOCKER: Yes.

DUNNING: So you could correlate that, for example with noise from your jet.

SHAFFERNOCKER: Yes. We rely on a single particle in the sensitive volume at a time and then prepare a real time history from the individual velocity determinations. From there you can go to a spectrum analysis, histogram, or rms.

DUNNING: And you can do it rapidly enough?

SHAFFERNOCKER: Yes. That's a function of how many particles you put through. On the compressor I think we got something around 20 or 30 particles per second because of the seeding technique. In the nozzle it was anywhere from 1,000 to 10,000.

PFEIFER: Have you measured the diameter of the particles and do you know if they are spherical particles?

SHAFFERNOCKER: My co-workers tell me they are one micron. The polystyrene particles were spherical. We tried two sizes on polystyrene - one micron and two microns just to see what the effect of the increased light intensity would be on the signal to noise ratio. There we were dealing with very low flow velocities - 100 feet per second. For the alumina used with the nozzle the average diameter (and it's not spherical) is on the order of 0.75 micron.

HUMPHREY: What difference did you see in the signal to noise ratio with your polystyrene particles?

SHAFFERNOCKER: The more light you get back, the better your signal to noise.

HUMPHREY: No I meant did you see appreciable improvement?

SHAFFERNOCKER: I don't think it was that significant. As it turned out with the Argon laser we were using the amount of modulation we had available to us it wasn't a significant contributing factor. We had enough to begin with, I guess that's the way to answer. It could be significant in some cases though at high flow velocities.

DUNNING: I am just going to comment on this question by Ron Humphrey. With one micron or three-quarter micron particles in Argon laser light you are already up under the little wiggles on the Mie scattering distribution and so one, two, or ten microns isn't going to make any difference. Below that it's going to start dropping off, but larger particles aren't going to affect it.

SHAFFERNOCKER: Yes, I didn't think it was. We just had the opportunity with the two sizes so we ran that part of the experiment.

TECHNICAL SESSION IV - TURBULENCE MEASUREMENTS

Session Chairman: J. Meyers

198 B

DOPPLER AMBIGUITY AND THE MEASUREMENT OF TURBULENCE

W. K. George and J. L. Lumley

The work I am going to talk about has existed in various forms for the last three years, the first presentation being by John Lumley at Rolla in '68[1]. It has been modified a number of times since then[2]. This represents the latest version and, I hope, the final one. It has been submitted for publication[3] and should be available in a number of months.

As a refresher for those who weren't here yesterday afternoon, the optical system that I am going to analyze in particular is a modified Goldstein system (see figure 1). Ours is a little different than most in that we have a polarization rotator at the laser, a polarizing beam splitter, and then another polarization rotator which may be adjusted so that both beams are vertically polarized. The idea is that by using the polarization rotator in combination with the polarized beam splitter, you never have to attenuate the light and can get maximum heterodying efficiency.

There are no optics in the receiving end. It is just an open photomultiplier tube. We haven't had a problem with stray light. In the terminology used yesterday, this is input aligned optics.

The scattering volume for Gaussian laser beams can be shown to be approximately Gaussian--that is, the surfaces of constant intensity of the scattered current are Gaussian. The current from a single particle can be represented by

$$i_{sp} = Ie^{-\left[\frac{x^2}{2\sigma_1^2} + \frac{y^2}{2\sigma_2^2} + \frac{z^2}{2\sigma_3^2}\right]}\cos \underline{K}\, x \qquad (1)$$

$\underline{x} = (x, y, z)$ represent the particle's position which is a function of time and σ_1, σ_2, σ_3 are measures of the scattering volume dimensions and are determined by the optical components used. $\underline{K}$ is the scattering wave number and is given by

$$\underline{K} = \frac{4\pi}{\lambda} \sin \theta/2 \qquad (2)$$

where θ is the scattering angle and λ is the wavelength of the light.

I will assume the particles track the flow, so $\underset{\sim}{x}$ is the Lagrangian position and is given by

$$\underset{\sim}{x}(\underset{\sim}{a},t) = \underset{\sim}{a} + \int_0^t \underset{\sim}{U}(a,t_1)\, dt_1 \qquad (3)$$

where $\underset{\sim}{a}$ is the initial particle position and $\underset{\sim}{U}(\underset{\sim}{a},t)$ is the Lagrangian velocity field. Substituting this expression into the cosine term above you can see that you obtain a constant phase depending upon the initial position of the particle, and a time-dependent phase depending upon the displacement of the particle--that is, the history of the velocity field. If one counts the zero-crossings due to this time-dependent phase, (i.e. differentiaties), a number proportion to the particle velocity is obtained.

Now this is where the fun comes in. Since there may be many particles in the scattering volume, what velocity is the velocimeter looking at? I say it is looking at an effective velocity, which is just an average over all particles in the volume at any instant. We call this velocity $u_o(t)$ and define it by

$$u_o(t) = \frac{1}{N(t)} \sum_{i=1}^{N(t)} \underset{\sim}{U}(\underset{\sim}{a}_i,t) \qquad (4)$$

It is more convenient to use the following integral definition for the effective velocity

$$u_o(t) = \frac{1}{\overline{N}} \int_{\text{initial volume}} \underset{\sim}{U}(\underset{\sim}{a},t)\, g(\underset{\sim}{a})\, d\underset{\sim}{a} \qquad (5)$$

where $g(\underset{\sim}{a})$ is a random function which contributes wherever there is a scatterer and $\overline{N}$ is the expected number of scatterers. If we further define the scattering volume in terms of the spatial dependence of the current, we may write

$$u_o(t) = \frac{1}{u} \int_{\text{all space}} U(\underset{\sim}{a},t)\, g(\underset{\sim}{a})\, W\,[\underset{\sim}{x}(\underset{\sim}{a},t)]\, d\underset{\sim}{a} \qquad (6)$$

where

$$W(\underset{\sim}{x}) = \frac{1}{(2\pi)^{3/2}\sigma_1\sigma_2\sigma_3}\, e^{-\left[\frac{x^2}{2\sigma_1^2} + \frac{y^2}{2\sigma_2^2} + \frac{z^2}{2\sigma_2^2}\right]} \qquad (7)$$

Using this effective velocity we can define an effective displacement which is the displacement experienced by a typical scattering particle.

$$\underline{\bar{X}}(t) = \int_0^t u_o(t_1)dt_1 \qquad (8)$$

Now we can decompose the motion of each particle into its initial position, the displacement of the field as a whole (this is time-dependent and is averaged over only the scattering volume) plus the deviation of the single particle from the field as a whole which we will call $\underset{\sim}{\Delta}(\underset{\sim}{a},t)$, that is,

$$x(\underset{\sim}{a},t) = a + \underline{\bar{X}} + \Delta(\underset{\sim}{a},t) \qquad (9)$$

where

$$\Delta(\underset{\sim}{a},t) = \int_0^t \left[\bar{U}(\underset{\sim}{a},t_1) - u_o(t_1)\right] dt_1 \qquad (10)$$

You can think of the scattering particles as moving through the volume somewhat randomly due to the turbulence. Each particle may be wandering slightly-- Δ is the wandering effect, if you will. To find Δ, we just subtracted the velocity of the field as a whole from the velocity of the particle.

Yesterday, I showed how, under certain restrictions $u_o(t)$ could be related to the Eulerian velocity field which is what we are usually after in this kind of measurement. I developed criteria for spacial resolution and showed how the spectrum was attenuated when the scattering volume was too large. Today, I am interested primarily in the deviations of the individual particles from the volume average, that is $\Delta(\underset{\sim}{a},t)$.

The Doppler signal current is given by the sum of the currents from the individual particles, that is

$$i(t) = \int_{\text{all space}} i(a,t)\, g(a)\, da \qquad (11)$$

It is difficult, but straightforward, to show that the Doppler current can be written as

$$i(t) = F(t) \cos \underline{K}\, x + G(t) \sin \underline{K}\, x \qquad (12)$$

This representation is similar to that used by Rice for the shot effect. All of the random phase information has been incorporated into the F and G including the Δ's. We may also write

$$i(t) = \left[F^2 + G^2\right]^{1/2} \cos\left[\underline{K}\, \underline{X} - \phi\right] \qquad (13)$$

where

$$\phi = \tan^{-1}\left(\frac{G}{F}\right) \qquad (14)$$

Recall that the velocity we would like to measure is contained in $\underline{X}(t)$. We may recover the velocity by clipping to remove the amplitude information and keeping only the zero-crossing information. The result is proportional to frequency, say ω_1, and is given by

$$\omega_1 = \underline{K}\, \frac{d\underline{X}}{dt} - \frac{d\phi}{dt} = \underline{K}\, u_o(t) - \dot{\phi}(t) \qquad (15)$$

Unfortunately, in addition to $u_o(t)$, we've also obtained the extraneous random phase information. The random phase ϕ includes the effects of the changing particle distribution, random velocities across the scattering volume, mean velocity gradients, and refractive index changes. We shall consider only the first two effects.

If the slewing rate of $\dot{\phi}(t)$ were significantly different from $u_o(t)$ we could build a detector to discriminate between the two and keep only the turbulence. Unfortunately, as we see later, the phase fluctuations are very broadband and, in fact, are almost white over the entire range of the turbulence. Thus we are always stuck with the random phase fluctuations.

We will compute the spectrum of the Doppler current. Let's assume that the turbulence (the effective displacement) and the particle derivations are independent. This can be justified as follows: first, they are uncorrelated by definition, second, we may take them to be statistically independent because fine scale turbulence is nearly independent of the large structure turbulence. We will assume that both the turbulent displacements $\underline{X}$ and the particle deviations have a Gaussian probability density. With these assumptions, we can compute the spectrum of the Doppler current. The result is shown in figure (2) and consists of two peaks centered at plus and minus $\omega_o = \underline{K}\, u_o$.

ω_o corresponds to the time average Doppler frequency corresponding to the mean velocity. The width of this peak depends on two things. It depends first on what I call $\Delta\omega_{u_o}$ which is proportional to the turbulence intensity. (It is not the turbulence intensity when the probability density is significantly non-Gaussian). Secondly, the spectral width depends on $\Delta\omega$ which is the Doppler ambiguity. The ambiguity broadenings that I will consider (and there are a number of them) are the transit time broadening and the broadening arising from the presence of velocity fluctuations across the scattering volume.

The transit time broadening is given by

$$\Delta\omega_L = \sigma_1/\sqrt{2}\ \ \overline{u}_o \tag{16}$$

where $\overline{u}_o$ is the mean velocity and σ_1 is the standard deviation of the sample volume in the direction of the flow.

The broadening due to the finite resolution of the sampling volume (or turbulent broadening) $\Delta\omega_T$ is given by

$$\Delta\omega_T = \sqrt{\frac{2}{15}}\ (\varepsilon/\nu)^{\frac{1}{2}}\ \ \underline{K}\,\sigma_2 \tag{17}$$

where ε is the rate of dissipation of turbulent energy and ν is the kinematic viscosity. $(\varepsilon/\nu)^{\frac{1}{2}}$ corresponds to the smallest dynamic scale of the turbulence and the linear dependence of $\Delta\omega_T$ on σ_2 is true only asympotically; the general dependence of $\Delta\omega_T$ on scattering volume size is shown in figure (3). It should be emphasized that $\Delta\omega_T$ arises from velocity fluctuation within the scattering volume.

The total ambiguous broadening $\Delta\omega$ is given by

$$(\Delta\omega)^2 = (\Delta\omega_T)^2 + (\Delta\omega_L)^2 \qquad (18)$$

(Note that the $\Delta\omega_T$ broadening appears to add to $\Delta\omega_{u_o}$ to make the total broadening minus the transit time broadening proportional to the turbulent energy*. This unfortunately is not true for the instantaneous signal.)

This is where I think that John Lumley and I have made our major contribution as I know no other analysis that treats the instantaneous velocities. The detector output as I said, is given by

$$\omega_1 = \underline{K}u_o(t) - \dot{\phi}(t) \qquad (19)$$

It is not difficult to show that u_o and $\dot{\phi}$ are statistically independent, hence their spectra are additive, i.e.

$$\text{Output Spectrum} = \underline{K}^2 F_{11}'(\omega) + N(\omega) \qquad (20)$$

where $F_{11}'(\omega)$ is the velocity spectrum and $N(\omega)$ is the spectrum of the phase fluctuations. The big question is then, what is N? Alternately, we may look at the correlation and ask, what is $\overline{\dot{\phi}(t)\,\dot{\phi}(t+\tau)}$?

On dimensional grounds we must have

$$N(\omega) \sim \Delta\omega \qquad (21)$$

since $\Delta\omega$ is the only parameter in the system. In other words, the ambiguity spectral height is proportional to the Doppler bandwidth $\Delta\omega$. In reference (2) it is shown that

$$\overline{\dot{\phi}^2} = \infty \qquad (22)$$

which implies that the correlation is singular at the origin. The infinite value of $\overline{\dot{\phi}^2}$ is a consequence of the non-stationarity of ϕ.

Computation shows that the height of $N(\omega)$ at $\omega=0$ is given by

$$N(0) = 0.77\,\Delta\omega \qquad (23)$$

The spectrum may be shown to be flat to a frequency of $\omega\sim\Delta\omega$ and to fall off as inverse frequency thereafter.

---

*This point was missed in the oral presentation and resulted in the controversy with R. Edwards.

If one considers the effect of an additive electronic noise to the Doppler signal current, the expression above may be modified to include the effect of the noise. The result:

$$N(o) = 0.77\ \Delta\omega \left\{ 1 + \frac{\Delta\omega_f}{\Delta\omega S^2} \right\} \qquad (24)$$

where $\Delta\omega_f$ is the noise bandwidth and S is the signal to noise ratio.

Figure (4) illustrates the shape of the ambiguity correlation $\overline{\phi(t)\phi(t+\tau)}$. Figure (5) shows the corresponding ambiguity along with Pao's spectrum for the turbulence in a plot which utilizes Kolmogorov scaling. Figures (6), (7), (8), and (9) represent respectively spectral measurements in laminar flow, spectral measurements in turbulent flow including ambiguity, corrected spectral measurements in turbulent flow, and finally the ambiguity spectral height in turbulent flow showing agreement with theory to within 10%. Figure (10) illustrates the effect of the ambiguity on correlation measurements; the small time behavior illustrates the effect of the low pass filtering on the ambiguity. The signal processing equipment used for these measurements is described in reference (2).

REFERENCES

(1) Lumley, J. L., George, W. K., and Kobashi, Y., "The Influence of Doppler Ambiguity and Noise on the Measurement of Turbulent Spectra Using a Laser Doppler Velocimeter", Proc. of the Symp. on the Measurement of Turbulence in Liquids, Univ. of Missouri at Rolla (September 1969).

(2) George, W. K., "An Analysis of the Laser Doppler Velocimeter and Its Application to the Measurement of Turbulence", Ph.D. Thesis, Dept. of Mechanics, the Johns Hopkins Univ., 1971.

(3) George, W. K. and Lumley, J. L., "The Laser Doppler Velocimeter and its Application to the Measurement of Turbulence", submitted to Journal of Fluid Mechanics.

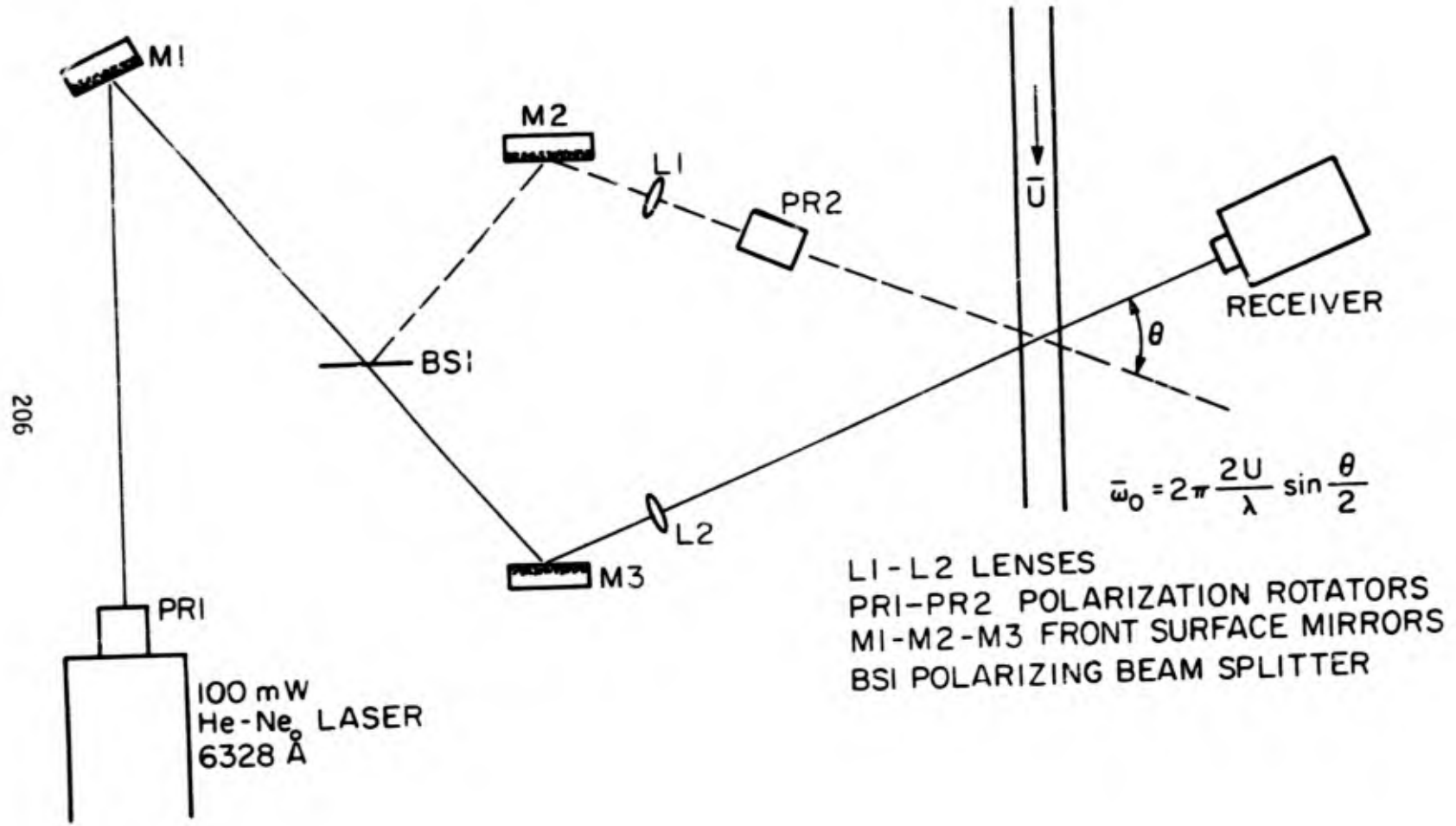

Figure 1. Optical Layout

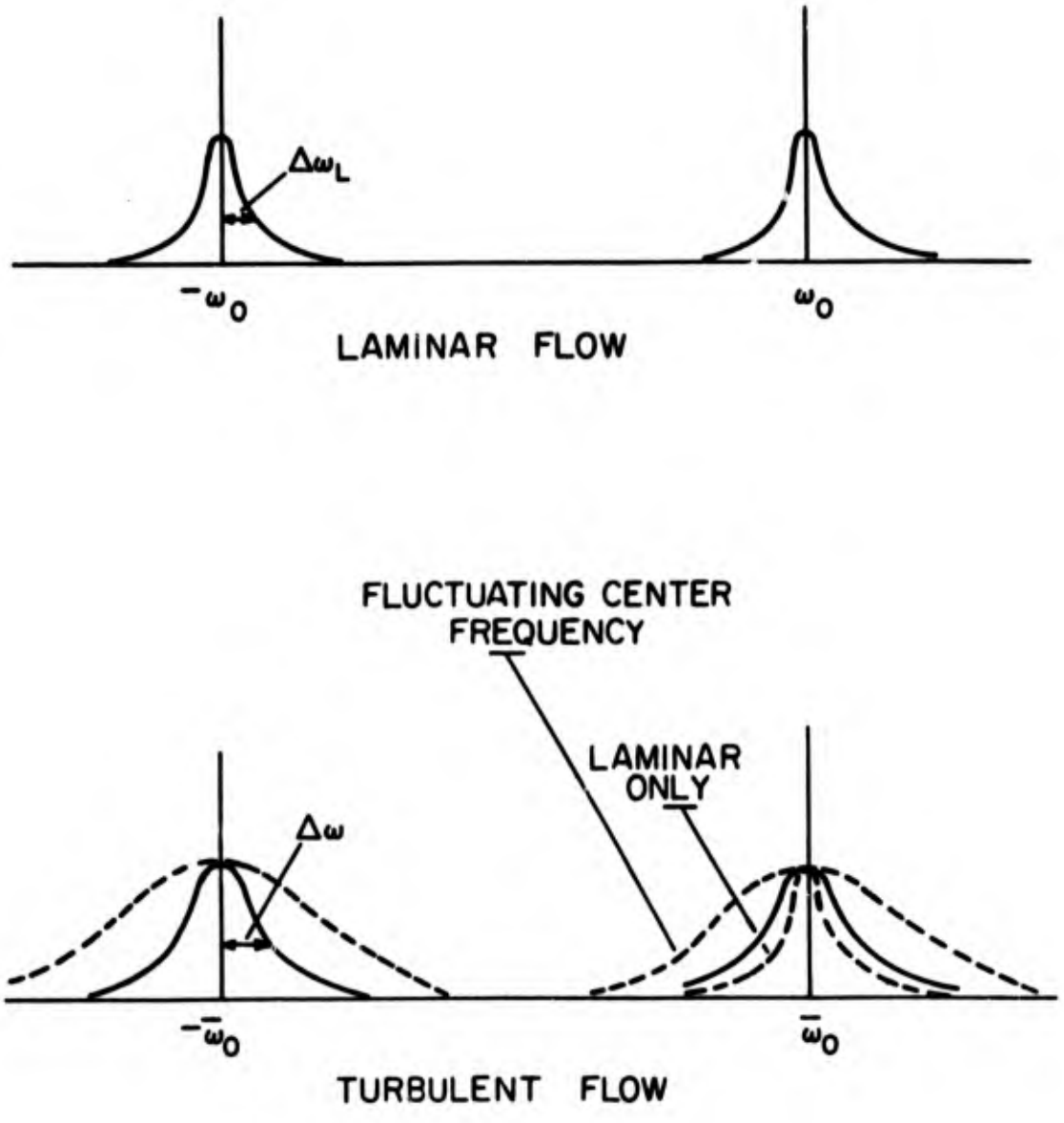

Figure 2. Spectrum of the Doppler Signal

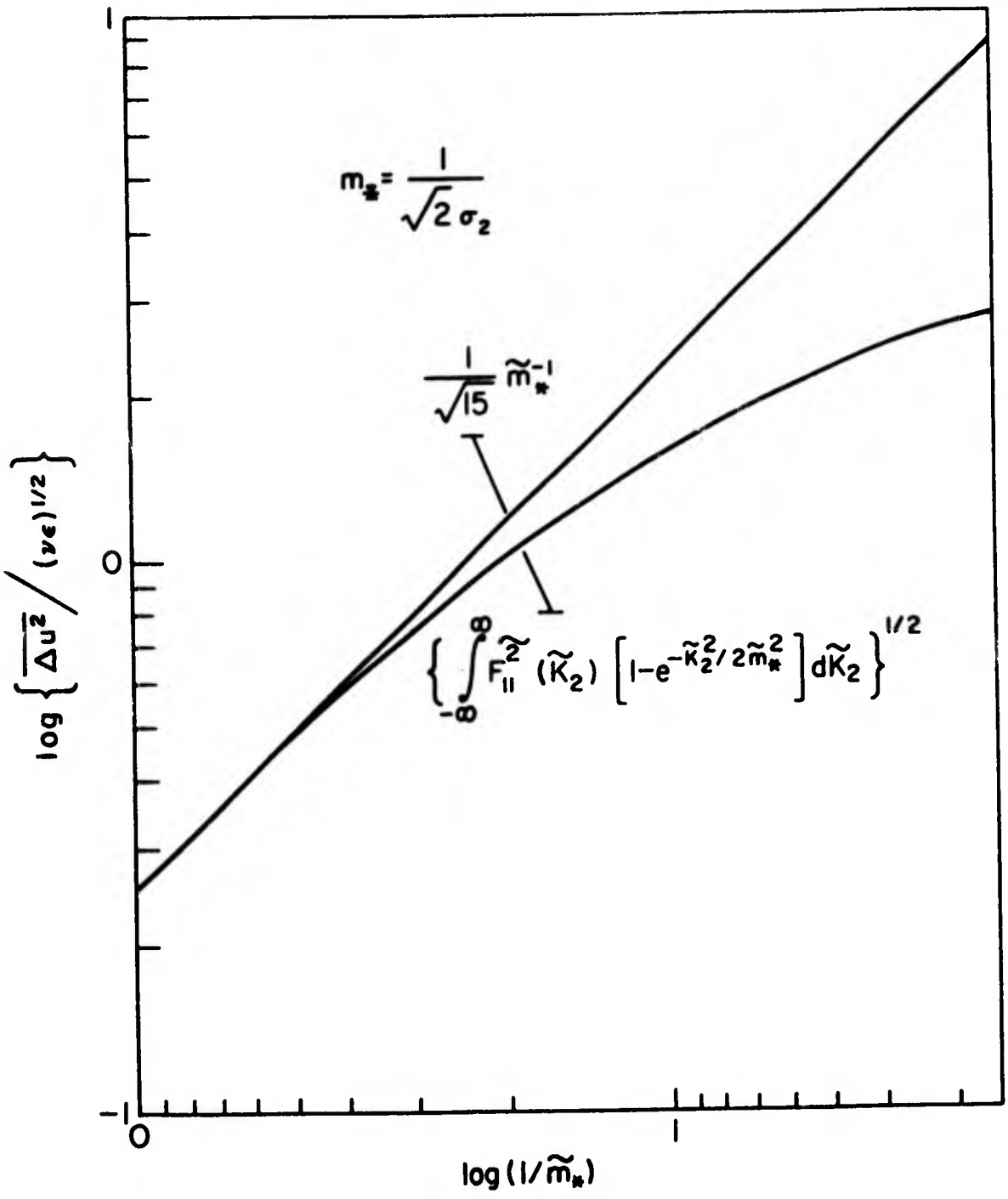

Figure 3. Nondimensional Turbulent Broadening $\Delta\omega_T^2 = K^2\,\overline{(\Delta u)^2}$

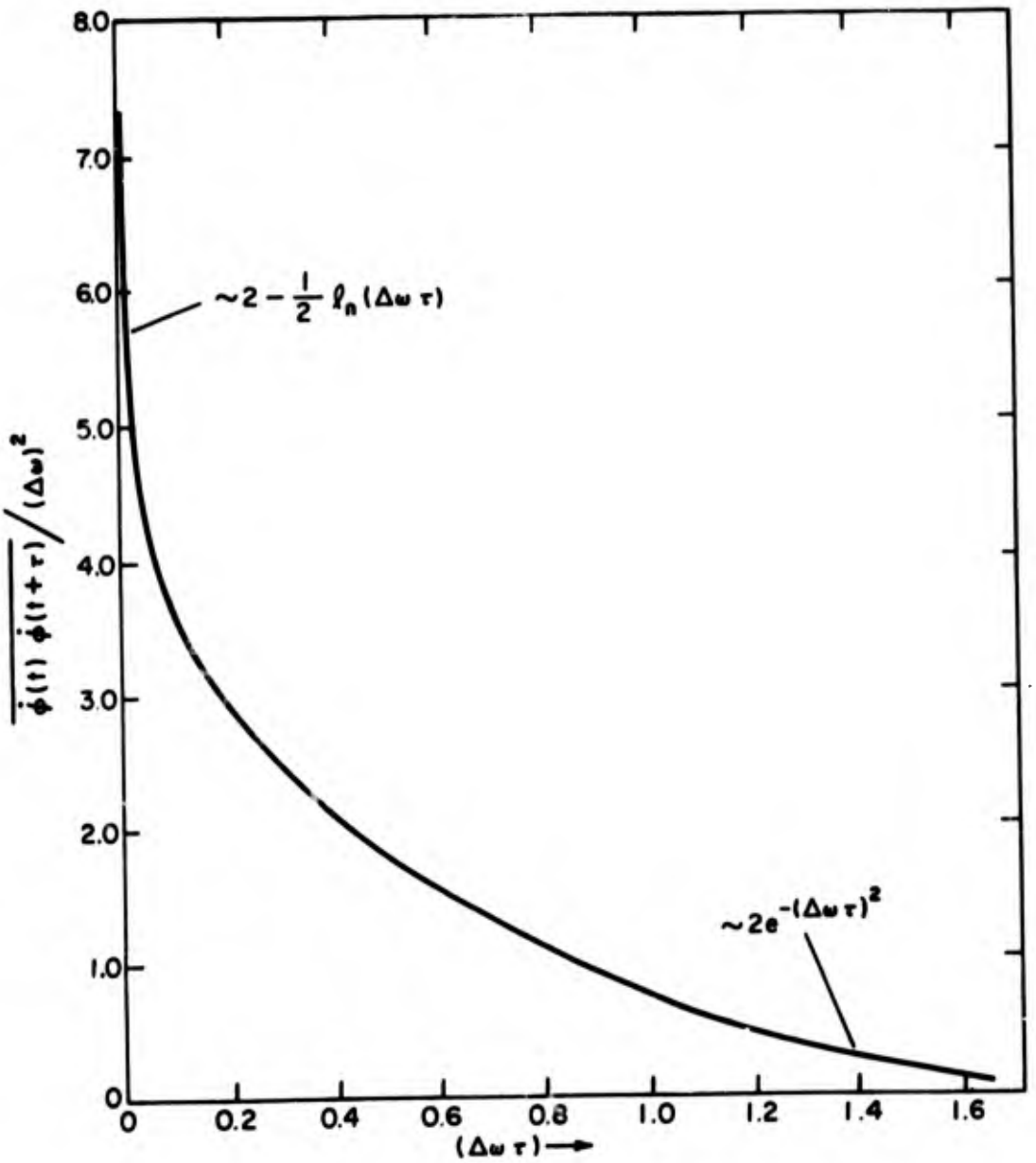

Figure 4. Correlation of Phase Fluctuations

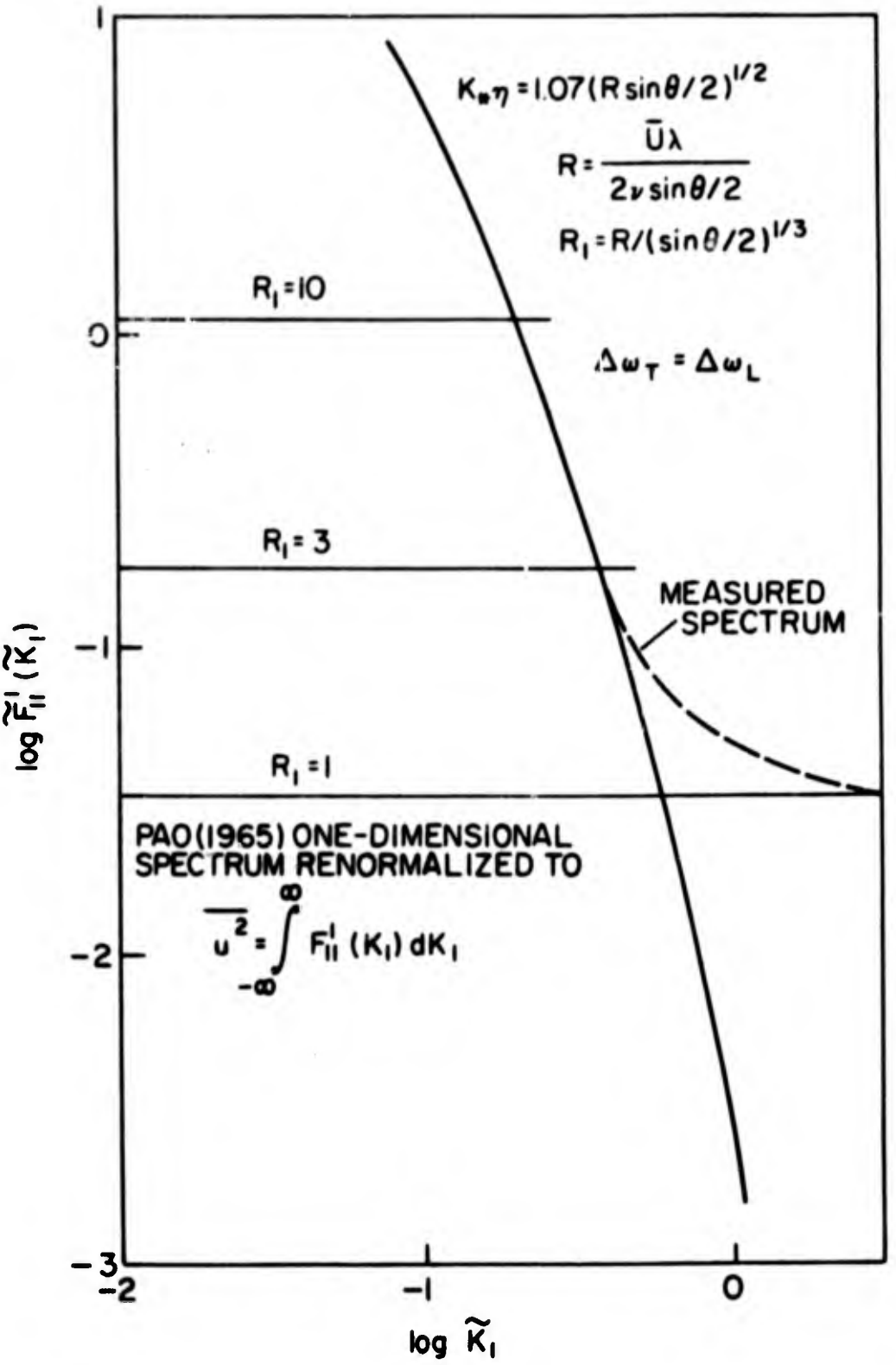

Figure 5. Optimum Ambiguity Spectra

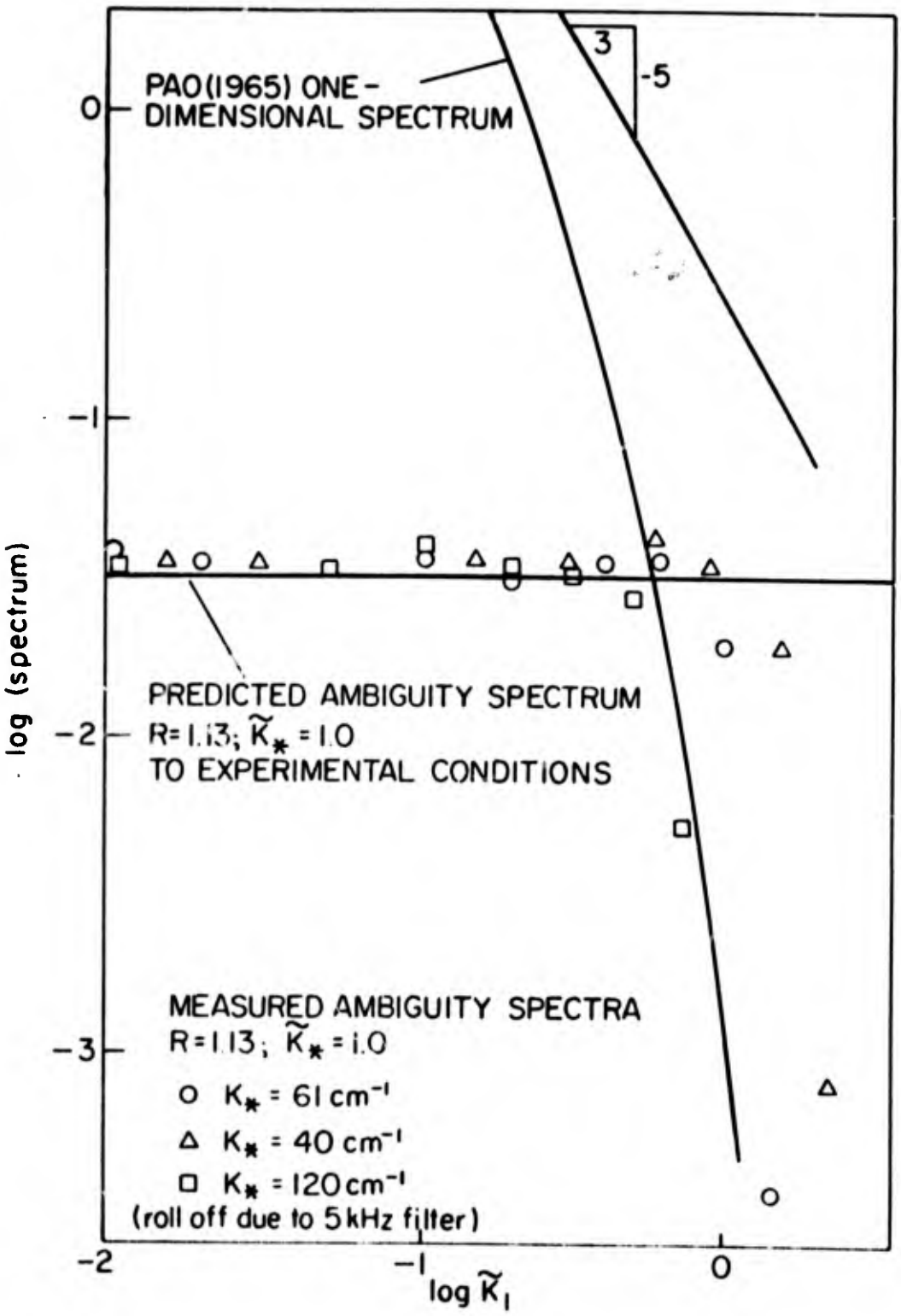

Figure 6. Comparison of Predicted and Measured Spectra in Laminar Flow

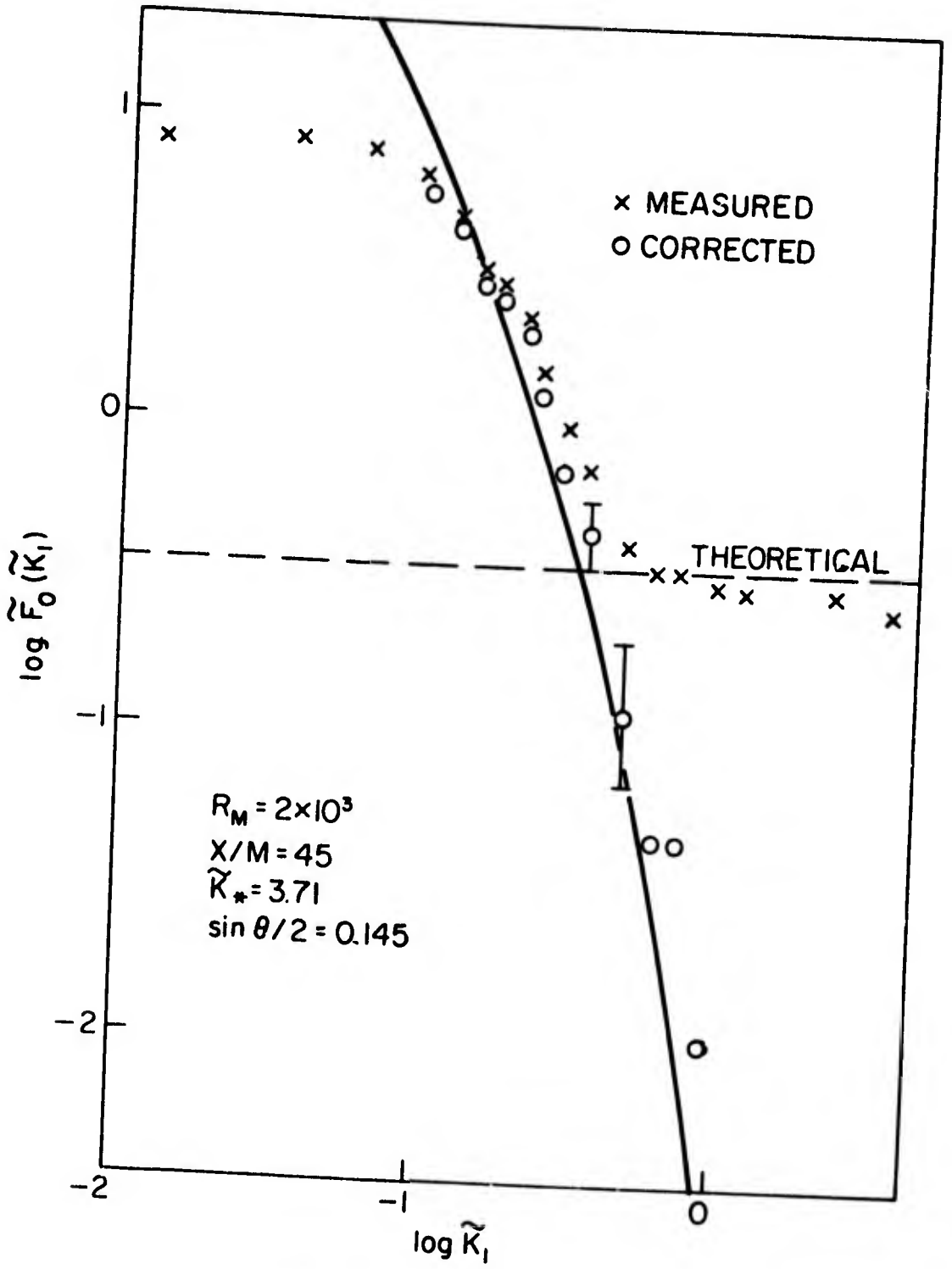

Figure 7. Measured Spectrum in Turbulent Flow Showing Correction for Ambiguity

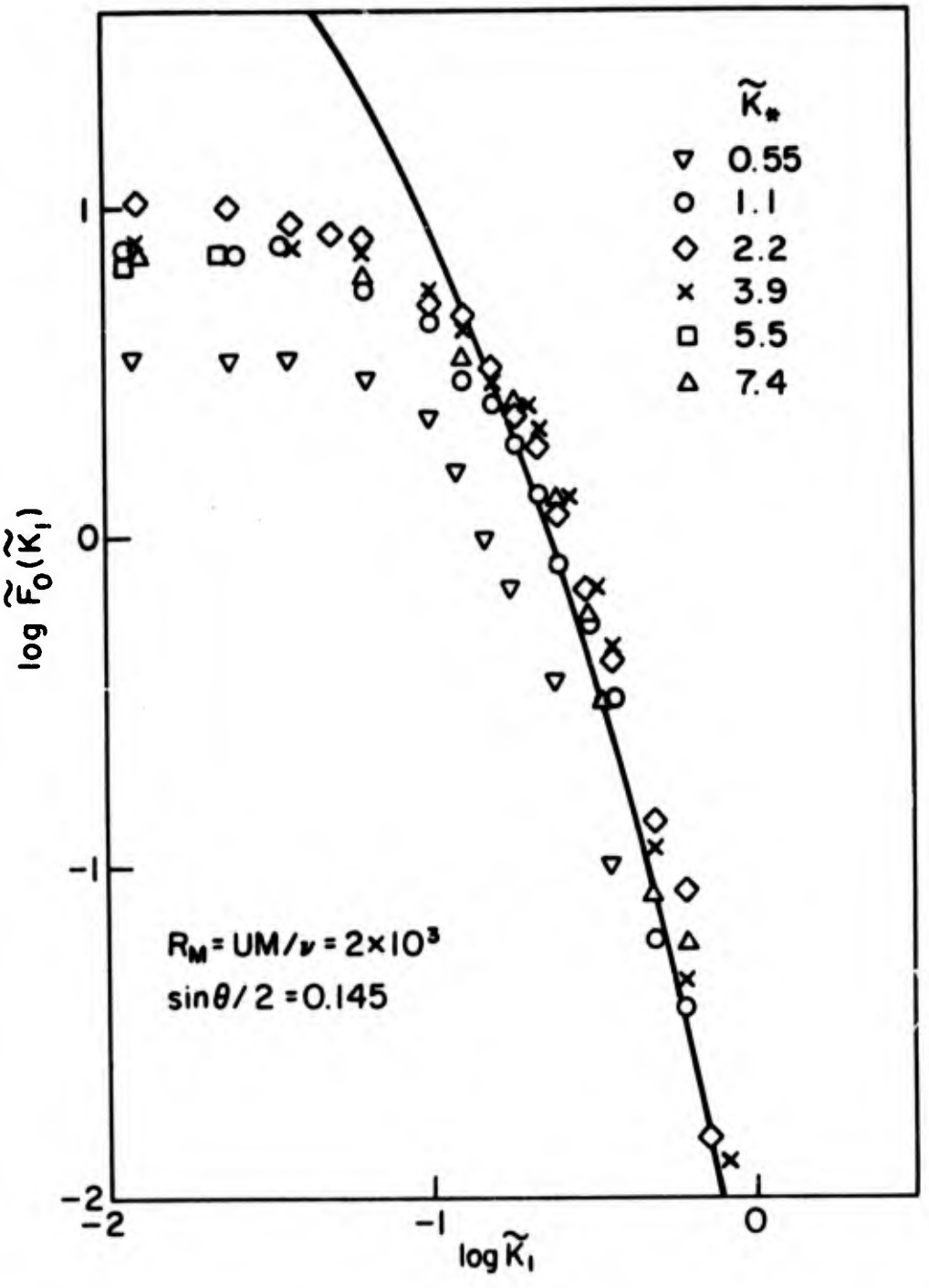

Figure 8. Corrected Spectra in Turbulent Flow

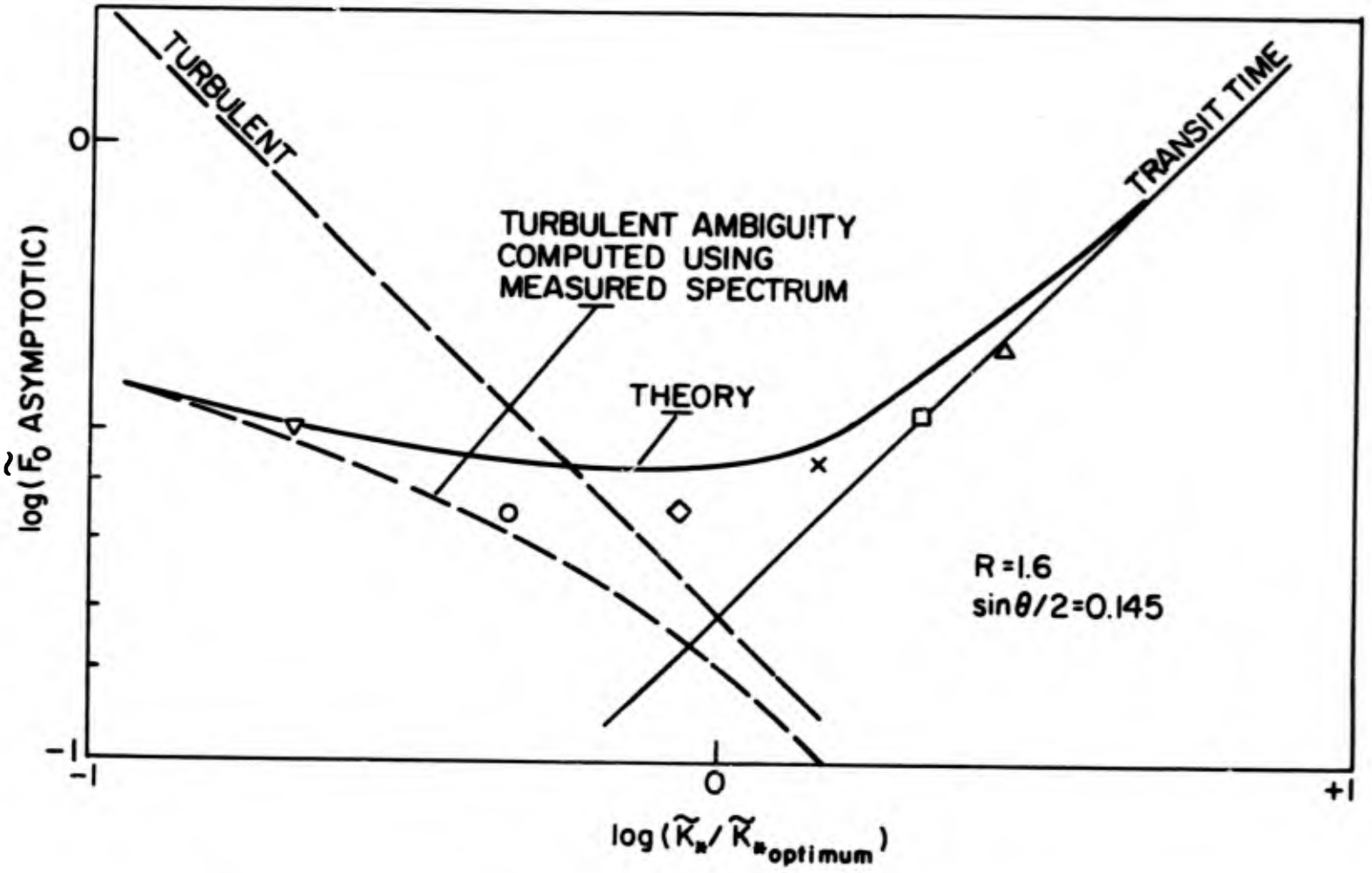

Figure 9. Comparison of Predicted and Measured Ambiguity Spectral Height in Turbulent Flow

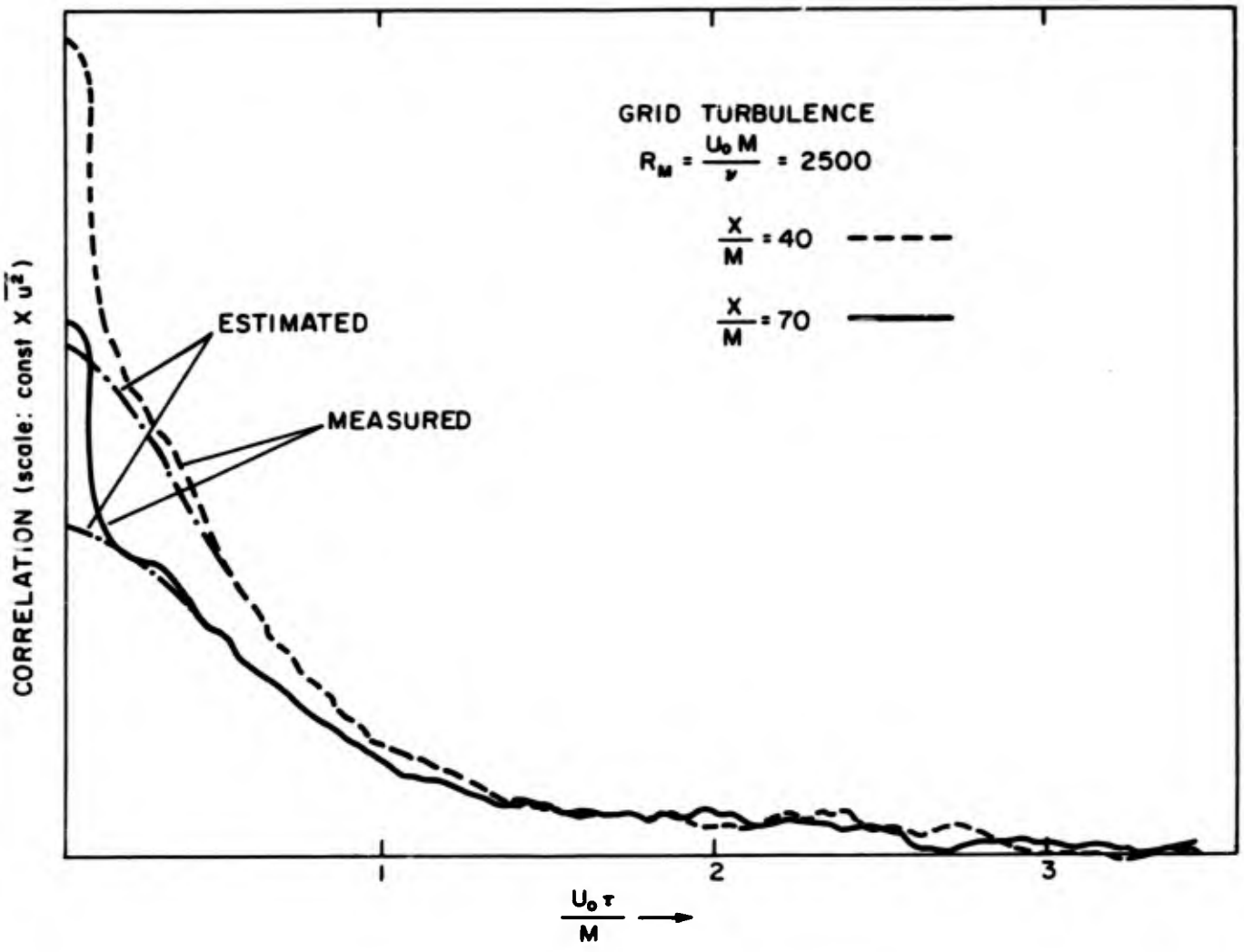

Figure 10. Measured Correlation in Turbulent Flow

DISCUSSION

ASHER: You mentioned of course that you were assuming more than three particles in the scattering volume. For frequency trackers that would necessarily need a high duty cycle and therefore the possibility of having multiple particles. I presume that your analysis would pertain completely.

GEORGE: Right. There is no difference between any of the frequency-voltage conversion techniques. I might point out that you have a little trouble understanding the noise bandwidth of the frequency tracker. Also, if you're working with a signal to noise ratio less than one or with low particle densities none of these effects is going to be very important. It's just the noise that's going to contribute this flat spectrum and the noise is going to vary the turbulence.

ASHER: This signal to noise that you talk about. In the counter approach you are talking about an instantaneous large S/N of 20 db where the average might go down to zero db. So you are way above the noise. I know from my own experience I can't even see the noise.

GEORGE: What do you mean by see - on the scope?

ASHER: Yes, on the scope.

GEORGE: Well the thing is it is filtered noise and filtered noise looks exactly like turbulence. The doppler ambiguity looks that way. They are all on the same bandwidth - you have a narrow band signal. They all look alike.

ASHER: Well I was talking about just spurious noise.

GEORGE: Yes, but you've filtered out the spurious noise so it doesn't exist.

ASHER: No, I'm talking about the raw signal.

GEORGE: I'm saying how can you tell the difference?

ASHER: Well one way to do it is to look on the scope and just see the signal when you reduce the incident light. You notice very quickly that you are getting into the dark current of the photo multiplier.

GEORGE: I've never gotten into the dark current of the photomultiplier, so I really don't think that's the problem.

ASHER: It is the problem.

GEORGE: I've used both reference beam and dual scatter systems. With the dual scatter system, I've usually been limited by the input amplifier following my photo diode. Now that's just lousy electronics design. The problem is you just can't see noise on a scope.

PIKE: From your early slide, your analysis was for the incoherent detection case. The setup you showed appeared to be a coherent case. Is there a difference in the way your analysis works? You summed at one point the current due to individual particles so this must be the coherent case.

GEORGE: No, there isn't any difference. You can show that you get the same kind of particle current dependence if you're working with the dual scatter or any other systems. Jim Whitelaw mentioned a paper where the author claims that by cutting your scattering volume down to within one fringe you get coherent detection. I don't want to comment on that because I'm not familiar with it. I would question really whether there is such a thing as coherent detection.

PIKE: Let me explain my terms. By coherent detection I mean the receiver is so small that the scattering volume forms one Airy ring at it, so every particle adds up being the same. Now your analysis does not apply in that case.

GEORGE: I don't know. I still suspect that the transit time is going to be there. Probably if you get the scattering volume down small enough it's a different problem.

PIKE: No, I'm not talking about the scattering volume. I'm talking about whether it's coherent detection or not, which is a function of the receiver size and the scattering volume.

EDWARDS: I wanted to comment on the differences of results in our analysis. Perhaps we don't differ on this one. We essentially say the length scale is one over the fringe spacing, not the sample volume size. The second thing we say is that the light from two different particles does not interact to contribute to the heterodyne spectrum. The consequence of that is no cusps.

GEORGE: I'm not saying the light from two particles interacts. I'm referring to the phase fluctuations.

PIKE: Could I ask whether that means Dr. Edwards thinks that he had done the analysis for the coherent detection case or not?

EDWARDS: Yes.

PIKE: Have you also done it for the incoherent detection case?

EDWARDS: No.

PIKE: So you have one incoherent and one coherent analysis.

EDWARDS: But we get the same answer for some things.

GEORGE: The only things we disagree on, by the way, is the existence of so called turbulent broadening due to the velocity gradients across the beam. We are in perfect agreement on everything else.

PIKE: I would be surprised if they came out the same.

APPLICATION OF A LASER DOPPLER VELOCITY METER IN TURBULENCE CHARACTERIZATION

M. K. Mazumder, P. C. McLeod, and M. K. Testerman

Department of Electronics and Instrumentation
University of Arkansas Graduate Institute of Technology
Little Rock, Arkansas 72203

Abstract

A differential method of optical heterodyning of the Doppler shifted scattered laser radiation for localized fluid flow measurements and its application to the characterization of the structure of turbulence are described. Characteristics of the Doppler signal from a turbulent flow field and the effect of system parameters on the instrumental spectral broadening and signal-to-noise ratio are discussed. Typical values of the instrumental spectral broadening were approximately 0.8 percent of the center frequency of the Doppler signal, and the signal-to-noise ratio was approximately 25 dB obtained from an air flow system using submicron dioctyl-phthalate scattering aerosol. An analysis on aerosol dynamics and scattering properties is given to determine the optimum particle size and concentration. The application of this method to the investigation of the decay of grid generated turbulence in a wind tunnel is described. Experimental data on the measurement of statistical parameters of turbulence, and on the energy decay at the final decay period are presented.

Introduction

A laser Doppler velocity meter has the essential features of an ideal instrument to measure the structure of turbulent fluid flow. The method provides an absolute method of velocity measurement, and does not require calibration. The flow field is not perturbed in the process of measurement. Its frequency response and spatial resolution are excellent. The method is applicable to both subsonic[1-8] and supersonic flow regions.[9,10] In spite of these advantages over hot wire anemometers, a laser Doppler velocity meter has several limitations in its application to the characterization of turbulence. One of the problems encountered in turbulence characterization comes from the instantaneous frequency spread of the Doppler signal. In turbulence measurement, the frequency spread may lead to a large error in the measurement of velocity fluctuations. This instrumental spectral broadening results in a low spatial resolution and a poor SNR. Further, FM demodulation of the Doppler signal becomes a difficult problem.

The receiving aperture broadening of the Doppler signal can be completely eliminated if a differential system[11] of heterodyning employing two incident beams is used. An investigation on the effect of system parameters on the performance of a differential laser Doppler velocity meter is presented here. The primary objective was to reduce the instrumental frequency spread by employing an optimum configuration in transmission and receiving optics and an optimum size range of the scattering aerosol. The method has been applied to the measurement of the decay of grid generated turbulence.

Instrumental Frequency Broadening

Figure 1 shows an experimental arrangement of a symmetrical heterodyning system employing two incident beams. The spatial frequency g_x of the inter-

ference fringes formed at the beam intersection of the two incident beams is given by

$$g_x = (2/\lambda_o) \sin \theta/2 \qquad (1)$$

where λ_o is the wavelength of the incident laser radiation. When a scattering particle passes through this fringe pattern, the scattered light will undergo amplitude fluctuation with a frequency f_c given by the product of the spatial frequency g_x and the component of the particle velocity along the direction of the fringe pattern. Thus,

$$f_c = Ug_x = (2U/\lambda_o) \sin \theta/2. \qquad (2)$$

The Doppler signal obtained in this method does not possess any receiving aperture broadening and the frequency f_c is independent of the scattering angle.[11]

The amplitude fluctuations of the scattered light will be simple harmonic in nature as an aerosol traverses through the interference fringe pattern formed by two parallel beams meeting at an angle θ. However in case of interference fringes formed by two converging beams, the resulting waveform will be distorted. This distortion will cause a frequency spread due to the finite convergence angle. Further, since each particle crosses the beam intersection as a discrete event, a frequency spread will arise due to the finite signal lifetime.

The major components of instrumental frequency broadening in a differential heterodyning process are (1) transmission aperture broadening (δf_a), (2) frequency spread due to the finite lifetime of the signal (δf_τ), and

(3) frequency spread arising from the velocity gradient present within the effective sensing volume (δf_s). Reduction of the instrumental broadening of the Doppler signal will have two advantages: (1) it will increase the accuracy of the system in turbulence structure measurement, and (2) it will increase SNR and, hence, frequency-to-voltage conversion will be possible by a comparatively simple method.

The transmission aperture broadening in a differential system can be written as[11]

$$\delta f_a / f_c = (2 \sin \alpha/2)(\cot \theta/2) \tag{3}$$

for velocity component U. Here θ is the angle subtended by the two incident beams at the point of velocity measurement and α is the angle of convergence of the incident beam focused by the lens L_1. It is desirable that θ should be large for a small aperture broadening. Increasing θ also decreases the effective length (ℓ) of the laser beam "probe" (sensing volume). This means that increasing θ would also result in a decrease of δf_s, the frequency spread arising due to the presence of the spatial velocity gradient in the sensing volume. The frequency spread arising from the finite size of the sensing volume can be calculated by determining the effective sensitive length (ℓ) of the "probe", and from the expected average spatial velocity gradient ($\partial u/\partial y$cm/sec/cm) at the point of measurement. Assuming diffraction limited optics, ℓ can be approximated as

$$\ell = 2.44 \lambda_0 / (2 \sin \alpha/2 \sin \theta/2) \tag{4}$$

and the frequency broadening can be expressed as

$$\delta f_s / f_c = \ell \langle (\partial u/\partial y) \rangle / \bar{U} \qquad (5)$$

where $\bar{U}$ represents the average velocity along the longitudinal axis (x) of the wind tunnel and δf_s represents the frequency spread arising from the average spatial velocity gradient $\langle (\partial u/\partial y) \rangle$ of the fluctuating velocity component u' (root means square value) along the lateral axis (y) of the wind tunnel. An expected value of this gradient can be computed by determining the Reynolds Number Re and the microscale of turbulence.

Figure 2 shows the variation of δf_a and δf_s as a function of $\alpha/2$. A velocity gradient of 500 sec^{-1} in the flow field was assumed to calculate δf_s. While the transmission aperture broadening decreases with the decrease of $\alpha/2$, the spread due to the finite scattering volume increases. This is due to the increase of the sensing volume since the blur diameter at the focal point increases as the aperture size in front of the focusing lens decreases. For a known value of θ and the average velocity gradient in the flow field, the convergence angle of the incident aperture diameter can be optimized. In Figure 2, α_1 indicates such an optimum value of the convergence angle for $\theta = 60^{o}$.

Sensing Volume

In turbulence characterization, the size of the laser beam "probe" within the flow field should be small compared to the microscale of turbulence but large enough to contain scattering particles at all times during the period of measurements. As mentioned earlier, a larger sensing volume introduces an appreciable broadening (δf_s) of the Doppler signal due to the spatial velocity gradients.

The size of the sensing volume depends both on the transmission and

receiving optics. If the incident beams are crossing at 0 at an angle θ, as shown in Figure 1, the volume of intersection of these two focused beams is

$$V = 2/3\ D_B^3 \left[1/\sin\theta + 1/(2\tan\theta)\right] \tag{6}$$

where the blur diameter D_B is given by

$$D_B = 2.44\ \lambda_o\ f_1/a$$

and f_1 is the focal length of lens L_1, λ_o is the wavelength of incident radiation, and a is the diameter of the transmission aperture. The effective scattering zone (shown as the shaded area in Figure 1) is the portion of this volume intersected by the depth of field of the imaging optics. To make this sensing volume small, lenses L_2 and L_3 should have minimum spherical aberrations. If uncorrected lenses are used, the lateral spherical aberration would determine the effective diameter (d) of the sensitive scattering zone. Figure 3 shows the effect of variation of $\Delta\theta$ on d if a plano-convex lens is used for L_2 (f_2 = 166 mm). The lower limit of d is set by the diffraction limit and the upper limit is set by the dimension D as determined by the transmission optics. D is the common diameter of the beam intersection, given by

$$D = D_B/(\cos\theta/2). \tag{7}$$

The length ℓ(equation 4) would depend primarily on the transmission optics since on-axis rays will not be blocked by the spatial filter (Figure 1), unless the optical axis of the spatial filter is tilted in a

plane perpendicular to the plane containing the transmission optical axes. The length (ℓ) decreases with the increase of the angle θ. However, reflection loss from the optical window of the wind tunnel increases with θ and scattering intensity decreases. The nature of variation of the length ℓ is plotted versus θ in Figure 4.

If, for example, $\theta = 60^{o}$, $f_1 = 700$ mm, $a = 4$ mm, $f_2 = 166$ mm, $x = 40$ mm and $\Delta\theta = 10^{o}$, the sensing volume can be characterized by $\ell = 550$ microns and $d = 4.5$ microns considering diffraction limited optics. The effective scattering volume is thus approximately 1×10^{-8} cm^3. This compares favorably with the dimension of a typical hot wire probe (wire diameter 10μ, length 1.5 mm, probe diameter 3 mm).

An estimation of the size of the sensing volume was made by placing a thin transluscent plate in the scattering zone and moving it along and perpendicular to the optical axis while recording the relative intensity of light falling on the photomultiplier. Simple lenses were used in the present experimental setup. Measurements on -3 dB points indicate that $\ell \approx 600$ microns and $d \approx 100$ microns.

Signal-to-Noise Ratio

In most applications of laser Doppler velocity meters, where the point of measurement is not far away from the receiver, the signal-to-noise ratio of the laser Doppler signal is determined by the noise content of the signal, i.e. SNR at the output will be limited by that of the incident scattered beam falling on the photocathode. To achieve this condition, signal power (power of the scattered beam falling on the detector) is made large so that the noise component of the signal is much larger compared to other noise components, such as thermal noise, stray light noise, dark current noise

and shot noise.

Since it is desired that, in a laser Doppler system, SNR should be high and δf should be low, it is possible to define a dimensionless quantity Q_s relating these two parameters. Designating this quantity as the "figure of merit" of the heterodyning system, Q_s can be defined by

$$Q_s = SNR/\ \delta f/f_c) \tag{8}$$

evaluated for a scattered beam intensity s at a unit distance from the scattering center and in the direction of the receiving aperture. For a comparative study between differential and local oscillator heterodyning systems, measurement of Q_s was made on the equal intensity scattered lobe (constant s) since SNR depends on the total signal power falling on the photocathode. Figure 5 shows a plot of Q_s versus P_s for the two heterodyning systems. From Fig. 5 it is observed that if the signal power P_s is greater than 10^{-10} watts, the differential system will have a larger value of "figure of merit". This advantage can be gained as long as P_s can be significantly increased by increasing receiving aperture.

Table I shows some experimental data on instrumental frequency broadening and signal-to-noise ratio. Measurements were made on laminar air flow using the differential heterodyning system.

A 50 mw He-Ne laser was used in this study. Typical SNR was, however, about 25 dB since a degradation of SNR was often caused by the relative vibration of the optical systems. When a 1.5 mw He-Ne laser was used, typical values of signal-to-noise ratio were about 10 dB. Instrumental frequency broadening (δf) was measured by using a communication receiver having a selectivity of 500 Hz. In general, the measured values of frequency spread

were lower than the computed figures. This is due to the fact that theoretical calculations were made based on the assumption that the intensity distribution across the transmission aperture is constant.

Aerosol Generation, Particle Dynamics and Scattering Properties

Localized fluid flow measurement using a laser Doppler method implies that there must be some scattering centers present in the fluid medium. The type of aerosol to be used would depend on the characteristics of the fluid medium and the flow system. The generation of a fairly monodisperse solid aerosol by dispersion of powders is quite difficult for a size range of present interest. One of the commonly used devices for generation of solid aerosol is the Wright dust feed mechanism[12] which uses dry compressed air for dispersion. Well fractionated solid powders can be used. If the generator is followed by an ilutriator, a suitable size range can be picked up for scattering aerosol. Aerosol generation by an atomizer nozzle of a modified Laskin[13] type can be used for generating liquid droplets in a size range of 0.1 to 3 microns diameter. Fairly uniform submicron aerosol (0.8 micron mass median diameter) of dioctyl-phthalate (DOP) was generated using an aerosol generator shown in Fig. 6. The aerosol output rate can be varied widely by controlling the number of atomizer nozzle and the applied pressure. Use of DOP or water droplets is advantageous because of minimum cleaning and corrosion problems in optical windows and wind tunnel equipment. One suitable method of generating submicron solid aerosol is by atomizing an aqueous solution of uranine (disodium salt of flourescein) in a nebulizer and subsequent drying of the aerosol. The generated aerosol preferably should be non-toxic and have a low electrostatic charge.

The size of the scattering aerosol suspended in the fluid medium should be small enough to follow the turbulent fluctuations of the fluid motion. If the particle inertia is large, such that it travels an appreciable distance independently, the particle will not follow the small eddies in the fluid. A measure of the particle inertia is its stop distance

$$S = \tau_p V_p \tag{9}$$

where s is the stop distance of the particle for it to come to rest when projected into still air with velocity V_p. The quantity of τ_p is the relaxation time[14] of the particle, which can be defined as

$$\tau_p = m_p/6\pi r_p \eta \tag{10}$$

where m_p is the mass of the particle, r_p is its radius and η is the viscosity of air, all in cgs units. How closely a suspended aerosol particle will follow the turbulent eddies would depend upon the ratio of the particle stop distance to the scale of turbulence. This ratio should be small. Figure 7 shows the stop distance plotted versus the particle diameter for two values of Reynolds number. In calculating the stop distance of a particle placed in a turbulent flow field, the estimated root mean square value of the fluctuating velocity components was considered.

Obviously, the desired size of aerosol is one that will follow the motion of an element of fluid but will not participate in the random motion of the gas molecules. Submicron particles have an appreciable Brownian movement. The mean square Brownian displacement of a particle can be

written as[12]

$$\overline{\Delta x^2} = 2RTt/(6\pi N\eta r_p) \tag{11}$$

where R is the gas constant, T is the absolute temperature, t is the time in seconds, η is the viscosity of the medium, N is the Avagardro number and r_p is the radius of the particle. The rms amplitude of this displacement is also plotted against particle radii in Figure 7. The average particle diameter should be such that $\overline{\Delta x^2}$ and s are minimum.

Evaluation of the scattering characteristics of aerosols in the fluid medium can be made from the Mie Theory if the size distribution and refractive index of aerosol particles are known. For spherical particles, the scattering intensity at an angle θ can be calculated for a wide range of aerosol parameters, given in the NBS table of scattering functions.[15] If the particles are separated by a distance large compared to their average radius, scattered intensities from more than one particle will be additive since there will be no permanent phase relationship between the radiation scattered by two different particles.

To gain a physical insight of the effect of aerosol paramters, Mie Theory can be simplified for approximate calculations. For a given θ, I_o and r_p an approximate value of $I(\theta)$ can be written in the form

$$I(\theta) = Knr_p^z \tag{12}$$

where K is a constant, r_p is the average particle radius, n is the aerosol number concentration per cc, and z depends on angle θ, aerosol size

parameter α_p and the refractive index of the particle. For polydisperse aerosol in the size range that can be used for turbulence measurement, it is expected that z would vary within the range of values of 2 to 4. This indicates that only the larger size fractions make primary contribution to the total scattering intensity. For DOP aerosol of 1 micron diameter, and λ_o = 6328 A, and $\theta = 30^o$, and for an incident laser beam power of 30 mw focused to an airy disk diameter of 100 microns, $I(\theta)$ is expected to be, from Mie Theory,

$$I(30^o) \approx 1 \times 10^{-7} \text{ w/particle} \tag{13}$$

at a distance of 50 cm from the scattering center.

Particulate concentration, n, should be sufficiently high for a high signal power. However, energy removed from the incident and the scattered beam will also increase in direct proportion to n. Further, a large aerosol concentration would effectively produce more heterogeneous aerosol due to a higher coagulation rate, since

$$dn/dt = (-k_{o/2})\, n^2 \tag{14}$$

where n is the instantaneous concentration in number of particles per unit volume, and K_o is the rate constant for still air which increases appreciably with turbulence. Thus, a fairly monodisperse aerosol will become polydisperse in short residence time due to coagulation if n is very high.

Decay of Turbulence at Low Reynolds Number

The purpose of the investigation on grid generated turbulence in a wind

tunnel was to illustrate the applicability of the laser Doppler velocity meter to the characterization of turbulence. Air flow with a low Reynolds number was investigated to indicate an advantage of laser Doppler velocity meter over hot wire anemometer where the latter looses its sensitivity at low air velocity. Decay of weak turbulence is also a subject of considerable recent interest.[16]

A channel of cross sectional area 3.8 cm x 3.8 cm and 16 meters long was selected for the present study. Air at room temperature was used as the fluid medium. Polydisperse submicron DOP aerosol of average diamter 0.8 micron and concentration of 10^7 particles/cc was used. The end connections to the air duct were made by flexible piping. The experimental setup is shown in Fig. 8. The flow could be adjusted by changing the blower speed. The channel was mounted on a movable frame so that the channel could be translated in the vertical and horizontal directions by known displacements. At the site of flow measurement in the duct, lucite windows (17 cm x 3 cm x 3 mm) were provided on the four sides.

FM demodulation of the Doppler signal was done by phase-locked loop FM detectors using Signetics NE 561B PLL integrated circuits. The demodulated output was fed to an active low pass filter to reject the high frequency noise arising due to occasional signal dropouts (due to time discontinutiy of the signal). The output of the filter can be directly recorded in a magnetic tape recorder for later processing of the signal. The demodulated Doppler signal was fed to a DISA 55D70 analog correlator for analog auto-correlation measurement of velocity as a function of time delay. For digital data processing, the recorded signal was digitized using an A/D converter for computer processing.

To examine the performance of the Doppler signal processing system, an

oscillatory laminar flow was established in the air channel by exciting the flow medium with a loud speaker. The speaker was connected through a Tee section to the air channel and when excited, the laminar flow was modulated sinusoidally. The detected velocity signal was displayed in an oscilloscope. This test was carried out at a different excitation frequency to determine the fidelity of the FM detection process.

A grid made of cylindrical rods (diameter 0.63 cm and spacing M = 1.27 cm) was placed at the upstream of the duct for turbulence generation. The separation x between the point of measurement and the turbulence generating grid was varied by moving the grid at the desired position. The velocity measurements were taken at a point far away from the turbulence generating grids and at the center of the pipe so that nearly isotropic conditions of the flow field were achieved.

The decay of turbulence expressed by the ratio of the mean velocity $\overline{U}$ and the r.m.s. value of the fluctuating component u' is plotted in Fig. 9 as a function of x/M where x is the distance between the turbulence generating grid and the point of measurement and M is the separation between the grids. For large x/M, a linear decay rate is expected from Taylor's relationship.[17]

$$\overline{U}/u't = \text{constant} + (5/A^2)(x/M).$$

From Fig. 9, A was calculated to have a value of 2.8.

Figure 10 shows a plot of velocity correlation against time delay for different values of x/M. The correlation coefficient was obtained by computing

$$R(\tau) = \frac{1}{T}\int_0^T u(t)\, u(t+\tau)dt/\overline{u^2} \qquad (15)$$

where τ is the time delay and T is the integration time large enough to include all small time scale fluctuations. The integral scale of turbulence along the x direction was measured using the relationship

$$x = \int_0^{\infty} R_x \, dx = \int_0^{X} R_x \, dx \tag{16}$$

where R_x is the correlation coefficient between U at two points at a distance x along the x axis, such that $R_x = 0$ for $x \quad X$. The energy spectrum of turbulence was obtained from the correlation plot.

If $R_x(\tau)$ is the velocity auto-correlation function, the energy spectrum,

$$G_u(f) = 4\int_0^{\infty} R_x(\tau) \cos(2\pi f\tau) d\tau. \tag{17}$$

Normalizing the energy spectrum with respect to the total energy $\overline{u^2}$, which is the total contribution from all frequency components,

$$\begin{aligned} \nu(f) &= G_u(f)/\overline{u^2} \\ \int_0^{\infty} \nu(f) \, df &= 1. \end{aligned} \tag{18}$$

The normalized energy spectrum is plotted in Fig. 11 for different values of x/M. The microscale of turbulence was obtained from the normalized energy spectrum.

$$\lambda = (\overline{U}/2\pi)\left[\int_0^{\infty} f^2 \nu(f) df\right]^{-1/2} . \tag{19}$$

Karman[17] has shown that for low Reynolds number

$$d\,\overline{u^2}/dt = -10\nu\,\overline{u^2}/\lambda^2 \qquad (20)$$

where t is the decay time measured with reference to the turbulence gen rating grid so that

$$t = x/\overline{U}. \qquad (21)$$

At the final decay period, the integral scale (ℓ) approaches nearly a constant value and the energy decay approaches an inve se square law relationship $\overline{u^2}/\,\overline{U}^2 \sim t^{-2}$ and the microscale (λ) increases with time such that

$$\lambda^2 = \text{const}\ x t. \qquad (22)$$

Figure 12 shows the energy decay and the variation of λ^2 with respect to the decay time t. Table II presents some of the compu ted and experimentally obtained values of turbulence decay parameters. With a two point velocity measurement system, it is possible to measure two point cross-correlation functions and to measure Reynolds stress. Frequency biasing by rotating diffraction grating[18] can be employed to measure velocity without directional ambiguity in cross-correlation measurement. Frequency translation of the Doppler signal is also helpful in supersonic flow measurement in maintaining the Doppler signal frequency within the useful range of signal processing equipment.

Acknowledgements

The authors are thankful to Professor R. W. Raible and Dr. J. G. Dodd

for helpful discussions and comments. This study was supported in part by NASA Grant NGL 04-001-007.

References

1. Yeh, Y. and Cummins, H. Z., Appl. Phys. Letters, 4; 176 (1964).

2. Foreman, J. W., Jr., George, E. W. and Lewis, R. A., Appl. Phys. Letters, 7; 77 (1965).

3. Foreman, et al., IEEE J. Quan. Electron., QE-2; 260 (1966).

4. Goldstein, R. J. and Hagen, W. F., Phys, Fluids, 10; 1349 (1967).

5. Huffaker, R. M., Appl. Opt., 9; 1026 (1970).

6. Berman, N. S., et al., AICHE J., 15; 323 (1969).

7. Angus, J. C., et al., Industrial and Engineering Chemistry, 61; 8 (1969).

8. Lennert, A. R., et al., "Laser Applications for Flow Field Diagnostics", Paper presented at the Second National Laser Industry Association Meeting, Los Angeles, California, Oct. 20-22, 1967. (Electro-Technology, Feb. 1970).

9. Yanta, W. J., Gates, D. F. and Brown, F. W., "The Use of Laser Doppler Velocimeter in Supersonic Flow", AIAA 6th Aerodynamic Testing Conference Albuquerque, New Mexico, March 10-12, 1971.

10. Jackson, D. M., J. Sci. Instr., 4; 173 (1971).

11. Mazumder, M. K. and Wankum, D. L., Appl. Opt., 9; 633 (1970).

12. Green, H. L. and Lane, W. R., "Particulate Clouds, Dusts, Smokes and Mists", E & F. N. Spon Ltd., London, U. K., 1964.

13. Parrish, E. C. and Schneider, R. W., "Tests of High Efficiency Filters and Filter Installations at ORNL", ORNL-3442, TID-4500 USAEC, June 1963.

14. Fuchs, N. A. "Mechanics of Aerosols", Pergamon Press, Elmsford, New York, 1964.

15. "Tables of Scattering Functions for Spherical Particles", Department of Commerce, National Bureau of Standards, Appl, Math., Series 4, January 1949.

16. Ling, S. C. and Huang, T. T., Phys. of Fluids, 13; 2912 (1970).

17. Friedlander, S. K. and Topper, L., "Turbulence, Classic Papers on Statistical Theory", Interscience Publication Inc., New York, N. Y., 1961.

18. Mazumder, M. K., Appl, Phys. Letters, 16; 462 (1970).

TABLE I

Effect of System Parameters on Instrumental Frequency Spread*

sin α/2	sin θ/2	$\delta f/f_c$ x 100% Calculated	$\delta f/f_c$ x 100% Observed	SNR dB
0.0028	0.1500	1.82	0.8	30
0.0040	0.5736	0.57	0.5	30
0.0075	0.0750	9.99	3.8	31
0.0143	0.2436	5.72	1.4	30
0.0143	0.1398	10.13	4.3	28

*Referred to Half-Power Points

TABLE II

Some Statistical Parameters of Turbulence at Low Reynolds Number

x/M	Decay Time t sec	u' cm/sec	Turbulence Intensity %	ℓ_x cm	$R\ell_x$	λ_x Calculated	λ_x Observed	ℓ_x/λ_x
12	0.396	5.7	14.86	1.08	41.5	0.51	0.54	2.0
18	0.595	4.5	11.68	1.20	36.4	0.58	0.70	1.7
24	0.792	2.5	6.50	2.16	36.7	0.75	1.00	2.1
30	0.990	1.7	4.46	2.72	31.4	0.94	1.38	1.96

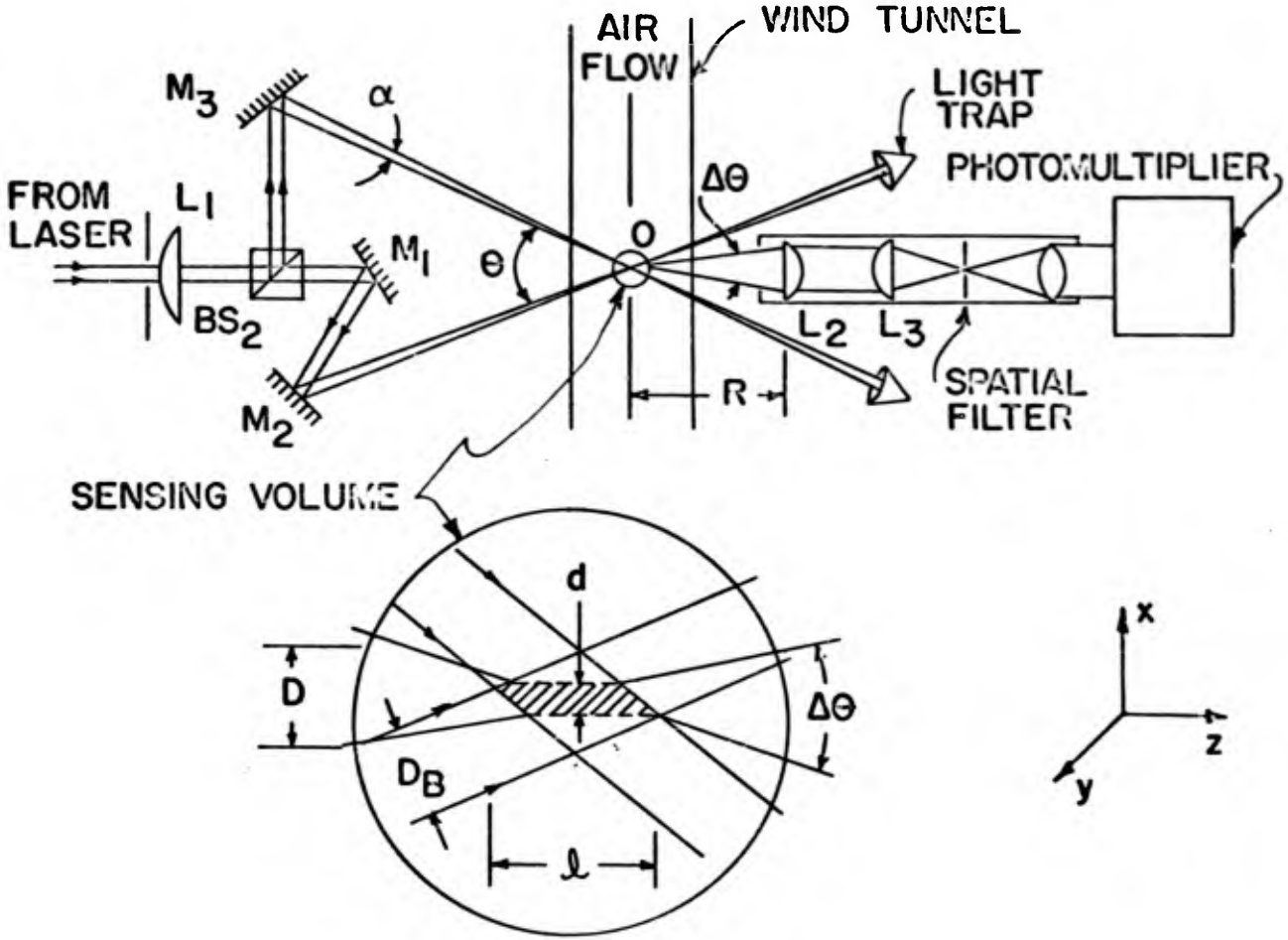

Figure 1. Differential heterodyning system

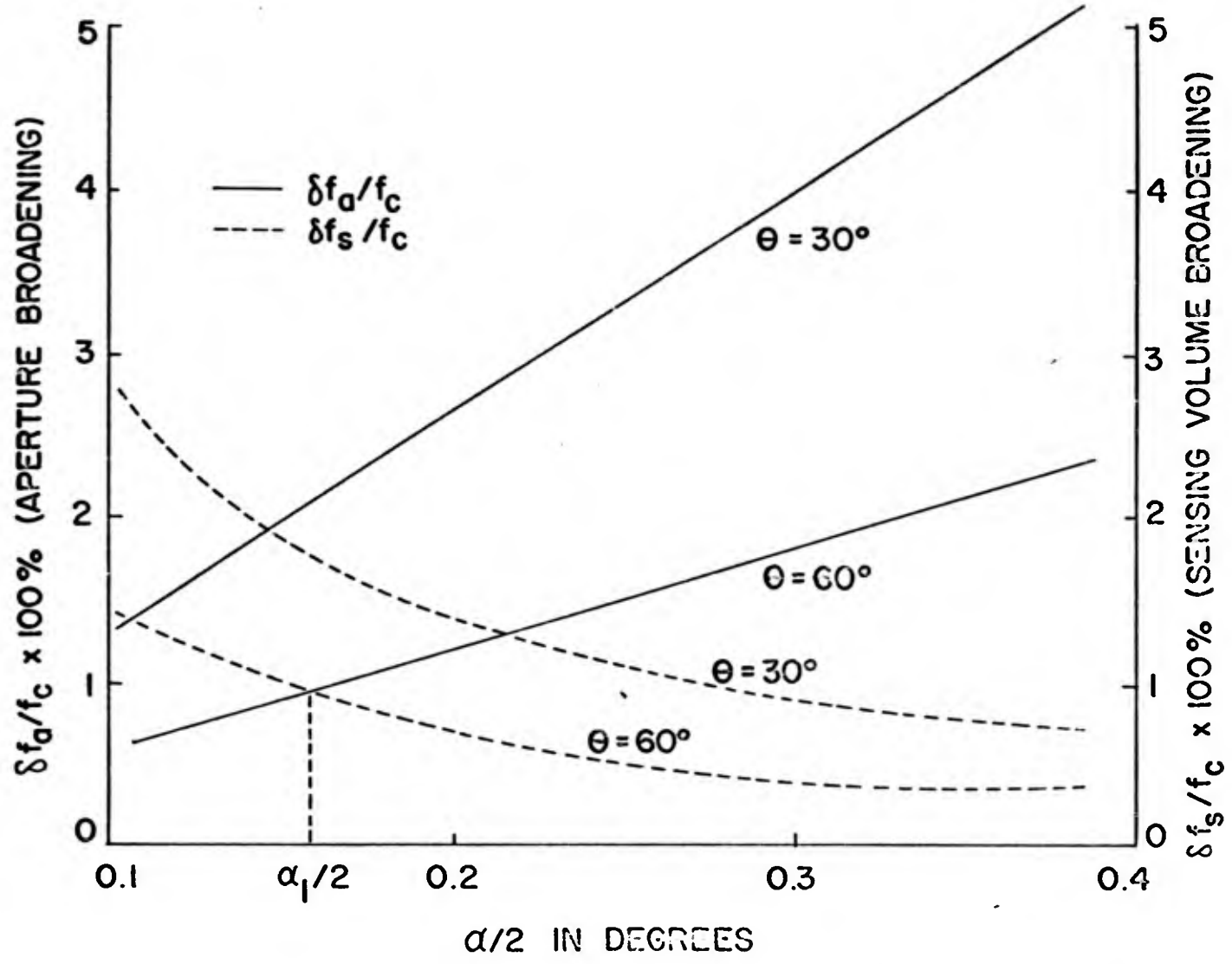

Figure 2. Variation of instrumental frequency broadenings of the Doppler signal due to finite sizes of aperture and sensing volume versus the convergence angle α. (A spatial velocity gradient of 500 sec^{-1} is assumed.)

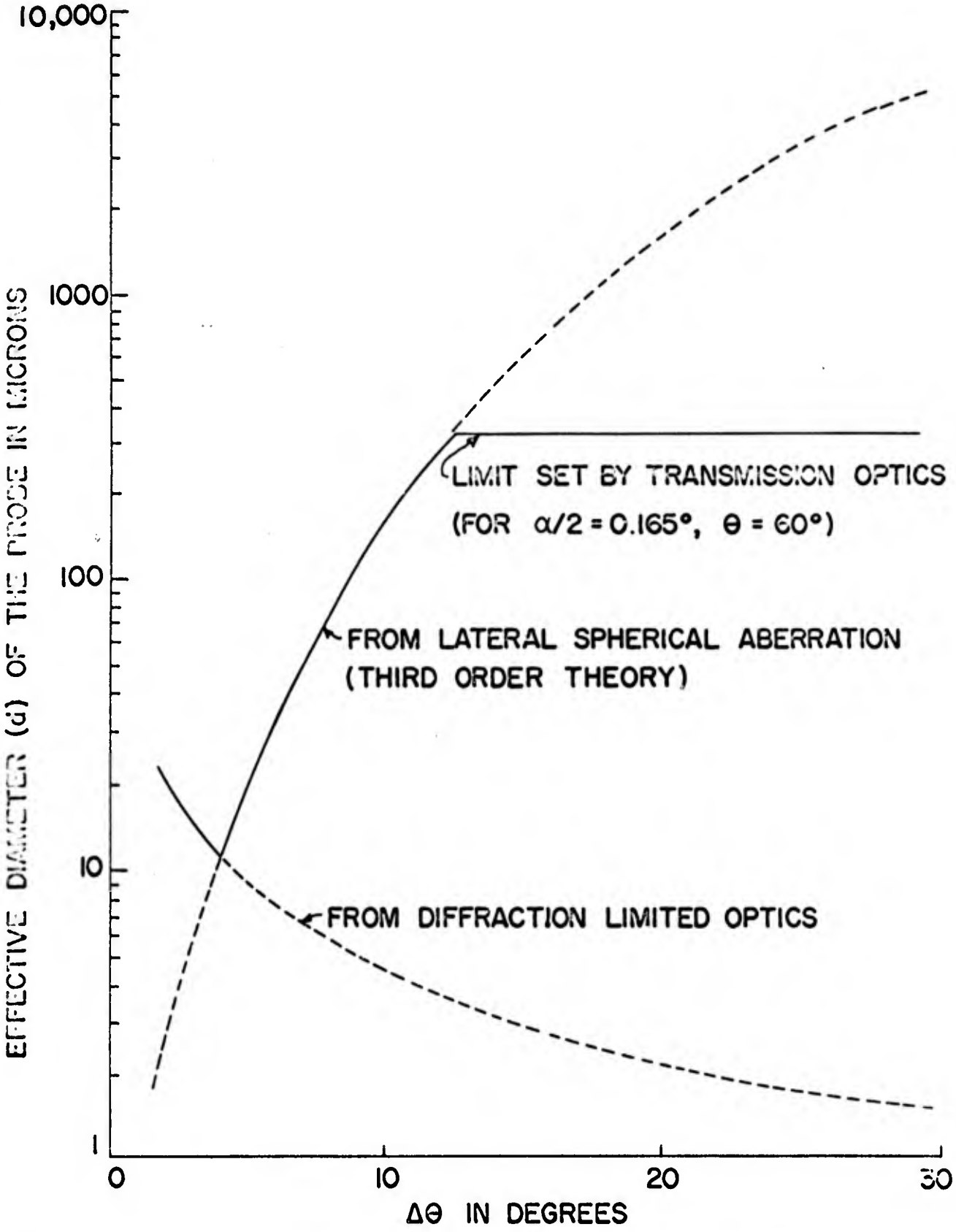

Figure 3. Effective diameter of the "laser beam probe" plotted versus the angle $\Delta\theta$ subtended by the receiving aperture at the center of the sensing volume

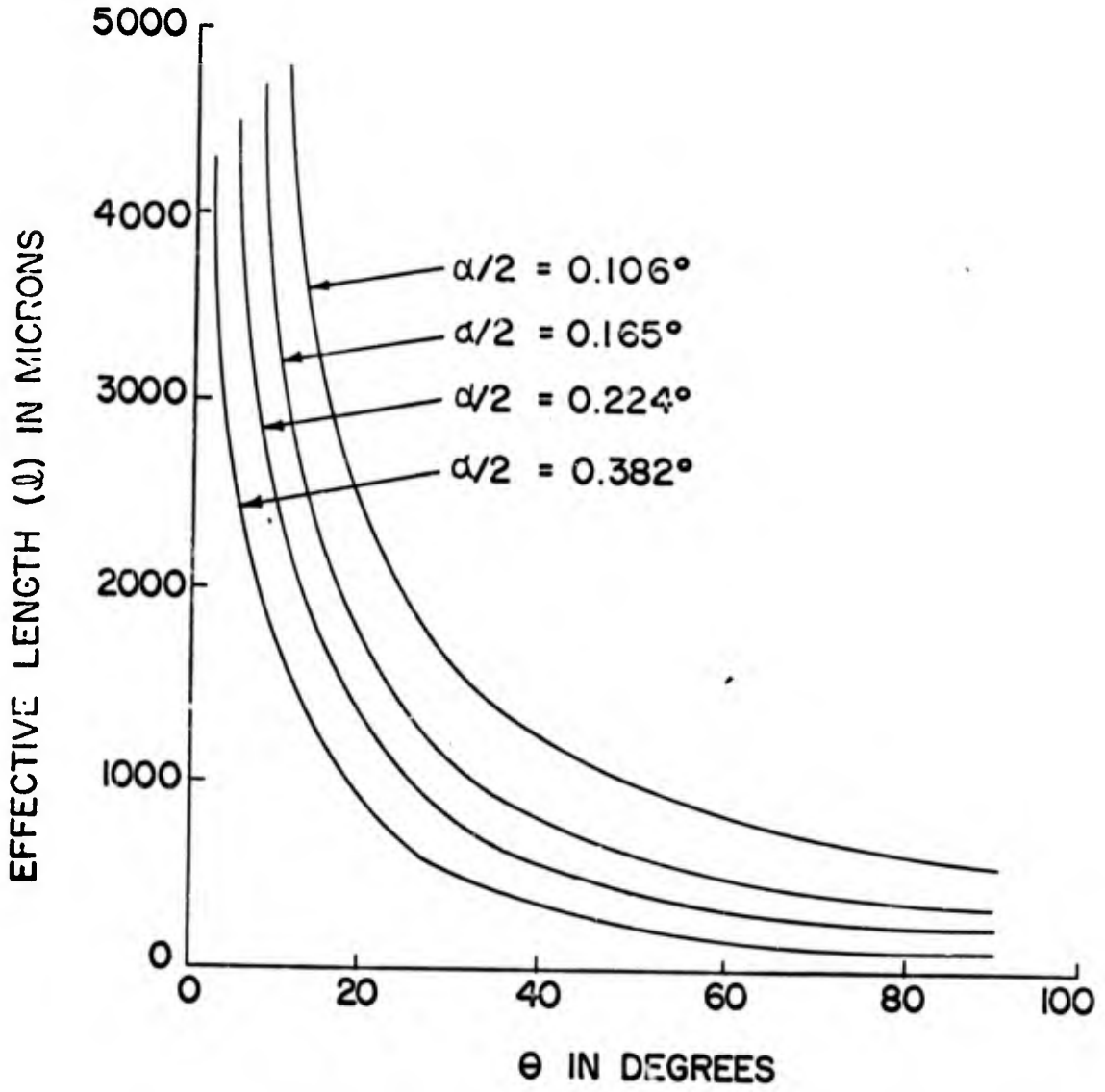

Figure 4. Effective length of the "laser beam probe" in the flow field plotted versus θ for different values of $\alpha/2$

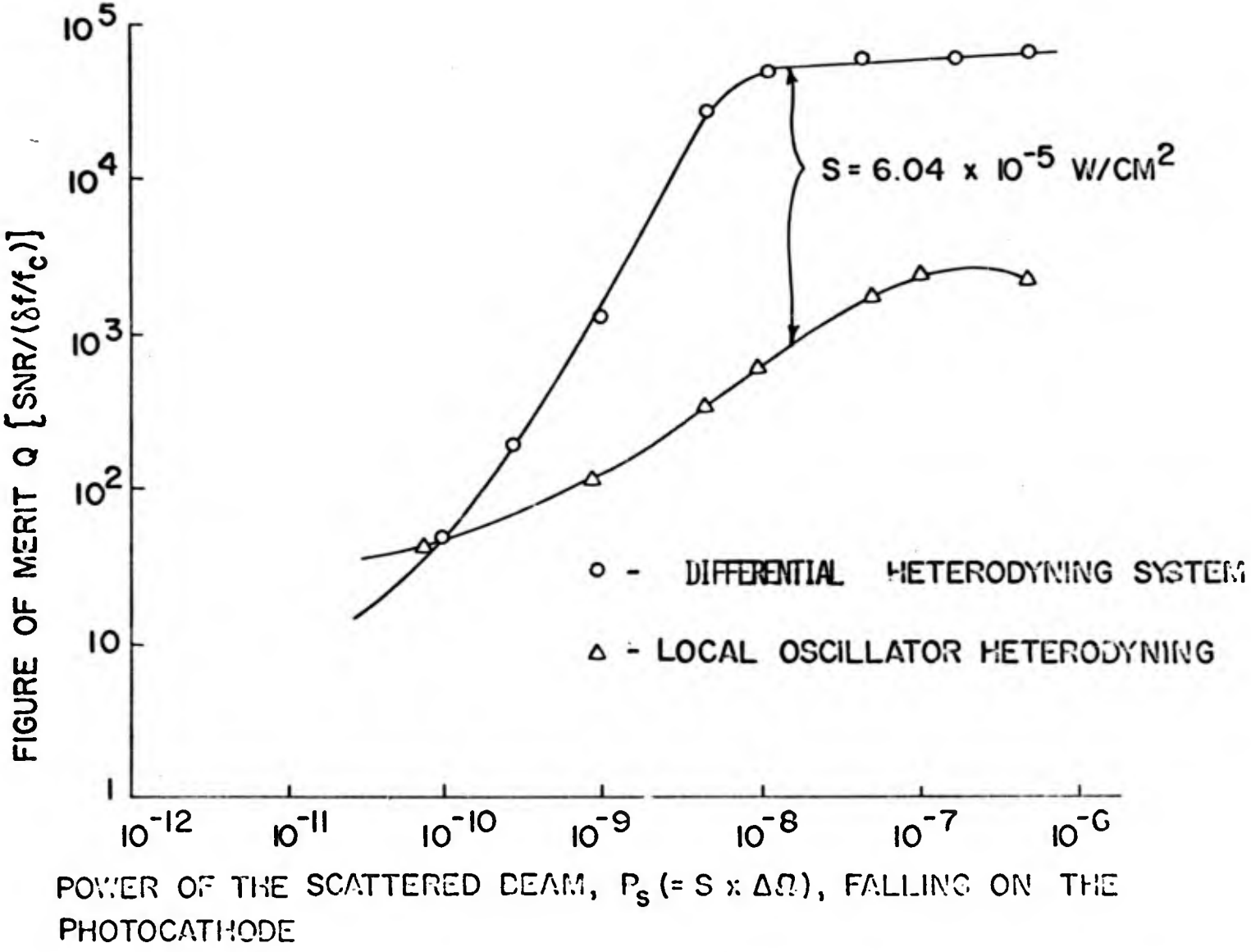

Figure 5. Figure of merit of the two heterodyning systems plotted versus P_s ($\Delta\Omega$ is the solid angle subtended by the receiving aperture at the point of measurement)

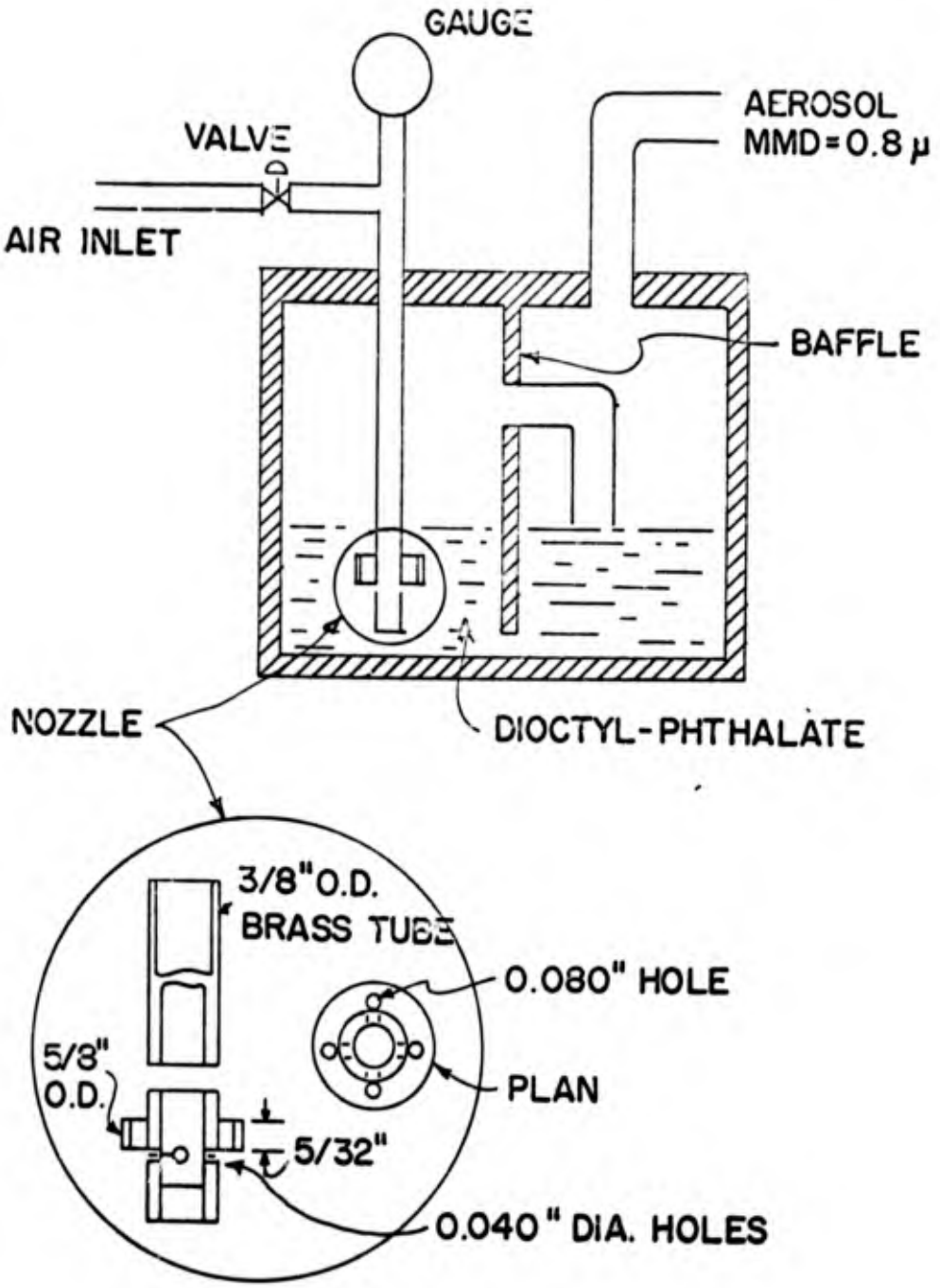

Figure 6. Schematic diagram of the DOP aerosal generator

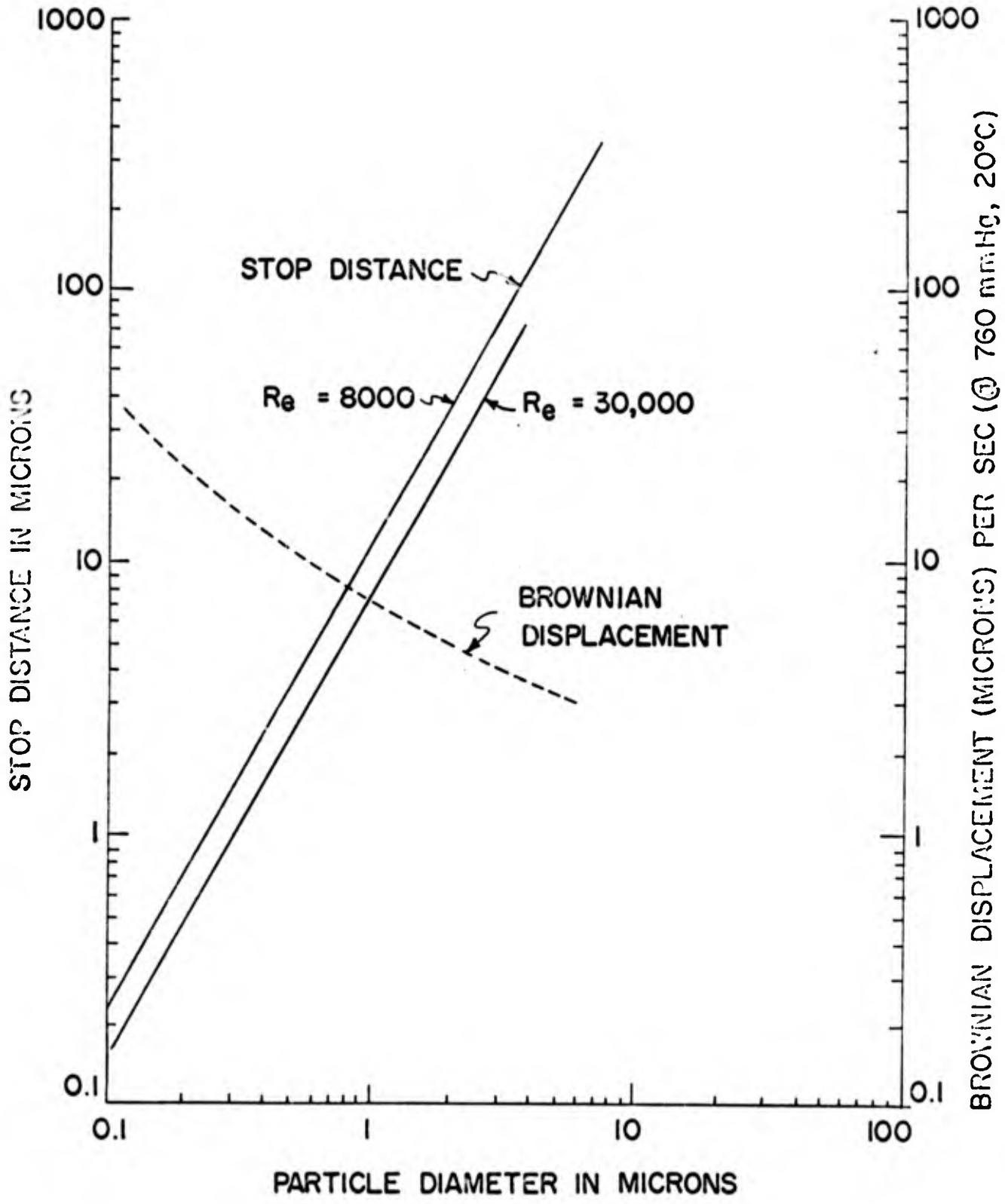

Figure 7. Stop distance and Brownian displacement for unit density spherical particles plotted versus particle diameter.

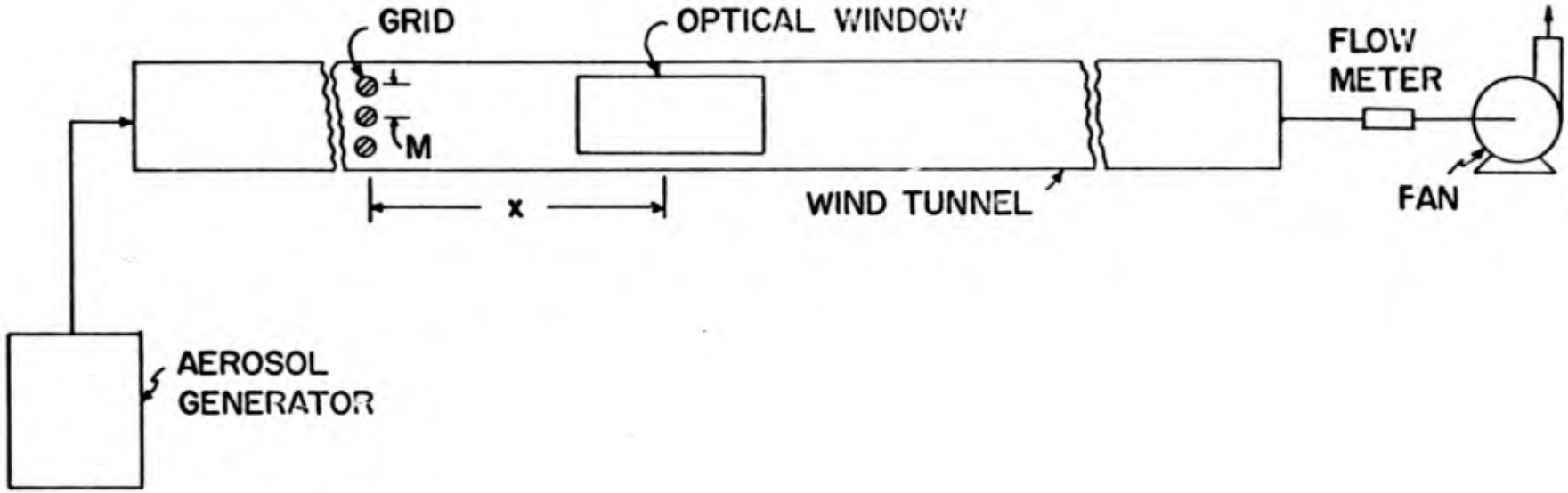

Figure 8. Schematic diagram of the flow system

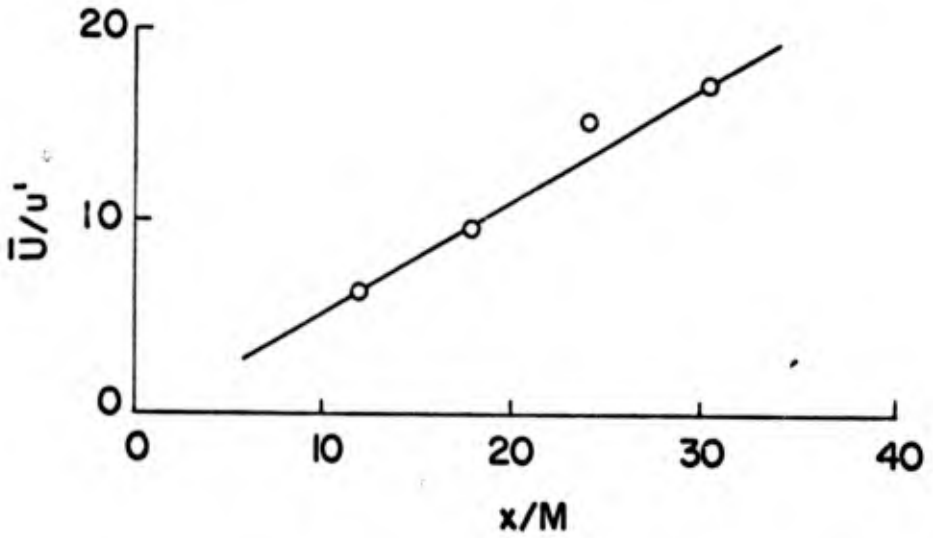

Figure 9. Decay of turbulence behind a grid of round bars

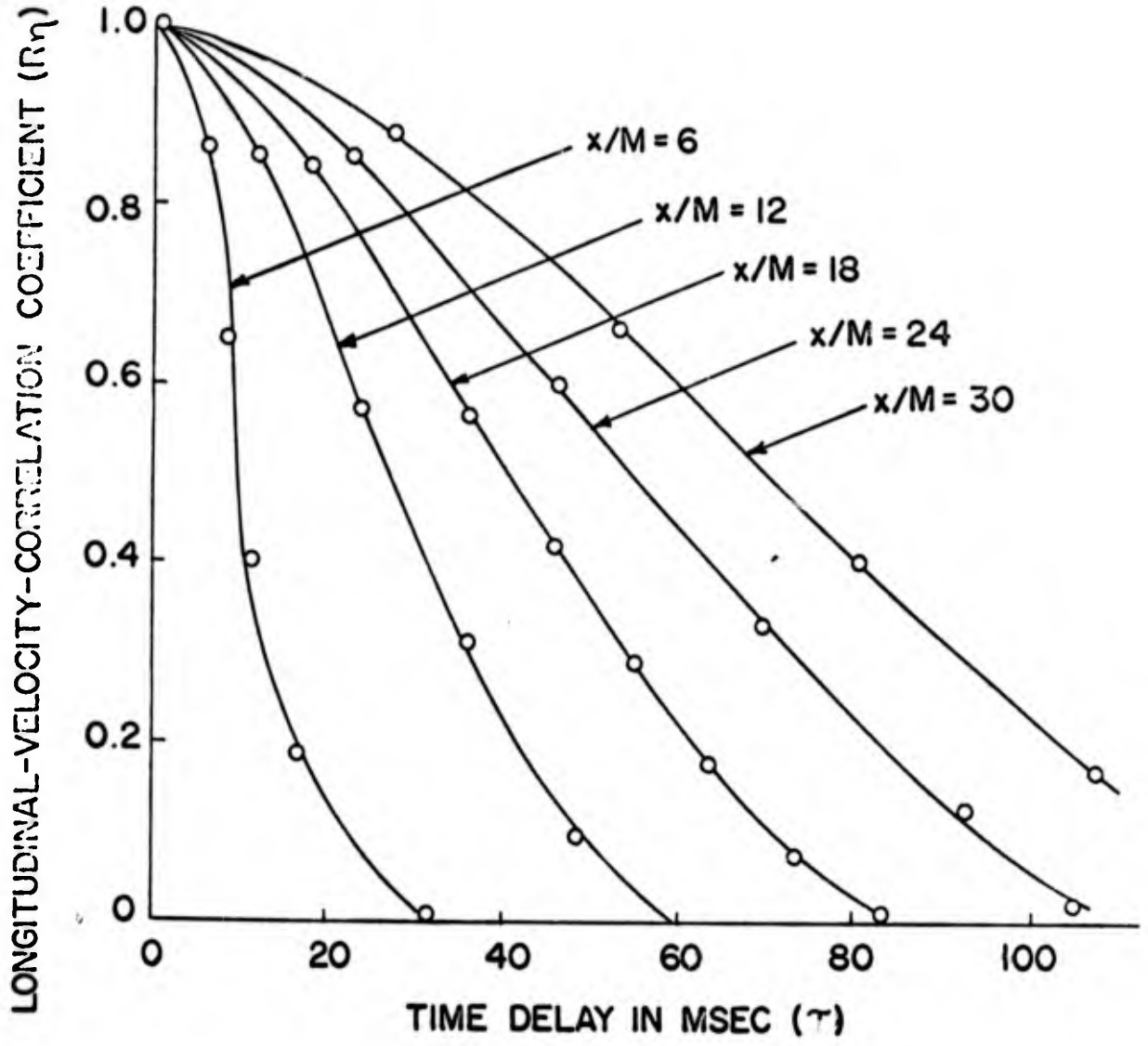

Figure 10. Velocity auto-correlation coefficient plotted versus delay time (digital correlation measurement)

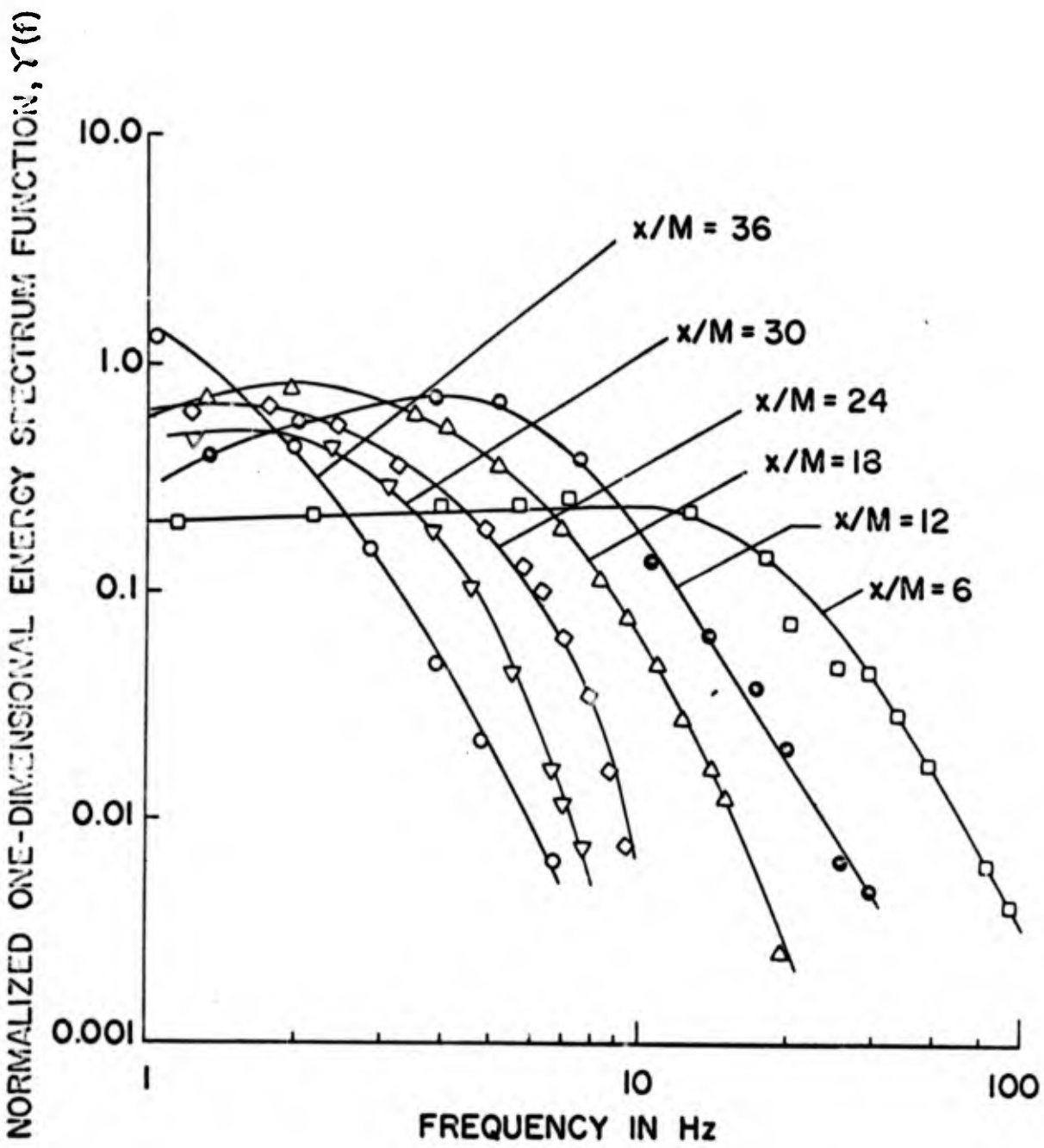

Figure 11. One-dimensional energy spectrum of turbulence of low Reynolds number

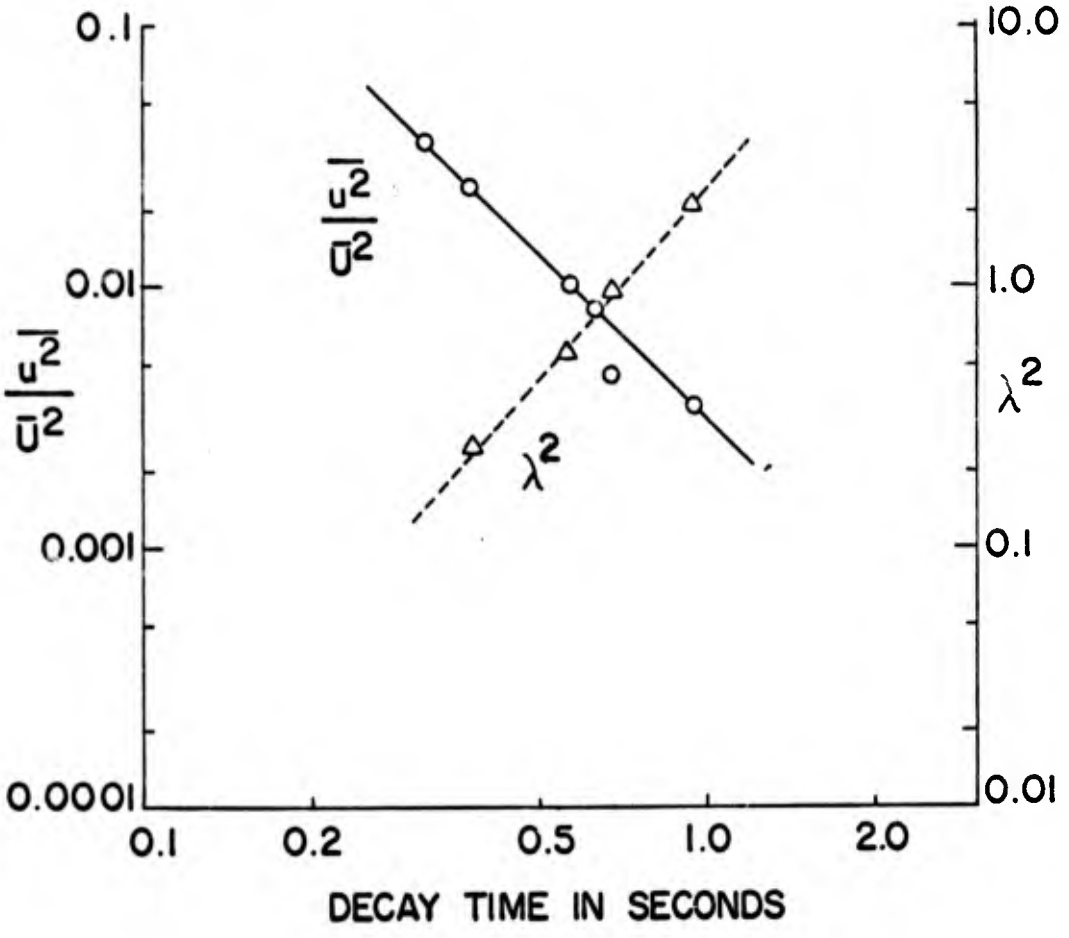

Figure 12. Energy decay of turbulence and λ^2 plotted versus decay time

GOLDSCHMIDT: What was your average velocity in the last set of measurements - the mean velocity in the wind tunnel?

MAZUMDER: We had a velocity of about fifty centimeters per second.

BOUTIER: Did you consider the laser beam divergence in the determination of the sensing volume?

MAZUMDER: What we have tried to show is that it is often possible to make an estimation of the sensing volume from the geometry of the receiving optics alone. If we use diffraction limited optics in the receiver and if we know the size of the pin hole used in the spatial filter, the sensing volume could be calculated easily. We actually measured the sensing volume by placing a very thin translucent screen (about ten microns) in the sensing volume and moving it along the longitudinal and transverse directions and plotting the DC current output of the photomultiplier against the spatial displacements of the transluscent scattering film.

EDWARDS: I noticed you did a dynamic calibration. Were you able to do an absolute dynamic calibration? In other words, were you able to know the ergs per square centimeter of sound power at a given point - where you measured?

MAZUMDER: Yes, it probably could be done. We really didn't go to that extent. A pressure transducer was placed in the acoustically excited flow medium and its output was displayed in a dual beam oscilloscope. The demodulated Doppler signal was displayed on the other channel of the oscilloscope. The ratio of the amplitudes of the acoustic excitation and the resultant oscillations of the flow borne particles were measured as a function of excitation frequency. Also, the Doppler signal displayed in the spectrum analyzer allowed us to measure the modulation index and the results agreed well with the data that were obtained from the demodulated signal output. This dynamic calibration could be carried out over a wide range of frequency but in our present set of experiments, the frequency range was limited by the relatively low cutoff frequency of the lowpass filter used in the phase locked loop detector.

Measurement of Turbulence by Optical Mixing Spectroscopy

C. P. Wang

Department of Applied Mechanics and Engineering Sciences

and

Institute for Pure and Applied Physical Sciences

University of California, San Diego, La Jolla, California 92037

Abstract

Using laser Doppler shift to measure turbulence is described in terms of optical mixing spectroscopy. The homodyne and heterodyne spectroscopy are discussed. By applying these to turbulent flow, the velocity probability density and the joint probability density can be obtained. A relation between the heterodyne power spectrum and the velocity spectrum of the turbulent flow is also obtained.

The author is indebted to Professors S. C. Lin and S. S. Penner for many helpful discussions. This research was supported by the Advanced Research Projects Agency of the Department of Defense and was monitored by the U.S. Army Research Office-Durham, Box CM, Duke Station, Durham, North Carolina 27706, under Contract DA-31-124-ARO-D-257.

I. INTRODUCTION

It is well known that when a light beam is scattered from a moving particle, its frequency will be shifted. This is called Doppler shift. Using this Doppler shift Yeh and Cummins,[1] Foreman et al.[2] and others have successfully measured the flow velocity by laser Doppler velocimeter.

Since the scattered light is scattered from a large number of particles in the flow, if all these particles are moving at the local flow velocity (this is likely to be the case), then the velocity distribution of the particles is the same as the velocity distribution of the flow. Hence it is possible to study the spatial structure of turbulent flow by analyzing the light scattered from these particles. Many investigators,[3,4,5] have done some work on the turbulence measurement by this laser Doppler technique. Recently, using the theory of optical mixing spectroscopy, Wang[6] formulated a new model for laser Doppler velocity measurement on turbulent flow. Here, based on this new model more detailed analysis is given.

In the approach here, we consider the laser beam incident on the scattering medium as the "carrier wave," the process of Doppler scattering as a modulation process and the scattered wave as a modulated wave which carries the information about the scattering medium. Then the information contained in the modulation is obtained through proper demodulation.

II. OPTICAL MIXING SPECTROSCOPY

The optical mixing spectroscopy[7,8] or light beating spectroscopy may be regarded as extensions into the optical region of devices and techniques which are conventional in radio frequency and microwave communications.

In general, a laser light is used as an incident light source, which is focused to a small scattering region to be measured. The light scattered from this scattering region is then collected by a lens and aperture system and falls on a photodetector. As is shown in Fig. 1, the output current of the photodetector is then fed to a spectrum analyzer which consists of a variable center frequency narrow band filter, a square law detector for the filter output, and a time averager to obtain the average power passing through the filter. The spectral power density thus obtained is called the homodyne spectrum. For a random stationary process this homodyne spectrum can be expressed as[7]

$$P_i^s(\omega) = 2\pi i_s^2 \delta(\omega) + \frac{i_s^2}{N} \int_{-\infty}^{\infty} \frac{R_{E^2}(\tau)}{R_{E^2}(0)} e^{i\omega\tau} d\tau + Ge i_s \qquad (1)$$

where i_s is the average current of the scattered light, N is the number of coherent areas ΔA on the photodetector, G is the gain of the photodetector, e is the charge of an electron, ω is the frequency in rad/sec, E(t) is the electric field of the scattered light, and $R_{E^2}(\tau)$ is the correlation function of $|E(t)|^2$, i.e.

$$R_{E^2}(\tau) \equiv \langle |E(t)|^2 \, |E(t+\tau)|^2 \rangle \qquad (2)$$

In Eq. (1), the first term is the dc component, which can easily be blocked out, the second term the signal spectrum and the last term corresponding to the shot noise which has a white spectrum. In general, the homodyne spectrometer not only removes the carrier frequency, but also has the effect of removing any phase information connected with the correlation function. That is, if $R_E(\tau) = \alpha(\tau) e^{i\varphi(\tau)}$, the homodyne spectrometer loses the phase information, $\varphi(\tau)$, which contains the important information on the absolute frequency shift or the absolute velocity of the scatterer.

To retain this phase information $\varphi(\tau)$, a reference signal is required. In general, this reference signal can be obtained in the following

three different arrangements,[9,10] 1) a local oscillator, or a reference light beam, may be used directly as the reference signal. This is called local oscillator heterodyne. 2) The scattered light from the same scattering region but by another coherent light beam incidented from a different direction may also be used as the reference signal. This is called differential heterodyne. 3) The scattered light from the same scattering region but collected in a different direction may also be used as the reference signal. This is called symmetric heterodyne. The relative merits of these arrangements are discussed in Ref. 9. Here, only the local oscillator heterodyne arrangement is discussed in detail. With minor modifications, the results can also be applied to the other arrangements.

Using the same light collecting and analyzing circuit system as used for homodyne spectrometer, but introducing a local oscillator or reference light beam,

$$E_{\ell o}(t) = E_o e^{-i\omega_o t} \quad . \tag{3}$$

Mixing this local oscillator field with the scattered field at the photodetector, we obtain a heterodyne spectrum. Assuming the average photocurrent due to the local oscillator is much larger than the average photocurrent due to the scattered light, the heterodyne spectrum can be expressed as[7]

$$P_i^H(\omega) \simeq 2\pi i_{\ell o}^2\, \delta(\omega) + \frac{4\epsilon^2}{N}\, i_{\ell o}\, i_s \int_{-\infty}^{\infty} \left\{ \frac{R_E(\tau)}{R_E(0)} \left[e^{i(\omega+\omega_o)\tau} + e^{-i(\omega+\omega_o)\tau} \right] \right\} d\tau$$

$$+ G e i_{\ell o}\,, \qquad (4)$$

where $i_{\ell o}$ is the average current of the local oscillator, and ϵ is the heterodyne mixing efficiency, i.e.

$$\epsilon^2 = \frac{\left| \frac{1}{\Delta A} \int_{\Delta A} E_{\ell o}(R) \cdot E^*_{sca}(R)\, dA \right|^2}{\langle E^2_{\ell o} \rangle_R \; \langle E^2_{sca} \rangle_R}\,. \qquad (5)$$

Here ΔA is the coherent area on the photodetector and R is the location of the photodetector. Physically, ϵ represents the degree to which the scattered wave front and the local oscillator has matched phase fronts over an area equal to a coherent area ΔA.

III. OPTICAL MIXING SPECTRUM OF TURBULENT FLOW

To study turbulent flow by optical mixing spectroscopy, a laser beam is used as incident light. The electric field of the light scattered from particle p, at location $\underset{\sim}{r}_p$, can be written as[6]

$$E_{sca}(t) \simeq A_p\, e^{-i(\omega_o t + \underset{\sim}{v}_p^K t) + i\varphi_p}\, \theta^{1/2}(t; \underset{\sim}{v}_p^K)\,, \qquad (6)$$

where A_p is the intensity of the scattered electron field, ω_o is the frequency of the incident light, $v_p^K = \left(\underset{\sim}{k} - \underset{\sim}{k}_o\right) \cdot v_p$, the velocity component parallel to $\underset{\sim}{k} - \underset{\sim}{k}_o$ and in the units of wavelength/sec, $\underset{\sim}{k}_o$ is the incident wave vector, $\underset{\sim}{k}$ is the scattered wave vector, φ_p is the phase factor which depends on the location of the scatterer, and $\theta(\underset{\sim}{r}_p)$ is the beam intensity distribution function. Now, we may define the probability density of velocity v_p^K, at $\underset{\sim}{r}_p$ to be $f(v_p^K; \underset{\sim}{r}_p)$. Then the correlation function of $E_{sca}(t)$ is

$$\frac{R_E(\tau)}{R_E(0)} = \frac{\langle E^*_{sca}(0)\, E_{sca}(\tau)\rangle}{\langle |E_{sca}(0)|^2\rangle}$$

$$= C' \int_V \frac{d\underset{\sim}{r}_p}{v} \int_{-\infty}^{\infty} dv_p^K \left\{ f(v_p^K; r_p)\ \theta(\tau; v_p^K)\ e^{-i(\omega_o \tau + v_p^K \tau)} \right\} \qquad (7)$$

where C' is a constant and v is the volume of the scattering region. The heterodyne spectrum then becomes

$$P_i^H(\omega) = C \int_{-\infty}^{\infty} \frac{R_E(\tau)}{R_E(0)}\, e^{i(\omega + \omega_o)\tau}\, d\tau$$

$$= C \int_V \frac{d\underset{\sim}{r}_p}{v} \int_{-\infty}^{\infty} dv_p^K \left\{ f(v_p^K; \underset{\sim}{r}_p)\ \theta(\omega; v_p^K) * \delta(\omega \pm v_p^K) \right\} \qquad (8)$$

where C is a constant, and * is the convolution product. Here the dc and short noise terms are not included. The effect of those two terms are discussed later. If some average value of v_p^K is used in θ, i.e. we assume

$$\theta(\omega; v_p^K) \simeq \theta'(\omega)$$

Then the spectrum becomes

$$P_i^H(\omega) = cf(\omega) * \theta'(\omega) \tag{9}$$

where $f(\omega)$ is the averaged probability density of velocity over the scattering region and $\theta'(\omega)$ is the averaged weighting function for the beam intensity profile. Usually, the half-width of $\theta'(\omega)$ is very narrow and can be approximated by a delta function. The heterodyne spectrum is then

$$P_i^H(\omega) \simeq cf(\omega) . \tag{10}$$

That is the spectrum obtained from heterodyne spectrometer corresponds to the probability density, $f(v_p^K)$, where v_p^K is simply replaced by ω, e.g., if the probability density is a Gaussian,

$$f(v_p^K) = \frac{1}{(2\pi)^{1/2}\sigma} \exp\left[\frac{-(v_p^K - \overline{v_p^K})^2}{2\sigma^2}\right]$$

where $\sigma = \left(\overline{(v_p^K - \bar{v}_p^K)^2} \right)^{1/2}$, then the heterodyne spectrum obtained is

$$P_i^H(\omega) \sim \frac{1}{\cdot \left(2\pi \overline{(\omega - \bar{\omega})^2} \right)^{1/2}} \exp \left[\frac{-(\omega - \bar{\omega})^2}{2\overline{(\omega - \bar{\omega})^2}} \right] .$$

Here the half-width of the spectrum corresponds to the rms velocity fluctuations.[3] However, if due to the finite beam width, $\theta'(\omega)$ may not be close to a delta function, then the measured spectrum is broadened by the convolution product of $f(\omega)$ and $\theta'(\omega)$. This is usually called Doppler ambiguity.[11] As is shown by Pike et al., the half-width of $\theta'(\omega)$ is proportional to the average velocity and inversely proportional to the beam width. Since $\theta'(\omega)$ is a known function, hence $f(\omega)$ can always be obtained from Eq. (9).

Similarly, for the homodyne spectrum, we have

$$\frac{R_{E^2}(\tau)}{R_{E^2}(0)} = c \iint \frac{d\underset{\sim}{r}_p \, d\underset{\sim}{r}_q}{v^2} \iint dv_p^K \, dv_q^K \left\{ f_J(v_p^K, v_q^K; \underset{\sim}{r}_p, \underset{\sim}{r}_q) \, \theta(\tau; v_q^K) \, \theta(\tau; v_p^K) \right.$$

$$\left. e^{i(v_p^K - v_q^K)\tau} \right\} + c \int \frac{d\underset{\sim}{r}_p}{v} \int dv_p^K \, f(v_p^K; \underset{\sim}{r}_p) \, \theta(\tau; v_p^K) \qquad (11)$$

where $f_J(v_p^K, v_q^K; \underset{\sim}{r}_p, \underset{\sim}{r}_q)$ is the joint density function of two velocities v_p^K and v_q^K at $\underset{\sim}{r}_p$ and $\underset{\sim}{r}_q$ respectively. The spectrum is then

$$P_i^S(\omega) = c\iint \frac{d\underset{\sim}{r}_p\, d\underset{\sim}{r}_q}{v^2} \iint dv_p^K\, dv_q^K \Big\{ f_J(v_p^K, v_q^K; \underset{\sim}{r}_p, \underset{\sim}{r}_q)\,[\theta(\omega; v_p^K)\,\theta(\omega; v_q^K)]$$

$$* \delta(\omega + v_p^K - v_q^K) \Big\} + c\int \frac{d\underset{\sim}{r}_p}{v} \int dv_p^K\, f(v_p^K; \underset{\sim}{r}_p)\,\theta(\omega; v_p^K) * \delta(\omega)$$

$$= c\int \frac{d\underset{\sim}{r}}{v} \int dv_p^K\, f_J(v_p^K, v_p^K + \omega; \underset{\sim}{r}) * [\theta'(\omega)]^2 + c\theta'(\omega)\,. \tag{12}$$

where $\underset{\sim}{r} = \underset{\sim}{r}_p - \underset{\sim}{r}_q$.

From this spectrum we can obtain the joint density function which can be used to calculate the velocity correlation functions. As shown by Bourke et al.,[5] this spectrum can also be used to measure the correlation length of the turbulent flow, i.e. the maximum r at which the spectrum width becomes constant.

As for the velocity correlation function and the power spectral density of a turbulent flow, a relation between the heterodyne power spectrum and the velocity spectrum of the turbulent flow is obtained.[12]

I.

$$P_i^H(\omega) = \int_{-\infty}^{\infty} \exp\left\{ -\frac{1}{\pi} \int_{-\infty}^{\infty} P_{v_1^K}(\omega) \left(\frac{\sin \frac{\omega\tau}{2}}{\omega} \right)^2 d\omega \right\} e^{-i(\omega - v_o^K)\tau} \, d\tau . \tag{13}$$

where v_o^K is the mean velocity, v_1^K is the fluctuation velocity, and $P_{v_1^K}(\omega)$ is the velocity spectrum. Because of the exponential and integral dependence, the velocity spectrum $P_{v_1^K}(\omega)$ is not sensitive to the variation of the heterodyne spectrum $P_i^H(\omega)$, hence various broadening effects, such as instrument broadening, Doppler ambiguity, etc. will not severely broaden the velocity spectrum $P_{v_1^K}(\omega)$.

VI. CONCLUSION

In conclusion, it has been demonstrated that a more complete picture of the laser Doppler velocity measurement is obtained by using the method of optical mixing spectroscopy. Using the measured homodyne spectrum and heterodyne spectrum various properties of the turbulent flow can be studied.

References

1. Y. Yeh and H. Z. Cummins, Appl. Phys. Letters 4, 176 (1964).
2. J. W. Foreman, Jr., E. W. George, J. L. Jetton, R. D. Lewis, J. R. Thornton and H. J. Watson, IEEE QE-2, 260 (1966).
3. R. J. Goldstein and W. F. Hagen, Phys. Fluids 10, 1349 (1967).
4. M. K. Mazumder and D. L. Wankum, Appl. Optics 9, 633 (1970).
5. P. J. Bourke, et al., J. Phys. A: Gen. Phys. 3, 216 (1970).
6. C. P. Wang, Appl. Phys. Letters 18, 522 (1971).
7. G. B. Benedek, "Optical Mixing Spectroscopy with Applications to Problems in Physics, Chemistry, Biology and Engineering," in Polarization, Matter and Radiation, Presses Universitaries de France, Paris, 1969.
8. H. Z. Cummins and H. L. Swinney, Progress in Optics, VIII, 135 (1970).
9. C. P. Wang, "A Unified Analysis on Laser Doppler Velocimeter" (unpublished).
10. F. Durst and J. H. Whitelaw, Proc. Roy. Soc. (London) A324, 157 (1971).
11. E. R. Pike, D. A. Jackson, P. J. Bourke and D. I. Page, J. Sci. Instr. (E), Ser. 2, 1, 727 (1968).
12. C. P. Wang, Appl. Phys. Letters (to appear May 1, 1972).

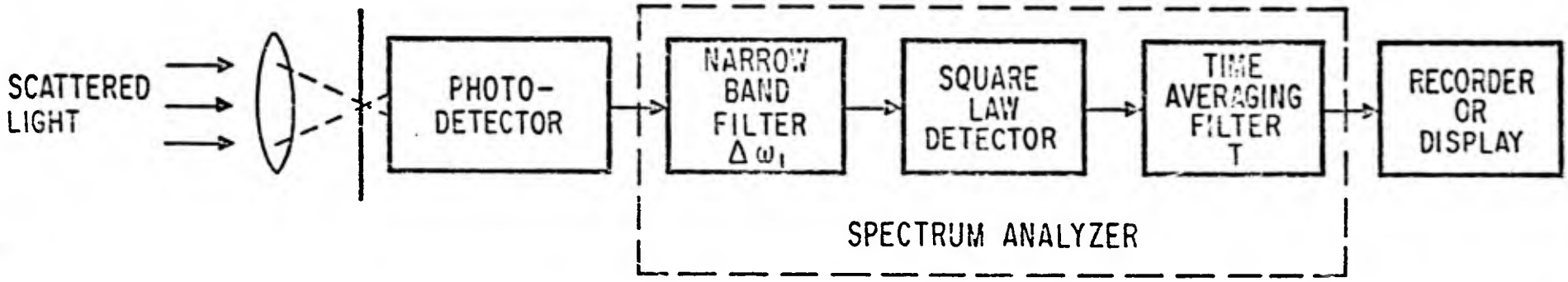

Figure 1. Block diagram of light collecting and spectrum analyzing system

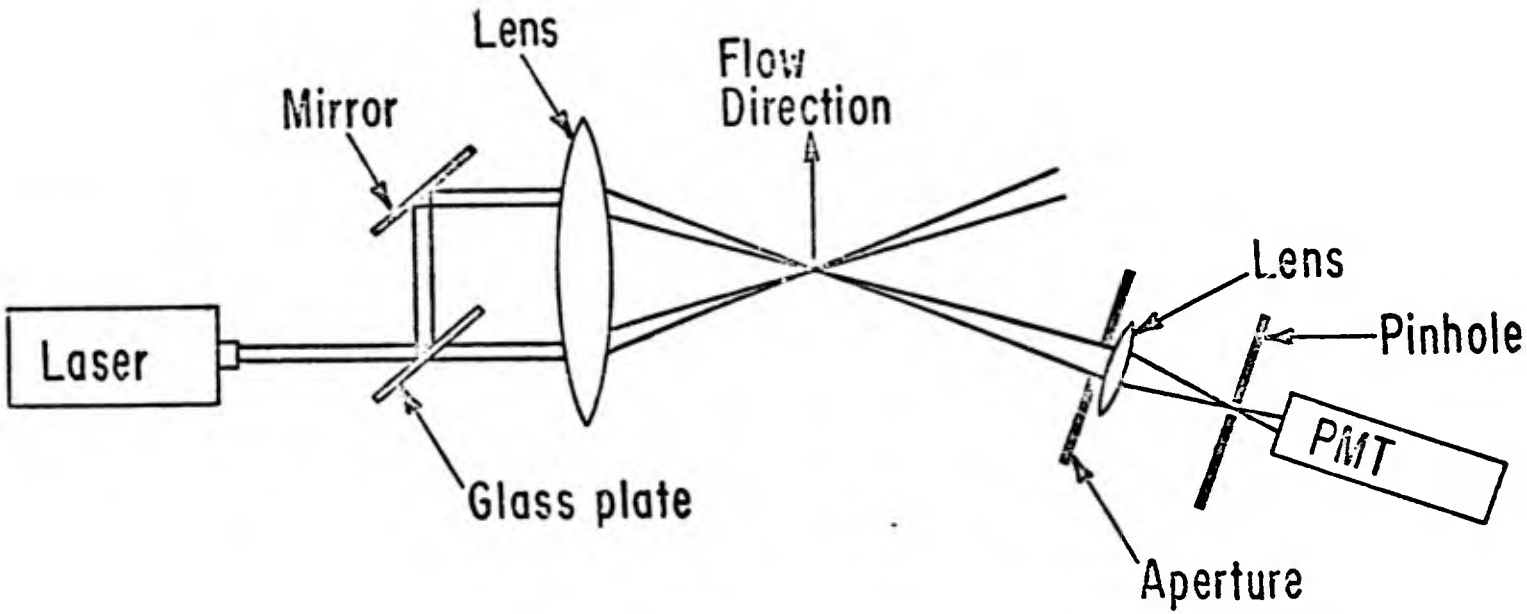

Figure 2. Local oscillator heterodyne arrangement

DISCUSSION

MAZUMDER: Did you use a helium-neon laser for your work?

WANG: No, we used a high power argon laser which we built. We can get thirty-five watts.

EDWARDS: What do you estimate the radiative half life of say a nitrogen molecule whic' you're exciting.

WANG: That's almost instantaneous for the Raman scattering. Is that the question you asked?

EDWARDS: No. I always had the impression that if you tried to scatter something by getting an individual molecule to absorb and re-excite, that the radiative half life would give problems.

WANG: What you mean is fluorescence. This is not fluorescence. This is almost instantaneous - a life time of 10^{-12} seconds.

PIKE: I would like to make a comment on nomenclature. I mentioned yesterday much of the work that we are discussing can be thought of as standard microwave stuff, and in microwave theory there are specific exact meanings to the words homodyne, heterodyne and so on. I would like to make a plea that these be used in optics as well. The meaning of homodyne in standard communication theory or radar theory is that one's local oscillator is at baseband. That is, one puts carrier information on at the same frequency as one takes it off again with a local oscillator. It's a heterodyne system. Homodyning is just heterodyning with a local oscillator tuned to the carrier frequency. There has been a lot of confusion in the field of optics because people used the term homodyne for a completely different process which is perhaps more picturesquely described as selfbeat, but which in radar we call intensity fluctuation spectroscopy. It is all very confusing and it would be very nice if people could agree to use well established terminology.

HUMPHREY: How are you proposing to separate the source of frequency of the different molecules - separating the velocity and density fluctuations.

WANG: Presumably the laser LDV is independent of the velocity fluctuation.

HUMPHREY: It isn't in reality is it?

WANG: Yes, it is independent because the energy involved in

velocity fluctuation is far less compared with the spectral line we are looking at.

MEYERS: One question that I have is not in the LDV regime. Have you considered measuring temperatures with Raman.

WANG: No, density fluctuations. Of course at constant pressures, temperature fluctuations are the same as density fluctuations.

MEYERS: So you can measure temperatures. I'm thinking of supersonic flows.

WANG: Yes. Then you have to get a profile instead of looking at one line. We haven't done the Raman work yet, but are proposing to do it. That's why I didn't present any data on that.

TURBULENCE MEASUREMENTS USING THE LASER DOPPLER VELOCIMETER

by

John W. Dunning, Jr.
NASA Lewis Research Center
Cleveland, Ohio

and

Neil S. Berman
Arizona State University
Tempe, Arizona

Although the laser Doppler velocimeter has been used for turbulence measurements in the past (1,2), no set of measurements in practical turbulent flows has been available to evaluate the instrument. In this work we examine in detail the photomultiplier signal representing the axial velocity of water within a glass pipe. We show that with proper analysis of the photomultiplier signal, the turbulent information that can be obtained in liquid flows is equivalent to recent hot film studies. In shear flows the signal from the laser Doppler velocimeter contains additional information which may be related to the average shear.

EXPERIMENTAL APPARATUS

The laser Doppler velocimeter located at the NASA Lewis Research Center is a one dimensional instrument with an optical arrangement of the Goldstein-Kreid type (3). A scattering angle of approximately 9.9 degrees as measured in water was used along with a Bragg tank which gave a static frequency shift of 30 MHz (zero velocity equals 30 MHz). The laser was a Spectra Physics Model 125. The frequency spectrum of photomultiplier signal could be directly displayed on a Hewlett-Pac 3 spectrum analyzer. Alternately the photomultiplier signal could be mixed with a signal from a local oscillator and the difference sent to an FM demodulator.

Two different demodulators were used, a fixed center frequency phase lock loop and a tunable discriminator which utilized pulse averaging demodulation.

The flow system was a recirculating water unit with an automatic level control on the head tank. The level in the head tank could be controlled to within ±1.5 mm. This is equivalent to a 0.1% control of total head. Glass pipes 1.9 cm, 2.54 cm, and 5.08 cm in diameter were used in the test section and measurements were made approximately 300 cm downstream of an entrance section. Water containing a small amount of 0.5 micron polystyrene spheres was used in the system.

SPECTRUM ANALYZER RESULTS

We consider first the spectrum analyzer display of the voltage or power in the signal as a function of frequency. This signal is the laser Doppler velocimeter frequency shift and is proportional to axial velocity. Figure 1 shows spectrum analyzer traces for turbulent flow using an average of several sweeps and a single sweep. Parameters for this figure are sweep width 10 kHz/division, band width 300 Hz, sweep time 0.2 seconds per sweep. The data were obtained with a 150 mm lens focusing the laser beam at the centerline of the 5.08 cm diameter pipe with a local mean velocity of 24.5 cm/sec (local N_{Re} = 14 000). Note that the single sweep has some width corresponding to the signal broadening due to the finite sample volume as discussed by Edwards et al. (4). It can be seen that the representation of turbulence requires long time averaging and some interpretation. The noise level is also significant. In laminar flow, similar spectrum analyzer traces in Figure 2 show no difference in signal broadening for multiple and single traces. Here the velocity is

5.25 cm/sec with the same pipe, optics and spectrum analyzer bandwidth. The other parameters are sweep width 2 kHz/division and sweep time 0.005 ms/division. The signal broadening of approximately 600 Hz at the one-half power point is considerably less than the 7500 Hz for turbulent flow. The 600 Hz can be calculated from the dimensions of the scattering volume and represents the finite volume broadening. In Figure 1 the finite volume broadening would be 2500 Hz, considerably less than the observed broadening which contains the turbulent fluctuations.

To obtain the turbulence intensity from the pictures of the spectrum analyzer traces, the finite volume broadening and noise must be subtracted. The analysis must also recognize that the white area on Figure 1 is bordered by the peaks of the single traces. The corrections are possible if Gaussian distributions are assumed but may be weighted by recent events on the screen. To avoid this problem the voltage or heights of the trace at discrete frequencies can be averaged over a suitable length of time. Figure 3 shows the result of a one second average at each point plotted as normalized power versus frequency. The solid line is a least squares fit of a Gaussian plus a linear function to the data. For this experiment at the centerline of a 2.54 cm diameter pipe, the local mean velocity was 292 cm/sec corresponding to a local Reynolds number of 86 000. The turbulence intensity was 3.1%. Using the analysis of Lumley and Panofsky (5), the "probable error" in the second moment for the one second average is ±20% and the "probable error" in the fourth moment is ±46%. The type of curve given in Figure 3 is equivalent to a velocity probability versus velocity curve and the error analyses of Lumley and Panofsky should hold.

In shear flows especially near the wall of a pipe, the probability distribution becomes wider. Figure 4 shows multiple sweeps and a single sweep on the spectrum analyzer for this case. Here the sweep width is 20 kHz/division, the bandwidth is 1.0 kHz and the sweep time is 0.02 sec/division. The location in the 5.08 cm diameter pipe is at $r/R = 0.92$ and the local mean velocity is 23.3 cm/sec. The single sweep is exactly the same as before with its width determined by the finite sample volume. The long time average, however, contains turbulence broadening, and an additional broadening due to velocity gradients in the radial direction. If this signal is treated the same as the previous one using a one second average per point, Figure 5 is obtained. The solid line represents the Gaussian plus linear fit. Obviously much longer averaging times are needed.

DEMODULATED SIGNAL

Spectrum analyzer averages or traces do not give information on the time variations of the turbulence. Therefore such information as the autocorrelation or the power density spectrum is unavailable from spectrum analyzer measurements. The probability density is available but is clouded by noise when a spectrum analyzer is used. FM demodulation techniques can be used to bypass the noise problem inherent in the spectrum analyzer and to yield a signal which can be processed to obtain the statistical data mentioned above. Basically we want to convert the frequency variations in the Doppler signal into voltage variations so that we may conveniently analyze the information content of the fluctuations. Figure 6 shows schematically the method used in this work. Optical heterodyning of the scattered and reference beams at the photomultiplier tube

gives a frequency shift, Δf, proportional to the instantaneous velocity, $\underline{u} + \underline{u}'$. This fluctuating frequency is heterodyned with a constant frequency, f, to move the signal to $|f - \Delta f|$, the center frequency of the FM demodulator. The demodulated output, after a low pass filter, is a voltage v proportional to the fluctuating velocity $\underline{u}'$. This voltage was recorded on an FM tape recorder. At a later time the tape was played back into an analog to digital conversion facility which digitized the fluctuating voltage signal and made a digital tape. In the analog to digital conversion, 13 bits were available to convert -10 to +10 volts to digital numbers from 0 to 8192. The digital tapes were processed on an IBM 360/67 computer to obtain power spectra, autocorrelations, and probability distributions.

As a test of the noise level of the electronics and the roll-off of the low pass filter a signal, frequency modulated by white noise, was made the input to the FM demodulator and processed as shown in Figure 6. The low pass filter was set at 500 Hz, and the digitizing rate at 8000 per second. The power spectrum is shown in Figure 7. The tape and digital noise level was extremely low at 2×10^{-2} mv^2/Hz.

A typical power spectral density at the centerline is shown in Figure 8 and is compared to the data of Resch (6) at the same Reynolds number. The local mean velocity was 54 cm/sec in the 2.54 cm pipe giving a local Reynolds number of 15 000 and a turbulence intensity of 3.9%. For purposes of digital analysis, the data was divided into two regions: 1) below 100 Hz was digitized at 1000 pts/sec for 16 seconds; 2) above 100 Hz was digitized at 8000 pts/sec for 2 seconds. The "probable errors" are greatest at the lower end of each frequency range and are estimated

to be 21% at 4 Hz and 12% at 100 Hz. The points shown were obtained by using the Fortran program "Rapsody" written by Brumbach (7). A Parzen filter was used to smooth the raw spectra. The interesting detail about this spectrum is the noise level appearing at 400 Hz. This is the finite volume effect. The spectrum of the finite volume broadening appears flat or perhaps slightly decreasing as frequency increases. If this level is subtracted from the spectrum, the turbulent spectrum falls on the values obtained by Resch. Similar results have been found by George and Lumley (8). The finite volume effect can also be seen in oscilloscope traces of the demodulated signal. In Figure 9 the top trace is the unfiltered signal including the high frequency finite volume effect. From the power spectrum for this experiment we can select 300 Hz as the frequency beyond which turbulence is negligible. When we use a 300 Hz low pass filter, we obtain the lower curve which represents the turbulence. It would be necessary to use such a filter to get meaningful autocorrelation and probability results for any turbulent data obtained from a laser Doppler velocimeter.

From a laminar flow analysis of the laser Doppler velocimeter (4), the standard deviation of the finite volume broadening can be used to determine the size of the sample volume in the axial direction and in the radial direction, σ_x and σ_z, respectively. For spot size we use the definition of Edwards, et al. (4). These spot sizes, which are only functions of the total optical system, are given for three different lenses in Table I. In turbulent flow (assuming Gaussian signals), for long time averages, the variance of the spectrum analyzer spectrum is approximately the sum of the variances of the turbulence broadening, the

finite volume broadening, and the velocity gradient broadening. The analysis of the demodulated signal is more complicated. Some results were given by Lumley, et al. (1) previously. We would predict, regardless of the absolute location of the finite volume broadening in the power spectral density, that the turbulent spectrum at low frequencies would be independent of the finite volume broadening. Further, the height of the spectrum of the finite volume broadening at zero frequency would be proportional to the mean velocity in the volume and the reciprocal of the axial dimension of the sample volume if no velocity gradients are present. If the finite volume broadening spectrum is flat at least as far out in frequency as the intersection with the turbulent curve, we can use the level at the intersection as representing the level at zero frequency.

To study the effect of sample volume size or lens focal length on the finite volume broadening spectra, we have performed several experiments whose results are given in Figures 10, 11, and 12. Figure 10 represents the tail of the spectrum from the flow in the 2.54 cm pipe at a mean local velocity at the centerline of 54 cm/sec. The local Reynolds number is 15 000 and the turbulence intensity is 3.9%. We have converted the vertical scale to units of Hz (deviation from the mean) squared per Hz frequency to compare the result to that predicted by George and Lumley (8). Although the height of the two flat portions of the curves, representing the finite volume broadening, varies correctly with the scattering volume size, the levels predicted by George and Lumley given by the marks on the right are high. The digitizing rate for this experiment was 8000 per sec and the low pass filter was set at 2500 Hz. An EMR Model

4140 tunable discriminator with a 5 pole Bessel low pass output filter was used with a center frequency of 200 kHz and a percent bandedge of ±30%. The sample time was 2 seconds. The waves in the spectrum are characteristic of the filter.

A similar experiment was run using a lower Reynolds number, 6000, and an EMR model 167 phase lock loop demodulator. The center frequency was 185 kHz and the bandedge deviation was ±16.5 kHz. An external 4 pole Butterworth bandpass filter (0.2-2000 Hz) was used before taping and a 6 pole Bessel low pass filter set at 2000 Hz was installed before the digitizer to obtain the data shown in Figure 11. For the two lenses used in Figure 10 the results are the same. Here at the centerline of a 1.9 cm pipe the velocity was 28 cm/sec and the turbulence intensity 3.9%. The finite volume broadening is low enough so that some drop off from a flat spectrum can be seen for the larger focal length lens and the spectrum could be interpreted to be higher than an extrapolation from the previous curve thus agreeing with the prediction of George and Lumley. Therefore, the 50 cm focal length lens was used and its spectrum is higher than predicted. The marks on the right side again are the values of George and Lumley. Clearly there is some other effect contributing. Since the effect increases with focal length, we suspect the velocity gradients across the sample volume in the radial direction.

Using the same apparatus and procedure as in Figure 11, we measured the spectrum at r/R approximately 0.8 where the velocity gradient for this low Reynolds number is quite high. The local mean velocity was 26 cm/sec, almost the same as the previous centerline run, but the turbulence intensity was doubled and equal to about 7.7%. In Figure 12 the

tails of the spectra for the three lenses are compared. The lines on the left are the centerline levels adjusted for the mean velocity difference. Note that the 3.75 cm focal length lens which gives a very small sample volume in all directions gives the same noise level as at the centerline, but the others are much higher. In fact the 50 cm focal length lens giving the largest radial dimension leads to a noise level considerably higher than that predicted for finite volume broadening alone. We conclude that the additional effect is due to velocity gradients. Although, again, the complete spectrum must be known before a proper analysis of the turbulence can be made, the additional information is related to the shear in the sample volume. George and Lumley predict that two point correlation experiments can be used to eliminate the finite volume broadening since when the volumes do not overlap the signals will not correlate. This may not be true for the additional source of broadening. Clearly there is more work to be done in use of the laser Doppler velocimeter in shear fields.

COMPARISON OF PROBABILITY DISTRIBUTIONS

FM demodulation and subsequent removal of the finite volume broadening leads to a remarkably noise free signal that can be used to obtain velocity probability distributions. Such a result can be compared to the spectrum analyzer trace. In Figure 13 we show the probability distribution at the centerline of the 2.54 cm pipe for the same run as Figure 3. The local Reynolds number was 86 000, mean local velocity, 292 cm/sec, and turbulence intensity 3.15%. For the digital analysis we used a rate of 1000 points/sec for 21.648 sec. Based on a significant frequency of 10 Hz, the "probable error" is 4% in the second moment and 10% for the fourth moment. The skewness of -0.516 and flatness of 3.23 agree with

recent data of Bose (9). This distribution appears on a semi-log plot to be decidedly non-Gaussian, however, the departure from Gaussian behavior within the first two standard deviations is small. When we compare Figures 3 and 13 on the same scales, Figure 14 is obtained. Here the solid line is the digital analysis and the dots correspond to the spectrum analyzer trace with the linear noise trends removed. The two curves can be made to coincide by subtracting the additional noise in the spectrum analyzer trace.

This noise appears to be a function of signal and is shaped by a band pass filter which follows the photomultiplier in the apparatus used in this study.

CONCLUSIONS

As a final demonstration of the ability of the laser Doppler velocimeter we show the complete corrected spectra in Figure 15 for the three Reynolds numbers that have been used in this work. The form is similar to that given by Resch and the area under the curve is normalized to 1. This graph shows that the data obtainable in liquid flows where the turbulence intensity is as large as that obtainable at pipe centerlines in fully developed flow is comparable to hot film work. We have also shown that additional information is available from the LDV signals in shear flows.

This paper has emphasized the correction of the unique pitfalls in the analysis of laser Doppler data. Without subtraction of the finite volume and other broadening, use of correct low pass filters, and sufficient averaging time, the data can be easily misinterpreted. We are confident that the laser Doppler technique is a valuable aid to the study

of turbulence and can provide low frequency turbulent information unobtainable by any other means.

REFERENCES

1. J. L. Lumley, W. K. George and Y. Kobashi, "The influence of ambiguity and noise on the measurement of turbulent spectra by Doppler scattering," in Turbulence Measurements in Liquids, ed. by G. K Patterson and J. C. Zakin, Department of Chemical Engineering, University of Missouri-Rolla, 1971.

2. R. J. Goldstein, R. J. Adrian and D. K. Kreid, "Turbulent and transition pipe flow of dilute aqueous polymer solutions," I & EC Fundamentals, 8, 498 (1969).

3. R. J. Goldstein, and D. K Kreid, J. Appl. Mech, "Measurement of Laminar Flow Development in a Square Duct Using a Laser Doppler Flowmeter," 34-E, 813 (1967).

4. R. V. Edwards, John C. Angus, M. J. French and J. W. Dunning, "Spectral analysis of the signal from the laser Doppler flowmeter: Time Independent Systems," J. Appl. Phys., 42, 837 (1971).

5. J. L. Lumley and H. A. Panofsky, "The structure of atmospheric turbulence," Interscience, New York, 1964.

6. F. Resch and M. Coantic, "Etude sur le fil chaud et le film chand dan L'eau," LaHouille Blanch 1969, 151 (1969).

7. R. P. Brumback, "Digital computer routines for power spectral analysis," AC Electronics, Santa Barbara, California, July 1968.

8. W. K. George and J. L. Lumley, "Limitations on the measurement of turbulence using a laser Doppler velocimeter," Preprint 1345 ASCE National Water Resources Engineering Meeting, Phoenix, Arizona, January, 1971.

9. B. Bose, "Some measurement in pipe flow," AIAA Journal, 9, 1405 (1971).

Table I

CHARACTERISTICS OF LENSES FROM LAMINAR FLOW

NOMINAL FOCAL LENGTH, CM	$\sigma_{x'}$ μM	$\sigma_{z'}$ μM
3.75	3	15
15	7	140
50	20	400

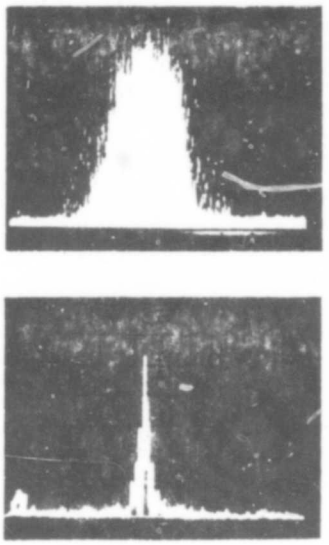

Figure 1

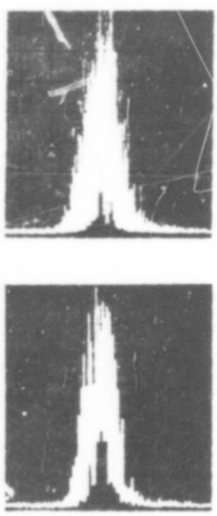

Figure 2

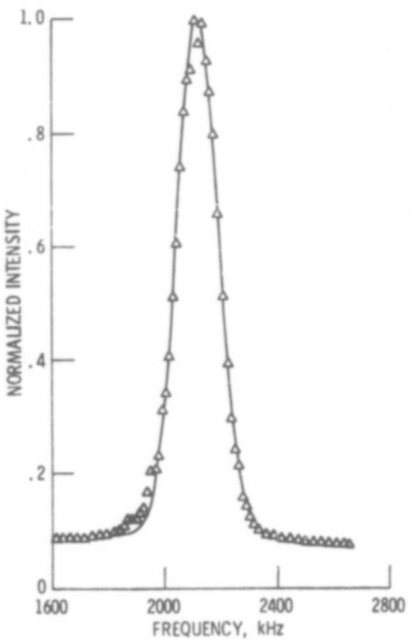

Figure 3

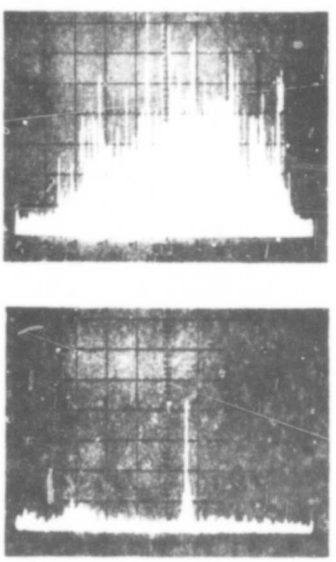

Figure 4

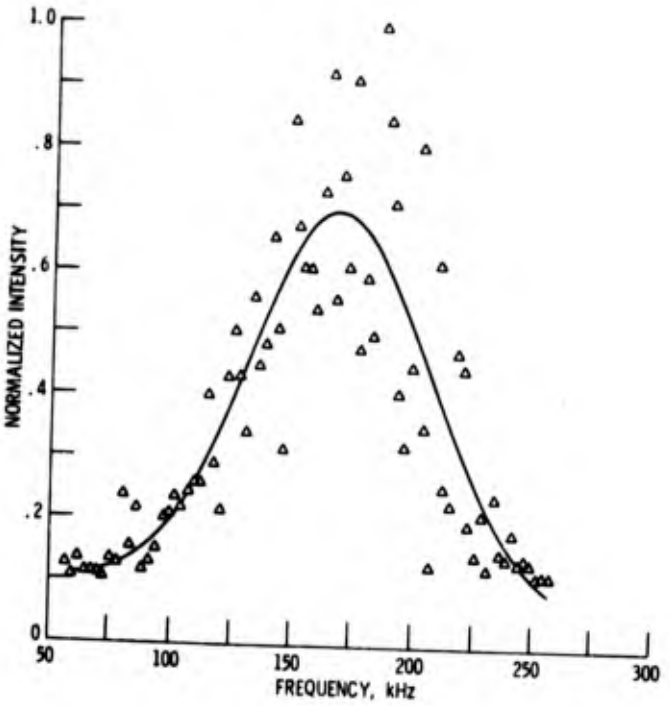

Figure 5

$$\Delta f = \frac{2\eta(\underline{u} + \underline{u}')}{\lambda} \sin\frac{\theta}{2}$$

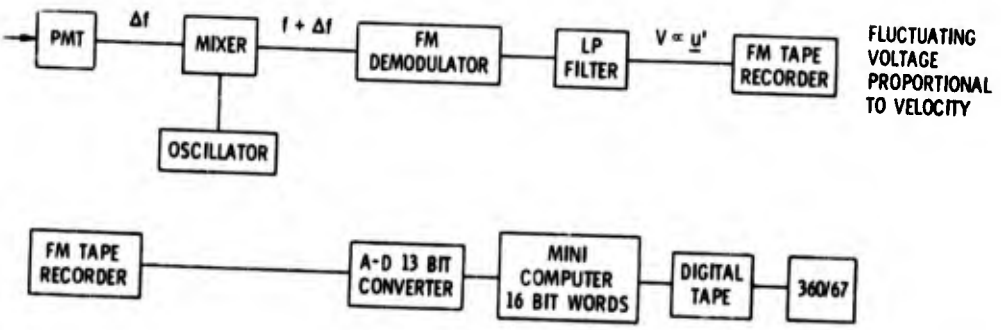

Figure 6

Figure 7

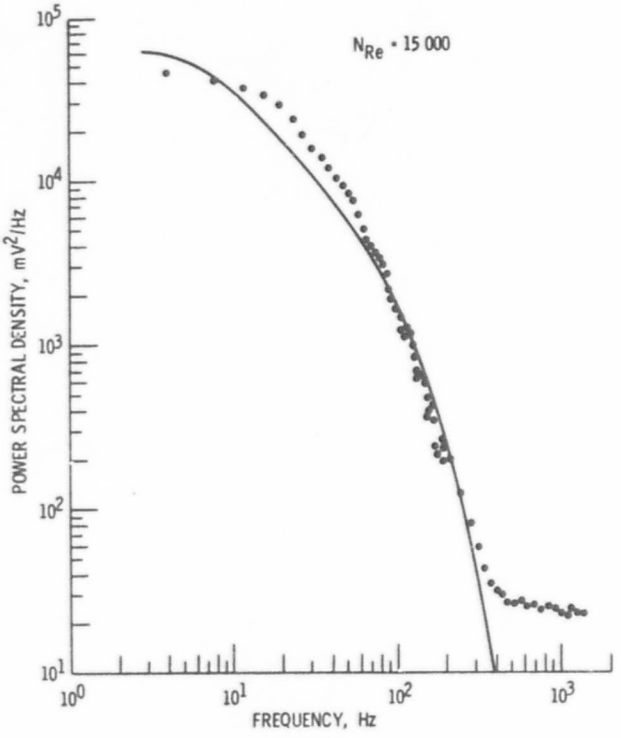

Figure 8

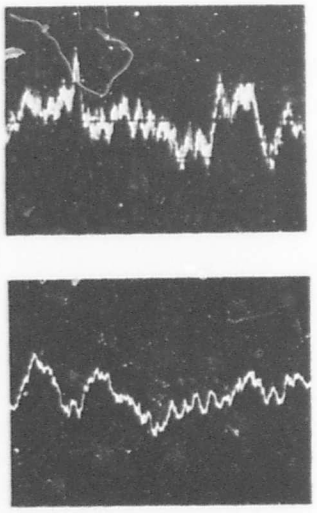

Figure 9

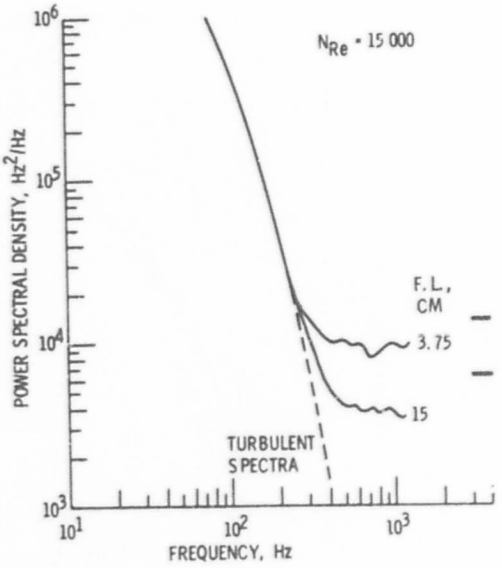

Figure 10

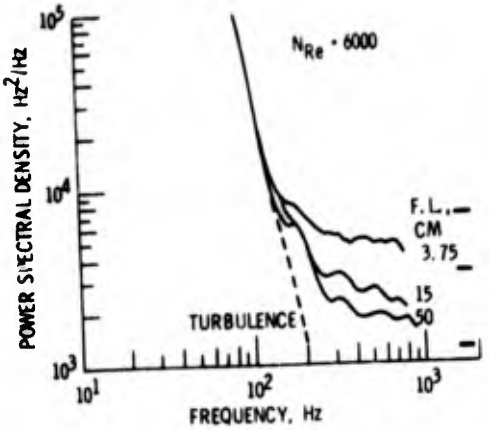

Figure 11

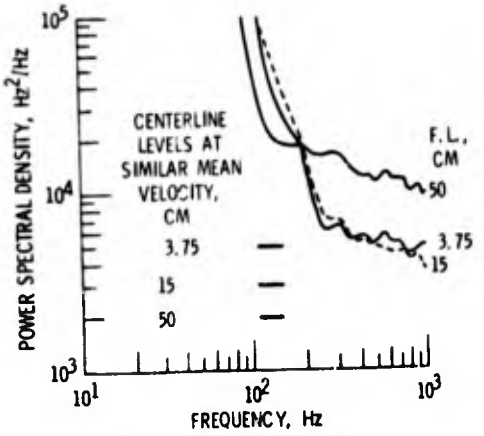

Figure 12

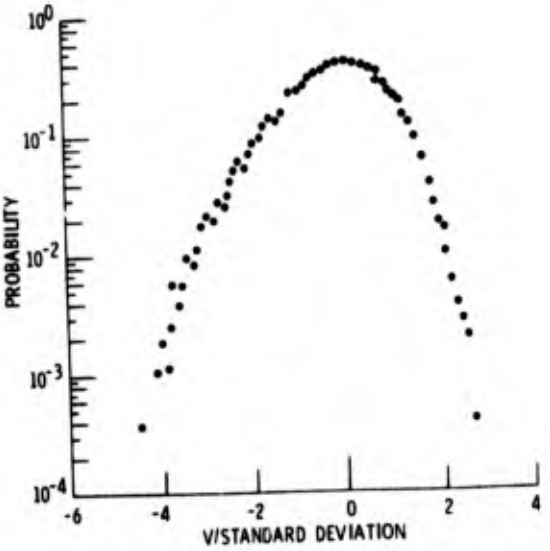

Figure 13

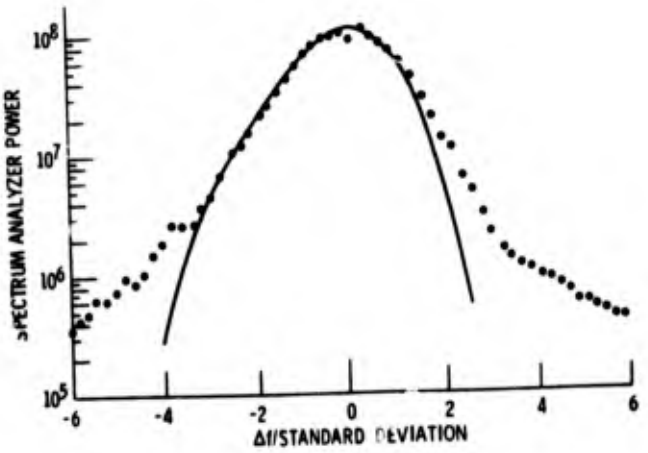

Figure 14

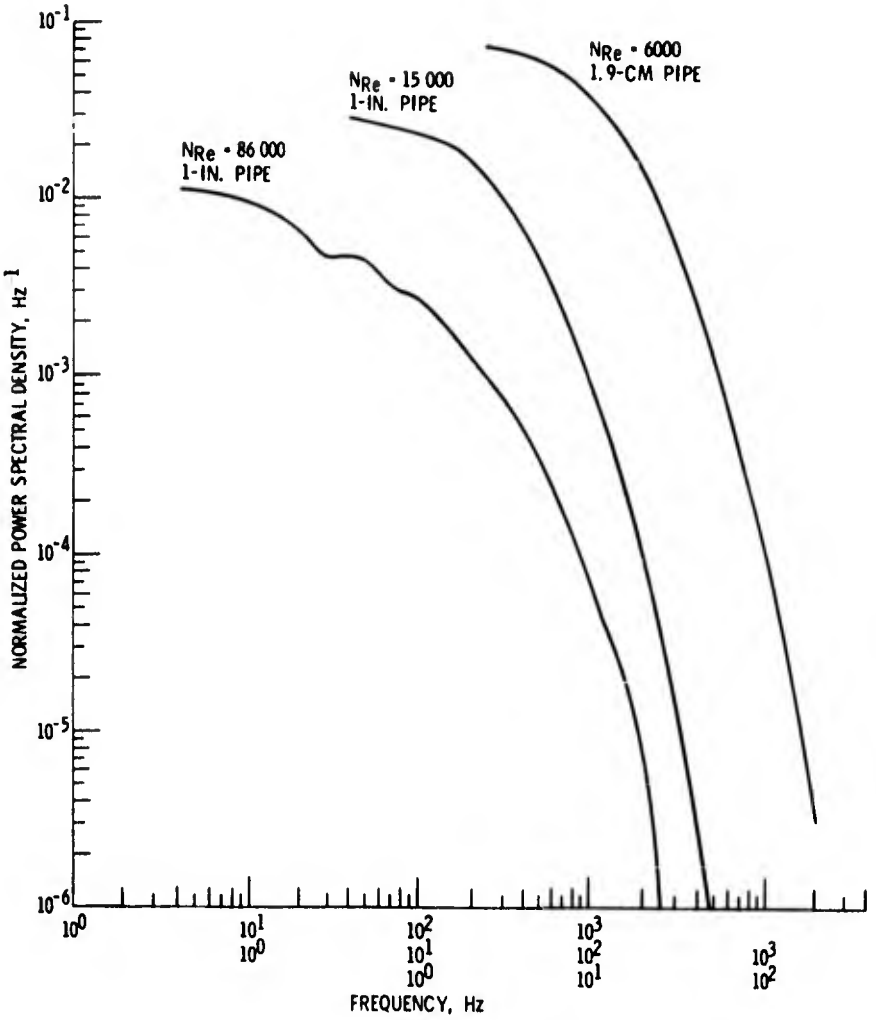
NRe = 6000
1.9-CM PIPE
NRe = 15 000
1-IN. PIPE
NRe = 86 000
1-IN. PIPE
NORMALIZED POWER SPECTRAL DENSITY, Hz⁻¹
FREQUENCY, Hz

Figure 15

GEORGE: When I showed the slide correlation, I remarked that we had pieced the asymptotic parts together. Our corrected analysis agrees with your result measured on the centerline with the exception of the 50 millimeter case. You mentioned you think you might have some velocity gradient problems. I would add that that may very well be turbulent broadening.

DUNNING: We hope to do an experiment this summer that will provide conclusive data in this area.

GEORGE: I made a calculation and concluded that on the centerline turbulent broadening is going to be the first one you see. You're really not going to see velocity gradient broadening until you get to extremely large sample volume sizes. Near the wall in the viscous sublayer the velocity gradient broadening will probably dominate the turbulent broadening. If you get into the logarithmic region they are all about the same.

DUNNING: I think what we really need is some conclusive data.

GEORGE: Yes. Some high Reynolds data - small microscale.

WELCH: I would like to make a statement first then ask a question. First, the spectrum analyzer and the scope can be used to play a number of games. One thing you can do if you have an infinite amount of time is just display the signal on the face of the scope and film it on single sweep. Of course you have to have a lot of volts in order to do this. As long as you realize that phase interference, volume doppler broadening and so forth are in there, in general you can pin these things down with the scope traces. You can actually see the phase interference producing modulation and you can see the bursts coming through. So you can get essentially the same general data if you have sufficient time. But we tried to get some data in a rectangular channel from about 300 kHz at a low velocity to whatever it was at 200 feet per second. Without any doctoring at all we ran into a situation where we had the broadening you both are talking about at about 1.5 orders of magnitude. We were never at the higher velocity before the noise - dropout noise, - phase interference, and so forth dominated. It began to level off at about 1.5 orders of magnitude.

DUNNING: You had a pretty low level of turbulence.

WELCH: Yes. Very small near the centerline. If you go to the wall then you've got other problems, of course.

DUNNING: This data, I should have said, was taken using water in one and two inch pipes with levels of turbulence around three or four percent. If you have higher levels of turbulence, then you're going to get a lot more turbulent energy spectrum. Bill's slides show this very nicely. He has a very low percent turbulence (about one percent) and he gets less than an order of magnitude of turbulent energy spectrum. The

spectrum of the signal can be approximated by the square root of the sum of the squares of the spectrum of the turbulence and the spectrum of the noise.

WELCH: We found the dropout rate to be the primary factor causing problems in our measurements. I'm just talking about that as a problem. I presume from what you said that the 1.5 order of magnitude figure is reasonable.

DUNNING: From your experiment, yes I would think so.

SHIH: I'd like to make some comments. I have a feeling listening to this talk this morning - particularly this session - that I'm back with the hot-wire people 10 years ago. It seems we are talking about the same things now. Can we come up and say which is better?

DUNNING: Each method has its own application. There are certainly some applications where the hot wire will have obvious advantages such as the measurement of the high frequency end of the turbulence spectrum.

SHIH: I think that's a big question though - particularly close to the wall. I have grave doubts whether we can get good measurements.

DUNNING: I think in the wall region may be where it's most valuable since the technique does not require a probe to disturb the flow.

SHIH: Number two comment is this. I think we should be thinking about three-dimensional flow. I think we've been playing this one-dimensional, two dimensional game too long.

DUNNING: You have to get it working first. You have to start somewhere.

ASHER: Just a little bit of rebuttal - you have to walk before you can run. I agree with you about the three-dimensional flows, but when you go into three-dimensional flows I would rather have a laser doppler system than some of the other techniques I have heard mentioned in private and also in public using a hot wire. If you've done it, you know what I mean. I was going to ask a question - if you could have done this data over again with some kind of quality control over the bursts that were coming in, the data that you were taking, perhaps this would alleviate some of the broadening that you saw. I think this was alluded to in the first response.

DUNNING: Let me put it this way. Some of this was done using a phase-lock-loop device from which I could get an idea of the dropout rate. Dropout rates were on the order of 5 to 10 percent and it didn't seem to affect us.

BERMAN: If we had gone further out in frequency then we might have seen it.

DUNNING: Right. Dropout on the phase-lock loop gives a short rise fine voltage excursion at the output. These rapid changes in the output contribute a white noise component to the spectrum which may be visible if one looks at a high enough frequency.

ASHER: I quess my comment is directed to anyone that feels these problems cannot be adequately taken care of. You made a major contribution and I think as we continue - as we start running faster and faster - these problems will be taken care of very easily. In fact I know they will.

DUNNING: It is a degree of sophistication.

GEORGE: John, you showed that you tried to improve the signal by cutting the filter right where the ambiguity began.

DUNNING: No, I didn't mean to imply that you could improve the signal by filtering. However, in order to obtain an auto correlation which represents that part of the turbulent spectrum that is not masked by noise (i.e. long correlation times) a filter should be used to eliminate the noise. Then one must take care not to place any significance in the correlation for times smaller than the reciprocal of the filter cutoff frequency.

TECHNICAL SESSION V - APPLICATIONS A

Session Chairman: W. Shaffernocker

284 B

LASER DOPPLER INSTRUMENTATION FOR FLUIDICS RESEARCH

by

Cornelius C. Shih
Professor and Chairman
Department of Fluid and Thermal Engineering
The University of Alabama in Huntsville

Introduction

Development of the laser Doppler heterodyne technique for velocity measurements was initiated by pioneers such as Yea and Cummins[1] several years ago. Since then, there have been numerous modifications and improvements of the technique based on the optical heterodyne principle. Further development of the technique has proved its general applicability to flows of both liquids and gases if a proper concentration of suspended particles or tracers and a sufficient power output of laser beam are made available in the flows.

In principle, this technique is based on the relationship between the flow velocity and the Doppler frequency shift of coherent, monochromatic light scattered from tracers suspended in a fluid flow. Two coherent monochromatic light beams with different frequencies resulting from the Doppler shift are then directed coincidentally onto the photosensitive surface of a photomultiplier tube, producing an optical heterodyne effect. This heterodyne effect leads to an output of electrical beat signal equal to the frequency difference between the two incident light beams. The velocity of the fluid flow can be determined through a measurement of the beat signal frequency, knowing geometric parameters of the optical system.

Advantages of the laser Doppler instrumentation over most conventional instruments for velocity measurement are: 1) no measuring probe to disturb the flow; 2) high frequency response in the instrumentation system suitable for transient flow applications; 3) small sampling volume in localized measurements; 4) simple and

[1] Yea, Y. and Cummins, H. Z., "Localized Fluid Flow Measurements with an He-Ne Laser Spectrometer", Appl. Phys. Letters, Vol. 4, pp 176-178, May 1964.

minimum calibration. It does, however, have some disadvantages as follows: 1) no sense of direction but magnitude of the velocity measurable by this technique; 2) critical and often tedious alignment and focusing of the optical apparatus; 3) slippage of tracers from the fluid flow; 4) requires transparent flow boundaries.

Despite the shortcomings mentioned, consideration of the advantages has overwhelmingly justified the application of laser Doppler instrumentation for the fluidics research. Specifically, flow characteristics in terms of velocity distribution over a rather small flow field in the fluidic device can be measured with this instrumental technique at better accuracy.

Therefore, projects have been initiated at the Fluid Dynamics Laboratory of the University of Alabama in Huntsville in order to achieve the following objectives:

1) Verify the feasibility of the instrumentation system with a spinning circular disc at regulated speeds of rotation which can be used as a means of calibration.

2) Determine the relationship between tracer concentration and laser power requirement with respect to the instrumentation feasibility for gas and liquid flows.

3) Design a laser Doppler instrumentation system for velocity measurement in a typical liquid amplifier and map velocity distribution curves in the two-dimensional flow field.

4) Design a laser Doppler instrumentation system for velocity measurement in a typical supersonic fluidic amplifier and map velocity distribution curves in the two-dimensional flow field.

5) Determine the feasibility of the instrumentation system with necessary modifications for measuring hot gas velocity associated with missile control systems.

Theoretical and Design Considerations

As the coherent and monochromatic laser beam is directed into a tracer-laden flow, it is scattered by the tracers causing the frequency shift of optical Doppler signal without perturbation of the flow field by photons. Through an

optical system, this Doppler frequency-shifted radiation is then mixed coincidentally with a known optical frequency of the local oscillator, i.e., the primary beam, to produce a sufficiently low beat frequency, resulting from the optical Doppler heterodyne phenomenon. The beat frequency, then, is converted into a voltage output through the photomultiplier and is represented with the intensity versus frequency relationship on a spectrum analyzer. The signal on the spectrum analyzer with a probability distribution function is a measure of the velocity distribution in a given scattering volume.

The equation of frequency shift due to the Doppler heterodyne effect on the scattered and incident beams is given by

$$f = \frac{(\cos\theta + \sin\beta)V}{\lambda} \tag{1}$$

where f denotes the frequency shift, V the tracer velocity, λ the wave length outside the fluid boundary, θ the angle formed by the incident beam and the fluid boundary, β the angle formed by the scattered beam and the normal of the fluid boundary as shown in Figure 1. The index of refraction can be shown to be excluded in Eq. (1). When the incident beam is oriented perpendicular to the flow direction, Eq. (1) may be simplified as

$$f = \frac{V \sin\beta}{\lambda} \tag{2}$$

Although the frequency shift f includes a sign describing the direction of a velocity vector, the electronic equipment measures only the magnitude of the frequency shift, resulting in only the magnitude of the velocity measured through this technique. However, the equations presented show that calibration of the instrumentation system for velocity versus frequency is theoretically simple and minimum provided that the wave length λ and scattering and incident angles β and θ are known.

While the instrumentation theory is rather simple, practical details in the design and development of a workable system of laser Doppler instrumentation are considerably difficult to learn and frequently through trial-and-error methods. Some valuable findings from previous experiences in theory and practice are summarized in the following guidelines for the design and development of the instrumentation system:

1) The power of a laser beam scattered by tracers is approximately proportional to the incident beam power and is inversely proportional to λ^4. Therefore, high output power and short wavelength are recommended in the selection of a laser.

2) The path length difference between the scattered and incident beams should be minimized.

3) The gas molecules cannot be used as scattering sources because of their high molecular activities compared with the flow velocity to be measured. This necessitates the use of natural or artificial contaminants or tracers. However, in liquid flows, the tracers may not be needed since the molecule mass of liquids is sufficiently large to ensure that the signal from the flow velocity surpasses the noise due to molecular activities.

4) In the design of an optical system, the scattering angle in the forward scattering direction must be small, say 5 to 10 degrees, in order to remain within the frequency response characteristics of conventional photomultipliers for high velocities up to 2000 or 3000 ft/sec and to reduce required tracer concentration for a given signal intensity.

5) According to a theoretical analysis of two-phase flow effects,[2] the frequency spectrum of motion of a one-micron particle is expected to follow the mean square motion of the fluid to within one percent. It may be deduced that the error due to tracer slippage from the fluid is negligible.

---

[2] Huffaker, R. M., Fuller, C. E. and Lawrence, T. R., "Application of Laser Doppler Velocity Instrumentation to the Measurement of Jet Turbulence", SAE Paper No. 690266.

Development of Instrumentation Systems

In order to prove the feasibility and gain competence in using the instrument, a one-dimensional assembly shown in Figure 1 was constructed with the forward scattering scheme. The scattering angle of 10 degrees was selected to gain a sufficiently high accuracy in readout, to remain within the frequency response characteristics and to reduce required concentration of tracers.

A transparent plastic disc rotated by a variable speed electric motor was used for the initial velocity measurements, serving at the same time as a calibrating device for the instrument. The surface of one side of the disc was roughened with sandpaper to enhance light scattering. With proper alignment and focusing, velocities ranging from 1 to 100 ft/sec were measured with excellent accuracy, resulting in the velocity coefficient calibrated to be unity. For the disc experiment, one milliwatt was sufficient as the power required for the laser.

After the disc experiment was successful, a one-inch diameter glass tube flowing water from the public water supply was placed in the instrumentation system for measuring velocity at the center of a tube section. By adding small concentrations of milk to the water, both laminar and turbulent flow velocities were measured even with the one milliwatt laser. However, with a 100 milliwatt laser, high quality measurements were obtained without adding contaminants to the water.

These initial experiments demonstrated that the accuracy of alignment, focusing and proper attenuation of the reference beam are important factors in obtaining good signals.

After completing these one-dimensional measurements, a two-dimensional system was designed and constructed for simultaneously measuring two orthogonal components of a velocity vector using a single photomultiplier tube. A schematic of the system is shown in Figure 2. The credibility of the technique was demonstrated by obtaining the two tangential velocity components of the rotating plastic wheel. A photograph of the spectrum analyzer trace, in which both velocity components of the rotating disc are evident, is presented in Figure 3.

The obvious advantage of this system is in the economy of using one photomultiplier tube for two components rather than two tubes for two components. However, efforts to obtain two-dimensional measurements in the fluid amplifier using the one-tube system were unsuccessful due to a combination of the increased alignment difficulty, the high turbulence level in the fluid and the low scattering particle concentration in the water from the public utility.

Instead of consuming excessive amounts of time for overcoming these technical difficulties, the two component measurements were made separately rather than simultaneously. This was accomplished by first surveying the flow field at predetermined locations with the optics adjusted to measure the velocity component parallel to the fluid amplifier center line. Then the optics were rotated so that the velocity component at 45 degrees from the center line was obtained at the same location and the same flow rate. The result was a two-dimensional survey of the flow field, although the components were not measured simultaneously as was originally planned. Figures 4 and 5 present a schematic of the subsequent instrumentation system and a general view of the optics assembly.

The bistable liquid amplifier of which the velocity survey was made is shown in Figure 6. The plexiglass upper and lower bounding surfaces provided transmittance of the reference and scattered beams through the flow field. Figure 7 illustrates an open loop water flow system used for providing water supply at a desired rate to the power nozzle and control port of the amplifier. The tank-amplifier assembly was mounted on a two-dimensional screw mechanism to permit precise movement of the fluid amplifier. Thus, the velocity survey was accomplished by maintaining the laser beam and optics stationary and moving the fluid amplifier so that the beam passed through the flow field at the desired measurement location. Figure 8 provides a general view of the two-dimensional experimental apparatus.

Two-Dimensional Velocity Surveys in the Bistable Liquid Amplifier

Velocity measurements in two components at 45 degrees of each other were made at many pre-selected locations throughout the flow field from the nozzle throat to a section 5/8-inches downstream of the flow splitter apex in the exit channels. The measurements were made by recording the Doppler shifted frequencies, as displayed on a spectrum analyzer, for each of the desired locations.

The quality of the Doppler shifted frequencies was observed to decrease with increasing flow rate and light scattering volume which is approximately 3.16×10^{-3} cm^3 in this study. In Figures 9 through 12, velocity measurements at the throat centerline represented by spectrum analyzer traces for various flow rates are shown. A comparison of the photographs shows that, as the velocity increases, the signal to noise ratio decreases and the signal spreads and becomes less distinct. This phenomenon may be attributed to increasing turbulence with increasing flow rate through the fluid amplifier.

Prior to the velocity survey, the type, size, and concentration of tracers in the tap water were determined through a series of sampling tests. The particles collected by a filter were primarily brown clay and ranged approximately from 5 to 20 microns in size. The concentration in the water was determined to be approximately 350 particles per cubic centimeter. This is much lower than the minimum concentration suggested by Foreman and Lewis[3] of 60,000 particles per cubic centimeter and indicates that better quality signals could probably be obtained by increasing the concentration.

The flow field was surveyed to obtain two-dimensional velocity vectors at pre-selected locations for various flow rates with and without control flow. Velocity components in a direction parallel to the fluid amplifier center line, $V_{(0)}$, and then in a direction at 45 degrees from the center line, $V_{(45)}$, were obtained as shown in Figure 13. The resultant velocity vector was determined by the following equations:

$$|\vec{V}| = \sqrt{V_{(0)}^2 + \left[\frac{V_{(45)}}{\cos 45^\circ} - V_{(0)}\right]^2} \qquad (3)$$

$$\psi = \cos^{-1} \frac{V_{(0)}}{|\vec{V}|} \qquad (4)$$

Due to the sign convention of downstream-positive and upstream-negative for the components, two possibilities exist for the resultant velocity magnitude, and four

[3] Foreman, J. W., Jr. and Lewis, R. D., "Effects of Optical Parameters in the Laser Doppler Velocimeter," Brown Engineering Company, Inc., Technical Note R-230, January 1967.

possibilities exist for the direction according to Equations (3) and (4), respectively.

Since the laser Doppler instrumentation cannot measure the flow direction, the appropriate signs for the velocity components in the recirculating region where the velocity directions were unknown were ascertained by flow visualization with dye and small air bubble injections. The flow paths of the dye and air bubbles were sketched for cases with and without control flow and presented in Figures 14 and 15. From these figures, component signs for locations within the recirculating region were determined, and the resultant velocity vectors were calculated for all locations using Equations (3) and (4). Typical results are graphically shown in Figures 16 through 19 for various flow conditions. The magnitude for each location is indicated, accompanied by an arrow which is both proportional to the magnitude (ft/sec) and in the direction of the velocity vector.

The flow fields were in general found to consist primarily of a main jet which was attached to one of the side walls and a large recirculating vortex which filled the remaining flow area. The recirculating region is characterized by a generally circular velocity pattern and a sharp reduction in velocity magnitude. However, the laser Doppler instrumentation failed to identify the separation bubble and the associated reattachment point for all the flow rates, because the bubble was too small.

In Figures 20 and 21, non-dimensionalized velocity components along the amplifier center line were plotted against the distance normal to the center line for various flow rates, representing a flow cross-section perpendicular to the center line in the fluid amplifier at a specified distance y (= 2.0 in.) downstream from the throat. A comparison of Figures 20 and 21 demonstrates the effect of control flow upon the velocity profiles showing the switch of flow. These figures also signify a similarity in velocity profiles for all flow rates tested for the Reynolds numbers at the throat ranging from 4,800 to 29,000.

Figure 22 presents a comparison of some of the velocity profiles obtained in this study with the mean profile from similar measurements by Bourque and Newman[4] in their study of jet reattachment to an inclined wall. The velocity profiles plotted are sufficiently far removed from the throat to ensure that no effects of reattachment

[4] Borque, C. and Newman, B. G., "Reattachment of a Two-Dimensional Incompressible Jet to an Adjacent Flat Plate," Aeronautical Quarterly, Vol. 11, August 1960.

are present. The normalizing velocity parameter is the maximum velocity Vm for each cross-section and the normalizing length $d_{m/2}$ is the larger distance from the wall at which the velocity equals one-half the maximum velocity for each cross-section. The comparison indicates a fair similarity. However, the data deviation in the region of the attached jet core may be attributed to the slight difference in the boundary geometry causing a circulating vortex adjacent to the attaching jet in the present study.

As a result of this study, the following recommendations may be in order for the improvement of the laser Doppler instrumentation for liquid amplifiers:

1. The signal quality can be improved by increasing the tracer concentration.
2. For long-duration tests, the concentration increase can best be accomplished by using a closed-loop system and adding the necessary contaminants.
3. Signal conditioning devices such as signal integrators can be used to aid in signal detection and tracking.
4. Better methods of aligning and focusing the beams are needed for obtaining signals of high quality.

Details of the study in this section are reported by Yarbrough in his M. S. thesis.[5]

Two-Dimensional Velocity Surveys in Supersonic Fluidic Amplifiers

A laser Doppler instrumentation system for velocity measurements in subsonic and supersonic jets has been developed and reported by Duggan and the author.[6] However, technical details of conducting a velocity survey in a supersonic fluidic amplifier are yet to be achieved.

---

[5] Yarbrough, J. W., "An Experimental Investigation of Velocity Fields in a Bistable Liquid Amplifier Using Laser Doppler Instrumentation," M. S. Thesis, The University of Alabama in Huntsville, 1970.

[6] Duggan, J. B. and Shih, C. C., "Development of a Laser Doppler Instrumentation System for Velocity Measurements in Subsonic and Supersonic Jets," Proceedings, AIAA Testing Conference, March 1971.

Feasibility Study of Velocity Measurement in Solid Propellant Rocket Exhaust

A preliminary experimental investigation was made to determine the feasibility of measuring velocities in the exhaust plumes of solid propellant rocket motors by use of the laser Doppler shift measurement technique. In addition, the use of magnetic tapes for recording transient test results was also studied. Although the data obtained from the single hot gas test did not provide a well defined exhaust velocity measurement, a velocity distribution in the vicinity of 4000 ft/sec was observed; and it was found that the data could be satisfactorily recorded on magnetic tape for thourough analyses at later times.

A schematic of the instrumentation system used in the hot gas tests is provided in Figure23. Due to the relatively short coherence length of the laser used, it was necessary to closely match the length of the reference and scattered beams. Also the relatively high intensity of the reference beam made it necessary to use a series of attenuators to lower its intensity so that an optimum ratio of scattered beam to reference beam intensity could be obtained. Mirrors were mounted on the walls of the facility to allow the laser to be positioned inside the blockhouse for protection. The receiver optics, photomultiplier tube, power supply, and low-noise preamplifier were enclosed in a heavy aluminum box which was rigidly mounted to a heavy support to prevent vibration during the test or damage in case of a motor failure.

The laser used in the test was the Raytheon Argon Ion Laser, Model LG-12. Its maximum power output at a wave length of 4880 Å was approximately 200 milliwatts but it could be adjusted to a much lower level for alignment purposes.

The spectrum analyzer used in the investigation provided the capability of viewing the complete range of expected frequencies simultaneously instead of only a small increment of frequencies as was possible previously. This spectrum analyzer was composed of two sections, both of which were manufactured by Hewlett-Packard. The RF Section was Model 8551 A, and the Display Section was Model 851 A.

The output of the spectrum analyzer was recorded on magnetic tape by use of the AMPEX FR 1200 unit at the hot gas test facility. The analysis of the data on the tape was performed at the Research Institute using the Honeywell Wideband 7620 tape unit. The signals recorded on the tape were viewed on an oscilloscope both with and without the use of the integrator.

In order to verify the alignment and adjustment of all components of the system, cold gas velocity measurements were made prior to the hot gas testing. Velocities were measured up to approximately 1800 ft/sec outside the exit of the sonic orifice. A needle valve spray arrangement as shown in Figure 24 was used to produce the mist particles for scattering light. Only short tests were made using water mist because the water particles froze and collected in the throat of the nozzle, quickly stopping it up.

After the alignment and operation of the system was verified, the hot gas test was performed. The 0.25 inch diameter sonic nozzle was used to form the jet. A relatively clean burning propellant (lot number LFT 3) was used in the test to produce the hot gas with its light scattering particles. The velocity was measured in the center of the jet at a distance of 5/64 inch downstream from the exit of the nozzle. The full scale tape recording voltage was selected to be 1 volt.

Evaluation of the data recorded on the tape during the hot gas test showed that a velocity of roughly 4000 ft/sec was measured. However, the maximum voltage of 1 volt was exceeded, and the peak of the Doppler shift signal was "chopped off." Therefore, it is impossible to determine the mean velocity at the jet center. Instead, a very broad signal was observed with no peak (Figure 25). The large width of the signal may have been caused by large variations in exhaust particle sizes and velocity gradients in the light scattering volume.

Based on these results it can be concluded that hot gas velocities above the sonic range can be measured and recorded. Since the peak of the signal was not obtained, it is not yet known how well the center velocity can be defined. The maximum velocity which can be measured in the exhaust plume is also still unknown. This information can only be gained by additional testing, but the present data show that the measurement of very high velocities in the hot exhaust gases may be possible.

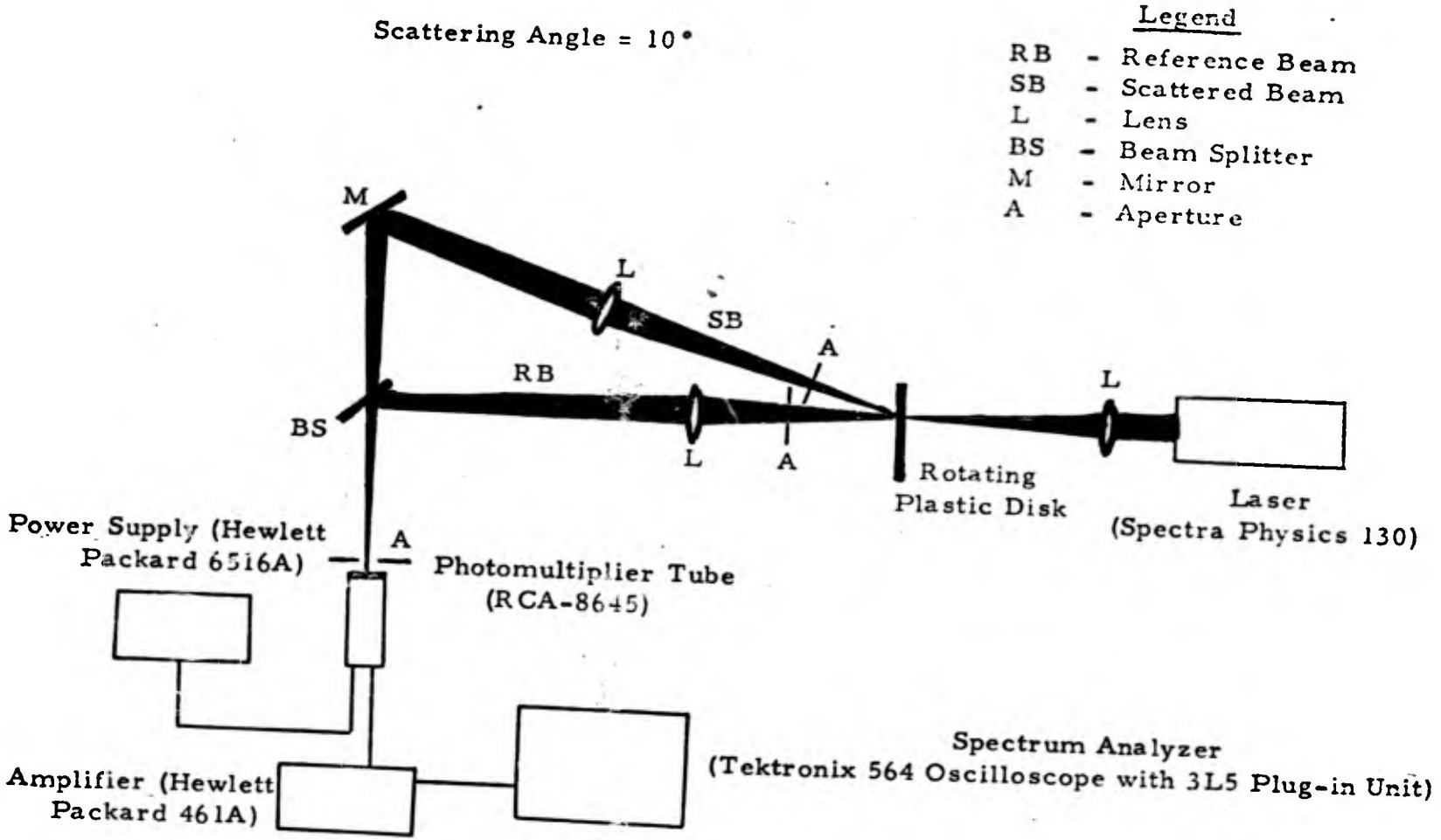

FIGURE 1. INITIAL LASER DOPPLER VELOCITY MEASURING SYSTEM

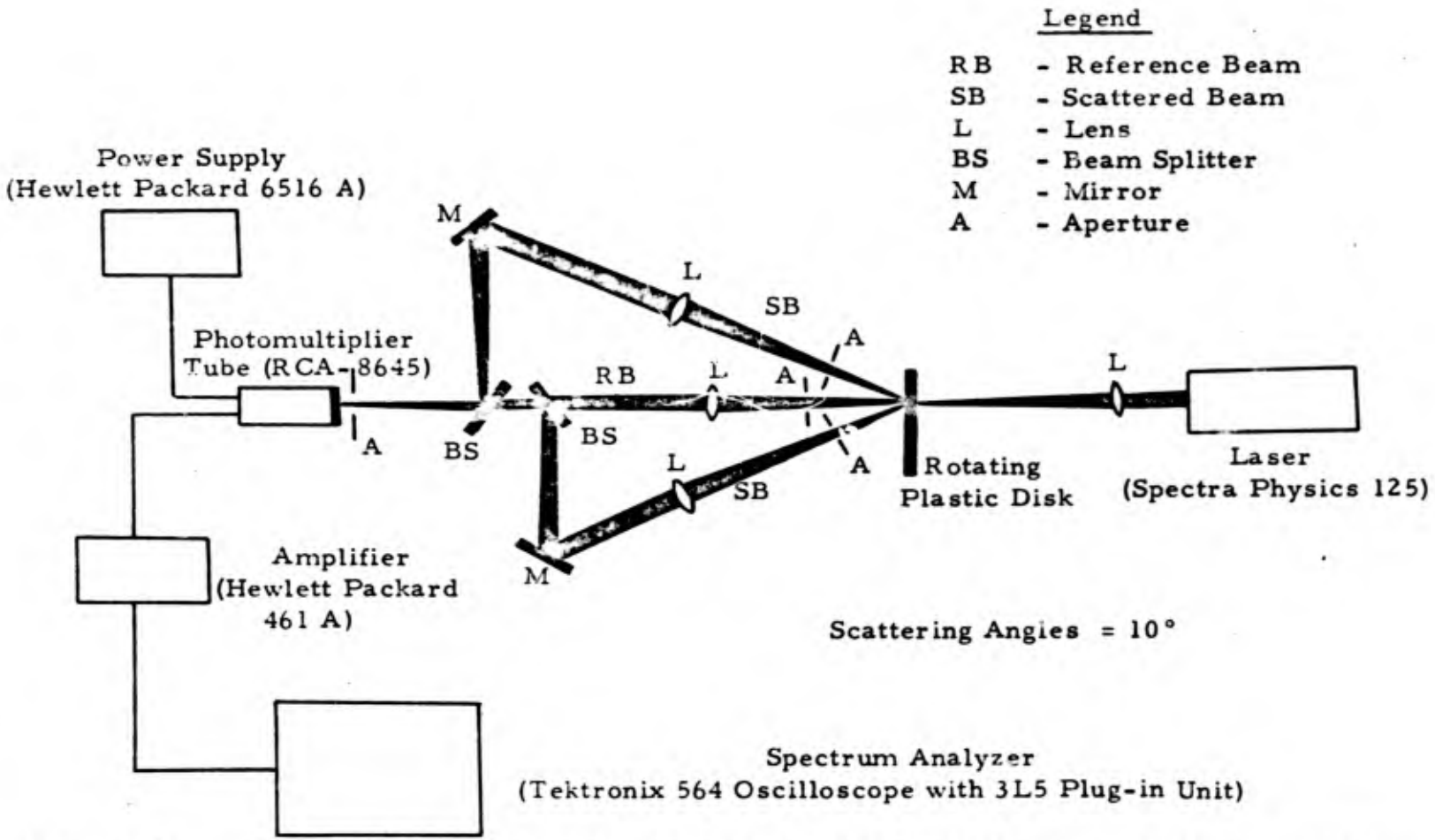

FIGURE 2 TWO-DIMENSIONAL LASER DOPPLER VELOCITY MEASURING SYSTEM USING ONE PHOTOMULTIPLIER TUBE

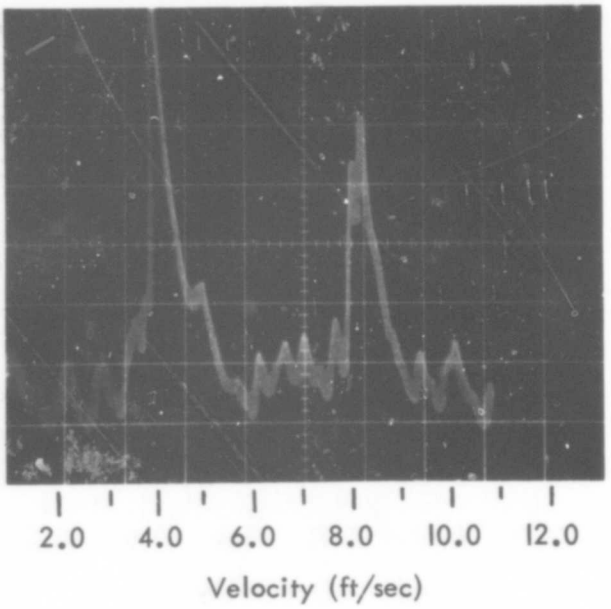

FIGURE 3. SPECTRUM ANALYZER TRACE AT MEAN VELOCITIES OF 4.2 FT/SEC AND 8.2 FT/SEC

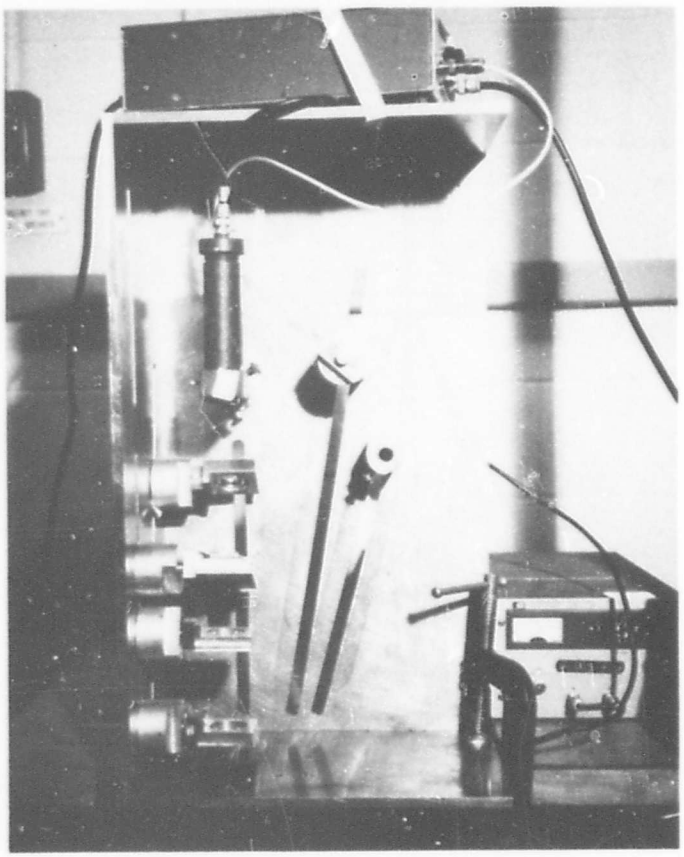

FIGURE 4. OPTICS ASSEMBLY

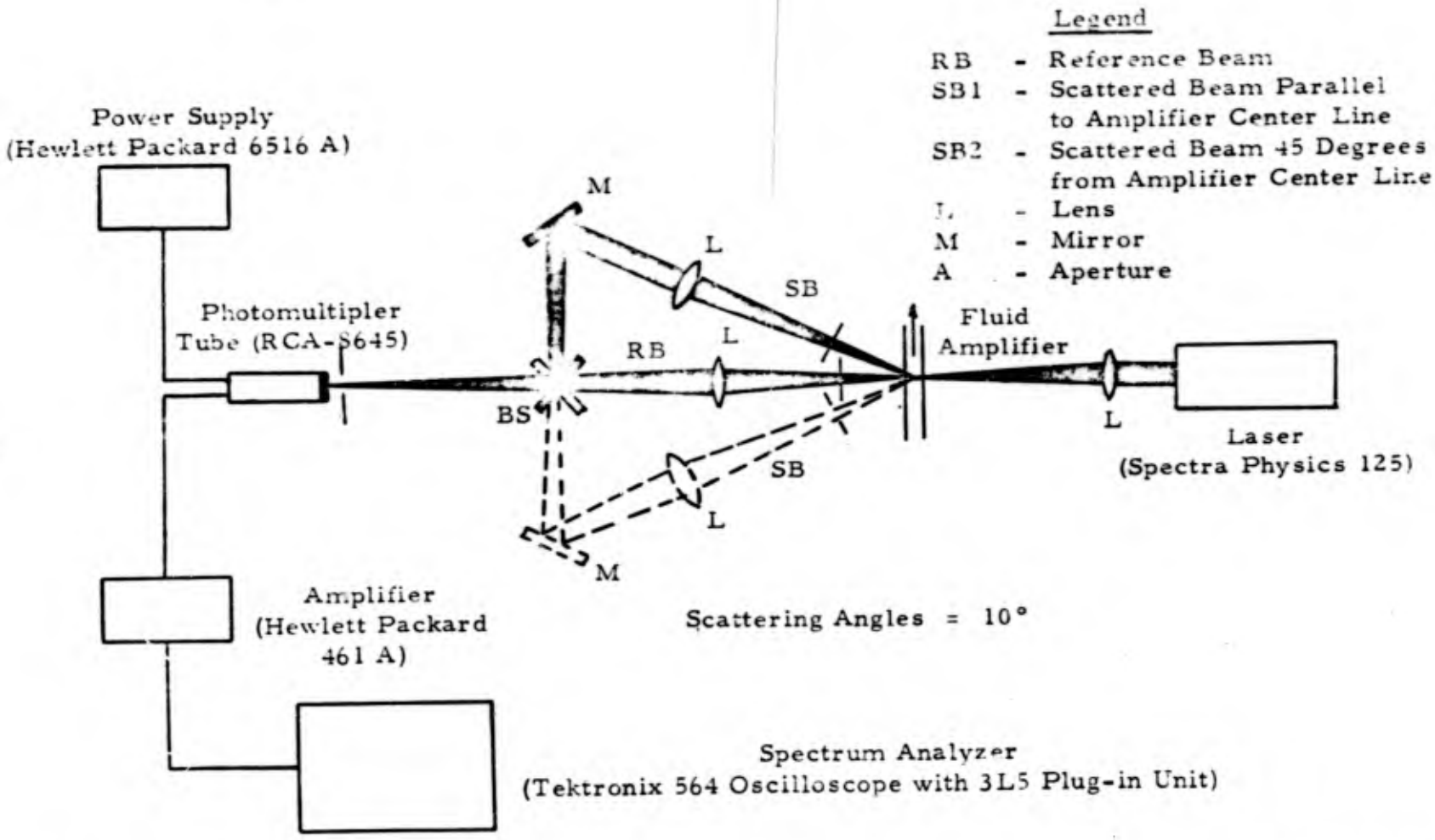

FIGURE 5. FINAL LASER DOPPLER VELOCITY MEASURING SYSTEM USED TO OBTAIN DATA

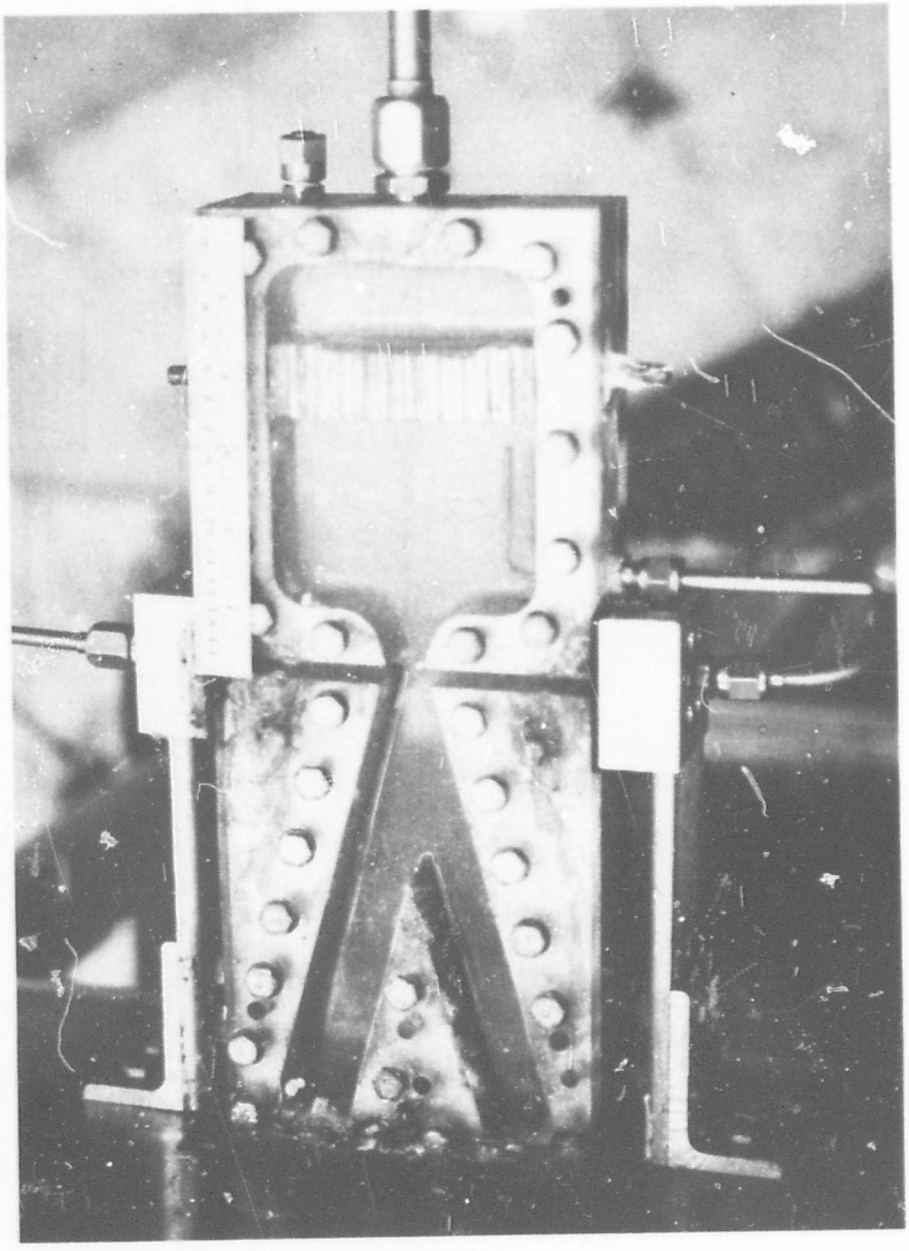

FIGURE 6. BISTABLE FLUID AMPLIFIER

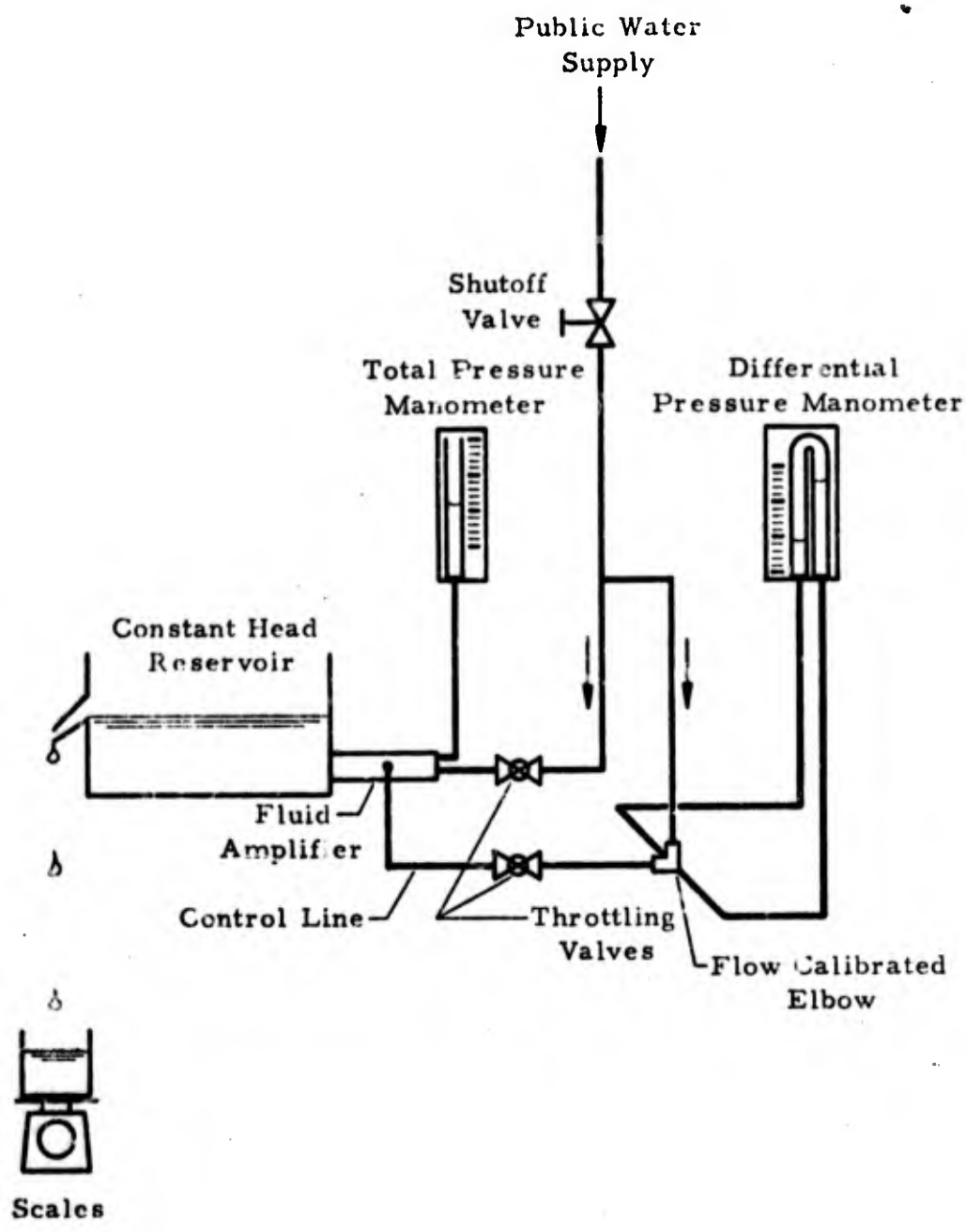

FIGURE 7. SCHEMATIC OF OPEN LOOP WATER FLOW SYSTEM

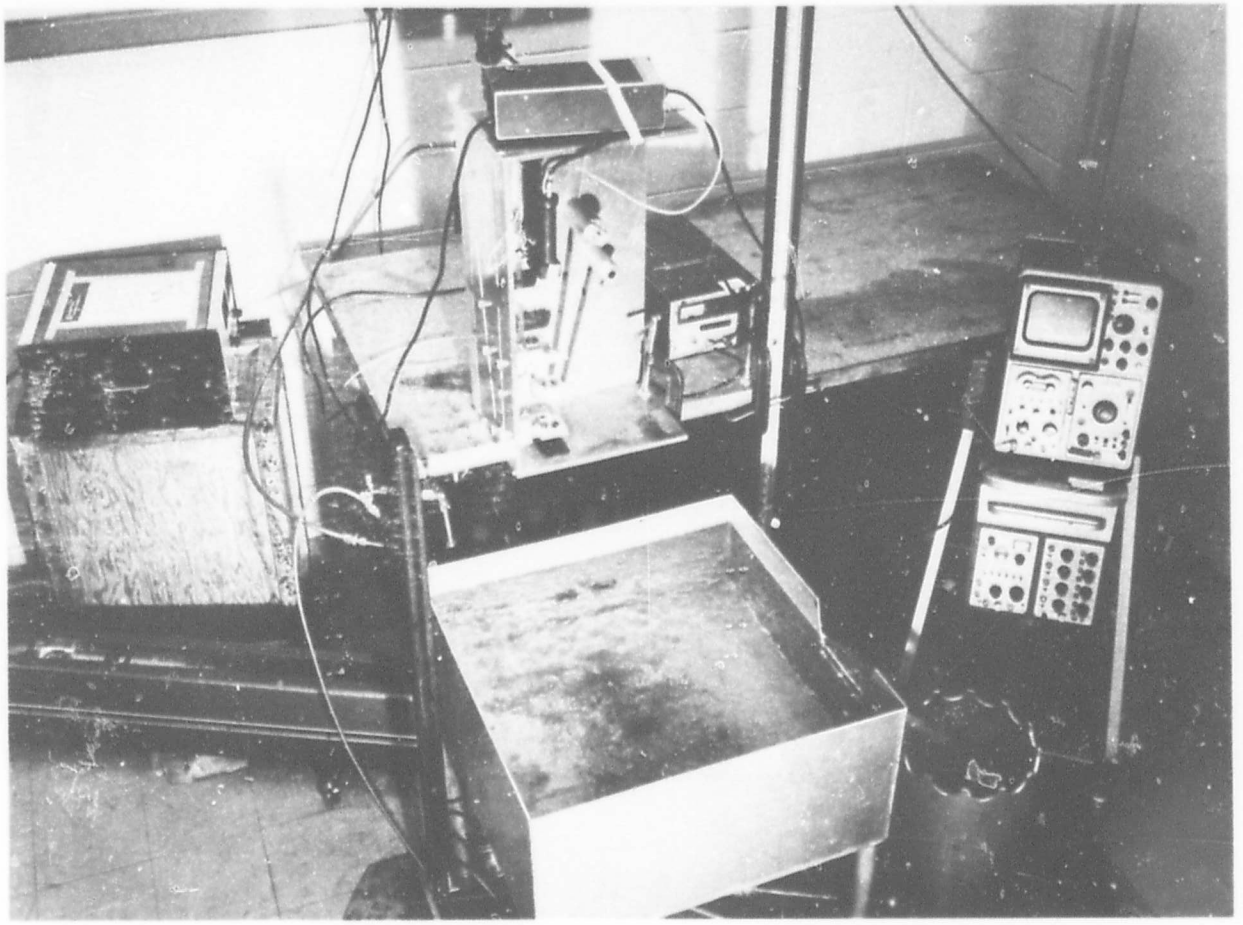

FIGURE 8. FINAL EXPERIMENTAL APPARATUS

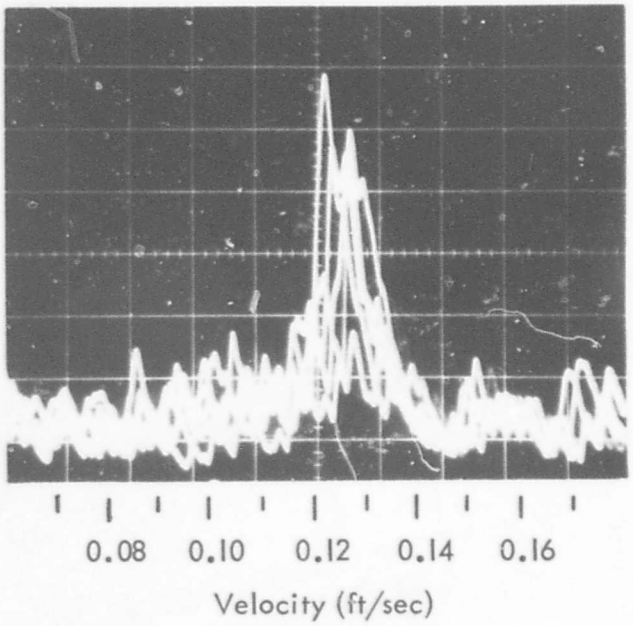

FIGURE 9. TYPICAL SPECTRUM ANALYZER TRACE AT MEAN VELOCITY OF 0.124 FT/SEC

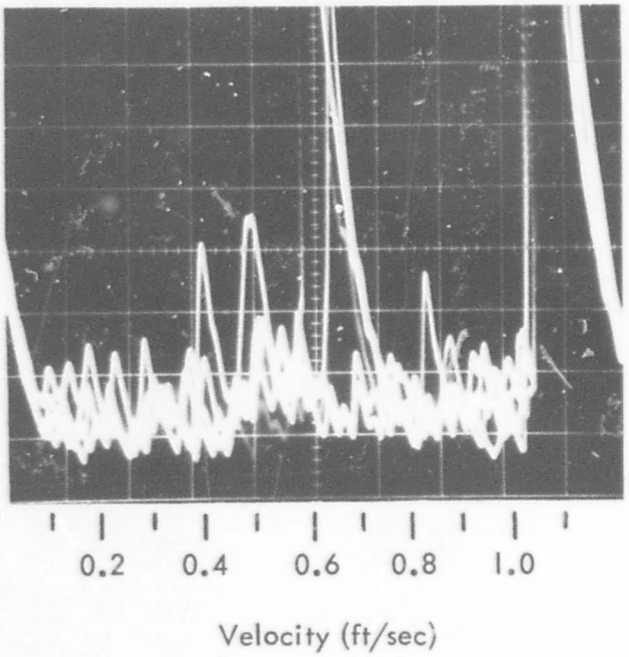

FIGURE 10. TYPICAL SPECTRUM ANALYZER TRACE AT MEAN VELOCITY OF 0.6 FT/SEC

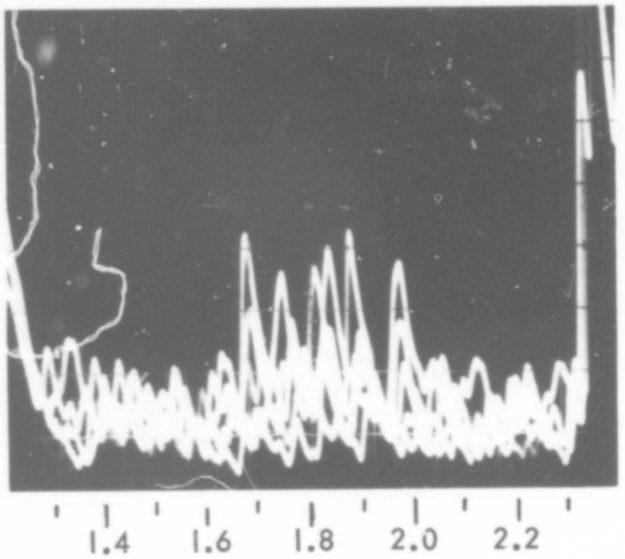

FIGURE 11. TYPICAL SPECTRUM ANALYZER TRACE AT MEAN VELOCITY OF 1.8 FT/SEC

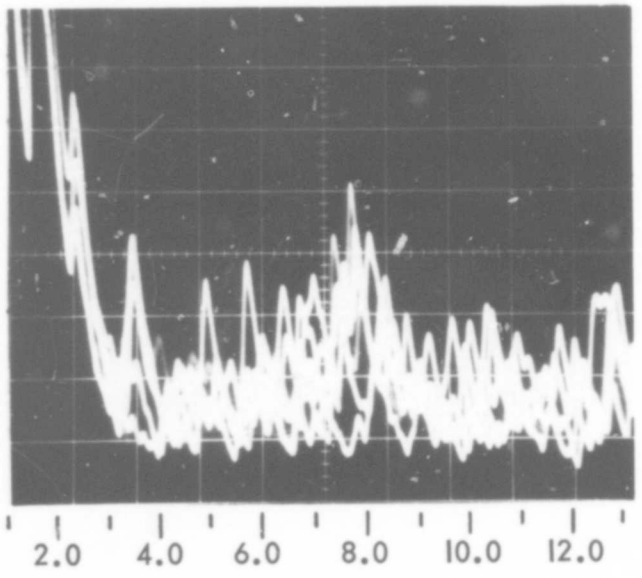

FIGURE 12. TYPICAL SPECTRUM ANALYZER TRACE AT MEAN VELOCITY OF 7.6 FT/SEC

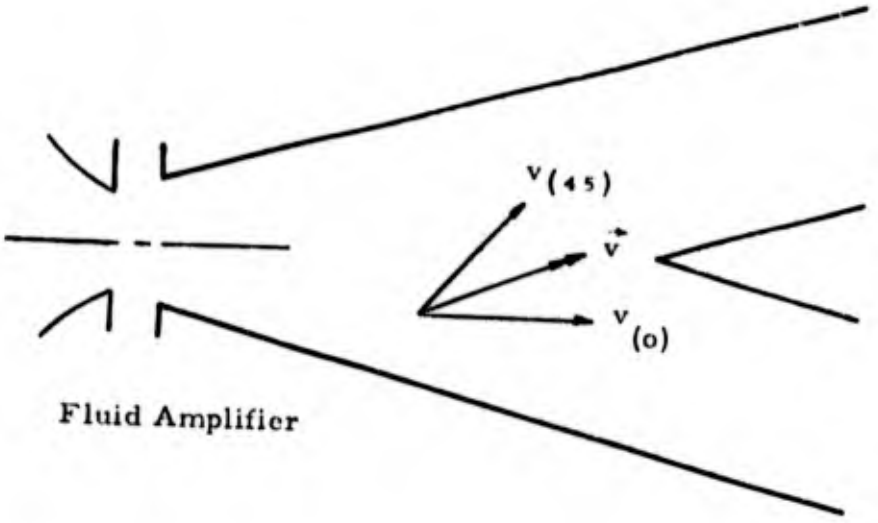

FIGURE 13. ORIENTATION OF MEASURED VELOCITY COMPONENTS

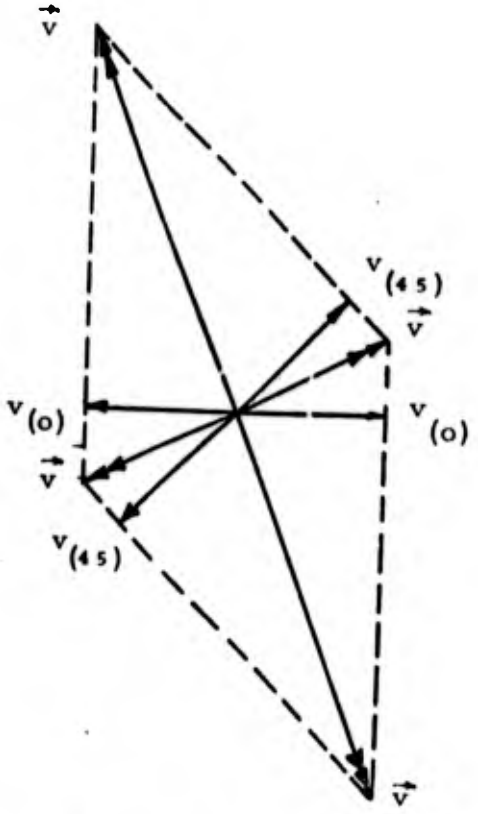

FIGURE 13a. POSSIBLE VELOCITY VECTORS FROM A GIVEN SET OF VELOCITY COMPONENTS

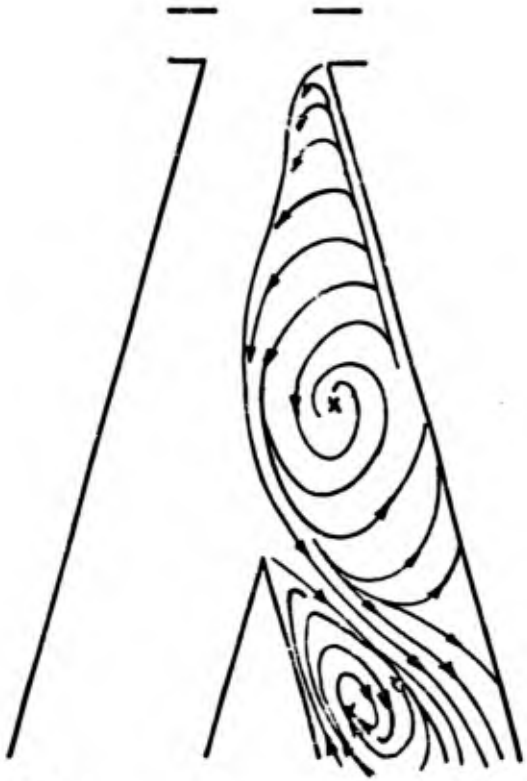

FIGURE 14. FLOW PATHS IN THE RECIRCULATING REGION WITH CONTROL FLOW OFF

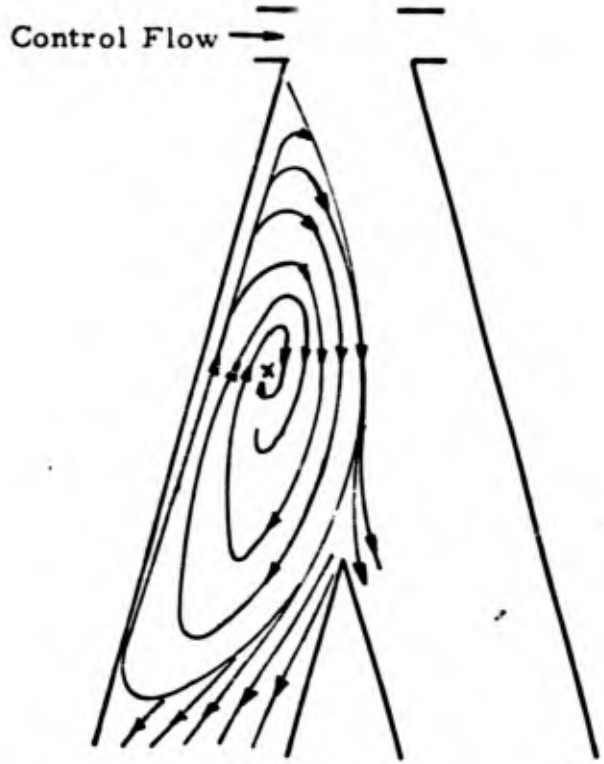

FIGURE 15. FLOW PATHS IN THE RECIRCULATING REGION WITH CONTROL FLOW ON

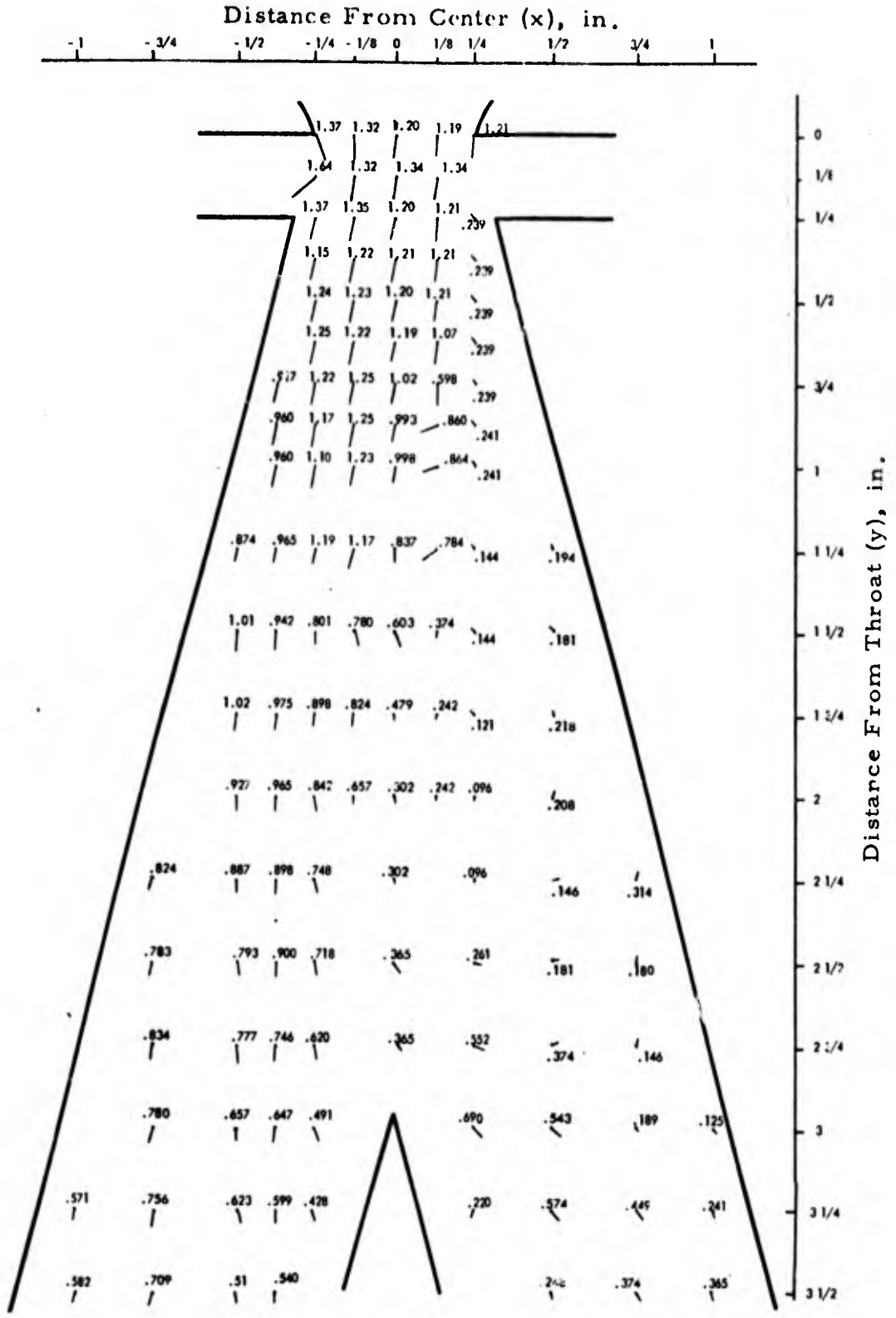

FIGURE 16. TWO-DIMENSIONAL VELOCITY FIELD AT FLOW RATE OF 0.268 LB/SEC WITH CONTROL FLOW OFF

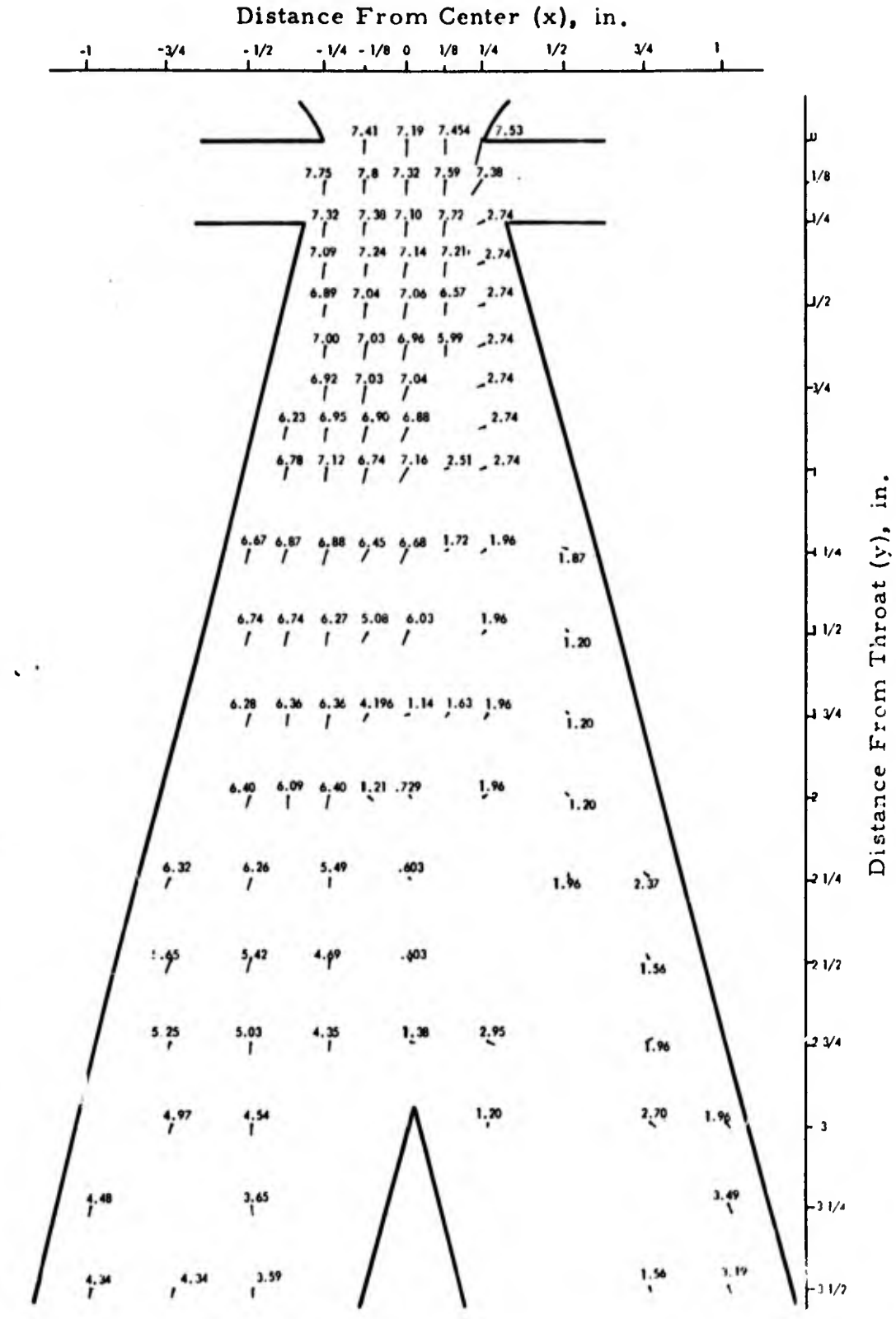

FIGURE 17. TWO-DIMENSIONAL VELOCITY FIELD AT FLOW RATE OF 1.58 LB/SEC WITH CONTROL FLOW OFF

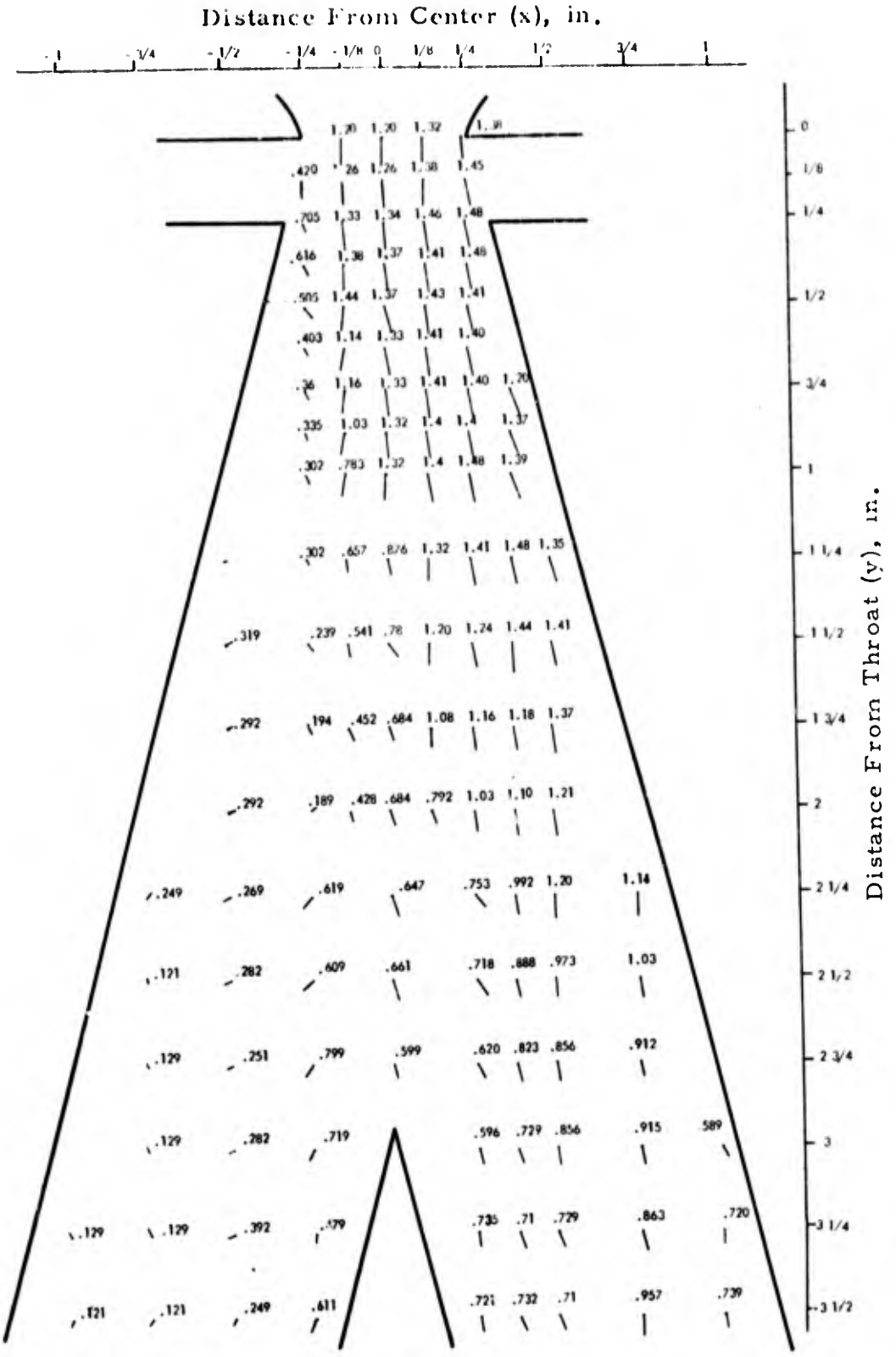

FIGURE 18. TWO-DIMENSIONAL VELOCITY FIELD AT FLOW RATE OF 0.292 LB/SEC WITH CONTROL FLOW ON

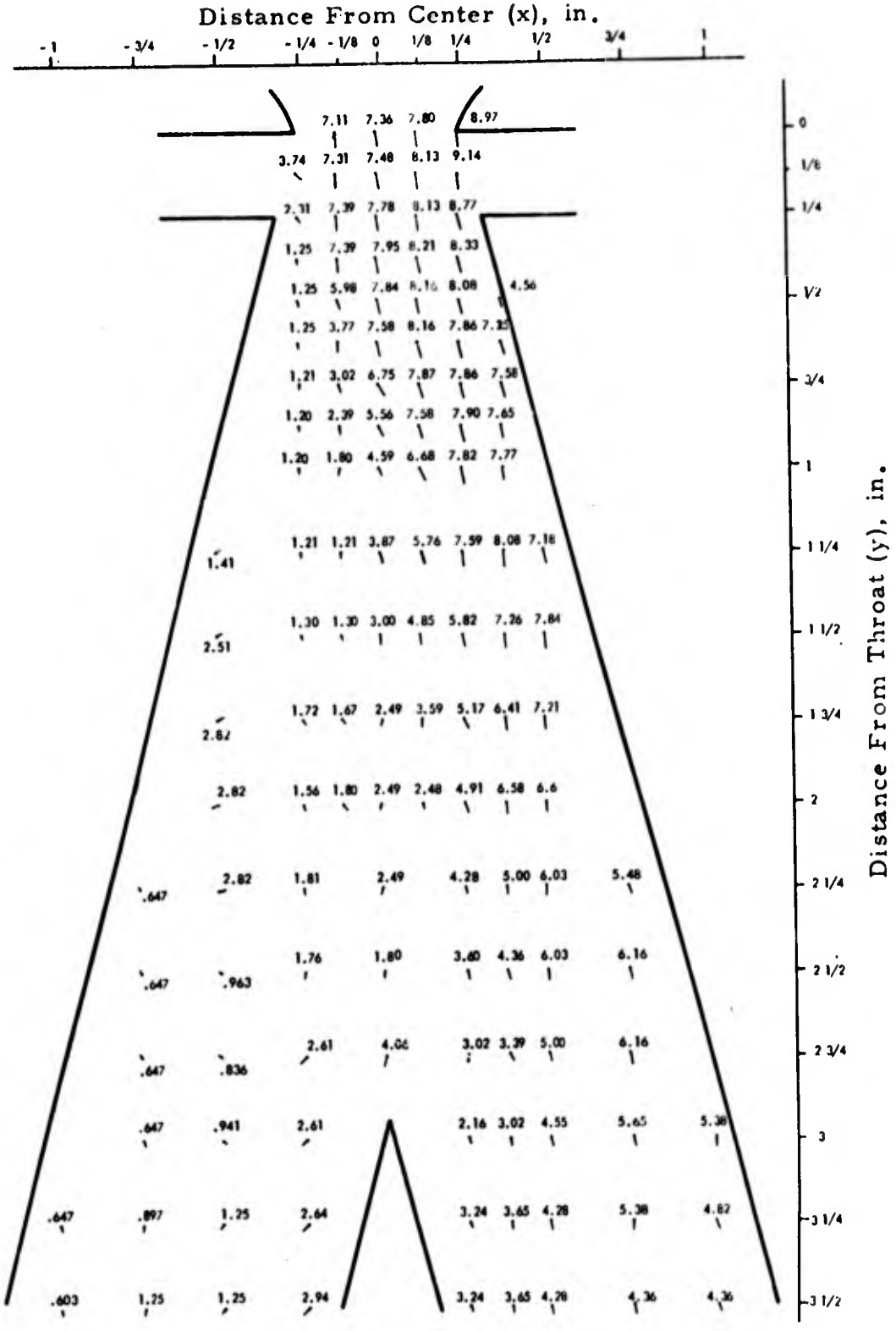

FIGURE 19. TWO-DIMENSIONAL VELOCITY FIELD AT FLOW RATE OF 1.71 LB/SEC WITH CONTROL FLOW ON

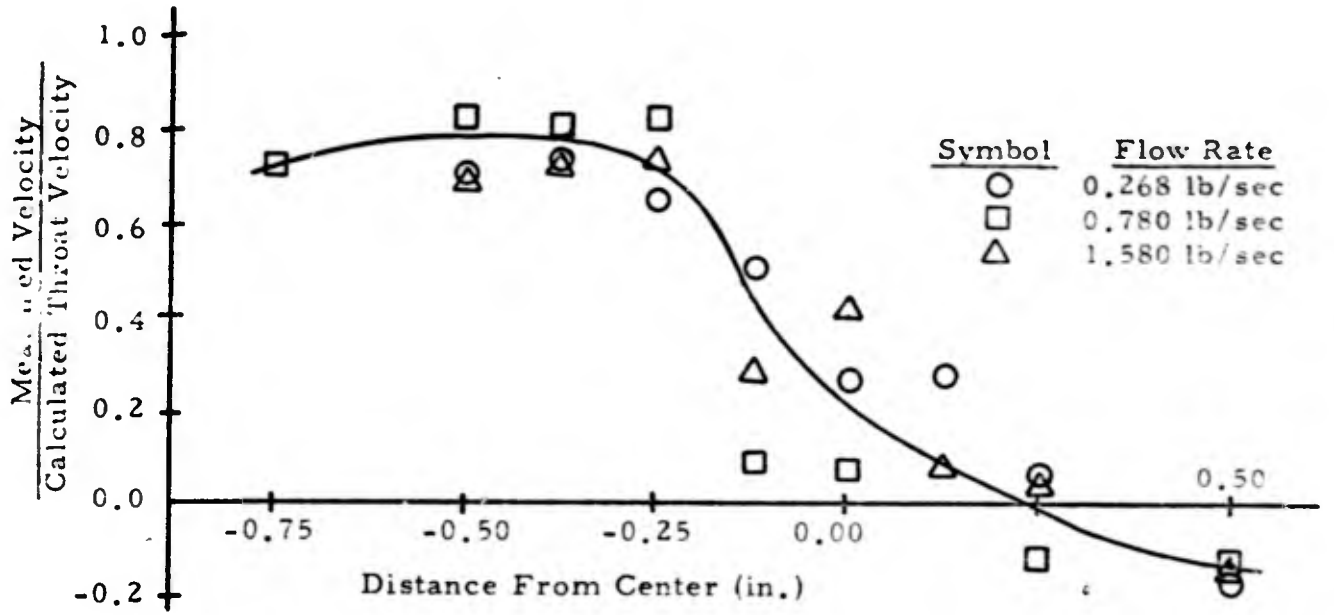

FIGURE 20. VELOCITY PROFILE AT y = 2.0 IN. WITH CONTROL FLOW OFF

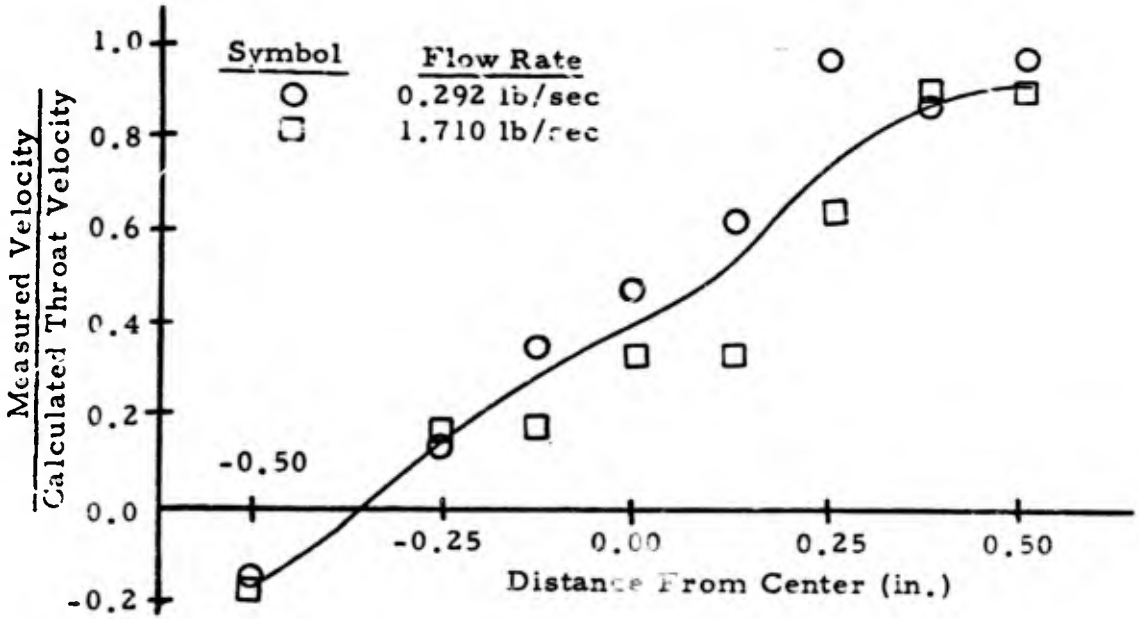

FIGURE 21. VELOCITY PROFILE AT y = 2.0 IN. WITH CONTROL FLOW ON

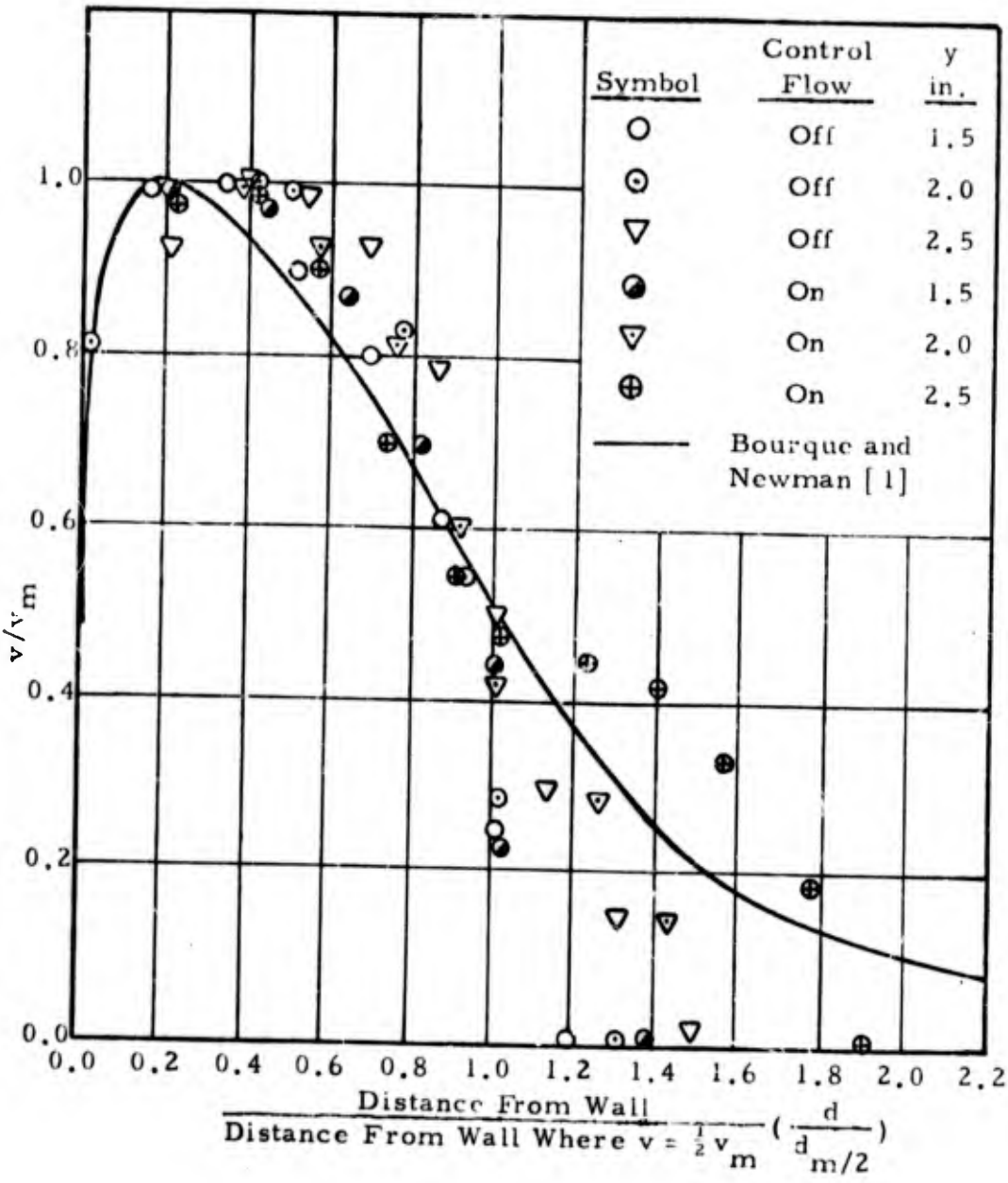

FIGURE 22. VELOCITY PROFILE COMPARISON

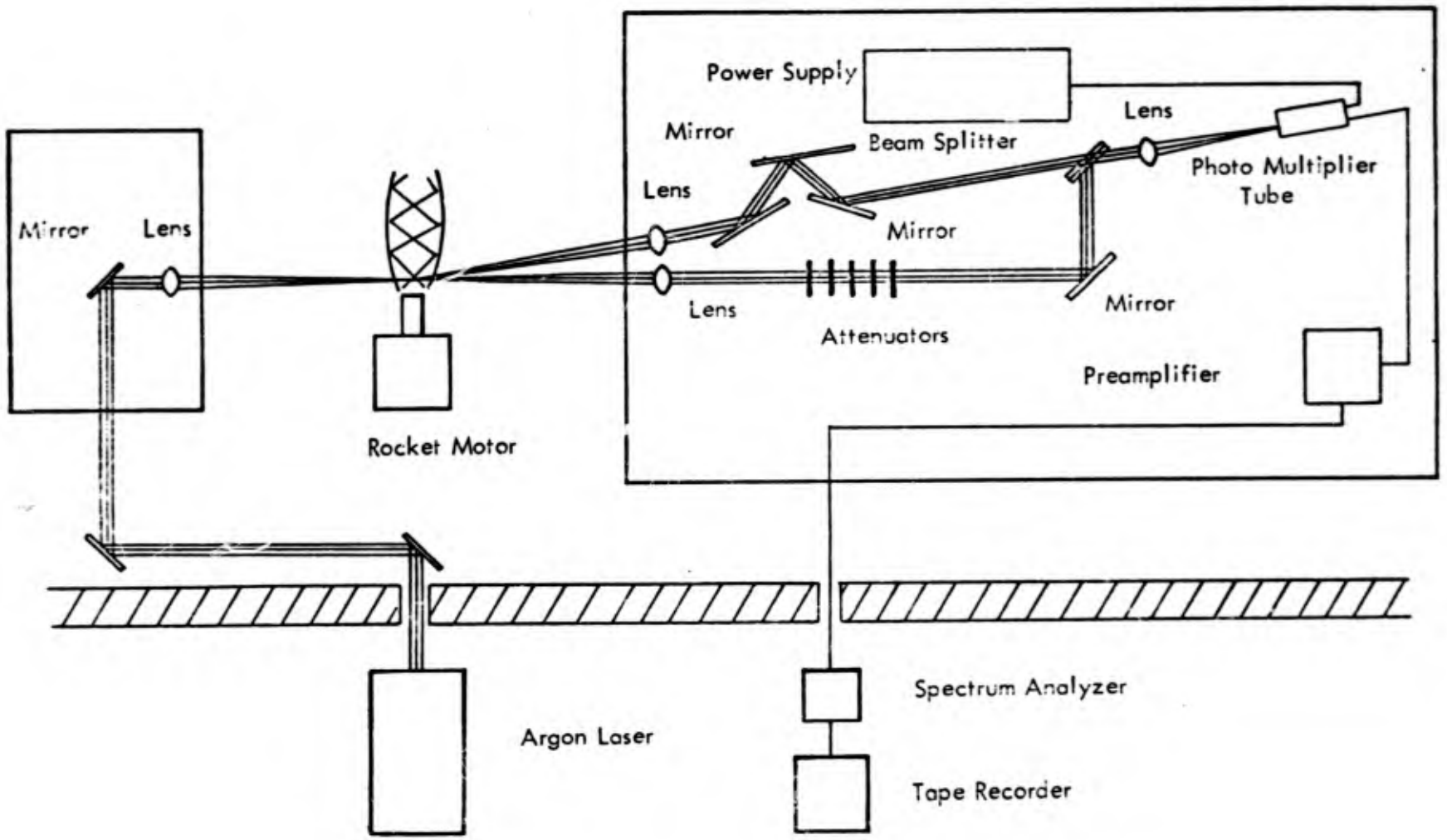

FIGURE 23: INSTRUMENTATION SYSTEM

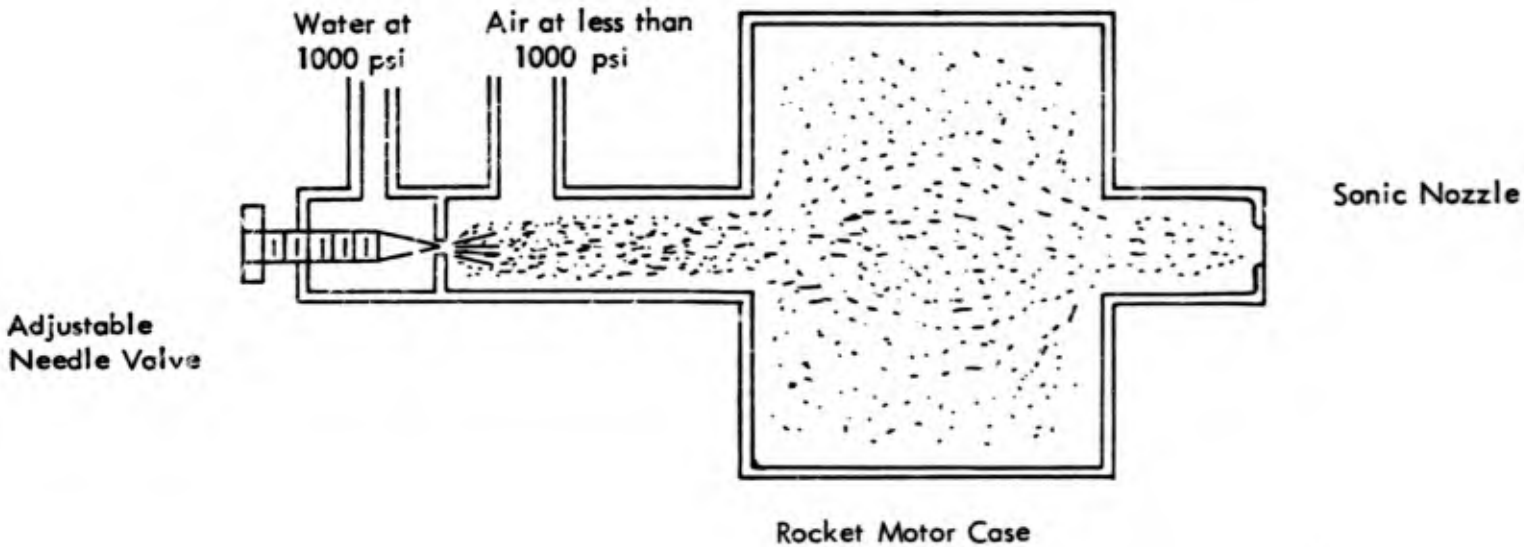

FIGURE 24: WATER MIST GENERATOR

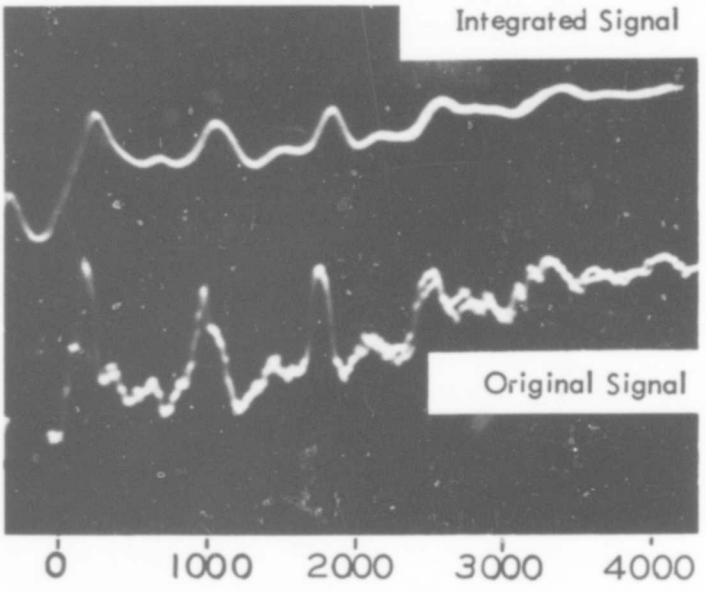

FIGURE 25

PHOTO DISPLAY OF ORIGINAL AND INTEGRATED HOT GAS SIGNALS
FROM THE LASER DOPPLER INSTRUMENTATION

ANGUS: Since the author brought it up earlier, I would like to make a couple of comments on the practicality of laser doppler flowmeters. They are also no good for measuring a lot of things like the mass in Jupiter and any number of extraneous things. The mistake one can make is trying to force it into the mold of a hot wire. It is not a hot wire and there is no particular sense in trying to make it duplicate things that hot wires do. The operational quantity of the hot wire - the most easily measured quanitities - have been velocities and velocity-correlation functions and that's the kind of theory that has developed for the description of turbulence.

Now the measurable quantity in turbulent flow for the laser doppler velocimeter is the space-time correlation function. It's a well-known quantity that has been known in turbulent theory for forty years. It just hasn't been used because there hasn't been a way of opertionally measuring it. Now there is. So I think we should not blame the doppler flowmeter for not measuring velocity-correlation functions so well but let's reorient our thoughts - think along the lines of what it does do. It measures the space-time correlation function.

Another minor comment is in regard to the business of transparency. I would regard that as a far less severe restriction than the restrictions on chemical reactivity and mechanical requirements that you run into with hot wires. You can't put hot wires into places that are highly chemically reactive - acid flows for example. With a laser flowmeter the tradeoff from the mechanical and chemical requirements to the business of transparency I think is trivial.

GOLDSCHMIDT: May I sketch rapidly something on the board. You hid something underneath the rug earlier and I'd like to bring it out once more. The question of whether a particle follows the flow or not is one that's concerned may people. I would like to show one curve (taken from "Turbulent Diffusion of Particles in Plane and Circular Jets", MSME Thesis, J.B. Lee, 1971; also prepared as Report HL 72-18 prepared for NSF G-K2729 and GK19317) that does not give an answer, but gives some kind of indirect suggestion as to what might be the case(*).

If we compare the turbulent transport coefficient for momentum in that stream, we have a ratio of what we might call the eddy diffusivity for the particles to the eddy viscosity for the transport of the momentum of the fluid itself (or the inverse of the Turbulent Schmidt Number). Suppose we plot this against a particle parameter Ψ_T which is the ratio of the particle response time to some time macroscale of the stream. What I want you to recognize is that as the particle size increases, or the density increases, so does the value of the abscissa. For the case of plane jets - particles suspended in two-dimensional plane jets - this curve will look as shown (see Figure 1) . The intercept will be something in the order of one, obviously, and it will increase within the range of the experiments that we have performed. There is a tremendous spread in the data - some of you have seen these curves. References 1 thru 6 contain the details if any of

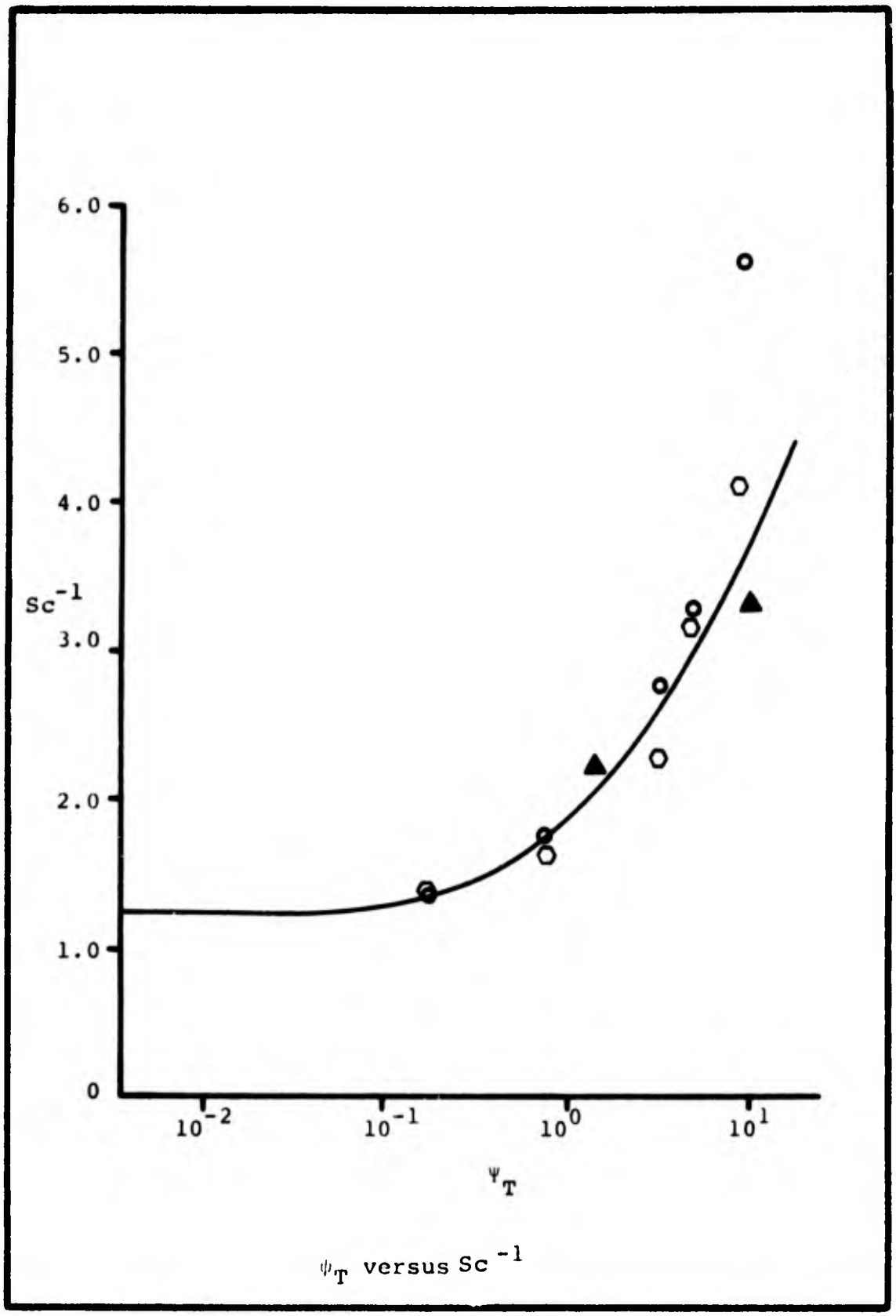

Figure 1

you are interested.

The point is that there is an increase of particle transport with size. This region where the value is close to one hopefully corresponds to that for the tracked particles in a laser anemometer system. This depends on the particle response time which is a function of its properties as well as the flow field that carries it. Certainly an infinite size particle would stand still, just being tickled by turbulence. So this curve has to go to zero somehow, and have a maximum before that. For neutrally buoyant particles this maximum appears to coincide with a particle whose size is equal to the turbulent macroscale. We are not saying that a particles does or does not follow the flow. We are saying that if we have particles someplace in this region, we may have transport coefficients which are far from equal to each other. Reynolds' analogy again once more violated. I'm not really answering the question - just bringing something out of the rug which might give us a yardstick to find out if we are safe or unsafe.

One final remark. Most of us using hot wires recognize that the best thing we can do is to do away with them. Maybe you people should take exactly the same attitude regarding laser doppler systems.

ASHER: I agree with you. Professor Shih mentioned the alignment, sensing direction, fluid transparency, etc. These things can be taken care of in most cases. Perhaps in your case, you should have used the hot wire. Your scale is not so small and you might have been happier with it because it is a fairly well-known thing. We have a fluidic business and we measured with our setup in twenty mil fluidic elements at Reynolds numbers less than 1000. With trivial flow velocities we were able to go right across the jet and go between side walls which were twenty to forty mils apart. So it can be done with very small scale and we got excellent results. (This is Bill Jones' work at the corporate R & D.)

You mentioned slippage of particles. This is a very important point. We talk about the response of particles, but we don't talk about slippage. We also have an interest in polymers used for drag reduction on torpedoes. My office mate has been interested in this. He once came up to me and said with seeding you're going to foul the flow up because near the boundaries you're changing the boundary layer. Now this could be true and this is the point that people who heavily seed should take into account. If you cannot heavily seed you do away with the turbulent ambiguity and, in addition, slippage of particles does not exist. You can try it out for yourself. If there are something like 10^4 particles per cc, you are going to have a slippage between particles and actually a drag reduction. If your particle density is lower than that, you're fine. It's really important.

REFERENCES

1. M.K. Householder and V.W. Goldschmidt, "Turbulent Diffusion and Schmidt Number of Small Particles" - Journal, of the Engineering Mechanics Division, ASCE, EM6, December 1969, pp. 1345-1367.

2. G. Ahmadi and V.W. Goldschmidt, "Kinematic Computer Simulation of the Turbulent Dispersion of Neutrally Buoyant Particles." Development in Mechanics, Vol. 5, Proceedings of the 11th Mid-western Mechanics Conference, Ed. by H.T. Weiss et al., The Iowa State University Press, August 1969, pp. 201-211.

3. G. Ahmadi and V.W. Goldschmidt, "Analytical Prediction of the Turbulent Diffusion of Small Solid Particles." Fluid Dynamics Symposium, Hamilton, Canada, August 1970.

4. G. Ahmadi and V.W. Goldschmidt, "Dynamic Simulation of the Turbulent Diffusion of Small Particles," Proceedings First International Conference on the Hydraulic Transport of Solids in Pipes (Hydrotransport 1), British Hydromechanics Research Association, Cranfield, September 1970 pp. F5-57 to F5-68.

5. G. Ahmadi and V.W. Goldschmidt, "Motion of Particles in a Turbulent Fluid - The Basset History Term," Transactions of the, ASME, Journal of Applied Mechanics, Vol. 38, Series E, No. 2, June 1971, pp. 568-569.

6. V.W. Goldschmidt, M.K. Householder, G. Ahmadi and S.C. Chuany, "Turbulent Diffusion of Small Particles Suspended in Turbulent Jets," Paper 4-2, International Symposium on Two-Phase Systems, Technoin, August 29 - September 2, 1971.

USE OF THE LDV IN SUBSONIC AND SUPERSONIC FLOW

William J. Yanta
Naval Ordnance Laboratory
Silver Spring, Maryland

What I'm going to talk about this morning are some results which we've obtained in supersonic flow and in low-speed channel flow. Some of the supersonic results were presented at the AIAA meeting last March in Albuquerque (Reference 1).

In Figure 1 is shown our Mach 3 wind tunnel. The test section is 2 1/2 inches by 2 1/2 inches. Flow goes from left to right. The supply air was one atmosphere at room conditions, so the velocity in the free-stream air was 2040 feet per second. A Pitot tube was used to measure the centerline Mach number and hence the centerline velocities.

One of the things that we are worried about is how the particle behaves when it is passing through a shock wave. What we have done is set up a computer program which includes some well-known drag relationships for small particles in supersonic flow. (References 1 and 2). Incidentally, this work is in rough draft form, and will probably be published at the beginning of the fall. If you are interested and will send me your name, I will be glad to send you a copy. Figure 2: What I've done here is taken the Mach 3 condition with room supply air and predicted how a particle reacts when it passes through an oblique shock wave. The particle size is the parameter. When it enters, it's going over 2,000 ft. per second. I'm only looking at the x-component of velocity plotted versus x in inches. The particle size range is from 0.2 micron up to 5 microns. The 0.2-micron particles come to equilibrium in back of the shock in less than 1/10 of an inch. If you have a five-micron particle, its inertia is quite high; it does not slow down very much.

Figure 3 shows the velocity lag along the centerline of the same nozzle. From the throat to the test section is about four inches. The throat is at x = 0 and we injected the particle in the settling chamber. I have plotted the lag between the particle velocity and the gas velocity as a function of particle size. You can see that a one-micron particle will lag up to about 50 feet per second just downstream of the throat. This indicates that if you want to keep the lag small the size must remain below one micron.

The problem is what do you use for particles. You want something that is non-toxic, non-corrosive, and non-flammable. After doing a lot of soul searching and considering restraints by people who run the wind tunnels, we finally chose water. There are a

couple of problems, though. First, water plays havoc with the thermodynamics of the system. Second, water droplets that are very small, say sub-micron, tend to evaporate at room conditions in about one millisecond (Reference 3). You really have problems in placing these small water droplets in the flow. So what do you do? Some years back, Reference 4, Archer and La Mer found that when you add a long chain alcohol to the water the evaporation rate is retarded. Concentrationwise we used about .03 percent to 0.5 percent dodecanol in water with a Laskin nozzle to generate water particles (Figure 4). The Laskin nozzle is simply a jet submerged under water. The jet shearing action generates a polydispersed aerosol. The dodecanol has a very low vapor pressure, and as the particle starts evaporating, the concentration of the dodecanol increases around the outer part of the particle forming a mono-layer of the dodecanol which retards the evaporation rate of the particle. As a result, you can increase the stability lifetime of the particle by a factor of a hundred. Now there is enough time to dump the particles into your supply chamber and get them down the nozzle before they evaporate.

Here are some of our results. Figure 5: across the oblique shock wave we measured the x-component of the velocity of the particles. You can see that there is some lag when compared to the gas velocity as predicted by our calculations. It takes about one-half of an inch before the particle comes into equilibrium with the flow in back of the shock. When you check against the computer calculations, you find that this particle size corresponds to a nominal two microns. This is in very good agreement with the predicted particle size for the configuration of Laskin nozzle that we used. Reference 5 at NRL had used Di-octyl phthalate and they found that the particle diameters were approximately one micron. So we checked with them closely: thus, there is some confidence here.

Next we measured the velocities of the particles along the centerline of the nozzle shown in Figure 6. Shown in comparison are measurements of the LDV, and Pitot probe measurements with and without the water aerosol. What we wanted to find out was whether there was any thermodynamic effect of the water on the flow. There was none when we added the aerosol. There is a lag or velocity difference between the LDV and the pitot measurements, as was expected. We measured the lag difference here also. It is an inaccurate measurement when you do it this way because you are measuring two absolute velocities and subtracting the differences. But we did it anyway and we found that when you compared the measured lag to the calculated lag the particles were again about two microns nominal diameter. When I say two, I mean that they were two microns plus or minus one micron. There was quite a bit of scatter in the measurements.

Now in Figure 7 are some measurements I have taken the last couple of weeks. We are using a pulse-type counter readout which we obtained from ARO and just put into operation. First, I wanted to check against a known flow so I used a two-dimensional subsonic

channel with a flow velocity of about 40 feet per second at atmospheric conditions. I first probed the flow with hot wires to determine the turbulent intensity measurements and the mean velocity measurements. The results are shown in Figure 7. So then we used the LDV using the natural seeding in the unfiltered air; the measurements are the circles. The centerline of the flow is at y = 0, and y = 1 is the nozzle wall since we were using a two-inch channel. We found there was quite a discrepancy particularly in the inner portion of the flow. We suspected the problem could be due to large particles since we were just drawing in room air, and it is a very dusty room. So we put an electrostatic filter in the front of the inlet to the channel. These results are shown in Figure 7. There was a marked increase in the velocity but it still is not in good agreement in the inner portion of the flow field.

In Figure 8 are shown the hot wire measurements and the standard deviations for the LDV data. You can see that the agreement is not that good. Probably, again, the particles are quite large.

Let me point out here that I took about 125 samples, with a maximum of two hundred samples, for each one of these five points. It is enough to give you the mean velocity but to find the standard deviation, as John Dunning pointed out this morning, you are going to need a lot of data points. In fact, if you assume the turbulence is Gaussian, you can determine from statistical tables the number of data points required for a certain level of confidence. For the second moment or the standard deviation which is the RMS value of turbulence, if you are going to be 90 percent confident that your measured standard deviation is within 5 percent of the population standard deviation, you need something like 550 data points. I only have about one hundred here, so the error band is probably like plus or minus 10 percent of the value on this data. This is for only 90-percent confidence. If you want to go to 99 percent, you are going to need well over 1000 data points. So a word of caution regarding the number of samples you are going to need if you are interested in the turbulence intensities.

If you are looking for mean velocity, just the mean value, then you can probably get away with less then one hundred samples unless your turbulence intensity is quite high. Now if you are going near the wall, your turbulence intensity can reach like 15 percent of the local value and you still need at least several hundred, maybe close to a thousand data points for just the mean velocity. Figure 9 is a histogram of the centerline velocity for 124 samples.

What we are going to try to do now for supersonic flow is filter out or eliminate all the particles and add our own. Using the Laskin nozzle again, and using Di-octyl phthalate, we will generate a polydispersed aerosol. You get a size distribution that looks Gaussian. To eliminate the large particles, you pass the aerosol through an impactor (Figure 10). The impactor is just a plate with small holes drilled through it, and placed approximately three hole diameters in back is an impacting or collecting plate. The aerosol

is then blown against the impacting plate. The small particles follow the flow and are carried around the impacting plate while the large particles impact against this plate and are essentially filtered out. The impactor does have a rather sharp cutoff so that by varying the hole size, you can control the cutoff size for the aerosol. Figure 14 shows the efficiency of the impactor from Reference 6. If you want 100 percent efficiency for a round hole you can work backwards and determine the particle size. We have not checked this curve, so I really don't know how good it is. Ranz and Wong did experimentally calibrate their system and they were in fair agreement with the theoretical curve. Their data was checked by other researchers and does seem to be fairly reliable. We hope to put this system into use this summer.

Author's Postscript: Since the presentation of these results, the LDV measurements have been retaken. These later measurements include turbulence intensity and shear stress distributions. Agreement with hot wire and Pitot surveys is excellent. These results will be presented at the January 1973 AIAA annual meeting.

REFERENCES

1. Yanta, W.J., Gates, D.F. and Brown, F.W., "The Use of a Laser Doppler Velocimeter In Supersonic Flow," AIAA Paper 71-287 AIAA 6th Aerodynamic Testing Conference, March 10-12, 1971

2. Neilson, J.H. and Gilchrist, A., "An Analytical and Experimental Investigation of the Trajectories of Particles Entrained by the Gas Flow in Nozzles," Journal of Fluid Mechanics, Vol. 35, Part 3, pp. 549-559, 1969

3. Eisner, H.S., Quince, B.W. and Slack, C., "The Stabilization of Water Mists by Insoluble Monolayers," Discussions of the Faraday Society, Vol. 30, 1960

4. Archer, R.J. and La Mer, V.K., "The Rate of Evaporation of Water Through Fatty Acid Monolayers," Journal of Physical Chemistry, Vol. 59, No. 3, 1955

5. Echols, W.H., and Young, J.A., "Studies of Portable Air-Operated Aerosol Generators," NRL Report 5929, U.S. Naval Research Laboratory, July 26, 1963

6. Ranz, W.E. and Wong, J.B., "Jet Impactors For Determining the Particle-Size Distributions of Aerosols," A.M.A. Archives of Industrial Hygiene and Occupational Medicine, Vol. 5, pp 464-477, 1950

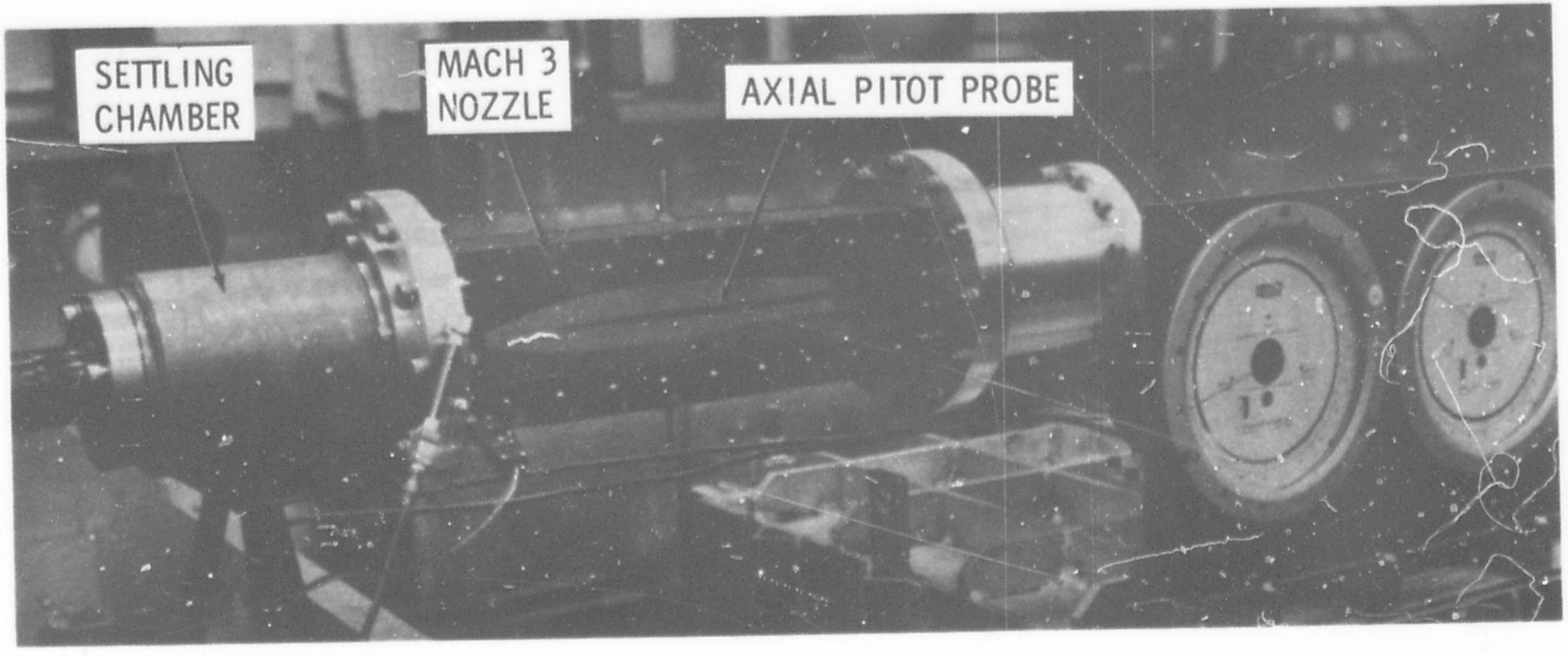

FIG. 1 MACH 3 WIND TUNNEL

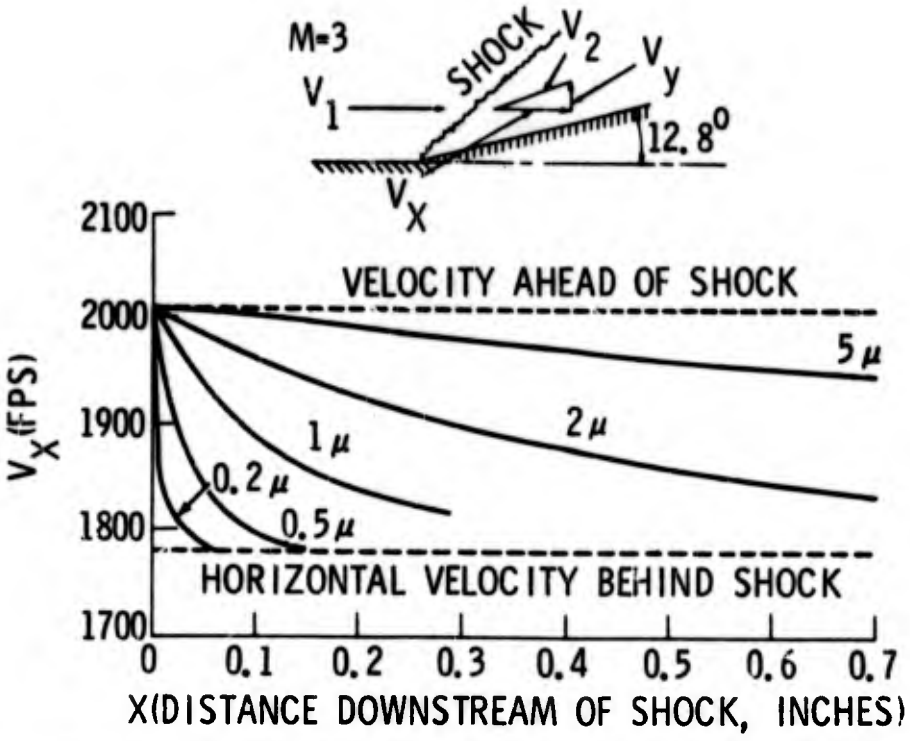

FIG. 2 PARTICLE HORIZONTAL VELOCITY COMPONENT BEHIND SHOCK

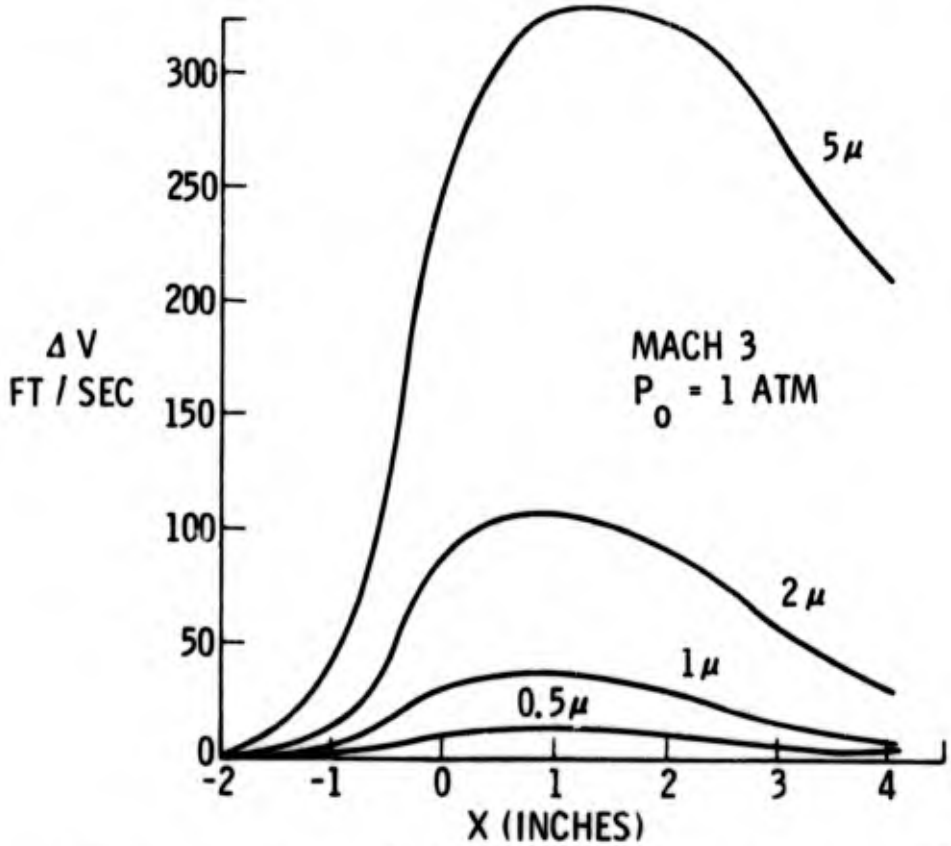

FIG. 3 PARTICLE VELOCITY LAG ALONG NOZZLE CENTERLINE

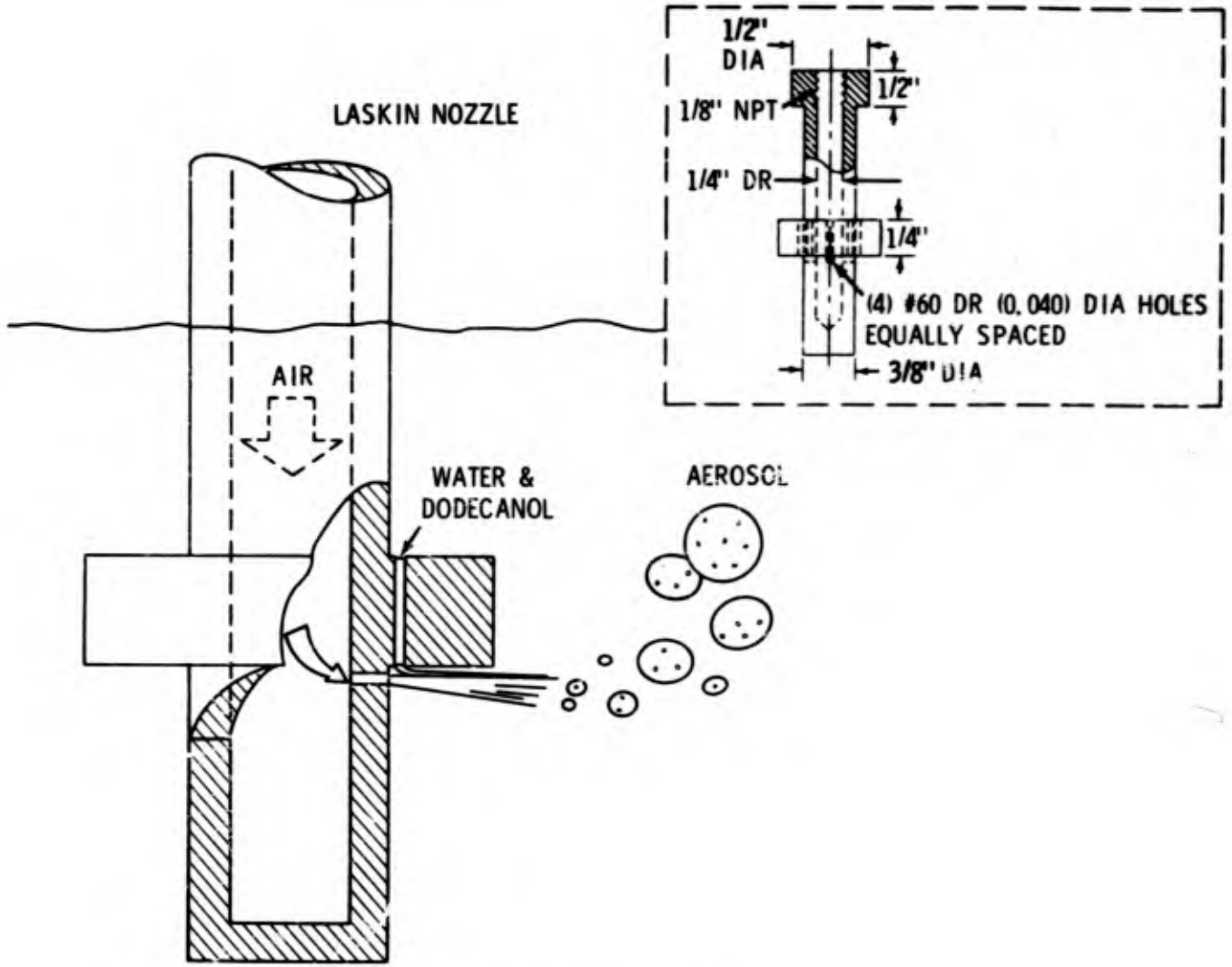

FIG. 4 LASKIN NOZZLE

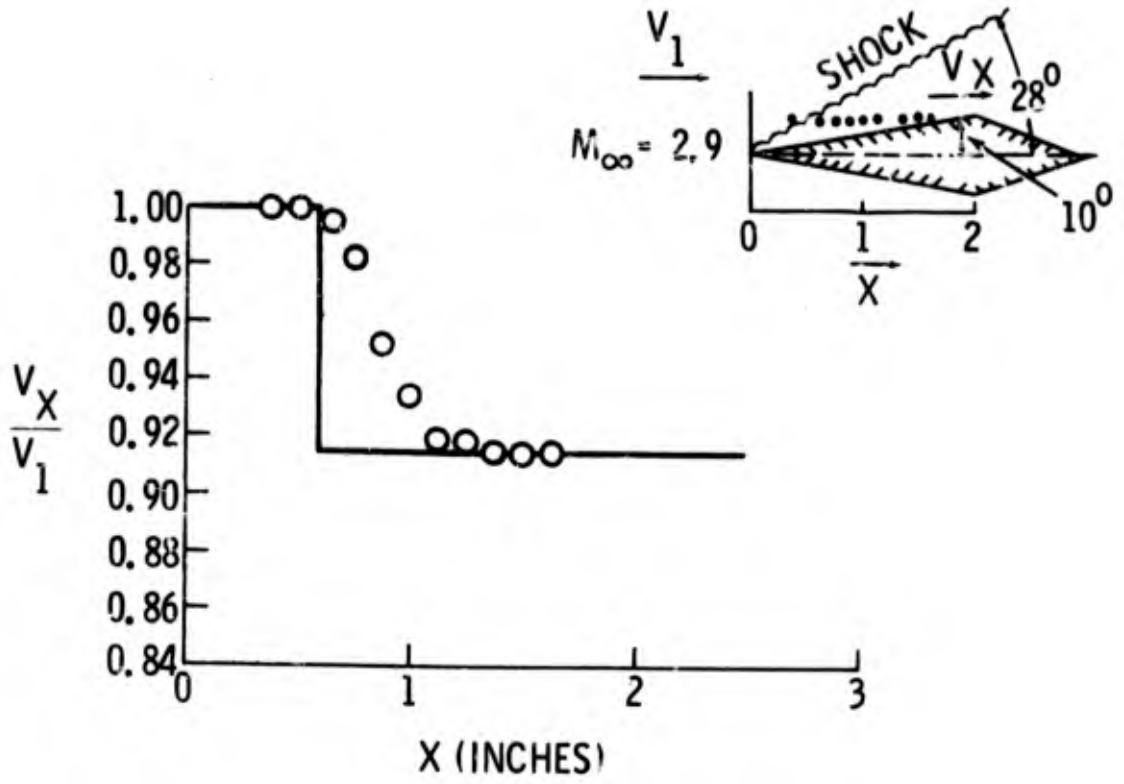

FIG. 5 VELOCITIES ACROSS OBLIQUE SHOCK

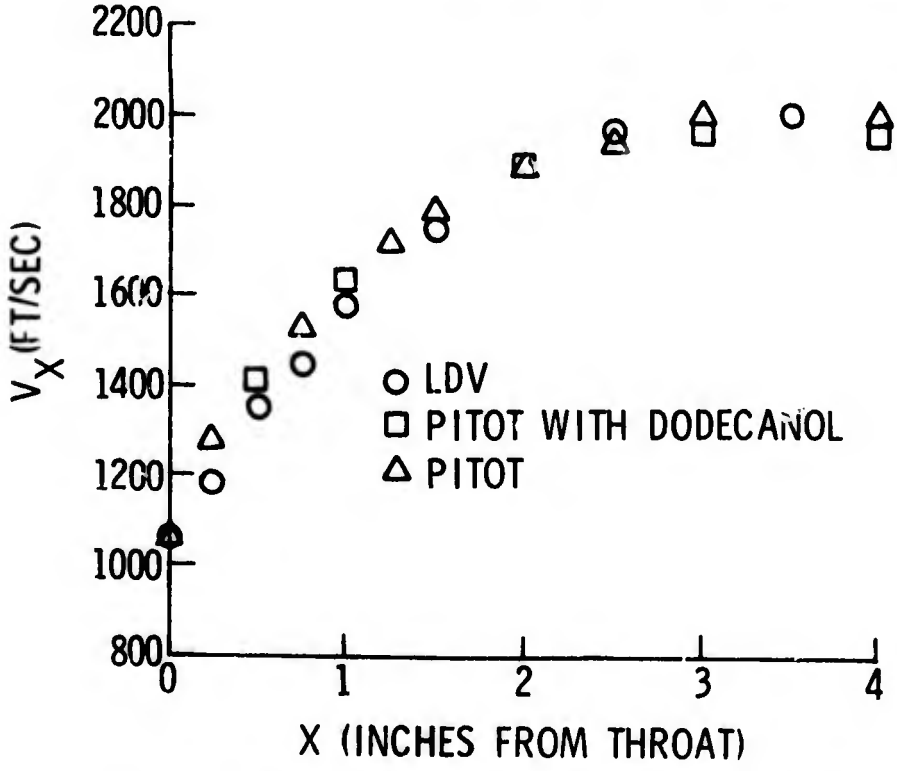

FIG. 6 NOZZLE CENTERLINE DISTRIBUTION

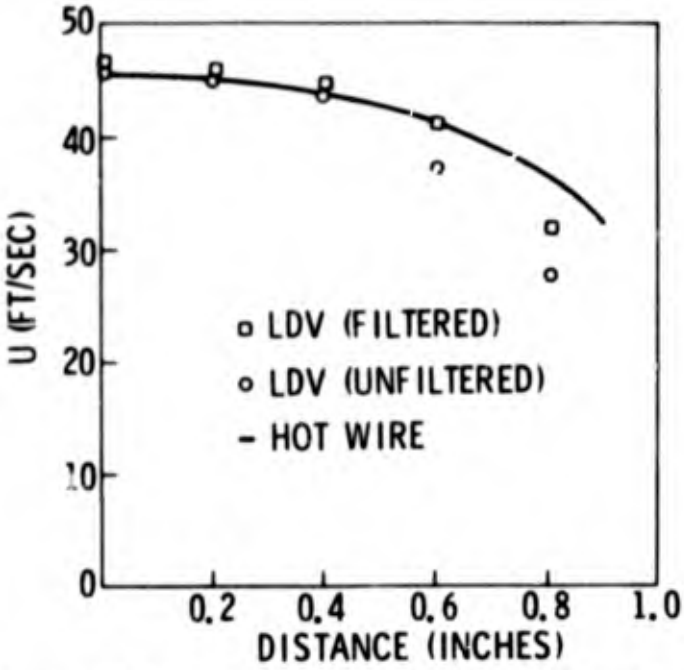

FIG. 7 MEAN VELOCITY PROFILE IN 2-D CHANNEL

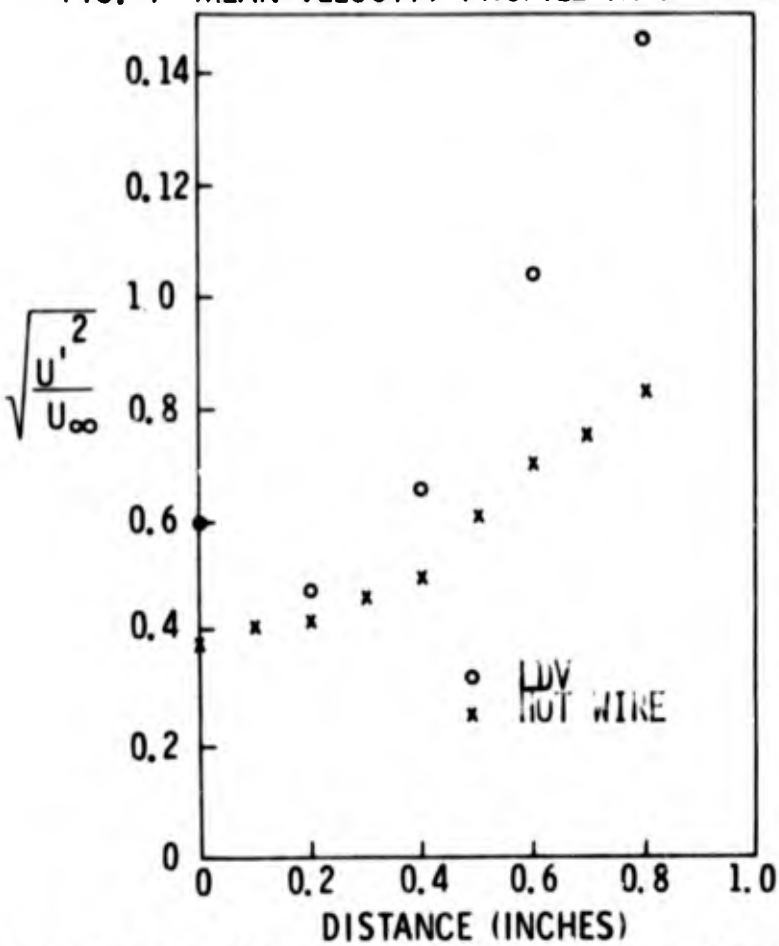

FIG. 8 TURBULANCE INTENSITIES ACROSS 2-D CHANNEL

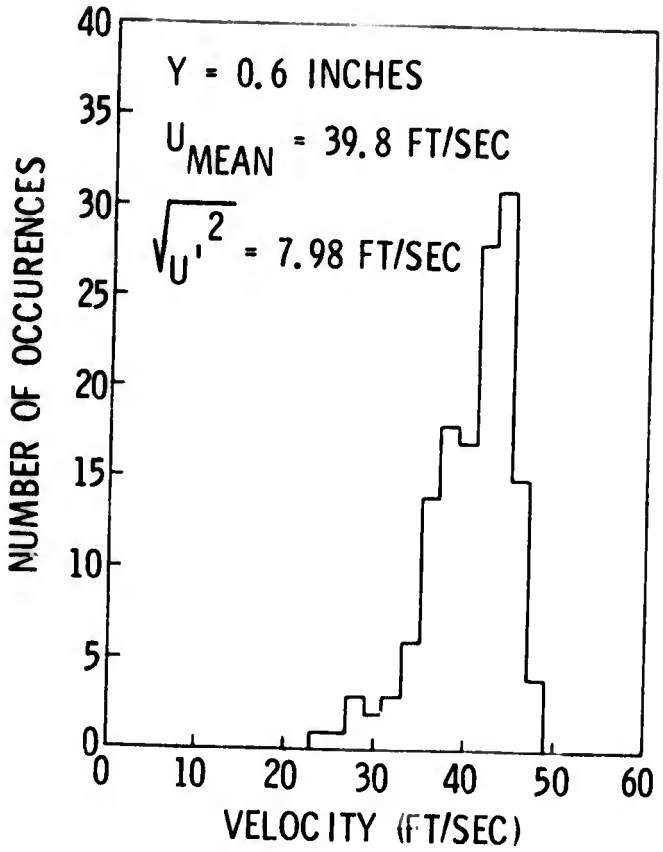

FIG. 9 HISTOGRAM OF VELOCITY DISTRIBUTION

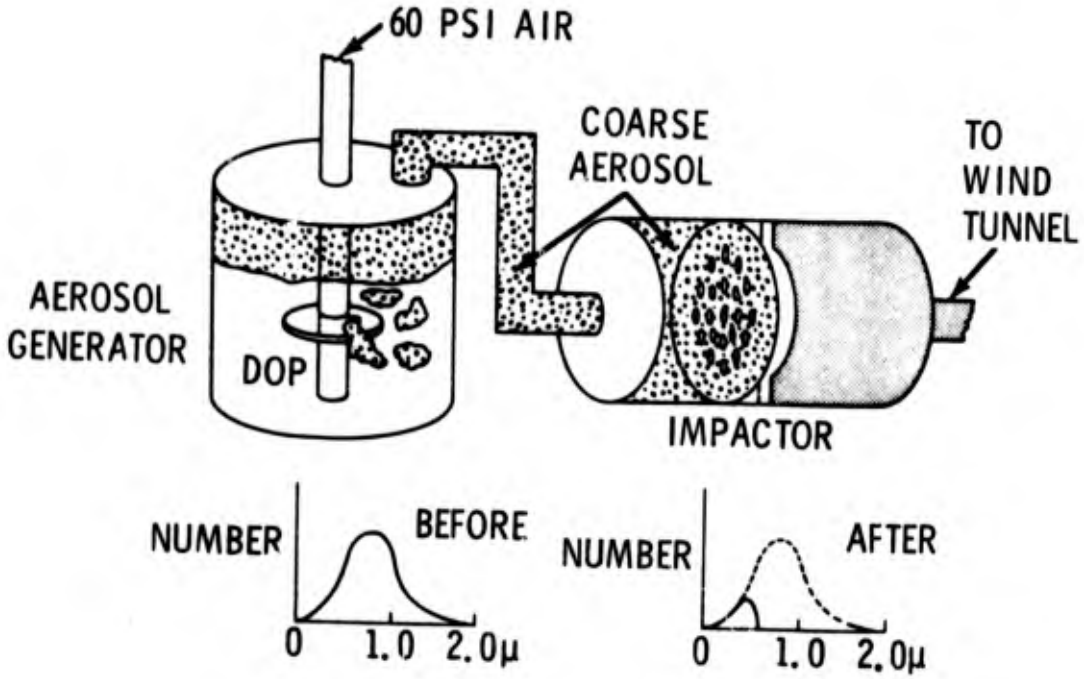

FIG. 10 LASKIN NOZZLE WITH IMPACTOR

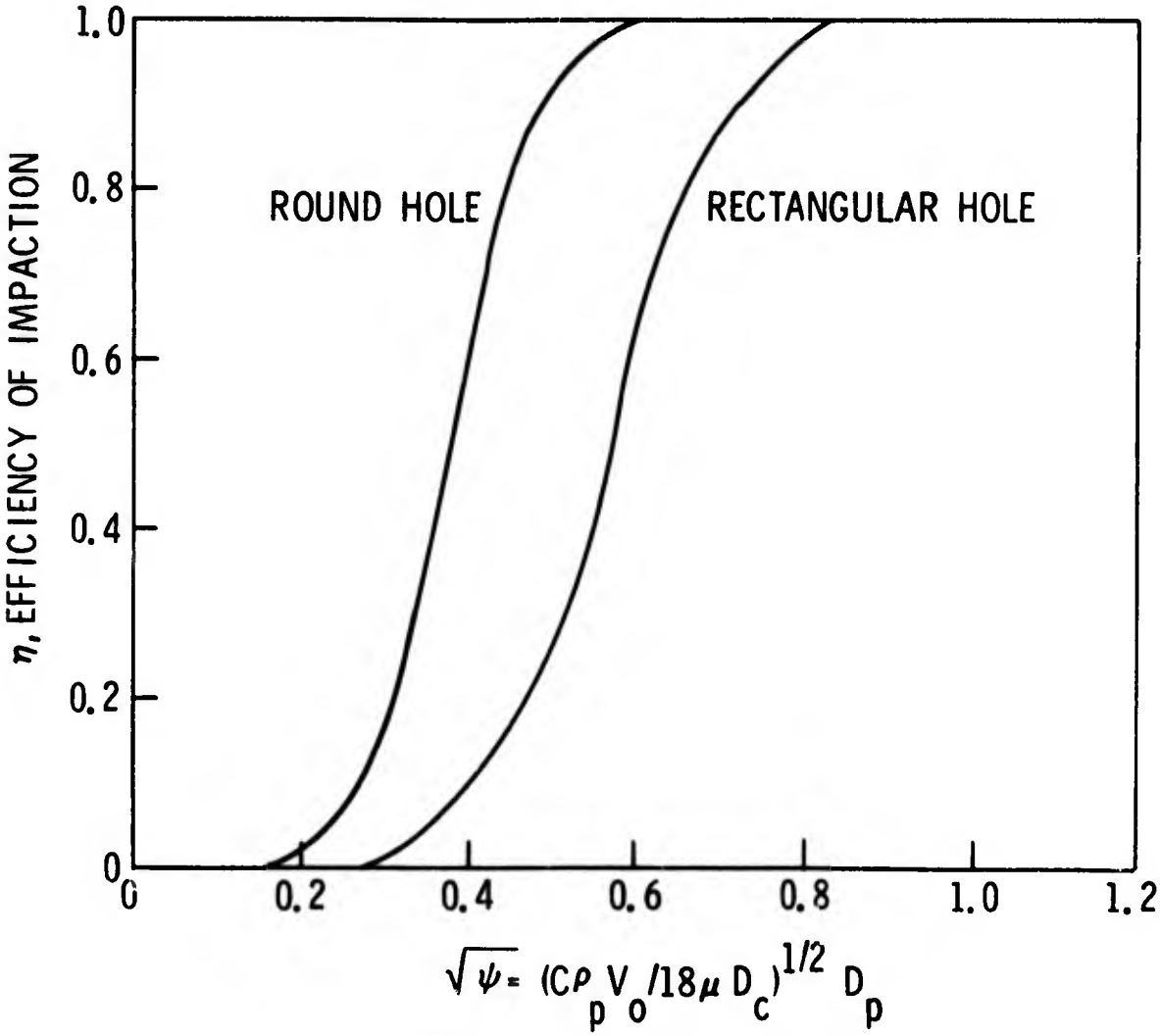

FIG. 11 EFFICIENCY CURVE FOR IMPACTOR

GEORGE: I noticed in that plot of turbulence intensity the difference between your measurements and the hot-wire measurements. You attributed that to statistical error. If this were a statistical error the points would be random. That's doppler ambiguity.

BERMAN: Yes, I agree with that. Also you indicated that there might be some effect of the particle size. I hope there will be some time this afternoon where I can present some calculations where I show this effect, but I don't think it would affect your data. There it would be almost wholly due to the finite transit time ambiguity if your scattering volume were small enough.

YANTA: My scattering volume was about 8 mils diameter.

BERMAN: How did you measure it?

YANTA: By calculation, knowing my input laser beam diameter and the focal length of the lens.

BERMAN: Usually the broadening is quite a bit smaller than that calculated because you don't align the optics. It can't really be determined unless you run an experiment with some known flow. What kind of particles did you use?

YANTA: I just used the room aerosol for that experiment.

QUESTION: The aerosol generator used Di-octyl phthalate?

YANTA: Yes

QUESTION: Isn't Di-octyl phthalate toxic?

YANTA: I understand it also might corrode plexiglas.

PIKE: It is very easy to get an estimate of this bandwidth time ambiguity if you have a set of calibrated pinholes. You know the focal volume is a three-dimensional Gaussian and you can determine its size with the pinholes. Then the bandwidth is one over the transit time.

MAZUMDER: Doesn't the air pressure to the Laskin nozzle affect the particle size?

YANTA: Yes, there might be a little bit of contention here, because the Laskin nozzle was done something like five years ago by people at NRL and they really didn't find that much difference in the size distribution by varying the pressure. It was very constant. For that particular jet size in the nozzle, the light scatter measurements that they performed are fairly reliable, I think. The particles were quite large, about 2 microns.

MAZUMDER: I was talking about the use of a lower pressure to reduce the number of large particles.

YANTA: You're right. The reason is that I tried to keep the orifice at sonic velocity. I also had to guess at the impactor jets. My hole size is about 0.015 inch. I have about forty of those little jets. I wanted to keep the velocity of the jets sonic also. When you work backwards, the aerosol is coming out on the back side of the jets at 15 psi, so I needed 60 psi input for both the jet and the impactor to be at sonic velocity. That's why we used the 60 psi. I agree that it might be better to keep this thing at a lower pressure, but I'm not sure I can be convinced that it's really going to affect the particle size very much.

LDV SYSTEMS DEVELOPMENT AND TESTING

by J.A. Asher, G.E. Corp. R&D

Our interest at General Electric Corporate R&D has been in turbulence measurements and providing a laser velocimeter system that will be capable of making these measurements.

We are using an axisymmetric air jet to determine whether or not this system development is successful. We also have a waveform generator that now fully simulates the doppler burst. Set on F.M. modulation the generator scans plus or minus 10% of a preset value of doppler frequency. So without even going to a laser we can check out a system in a fairly objective way. We have done particle seeding evaluation. I'm going to be mentioning more about that at the end of the talk. We are interested in eventually getting to multi-dimensional, the turbulence measurements. We will be developing a system for correlations of frequency spectra. Recently we have done propane flame traverses.

In the development of the laser velocimeter at G.E. our choices have been:

(a) Dual Beam. One advantage is ease of alignment. I can go into a lab after having it completely down and after ten minutes have it completely aligned. It is relatively insensitive to vibration.

(b) A Counting Signal Processor. It is not at all degraded by low duty cycles. This means that we can reduce our seeding requirement. The reduction in seeding requirement is a real advantage for those who are trying to produce this seeding, as they know. It also reduces a turbulence ambiguity that has been talked about, and it prevents a change in the character of the flow.

(c) A High Speed Data Acquisition Rate. We work up to a hundred kilohertz data acquisition rate at the present time and because we are using the doppler burst itself, not an average signal, we have a high signal to noise ratio.

(d) Seeding. We have chosen to put in a chemical particulate such as aluminum oxide (Fig. 1). These types of particles are very well size graded. We know from our electro-photomicrographs the actual size distribution. Perhaps we should incorporate something like Bill Yanta (NOL) described for making that size distribution even smaller than it is. We use a fluidized bed for injection of these particles.

We can provide a constant data acquisition rate through the use of a single throttle valve. The dangers due to the use of these particles (none known to exist) to machinery and personnel, as well as any toxic effects are known before you start. Conversely by using intrinsic particles you never know what you may be dragging in from the outside. The frequency response and relaxation times of the injected particles are known and that is an extremely important point.

I can't over-emphasize how well and simple the fluidizing bed has worked for us. Linde or Adolf-Meller produces these agglomerate-free powders. There are ways to provide an even higher degree of agglomerated-free particles using highly underexpanded jets. But in our case we have had great success without this. We pump in air, and the particles and air at the exit come into a venturi. The shearing effect between the main flow and our seeding flow has been sufficient to do away with all the agglomerates as far as we can see.

Figure 2 shows the data acquisition system. As I mentioned, we have a calibrator oscillator which we can use to fully simulate the photomultiplier input. In other words, with it we can forget the LDV optical setup. From Figure 2 we show a pre-amp, filter, and limiter. The hard limiter is used for defining the Doppler modulation zero crossings. The logic is for the direct counting and is emitter-coupled type. We go into a pulse-width-to-height converter which is sometimes known as a TAC (Time-to-Amplitude Converter). At this point there is the option of going into either a computed or real time output. We are able to determine our acquisition count rate, that is the number of velocity points that we are getting per second from a conventional counter. This defines your upper limit of turbulent frequency response (one-half the data rate).

For the computed case, we have a pulse height analyzer (PHA) in which we store information. There are 256 channels. The pulse height proportional to the time associated with the passage of the particle past a preset number of fringes is stored in the PHA. The smallest heights are placed in the first channels. A preset incremental voltage exists between adjacent PHA channels.

We have now an option to go low or high speed. At high speed it takes about 18 seconds to feed the data from the pulse height analyzer through a communication terminal to a remotely connected (through phone wires) main computer. We go into a G.E. 4020 computer, and automatically have a disc file made in the G.E. 605 main computer. A high speed printer for readout of calculations and histograms can then be easily accessed.

The other way, at slow speed, goes right into a teletype, and into the 605 directly. Teletype output, of course, is an option in both cases and gives us immediate results.

The real time output is going to allow us to provide these immediate results in a simplified manner. Here we have a sample-and-hold.

There is an option in choosing the voltage droop of the sample-and-hold circuit. One can use an A to D and a D to A sample-and-hold. This is restricted to 20 kilohertz acquisition rate but it has no droop. We also use a fast track-and-hold manufactured by Dynamic Measurements. It has a droop of one millivolt per millisecond, which is normally a very slow droop when you have a signal level of up to 10 volts and data updates at the kilohertz rate. From the sample-and-hold we go through a divider. Remember the signal coming out of this pulse-width-to-height converter is the inverse of the velocity. This is normally stored in the pulse height analyzer, but when we want a real time output, it is desirable to view the velocity directly. So we go through an analog divider, in this case a PAR divider where a preset numerator is used as an analog of the fringe spacing.

We go out into an integrating DVM with this signal where the mean velocities are measured. An RMS meter is used for determining turbulence level. The tape recorder can also be used for a permanent record and the input for the turbulence spectrum measurements.

The signal processor that we have developed is a direct counter; it has a wide doppler frequency window and high data acquisition rate, up to 100 kilohertz. The minimum acquisition rate goes right down to zero. For the low data rates trouble develops when using a track and hold that has droop. That's why the no droop type perhaps is satisfactory for that use.

Our data output is computed in real time and from tape. We have data transmittal inhibits which are adjustable. They are very important. They have been mentioned in brief by other people here. Let me go into them now.

There is a low level doppler modulation where this can imply that you can get a possible error in transit time. This is due to the particle diameter being too small or the particle passage might be through the side of the scattering volume.

There's a high level doppler modulation alarm. This alarm indicates that the particles are too large and we have to worry about our turbulence frequency response.

There is a high level pedestal alarm. This is generated normally because the particles are large with respect to the fringe spacing and this will give you quite an error in your transit time.

The doppler dropout perhaps is the most important, and sometimes can be used instead of all three of these other alarms. Essentially what this does is use two time-to-amplitude-converters or what I call transit time to height converters. These two TAC's output signals are compared and if they are not within certain error limits, the signal is deleted.

We have set up each inhibit on a read out meter so that we can determine its occurrence.

This is a sample of the output we get from a high speed printer (Fig. 3). Sample time in this case was 27 seconds, and we have 34,000 counts. Figs. 4 and 5 show probability distributions on the centerline for jet Mach numbers = 0.3 and 1.2. At x/d = 7 and 10 the histograms are becoming very widely distributed where you need more data samples to provide a truly time independent distribution.

Fig. 6 shows the results of an analytical analysis of particles going through a shock. It gives you an idea of how long the relaxation times can be. This is very similar to what Bill Yanta reported from his experimental study. A particle of 3.5 specific gravity has to be on the order of 0.1 microns to accurately follow the fluid through a strong shock front.

FIG. 1. ELECTRON PHOTOMICROGRAPH OF ALUMINUM OXIDE (Al_2O_3)
Vendor Specification, 0.3 μ

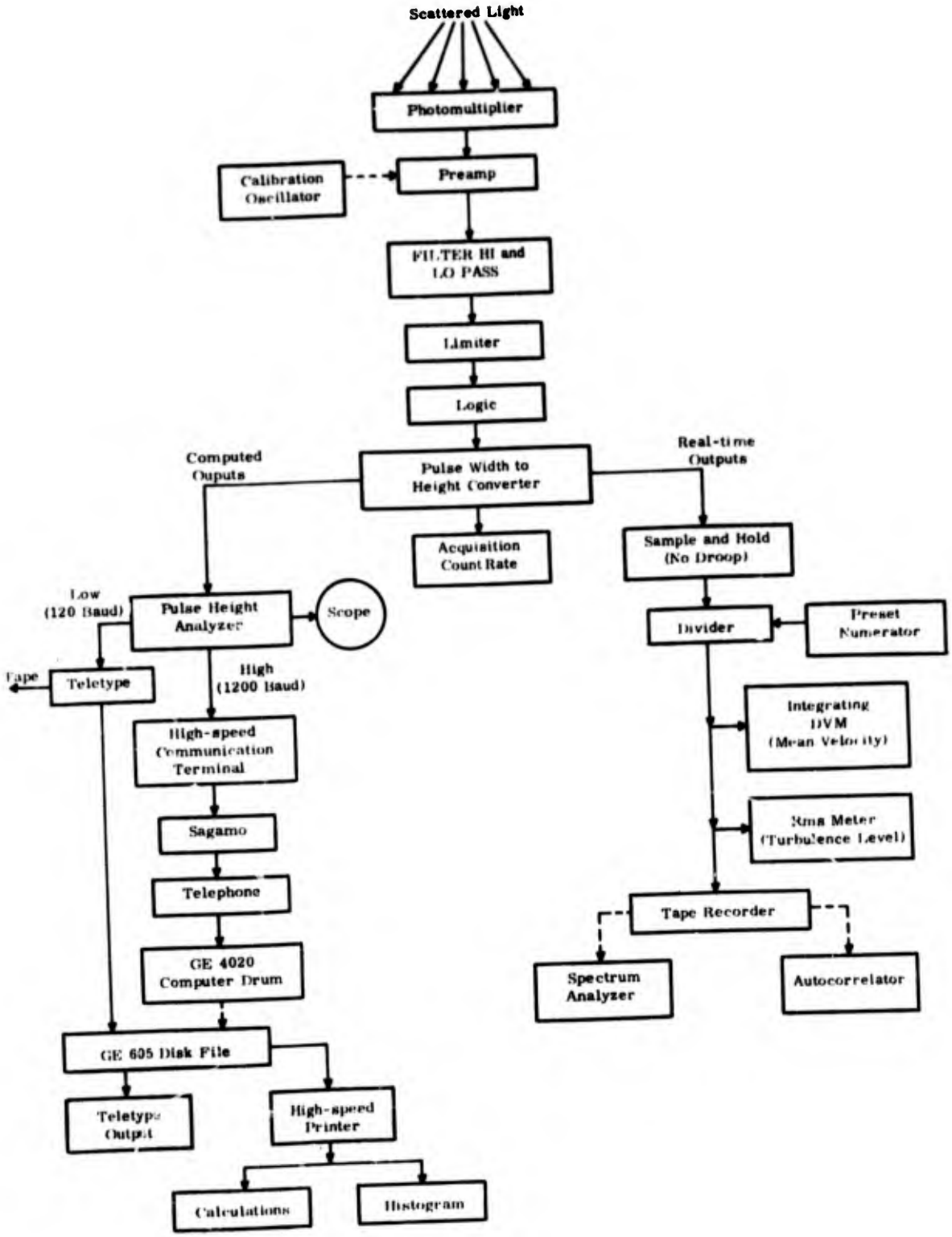

FIGURE 2. General Electric Corp. R&D Data Acquisition and Reduction System.

FIG. 3. Typical Laser Velocimeter Data Readout.

FIG. 4. Laser Velocimeter Velocity Probability Distributions for Air Jet Mach Number = 0.3.

x/d	$\bar{u}/U_{EXIT}$	u'/U_{EXIT}
3	0.995	0.041
5	0.993	0.050
7	0.897	0.127
10	0.633	0.156

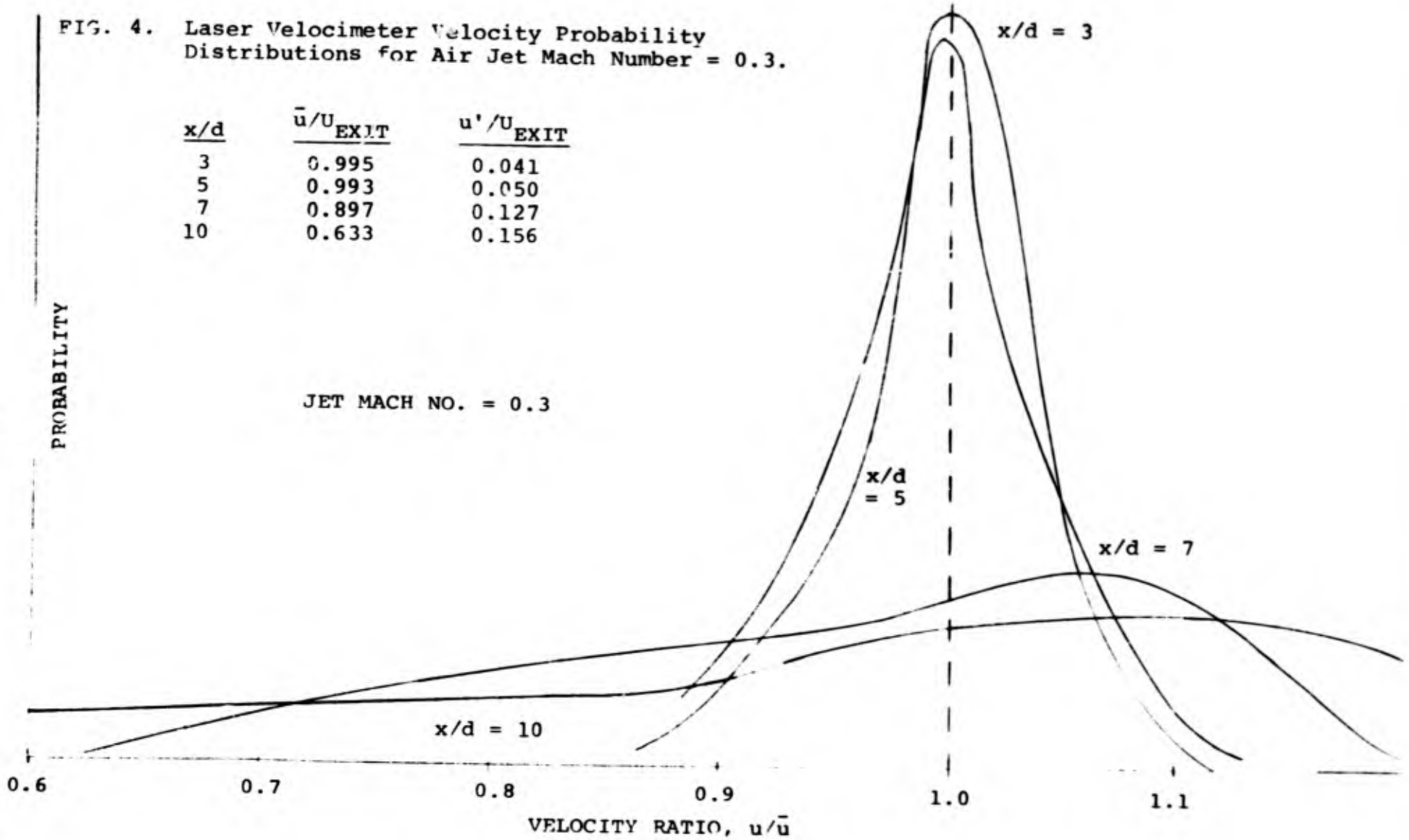

FIG. 5. Laser Velocimeter Velocity Probability Distributions for Air Jet Mach Number = 1.2.

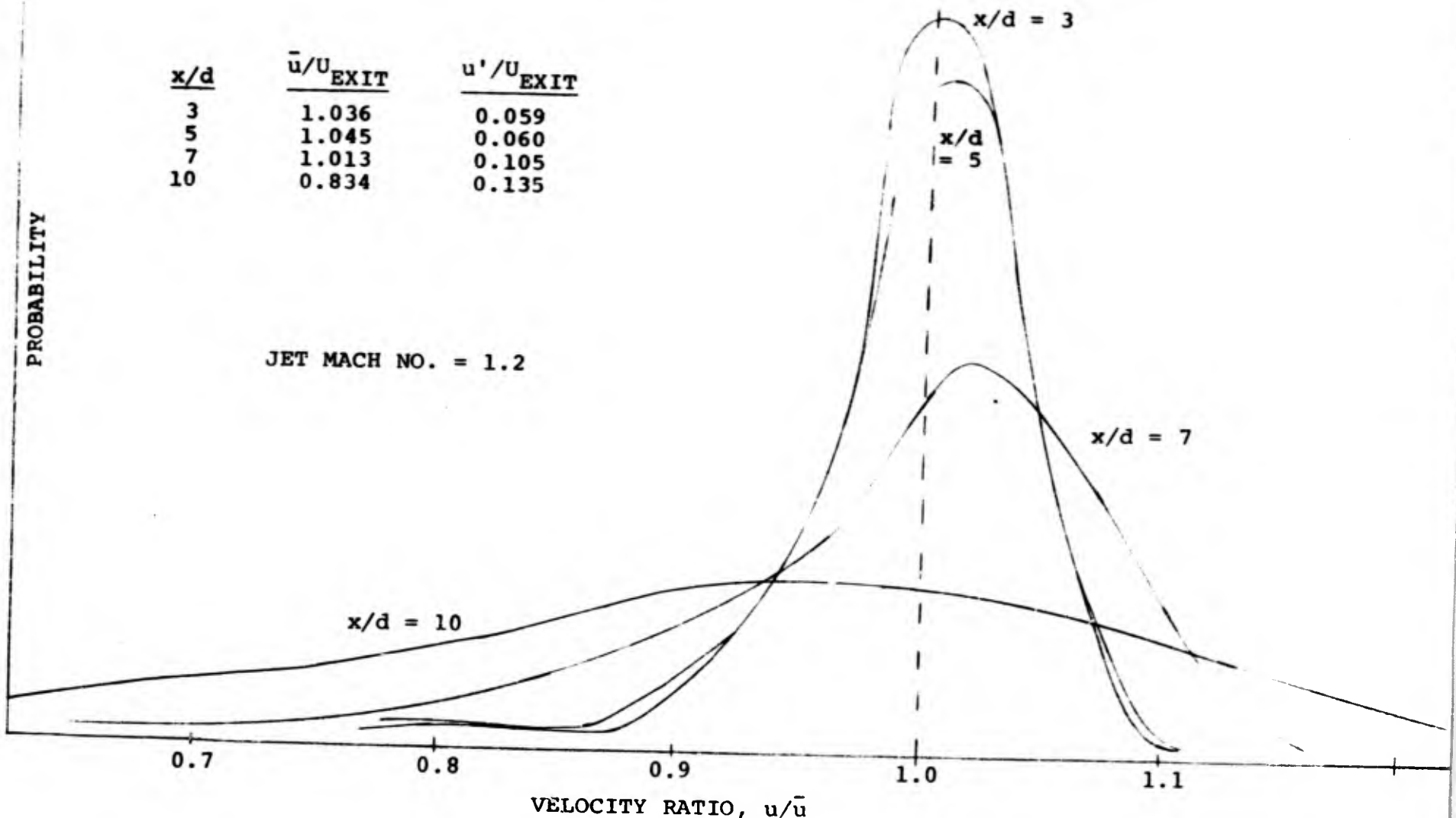

x/d	$\bar{u}/U_{EXIT}$	u'/U_{EXIT}
3	1.036	0.059
5	1.045	0.060
7	1.013	0.105
10	0.834	0.135

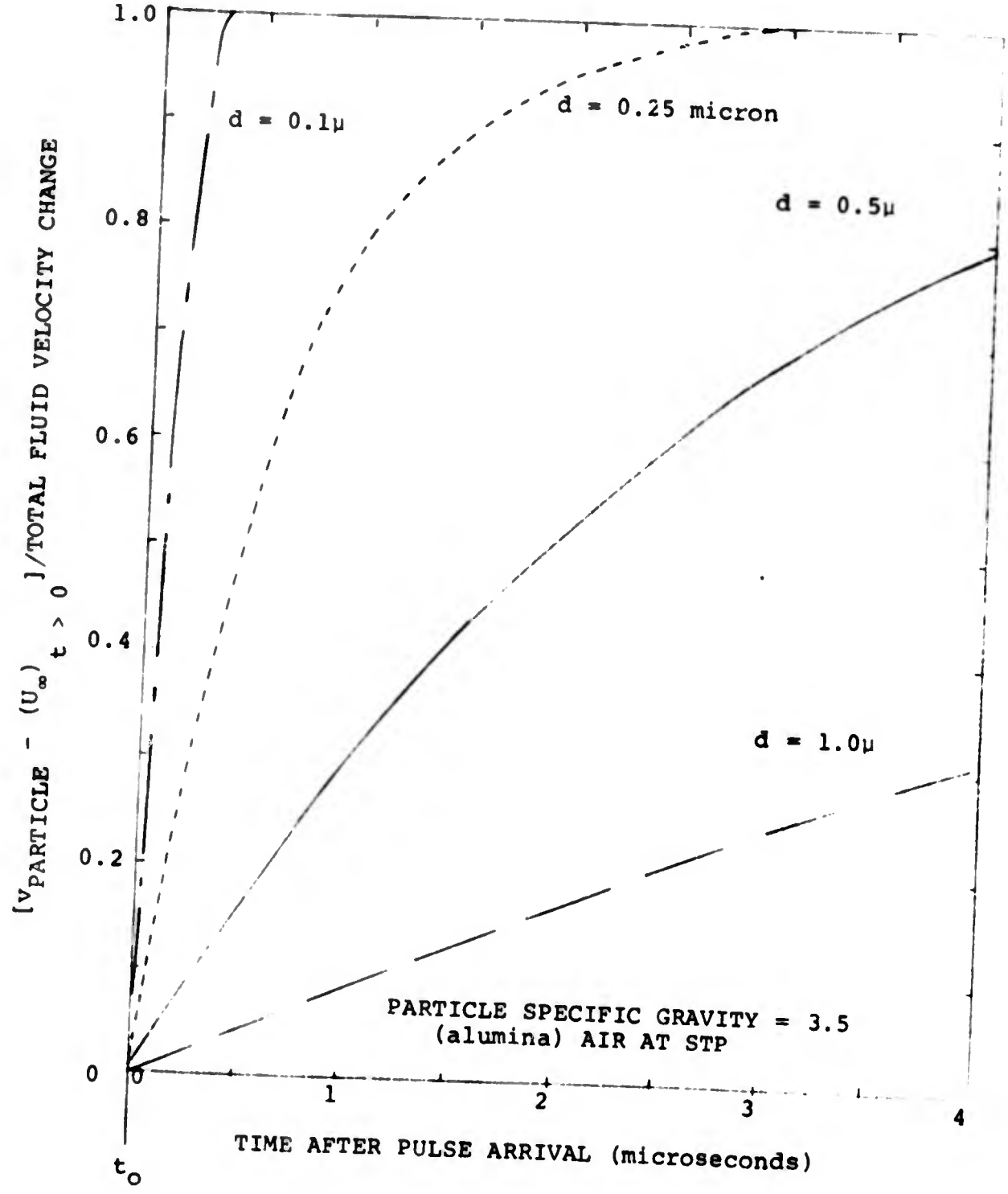

Fig. 6. Particle Movement with Step Change in Velocity for Various Particle Diameters.

DISCUSSION

FRANCIS: Does the data rate of 100 kilohertz infer that 100,000 particles per second are going through the focal volume?

ASHER: No, it actually infers that you have greater than that. Paul Mossey, of Evendale, has been using this circuit in very large jet flows. He found that with all the dropout inhibits he has been using (fairly similar to ours) that he has been getting something like only 30 percent successes which means about 70 percent failures. So if you want to have a data acquisition rate of 100,000 it means you're going to have to have 300,000 particles going through.

SHAFFERNOCKER: Andy Lennert may have some data, too.

LENNERT: Yes, that number is about right.

ASHER: I want to go a little bit further into that because it's a good point. Now you ask the question, what is the maximum number of particles you can pack through there if there is only one at a time? For the high velocity flows that Paul was working with (where the dropout does occur most frequently, obviously) the number was something like five million particles per second going through the scattering volume. It goes up as the velocity increases and that is fortunate because the design frequency response goes up as well.

PIKE: I could make a comment on the question that has risen this morning regarding statistical accuracy in processing data. You proved that there is some similarity between the laser doppler work and some well established work in optical mixing spectroscopy. In that field there are vast amounts of literature on the question of statistical accuracy in such measurements. Although it is not directly applicable, I would think it could be made so with a certain amount of modification. Basically the numbers that come up are just a total number of photons that you can detect from the whole experiment and the number of doppler cycles that have elapsed in the whole experiment. If you make the right combination of these, you get the accuracy estimate whether it's rms turbulence or whatever. There is a lot of interesting work to be done there.

ASHER: There is one thing I would like to add. When Bill Yanta made measurements out to the side of the jet where the turbulence level was highest and he had the greatest errors, that was also the position where he had the widest distribution. This means his second moment is going to be worse unless he has a commensurably increased number of samples, and he did not. That's why I feel that there is a possibility of large error.

HAUER: I take it that you disagree with what George has said as far as the limiting factor being instrumental broadening in this case. Or is this a statistical matter?

ASHER: As far as the direct counting is concerned, my personal belief is that using multiple particles in the scattering volume is extremely hazardous to one's health - especially when you try to publish the work! I do not believe that it is necessary under most conditions to ever have multiple particles in your scattering volume. If you do because of the LDV signal processor that you are using, that's a problem that I personally can't help. For most scattering volumes that you are talking about, you have sufficient number of particles to get a 50 percent duty cycle - where you are not going to have the probability of multiple particles. You will be able to get your data and most of the turbulent ambiguity will be reduced. There is another turbulent ambiguity I think that the signal processor reduces as well.

YANTA: In my experiments I was getting only about three particles per second. The duty cycle was very low.

WHITELAW: One point regarding the effects on health of particles.

ASHER: Alumina is nontoxic - that's what they say.

WHITELAW: The long term effect of small particles in the lung is not really known. I tried to find out for various substances from the British Health Service. It's a good establishment and they said that if you are putting particles in the atmosphere it's exactly what we don't want you to do.

ASHER: We have Environment I right by us and they measured the small particle content in the air. It's vast because most of it just stays in the air from the stacks that generate.

TECHNICAL SESSION VI - APPLICATIONS B

Session Chairman: B.Z. Jenkins

349B

LDV FOR CHARACTERIZING AIRCRAFT TRAILING VORTICES

By

A. E. Lennert, W. M. Farmer, J. O. Hornkohl

ABSTRACT

A prototype laser velocimeter is being built to perform proof-of-principle measurements on trailing vortices stemming from wing tips of aircraft. The velocimeter to be used is a three-component dual scatter system to not only measure the magnitude of the velocity components simultaneously but will also determine directionality. An in-house developed read-out system will be used to process the data. A description of the laser velocimeter including the signal conditioner and data processor is presented. Included are the expected operating parameters for the field experiments to be conducted.

The research reported in this paper was sponsored by Arnold Engineering Development Center, Air Force Systems Command, Arnold Air Force Station, Tennessee, under Contract No. F40600-72-C-0003 with ARO, Inc. Further reproduction is authorized to satisfy the needs of the U. S. Government.

This research is supported by National Aeronautics and Space Administration, Langley, Virginia, under Contract No. L-52080.

NOMENCLATURE

A	Area
D_f	$1/e^2$ beam diameter at focal region
DS	Dual Scatter System
FL	Focal length
N_e	Effective number of fringes
N_s	Number of stationary fringes
R	Range
R_2 R_1	Radius of telescope
S/N	Signal to noise ratio
LO	Local oscillator or reference beam system
d	Peak to peak fringe spacing
d_b	beam diameter at transmitter lens
d_s	Beam separation at transmitter lens
f_o	Light frequency
f_D	Doppler frequency
f_m	Modulation frequency
k	Propagation vector $\frac{2\pi}{\lambda}$
n	Number of fringes, within $1/e^2$ intensity
v	Velocity in focal volume
λ	Wavelength of light
θ	Angle between transmitted laser beams

Subscripts

o	Original beam
s	Scattered beam
R_1	Receiver telescope
t	Transmitter telescope

LDV FOR CHARACTERIZING AIRCRAFT TRAILING VORTICES

By

A. E. Lennert, W. M. Farmer, J. O. Hornkohl

INTRODUCTION

From the reports of numerous incidents and accidents (Ref. 1) during the past few years it is evident that the trailing vortices stemming from the region near the wing tip of large aircraft create a severe hazard to penetrating light aircraft. Attempts have been made to understand the creation and decay of these wing tip vortices; however, substantiating measurements to correlate the theories have not met with too great a success. Prior to the development of the LDV measuring technique, the only quantitative data acquired of the trailing vortices were by means of flying an aircraft down a cross-wind runway to permit the action of the crosswind to cause the wing tip vortices to drift past a measurement station. The measurement station generally comprised a tower located at some distance from the edge of a runway upon which mechanical anemometer were suspended. Simultaneously smoke was also released such as to make the vortices visible (Ref. 1).

A number of such measurements have been made utilizing cup anemometers and compared with a one component CO_2 LDV system. In the experiment a 20 watt CO_2 gas laser (Ref. 1) was used in conjunction with a 12 inch transmitter-receiver telescope system such that the transmitter beam could be focused near a cup anemometer. Radiation scattered from smoke particles traversing the focal region of the laser beam was collected by the same telescope system. The scattered radiation was imaged on a detector. The signal from the detector passed through a signal conditioning system that yielded the particulate velocity. Preliminary data were taken comparing the cup anemometer with the CO_2 LDV system and are included in Fig. 1. The top set of curves compares the measurements of both systems under steady wind conditions. It is readily noticed that the velocity changes measured by the LDV system are much more sensitive than those acquired by the anemometer. In the lower set of curves, taken under variable wind conditions, the enhanced sensitivity of the LDV system over the anemometer data is much more noticeable. In both curves directionality is not included in the LDV data.

Although the use of the CO_2 laser has proven moderately successfuly, there is still the spatial resolution and S/N problems that must be overcome to effectively perform detailed measurements of the trailing vortex. For a given

transmitting lens the spatial resolution of a LDV system is directly proportional to the wavelength and the transmitted beam f number, hence it becomes obvious that for constant f numbers, a shorter wavelength gives better the resolution. Furthermore, it has been shown that for Burst type signals dual-scatter LDV systems give better S/N (Ref. 2). For these reasons an argon laser LDV system is being constructed to perform measurements of trailing vortices at remote distances. Proof-of-principal measurements were made at the AEDC airport, under NASA sponsorship and with the assistance of NASA-Langley personnel. As in previous measurements a tower with three anemometers was erected, by the Langley personnel, to correlate both LDV and anemometer data. The vortex, created by a C47 aircraft flying at approximately 50 feet above the ground, was to be measured. Visual contact with the vortex was established by smoke bombs mounted on the wing tips of the aircraft. In addition, a smoke bomb tower was erected near the anemometer tower to visually ascertain the vortex flow field (Fig. 2). The LDV system, schematically illustrated in Fig. 3, and a photograph in Fig. 4, was checked out on the aircraft run-up pad where the flow field measurements were to be made. The probe volume was established at 1 foot from the center anemometer. The entire LDV telescope system was moved approximately 180 feet off the side of the runway.

Measurements were made at an elevation of approximately 30 feet above the ground plane and the horizontal distance between the telescope and the anemometer tower was approximately 120 feet. The aircraft flew a parallel pattern to the telescope line-of-sight such that the background wind velocity would drift the vortex through the probe volume and the anemometers mounted on a tower. A major interface problem arose between the transmitting-collecting optics of the LDV unit and the automatic readout resulting in no rapid data acquisition. The experimental results depended solely upon acquiring photographic data from oscilloscope recordings. In many cases the sudden arrival of the trailing vortex produced tremendous amounts of data such that the analysis of the oscilloscope traces was impossible. It was, therefore, difficult to correlate the LDV data with that of the rotating anemometers; nevertheless, proof-of-principal data including background wind velocity, that compared favorable with the data acquired from flight operations, in addition to vortex flow field data were acquired and photographs of typical data are shown in Fig. 5.

For the past year additional development activity centered about modifying the Laser Velocimeter (LV) with particular emphasis placed upon the Doppler Data Processor system. The unit now covers the low frequency domain required

for trailing vortex data. Additional laboratory results verified improvements and full scale experiments are currently being scheduled at the Malabar site of the Range Measurements Laboratory at Patrick Air Force Base to acquire simultaneous three component velocity vector data (vector magnitudes and direction) of the trailing vortices.

The remaining portions of this report will outline the prototype LDV design to perform the full scale, three-component, remote measurements, including directionality over a range from 200 - 1000 feet.

SECTION II

PERFORMANCE ANALYSIS OF REMOTE SENSING LASER VELOCIMETERS

In view of the success (Ref. 2, 3, 4) that has been achieved in applying dual scatter laser velocimeters for wind tunnel measurements a performance analysis was completed to ascertain the feasibility of utilizing shorter wavelengths for remote sensing applications. The study was made to ascertain the dependence of the scatter signal power as a function of range, wavelength, laser power, and signal to noise ratio for ranges greater than 10 meters (Ref. 5, 6). In addition, a comparison between the performance of local oscillator and dual scatter systems, particularly in a

turbulent atmosphere, was also necessary to determine which system should be selected.

An analysis was performed utilizing signal to noise power ratio, S_r , as a common denominator (Ref. 6). The relative performance of the dual scatter and the local oscillator LDV systems was made using a basic comparative performance figure S_r of the two systems defined as:

$$S_r = \frac{(S/N)_{DS}}{(S/N)_{LO}} \qquad (1)$$

Since the S/N values were determined at the output of the signal detector they are biased toward the optical and detector performance for each of the systems. The parameters used in performing the analysis are included in Table 1. The summary of the results of the study are included in Figs. 6, 7, 8, and 9. Figure 6 contains a plot of the S_r of the CW signals in both turbulent and quiescent atmospheres as a function of range. In this particular case, both the dual scatter and the local oscillator systems were operated at a wavelength of 5000 A° and transmitted through the same set of optics such that the system could measure 3 orthogonal velocity components. It is seen that in either a quiescent or turbulent atmosphere and regardless of propagation path (vertical, horizontal, or at a 45° angle) the

signal to noise ratio criteria indicate the dual scatter will outperform the local oscillator system within a range of 1000 meters. In a quiescent atmosphere the dual scatter outperforms the local oscillator at any range whereas in the slant height and horizontal propagation cases the local oscillator systems outperform the dual scatter beyond a range of approximately 2000 meters. In Fig. 7, a comparison is made of a dual scatter system operating at 0.5 micrometers with a local oscillator system operating at 10.6 micrometers. In a turbulent atmosphere the local oscillator system outperforms the dual scatter system beyond the range of approximately 700 meters for all propagation paths considered. In the case of a quiescent atmosphere the local oscillator will again outperform a dual scatter beyond a range of approximately 700 meters. Within this range the dual scatter system outperforms the local oscillator in every case. In both Figs. 6 and 7, the signals are CW.

This situation changes, however, when burst signals are detected. Comparing the local oscillator and dual scatter system operating at 0.5 micrometers in both the turbulent and quiescent atmosphere (Fig. 7) it is found, regardless of the propagation path, that the dual scatter will outperform the local oscillator.

In a quiescent atmosphere the signal to noise ratio of the dual scatter system is invariable several orders of

magnitude greater than the local oscillator system. In Fig. 9, a comparison is made of the dual scatter operating at 0.5 micrometers and the local oscillator at 10.6 micrometers in both a quiescent and turbulent atmosphere. From the figure, it is readily seen that for burst type signals the dual scatter system outperforms the local oscillator beyond a range of approximately 25 meters in the case of a turbulent atmosphere. In the case of a quiescent atmosphere the dual scatter LDV system outperforms the local oscillator within a range of interest (up to 350 meters).

The results can be briefly summarized as follows: (1) If the LDV signals are of a burst nature the dual scatter system offers inherently higher signal to noise ratios than the local oscillator signals. For the case of CW signals, there are conditions where the local oscillator system offers superior performance. (2) The use of the long wavelength with the local oscillator system tends to cancel the limiting aperture effects due to turbulence degradation. (3) When long wavelengths are used in local oscillator systems, the output beam diameter or the power must be increased accordingly. In the event the wavelength is increased by an order of magnitude, over a previous wavelength, and the original input beam diameter is constant the power must be increased by two orders of magnitude to maintain the same signal noise ratio. (4) The local oscillator system exhibits the worst

performance for vertical propagation and the best for parallel or horizontal path propagation, whereas the dual scatter systems are essentially independent of observation angle. (5) The local oscillator system operates most efficiently in a quiescent atmosphere at very long ranges. This increase in performance can be attributed to an increase in the number of scatter centers available as the probe volume increases.

SECTION III

THEORY OF THE DUAL SCATTER LASER VELOCIMETER

The Doppler theory inherent with the local oscillator and the dual scatter LDV is well understood and shall not be considered. However, for the sake of clarity an alternative analysis (Ref. 7) of the DS system is presented such that the physical phenomena inherent with the masuring technique will be easily understood. The laser source is split up into two beams, for each velocity component, and focused to a diffraction limited region of Gaussian intensity containing essentially planer wavefronts of radiation. In view of the coherence characteristics of the source the beams will interfere constructively and destructively to establish

a set of closely spaced, planer, interference fringes at the beam crossover, or focal, region. The peak to peak fringe spacing, d, is readily shown to be:

$$d = \frac{\lambda}{2 \sin \frac{\theta}{2}} \tag{2}$$

the $1/e^2$ diameter of the focal region is:

$$D_f = \frac{4}{\pi} \lambda \frac{F.L.}{d_B} \tag{3}$$

the number of fringes contained in a focal volume can be determined by dividing the peak-to-peak fringe spacing into the focal diameter as follows:

$$n = \frac{4}{\pi} \frac{FL}{d_b} 2 \sin \theta/2 = \frac{8}{\pi} \frac{FL}{d_b} \sin \theta_2 \tag{4}$$

This can be further simplified by assuming $\theta/2 \angle\angle 1$ such that $2 \sin \theta/2 \approx \theta$, where θ is the separation of the two beams at the transmitter divided by the range. With this approximation:

$$n = \frac{4}{\pi} \frac{d_s}{d_b} \tag{5}$$

As a particle traverses the focal volume at a velocity v the interference fringes are cut at a rate of:

$$\frac{\lambda}{2v \sin \theta/2} = \frac{1}{f_D} \qquad (6a)$$

$$f_D = \frac{2v \sin \theta/2}{\lambda} \qquad (6b)$$

which is exactly the period of the Doppler frequency and the Doppler shift frequency respectively. Since the particle traversing the fringes repetitively scatters light it will generate an alternating, fluctuating, current with a frequency proportional to the rate at which the particle intercepts the fringes. It has also been shown that only one component of velocity, mainly the component normal to the interference fringes, is measured. It is straightforward to add additional optics to determine the second and third velocity component.

The unique feature of the dual scatter technique is that it is possible to place the receiver optics in any position since the viewing direction does not affect the measurements. In general, however, the operation of the dual scatter system is close to the axis for optimum operation. This is predicated upon light scattering phenomena and not upon the instrument. Furthermore the dual scatter technique is extremely sensitive- resulting in higher S/N ratios than the local oscillator in that light is premixed before the scattering event results hence the technique is insensitive to any perturbations that affect the local oscillator systems. In addition, the S/N for the dual scatter system is independent

of the number of scatter centers in the probe volumn whereas for the LO the S/N is functionally dependent upon n for enhanced values of S/N.

In view of burst type signals acquired by a dual-scatter system a data acquisition system must be designed to accommodate these signals. A Doppler Data Processing System has been developed which is essentially a burst measuring device and will be described in the following section. The fundamental problem inherent with any of the present LV systems, such as described, is the ambiguity in the direction of the velocity vector. The Doppler signals yield only the absolute values of frequency or velocity but have 180° ambiguity in the direction. By including Bragg cells to modulate the laser beam at a known frequency it is possible to acquire directionality and hence, true vector velocities. This is readily shown in the following dual scatter analysis (Ref. 8).

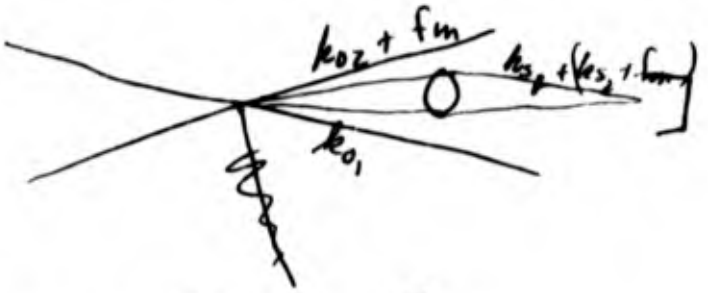

$$f_{D1} = f_o \pm \vec{v} \cdot (\vec{k}_{s1} - \vec{k}_{o1}) \qquad (7a)$$

$$f_{D2} = f_o + f_m \pm \vec{v} \cdot (\vec{k}_{s2} - \vec{k}_{o2}) \qquad (7b)$$

Since the particles scatter light from the same point the scattered propagation vector disappears when the difference frequency is obtained e.g.:

$$f_D = (f_{D1} - f_{D2}) = \mp \vec{v} \cdot (\vec{k}_{02} - \vec{k}_{01}) - f_m \qquad (8a)$$

$$f_D = (f_{D2} - f_{D1}) = f_m \pm \vec{v} \cdot (\vec{k}_{01} - \vec{k}_{02}) \qquad (8b)$$

When the particles are traversing the focal volume in the direction of the moving fringes the Doppler frequency will be lower than the modulation frequency. Conversely, if the particles are traversing opposite to the direction of the traveling fringes the measured frequency would be higher than the modulation frequency. In this manner the directional ambiguity is resolved. Furthermore, since the modulation frequency is superimposed upon stationary fringes the number of effective fringes (stationary plus traveling) within the focal volume becomes:

$$N_e = N_s \left(\frac{f_m}{f_D} \pm 1\right) \qquad (9)$$

The result of imposing traveling fringes upon the focal volume increases the net number of fringes and hence within the same counting interval of a Data Conditioning and Processing system, such as developed by Kalb (9), greater accuracy of the measurements is realized.

SECTION IV

TRAILING VORTEX TEST PARAMETERS

A prototype laser velocimeter system has been designed for mapping trailing vortices using the Malabar site equipment of the Range Measurements Laboratory (RML) at Patrick Air Force Base. In this particular experiment two argon laser sources will be used. Each of the sources will be modulated at a known frequency e.g., 15 MHz, 25 MHz and 30 MHz respectively. The 15 and 25 MHz modulated transmitting beams will be transmitted by a 36 inch telescope. This telescope system will be used to ascertain the vertical and horizonal components of velocity. A second telescope, 24 inches in diameter, will be used to transmit the 30 MHz modulated beams that will be used to determine the third velocity component. The range of operation for the experiment will be between 200 and 1000 feet. The test setup is schematically illustrated in Fig. 10, a third telescope, 48 inches in diameter, located approximately 450 feet from the 36 inch telescope and approximately 300 feet from the 24 inch telescope will be the receiving telescope for all three components of velocity. The received signal will be focused through a pin hole and narrow band filter onto a photomultiplier tube. From the photomultiplier tube assembly the signal passes

through a dual output wideband amplifier to increase the signal level by means of a gain adjust. Figure 11 contains a schematic diagram of the signal preconditioning system. The input passband frequency (3 db level) of the amplifier is 30 MHz. One output signal carries the 15 MHz signal through its respective filter-wideband amplifier network and the 25 MHz portion passes through its respective network. In a similar manner, the 30 MHz signal passes through its amplifier filter network. All three signals enter their respective mixers where a reference oscillator frequency heterodynes with the respective signals to downshift the frequence before passing into a low pass amplifier, with a variable frequency adjust, and then into a Doppler processor. Each individual component will pass through its own respective Doppler Data Processor and then into the Data Acquisition System.

A. Doppler Data Processor

The frequency burst signal processing electronics system schematically shown in Fig. 12 is a hybrid analog-digital signal conditioning and processing instrument termed a Doppler Data Processor (DDP) (Ref. 9). The functions of the DDP are (1) to filter out extraneous noise, (2) to determine the average period of at least eight cycles of the Doppler shift signal, (3) to negate a data recording cycle when the period of eight cycles is not equal to twice the period of the first four cycles, and (4) to provide a visual

display and a binary coded decimal output of the period of the Doppler signal. The data acquisition system will employ an incremental magnetic tape system for mass data recording and compatibility with subsequent digital computer computations.

The photodetector signal for a small scatter particle passing near the geometric center of the probe volume is indicated in Fig. 13a. Ideally, the D.C. shift of the signal is comparable in magnitude to the A.C. or Doppler signal portion. Photodetector shot noise generated by the D.C. shift as well as background radiation tends to obscure the Doppler signal information. A bandpass amplifier is used to remove much of this D.C. shift and to minimize the associated shot noise.

A representative signal introduced at the input to the DDP is shown in Fig. 13a. The bandpass amplifier (Fig. 12) output signal is shown in Fig. 13b. The Schmitt trigger (Fig. 12) output signal is shown in Fig. 13c. An oscilloscope triggered gate at the output of the Schmitt trigger prevents passage of pulses to the A-B-C-D ripple counter when the signal level at the oscilloscope is below a certain selectable trigger point. This technique has proven to be a valuable means of signal level selection and noise rejection.

The gated signal applied to the A-B-C-D binary ripple counter produces a single rectangular wave signal or "pulse" at the D Binary output Fig. 13f with a time duration equal to the total period of the first eight pulses in the

gated pulse train. At this point Binary D is inhibited from further toggling by Binary I until a recycle control pulse is received. The D Binary pulse becomes the gating signal for the main gate pulse stretcher Fig. 13g which produces a resultant pulse precisely stretched in time by 125 times the D Binary pulse. Precision current sources contained within the pulse stretcher permit very precise time duration extention of the D Binary pulse width. The stretched pulse controls the main gate of a conventional frequency counter. During the stretched pulse interval, precisely timed clock pulses from a crystal controlled oscillator pass through the main gate and accumulate in the counter decimal counting units (Fig. 12). The resultant counter visual display reads the average period of the Doppler signal information in nanosecond units. The pulse stretching technique is useful for short burst signal period determination at frequencies extending from 100 KHz to 100 MHz. At lower frequencies the main gate pulse stretcher is not required.

The circuits described thus far measure the average period of both periodic and non-periodic signals. When the signal pulse train becomes non-periodic during this time period due to included noise spikes, peak fringe intensity irregularities, or large fluctuations in peak signal amplitude, additional circuity has been included to detect this condition and prevent the recording of a data point. Details of the techniques are included in Ref. 9, and will not be further discussed.

Six parameters will be recorded from TS-ER's laser velocimeter instrumentation by RML's data acquisition and computing equipment. These six parameters represent three velocity measurements, each consisting of the shifted Doppler frequency and the local oscillator frequency.

The Range Measurements Laboratory's (RML) system records all range parameters each one tenth of a second. These include the elevation angle, azimuth angle, and range setting of each telescope as well as time, and other parameters. The LV data will be recorded at this rate.

One scan of these parameters will be recorded on magnetic tape as one 600 word record. The parameters of interest to the Trailing Vortex Study will be picked from each record to be entered into the data reduction program that will resolve the three velocity components into one velocity vector.

To interface the Hewlett-Packard HP5245M electronic counters with the XDS Sigma 7 digital computer, the voltage levels will be converted from + 18 and - 8 volts to + 5 and 0 volts for logic levels of "1" and "0" respectively. These signals will be transmitted approximately 200 feet from the velocimeter equipment to the computer. This part of the interface is being handled by RML personnel.

The data reduction can be broken down into three distinct manipulations. The first involves the determination of the individual velocity components from the basic frequency

measurements. The second consists of resolving the measured velocity components into a common co-ordinate system using the elevation and aximuth angles of the transmitting telescopes. The third consists of presenting the data in a meaningful format, such as tabulated data or a plot of velocity vs location.

To resolve the individual velocity components into a common co-ordinate system involves rotation of the co-ordinate system of two of the velocities through the elevation and aximuth angles of their transmitting telescope and rotation of the co-ordinate system of the other velocity through the aximuth angle of its transmitting telescope. This converts the three measured velocities into one velocity vector in a co-ordinate system centered on one of the transmitting telescopes. Transformation of the velocity vector to a convenient co-ordinate system for data display is then straightforward.

This information will then be tabulated or plotted as velocity magnitude and angle versus time, time rate of velocity measurements, measured velocity components versus time, etc.

The parameters to be encountered during the next series of experiments, to be conducted at the test site at Patrick Air Force Base, were determined by scaling experimental data acquired with a mock-up of the system at the AEDC. An 8 inch diameter and a 10 inch diameter telescope system was used for the transmitter and receiver respectively. A CRL 53G laser, operating in a 5145 Å line, was used as the laser source. Two component measurements were made of atmospheric conditions at a range of approximately 80 feet. The vertical and horizonal components were modulated at a frequency of 15 and 25 MHz respectively. Typical data that were acquired are shown in Fig. 14.

It has been determined (Ref. 6) that the scattered signal power is inversely proportional to the wavelength cubed and the fourth power of the range $(\frac{1}{R^4})$. In addition, the signal power is proportional to the area ratio of both the transmitting and receiving telescopes. The laser power required as a function of range and transmitting-receiving optics is shown in Fig. 15. The scaling was as follows:

$$R_2 = \left(\frac{A_{R2}}{A_{R1}}\right)^{1/2} \left(\frac{A_{t2}}{A_{t1}}\right)^{1/2} R_1 \qquad (10)$$

Figure 16, 17, 18 are plots of the Doppler frequency as a function of the range and velocity. Included are the additional parameters of modulation frequency, the wavelength, and the diameter of the transmitting and receiving telescopes.

Figure 16 and 17 are plots where a 3 foot telescope is used for transmission for a modulation frequency of 15 and 25 MHz. In Figure 18, the data are plotted for a 2 foot telescope and a modulation frequency of 30 MHz. The data were acquired by the use of Equation 5. Figure 19, the fringe spacing is plotted as a function of range under varying conditions of Bragg cell frequency. The 15 and 25 MHz plots were made using the 3 foot diameter transmitting telescope and the 30 MHz plot for the case of a 2 foot transmitting telescope. Figure 20, the transmitter probe volume length as a function of range is plotted again with the modulation frequency being the third parameter.

REFERENCES

1. Air Transportation and Society, Volume Two/Appendix II, September 15, 1971.

2. Lennert, A. E., Brayton, D. B., Crosswy, F. L., et al. "Summary Report of the Development of a Laser Velocimeter to be Used in AEDC Wind Tunnels", AEDC-TR-70-101 (AD871321), July, 1970.

3. Lennert, A. E., Smith, F. H., Jr., and Kalb, H. T., "Application of Dual Scatter, Laser, Doppler Velocimeters for Wind Tunnel Measurements", Presented at the von Karman Institute for Fluid Dynamics, Rhode-Saint-Genese, Belgium, June 21-23, 1971.

4. Smith, F. H., Lennert, A. E., Hornkohl, J. O., "Velocity Measurements in Aerodynamic Wind Tunnel (IT) Using a Laser Doppler Velocimeter", AEDC-TR-71-165, February, 1972.

5. Farmer, W. M., Hornkohl, J. O., and Brayton, D. B., "A Relative Performance Analysis of Atmospheric Laser Doppler Velocimeter Methods", EOSD conference paper, N. Y., N. Y. September, 1971.

6. Farmer, W. M. and Brayton, D. B., "Analysis of Atmospheric Laser Doppler Velocimeter", Applied Optics, Vol. 10, No. 10, October, 1971.

7. Rudd, M. J. J. Phys. E2, 55 (1969).

8. Mazumder, M. K. Applied Physics Letters, Vol. 16, No. 11, June 1, 1971.

9. Brayton, D. B., Kalb, H. T. and Crosswy, F. L., "A Two Component Dual Scatter Laser Velocimeter with Frequency Burst Signal Readout," Submitted to Applied Optics.

GROUND-WIND DATA FROM CO_2 LASER DOPPLER SYSTEM

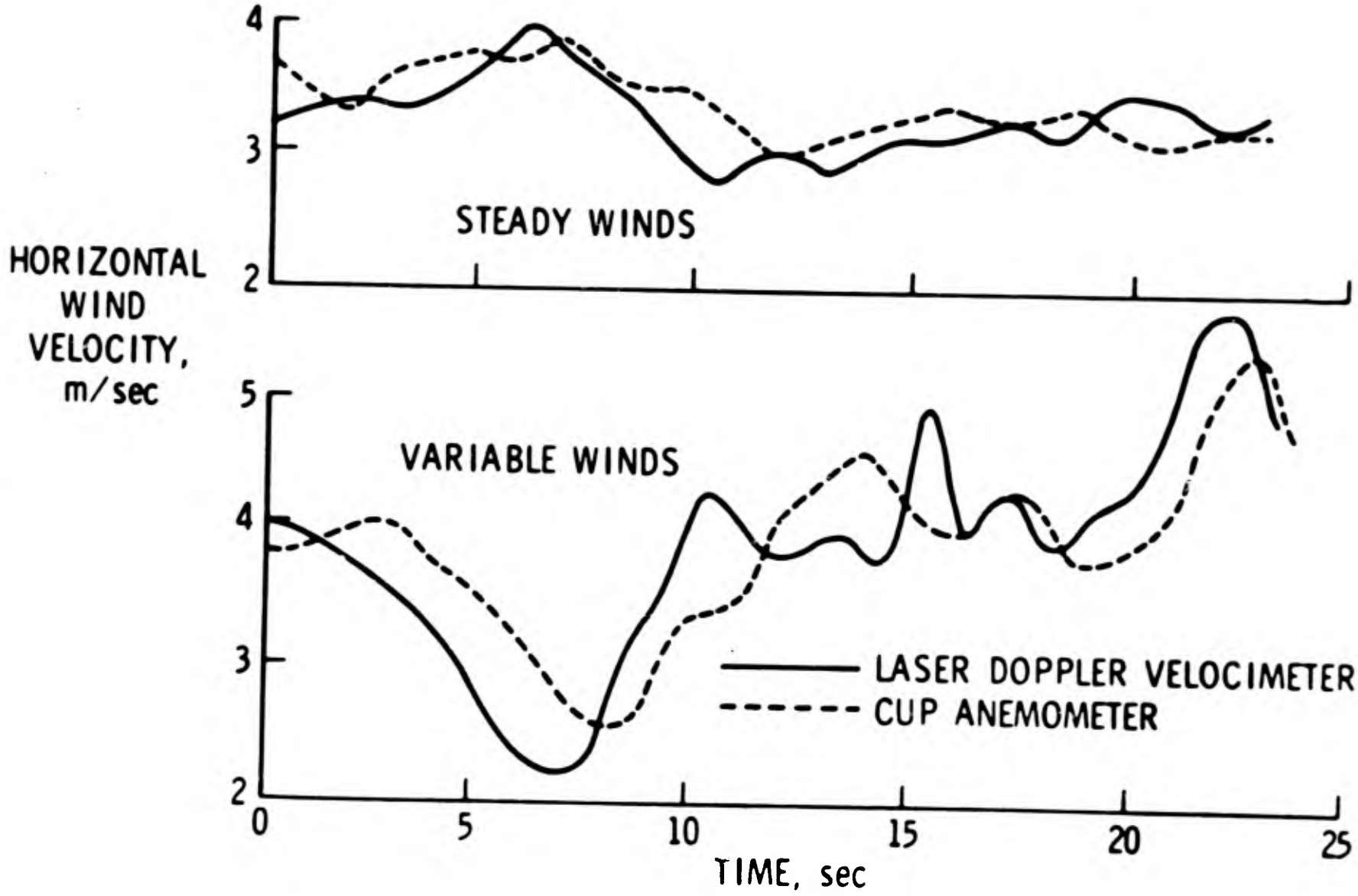

Figure 1

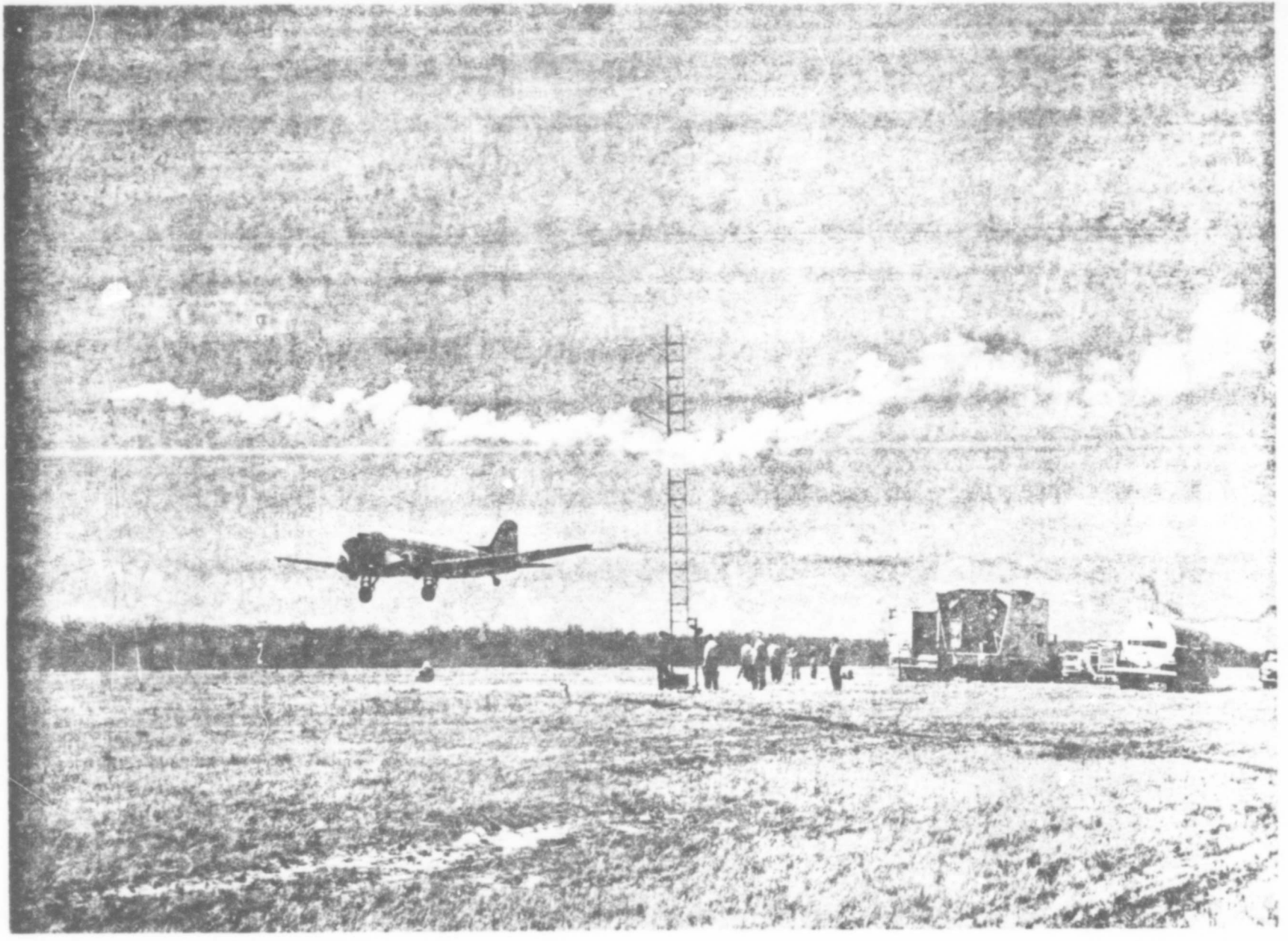

Figure 2

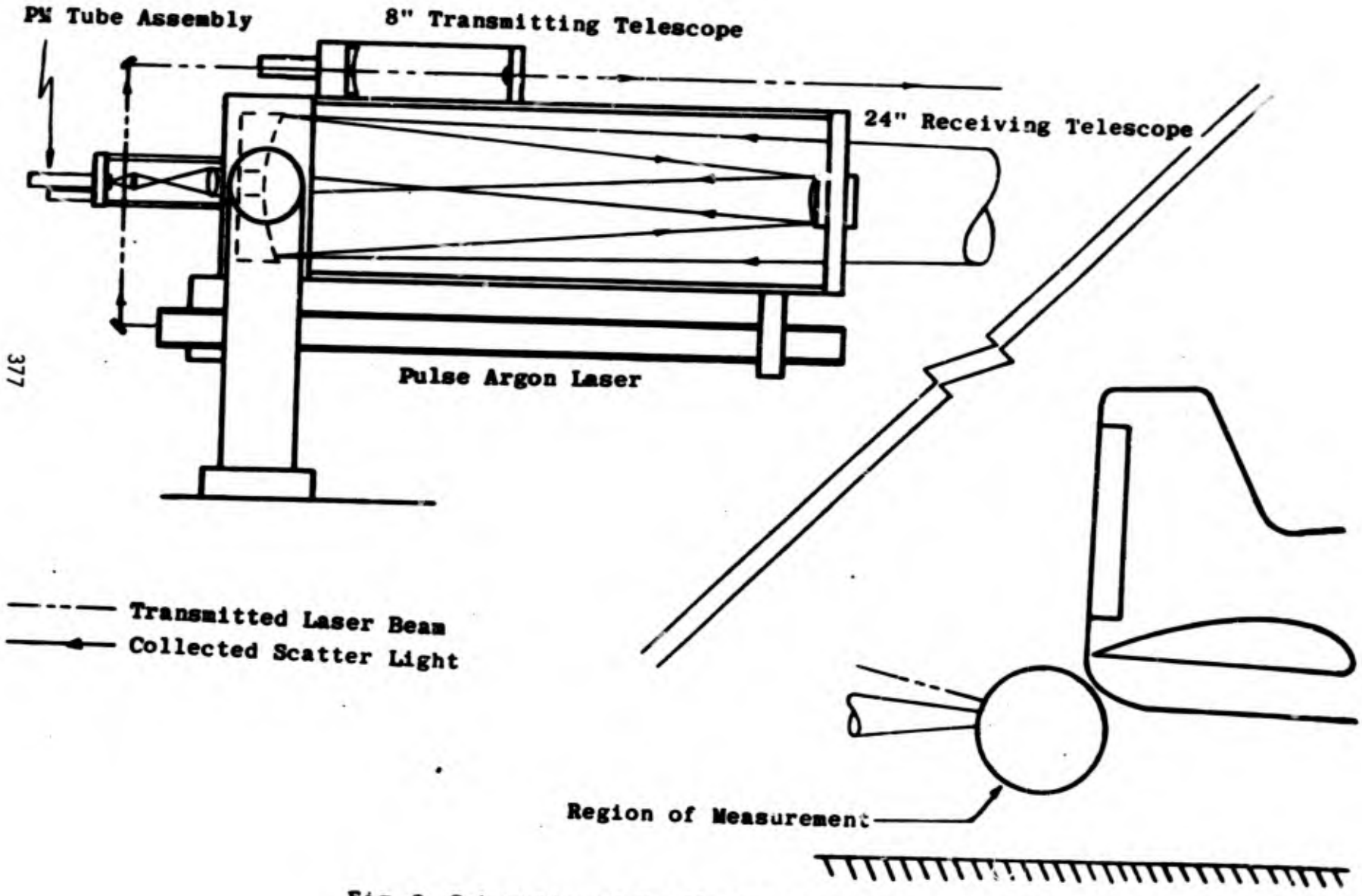

Fig. 3 Schematic of Prefli ht Test Set-up

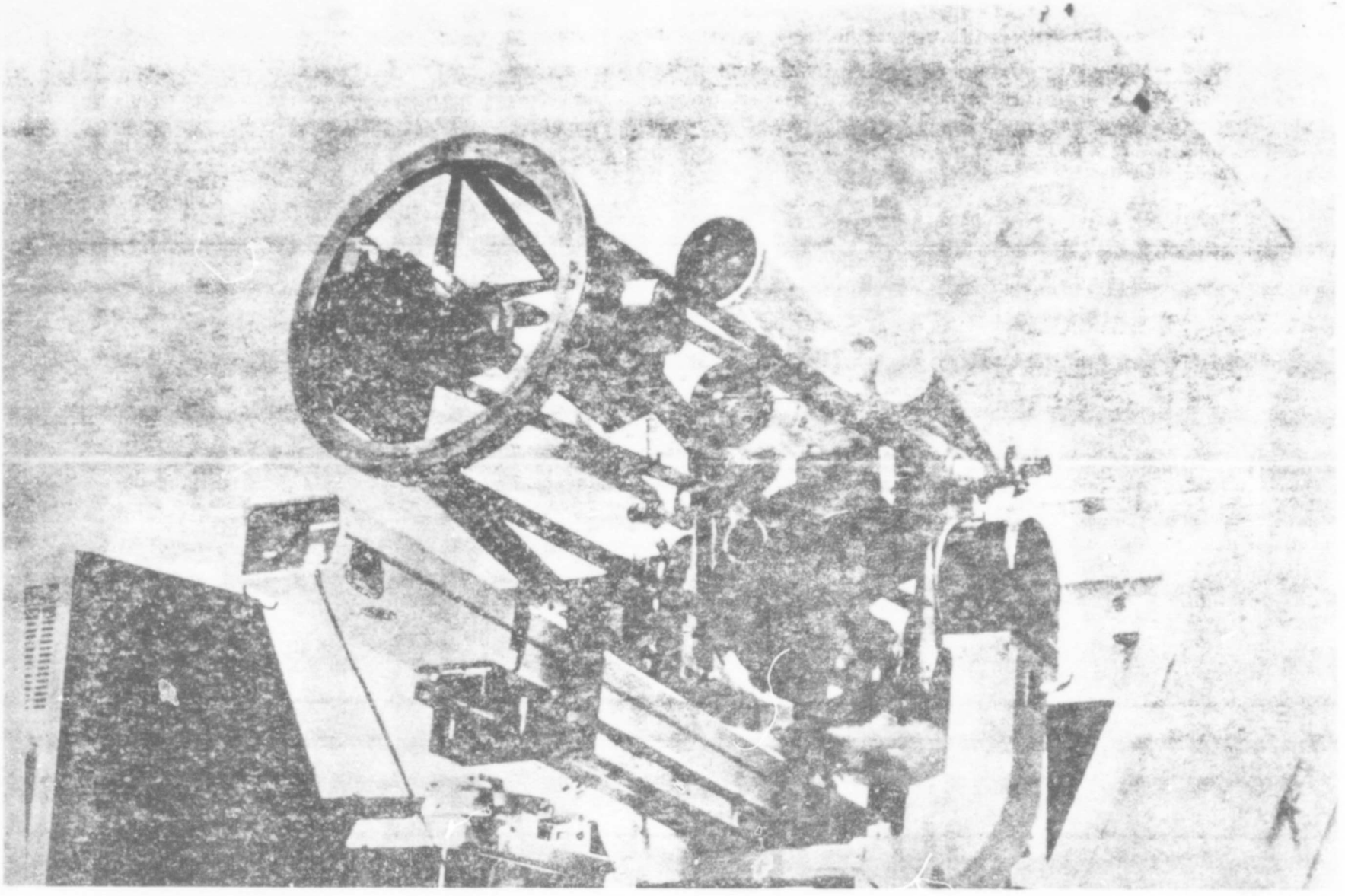

Fig. 4

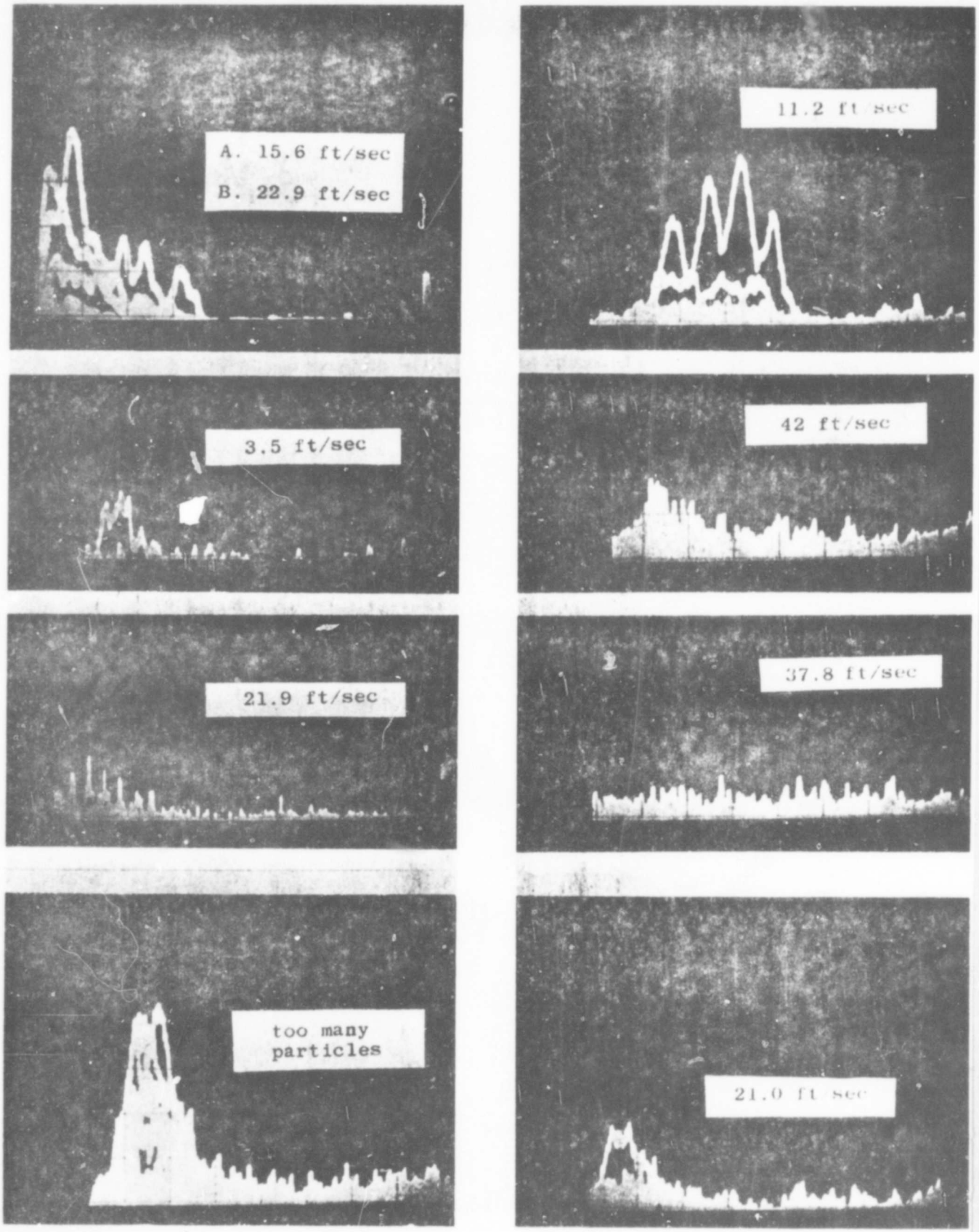
A. 15.6 ft/sec
B. 22.9 ft/sec
11.2 ft/sec
3.5 ft/sec
42 ft/sec
21.9 ft/sec
37.8 ft/sec
too many particles
21.0 ft/sec

Fig. 5

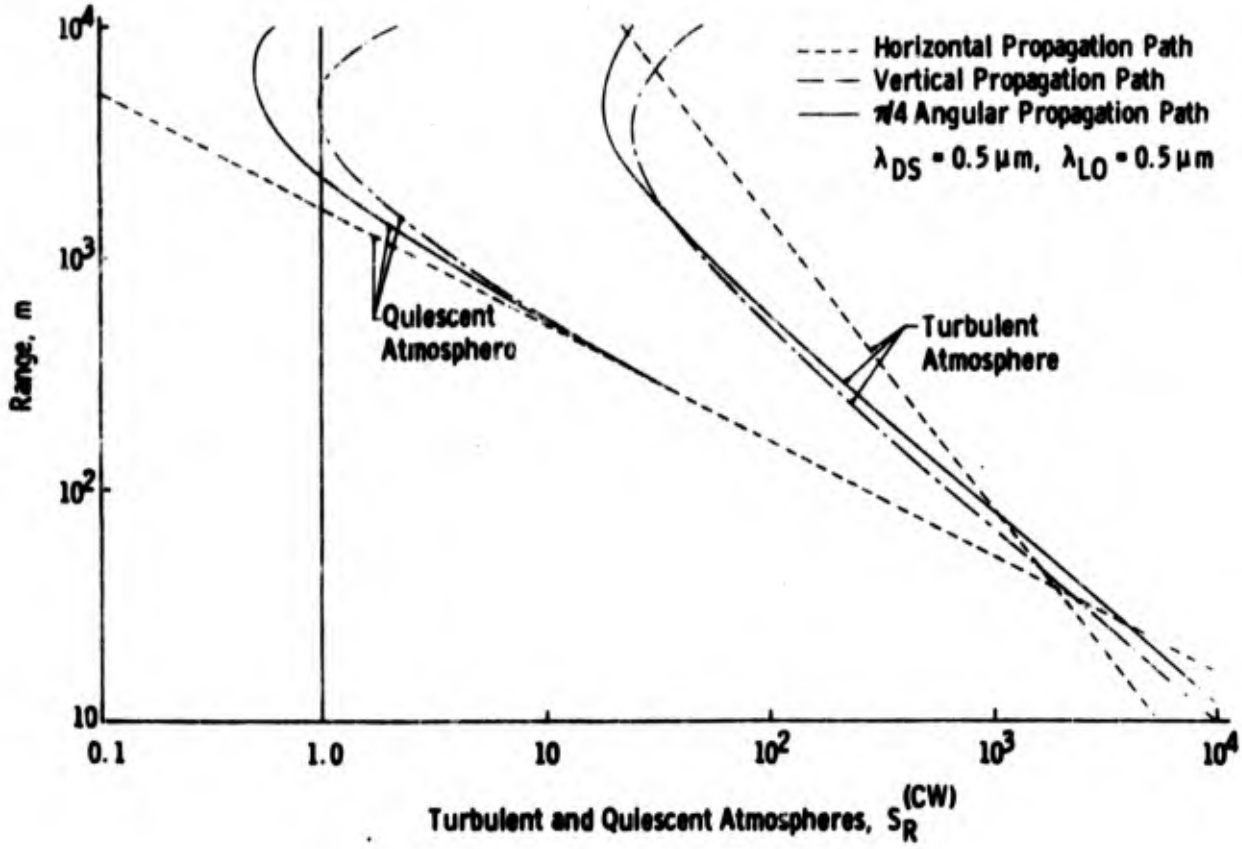

Fig. 6 LDV Operation in Turbulent and Quiescent Atmospheres, $S_R^{(CW)}$

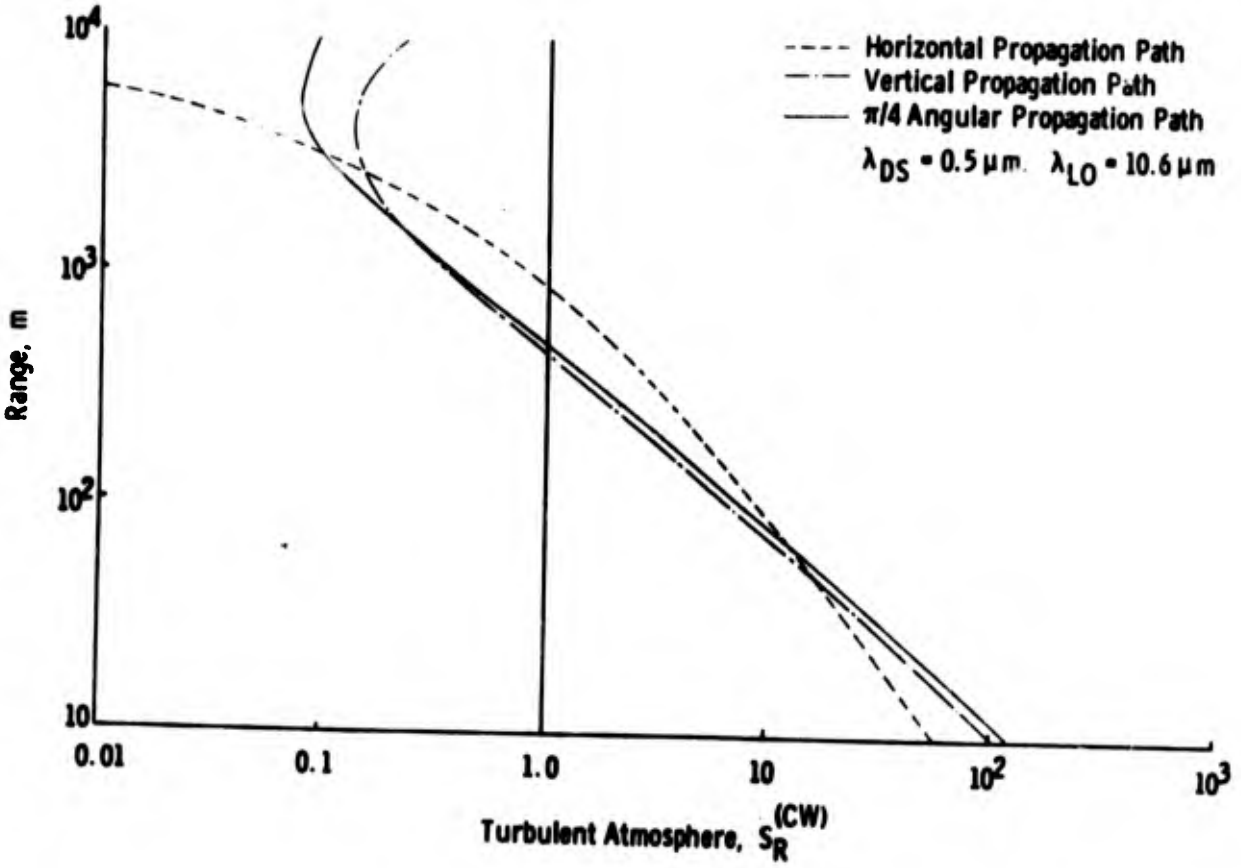

a. Turbulent Atmosphere

Fig. 7 LDV Operation, $S_R^{(CW)}$

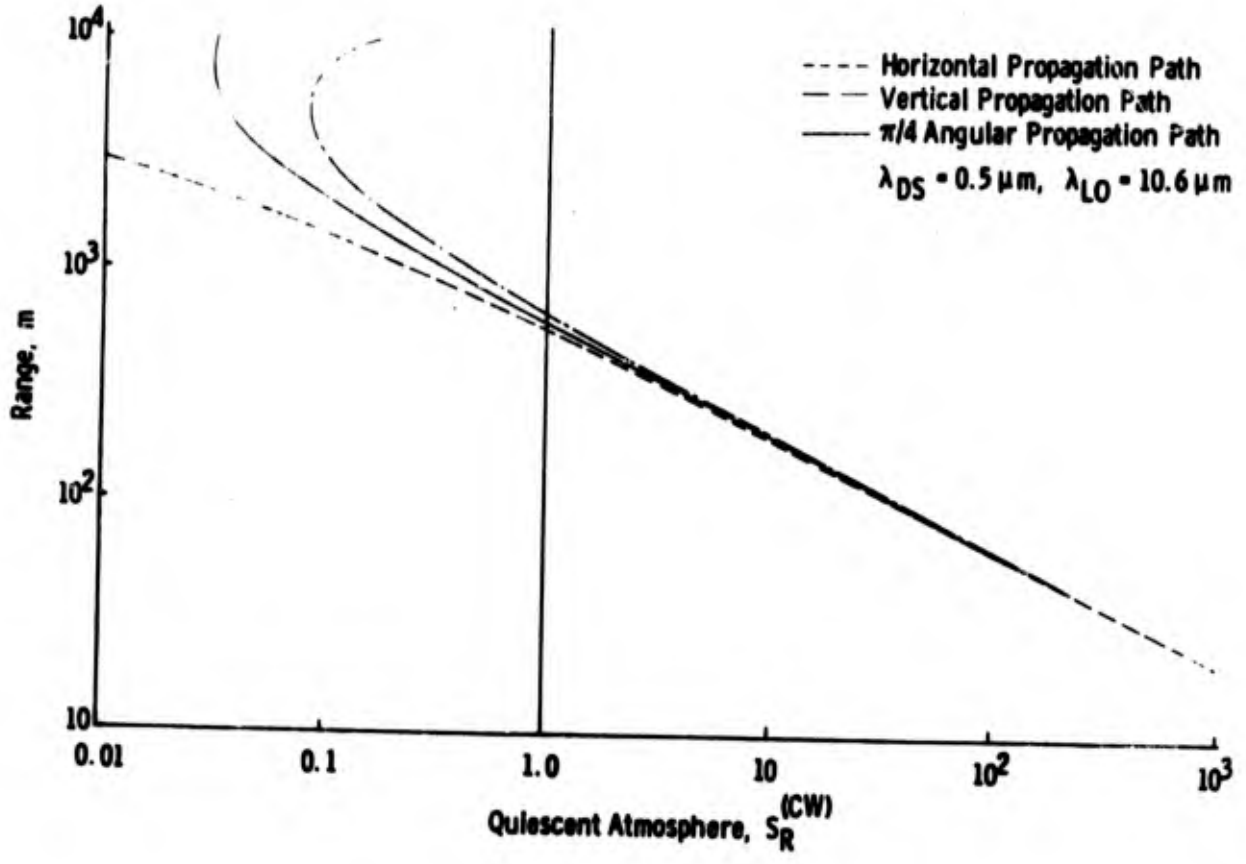

b. Quiescent Atmosphere
Fig. 7 Concluded

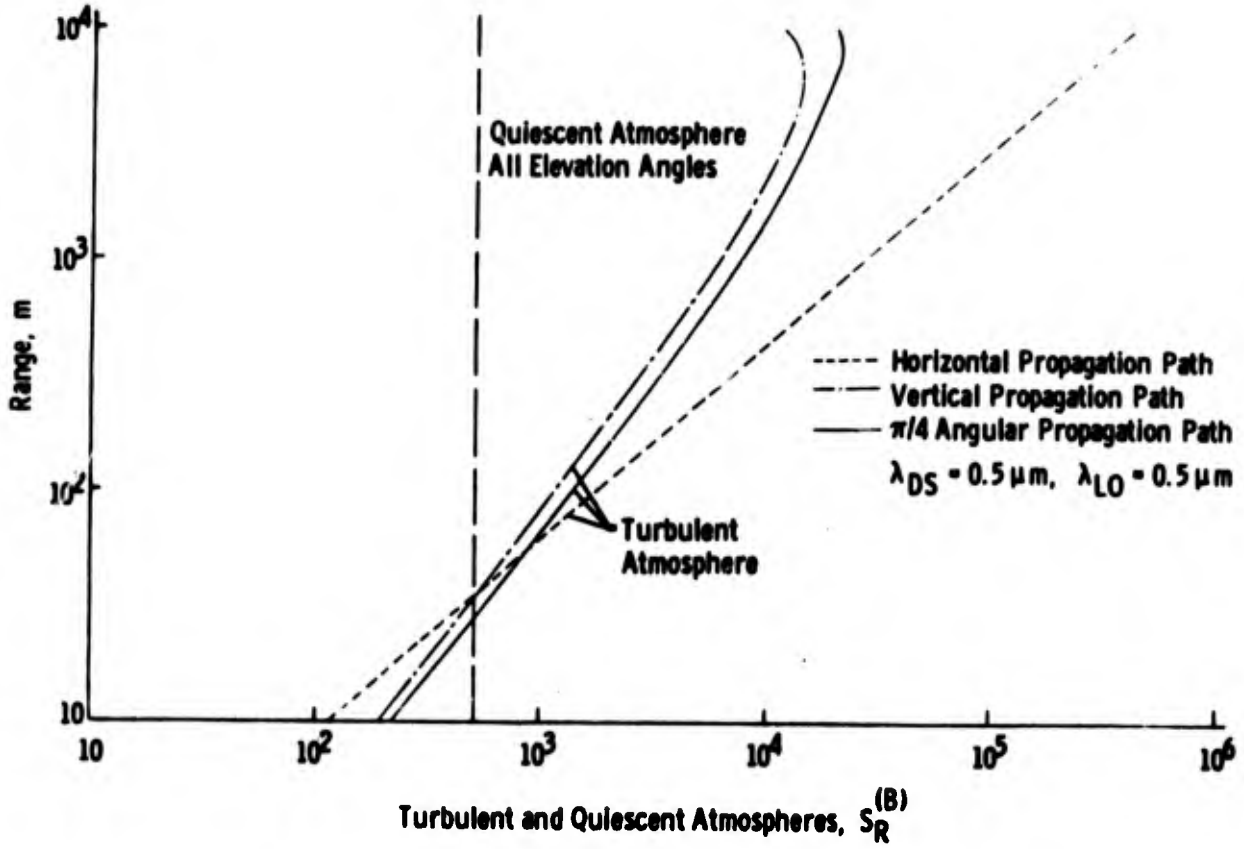

Fig. 8 LDV Operation in Turbulent and Quiescent Atmospheres, $S_R^{(B)}$, λ_{DS} = 0.5 μm, λ_{LO} = 0.5 μm

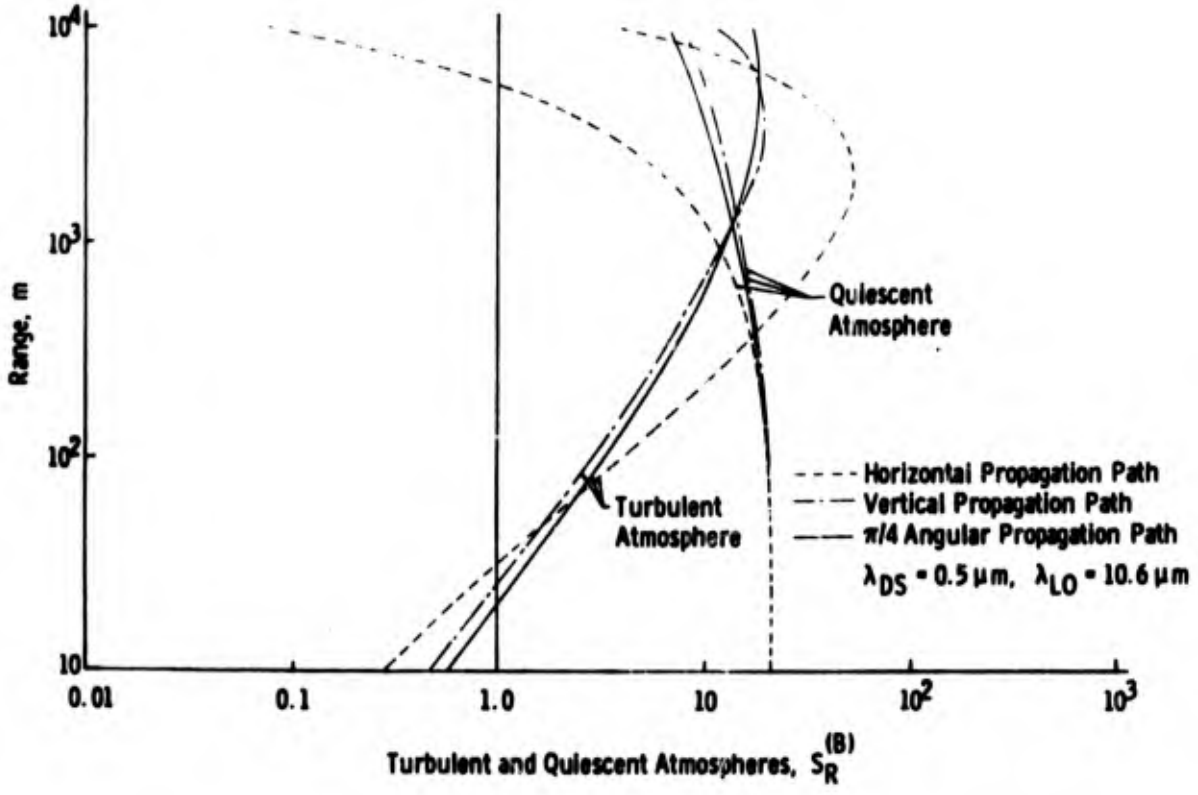

Fig. 9 LDV Operation in Turbulent and Quiescent Atmospheres, $S_R^{(B)}$, λ_{DS} = 0.5 μm, λ_{LO} = 10.6 μm

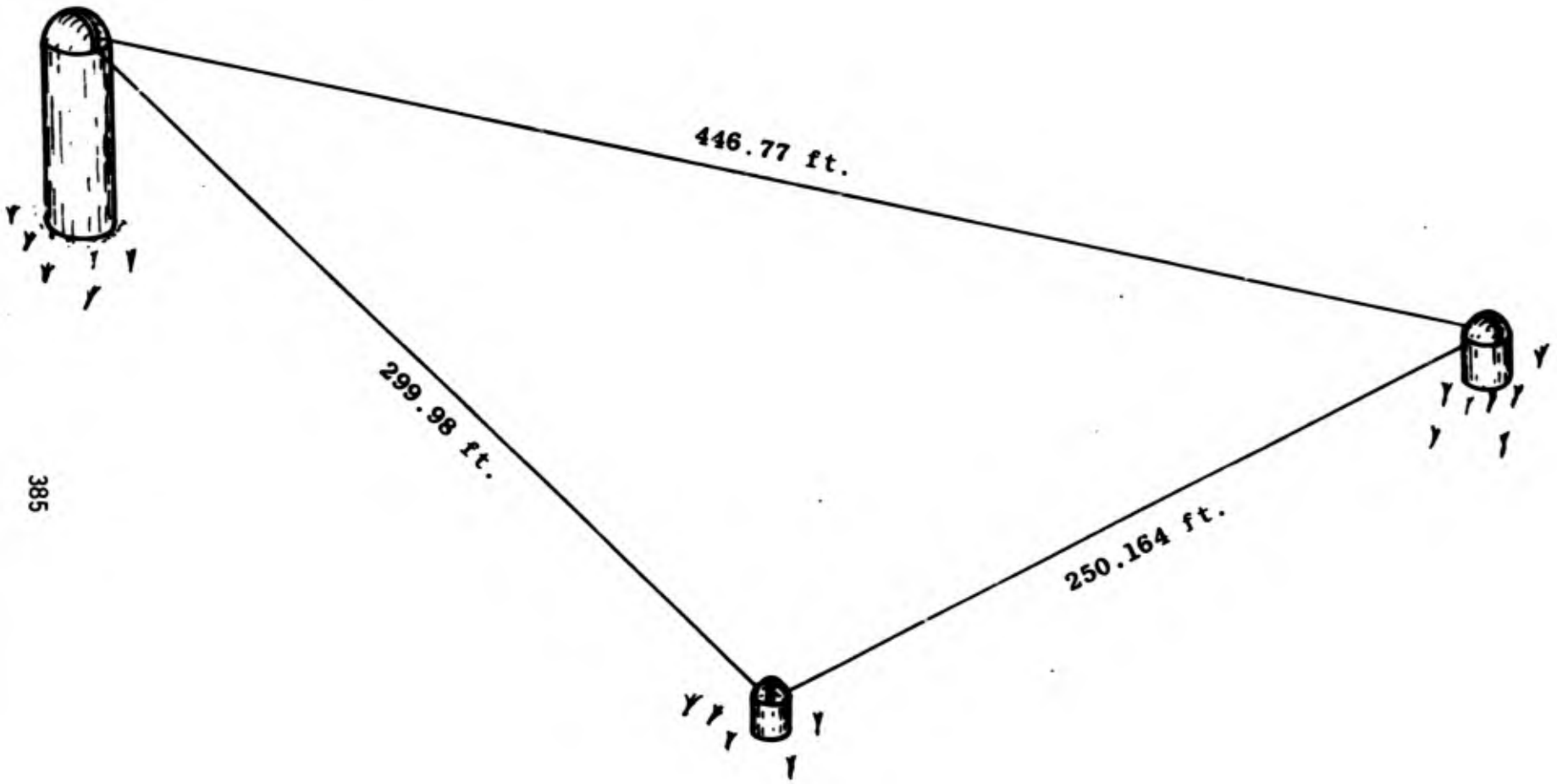

SCHEMATIC OF THREE-COMPONENT LDV

Figure 10

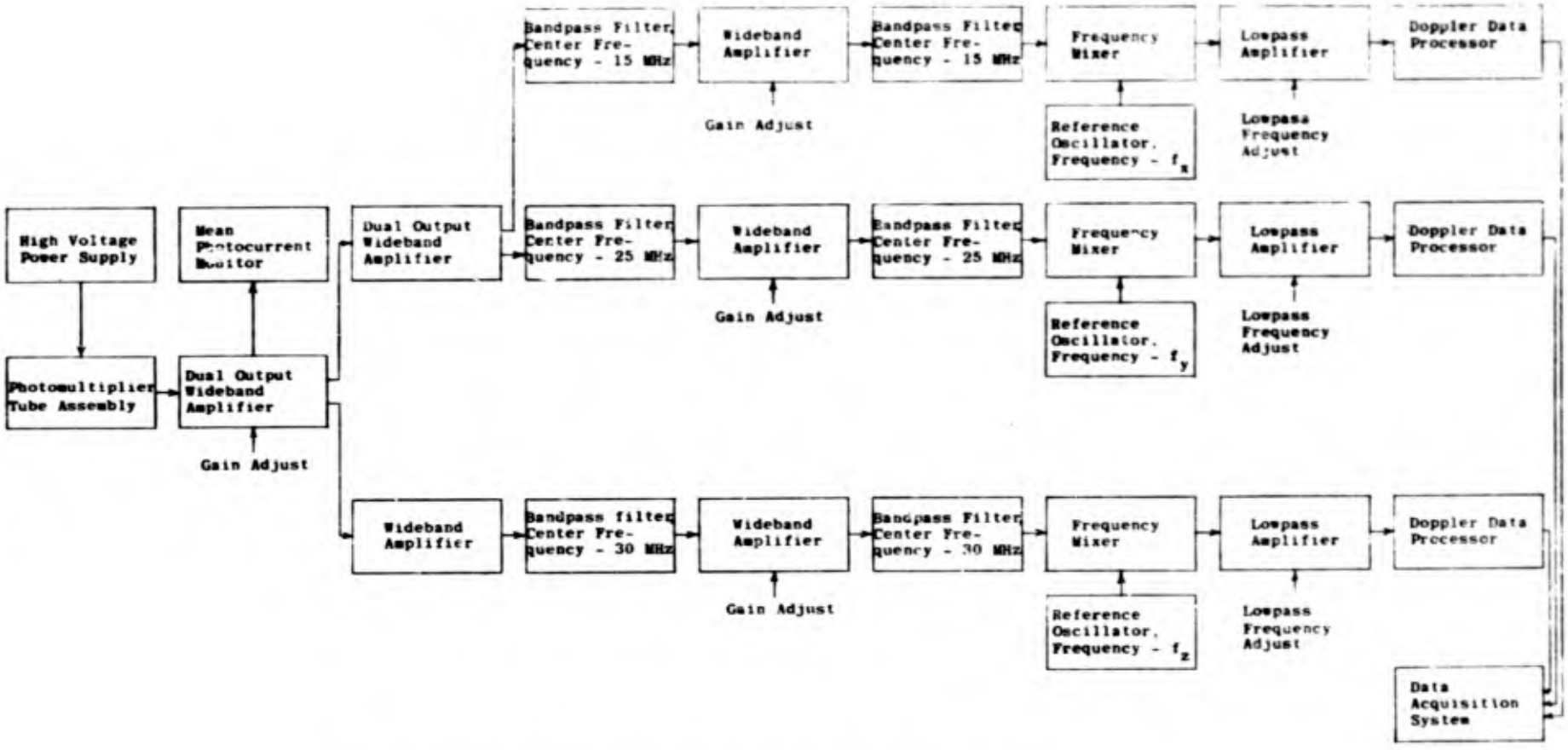

SIGNAL SPLITTER AND SPECTRUM TRANSLATOR FOR THE VELOCITY VECTOR LDV SYSTEM

FIGURE 11

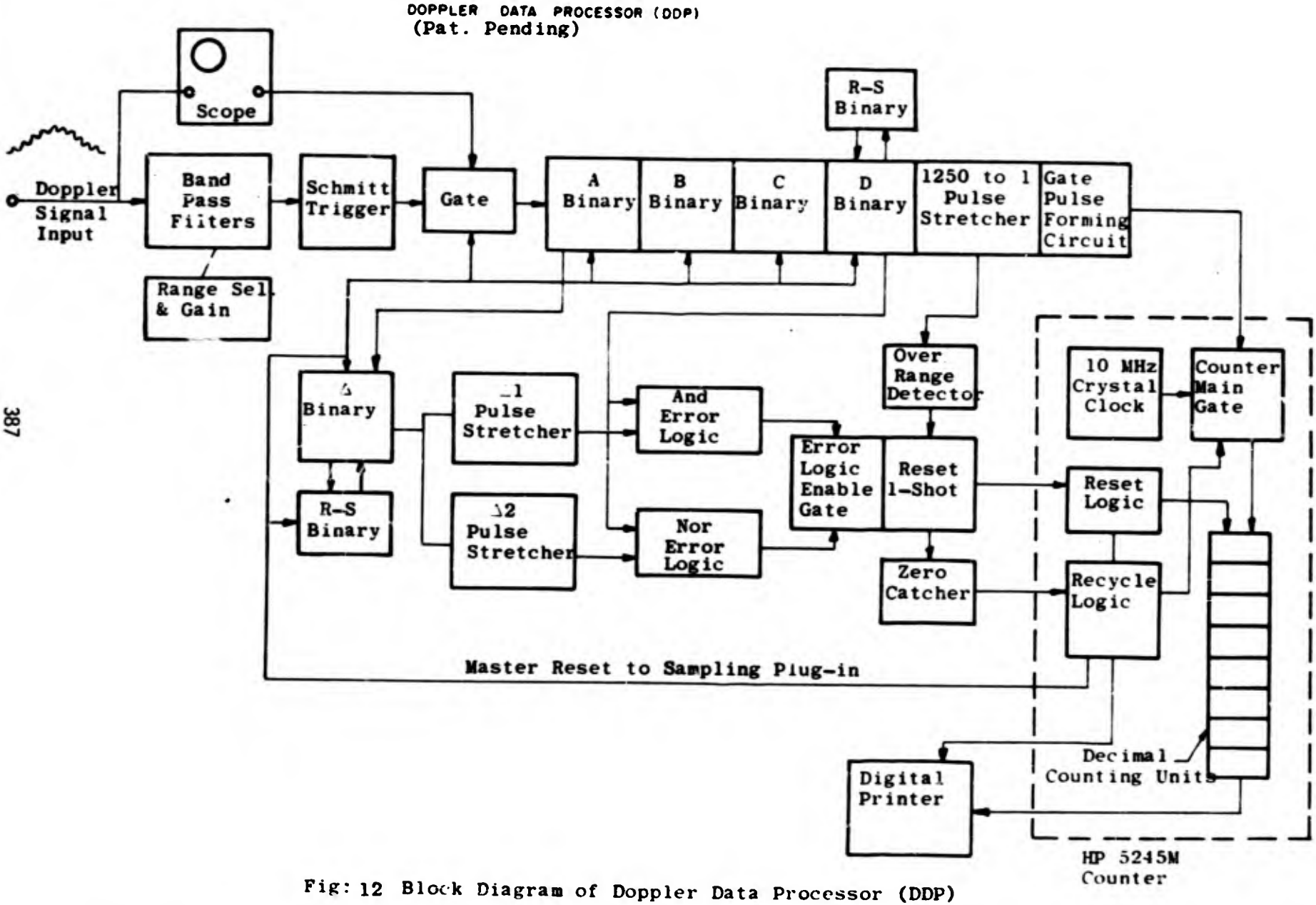

Fig: 12 Block Diagram of Doppler Data Processor (DDP)

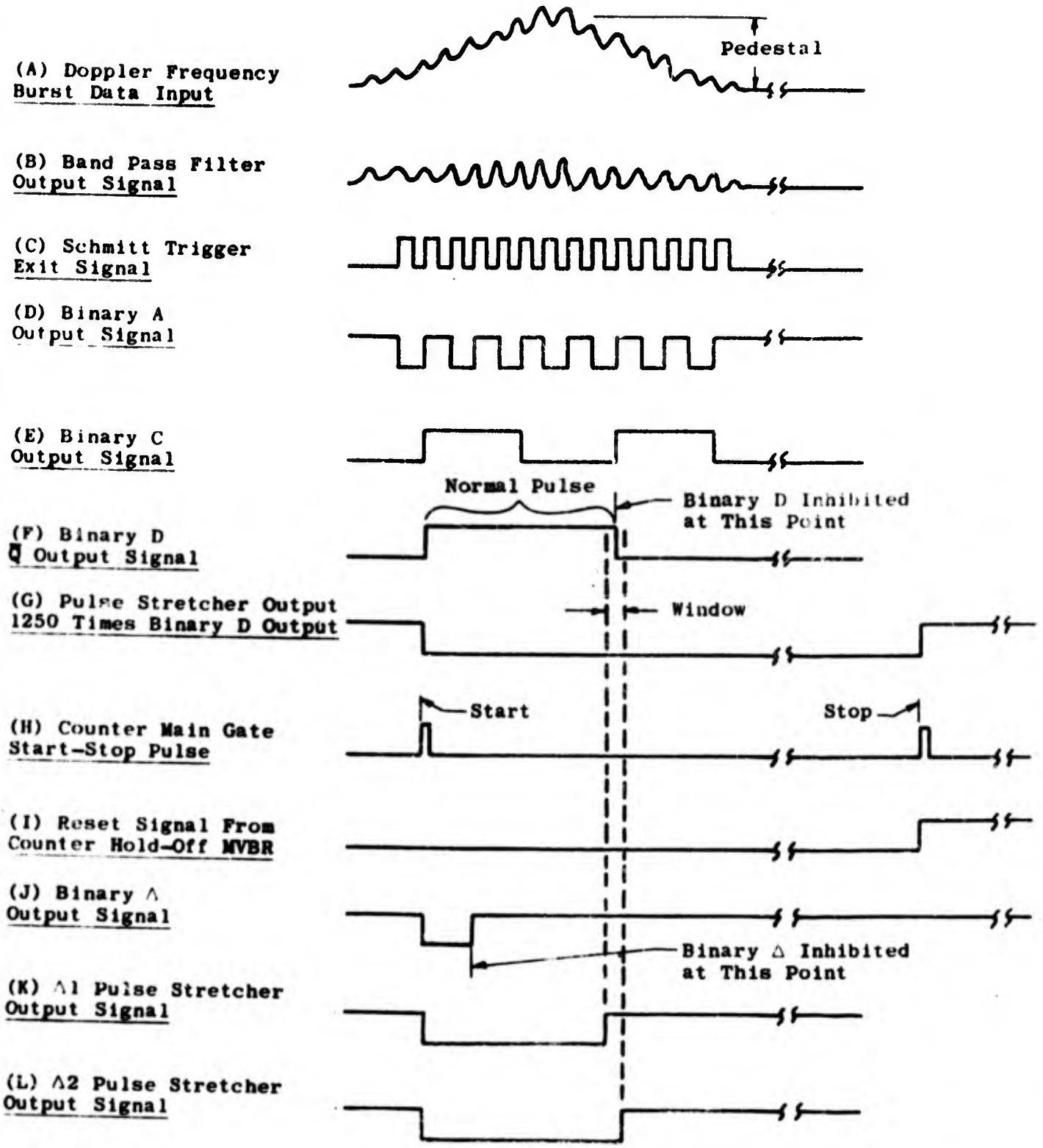

Fig. 13 Doppler Data Processor Logic

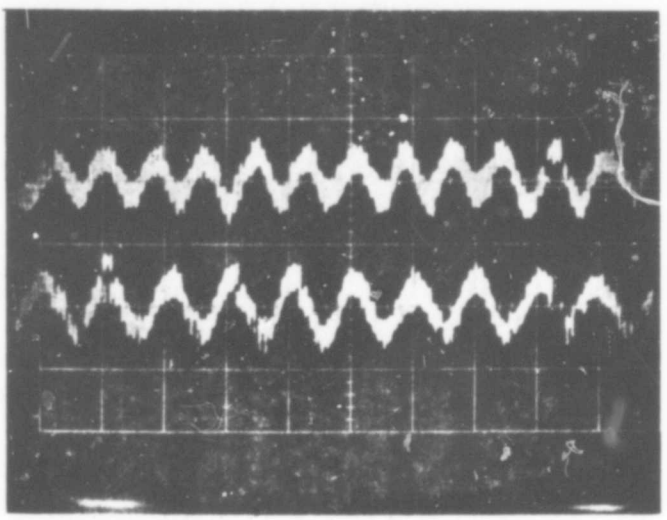

Fig 14 2 component, simultaneously acquired, LV signals

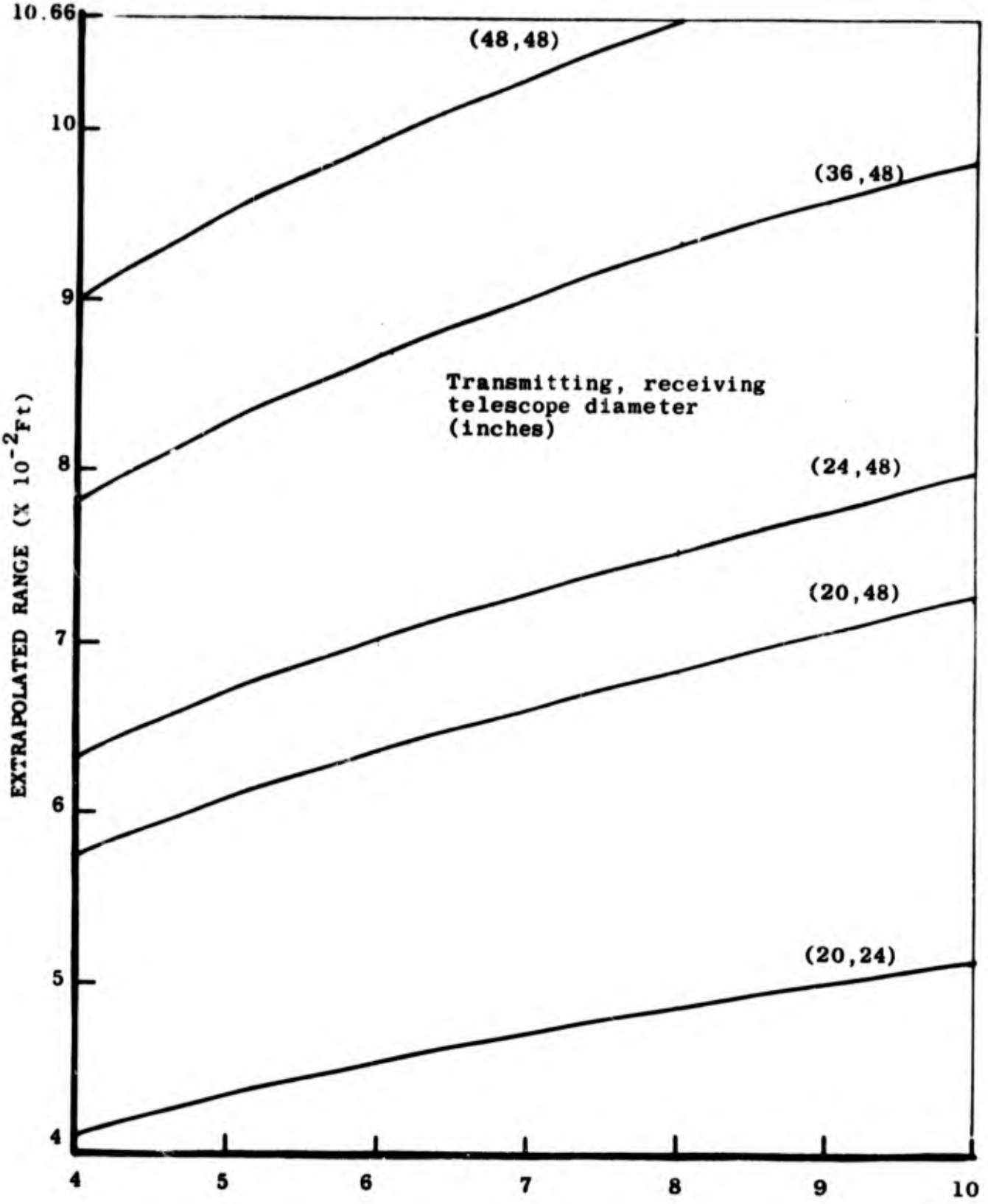

Fig.15 RANGE-LASER POWER RELATIONSHIP

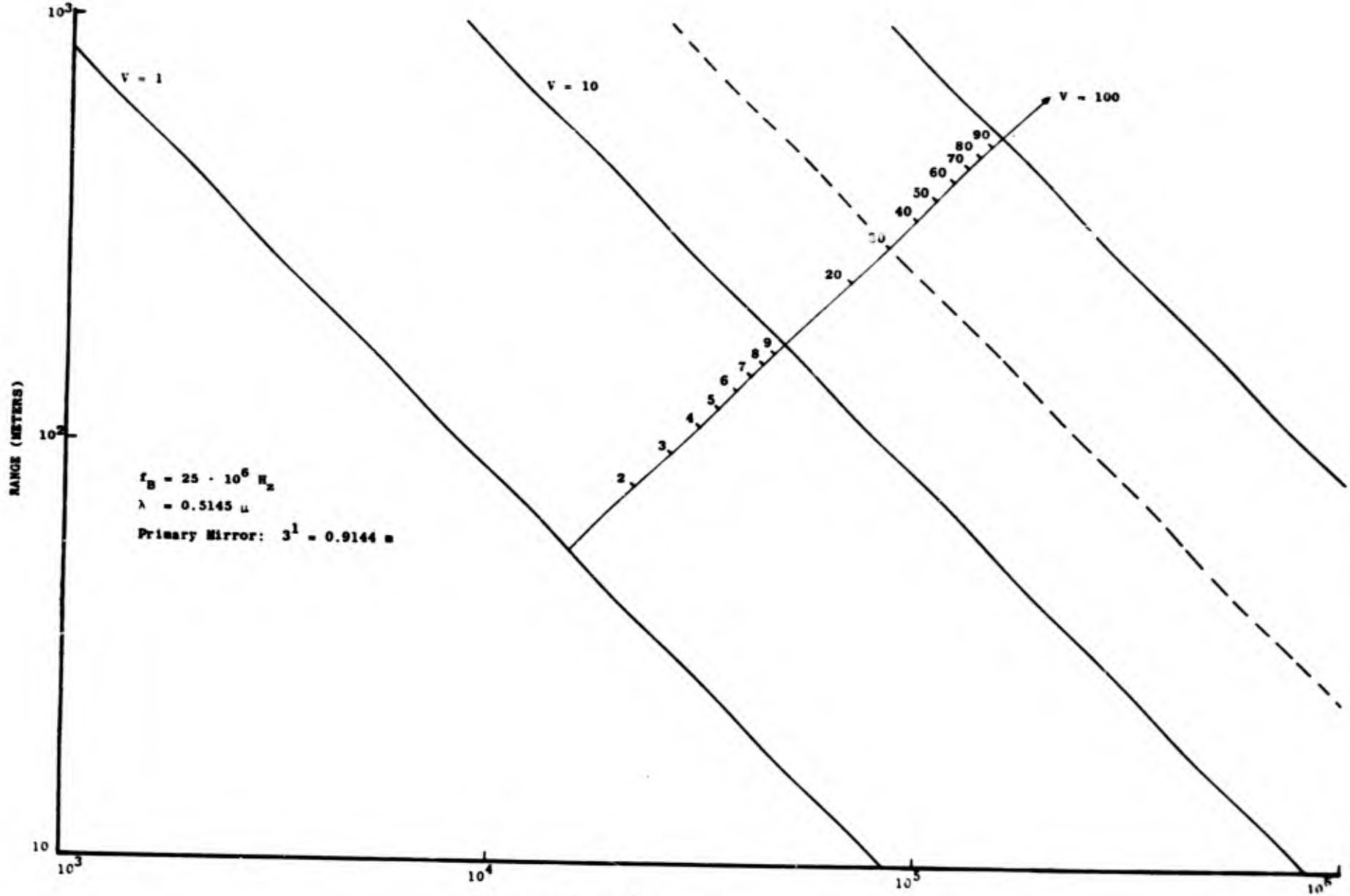

FIGURE 16 DOPPLER FREQUENCY (Hz)

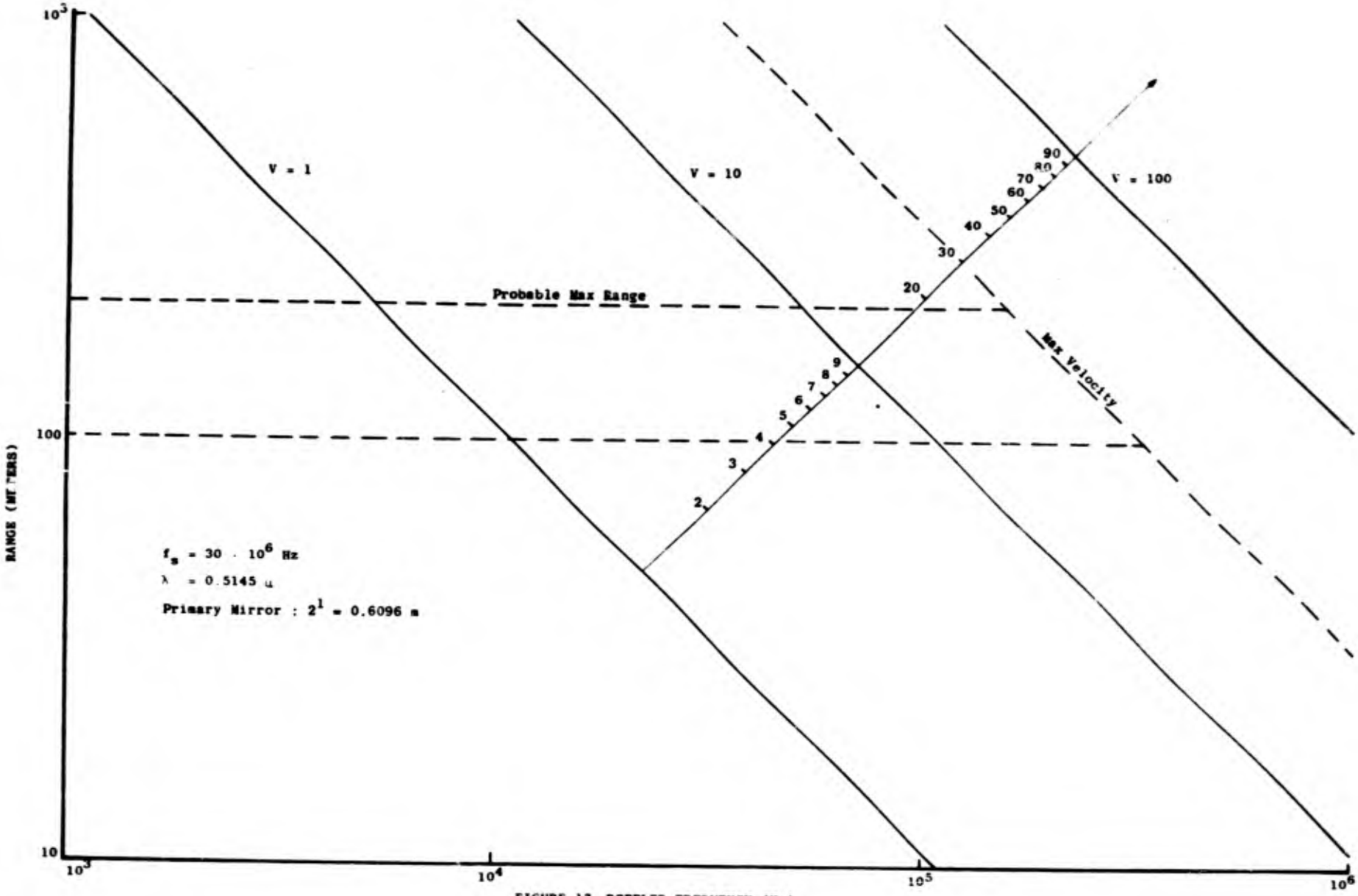

FIGURE 17 DOPPLER FREQUENCY (Hz)

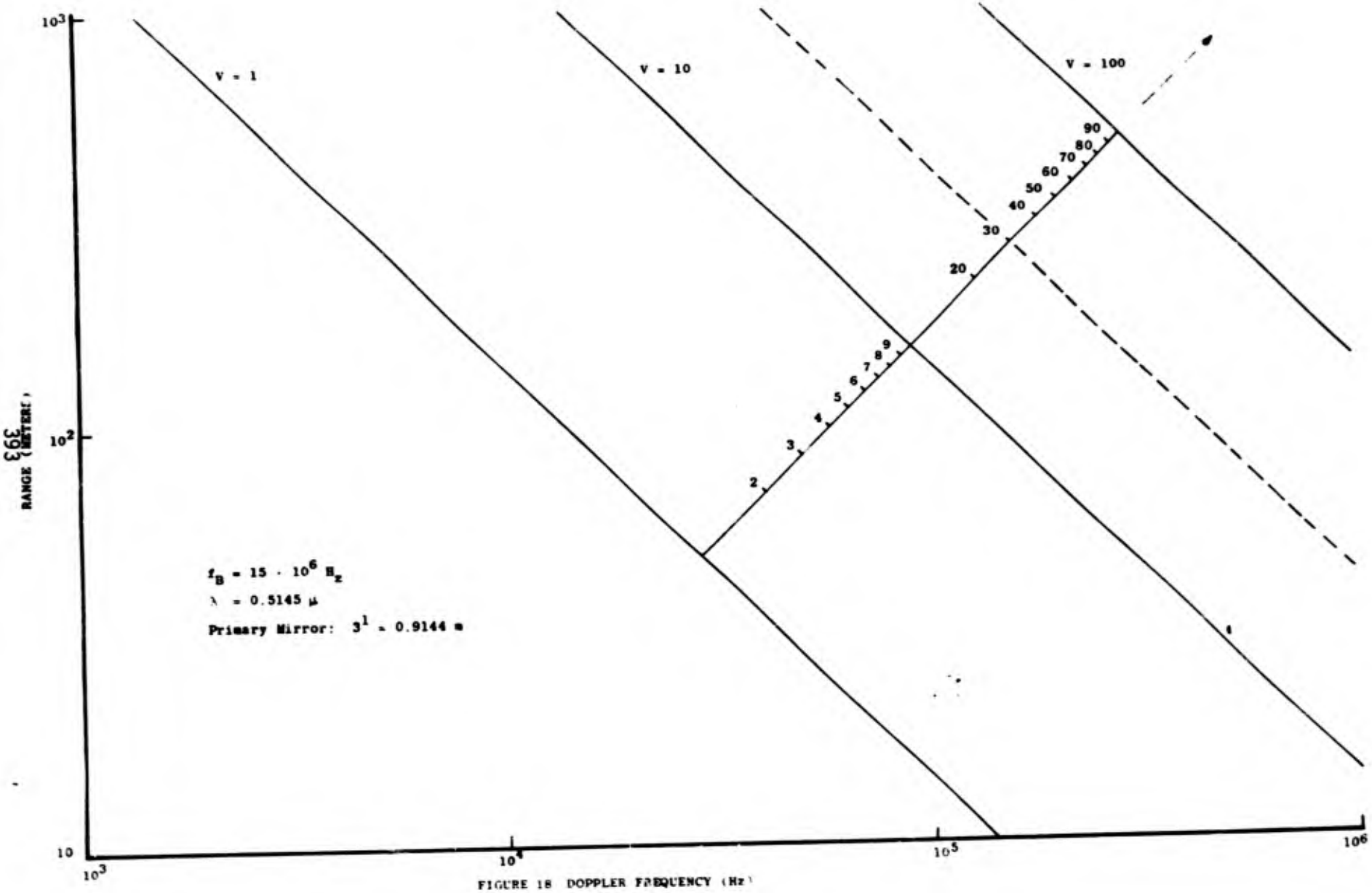

FIGURE 18 DOPPLER FREQUENCY (Hz)

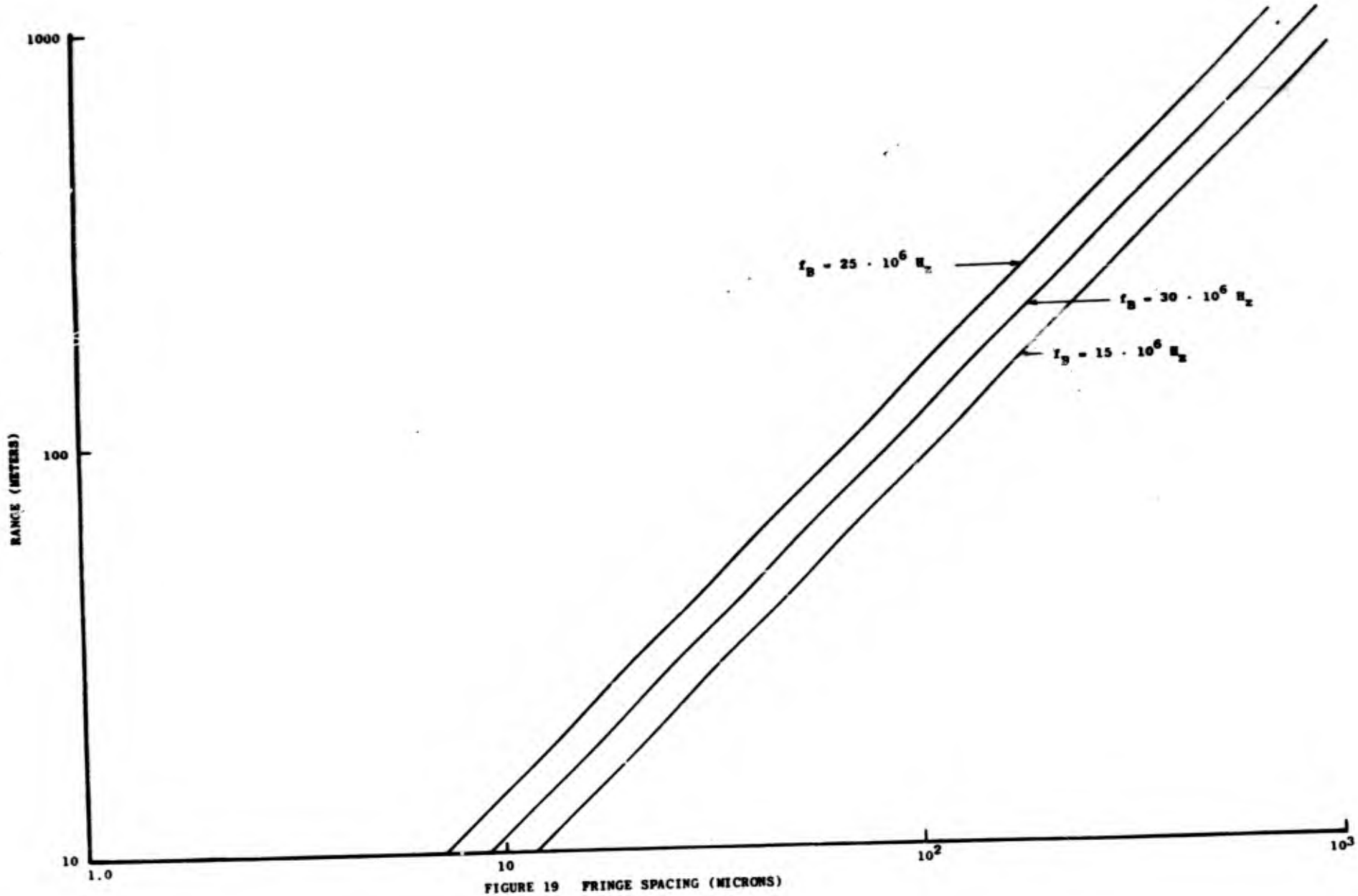

FIGURE 19 FRINGE SPACING (MICRONS)

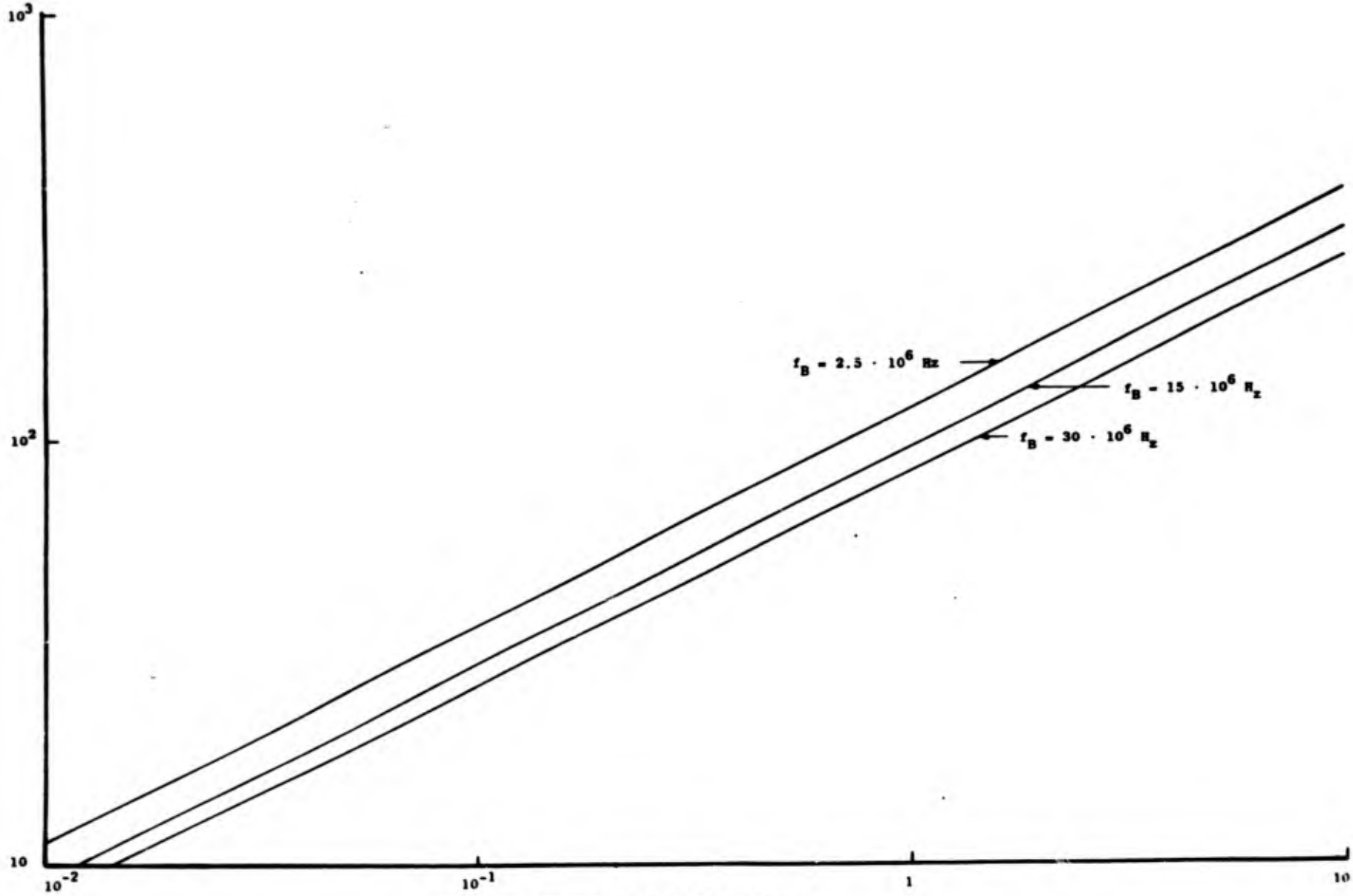

FIGURE 20 TRANSMITTED PROBE VOLUME LENGTH

SIGNAL CHARACTERISTICS AND SIGNAL CONDITIONING ELECTRONICS FOR A VECTOR VELOCITY LASER VELOCIMETER

F. L. Crosswy, J. O. Hornkohl and A. E. Lennert

Experimental Research/Technical Staff
Office of the Managing Director
ARO, Inc.
Arnold Air Force Station, Tennessee

The research reported in this paper was sponsored by Arnold Engineering Development Center (AEDC), Air Force Systems Command, Arnold Air Force Station, Tennessee, under contract #F40600-72-C-0003 with ARO, Inc. Further reporduction is authorized to satisfy the needs of the U. S. Government.

This research supported by National Aeronautics and Space Adminsistration, Langley, Virginia, under contract #L-52080.

ABSTRACT

The signal conditioning electronics used to interface a recently developed Bragg cell type vector velocity laser velocimeter (LV) to a signal processor and data acquisition system are described. The Bragg cell LV eliminates the 180° velocity direction ambiguity problem of the conventional LV but in turn imposes a unique signal conditioning problem. The signal characteristics and the signal conditioning problem are defined and signal conditioning electronic circuits are described. Initial LV system evaluation data are presented for two orthogonal velocity component, atmospheric wind measurements. The Bragg cell LV electronics system is shown to be readily expandable to a three dimensional vector velocity measurement system.

SECTION I

INTRODUCTION

A new self-aligned laser velocimeter (LV) optical system utilizing a unique two-dimensional ultrasonic Bragg cell has been recently developed.[1] A signal processor and data acquisition system for conventional LV systems (without Bragg cell or other optical frequency translation device) has also been recently reported.[2] The purpose of this paper is to define the signal conditioning problem and to describe the signal conditioning instrument which has been developed to interface the new optics system to the signal processor and data acquisition system.

The new LV system is described here as a "vector velocity" measurement device as opposed to the conventional LV system which effects velocity magnitude measurements with a 180° direction ambiguity, i.e., the conventional LV cannot differentiate between the velocity vectors $\bar{v}$ and $-\bar{v}$. The Bragg cell LV eliminates the 180° ambiguity but in turn imposes a unique set of signal conditioning and data acquisition problems.

The complete vector velocity LV system consists of four major subsystems as shown in the functional block diagram, Figure 1. Subsystems 1, 3 and 4 are briefly discussed to define the interface design constraints imposed upon subsystem 2, the signal conditioning subsystem. Time and frequency domain

signal characteristics, essential for the design of subsystem 2, are derived and compared with those of the conventional LV system. A discussion of subsystem and overall LV system accuracy and precision is next presented. The signal conditioning instrument is then discussed in some detail, from concept through circuit schematic to fabrication and packaging. Finally, the directionality capabilities of the new LV system are demonstrated by data produced in the laboratory and in a field test.

SECTION II

OPTICAL SYSTEM DESIGN CONCEPTS

The first LV systems reported were the output aligned, reference beam type[3,4,5] and were quite difficult to use because of the tedious adjustment procedures required to properly align the laser radiation wavefronts at the photodetecting surface. The input aligned (crossed beam), reference beam LV[6] was an improvement since alignment tedium was significantly reduced. The ultimate in operational simplicity at AEDC was achieved with the introduction of the self-aligned, input aligned (crossed beam) LV.[7,8] The self-aligned approach can be used to implement either the reference beam or the dual scatter (differential Doppler) type LV.[9,10] Self-aligning techniques significantly reduce the alignment problems experienced with non-self-aligned systems. However, all these systems possess at least one common potential deficiency--the 180°

direction ambiguity. This deficiency is unimportant for applications where the velocity direction is known a priori. However, in such applications as atmospheric wind velocity studies, turbulent fluid flow measurements and oscillatory fluid flow measurements, the velocity direction at each instant of time is generally unknown and may be as important as the velocity amplitude.

The directional ambiguity problem has been solved by utilizing somwhat more sophisticated LV systems which incorporate an optical frequency translation device such as a Bragg cell or rotating diffraction grating.[11,12] The net effect of the optical frequency translator is to provide a carrier signal with frequency f_o. Then, LV measurement of the velocity vector $\vec{v}$ produces a signal with frequency $f_o + f_D$ ($f_D \propto |\vec{v}|$) whereas measurement of the velocity vector $-\vec{v}$ produces a signal with frequency $f_o - f_D$. The plus or minus deviation of f_D from f_o resolves the directional ambiguity problem.

SECTION III

NEW VECTOR VELOCITY LV OPTICAL SYSTEM

The new LV system is a crossed beam, self-aligned, dual scatter type and its operation is readily described in terms of an interference fringe model.[1] Therefore, subsequent discussions will be in terms of this fringe model as opposed to the Doppler shift-optical heterodyne detection interpretation. The principal component is a novel, two-dimensional, ultrasonic Bragg cell,

developed at AEDC, which permits (1) exploitation of self-aligning techniques and (2) simultaneous vector velocity measurements for two orthogonal velocity components.[1] A simplified schematic of the optical subsystem is shown in Figure 2. The incoming laser beam is diffracted by the orthogonal ultrasonic traveling waves in the Bragg cell. When properly adjusted, the cell produces four equally intense beams, three diffracted beams and a portion of the original undiffracted beam. These four beams originate from the same region inside the cell, travel similar optical paths, and are automatically brought to a common focus by the transmitting optics; therefore, the system is said to be "self-aligned."[1]

The optical frequency of the diffracted beams can be optionally upshifted or downshifted by proper orientation of the Bragg cell with respect to the incoming laser beam. Figure 3 illustrates the possible four beam output combinations that may be chosen for transmission.[1]

The respective Bragg orders are shown in parentheses with the horizontal value shown first below the dot representing the diffracted beam. The optical frequency of the diffracted beam is shown above the dot. The moving interference fringe planes[1] produced in the probe volume by any two beams are oriented perpendicular to the line connecting the two dots representing these two beams. The direction of fringe travel in the probe volume is the same as that of the ultrasonic wave vector, $\underset{\sim}{K}$ (i), for non-inverting transmitting optics whereas

the direction of fringe travel is opposite to $\underset{\sim}{K}$ (i) for inverting transmitting optics. The relative length of any side of the rectangle is directly proportional to the associated ultrasonic frequency.

SECTION IV

SIGNAL CHARACTERISTICS

There is no advantage in choosing one four-beam set over any of the other three possibilities shown in Figure 3. Therefore, in the following discussions the beam set (0,0), (1,0), (1,1) and (0,1) is selected.

4.1 Optical Component Constraints

The diffraction cell producing the four beam pattern is operated in the Bragg mode as opposed to the Raman-Nath mode since Bragg mode operation permits concentration of the diffracted light in a single order. Bragg mode operation requires adherence to the Bragg law[13]

$$n\lambda = 2\Lambda \sin\phi = 2\Lambda \sin\theta \qquad (1)$$

and to the condition[13]

$$w f_o^2 = 2\mu v^2 N/n\lambda = 1.2(10^{15}) \qquad (2)$$

where ϕ and θ are the angles of the incident and reflected laser beams with respect to the ultrasonic wavefronts, λ and Λ are the laser light and sound wavelengths respectively, n is the

diffraction order, w is the diameter of the ultrasonic beam in cm., f_o is the ultrasonic frequency in hertz, μ is the index of refraction for water, v is the velocity of sound in water and N is the number of ultrasonic wavefronts traversed by a laser light ray in passing through the Bragg cell. For the system shown in Figure 2, n = 1, N = 1 and $\lambda = 5.145\ (10^{-4})$ cm.

The maximum practical dimension, w, is dictated by the diameter of the ultrasonic driving device and is 2.54 cm. for the piezoelectric quartz crystal driver used in the system shown in Figure 2. This constraint on w then necessitates the use of an ultrasonic drive frequency, f_o, in the range of tens of megahertz (Eq. 2). We have chosen (see Figs. 2 & 3) $f_o(1)$ = 25 MHz and $f_o(2)$ = 15 MHz. The optical spectrum at the output of the Bragg cell for this selection is shown in Figure 4. Each of the four beams is represented in the frequency domain by a frequency impulse function. The intensities of the four beams can easily be made equal by adjusting the electrical input power to the piezoelectric drivers.

The LV system can be successfully operated with or without the polarization rotation plates shown in Figure 2. In either case, each set of two beams with a non-orthogonal polarization relationship will form moving interference fringes in the probe volume.[1] The fringes formed by beam pairs (0,0) with (1,0) and by (0,1) with (1,1) propagate horizontally across

the probe volume at the rate

$$\left|f_\ell-[f_\ell+f_o(1)]\right| = \left|f_\ell+f_o(2)-[f_\ell+f_o(1)+f_o(2)]\right| = f_o(1) = 25\ \text{MHz}$$

and are therefore, used for the horizontal velocity component measurements. By the same considerations, beam pairs (0,0) with (0,1)& (1,0) with (1,1) produce fringes which travel vertically at the rate $f_o(2)$ = 15 MHz. When the polarization rotation plates are not used, beams (0,0) and (1,1) interfere to produce fringes which move diagonally at the rate $f_o(3)$ = 40 MHz and beams (1,0) and (0,1) produce fringes which move diagonally at the rate $f_o(4)$ = 10 MHz. The polarization rotation plates produce an orthogonal polarization relationship between the diagonal beams and thereby eliminate the diagonal fringes.

A light scattering particle passing through the probe volume produces a unique signal for each fringe set with frequency, f_{SC}, given by[1]

$$f_{SC} = f_o \pm f_D \qquad (3)$$

where f_D is directly proportional to the velocity magnitude of the particle and is the "Doppler" frequency of the conventional type LV. A motionless scatter particle in the probe volume produces a sinusoidal signal with frequency $f_{SC} = f_o$. A particle traveling in the same direction as the moving fringes produces a signal with frequency $f_{SC} = f_o - f_D$ while a particle traveling in a direction opposite that of the moving fringes produces a signal with frequency $f_{SC} = f_o + f_D$. The photodetected signal spectrum produced by a motionless particle is shown in Figure 5 which illustrates the velocity component carrier signals

when polarization rotators are not used. Use of the polarization rotators eliminates the diagonal velocity component carrier signals at 10 and 40 MHz and thereby eliminates possible interference with the signals centered at 15 and 25 MHz. The diagonal carrier signal amplitudes are half that of either the vertical or horizontal since only two of the four beams are used to form the diagonal fringes whereas all four beams are used to form the vertical and horizontal fringes.

4.2 Time and Frequency Domain Characteristics

The scattered radiation intensity envelope for scatter particle trajectories close to the geometric center of the probe volume is gaussian for laser operation in the TEM_{oo} mode, the preferred mode for LV applications. The corresponding photodetected time domain signal for a single scatter particle traversing a fringe set for the conventional dual scatter LV is given by

$$x_1(t) = A_p \exp\{-[2\sqrt{2}(t-t_o)/\tau]^2\} + A_s \exp\{-[2\sqrt{2}(t-t_o)/\tau]^2\} \cos 2\pi f_D t \quad (4a)$$

while the time domain signal for the same scatter particle and trajectory for a dual scatter LV with an optical frequency translator is given by

$$x_2(t) = A_p \exp\{-[2\sqrt{2}(t-t_o)/\tau]^2\} + A_s \exp\{-[2\sqrt{2}(t-t_o)/\tau]^2\} \cos 2\pi (f_o \pm f_D) t \quad (4b)$$

where f_D is the "Doppler" frequency, f_o is the carrier frequency and is the time required for the scatter particle to transit the probe volume outer boundaries. This boundary is defined by

the surface of that ellipsoid where the laser radiation intensity is e^{-2} times the maximum intensity near the geometric center of the probe volume.[10] The quantity, e, is the base of the Naperian logarithm. Equations 4a and 4b are represented in Figures 6a and 6b respectively. The signals are seen to consist of two distinct summed waveforms, (1) a gaussian pulse or "pedestal" waveform with peak amplitude A_p and a gaussian amplitude modulated sinusoid with peak amplitude A_s. Note that the signal parameters A_p, A_s, τ and f_D are the same for both type LV systems provided that laser radiation intensity in the probe volume, probe volume dimensions and fringe spacing are set up to be identical.

The "Doppler" frequency is given by[10]

$$f_D = v/d = \frac{2v\sin\theta/2}{\lambda} \qquad (5)$$

where v is the magnitude of the scatter particle velocity, d is the probe volume fringe spacing, θ is the angle between the crossed laser beams and λ is the wavelength of the laser radiation. The parameter τ is related to f_D by

$$\frac{1}{\tau}/f_D = 1/N = \frac{\lambda}{2b_o\tan\theta/2} \qquad (6)$$

where N is the number of fringes set up within the probe volume (e^{-2}) maximum intensity contour and $2b_o$ is the gaussian diffraction limited laser beam diameter in the probe volume.

The signal amplitudes A_p and A_s are directly proportional to the peak laser radiation intensity within the probe volume. The ratio A_s/A_p is related to scatter particle size with respect to the fringe spacing.[14] In general, large particles produce small A_s/A_p ratios and vice versa. In wind tunnel LV applications at AEDC using intrinsic test section aerosol scatter particles, the A_s/A_p ratio has been observed to vary from 0 to 0.5.

An important requirement of an LV signal conditioner is to attenuate the pedestal waveform but enhance the sinusoidal waveform since the frequency of the sinusoid conveys the velocity information and presence of the pedestal waveform interferes with frequency or period measurement circuitry. The pedestal waveform can be practically eliminated by utilizing a relatively sophisticated balanced optical photodetector scheme instead of the conventional photodetector.[15] However, simple electronic filters can be used to separate the sinusoid from the pedestal provided that

$$e/2\tau \ll f_{sc} \tag{7a}$$

and

$$2A_s \simeq A_p \tag{7b}$$

The significance of conditions 7a and 7b in comparing the conventional LV and the LV with optical frequency translation can be deduced by observation of the Fourier transforms of Equations 4a and 4b. Using the frequency translation theorem and the gaussian function transform pair relationship, the

Fourier transforms of Equations 4a and 4b are found to be respectively

$$X_1(f) = \left(\frac{A_p\tau}{2}\right)\left(\sqrt{\frac{\pi}{2}}\right)\exp\left\{-\left[\frac{\pi f\tau}{2\sqrt{2}}\right]^2\right\} + \left(\frac{A_s\tau}{4}\right)\left(\sqrt{\frac{\pi}{2}}\right)\exp\left\{-\left[\frac{\pi(f+f_0)\tau}{2\sqrt{2}}\right]^2\right\} \quad (8a)$$
$$+\left(\frac{A_s\tau}{4}\right)\left(\sqrt{\frac{\pi}{2}}\right)\exp\left\{-\left[\frac{\pi(f-f_0)\tau}{2\sqrt{2}}\right]^2\right\}$$

$$X_2(f) = \left(\frac{A_p\tau}{2}\right)\left(\sqrt{\frac{\pi}{2}}\right)\exp\left\{-\left[\frac{\pi f\tau}{2\sqrt{2}}\right]^2\right\} + \left(\frac{A_s\tau}{4}\right)\left(\sqrt{\frac{\pi}{2}}\right)\exp\left\{-\left[\frac{\pi(f+f_0\pm f_0)\tau}{2\sqrt{2}}\right]^2\right\} \quad (8b)$$
$$+\left(\frac{A_s\tau}{4}\right)\left(\sqrt{\frac{\pi}{2}}\right)\exp\left\{-\left[\frac{\pi(f-f_0\mp f_0)\tau}{2\sqrt{2}}\right]^2\right\}$$

Equations 8a and 8b are plotted in Figures 7a and 7b respectively.* The sinusoid signal bandwidth (10% amplitude points) is $\frac{e}{\tau}$ while the pedestal bandwidth (10%) is $\frac{e}{2\tau}$ for both the conventional LV and the LV with frequency translator. However, Figure 7a shows that the conventional LV can violate the inequality set forth in Equation 7a and produce overlapping spectra. This in turn negates the possibility of using simple filter techniques to separate the sinusoidal signal from the pedestal. For example, Equation 6 shows that $1/\tau$ becomes a larger percentage of f_D as N is reduced so that when N = 2 the $\frac{1}{\tau}$ point is 0.5 f_D and spectra separation by simple filter techniqes is impossible. This particular case is shown in Figure 7a. Filter techniques are effective for $N \geq 5$ approximately, except when condition 7b is violated. This condition is violated when scatter particles, large compared to the fringe spacing, pass through

*Only the positive frequency spectrum is shown since the negative frequency spectrum contributes nothing to the explanations.

the probe volume and produce a significant portion of the pedestal spectra within the sinusoid spectral bandwidth ($A_p >> 2A_s$).

Figure 7b shows that the LV with optical frequency translator produces a signal which can always be made to satisfy inequality 7a and can be made immune to condition 7b by choosing f_o large enough to adequately separate the pedestal and sinusoid spectra. The most fundamental form of filter, an RC highpass section, can now be effectively used to separate the spectra.

Two additional advantages, from a signal conditioning point of view, are gained by using an LV with optical frequency translator. A minimum number of eight sinusoid cycles per scatter particle transit is required for operation of subsystem 3 shown in Figure 1. Particle trajectories nearly parallel to one of the orthogonal LV measurement axis can produce fewer than eight cycles in the second velocity component signal. This is a brief statement of the "flow direction dead zone" problem discussed in some detail in Ref. 2. The number of sinusoid cycles per particle transit, N_{BC}, produced by the Bragg cell LV relative to the conventional LV, N_{CON}, is in the most general case given by:

$$\frac{N_{BC}}{N_{CON}} = \left| \frac{f_{IF}}{f_D} \pm 1 \right| = \left| \frac{f_o - f_{ho}}{f_D} \pm 1 \right| \qquad (9)$$

Where f_{IF} is the output frequency generated by an electronic frequency heterodyne device given the input signal frequency $f_o \pm f_D$ from the LV photodetector and f_{ho} from a heterodyne oscillator. Equation 9 shows that if f_{IF} is chosen to be much greater than f_D then the number of signal cycles, N_{BC}, can be made much greater than N_{CON} and the requirements of subsystem 3 can be satisfied. The second additional advantage is that N_{CON} can optically be made as small as one in a Bragg cell LV system in order to concentrate the available laser power into as few fringes as possible which in turn produces maximum scattered intensity per scatter particle fringe crossing.

4.3 Information Spectra

Figure 5 shows the spectra of the four carrier signals produced by a motionless scatter particle or scattering surface inserted into the probe volume whereas each particle of a dynamic particle field will produce a signal spectrum as shown in Figure 7b. Those particles with the maximum velocity deviation from the mean value of the particle field velocity distribution will dictate the bandwidth, W, of the velocity information spectrum. It follows from this discussion and Figure 7b that the velocity information bandwidth is given by:

$$W = 2 \left| f_{D\ mean} - (f_{D\ max} + \frac{e}{2\tau}) \right| \qquad (10)$$

where $f_{D\ mean}$ is the mean "Doppler" frequency produced by the dynamic particle field and $f_{D\ max}$ is the maximum "Doppler" frequency produced by this same field. This bandwidth, W, is the bandwidth which must be accommodated by the signal conditioning instrument, subsystem 2.

Information spectra for the special case of an isotropic velocity distribution with zero mean is depicted in Figure 8. Bandpass filter techniques are used to separate the four information spectra prior to further signal conditioning and data acquisition operations. Simple filters can be used as long as adjacent information spectra are sufficiently attenuated. Overlapping information spectra represent the ultimate limits on component velocity magnitudes which can be accommodated regardless of the type filter used. Figure 8 shows that the first limit is reached when the spectrum centered at 10 MHz overlaps the one centered at 15 MHz. However, this problem can be resolved by use of the polarization rotators (Fig. 2) which eliminate the spectra centered at 10 and 40 MHz. The next limit is reached when the spectra centered at 15 and 25 MHz begin to overlap. At this point, accommodation of still greater velocities obviously requires that the velocity information spectra be further separated by using a greater frequency interval between the carriers.

4.4 Information Spectrum Translation

Equation 2, given the practical constraint that $w \leq 2.54$ cm., shows that proper Bragg cell operation requires a drive frequency (carrier frequency), f_o, in the order of 10^7 Hz. On the other hand, low velocity LV applications such as atmospheric wind velocity measurements may produce signal frequency deviations about the carrier in the 10^3 Hz. range. This situation requires a signal frequency (or period) measurement accuracy in the order

of 0.01%. Subsystem 3 shown in Figure 1 has a nominal accuracy specification of 1% of its full scale setting which is not compatible with the 0.01% requirement. Subsystem 2 solves this problem, utilizing electronic heterodyning techniques, by translating the velocity information spectra to a lower carrier frequency. Translation by two decades in frequency results in a carrier of order 10^5 with the same 10^3 Hz deviation. The measurement accuracy requirement is now 1% which is compatible with the subsystem 3 specification.

SECTION V

SYSTEM ACCURACY AND PRECISION

The following specifications of accuracy and precision are definitely not intended to be taken as limits, rather they are specifications attainable by calibration procedures and equipment at AEDC.

5.1 Subsystem 1

The accuracy and precision specifications for subsystem 1 (Fig. 1 & 2) are determined solely by the accuracy and precision associated with the measurements of θ (Eq. 5), the oreintation of the probe volume fringe planes with respect to the velocity measurement plane and the frequencies of the Bragg cell drivers. The velocity measurement plane is defined by the two orthogonal velocity components to be measured. For a horizontal wind tunnel this plane is usually defined by the local vertical and the longitudinal axis of the tunnel.

The angle θ can be calculated from $\frac{\theta}{2} = \tan^{-1}\frac{d}{2L}$ where L is the distance from the center of the probe volume to a reference plane situated to intercept the beams diverging from the probe volume and d is the distance between two applicable beams at the surface of this plane. The reference plane is oriented parallel to the velocity measurement plane.

The orientation of the probe volume fringes with respect to the measurement plane can be determined by observing the angular orientations of the lines defined by appropriate pairs of beams projected onto the reference plane. For example, the pair of beams which are used for the vertical velocity component measurement should define a vertical line on the reference plane whereas the pair of beams used for the horizontal velocity component measurement should define a horizontal line on the reference plane.

Conventional optical tooling techniques utilizing horizontal and vertical tooling bars and optical transits can be exploited to determine L and d with a systematic error no greater than 1 part in 10^4. However, the random error of these measurements can be as much as 1 part in 10^3 because of the uncertainties in the location of the geometric center of the probe volume and the centers of the beams intersecting the reference plane. Given the accuracy specification 0.01% and the precision specification 0.1% in determining L and d, the angle θ and therefore, the relation of v to f_D should be determinable to within 0.2%.

Optical tooling techniques can also be used to angularly align the probe volume fringes with respect to the reference plane with a systematic error or resolution specification better than 1 part in 10^5. Again, however, the uncertainties in locating the centers of the beams projected upon the reference plane can produce random errors as great as 1 part in 10^4.

The Bragg cell drive signal frequency can be determined with a systematic error no greater than 1 part in 10^8 and a random error less than 5 parts in 10^9 by using an electronic frequency counter. The counter can be calibrated to within 3 parts in 10^{10} by a calibration system referenced to an NBS frequency standard signal transmitted by WWVB. The counter time base aging rate specification is less than 5 parts in 10^{10} per 24 hours and its short term (1 second average) fractional frequency deviation, or random error, is less than 5 parts in 10^{11}. These specifications show that the introduction of the Bragg cell into an otherwise conventional LV system does not degrade the overall system accuracy and precision.

The accuracy and precision specifications for measurement of the probe volume fringe orientations and the Bragg cell driver frequencies are at least an order of magnitude greater than those for determination of the angle θ. Therefore,

considering only subsystem 1, the velocity component vectors should be determinable to within 0.2% of the actual values.

5.2 Subsystem 2

The primary functions of subsystem 2 are listed in Figure 1. The photodetection, amplification and bandpass and lowpass filtering operations do not alter the velocity information signal frequencies and, therefore, do not degrade the LV system accuracy and precision. On the other hand, the spectrum translation function requires that the entire velocity information spectrum be translated to a lower frequency carrier. This function can be executed with high accuracy and precision by using a crystal controlled oscillator in the heterodyning process. An ultimate systematic error of 1 part in 10^8 and a random error less than 5 parts in 10^9 can be achieved by monitoring the crystal oscillator with the same type frequency counter used to monitor the Bragg cell driver frequency. Therefore, when properly utilized, subsystem 2 should introduce no appreciable error into the overall LV system.

5.3 Subsystem 3

The primary functions of subsystem 3 are listed in Figure 1. This subsystem is termed the Doppler Data Processor (DDP). Given a signal of high signal-to-noise (S/N) ratio (S/N > 20db) such as provided by a laboratory oscillator, the DDP will determine the signal period with a combined systematic and random error less than 2 parts in $10.^{3\ 2}$ However, dependent upon a complexity of factors including available laser power,

scatter particle size, scattering angle, background light level, etc., an LV system may produce signals with S/N ratios much less than 20 db. Error logic circuitry in the DDP is relied upon to limit the combined systematic and random error to less than 2 parts in 10^2 by sensing and rejecting low S/N ratio signals.[2]

5.4 Subsystem 4

Subsystem 4 is a digital computer accepting up to seven significant digit data. Therefore, barring programming errors, this subsystem will not degrade the overall LV system accuracy and precision specifications.

5.5 Overall System Accuracy and Precision

Given high S/N ratio signals the combined systematic and random error of the overall LV system is dictated by subsystems 1 and 3 and can be as low as 0.4%.

As with any opto-electronic measurement device low S/N ratio conditions ultimately limit the usefulness of the entire LV system. The DDP is presently adjusted to limit the overall LV system systematic and random error to less than 2 parts in 10^2 for poor S/N ratio signals. Data from poor S/N ratio signals are rejected by the DDP and are not recorded.

SECTION VI

SIGNAL CONDITIONING INSTRUMENT

A block diagram of subsystem 2 is shown in Figure 9 and a photograph is shown in Figure 10. This subsystem consists

of three major assemblies: (1) a photodetector assembly, (2) a set of nine crystal controlled, heterodyne or spectrum translation oscillators and (3) an instrument termed a "Signal Separator and Spectrum Translator (SSST)."

6.1 Photodetector Assembly

The photodetector assembly consists of a 931A photomultiplier (PM) tube,its enclosure and high voltage power supply, a dual output preamplifier and an instrument to monitor the mean photocurrent level. The PM tube enclosure provides electrostatic, magnetic and electromagnetic shielding, and contains an optical interference filter to attenuate spurious radiation and an iris diaghram type variable aperture.

The preamplifier provides three primary functions: (1) connects directly to the PM tube enclosure to minimize the parasitic capacitance loading the PM tube anode and thereby maximize frequency response, (2) boosts the signal level before introduction onto a transmission line where noise pickup might occur and (3) provides required frequency response bandwidth and output impedance to drive a 50 ohm transmission line.[9] These functions can be provided by any one of several integrated circuit video amplifiers. We presently use the μA733 amplifier which provides a gain variation from 10 to 100 and a usable bandwidth beyond 100 MHz.

Because of spectra separation (Fig. 7b) the "Doppler" signal is passed but the pedestal waveform is effectively eliminated by a simple RC highpass section coupling the photo-

detector signal into the preamplifier input. The preamplifier passband is presently required to pass 15, 25, and 30 MHz carriers. As explained previously, the 15 and 25 MHz carriers are being used to convey two orthogonal components of velocity information. The 30 MHz carrier is used to convey a third non-orthogonal component of velocity information in a two laser technique described in Reference 16. Each SSST instrument is designed to accommodate two different carrier signals. One of the preamplifier outputs provides the input signal for the 15 and 25 MHz SSST instrument while the other output drives the 30 MHz SSST instrument. The following descriptions of the SSST instrument will be solely in terms of the 15 and 25 MHz unit since the operating principles of the 30 MHz unit are identical. The crystal controlled oscillators used in subsystem 2 are commercially available and will not be discussed further.

6.2 Signal Separator and Spectrum Translator

A schematic diagram of the 15 and 25 MHz SSST instrument is shown in Figure 11. The operational amplifier circuit (IC1-MC1539L) is used to monitor the mean photocurrent level when the separate photocurrent monitoring device (Figs. 9 & 10) is not used. The separate device is not required when the photodetected signals are large amplitude.

The integrated circuit, IC2, is a μA733 video amplifier with a nominal gain of 100. The output at pin 8 is used for the 15 MHz channel while the output at pin 7 is used for the 25 MHz channel. Separation of the velocity information spectra

(See Fig. 8) is accomplished by the T-section filters F1, F2, F3 and F4. Filters F1 and F2 are tuned to pass 15 MHz while F3 and F4 are tuned to pass 25 MHz. All filters have a nominal 1 MHz 3db bandwidth and 50 ohm input and output impedances. Since the 15 and 25 MHz channels are identical except for the filters the remaining discussion is in terms of the 15 MHz channel only.

A nominal gain variation 10-50 is provided by IC4. The output of filter F2 drives the 50 ohm signal port of mixer MX2 while the local oscillator port is driven by emitter follower Q1. The emitter follower in turn is driven by a limiter amplifier implemented by the CA3049 integrated circuit, IC5. The limiting level is set at 1.2 volts peak-to-peak which is optimum for operation of the mixer. A second limiter output drives emitter follower Q2 which in turn provides a front panel output for precise counter monitoring of the heterodyne oscillator frequency. The input signal to the limiter amplifier is furnished by one of the three external heterodyne oscillators at 15.1, 15.2 or 15.5 MHz. The velocity information signals at the input to the mixer are centered at 15 MHz whereas these same signals are centered at 100, 200 or 500 KHz at the mixer output depending upon which heterodyne oscillator is selected.

The output of mixer MX2 is coupled to the input of a lowpass amplifier implemented by the CA3049 integrated circuit IC6. The lowpass cutoff frequency is selected by an eleven

position switch and can be varied in a 1,3,5 sequence from 1 KHz to 3 MHz (see Fig. 11). The lowpass frequency is always set as low as possible in order to reject noise outside the frequency bandwidth of interest. The lowpass cutoff frequency, f_2, is given by $f_2 = (4\pi RC)^{-1}$ where R is the value of resistor R59 or R63 and C is the value of the capacitor selected by the eleven position switch. The differential outputs of the lowpass amplifier drive emitter followers Q7 and Q8 which in turn furnish two front panel outputs. One of these outputs normally serves as input to an oscilloscope while the second output provides the input signal to the DDP instrument.

6.3 Fabrication and Packaging

Figure 12 shows the front panel and the printed circuit board for the SSST instrument. Ground plane printed circuit board construction was exploited to minimize interaction of the 15 and 25 MHz channels. Standard Nuclear Instrument Module (NIM) enclosures were used to package the SSST instruments as well as the Bragg cell reference oscillators and the heterodyne oscillators. These NIM modules plug into a NIM bin power supply assembly which fits a standard 19" rack. The NIM module-NIM bin approach has been found to be quite practical and economical for prototype or finished instrument packaging. A photographic film positive of the front panel lettering is attached to the prototype SSST to label the switch and connector functions.

SECTION VII

SYSTEM EVALUATION

Two initial evaluations of the system concept shown in Figure 1 were conducted: (1) a laboratory test using an LV system sutiable for wind tunnel applications, and (2) a field test using an atmospheric research type LV system. The primary purpose of the two tests was to demonstrate that the new LV systems could simultaneously resolve the 180° directional ambiguity problem for two orthogonal velocity components. Precise determination of the velocity component magnitudes was not required for these evaluations. Therefore, the θ angles (Eq. 5) and the orientation of the two orthogonal measurement axes with respect to the local vertical were not precisely determined.

7.1 Laboratory Test

The LV system was set up in the forward scatter configuration with the geometric centerline of the transmitting and receiving optics intercepting at a 12° angle at the probe volume. The transmitting optics focal length was 1.1 meters and the receiving optics was located 0.7 meters from the probe volume. The laser power was 10 mw. at 4880Å . The system was set up to simultaneously detect the vertical and horizontal velocity components of intrinsic room aerosols. The translated carrier frequency was set at 20 KHz for both output signals and the SSST lowpass amplifier cutoff frequencies were set at 30 KHz.

The air velocity vector was expected to fluctuate somewhat randomly in direction and magnitude and this was verified by observation of oscilloscope displays of the two output signals from the SSST. Figure 13 is typical of the signals produced by the LV system and the directionality capabilities are clearly demonstrated. Figure 13a shows that the vertical component is in the -y direction with the horizontal component in the -x direction whereas Figure 13b shows that the vertical component is still in the -y direction but the horizontal component has shifted to the +x direction. The quality of the oscilloscope displays was somewhat degraded by the effects of the chopper technique used to simultaneously dsiplay the two waveforms but the actual S/N ratios were compatible with the DDP instrument.

7.2 Field Test

The atmospheric research type LV consists of an 18-inch diameter telescope type transmitter and an 8-inch diameter telescope type receiver. The receiver is mounted directly atop the transmitter so that the system operates in a backscatter configuration. The laser power was set at 3 watts at 5145Å. The system was set up to simultaneously detect the vertical and horizontal velocity components of intrinsic atmoshperic aerosols at a range of 30.5 meters and 2.2 meters above the ground. The translated carrier frequency was set at 100 KHz for both output signals and the SSST lowpass amplifier cutoff frequencies were set at 100 KHz.

Figure 14 is typical of the signal waveforms recorded during the field test. The fluctuation of the vertical velocity component from the +y direction in Figure 14a to the -y direction in Figure 14b clearly demonstrates the directional measurement capabilities of the LV system. The quality of the oscilloscope displays shown in Figure 14 was again degraded by the chopper technique used to simultaneously display the two waveforms. The signal frequencies in Figure 14 are closer to the 1 MHz oscilloscope chopper frequency than are the signal frequencies in Figure 13. Therefore, the waveform presentation in Figure 14 is poorer than that in Figure 13. However, the actual S/N ratios of the signals typified by Figure 14 were compatible with the DDP instrument.

SECTION VIII

SUMMARY AND CONCLUSIONS

A newly developed LV system which simultaneously measures the magnitude and direction of two orthogonal velocity components of light scattering particles has been summarily described. Functional descriptions of the four major subsystems comprising the LV system were provided. Only subsystem 2, the photodetection and signal conditioning subsystem, has been described in detail since the other subsystems are treated in other literature. The signal conditioning problem was defined in terms of the basic physical

aspects of laser velocimetry, subsystem dictated constraints, and accuracy and precision characteristics. The signal characteristics in the time and frequency domains were derived which showed that the new system quite simply resolves the pedestal waveform suppression problem associated with certain (small N) conventional LV systems. The new LV system also provides a solution for the "flow direction dead zone" problem characteristic of conventional LV systems with small N, where N is the number of fringe planes set up in the probe volume. Conventional LV systems are restricted to a lower limit on N of 5-10, whereas the new system can function with an N value as low as N = 1. Detailed circuit schematic diagrams of the signal conditioning subsystem were provided. Data from initial evaluation tests was presented to show that the system is capable of resolving the 180° directional ambiguity problem characteristic of all conventional LV systems. An overall system error as low as 0.4% for certain applications (those producing a high S/N ratio) should be obtainable following careful alignment and calibration procedures.

Brief mention was made of the fact that initial LV design criteria provided for future inclusion of a third non-orthogonal velocity component using a carrier frequency at 30 MHz (see Fig. 8). Recent successful operation of a laboratory model, 3 velocity component, Bragg cell type LV has verified the feasibility of the concept.

The atmospheric wind velocity measurement applications to date have produced relatively low data rate frequency burst samples (<10 samples per second) of velocity. This rate is well below the Nyquist rate required for comprehensive fluid flow turbulence measurements. However, recent experiments with a relatively high power, 10w, argon laser and an LV optical subsystem defining a quite small probe volume shows promise of producing at least an order of magnitude increase in the data sample rate when using atmospheric aerosals as scatter particles. The addition of artificial scatter particles, however undesirable, can produce essentially continuous wave signals. To take full advantage of the increased velocity sample rate, FM demodulator and spectrum analysis instrumentation is being assembled to operate in parallel with the DDP instrument.

REFERENCES

1. Hornkohl, J. O. and Farmer, W. M. "A New Self-Aligning Laser Doppler Velocimeter Utilizing A Two-Dimensional Ultrasonic Bragg Cell." Submitted for publication in Applied Optics.

2. Brayton, D. B., Kalb, H. T. and Crosswy, F. L., "A Two-Component, Dual-Scatter Laser Doppler Velocimeter With Frequency Burst Signal Readout", To be published in Applied Optics.

3. Yeh, Y. and Cummins, H. Z., "Localized Fluid Flow Measurements with an He-Ne Laser Spectrometer." Applied Physics Letters, Vol. 4, No. 10, May 1964 pp. 176-178.

4. Foreman, J. W., George, E. W., and Lewis, R. D.,"Measurement of Localized Flow Velocities in Gases with a Laser Doppler Flowmeter." Applied Physics Letters, Vol. 7, No. 77, 1965.

5. Shipp, J. I., Hines, R. H. and Dunnill, W. A. "Development of a Laser Velocimeter System." AEDC-TR-67-175, October, 1967.

6. Goldstein, R. J. and Hagen, W. F., "Turbulent Flow Measurements Utilizing the Doppler Shift of Scattered Laser Radiation." Physics of Fluids, Vol. 10, June 1967, pp. 1,349-1,352.

7. Brayton, D. B., "A Simple Laser Doppler Velocimeter with Self-Aligning Optics." Proceedings of the Electro-Optics Systems Design Conference, New York City, Sept. 16-18, 1969, pp. 168-177.

8. Mayo, W. T., "Simplified Laser Doppler Velocimeter Optics." Journal of Scientific Instruments (J. Phys. E) Vol.3, 1970, pp. 235-237.

9. Lennert, A. E., Brayton, D. B. and Crosswy, F. L., "Summary Report of the Development of a Laser Velocimeter to be Used in AEDC Wind Tunnels." AEDC-TR-70-101, July 1970.

10. Brayton, D. B. and Goethert, W. H., "A New Dual-Scatter Laser Doppler-Shift Velocity Measuring Technique." I.S.A. Transactions, Vol. 10, No. 1, 1971, pp. 40-50.

11. Denison, E. B. and Stevenson, W. H., "Oscillatory Flow Measurements with a Directionally Sensitive Laser Velocimeter." The Review of Scientific Instruments, Vol. 41, No. 10, October 1970, pp. 1,475-1,478.

12. Maxumder, M. K. "Laser Doppler Velocity Measurement Without Directional Ambiguity By Using Frequency Shifted Incident Beams." Applied Physics Letters, Vol. 16, No. 11, June 1970, pp. 462-464.

13. Willard, G. W. "Criteria for Normal and Abnormal Ultrasonic Light Diffraction Effects." The Journal of the Acoustical Society of America, Vol. 21, No. 2, March 1949, pp. 101-108.

14. Farmer, W. M. "On the Measurement of Particle Size, Number Density, and Velocity Using a Laser Interferometer," Applied Optics, to be published Nov. 1972.

15. Goethert, W. H.,"Balanced Detection for the Dual-Scatter Laser Doppler Velocimeter." AEDC-TR-71-70. June 1971.

16. Farmer, W. M., "Determination of a Third Orthogonal Velocity Component Using Two Rotationally Displaced Laser Doppler Velocimeter Systems." Applied Optics, Vol. II, April 1972, pp. 770-774.

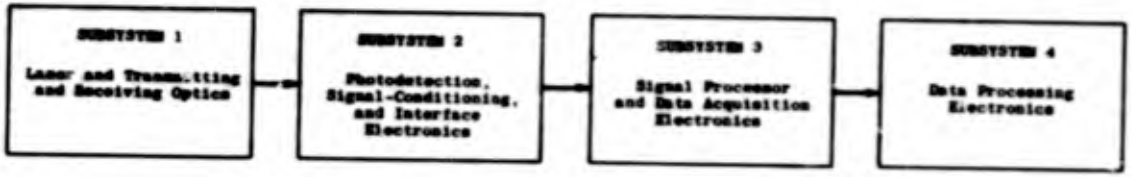

SUBSYSTEM 1 FUNCTIONS

(1) Provide proper laser power and polarization

(2) Split input laser beam into four equal power output beams

(3) Shift the optical frequency of three of the output beams in order to ultimately provide four velocity information carrier signals

(4) Optionally rotate the polarization of three of the output beams to eliminate two of the four carriers

(5) Define the probe volume by transmitting and intersecting the four output beams at a common cross and focus point

(6) Provide scattered laser radiation receiving optics

(7) Provide receiver aperture and interference filter discrimination against spurious light

SUBSYSTEM 2 FUNCTIONS

(1) Photodetect the scattered laser signal radiation

(2) Amplify the photodetected signal

(3) Bandpass filter the signal to separate the carrier-centered velocity information spectra from each other and from wideband noise outside the information bandwidth

(4) Translate the velocity information spectra to low frequency carriers to accommodate the accuracy specification of Subsystem 3

(5) Provide selectable cutoff frequency low pass filters to accommodate the information bandwidth and attenuate noise and spurious signals outside this bandwidth

(6) Provide above functions for up to three velocity components

SUBSYSTEM 3 FUNCTIONS

(1) Simultaneously accept up to three velocity component signals

(2) Apply logic decision circuitry to accept valid signals but reject spurious signals

(3) Determine period of valid signals

(4) Encode period information and record on paper tape and/or magnetic tape

(5) Record other experiment variables - time, temperature, position, etc., as required

SUBSYSTEM 4 FUNCTIONS

(1) Convert signal period information to velocity information

(2) Compute mean velocity, rms deviation, turbulence intensity, etc., as required

(3) Tabulate and/or plot velocity data

Fig. 1 Vector Velocity LV Subsystems Functional Block Diagram

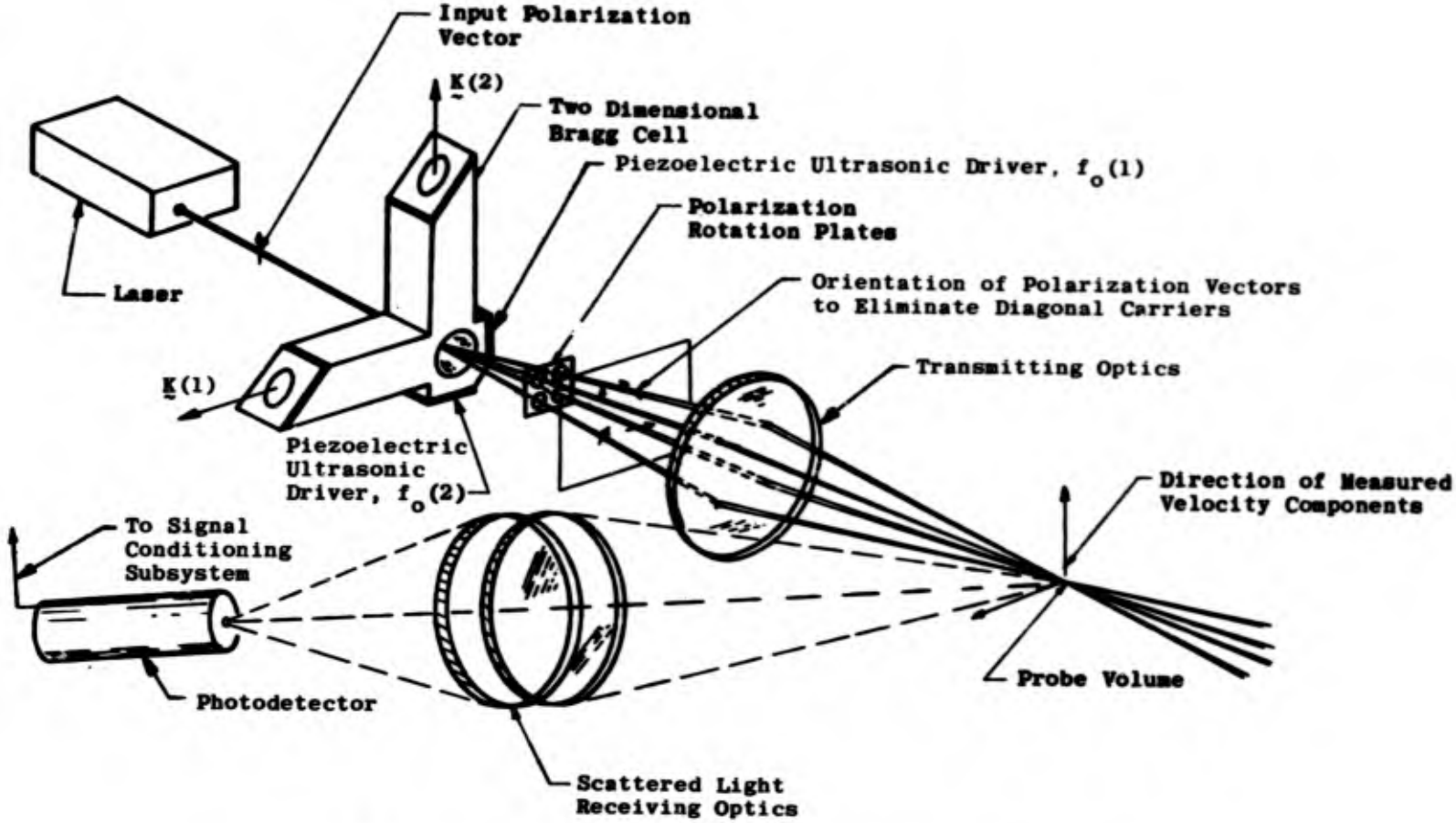

Fig. 2 Vector Velocity LV Optical Subsystem Schematic

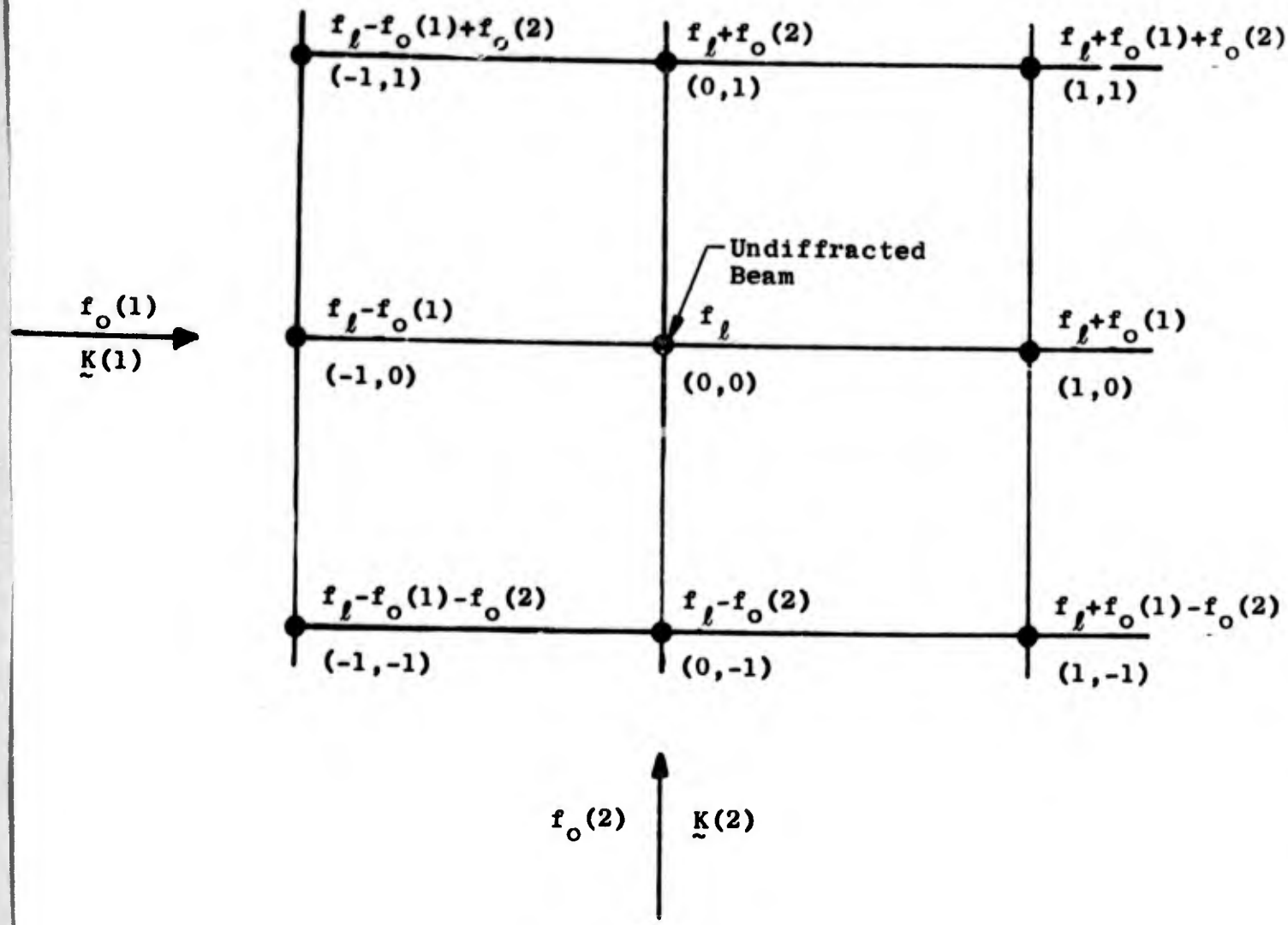

Fig. 3 Diagram Of Possible Beam and Frequency Combinations Using A Two-Dimensional Bragg Cell

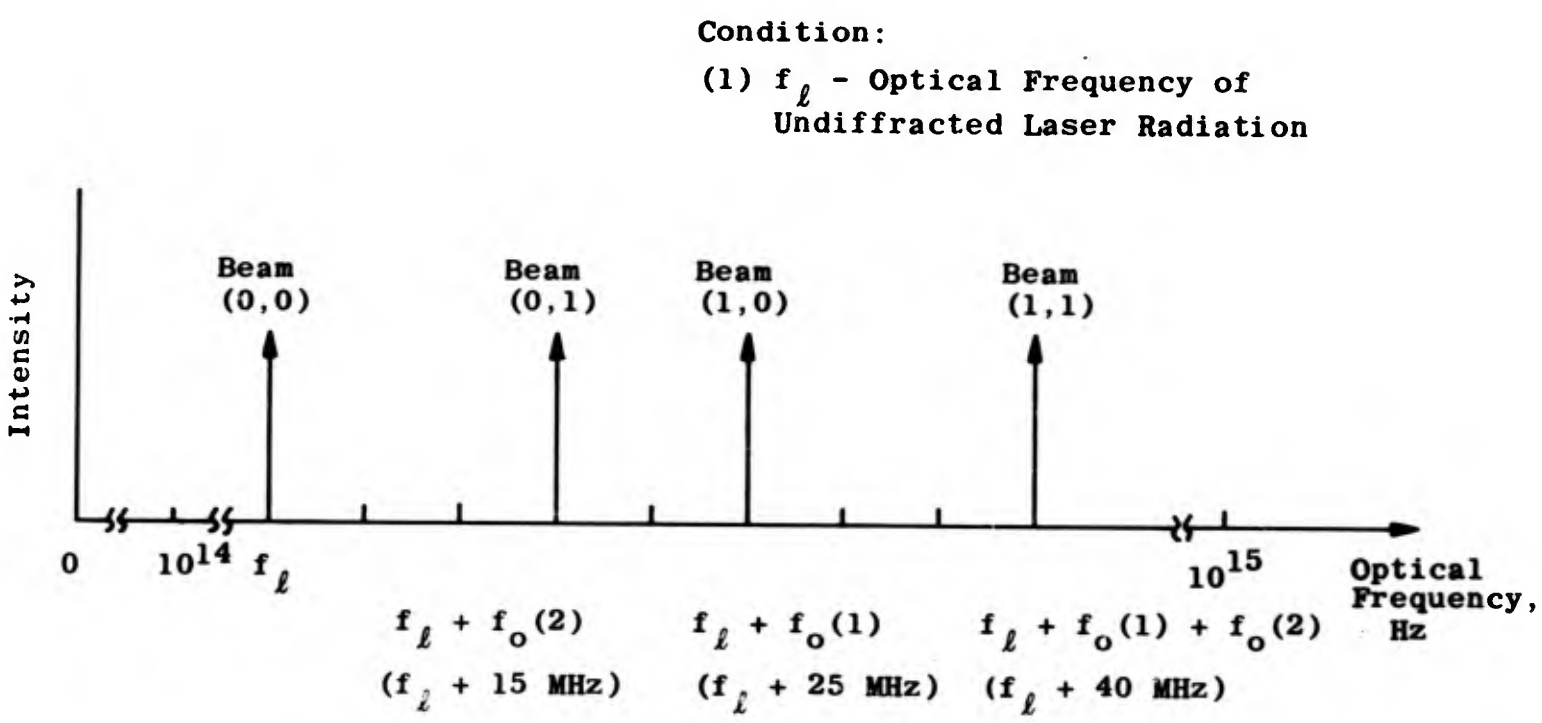

Fig. 4 Optical Intensity Spectrum at the Output of the Bragg Cell

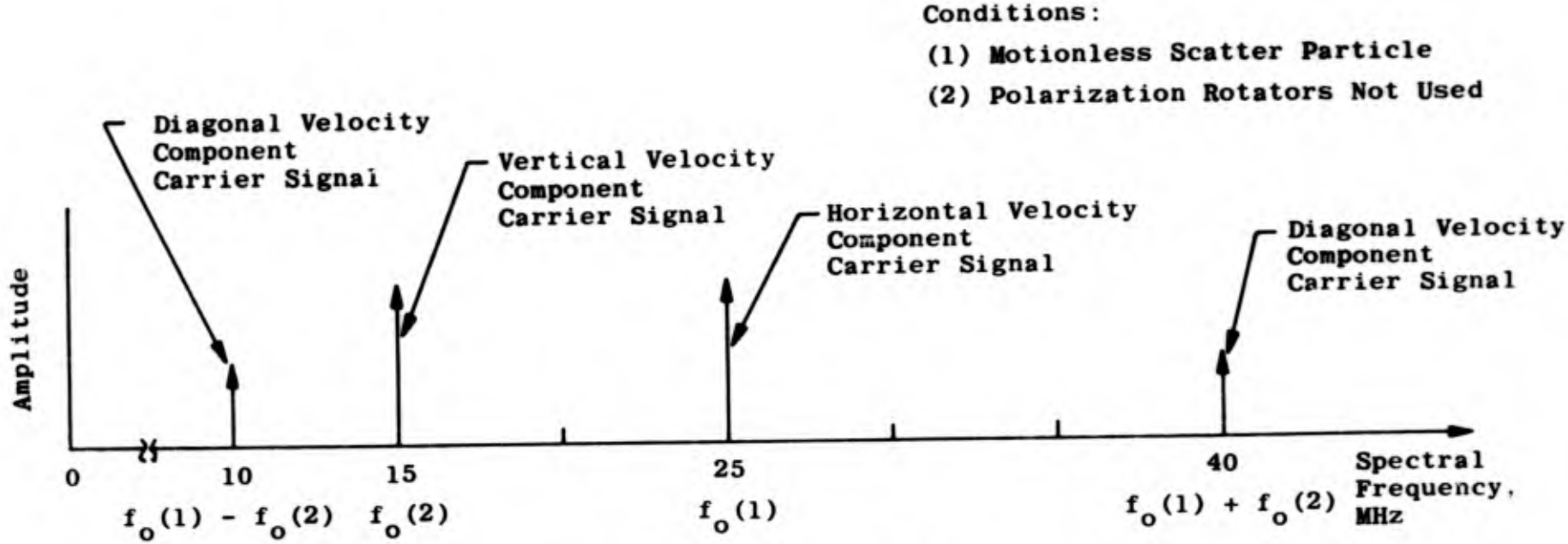

Fig. 5 Photodetected Signal Spectrum for Motionless Scatter Particle Illustrating Velocity Component Carrier Signals

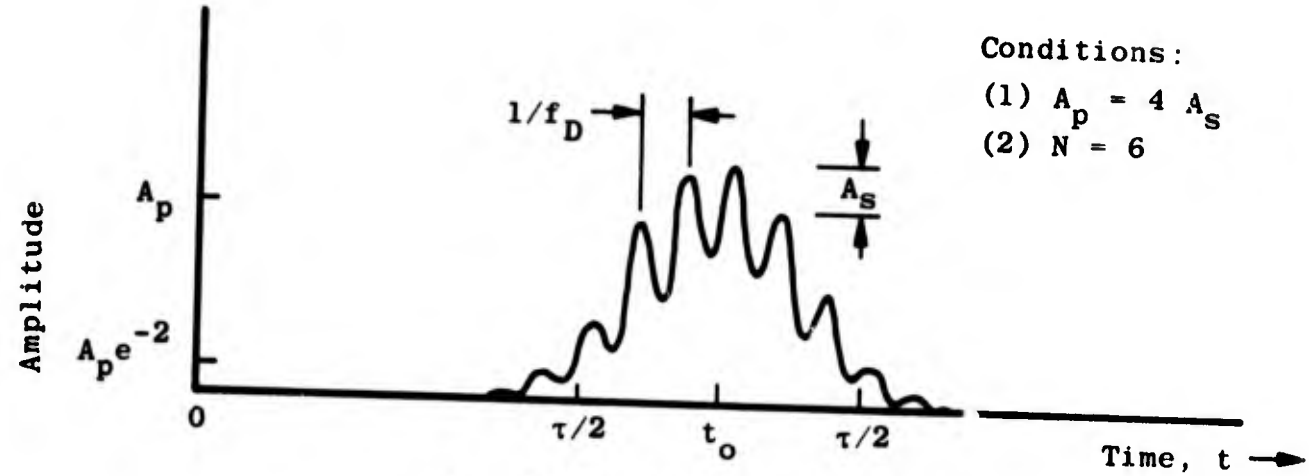

a. Conventional LV System

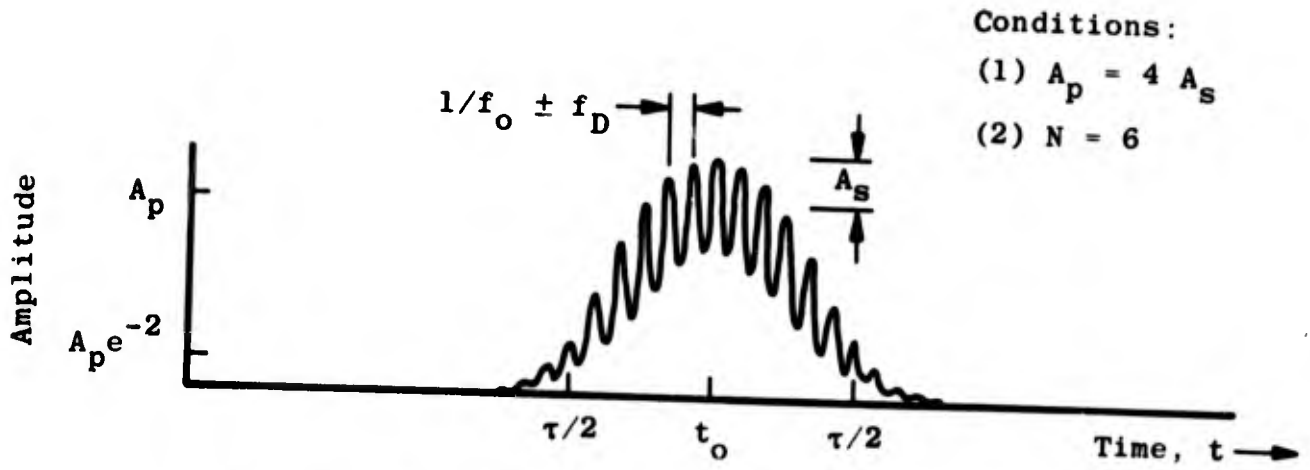

b. LV System with Optical Frequency Translator

Fig. 6 Time Domain Signals - Single Scatter Particle Traversing the Probe Volume

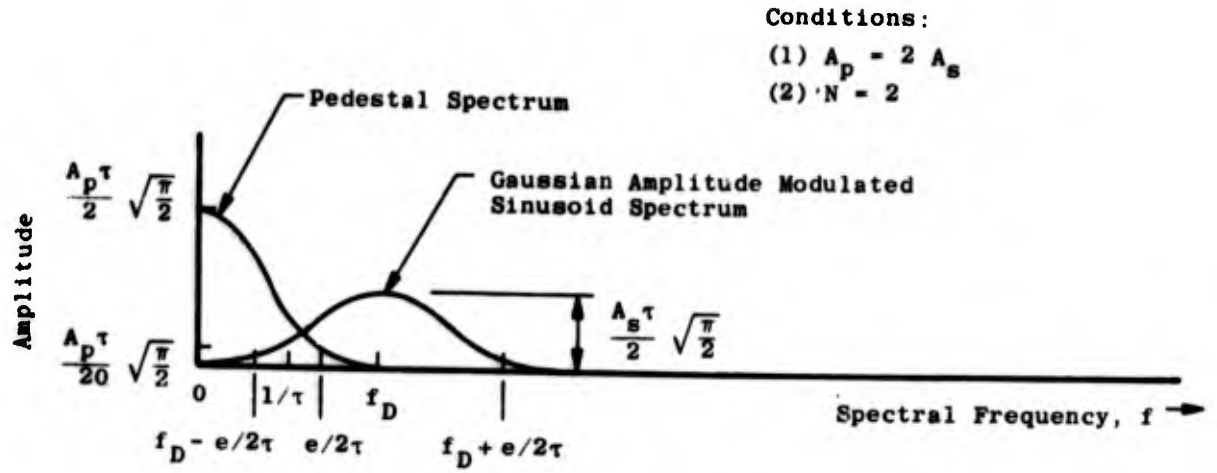

a. Conventional LV System

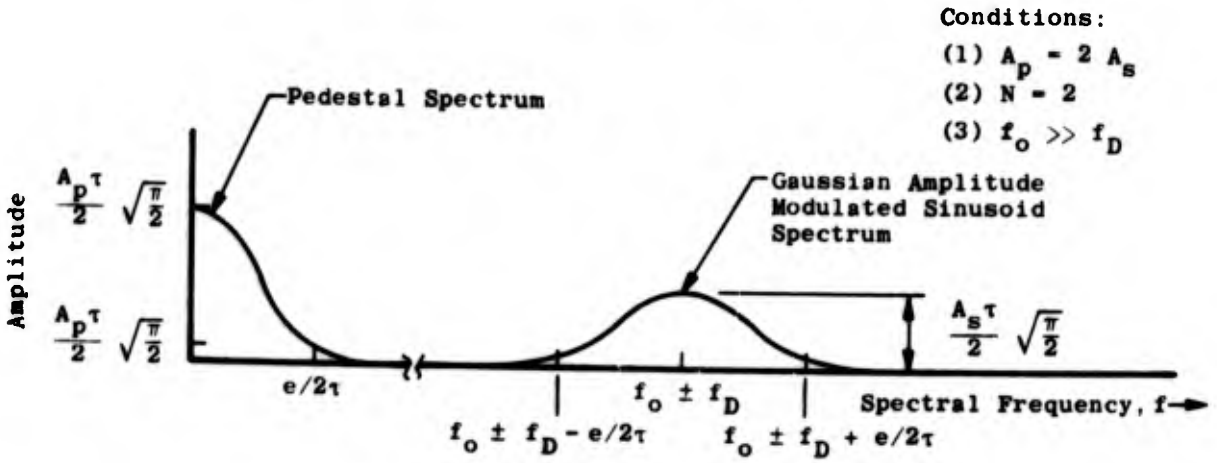

b. LV System with Optical Frequency Translator

Fig. 7 Frequency Domain Signal Representation - Single Scatter Particle Traversing the Probe Volume

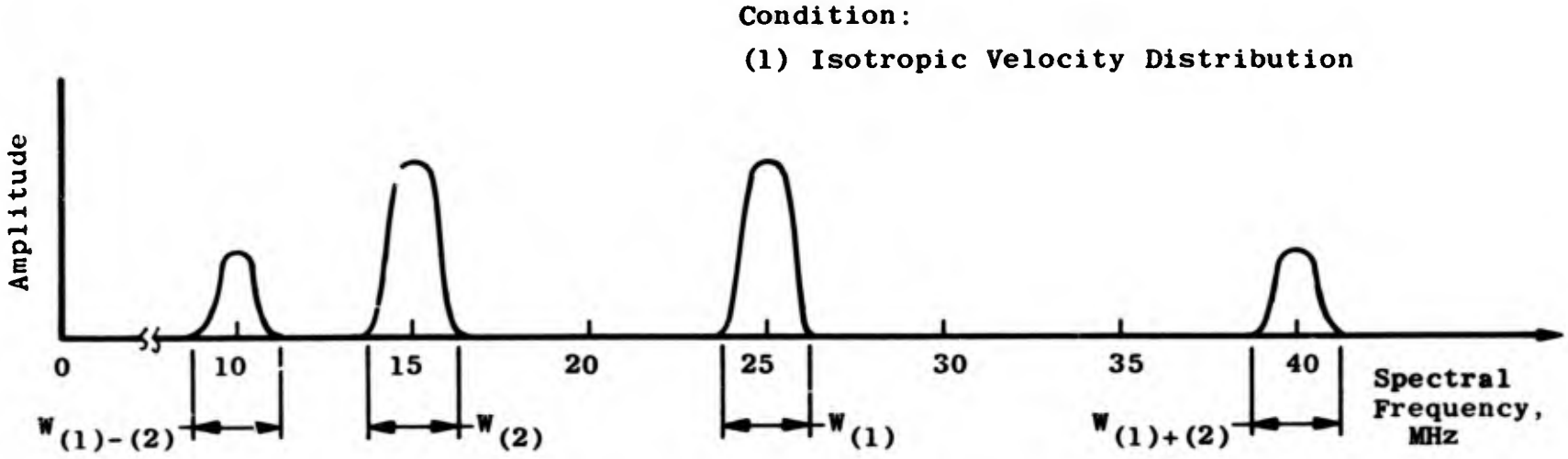

Fig. 8 Velocity Information Spectra Illustrating Relationship of Adjacent Spectra

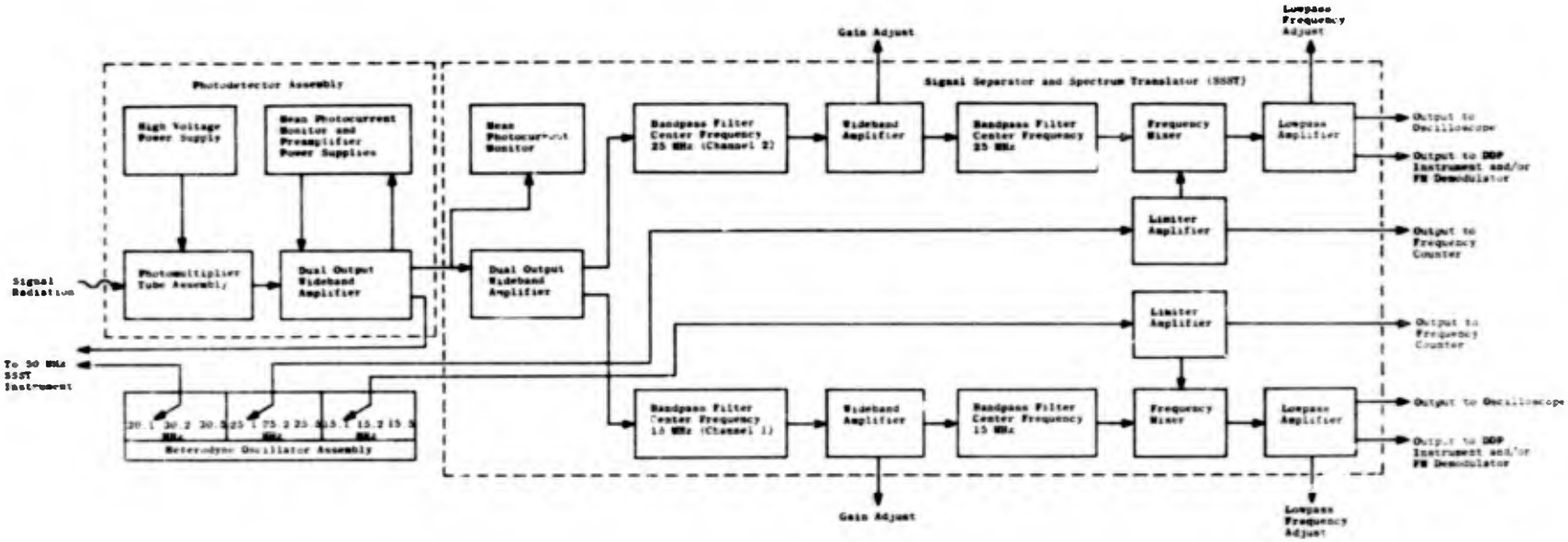

Fig. 9 Block Diagram of the Photodetection, Signal-Conditioning, and Interface Electronics, Subsystem 2

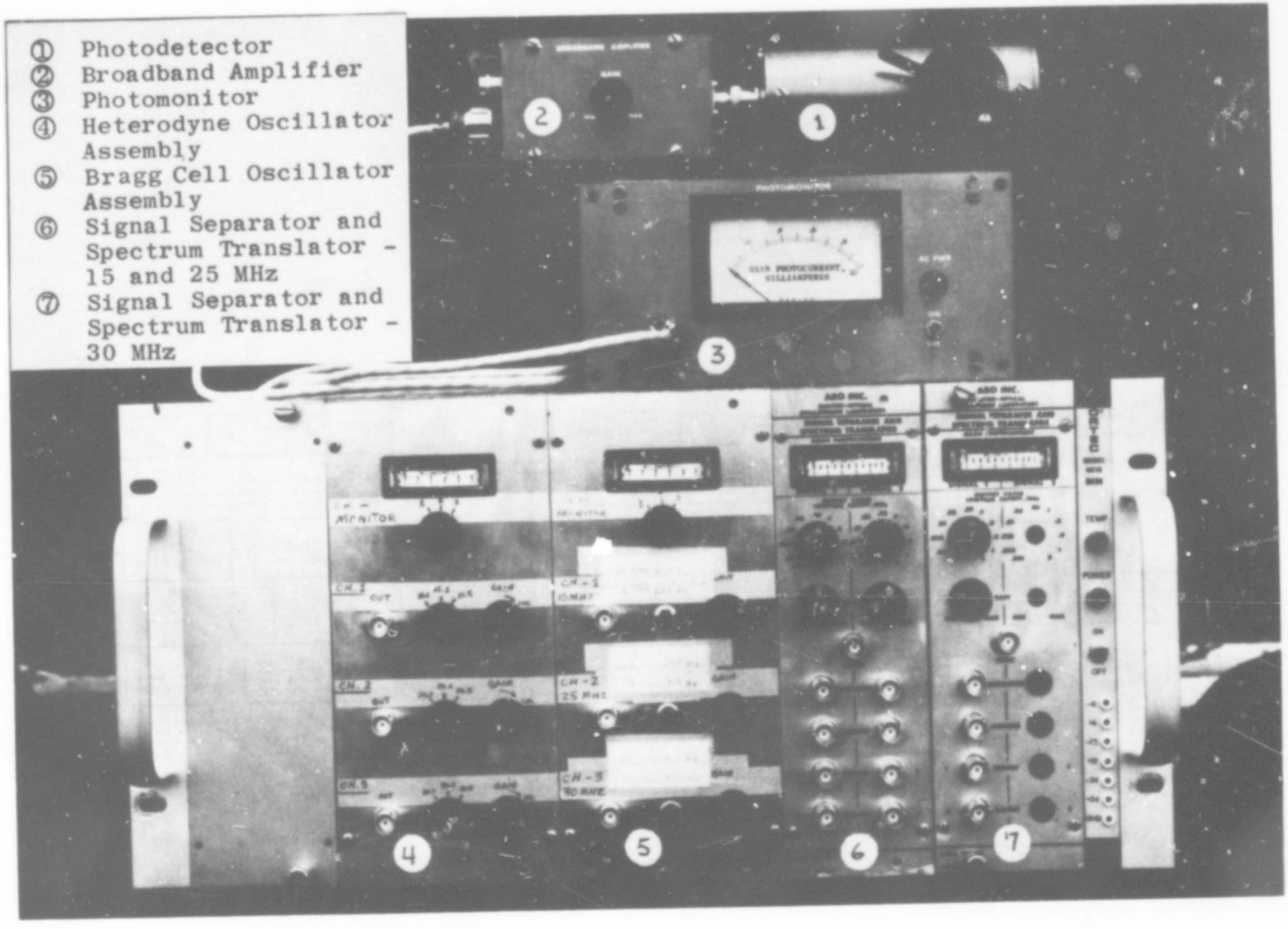

Fig. 10 Photodetection, Signal-Conditioning, and Interface Electronics Subsystem 2

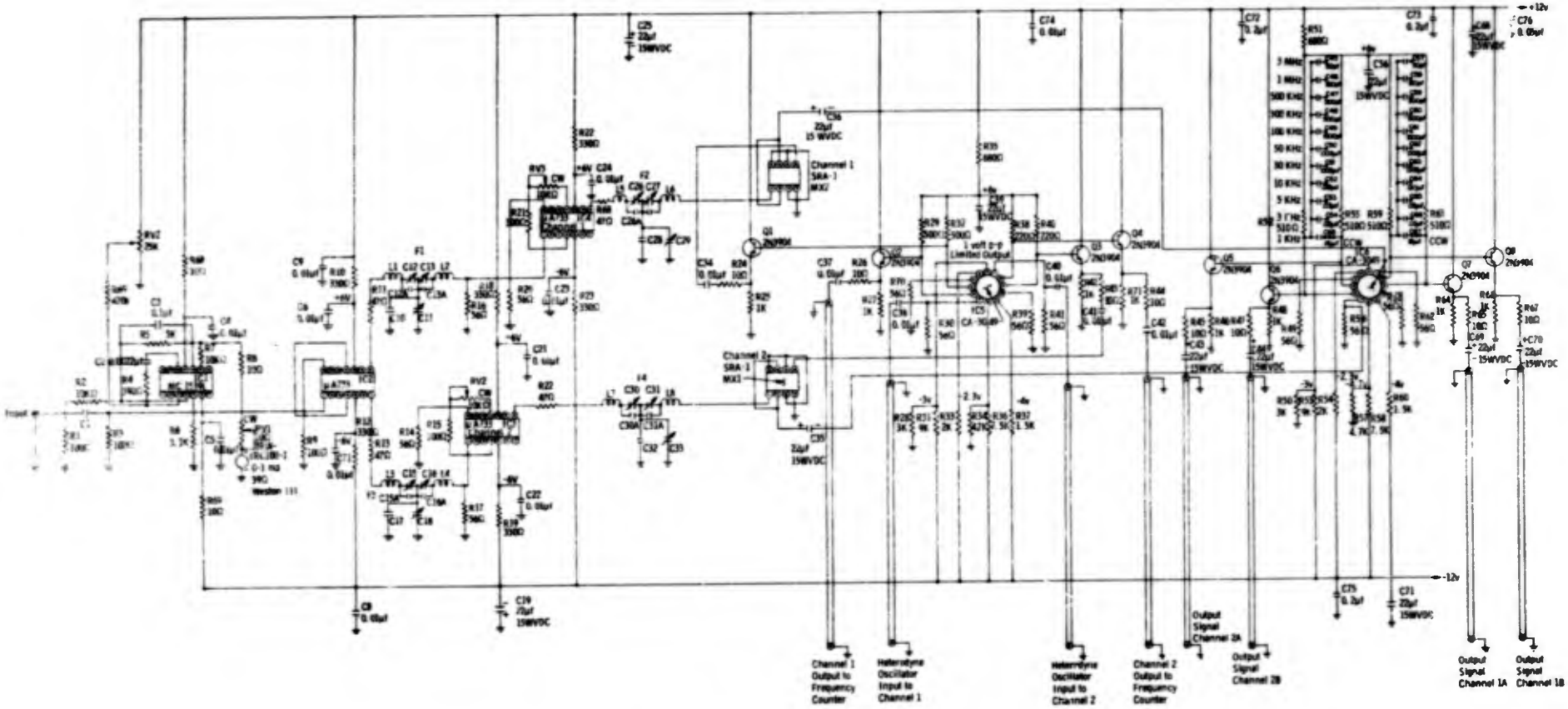

Fig. 11 Schematic Diagram of Signal Separator and Spectrum Translator

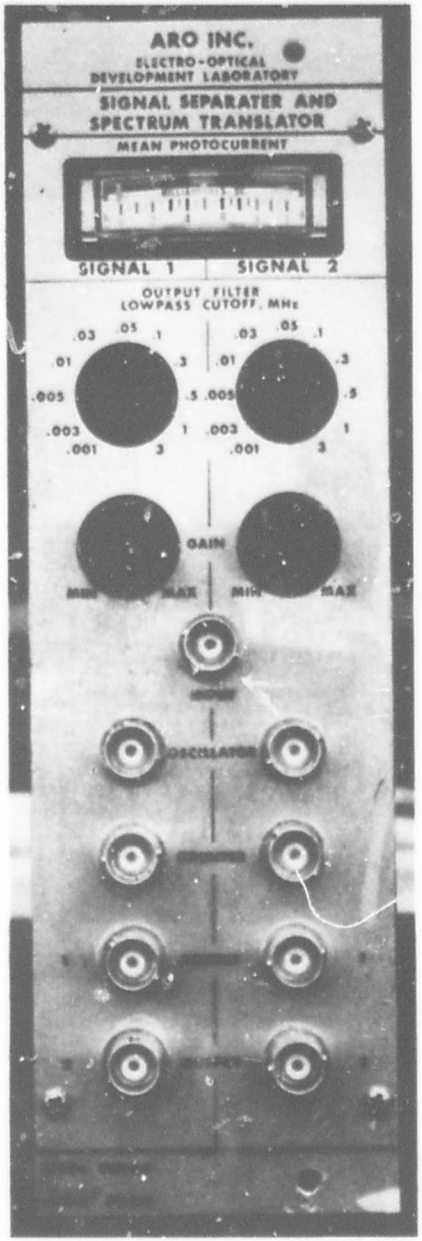

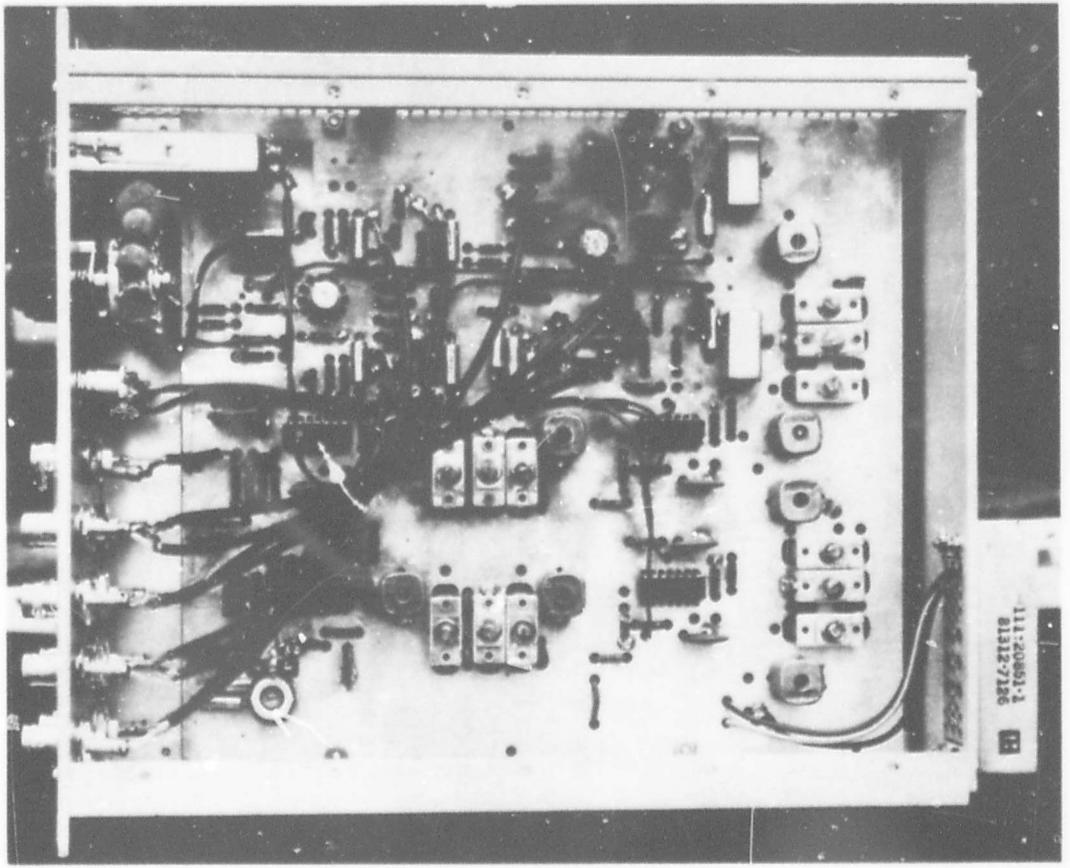

Fig. 12 Fabrication Details of Signal Separator and Spectrum Translator

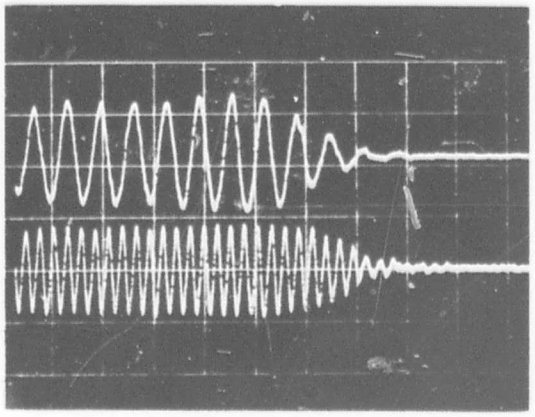

Horizontal, 7.6 kHz

Vertical, 18.3 kHz

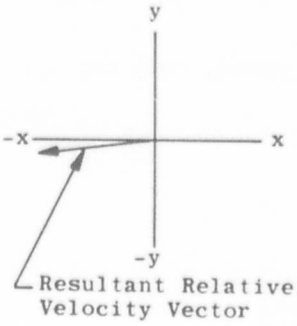

a.

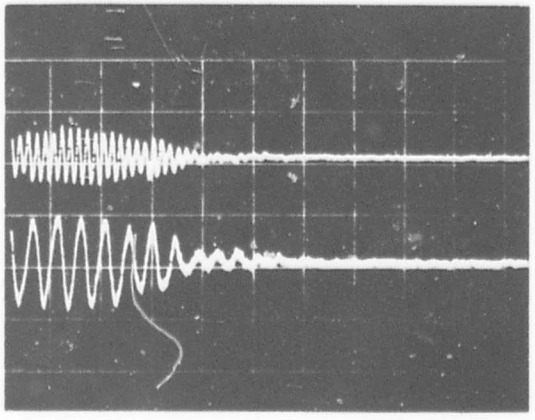

Horizontal, 30 kHz

Vertical, 10.6 kHz

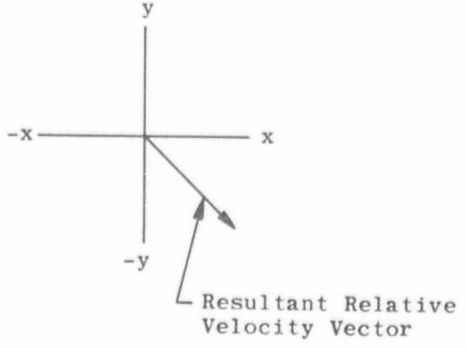

b.

Fig. 13 Directionality Evaluation - Laboratory Test
Conditions:
(1) Translated Carrier Frequency - 20 kHz Both Traces
(2) Vertical Scale - 0.5 v/div.
(3) Horizontal Scale - 0.2 msec/div.
(4) Intrinsic Room Aerosol Scattering Particles

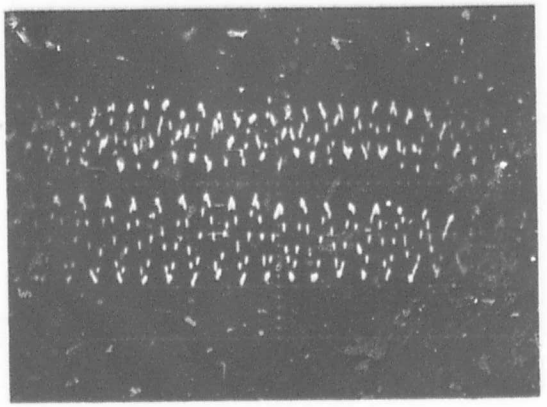

Horizontal, 138.79 kHz

Vertical, 100.48 kHz

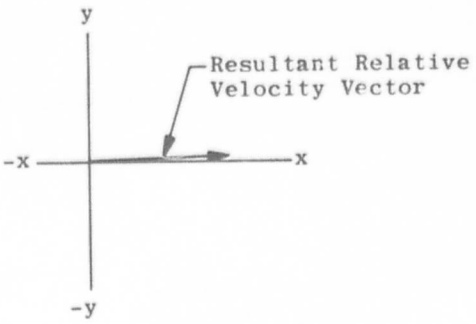

a.

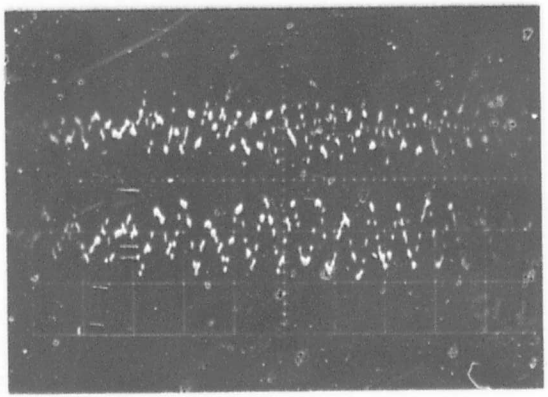

Horizontal, 155.0 kHz

Vertical, 92.52 kHz

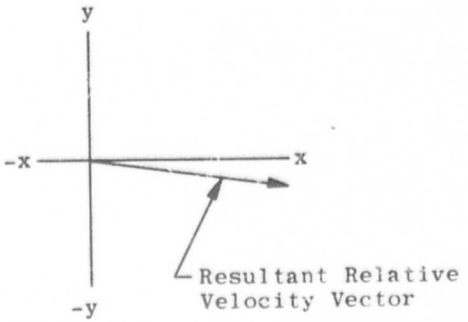

b.

Fig. 14 Directionality Evaluation - Field Test
Conditions:
(1) Translated Carrier Frequency - 100 kHz Both Traces
(2) Vertical Scale - 0.5 v/div.
(3) Horizontal Scale - 20 μsec/div.
(4) Intrinsic Atmospheric Scattering Particles

DISCUSSION

PFEIFER: How broad is your window with respect to the pulse lengths?

CROSSWY: We can adjust it so that if the periodicity does not check within 0.5 percent it will reject the data. Our data rate goes down because it has to be a very pure waveform before we accept it. If we are willing to tolerate less accurate data, say one or two percent, we open our window. As we open the window, the data rate goes up.

LENNERT: We are limited right now in terms of the switching circuitry. Last year we were stretching the pulses 1250 times. We have improved the switching rate to get down to 125 and by next year we feel we will be going direct instead of using artifacts.

VOM STEIN: What is the precision of your pulse stretcher?

CROSSWY: I guess the best way to answer that is on the basis of putting in a known signal. We start out with a CW signal from an oscillator and then generate a burst signal with a modulating scheme. Thus we start with a precisely known frequency and then read the instrument. We put a nominal specification of 1 percent on this measurement. Actually in the laboratory with this type signal we do much better - sometimes 0.1 percent.

ANGUS: What information are you going to learn that you wouldn't learn from a smoke grenade and three orthogonal movie cameras?

LENNERT: What we are trying to do is to make a number of detailed measurements across the wake region. Our design criteria reads that we want to measure a region of about 100 feet with a minimum of 100 data points per second and an accuracy of $\pm$ 50 feet per seconds throughout the range. In the tests that we are planning at Patrick, we hope to get the background wind velocity and direction and include that as an error in the system.

ANGUS: Yes, but what is that data going to enable a pilot or airport designer to do that he wouldn't be able to learn from a smoke grenade?

LENNERT: First of all we are trying to get detailed information with regard to the outer wake turbulence as well as the inner scale breakup and to use this as diagnostic tool to try to affect design. We

want to get detailed quantitative design information as opposed to qualitative information.

DUNNING: Design for what - for the spacing of airplanes or for the airplanes?

LENNERT: We want quantitative information in regard to the effectiveness of some device you might install on the aircraft to minimize the wake.

PIKE: Can you tell me what time it takes to obtain your information - the 100 data points, is that one velocity?

LENNERT: We want 100 data points per second minimum.

PIKE: But how many of those do you need to specify the velocity? Presumably the velocity is not changing very fast. Are you looking at 100 points in space in one second?

LENNERT: Yes. We hope to get three components simultaneously at each individual data point. We hope to get more than one data point per station or if we track continuously we hope to get more than 100 data points over a 100 foot span.

PIKE: This experiment looks very much like the one I discussed yesterday except ours was in a wind tunnel. I hope I will have enough time this afternoon to talk about our atmospheric work. I seriously believe that photon correlation should be used for this.

LENNERT: Well, there are other applications such as looking at chopper blade rotation on the outdoor test range. In other words the applications are much more than just this one particular case.

PIKE: Yes, but the signal processing is expensive. You might be able to pick up a factor of 10^2. How much does the 48 inch mirror cost you - $10,000?

LENNERT: No, it will cost more than that.

PIKE: How much is your laser? How many watts?

LENNERT: Well, in the particular measurements that we are making now it runs about $18,000 for 4 watts in the 4880 line and 5.5 watts in the 5148 line.

PIKE: You really are using a sledge hammer. You did mention Farmer and Brayton's paper. I should say that it's all wrong. I hope you didn't base all your calculations on that paper.

LENNERT: Well, we are using measurements that we are making outdoors where we have an 8 inch telescope. We have scaled up to the full scale unit and have some detailed plots with regard to the power required as a function of range and different telescope systems for the data acquisition rate in which we are particularly interested. So I say to each his own. We could sit down and yell at each other for two or three years and no one is going to change his mind until they see the final product.

HAUER: I guess my question is really the same as Dr. Pike's, but you know we were hearing this morning what really large sample sizes are necessary for obtaining turbulence information. It-sounds to me that at 100 per second you are talking about very long time constants in atmospheric phenomena. How about getting the inner scale.

LENNERT: Well, this is a problem. I have a feeling that when we get involved in the program and go into more detail - particularly inside the core where we have the high frequency motion - that we will probably need considerable probing in that inner region.

REYNOLDS: Is the basic aim of the first shot just to get general information on mean velocities and not on detailed turbulence?

LENNERT: Initially that is right.

ORLOFF: If you're not going to see the vortex, how are you going to know where you are?

LENNERT: The telescope has the capability of zooming. The telescope can be positioned within an arc second. So we will be programming the zooming characteristics of the telescope system and use that for the position indicator. It will all be slaved together in that particular experiment. We do this at the present time rather crudely at home with two telescopes slaved together.

UNIDENTIFIED: You have to know where the vortex is.

LENNERT: That's right. We know the wind velocity. We know where the aircraft is flying in the first go around and we will be sweeping this range. Once we determine the characteristics of the vortex, we can superimpose that on the velocity characteristics of the flow field.

WIND TUNNEL MEASUREMENTS

LDV CHARACTERISTICS

James F. Meyers* and William V. Feller**

NASA Langley Research Center

Hampton, Virginia

The laser Doppler velocimeter used at NASA Langley is a crossed-beam dual-scatter optics system that can be either used in forward-scatter or back-scatter modes. The signal processing is performed by either a high speed oscilloscope, spectrum analyzer, or a wide-band frequency tracker. A good deal of theoretical work has been done to determine the LDV output characteristics such as signal-to-noise ratio based only on the physical characteristics of the LDV optics system in use, and the particles in the flow (Ref. 1). Also, work has been performed on determining the response of a given particle to flow fluctuation. A fully developed turbulent pipe flow is being used now as a test bed for determining the operational characteristics of the LDV system.

To begin, we use equation 1 for determining the scattered power collected by the receiving optics. This is the equation where we have expressed the scattered power as a function of F, q, σ_{mie}, ΔV, and Ω.

$$P_{sc} = F\ q\ \sigma_{mie}\ \Delta V\ \Omega \qquad (1)$$

F - laser power intensity at the sample volume in the flow

q - transmissivity of the medium (for gases q = 1)

σ_{mie} - scattering cross section of the particle.

---

*Aero-Space Technologist, Instrument Research Division
**Aero-Space Technologist, Hypersonic Vehicles Division

ΔV - volume of the ellipsoid defined by the crossing of the two beams

Ω - the effective area of the receiving optics divided by the squared focal length.

Further

$$F = \frac{q\ P}{A_{cl}} \tag{2}$$

where P - input laser power

A_{cl} - cross-sectional area of the sample volume based on the Airy disk.

The Airy disk diameter may be defined:

$$D_a = \frac{1.22\ \lambda\ F_1}{D} \tag{3}$$

where λ - input laser wavelength

F_1 - focal length of the input focusing lens

D - diameter of the input laser beam

The sample volume, ΔV, is defined by:

$$\Delta V = \frac{\pi\ D_a^3}{6\ \sin\ \varphi} \tag{4}$$

where φ - angle between the crossed laser beams

The Mie scattering cross section, σ_{mie}, is found by the following equation (Ref. 2):

$$\sigma_{mie} = \frac{1}{K^2} \sum r\ i\ (\alpha,\ n,\ \theta)\ N_{mie} \tag{5}$$

where K - wave number of incident radiation.

$i\ (\alpha,\ n,\ \theta)$ - scattering intensity function of the particle size-to-wavelength ratio, index of refraction, and scattering angle.

N_{mie} - number of particles of radius r

We can take the scattering cross section for a given particle of a given radius that is passing thru the sample volume ellipsoid and calculate the power collected from its scattered radiation. The summation in the scattering cross-section equation can be converted to an integral that contains the particle size distribution of the seeding mechanism. In the natural atmosphere it is the Junge distribution, $1/R^3$, but for a particle generator, the distribution could be Gaussian, rectangular, or what have you. It doesn't matter. That is all input and the program gives the collected scattered power. So now you can take your physical information on tunnels; run through a few LDV configurations, and find the optimum system.

Figure 1 shows one such run through the computer program. The vertical axis is scattered power in watts as a function of the cross beam angle based on a λ of 5145 $\mathring{A}$ and 0.3 micron diameter alumina particles, with an input laser power of 1.25 watts. The ordinate is average scattered power over a long time based on 1,000 particles per cc, which is in the neighborhood of a 1% duty cycle. From this scattered power we can go through equation 6 and calculate the effective signal-to-noise ratio. It's a simple equation that is used by several researchers.

$$S/N = \frac{\eta P_{sc}}{2 \Delta f \beta h \nu} \qquad (6)$$

Signal-to-noise ratio is equal to the quantum efficiency of the photomultiplier tube, η, times the scattered power from equation 1, divided by twice the noise bandwidth of the instrumentation. Beta is the statistical factor due to dynode emission in the photomultiplier tube and $h\nu$ is the photon energy. Using the results for scattered power from Figure 1, the signal-to-noise ratio is presented in Figure 2.

If we have given that there is one particle in the sample volume, the dependence on volume in the equation is removed and the signal-to-noise for single particle scatter may be calculated. The results from this calculation for single particles based on the inputs for Figures 1 and 2 are given by the dashed line in Figure 3. Also in this Figure, the time average signal-to-noise ratio is given as a function of particle number density. As you can see, this is the expected linear function until it reaches the point where you have 100% duty cycle and it levels off for the dual-scatter system. The signal-to-noise ratio for the reference-scatter system will begin with a little lower slope but will not level off as the dual-scatter configuration does.

Figure 4 shows the equations we used to study the motion of the seeding particles. The drag coefficient taken from reference 3 is empirical in origin, and contains the Stokes relation, 24/Re, but with correction terms that take the drag coefficient to the free molecule limiting value at small Reynolds numbers, and to an experimental value of 0.4 at high Reynolds numbers. The velocity in the Mach number and Reynolds number is a relative value, the difference between gas velocity and particle velocity.

The particle motion is expressed by Newton's law, F = m a, written in terms of the relative Mach number and Reynolds number. The acceleration of the particle is given by the bottom equation, which is dependent upon the particle diameter, D, particle density, ρ_p, Reynolds number, Re, the viscosity of the gas, μ, the drag coefficient, C_D, and the velocity difference between the gas and the particle, $(V_g - V_p)$.*

*However, see the discussion after this paper.

Figure 5 shows the response function for a 1 micron alumina particle. We assume a fluctuating air flow with a mean velocity of 100 m/s which is fluctuating by 10 m/s, at standard atmosphere density. Thus the air velocity is oscillating from 90 to 110 m/s over a range of frequencies. The response function plotted is the ratio of the amplitude of the particle velocity fluctuation to the amplitude of the fluid velocity fluctuation, after an initial transient (always very short, a few cycles). The response starts with 100% at low frequencies and then starts rolling off at about 1 kHz. The results using Stoke's drag law do not differ very much from those using the corrected Stoke's law for the 1 micron particle, showing that low Reynolds number effects are not too large for this size particle and gas density. An arbitrary wave form, like turbulence, can be considered to be a superposition of sine waves of varying frequency, so this plot of the particle's response or transfer function (called a Bode plot in electrical engineering) is a measure of the accuracy with which the particles follow the fluid flow.

The Bode plot for a 0.3 micron alumina particle is given in Figure 6. As you can see, there is quite a difference now between the prediction by the "exact" drag law and by Stoke's equation under the same conditions, that is with 0.3 micron particles and the same driving function.

On Figure 7 we are showing the "exact" equation for alumina in three different particle sizes. Choosing a response ratio of, say 90%, you can find out where the effective information rolls off as far as turbulence frequency is concerned.

Now why alumina? Why not kerosene, or DOP, why not something else? Even though alumina is heavy, (its specific gravity is 3.65), it is nice because it is available commercially with a very narrow size distribution if it doesn't

clump. So, we can then take our turbulence output and play the same game the hot wire people do. Make an amplifier that inverts the particle's Bode plot and then correct the turbulence data out to 100 kHz by placing the amplifier in the output line of the tracker. It looks good on paper, but we won't know for awhile if it works.

In Figure 8 we are trying to determine slippage of the particle as a function of frequency. This is the phase lag which drops quite abruptly. To find the actual slippage, you have to take into consideration the frequency. For example for a 1.0 micron particle there is a 30° phase lag at 1 kHz which can be converted to give an actual time lag or distance lag.

Now going to the experimental setup to give an idea of what the test bed looks like. We have a Spectra Physics model 125 He/Ne laser. We bring the beam up, as shown in Figure 9, split it in the optics box, and take just one component. Why one component? Because we have only one component of electronics. We focus the two beams in the jet formed by a turbulent pipe flow exhausting into the room. The collected scattered light is brought to the photomultiplier tube.

The way this instrument is set up, we can rotate the entire optical system plus or minus 45° around a vertical axis, take our points and do a Reynolds stress analysis. The carriage is motorized so we can scan across the flow and obtain velocity profiles.

Using a wideband frequency trakcer, we can also get turbulent profiles. Right now the data we have is just turbulence intensity obtained by taking the AC output of the tracker and running it through an RMS meter. The AC output can also be run into a spectrum analyzer, a correlator, or what have you, to find the information that you are looking for. As we scan the focal volume across the flow we get real time output data.

In Figure 10 the solid line is the mean velocity profile as we scanned across the jet issuing from the end of a long pipe, in which we expect fully developed turbulent pipe flow. The dashed line is the velocity calculated from pitot pressures taken 5 millimeters downstream of the LDV sample volume. There is a difference of about 5%, as you can see. We think this is due to the large particles lagging in the flow.

At each edge of the flow is an example of the problem I mentioned yesterday. The tracker output curve wanders off to erroneous values at both edges of the flow, where the duty cycle has fallen, and the tracker is trying to include that noise spike. I think it is inherent, and the problem can develop in all tracking systems. I think it is in our system because of our input AGC amplifier. The amplifier doesn't give you white noise out for white noise in, and this is a problem. If you have a good amplifier in the front end, you may not even see this. We are now trying to correct this but right now when the duty cycle gets low, that is the end of our good data.

The next figure, Figure 11, shows a scan across the flow of the mean velocity and the turbulent intensity. You can see the turbulent intensity is fairly low in the center and then peaks near the edge where the mean flow shows the largest velocity gradient, as expected from hot wire measurements. Again, where the duty cycle falls off, the tracker output wanders off and gives unreal outputs.

Figure 12 was taken 9 inches or 23 centimeters downstream of the end of the pipe flow. Comparing with the previous figure that was taken very close to the exit, you can see how the core of the flow is now narrower. The turbulence peaks are coming closer together, and the mixing region at each edge is getting wider.

This is some of the work that we are trying to do. We are using a test bed to find out exactly what the characteristics of the LDV are before we use expensive tunnel time in a Mach 6 tunnel to study turbulent boundary layers. By using this test bed, we hope to find out all the problems, or as many as we can, so that when we use the instrument in a wind tunnel, we can use it with confidence.

REFERENCES

1. Meyers, J. F.: Investigation and Calculations of Basic Parameters for the Application of the Laser Doppler Velocimeter. NASA TN D-6125, April 1971.
2. McCormick, M. P.: Laser Backscatter Measurements of the Lower Atmosphere. Ph. D. Thesis, College of William and Mary in Virginia, 1967.
3. Cuddihy, W. F., Beckwith, I. E., and Schroeder, L. C.: A Solution to the Problem of Communications Blackout of Hypersonic Re-entry Vehicles. Proceedings of the Anti-Missile Research Advisory Council Meeting, Aberdeen, Md., October 22-24, 1963.
4. Fridman, J. D., Meister, K. A., and Young, R. M.: Wide Band Frequency Trackers in Laser Doppler Velocimeter Systems. 17th National Aerospace Instrumentation Symposium, I.S.A., May 10-12, 1971, Las Vegas, Nev.

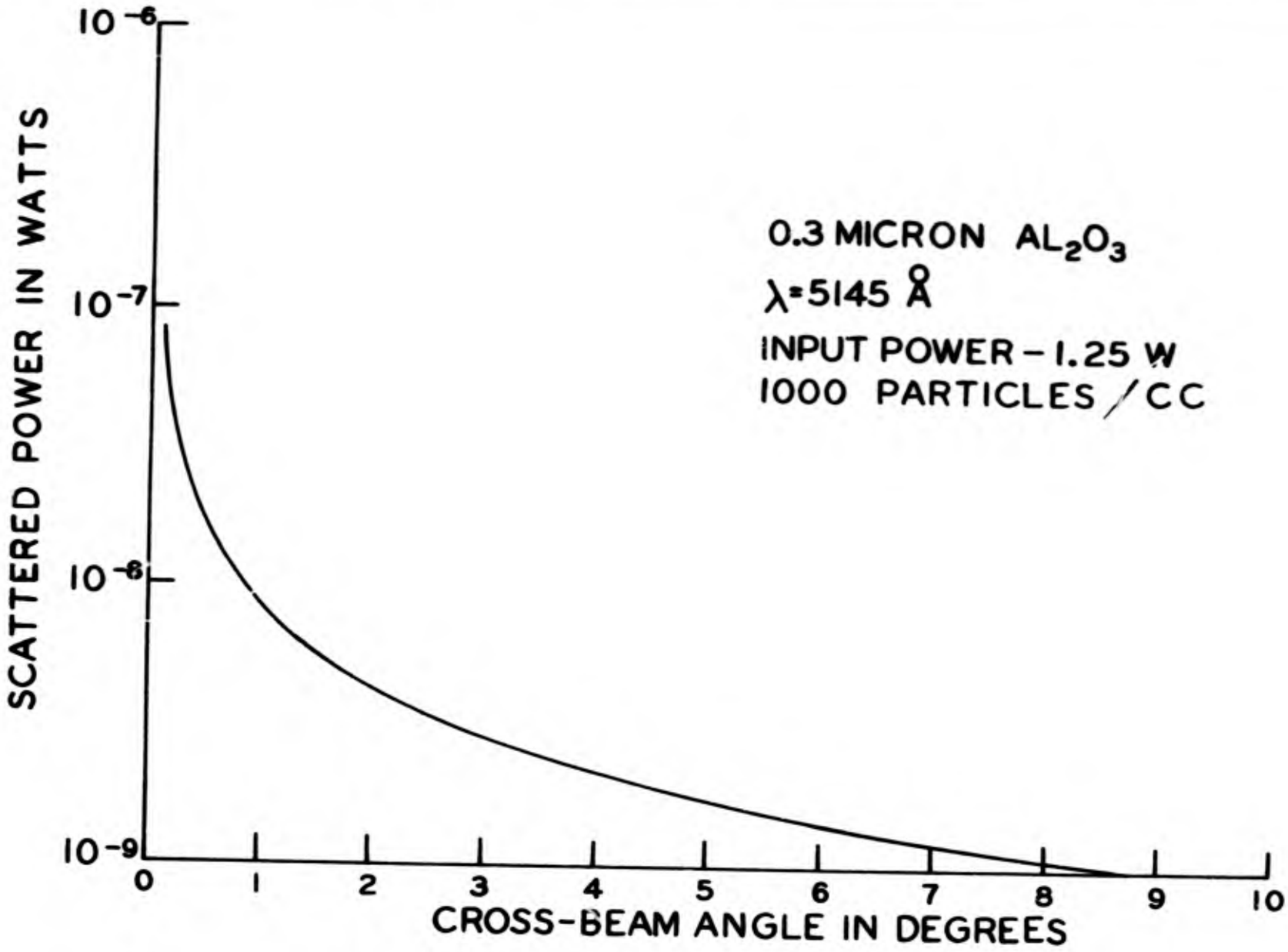

Figure 1. Time averaged scattered power collected by the LDV receiving optics

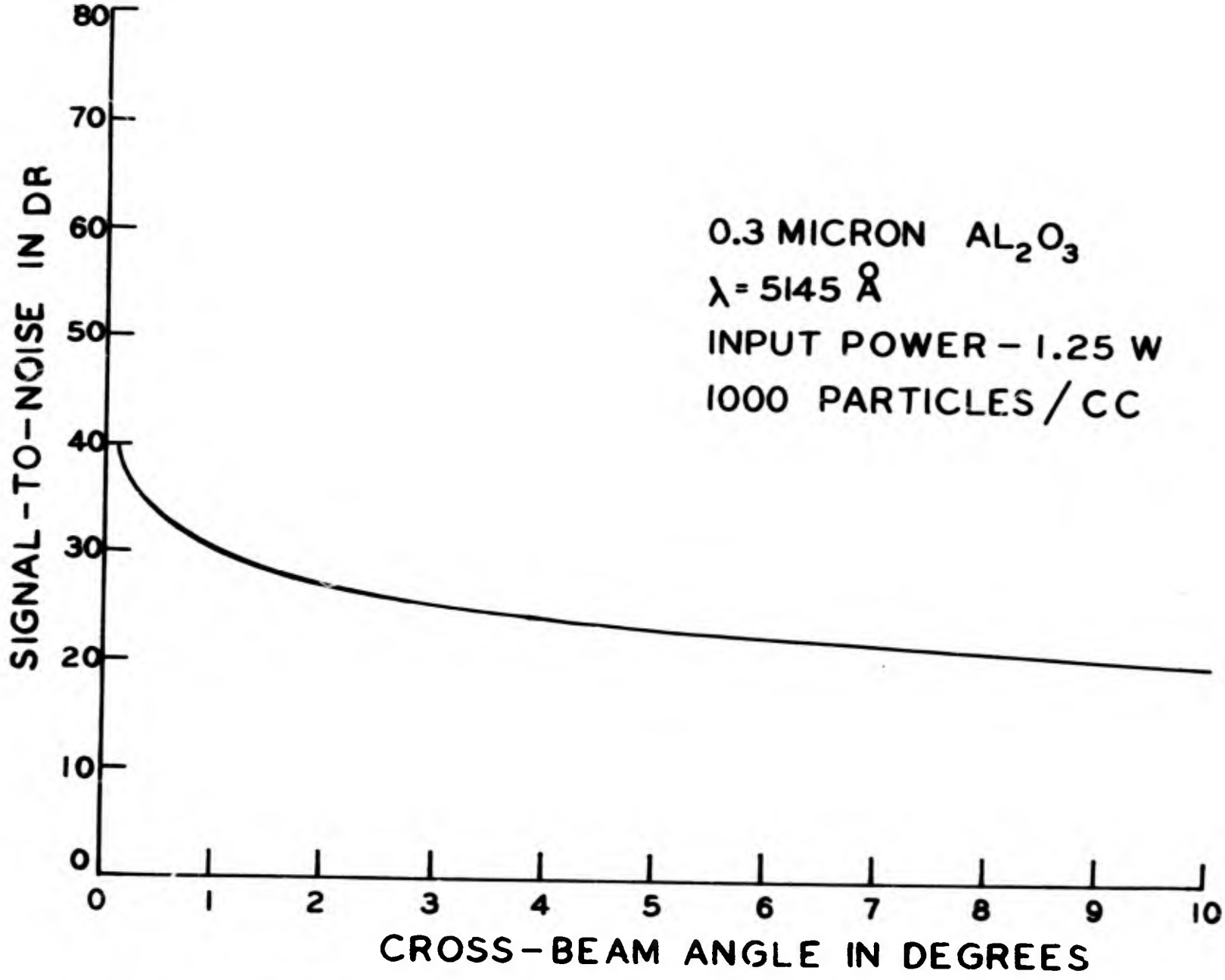

Figure 2. Time averaged signal-to-noise ratio of the LDV output signal

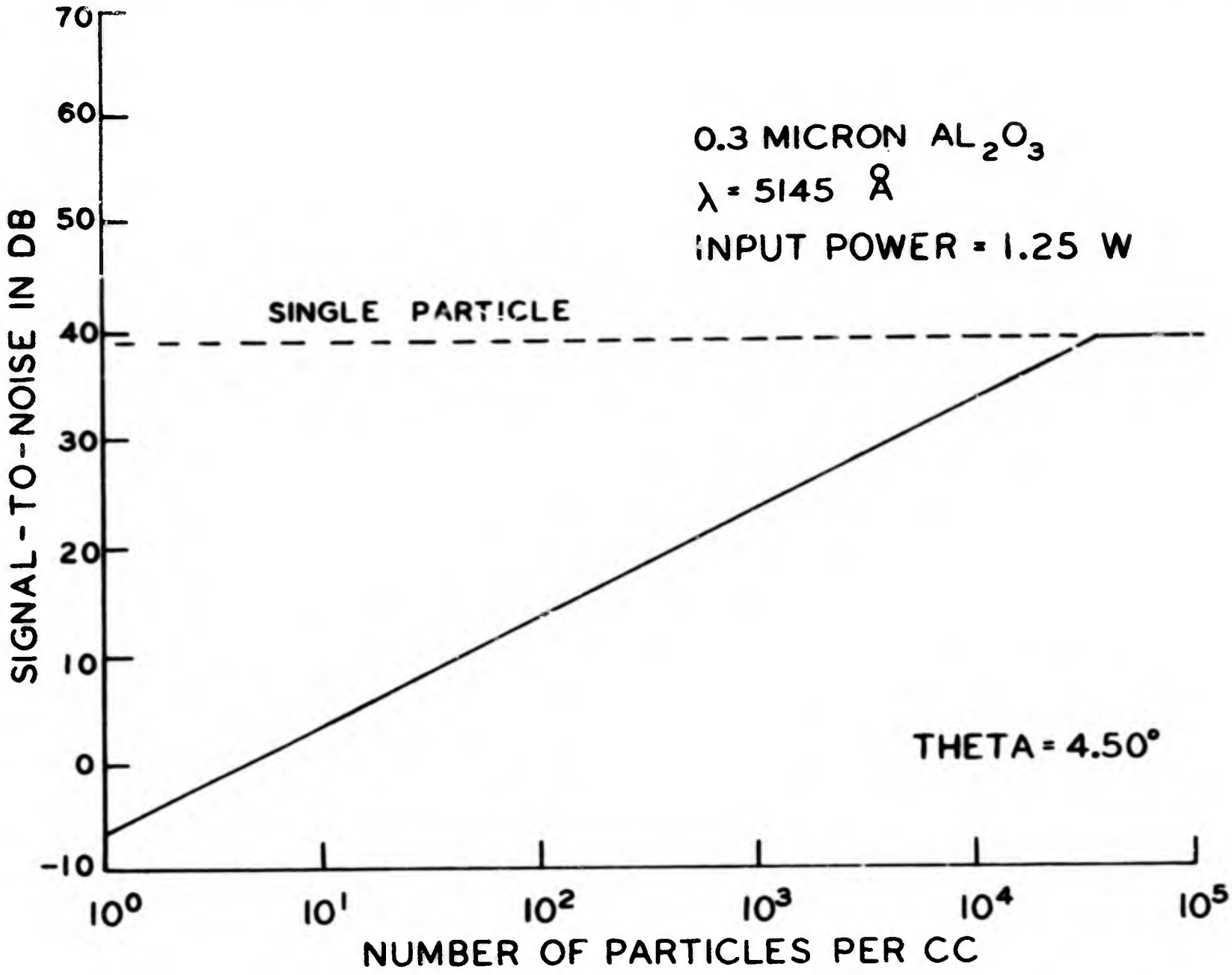

Figure 3. Time averaged signal-to-noise ratio as a function of particle density

PARTICLE MOTION

$$C_D = \frac{\bar{C}_D + \frac{51.1\,M}{Re}}{1.0 + 0.256\,M\left(\bar{C}_D + \frac{51.1\,M}{Re}\right)}$$

$$\bar{C}_D = \frac{24.0}{Re} + 0.4 + 1.6\ e^{-0.028\,Re^{0.82}}$$

$$\frac{dV_p}{dt} = \frac{3}{4}\,\frac{\mu_g Re\ C_D\ (V_g - V_p)}{D^2\ \rho_p}$$

Figure 4. Equations used for the motion of a particle in a fluctuating flow

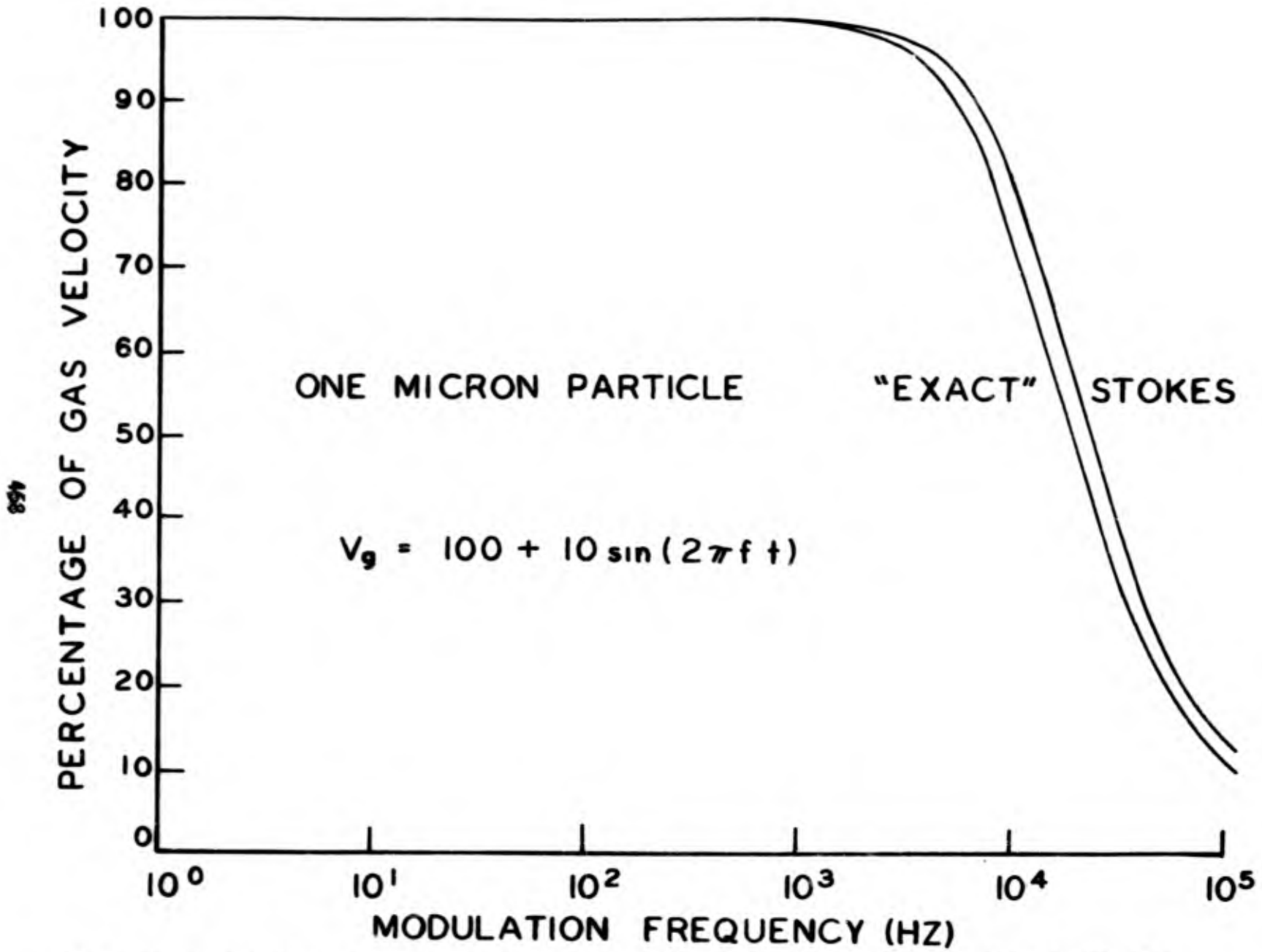

Figure 5. Amplitude response of a particle in a fluctuating flow: 1.0 micron Alumina particle

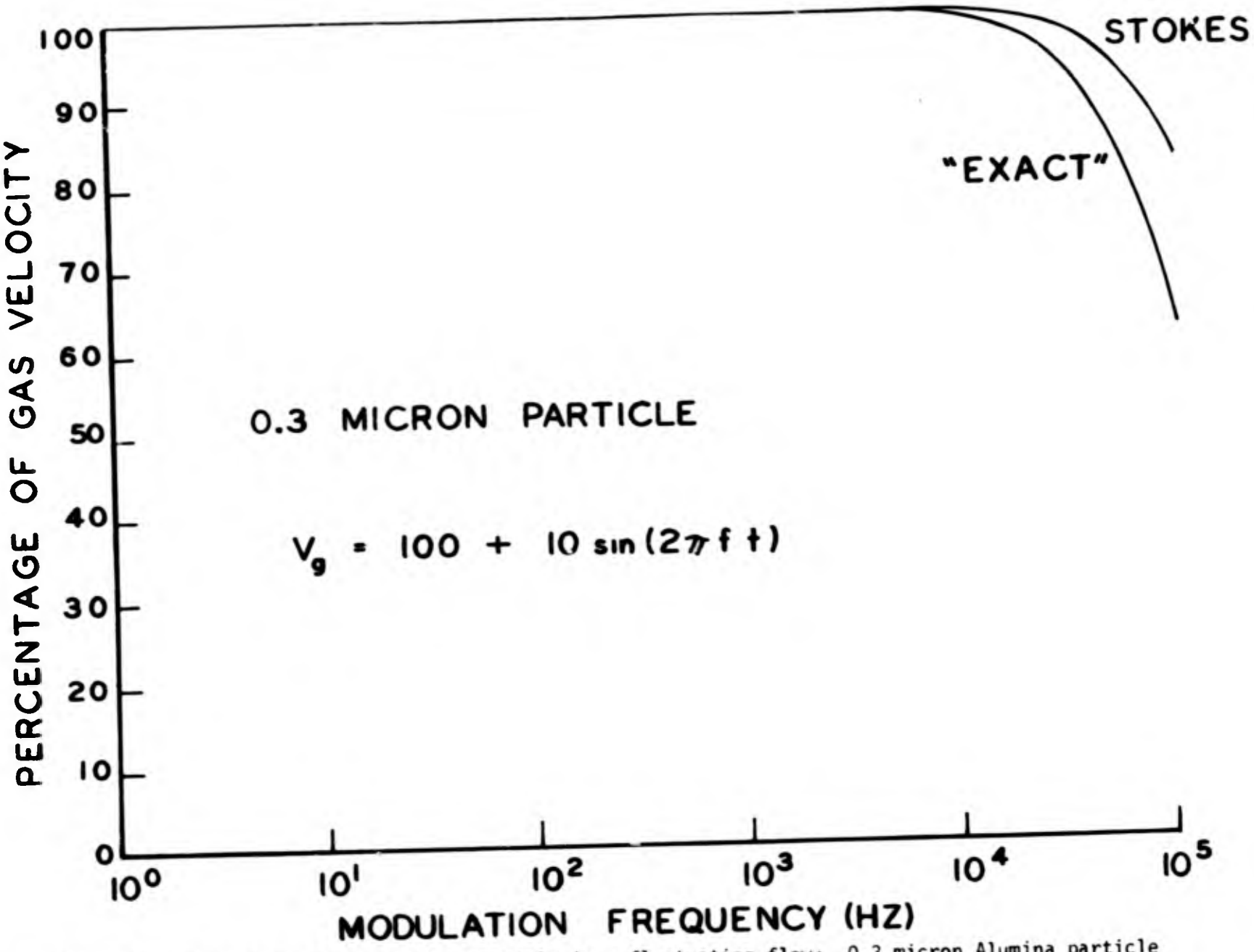

Figure 6. Amplitude response of a particle in a fluctuating flow: 0.3 micron Alumina particle

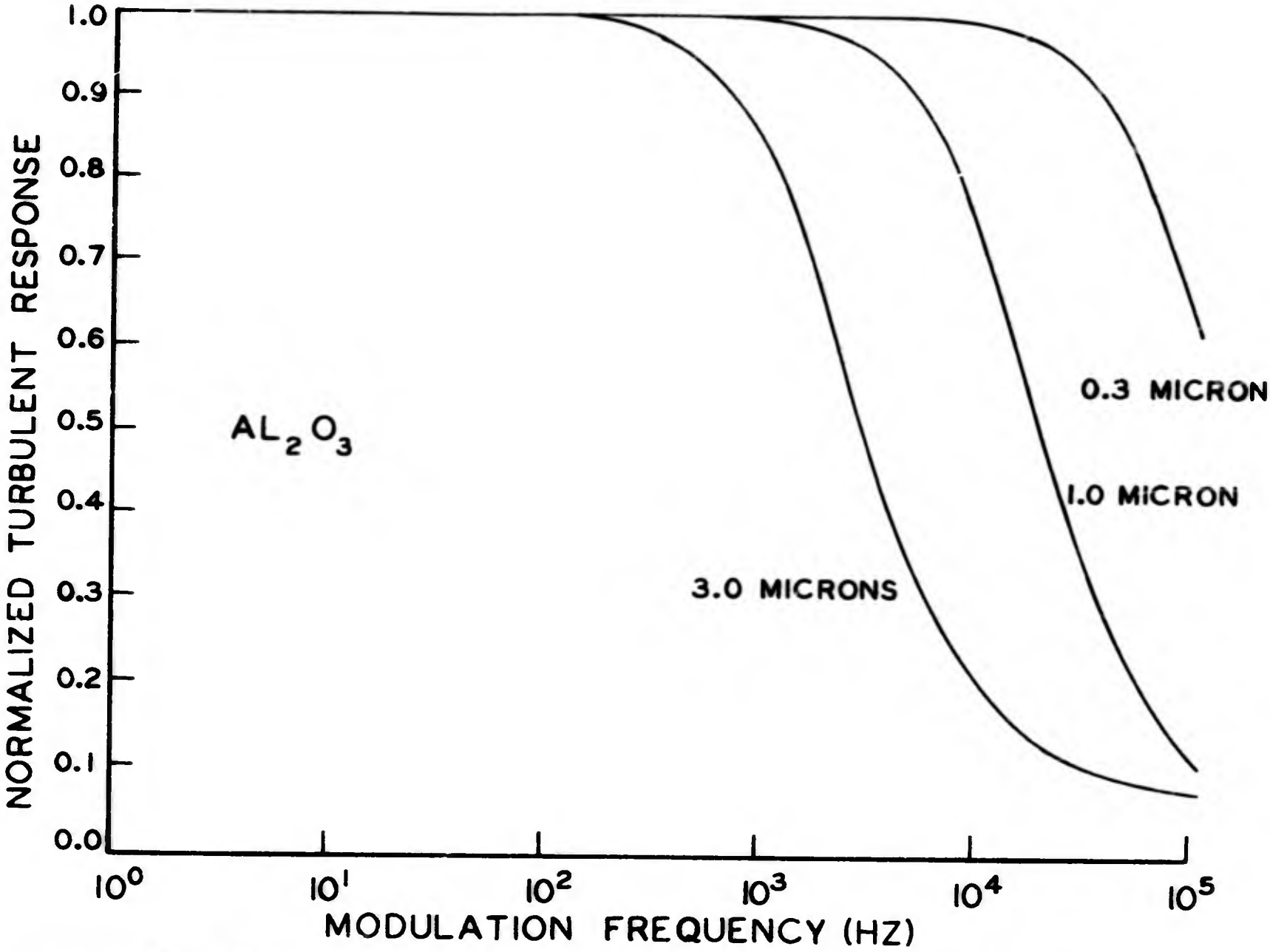

Figure 7. Amplitude response to a 10% fluctuation of flow velocity using the "exact" drag law

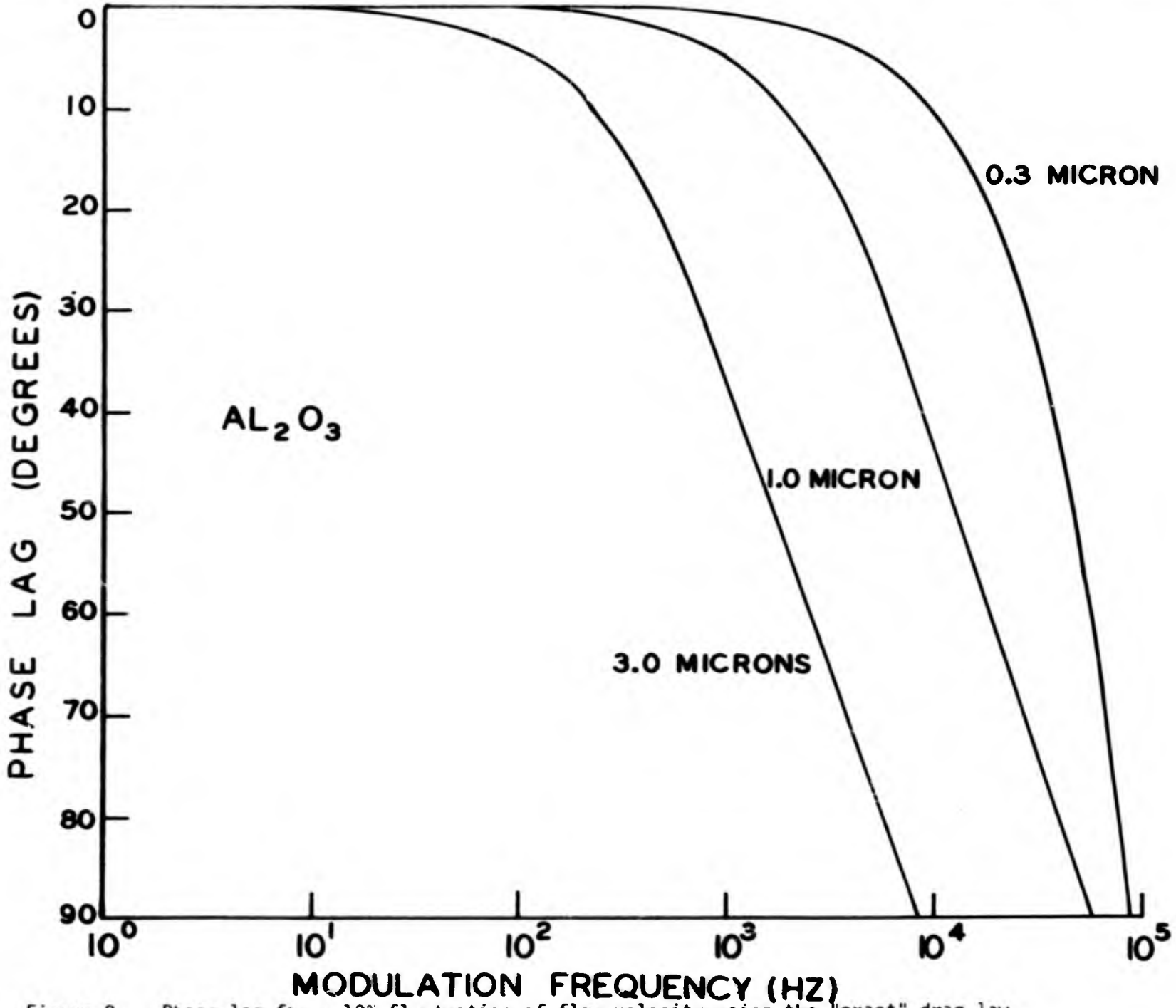

Figure 8. Phase lag for a 10% fluctuation of flow velocity using the "exact" drag law

Figure 9. LDV setup for a 2-inch subsonic free jet

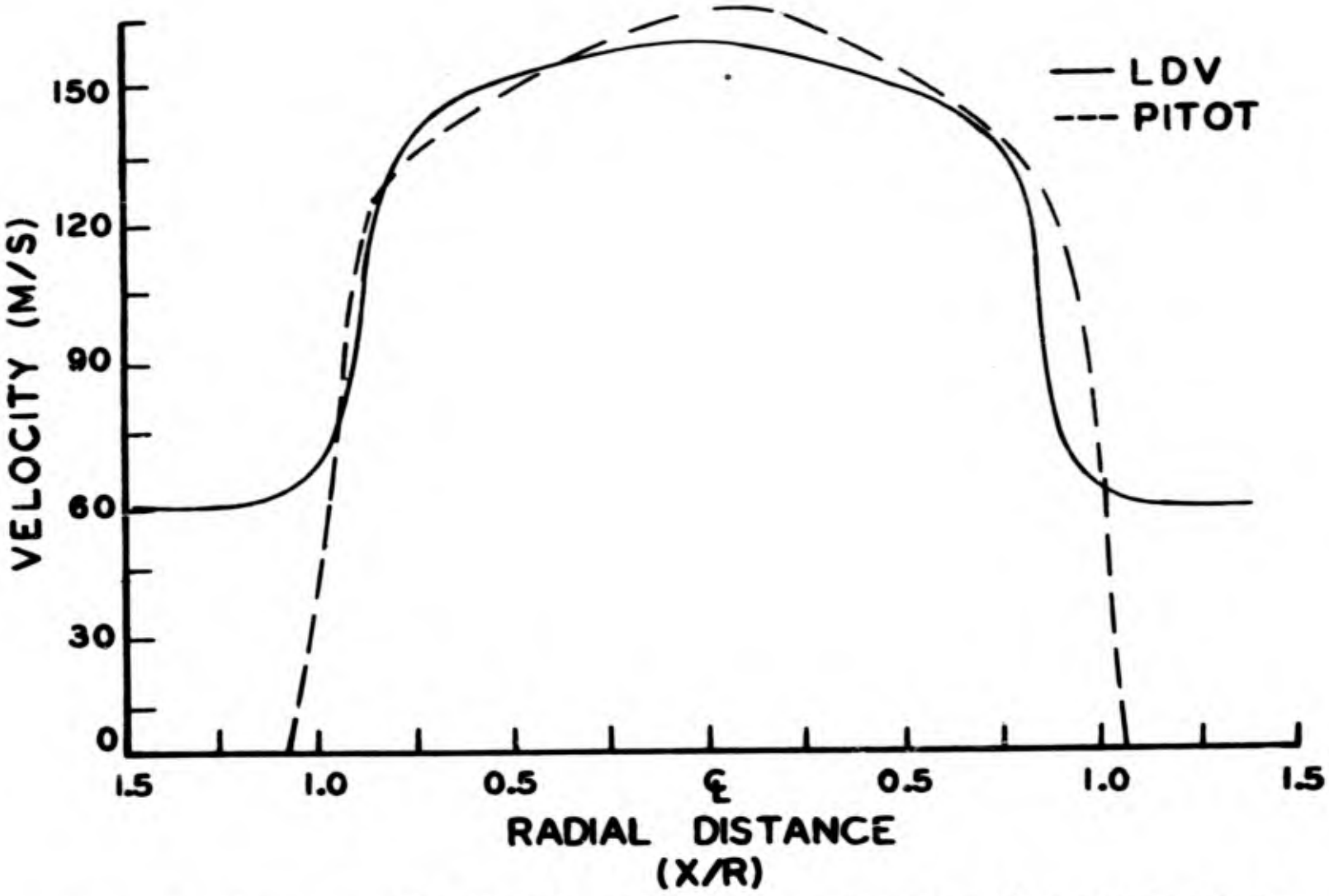

Figure 10. Comparison of LDV and Pitot velocity measurements in the 2-inch subsonic free jet

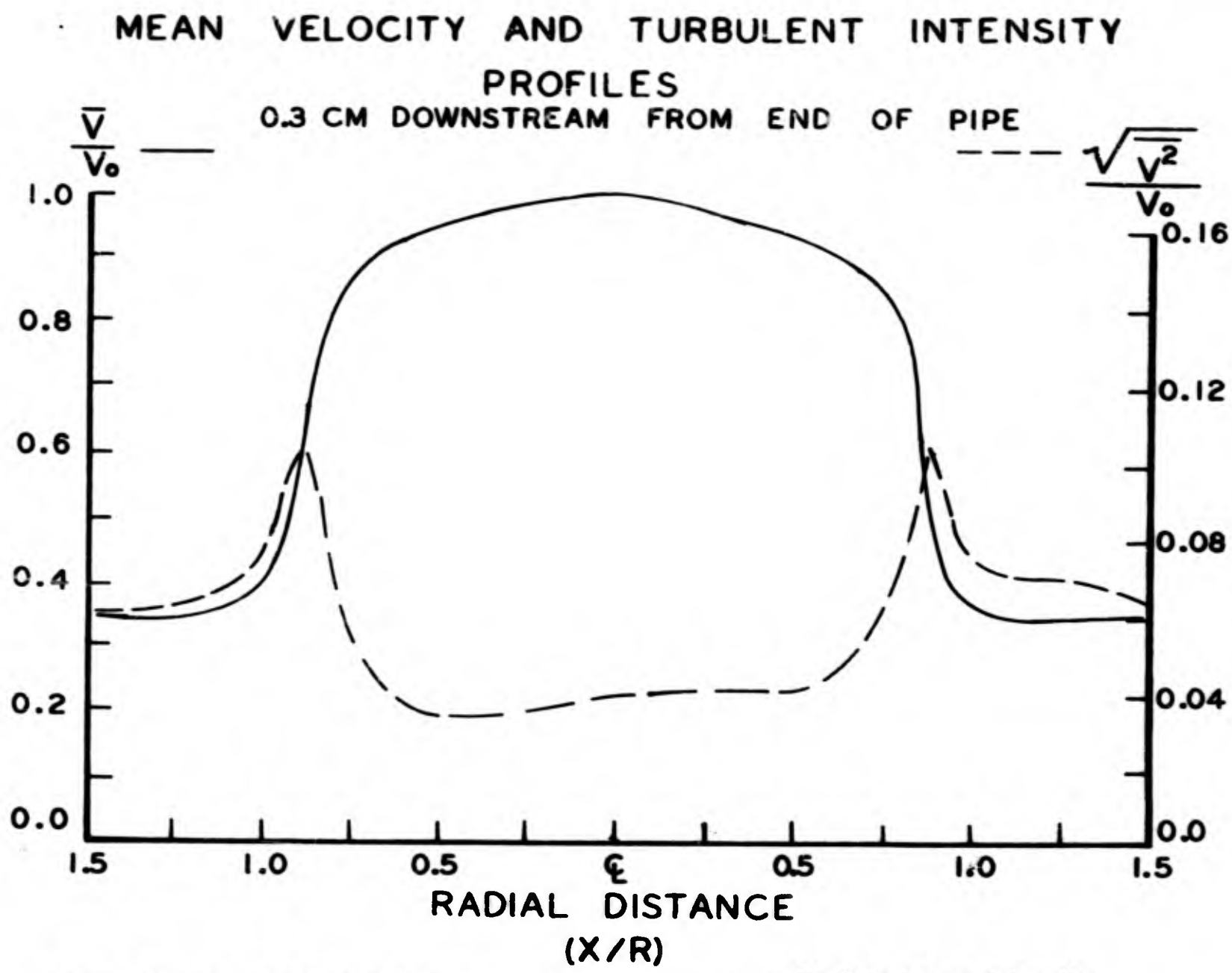

Figure 11. Mean velocity and turbulent intensity profiles at the 2-inch free jet exit

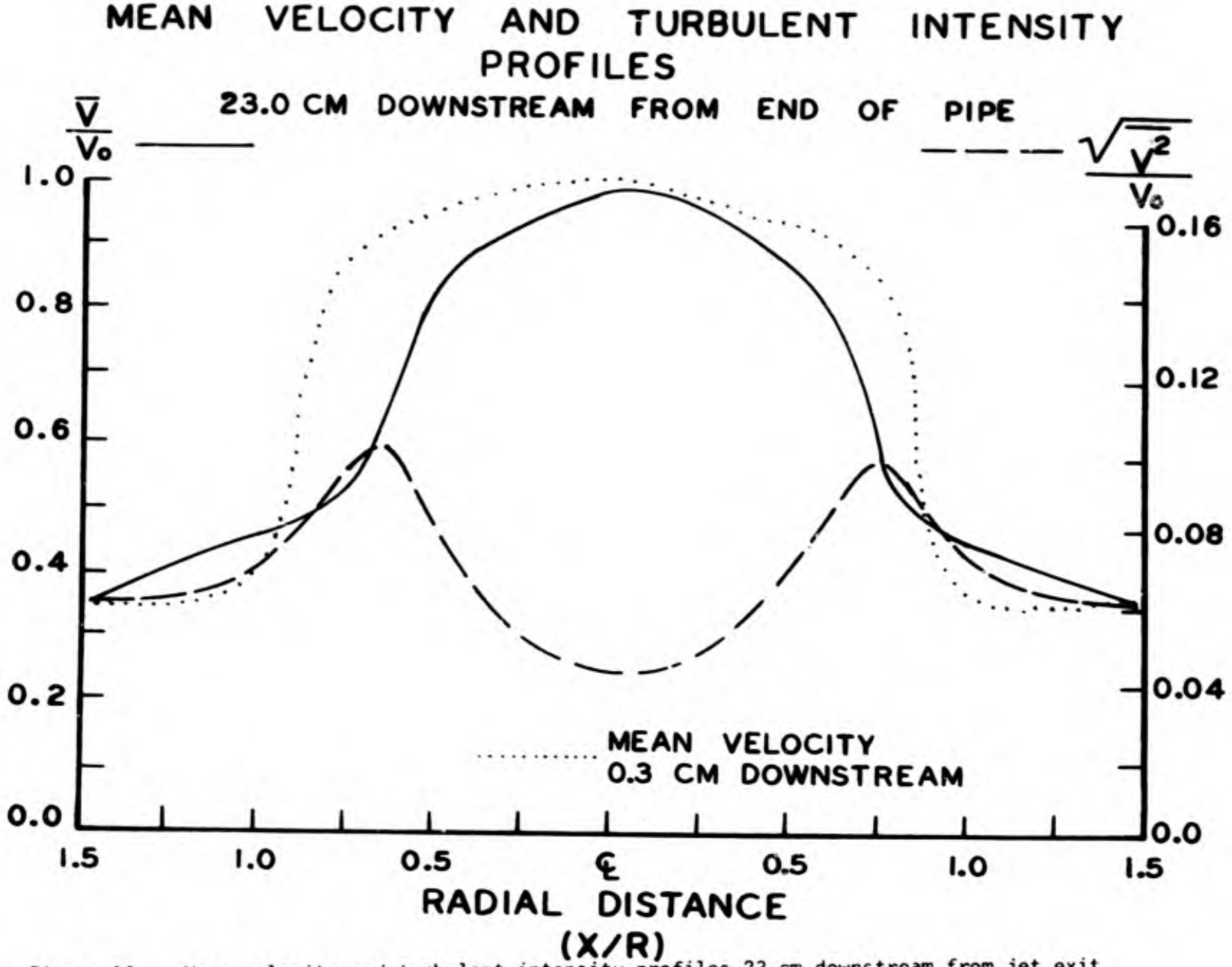

Figure 12. Mean velocity and turbulent intensity profiles 23-cm downstream from jet exit

DISCUSSION

GOLDSCHMIDT: I would like to go to your curve of particle velocity lag versus frequency. There are two fallacies in what you presented to us: First of all, the assumption that the equations are as simple as presented. I think Lumley alerted us to the necessity of carrying most of the terms of the equation of motion for the particles. To be more specific, there is a coupling term and a nonlinear term which you don't have. Soo and some of his co-workers have also stressed the need of some of these terms even in the range of size particles that you have. One of our students attacked numerically the equations for a particle. An interesting result is the fact that you might get an increase of velocity at certain frequencies due to the nonlinear coupling phenomena.

The second fallacy is the assumption that we can take a look at the sinusoidal component as being a representative of what we would have if we added these to get a turbulent flow. The fact is the problem is nonlinear and we cannot add these components individually. So your dream to build on an amplifier that compensates will fail.

GEORGE: That's all right, your spectrum will still be flat to 100 kHz because of the ambiguity.

MEYERS: The corrections that we used are supposedly pretty good. The nonlinear terms are taken into account so we can go down to the free molecular limit where we have very long mean free paths of the molecules all the way up to a continuum flow. I have to beg off on this question because I did not do the work on this. I am just presenting it, so I am not able to argue with you.

ORLOFF: What is the trend in the rolloff characteristics for velocity below and above that calculated? It looked like you have about a hundred meters per second.

MEYERS: A hundred meters per second, yes.

ORLOFF: What is the trend above and below that?

MEYERS: As long as you're subsonic, I have confidence in these. If you go supersonic, I don't know yet. When you go supersonic your densities and temperatures change. This is based on one atmosphere pressure. It's only under one specific set of tunnel conditions that these hold. For another tunnel condition you just throw in the program again and out pops your answer.

ORLOFF: What I meant was if you were to lower your mean velocity but keep the same percentage of turbulence, what increase would you get in your turbulence response?

MEYERS: No. I have some velocity versus time plots which show that the mean velocity, even for very large particles, comes up very quickly. If you start with a gas at normal conditions and inject a particle at rest it comes up very quickly. Then you have your lag behind your sinusoid. It doesn't matter how far it has to go to reach the main velocity. It will get there. The trick is that your distance from injection to equalization will change depending upon how high the velocity is.

GOLDSCHMIDT: These are still based on the equation you showed us on the board - an inertial force is equal to this corrected drag force only. Correct?

MEYERS: Yes.

GOLDSCHMIDT: That's the equation which I claim is incomplete. F = ma, but there are more forces.

AUTHOR'S AFTERWORD

Dr. Goldschmidt is of course correct that the equation of motion for a single particle is given here is incomplete. However, for the case of interest to us, of particles in air, the density of the particle is very much greater than the density of the fluid, and as shown by Hinze (Turbulence, 1959, pp 352-364), the additional terms involving acceleration of the air may be neglected to good approximation.

In re-examining the question of the frequency response required in order that particles will follow turbulent fluctuations, we realized that we had been wrong in assuming that the frequency response required of the particles could be estimated from the frequencies measured with hot wires. The considerations which led us to this conclusion, while not new, may not be generally appreciated in connection with the LDV seeding problem, so we would like to call attention to them.

A hot-wire probe is fixed with respect to a tunnel or surface, and samples the fluctuations that are convected past it at some mean velocity. The frequency that the wire must follow to describe the turbulence depends on the wave number (reciprocal of distance between fluctuations) and on the mean velocity. For the small scale turbulence in a hypersonic boundary layer, this frequency becomes very large, on the order of 10^5 Hz.

The response required of our seeding particles is altogether different. The particles, injected into the flow somewhere well upstream of the sample volume, can be considered to be nearly embedded in the local flow. Each particle must respond to changes in the velocity of the local air volume in which it is embedded, as this volume becomes entrained in a growing eddy or leaves a decaying one. The appropriate index for the particle response is the ratio of a

relaxation distance or time, over which the particle reaches some fraction of an impulsive gas velocity change, to the length or time scale of the turbulence. Frequency, in this (Lagrangian) frame of reference is difficult to assess, but is certainly not the same as the Eulerian frequency sensed by the hot-wire. Our opinion, subject to further study, is that the frequency range involved in a hypersonic turbulent boundary layer may not be very much different from that in a low speed one in the Lagrangian frame of reference, perhaps on the order of 10^3-10^4 Hz, compared to the 10^5 Hz estimated from hot-wire data.

The readout system of the LDV, however, is sampling the velocity information from a succession of particles convected through the sample volume. The LDV must therefore have the same frequency response as the hot-wire system, to describe the same flow equally well.

Laser Doppler Program for Velocity Turbulence Measurement

M. Huffaker
Marshall Space Flight Center

I'd like to review our programs at the Marshall Space Flight Center for the development of Laser Doppler systems. We have two main programs outlined in Figure 1: One is for trailing vortex measurements and in connection with airport warning systems and the other is the development of a clear air turbulence on board measuring and warning system for airplanes. In the trailing vortex program, there are field tests for the measurement of wind velocity and turbulence. These consist of a number of things. One is to compare the Laser Doppler system with standard weather instruments and anemometers such as cup anemometers. The measurement program also involves evaluating components, optics, detectors, optics configurations, efficiency of systems, range resolutions, and overall performance of Laser Doppler systems in the atmosphere. These measurements have been going on for about 3½ years, and quite a lot of data are available.

Also, in the trailing vortex program is the development of a three-dimensional low altitude research system for the measurement of the detailed properties of trailing vortices. The structure of the airplane trailing vortex is not known. The decayed properties are not known and a detailed velocity structure of the vortex is needed for an adequate understanding of the decay rate, the strength of the vortex, and effect of the atmosphere on those parameters. The first phase of this study is near completion.

We have another program that started in 1963 and has continued recently at a smaller level of effort. We have a three-dimensional argon system. It is a reference beam system which has been used for three-dimensional velocity measurements in jets and in wind tunnel type flows. We have with this system three trackers that were developed over the past several years to follow the flow up to frequencies of around 200 megacycles with deviation rates of up to 100 KC over ranges in frequency of plus or minus 30 or 40 megacycles. These have been used in jets and compared with hot wire data and these agree quite well. One of our programs going on now is to do a very detailed and precise measurement of the three-dimensional turbulent properties in a pipe flow. We selected the pipe because this was considered one of the more well known turbulent flows. We wanted to do one experiment as well as could be done and to account for all of the errors in the measurement.

The other part of the trailing vortex program is to determine whether a Doppler System like this can work in the airport environment and be used as an airport warning system for trailing vortices and for wind shears in the airport area. Can such a Doppler system work? What are its range limitations? What are its safety problems? What are the configurations? What are the requirements for a system to work in the airport area? What constitutes a warning system? These studies are near completion.

Our other major program is the development of a clear air turbulence detection system. The clear air turbulence detection system was started around 1967 and the hardware has been built. It's scheduled for flight testing on the Ames Convair 990 in June of this year.

I would like to briefly review some of the particular results of these programs and to show you some of the equipment and examples of the data that have been taken on our systems. Figure 2 is our three-dimensional system that is used to measure velocity and turbulence in our wind tunnels. The angles are adjustable, and we can move them out quite wide. This was done about six years ago, so it is not necessarily optimized in terms of overall signal to noise. But we do get adequate signal to noise of 30 to 40 db with added tracers in the flow. We get about 15 db from the natural contaminates in the air. Its main application is for turbulent types of flows. For that we feel that we have to add a sufficient number of particles to give us a continuous sample.

Figure 3 is an example of one component of the data that can be taken in a wind tunnel with the three-dimensional system. Hundreds of data points were taken around a wing tip that was placed in a 7 inch wind tunnel. The three-dimensional velocity field was measured at various downstream locations. This was done with good spacial resolution across, as you can see. This is an example of the kinds of mean velocity data that you can get. The three-dimensional system has a Bragg cell incorporated into it so that we can resolve the vector ambiguity.

We are currently using an LDV configuration for the three-dimensional pipe flow tests, using larger scattering angles. These results should be available in about two months. Everything looks good so far.

One of the tests that we wanted to do is to compare with standard anemometers to determine whether the Doppler system really compared with the cup anemometer or other types of sensors. We have done this at Huntsville and also at Fort Collins, Colorado. Figure 4 illustrates the test arrangement. One of the reasons for going to Colorado was the very low particle levels that we could get, and we wanted the particle concentration levels to be one of the variables in

the evaluation. We also want to evaluate this for operation in high winds, rain, snow, and fog, that is, under all types of weather conditions. We have made measurements to two miles with the system with very little difficulty. Signal to noise is a thousand to ten thousand to one from a single particle. The comparison tests were done at altitudes near the towers which were at a distance of 80 to 100 feet.

Figure 5 is a comparison of the turbulence spectra, as taken with the cup anemometer (the bottom trace) and the Laser Doppler systems (the top trace). We see a remarkable agreement between the two and I hear some comments that this is Doppler ambiguity, but I don't think so. When we also make hot wire measurements, the hot wire follows the top trace identically. It's a beautiful comparison when the hot wire data are sketched on top of that. (Question: What was your highest frequency?) Answer: One cycle. (Comment: That is not Doppler ambiguity). It is also in the data processing. It is a fold-back problem. But the velocity time history that you get from the cup anemometer, and the time history as taken with the Laser Doppler system, agree identically. You can even see the higher response in the Doppler system versus the poor time response if you look at the short time comparison.

We want to go to three-dimensional systems. We also want to show three-dimensional comparisons with three-dimensional standard wind anemometers. We have just completed these measurements with the three-dimensional Laser Doppler system and with a three-dimensional propellor type of sensor. Figure 6 illustrates the three-dimensional test site configuration. Comparing the u, v, and w velocity components from the Laser Doppler with u, v, and w components from the propeller type anemometers, the agreement is quite good (see Figure 7).

Figure 8 is an artist's concept of a three-dimensional Laser Doppler scanning system. This system has applications other than for trailing vortex research. It would be a general atmospheric meteorological research tool.

On our clear air turbulence program, we will see the Ames Convair 990. The Convair 990 will have a pod attached to the side of the aircraft and will contain a 14" germanium window (see Figure 9). It is a pulsed system. The pulse length is variable and is 2, 4, 8, or 10 microseconds. The power is 5 to 10 kilowatts peak power. Using 12 inch optics, you can look into the beam and you won't feel it. The energy in the beam is approximately .01 watt/cm^2. It is completely safe.

Figure 10 is a picture of the hardware. It uses a very stable CO_2 laser for stability, with very narrow line width. The low power laser goes into a modulator which gives the selected pulse length. The signals then go into the power amplifier and this gains the signal up to the required power level of 5 to 10 kilowatts. Then it goes into the telescope and the signals come back and are mixed with the local oscillator. The system is going through a ground check-out at the contractor's plant now. It is scheduled for flight testing in August of this year.

To show that the Doppler system can measure and detect vortices was a problem that became increasingly important several years ago due to the advent of large jumbo jets. We wanted to show that Doppler systems can measure and detect trailing vortices to demonstrate the capability of Laser Doppler systems.

This vortex measuring program was done about 2½ years ago. Figure 1 shows what the wind signal looks like on a spectrum analyzer. The spectrum analyzer is an unacceptable means of data processing. It is a very inefficient means of data processing but does give the experimenter a quick look capability for visualizing the flow velocity. The scale is approximately 1.5 megacycles across which represents 26 feet per sec. and this shows just the normal wind velocity as it is coming through the sensitive volume. The spectrum is swept at about a millisecond rate. As the vortex comes through, you see the edge of the vortex and the velocity distribution changes. Then as the vortex drifts across, the velocity distribution increases and then decreases. By these measurements, it was much higher than we had expected. We did not expect velocities greater than about 25 feet per second. It was up around 35 feet per second in that particular vortex. After the vortex goes through, the Laser Doppler system measures the normal wind velocity.

If there is time, there is a three minute movie to show you what Doppler signals look like in the atmosphere and for a vortex type flow.

Comments during the movie: That was one of a few shots that I have seen showing the actual vortex breakdown. You could see the details of the inner flow structure which is quite fascinating.

There are about two shots here of some vortices. Again this is from a DC 3. The velocities you can get from 747 or 727, are in the order of 180 miles per hour center peak speed. You can see that they are concerned about this effect in an airplane like the DC9 or 737. It was surprising to us that a DC 3 could generate such a vortex.

One of the vortex problems is that you are unable to predict the lingering time over an airport area. Sometimes they have been known to stay a long time over a runway and this all depends upon the atmospheric conditions. This is from a little DC 3.

We are looking about ten feet upwind of the smoke and about ten feet closer to the airplane flight path to make sure that there is no contaminate in the area where we are looking. We only use the smoke to show the correlation between detection with the Laser Doppler system and then a few seconds later the smoke visualization.

Now you see the velocity beginning to change as the second vortex comes through, and then the velocity distribution goes completely off scale. Again, we are 20 to 30 db down in processing with this way of visualizing.

This is a run without any smoke, but just looking at the same position; we had the plane then fly by just to give a comparative measurement. That is the vortex as it is passing. Again the second vortex goes through and it just goes completely off scale. We should have set our scale higher. Then we have just the normal wind and turbulence.

I. TRAILING VORTEX MEASURING AND AIRPORT WARNING SYSTEMS.

1. FIELD TESTS OF WIND VELOCITY AND TURBULENCE

   A comparison with standard weather instruments and anemometers will be made.

2. DEVELOPMENT OF 3-D LOW ALTITUDE RESEARCH SYSTEM

   For measuring trailing vortices behind aircraft (also wind and turbulence profiles, etc.)

3. WIND TUNNEL VORTEX MEASUREMENTS

   Small, in-house effort, using available system.

4. CONCEPTUAL DESIGN STUDY OF AN AIRPORT WARNING SYSTEM

   Phase A - type study of an airport trailing vortex warning system.

II. DEVELOPMENT OF A CAT ON - BOARD MEASURING SYSTEM.

CAT RESEARCH INSTRUMENT DEVELOPMENT

A RESEARCH SYSTEM WILL BE FLIGHT TESTED TO PROVE THE FEASIBILITY OF DEVELOPING AN OPERATIONAL SYSTEM

Figure 1. Marshall Space Flight Center LDV Programs

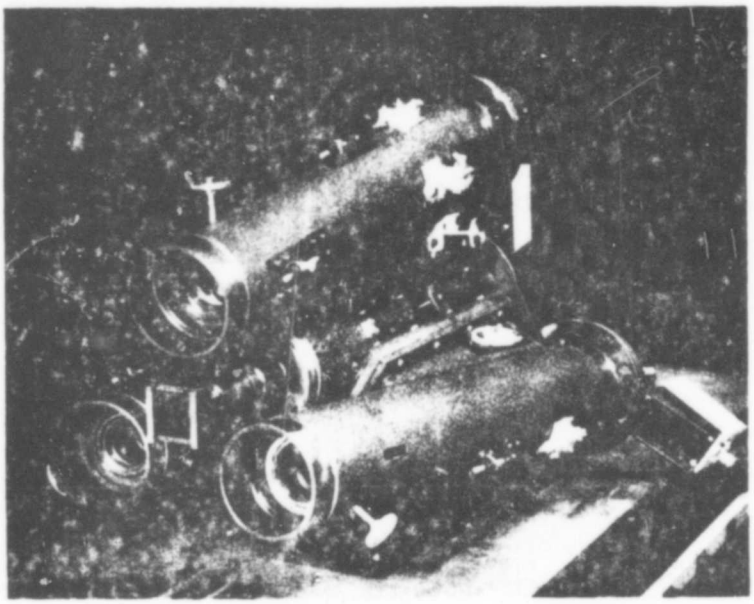

3-DIMENSIONAL VELOCITY INSTRUMENT

Fig. 2

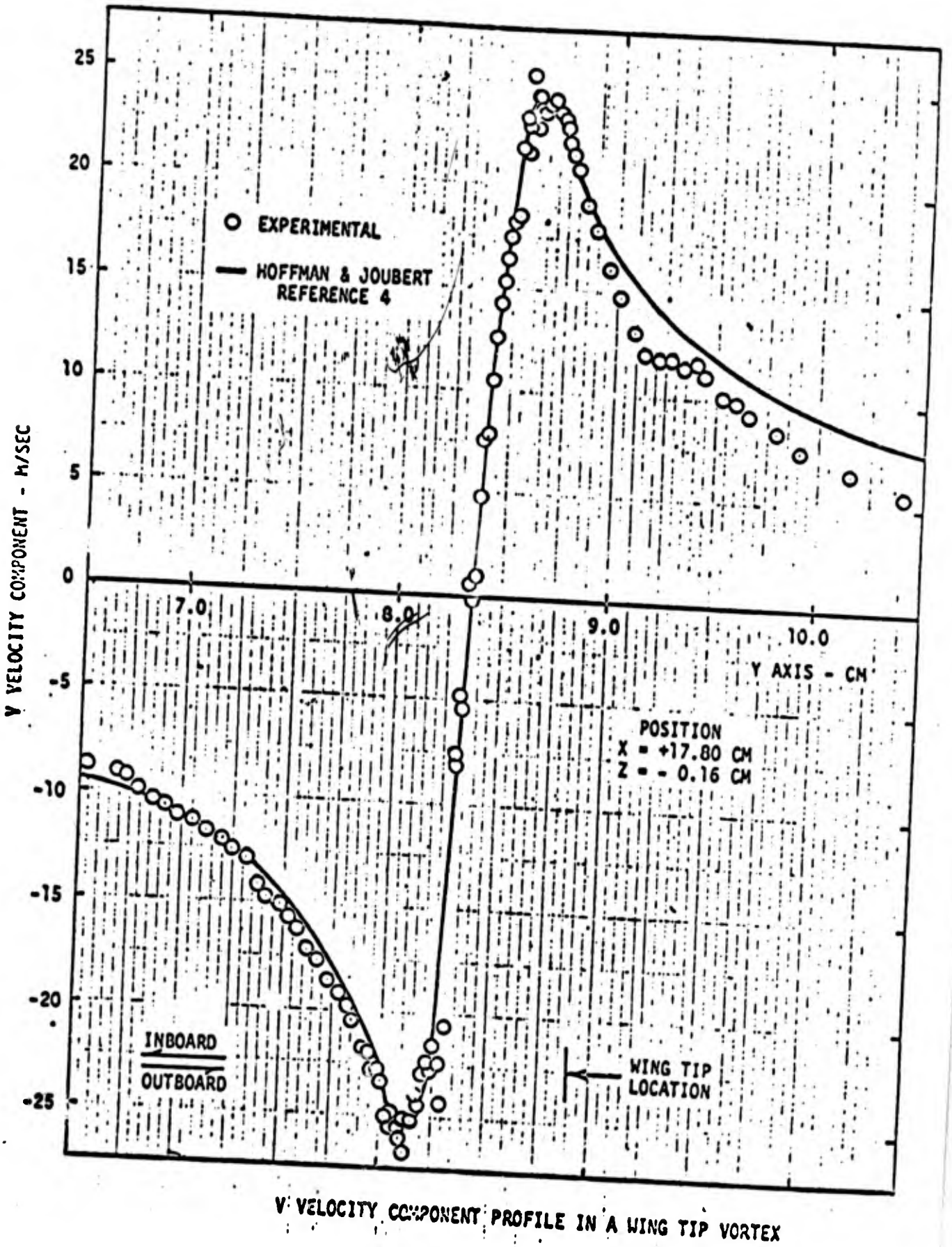

V VELOCITY COMPONENT PROFILE IN A WING TIP VORTEX

Fig. 3

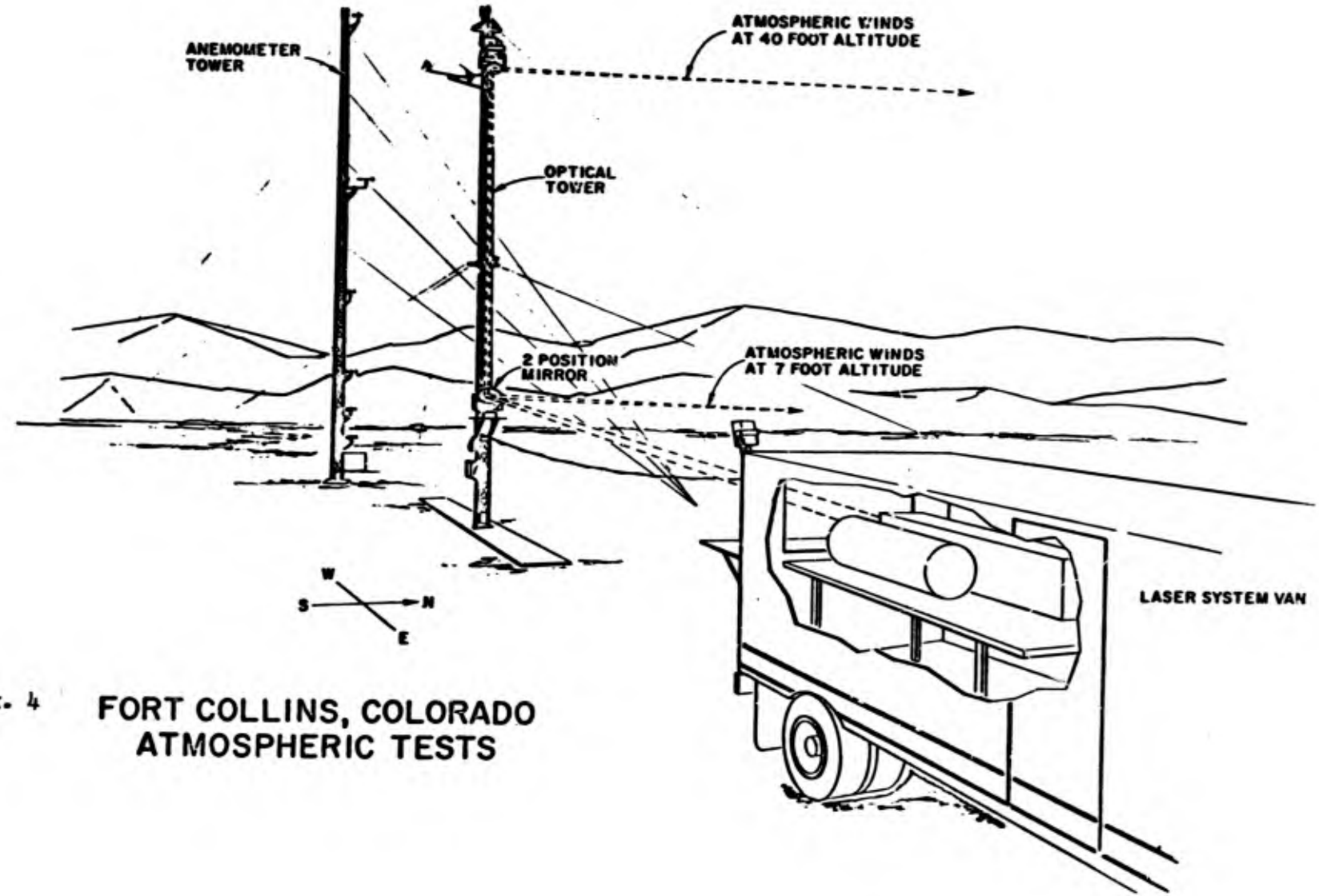

Fig. 4 FORT COLLINS, COLORADO ATMOSPHERIC TESTS

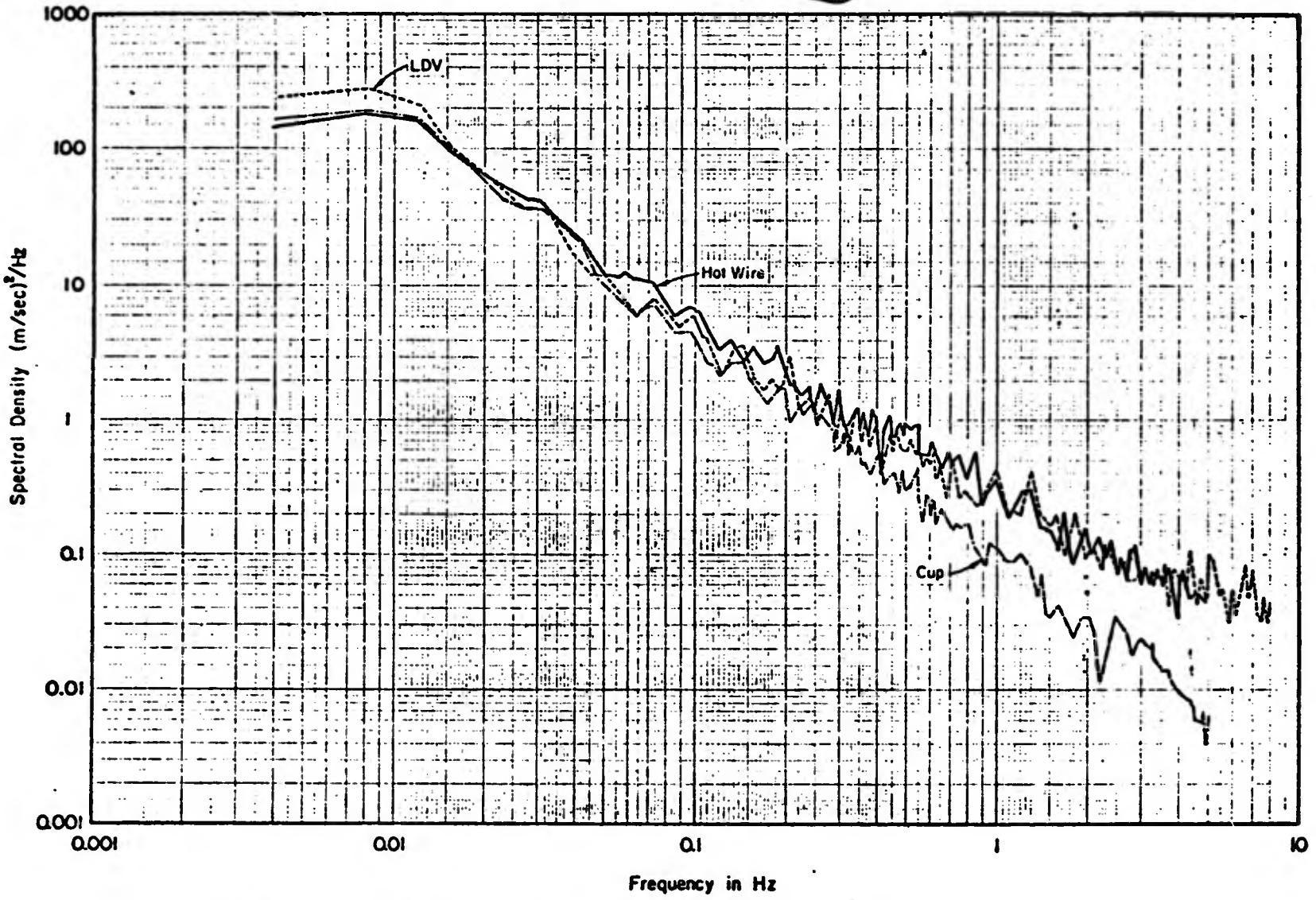

Fig. 5 Comparison of spectral density distributions for Test 32701.

3D TEST SITE CONFIGURATION

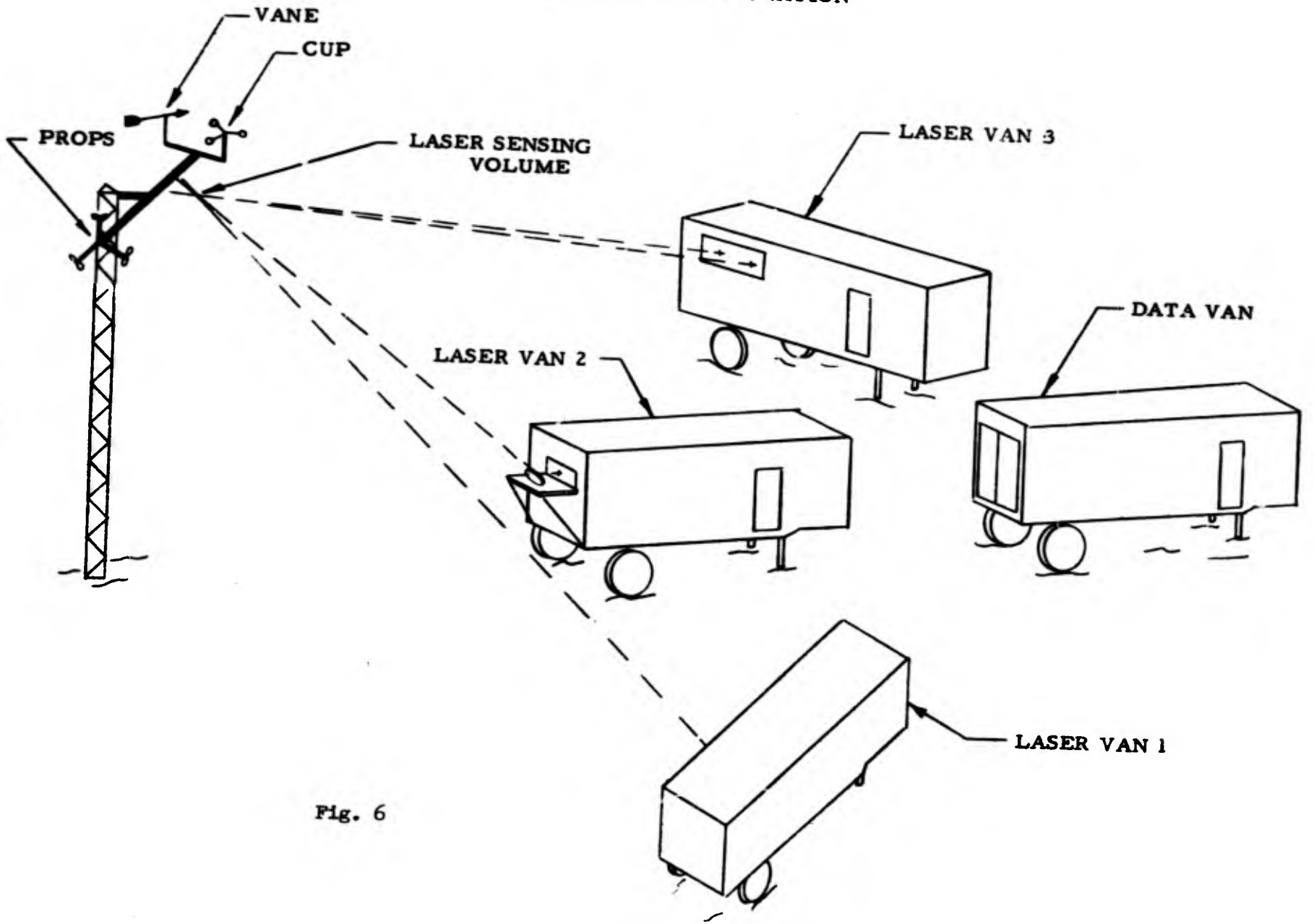

Fig. 6

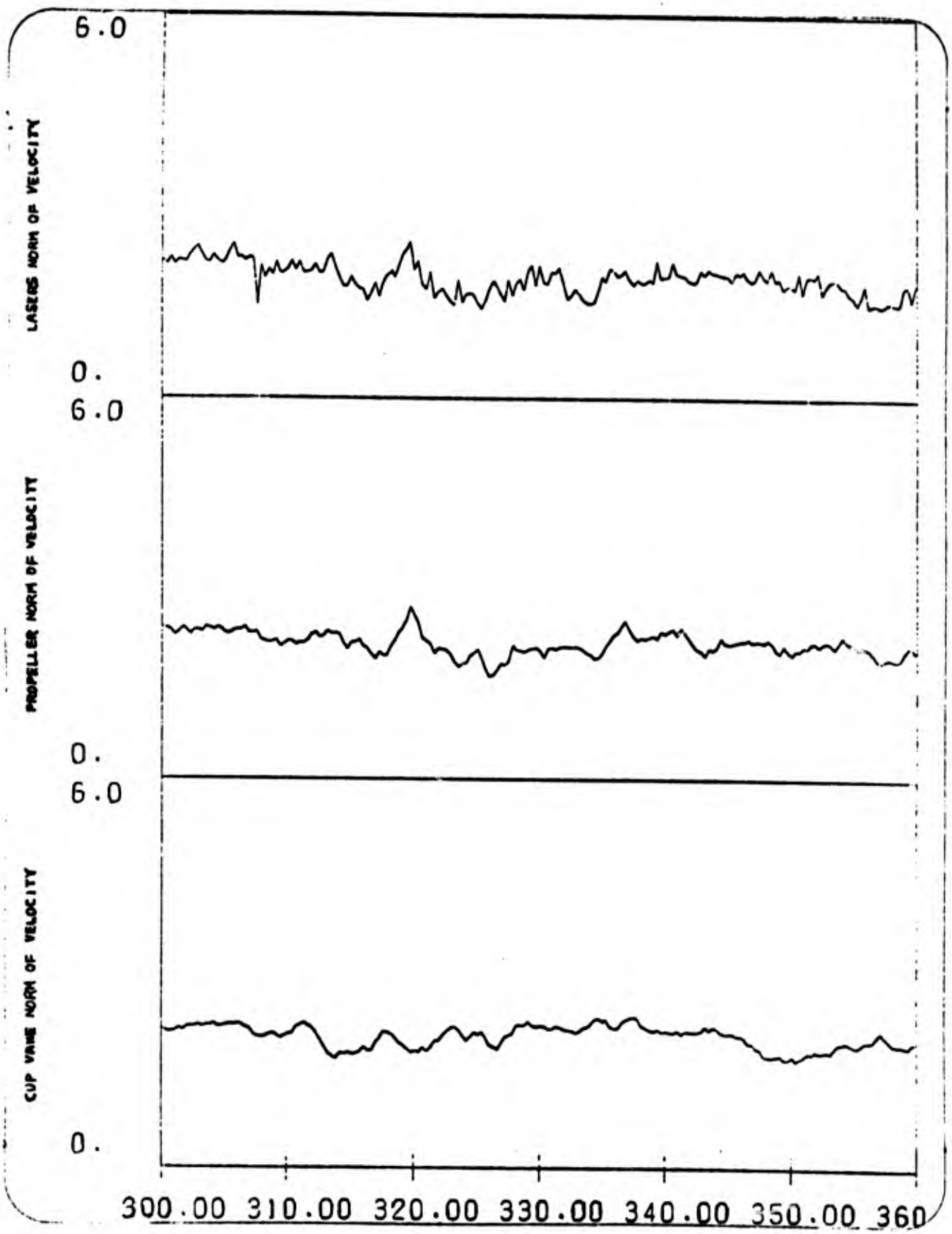
6.0
LASERS NORM OF VELOCITY
0.
6.0
PROPELLER NORM OF VELOCITY
0.
6.0
CUP VANE NORM OF VELOCITY
0.
300.00 310.00 320.00 330.00 340.00 350.00 360

Fig. 7

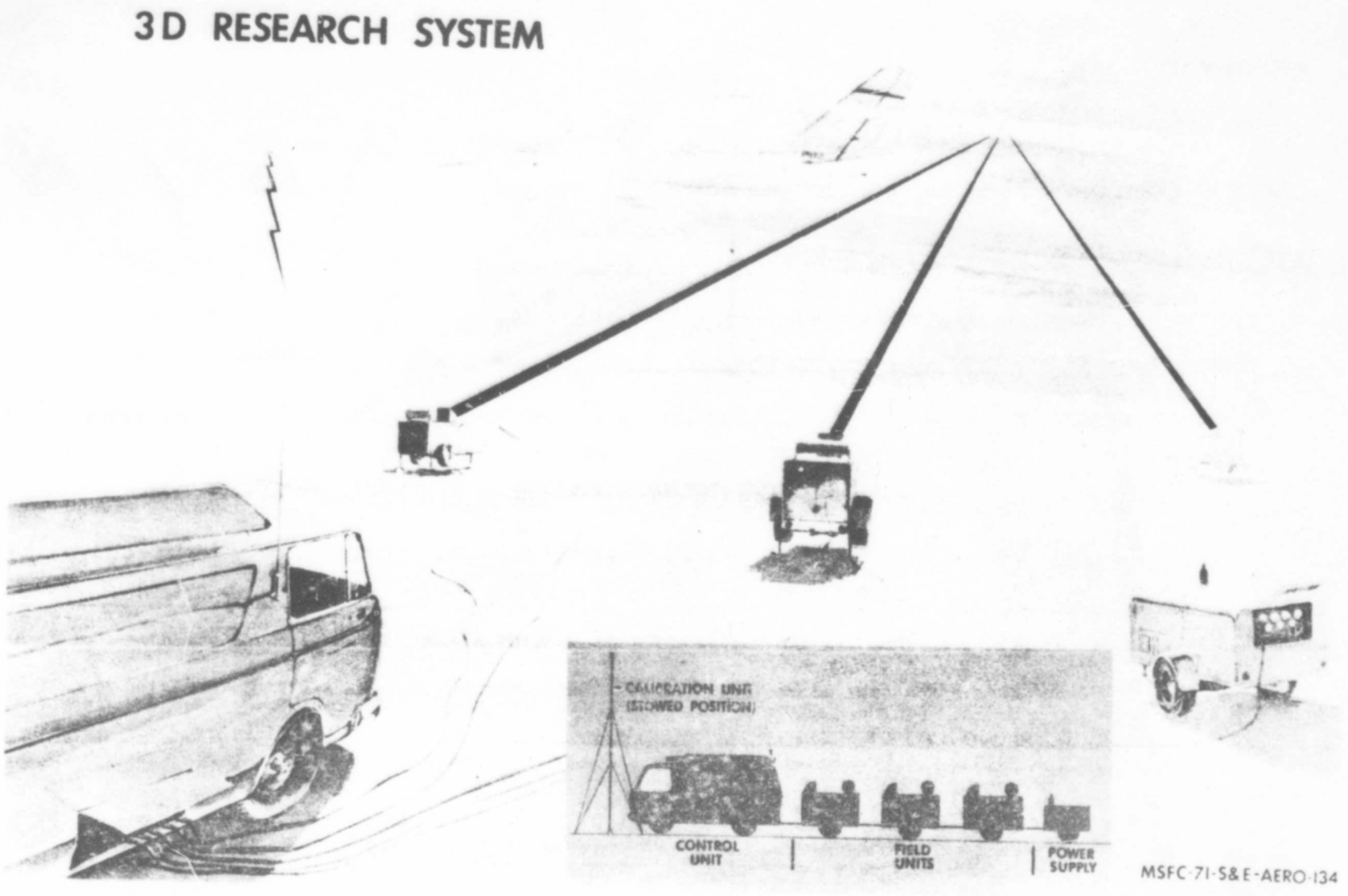
3D RESEARCH SYSTEM
CALIBRATION UNIT (STOWED POSITION)
CONTROL UNIT
FIELD UNITS
POWER SUPPLY
MSFC-71-S&E-AERO-134

Fig. 8

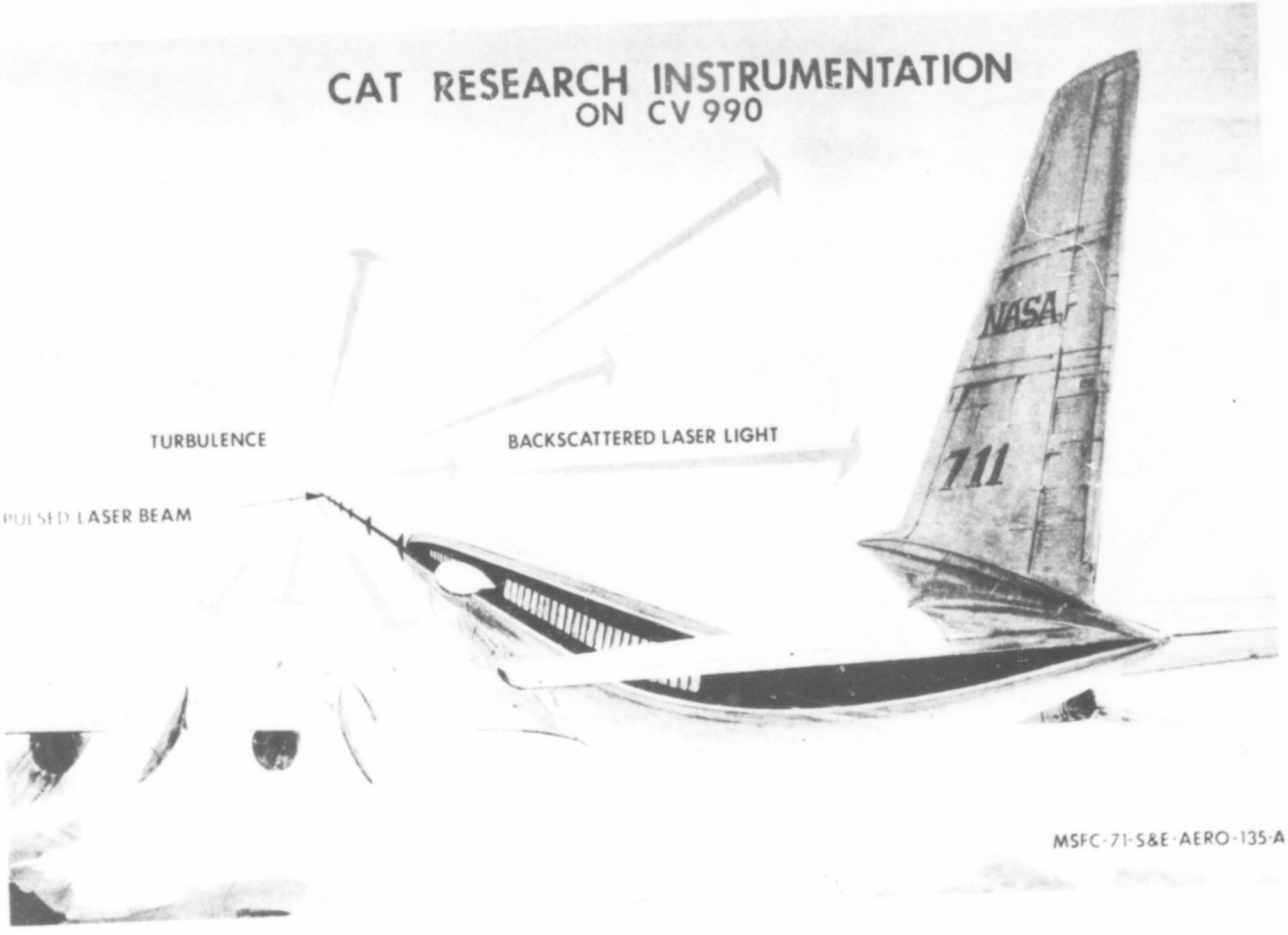
CAT RESEARCH INSTRUMENTATION
ON CV 990
TURBULENCE
BACKSCATTERED LASER LIGHT
PULSED LASER BEAM
NASA
711
MSFC-71-S&E-AERO-135-A

Fig. 9

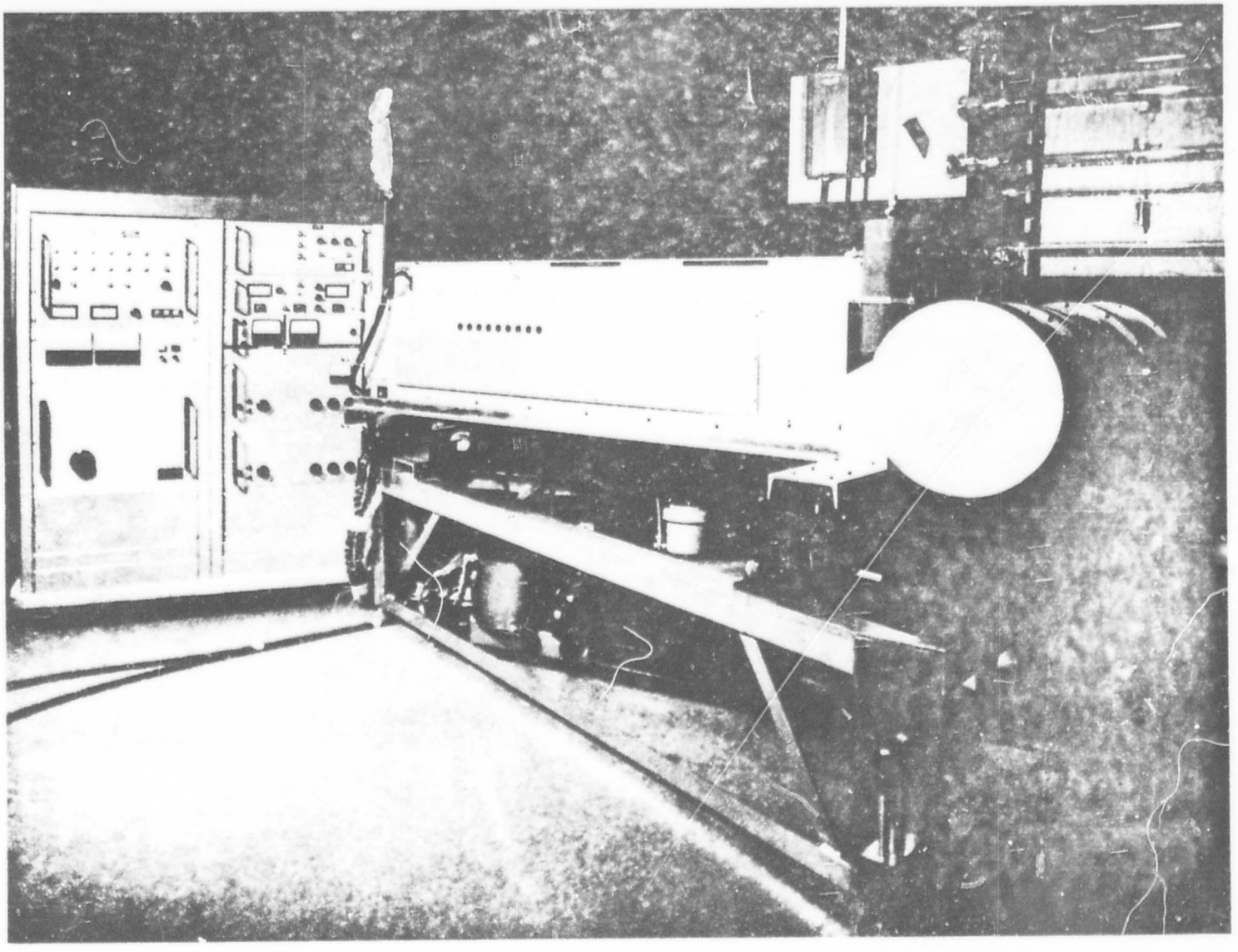

Fig. 10 CAT Transmitter

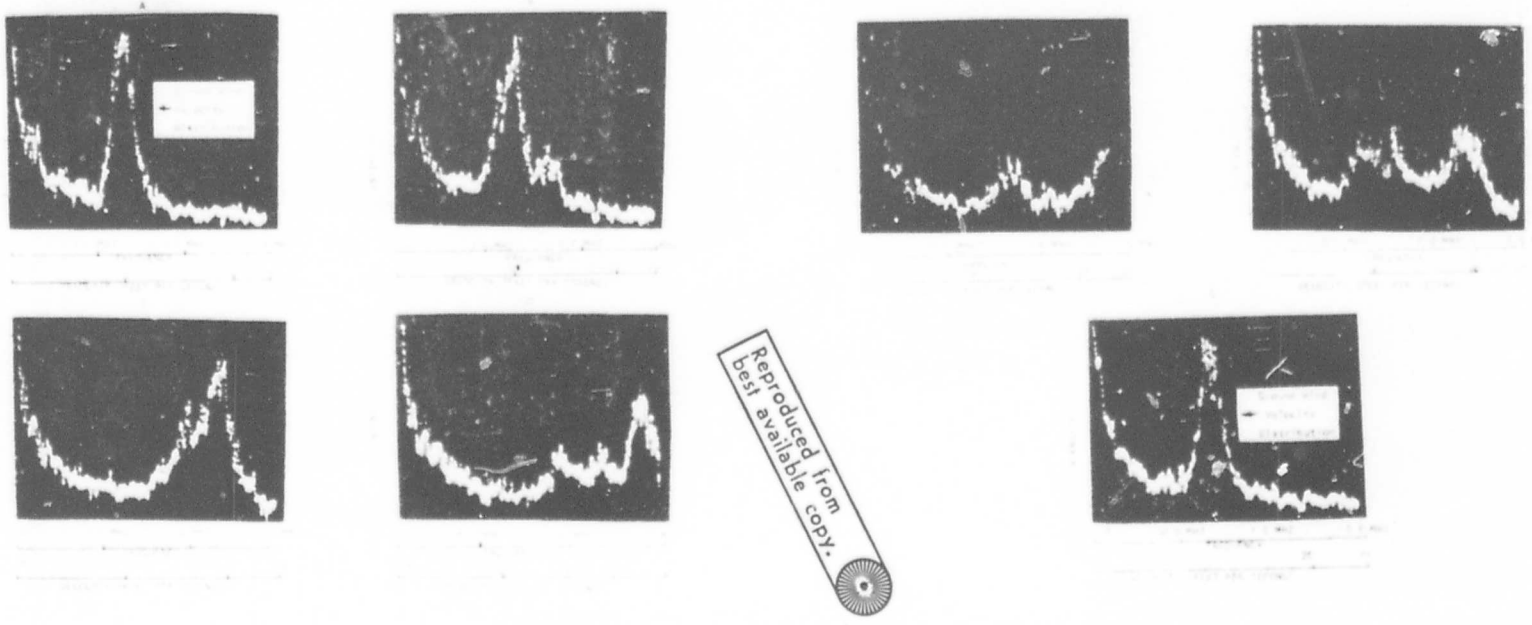

Fig. 11 TIME SEQUENCE DISPLAY OF THE VELOCITY STRUCTURE OF A TRAILING VORTEX USING A LASER VELOCIMETER

DISCUSSION

PIKE: Was the detector cooled with helium or nitrogen?

HUFFAKER: We have used both. For these we used copper doped germanium at liquid helium temperatures - these are CO_2 lasers at ten microns. For the wind tunnel program we used argon lasers. For the atmosphere we used CO_2.

PIKE: For laser power, you talked about a two-mile range. What is the laser power for that?

HUFFAKER: The laser power has generally been about 10 watts.

PIKE: The volume you are looking at at two miles is large?

HUFFAKER: Quite right. No detailed measurements have been made at those ranges. So far we have been using a single mirror concept - using the depth-of-focus approach in which the volume gets worse as it goes out. As we change the range we see the difference in velocity distribution as we go out to ranges of that order.

PIKE: And the transmitter diameter?

HUFFAKER: Twelve inches.

MEASUREMENT OF SUPERSONIC VELOCITY AND TURBULENCE BY LASER ANEMOMETRY*

D. A. Jackson and D. M. Paul**

The Physics Laboratory,
University of Kent,
Canterbury,
Kent, England.

ABSTRACT

A laser anemometer which directly measures the frequency change in light scattered from flow borne oil droplets has been used to measure mean velocity and turbulence widths in supersonic flows. Experiments have been performed in wind tunnels and free jets.

*Unfortunately Prof. Jackson was unable to complete final travel arrangements, and was unable to present this paper at the Workshop as planned. We are glad to publish the paper as submitted and feel that it adds to these proceedings. Ed.

**Supported by a Harwell Fellowship, now with Shell, Applied Physics Division, Thornton, Chester.

INTRODUCTION

Laser doppler techniques have been developed by several authors[1] and applied to the study of flow profiles.

The main advantages of this technique over Pitot tubes and hot wire anemometers are (a) absolute velocity measurements which is sensitive to only one component of the flow, and (b) non interference with the flow pattern, coupled with high spatial resolution.

The basic principle of flow measurement based upon the detection of the doppler frequency shift of light scattered from particles suspended in the flow is shown in Fig. 1. The scattered light is detected at an angle θ away from the incident direction. The mean frequency shift is $2n\,\bar{V}/\lambda \sin \theta/2$ where $\bar{V}$ is in the direction of Q, i.e. along the bisector of the angle between the incident beam and the scattered beam. If a symmetrical geometry is used then V will correspond to the velocity component along the axis of the flow.

The frequency shift therefore depends upon the scattering geometry, hence the measured instrumental width will depend on the solid angle of acceptance of the collecting optics. There are other causes of frequency broadening due to the finite lifetime of the particle in the field of view (ambiguity broadening in radar terminology[2]). This ambiguity broadening also sets a limit to the spatial resolution in the probe region. A further complication is that since the particles must be small in order to follow turbulent flows at high speed the light will tend to be scattered mainly in the forward direction, curve 'e' Fig. 2. It is therefore necessary to analyse the angular dependence of the amount of light which can be detected for a given instrumental bandwidth.

The results of this analysis[3] are shown in Fig. 2 where curve 'f' represents the angular variation of the amount of light scattered from .5μ particles which can be collected to give a 1% instrumental frequency broadening. This curve was plotted assuming the volume of the scattering region was sufficiently large that there was no ambiguity broadening. However, if we wish to restrict the spatial resolution to that obtainable by pitot tubes and hot wire probes there is a lower limit to the usable scattering angles and these are shown for several spatial resolutions by the vertical lines in Fig. 2. For example, if we require a spatial resolution of 10^{-2} cms coupled with a capability of measuring turbulent levels of 1% or greater, then the smallest scattering angle that can be used is 30° whatever the velocity.

The most frequently used technique is that of optical heterodyning[1] in which the doppler shifted light is mixed with an unshifted reference beam on a square law detector. Flow measurement by heterodyning has proved extremely successful when the mean velocities are low such that the frequency shifts are less than 100 MHz. However, if we wish to study turbulence profiles at high velocities, i.e.~100-1000

meters/sec at the spatial resolution previously quoted, then the doppler frequency shift will lie in the range 100-1000 MHz, Fig. 2. Such high frequency shifts are beyond the range of all but the most expensive photomultipliers. Also amplification at such high frequencies requires special electronic techniques.

An attractive alternative method of velocity measurement is to directly measure the frequency shift of the scattered light. This may be achieved using high resolution Fabry-Perot interferometers, which are capable of measuring frequency changes from ~5 MHz up to 500 GHz with a bandwidth of 1 MHz. A further advantage of the Fabry-Perot system over the heterodyne technique is that it uniquely measures the sense of direction of the flow. We have previously[4] reported some preliminary measurements where the velocity of ice particles suspended in streamline supersonic flows (Mach 1 - 3) were determined using a confocal Fabry-Perot to analyse the spectrum of the scattered light.

Mean velocities were compared with those obtained using conventional Pitot tubes and the results were found to be in good agreement. No detailed measurements of turbulence levels were made at that time but a superficial analysis of turbulence profiles behind a wedge was carried out; representative spectra are shown in Fig. 3(a), where it can be seen that the mean velocity increases as the turbulence decreases as one moves away from the wedge.

The ice particles were formed during the rapid expansion (of humid air) in the throat of the wind tunnel. Ice particles however, are not the most suitable particles since (1) wind tunnels are usually operated with dry air (water vapour (or ice) leads to rapid erosion of test sections), (2) the particle size is likely to be variable hence not all the particles faithfully follow the flow, and (3) the particles size is dependent on the mean flow velocity (unpublished results - determined from radial scattering distribution). In experiments in regions of high turbulence (2) and (3) are likely to lead to erroneous results since the scattering coefficient will be velocity dependent.

In order therefore, to establish that the laser doppler technique can exploit its inherent advantages over hot wire and Pitot tube measuring devices, it is necessary to develop a probe particle which is more suitable for wind tunnel environments. There are several alternatives, e.g. tobacco smoke, hydrogen chloride - ammonia vapour mixture, oil - air mixture, etc.,

We have found that the oil - air mixture is the easiest to inject into the flow stream in the case of free jets. Results are presented here of measurements of V and ΔV in a jet seeded with 0.5μ oil droplets. Further work is in hand to establish that such a mixture is suitable for injection into a full-scale wind tunnel.

Measurements in a Free Oil Jet

The experimental arrangement is shown in Fig. 4 in which a symmetrical scattering geometry is used such that only the velocity component along the axis of the jet is sampled. Detail of the jet and generator of the oil droplets is shown in insert Fig. 4. The smoke from the generator (supplied by Taylor Industries), is forced into the mixing chamber by CO_2 where it is mixed with compressed air and allowed to escape into the atmosphere through a tapered nozzle. The nozzle diameter was such that differential pressures up to 4 atmospheres could easily be obtained. The smoke concentration was essentially governed by the differential pressure between the compressed air and the CO_2 pressure.

The laser (Coherent Radiation Laboratory model 52A) was operated in a single longitudinal mode by an intra-cavity etalon. The scattered light was focussed into a confocal piezoelectrically scanned Fabry-Perot (CRL 570)(5) free spectral range 2 GHz - resolution 7 MHz driven by the 150 V sawtooth ramp of a Tektronic 531Δ oscilloscope. The transmitted light was detected by an EMI 9558A photomultiplier, the output of which was fed to the oscilloscope, or an X-Y recorder.

The Fabry-Perot system was initially aligned for maximum frequency resolution by detecting the light scattered from a diffuse scatterer placed at the desired probe region. When this was removed and smoke allowed to flow at a few cms/sec (such that the change in frequency would be < 1 MHz) there was no observable change in the profile.

The scattering volume was determined by a stop placed in front of the Fabry-Perot, spatial resolutions of better than .01 mm were easily obtainable. At such spatial resolutions, and with moderate smoke intensities (i.e. mist rather than fog) the detector currents were typically 10^{-6} amps with the tube operated at 1000 V (- 180 A/Lumen), even at the highest velocities.

The construction of the jet was such that it was possible to vary its axis with respect to the optical sampling volume without disturbing the optical arrangement.

The mean velocity was measured at about 10 nozzle diameters from the jet nozzle, typical (time averaged) spectra are shown in Fig. 5 where an obvious feature is the marked asymmetry of the profile, which appears to be pressure (and hence velocity) independent, indicating that this is a feature of the construction of the mixing chamber and nozzle shape rather than because the oil droplets are not following the flow (similar experiments with a convergent-divergent nozzle gave a gaussian distribution along the axis of the jet), Fig. 3(b).

The variation of mean velocity as a function of pressure is shown in Fig. 6 which shows that above a differential pressure of

~1.5 atmospheres there is only a slight increase in the mean velocity, indicating a limit to the mean flow set by the nozzle size.

A further set of measurements was performed to observe the variation of mean velocity and velocity spread as a function of radial distance from the axis of the jet. Typical spectra are shown in Fig. 5 where the character is seen to change as one moves away from the axis of the jet, in that the profile appears to become more and more gaussian in shape as one would expect in a highly turbulent region. The normalized velocity ($u_r/u_{r=0}$) as a function of r/R is shown in Fig. 7 and compared with the experimental and theoretical results given in a review of Siddharther[6] for supersonic jets of Mach No. between 1 and 3. Our results are seen to be in a very good agreement, the deviation probably being because we used the peak of the distribution to define the mean velocity rather than $\bar{U}^2$. The variation of the percentage turbulence against r/R is also shown, where the maximum percentage turbulence is 50%. Local turbulence levels at the edge of the flow are ~100%. Such high turbulence levels cannot usually be accurately measured by hot wire anemometers[7].

Instantaneous Velocity Measurement

In many applications it is desirable to follow the time variation of the mean velocity rather than the time average velocity.

We have outlined a scheme[8] by which it should be possible to modify the Fabry-Perot system such that it will present instantaneous velocity fluctuations. This is simply acheived by "aperturing" the output of the Fabry-Perot so that the intensity of the transmitted light now corresponds to a frequency (the Fabry-Perot is now no longer driven).

Shear Stress Measurements

If the spectrum of the scattered light is simultaneously analysed at the scattering angles θ and $-(180 - \theta)$, Fig. 1, then $\bar{V}_x$ and $\bar{V}_y$ can be measured. In principle by using "apertured" Fabry-Perots it should be possible to follow the time variation of $\bar{V}_x$ and $\bar{V}_y$ and if the signals corresponding to $\bar{V}_x$ and $\bar{V}_y$ are multiplied together one would obtain $\bar{V}_x\bar{V}_y$, the shear stress.

CONCLUSION

We may conclude that the laser technique for measuring high speed flows is complementary to the previously used hot wire and Pitot tube probes, and also that it is possible to operate it in regions of very high turbulence causing the acquisition of data hitherto inaccessible. Further development of the system should enable instantaneous measurement of mean velocities as well as the time development of Reynolds shear stress.

REFERENCES

1. Benedek, G. B., 1968, Polarisation Matiere et Rayonnement, Livre de Jubile en L'honneur du Professeur A. Kostler (Paris: Presses Universitaires de France).

2. Pike, E. P., Jackson, D. A., Bourke, P. J. and Page, D. I., J. Sci. Insturm., 2, 111, (1968).

3. Jackson, D. A. and Paul, D. M., J. Sci. Insturm. 4, 173, 1971.

4. Jackson, D. A. and Paul, D. M., Physics Letters, 32A, 77, (1970).

5. Hercher, M., Applied Optics, 7, 951, (1968).

6. Siddhather, M., Imperial College Report.

7. Durst, F, and Whitelaw, J., Imperial College London Report.

8. Paul, D. M. and Jackson, D. A., J. Sci. Insturm. 4, 170. 1971.

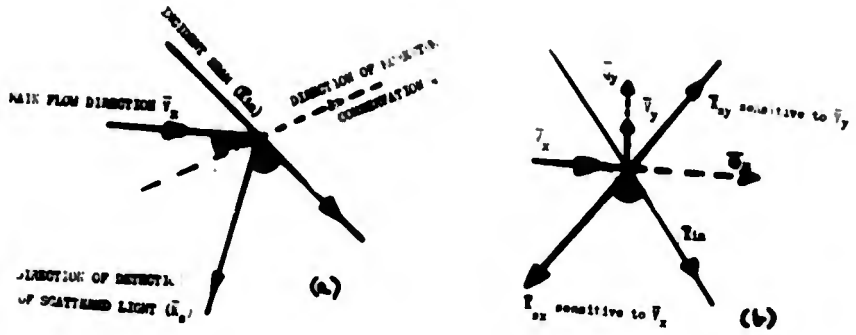

Figure 1. (a) The scattered light is detected at an angle θ to the incident beam. The momentum transfer $\overline{Q} = \overline{\Sigma}\,\overline{K}_{(in)} \sin \theta/2$ and the doppler frequency change is $\overline{Q} \cdot \overline{V} = 2n\,\overline{V}/\lambda \sin \theta/2 \cos \beta$. If $\overline{Q}$ lies along $\overline{V}_x$ (Figure 1(b)) corresponding to a symmetrical scattering geometry, then the frequency shift is $2n\,\overline{V}_x/\lambda \sin \theta/2$. Detection of the scattered light along $\overline{K}_{sy}$ enables the component $\overline{V}_y$ to be measured.

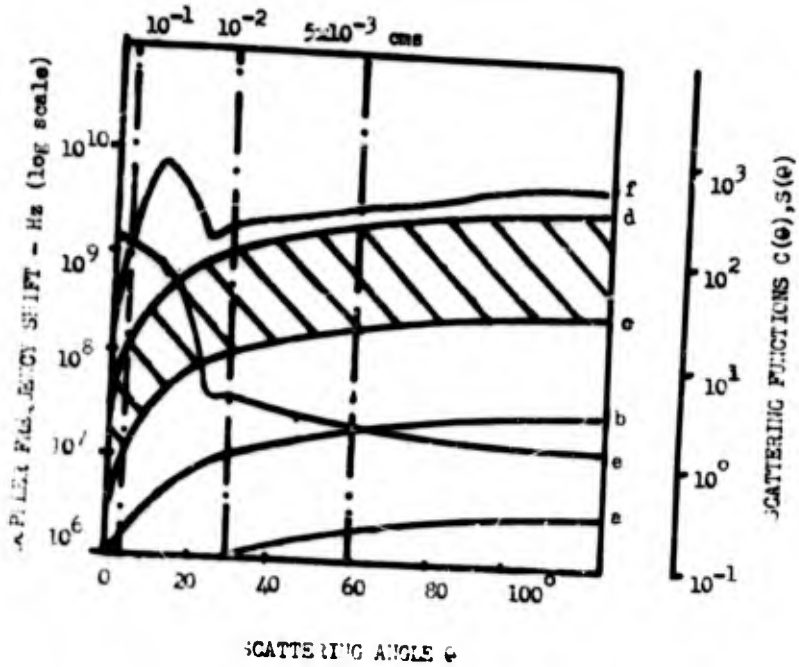

Figure 2. Curves 'a', 'b', 'c' and 'd' are the frequency shifts as a function of scattering angle θ, for flow velocities 1, 10, 100 and 1000 meters/sec respectively.

The shaded area 'c'-'d' corresponds to the transonic region between 100-1000 meters/sec.

Curve 'e' is the angular scattering coefficient for light (5000 Å) scattered from .5μ particles, $C(\theta)$.

Curve 'f' is the angular variation of the amount of light which can be collected to give a 1% frequency broadening, $S(\theta)$.

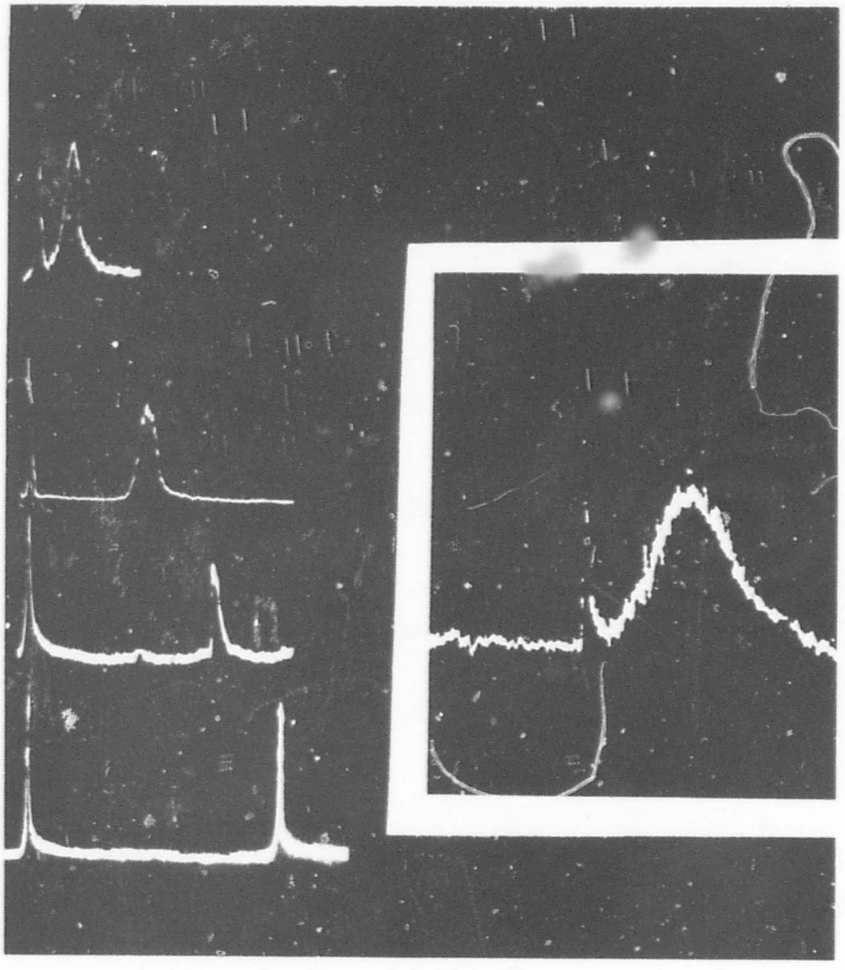

Figure 3. (a) Shows the variation of mean velocity and turbulence behind a wedge in a Mach 1.6 wind tunnel using ice particles as 'probe particles'. The distances behind the wedge are ~1cm, ~5cms, ~10cms, ~25cms. The maximum frequency shift corresponds to 930 MHz.

(b) Turbulence profile from a 'divergent-convergent' free 'oil-jet'.

The peak on the left in each figure is that of the reference unshifted laser light. The width of this peak corresponds to the bandwidth of the Fabry-Perot.

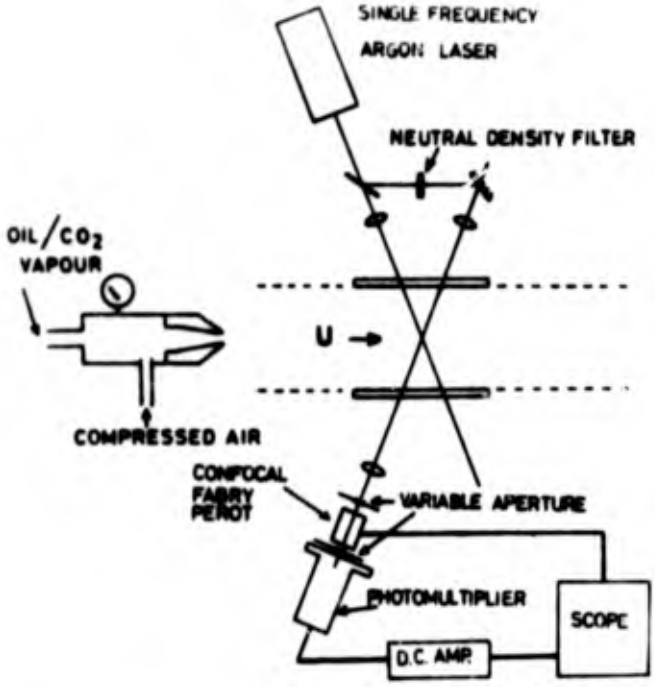

Figure 4. Optical arrangement showing the system used to match the reference and signal beams into the analyzing optics.

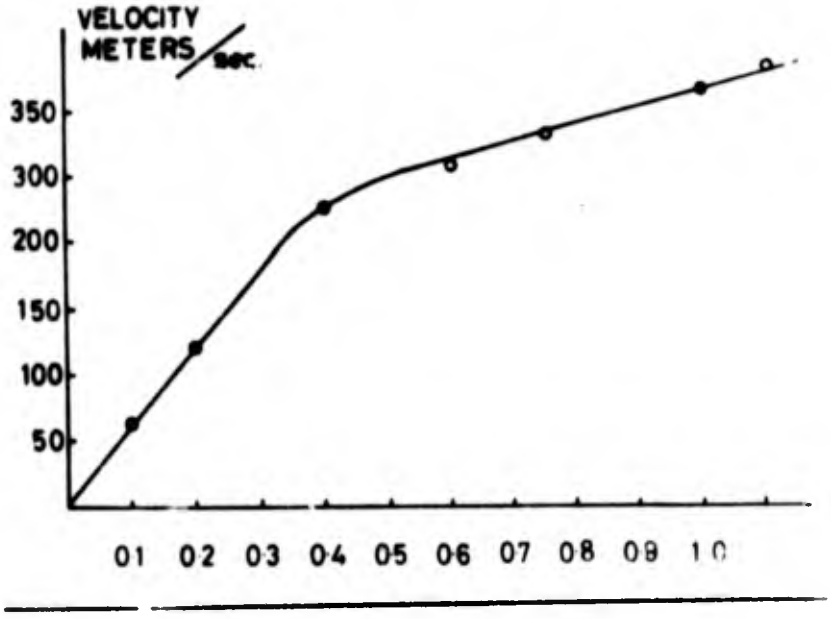

Figure 5. Typical spectra of the free jet at 10 nozzle diameters from the nozzle.
(1) - on axis where the differential pressure is 0.1 atoms.
(2) - on axis where the differential pressure is 1 atom.
(3) - 2.5mm off axis where the differential pressure is 1 atom.
(4) - 3.5mm off axis where the differential pressure is 1 atom.

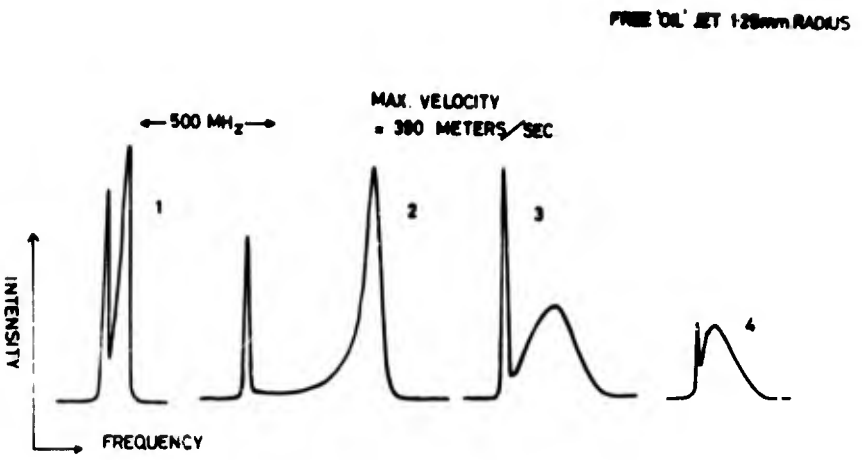

Figure 6. Variation of core velocity with differential pressure.

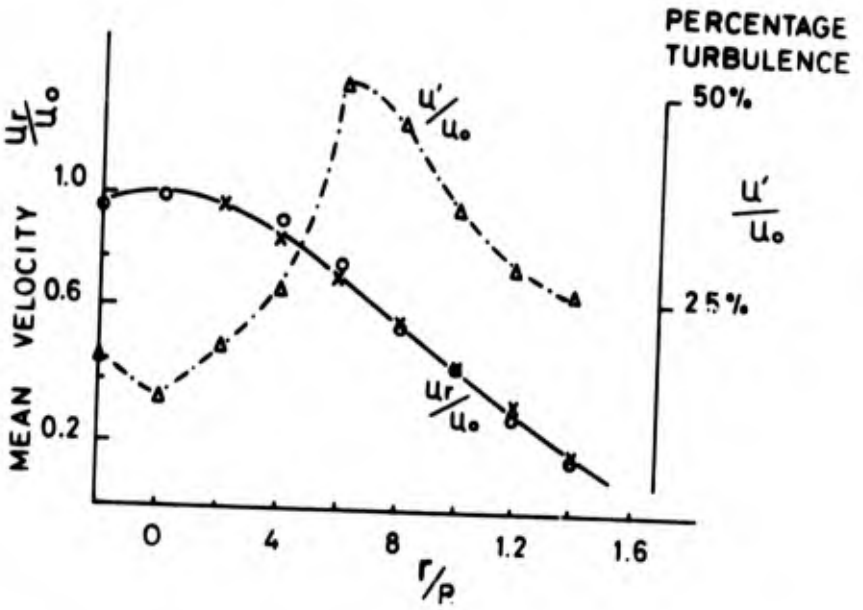

Figure 7. The variation of the mean velocity and turbulence width as a function of radial distance r from the axis of the jet. R = r is the point where the velocity is half its value on the jet axis at the same axial station. The core velocity was 390 meters/sec.
O - Experimental points from present measurements.
X - Normalized data points taken from Siddhartha[6].
- Predicted curve from [6].
Δ - Percentage turbulence data points.

DISCUSSION OF THE LDV FRINGE MODEL

C. P. Wang

University of California
San Diego

La Jolla, California

I would like to raise a question about the fringe model. As I understand it, the fringe model says that you have a set of fringes generated by two crossed laser beams. As the particle goes through these fringes it is in a dark region and doesn't block any light. In a bright region you block more light and so on. So the intensities fluctuate and give you a frequency and that happens to be the doppler frequency. Now my question is a hypothetical question. Suppose you have a square particle like the slide Professor Whitelaw showed yesterday and the width of this particle is exactly the same dimension as these fringes. This particle moving through won't change anything. The intensity will stay the same so you won't get any signal. Or let's exaggerate a little more. You could have a very fine wire and pull this wire through. You won't get any signal if you assume a fringe model. But you do get the same doppler frequency shift if you use the scattering model.

DISCUSSION

PIKE: If your wire is perfectly smooth, you won't get any signal in any case.

WANG: But you still get scattered light.

PIKE: Well then if the wire is not smooth you still have particles in effect.

WANG: O.K. so let's limit it to a square particle. You always get scattered light. Then how do you explain it?

ASHER: Your signal is made up of low frequency components. It has particles starting out just entering your scattering volume. When it ends, there is no scattered light before and after. In between there should just be the step function of scattered light. That's it. Now with the infinitely long wire that you've shown, you will keep pulling for the rest of your life. All you've done is change the DC level.

PIKE: The technical answer is very straightforward. That is that you've got to assume that in that volume there is a random spacial distribution of scattering centers and then this formally is just a well-known two-dimensional random walk problem. Even with scattering particles that aren't the same size the answer is that the total scattering is proportional to $\sqrt{n}$. It is a statistical problem and you could find a situation with no signal at all. If you put in square particles one in each fringe you just balance it all out. You could get zero intensity.

WANG: You mean you don't get a signal when you assume a fringe model - you won't get any frequency?

PIKE: It does not depend upon the shape or size of the particle. It depends on the spatial position. You can put some dots on the board in such a way that at the receiver end you will add up all the signals and get nothing.

WANG: You mean you cannot visualize a physical picture like this?

PIKE: Yes. The next minute when your wire is in a different position and the scratches and bumps are in different places then maybe the signal will add up to something. If you take the statistical average of what you find that there is a two-dimensional gaussian distribution of the electric field vector and the mean square power is related to the square root of the number of particles.

HAUER: You are talking about one case where you have a single particle that's large compared to the fringe spacing and, in the second case, you are talking about the superposition of random scatters in the probe volume. You are talking about two different cases, are you not?

PIKE: No. I tried to make it the same.

HAUER: I don't think you can consider them in the same way.

PIKE: There is of course the difference between coherent detection and incoherent detection which apparently is not very well understood by people.

WANG: From the fringe model I don't see how the coherent-incoherent business comes in.

PIKE: If you have a coherent detection the receiver aperture is so small that any particle in that fringe volume always has the same angle in its electric vector. Therefore, they add up as n and not $\sqrt{n}$.

WANG: Right. This is if you assume the scattering model.

PIKE: You do have scattering, that's for sure, otherwise you won't have any signal.

GEORGE: The fringe idea was begun probably by Rudd a number of years ago. He made up a theory that if particles crossed the beam they blocked the light. He even went a little further and said that because it blocked the light, you get a better signal to noise ratio. That is a myth. It's nonsense. The particles are essentially acting like a collection of linear oscillators which are responding to two separate inputs. I think when you consider it in that light the problem doesn't exist. I think the problem in your mind is this whole myth about particles blocking light.

WANG: So you say that blocking light is the wrong concept.

GEORGE: In my mind, yes.

WANG: O.K. That's just what I wanted to know.

WHITELAW: I think you're right. The problem arises from thinking of the fringe or cross beam system as something different from the reference beam system. Both systems operate on a doppler shift principle.

GEORGE: The idea of fringes is just a convenient peg to hang discussion on.

WHITELAW: The point I was trying to make was that the strength of the signal you get out will be related to the size of the particle relative to the fringe distance. That's true. If you measure with a particular fringe system and put in particles of different sizes, you will measure a decrease in signal strength for particular sizes.

WANG: But you couldn't see that from the scattering model.

WHITELAW: You can't see it conceptually. You can see it if you do an analysis. You will get something that says the intensity of scattered light divided by some normalizing intensity is a function of the size of the particles divided by the fringe spacing. We made it easy and just did the integration for the square particles.

PIKE: This is a curious feature that a very basic question like this is just not written down in the literature. I don't think I could recommend a paper except perhaps the recent one by Les Drain. I do have a set of pictures of slides that were extracted from a lecture I gave last year in which I think all of these questions are layed out in very bare form.

STEVENSON: Could I make one final comment here. I said yesterday in my talk that you really don't have a fringe system in any case. What you have is an electromagnetic field distribution. As long as there is nothing to scatter from there is no light scattered. Only when the particle comes into this region does light leave in any direction other than the direction that the beams are travelling originally. When the particle moves into a high electric field region it scatters light to the detector. When it moves into the region where the field is zero, there is no light scattered. You will notice that this takes place in a time less than one doppler cycle. So you're not really getting doppler information when you are passing through less than one cycle. Does that shed any light on the problem?

WANG: The way I understood the fringe model is that you were blocking the light. Obviously this isn't true.

WHITELAW: Does anyone remember the paper on optical anemometry by Gaster about 1963. He used a rotating grating. Essentially I believe he did what you are talking about - blocking out light. I'm not sure if anyone would agree or not. The rotation of the disc generated a moving fringe pattern.

STEVENSON: You're just collecting the diffracted orders?

WHITELAW: That's right this is an intensity device as opposed to a frequency device.

SHENKER: Could you comment on leaving the particle stationary and moving the fringes? Should you get any output?

WANG: Yes. Just by relativity.

LENNERT: In fact, there are other things you can do. For instance in some of the experiments we ran with a crossbeam system we took a very fine wire and went to different portions of the focal region. When you come in close to the $1/e^2$ region you can see the doppler signal as two peaks - in other words two superpositioned signals one after the other. It is not a matter of blocking light, it's a matter of scattering light. As you're going through an alternately light and dark region, you have the intensity modulation which is the doppler signal riding upon the D.C. level. You can make an analysis in terms of a fringe visibility function. If the particle size becomes larger than the dimensions of the fringe spacing, then you start getting decreased amplitude or resolution from fringe to fringe. Ultimately when the particle sizes are very large, all you get is a D.C. level of varying intensity. That is one means of discriminating against certain particle sizes - by tightening up or relaxing the fringe spacing in the focal volume.

JOHNSON: If I recall in Rudd's initial model he collected both incident beams. In this case the dominant factor would be blocking the light.

PIKE: No, I don't think that is quite true, because a one-micron particle really wouldn't block the light very much.

JOHNSON: You wouldn't have a very good signal to noise ratio because you've got a tremendous power level.

PIKE: It's well-known that light goes around corners and makes diffraction patterns.

JOHNSON: In his original paper he actually had his lens collecting the beam - for sure it wouldn't work very well.

DUNNING: That's right then in his next paper, they showed a great significant increase in signal to noise ratio by blocking out the two beams.

GEORGE: With regard to "blocking" in a more general context, it has been suggested for heterodyne systems that you can just keep adding particles. I refer you to the analysis by Melling, one of Dr. Whitelaw's students. He points out that when the particle concentration gets too high you start attenuating the laser beam because of the multiple scattering in the probe volume. So you don't want to just keep pumping in more and more particles, you're going to hurt yourself.

AN ANALYSIS OF THE DATA ACQUISITION RATE OF AN ATMOSPHERIC, BACK-SCATTER LASER DOPPLER VELOCIMETER

By

D. B. Brayton

Experimental Research/Technical Staff
Office of the Managing Director
ARO, Inc.
Arnold Air Force Station, Tennessee 37389

ABSTRACT

A theoretical analysis is summarized which predicts the data acquisition rate (# signal bursts/second) of an atmospheric, dual scatter, backscatter LDV. A model atmospheric aerosol consisting of spherical particles of constant index of refraction and known size distribution is used in the analysis. The results predict the rate of reception of single particle Doppler bursts above a prescribed level of signal-to-noise ratio. The results can be used to compare the performance of different optical schemes and to optimize a particular system design.

The research reported in this paper was sponsored by Arnold Engineering Development Center, Air Force Systems Command, Arnold Air Force Station, Tennessee, under Contract No. F40600-72-C-0003 with ARO, Inc. Further reproduction is authorized to satisfy the needs of the U. S. Government.

Let it be assumed that the aerosol particles contained within the lower elevation of the earth's atmosphere are essentially spherical in nature and are characterized by a constant index of retraction. A knowledge of three parameters then completely specifies the light scattering characteristics of such an atmosphere: (1) the particle index of refraction, n, (2) the particle size distribution function dN/dr and (3) the single particle Mie intensity function $i(\theta_s)$. dN/dr has been experimentally measured and is relatively constant throughout the earths lower atmosphere[1,2,3]; dN/dr is plotted in Figure 1[3]. $i(\theta_s)$ is available from the theory of Mie[4]. Since $i(\theta_s)$ depends upon the dielectric constant and conductivity of the scatterer, an average index of refraction representative of the atmospheric aerosol must be chosen. A reasonable estimate is n = 1.5[2]. For n = 1.5, i(180°) has been conveniently tabulated versus the particle size parameter $\alpha = 2\pi r/\lambda$ by reference 5. Thus the light scattering characteristics of the atmospheric aerosol are completely specified.

The number of particles per unit volume within the size range $\Delta r/2$ of particle radius r is (dN/dr) Δr. Assuming Δr is small each of these particles has a differential scatter cross section $\frac{d\sigma}{d\Omega}(\theta_s) = i(\theta_s)\left(\frac{\lambda}{2\pi}\right)^2$ such that when illuminated by a beam of intensity $\downarrow$ it will scatter a power $\frac{d\sigma}{d\Omega}(\theta_s) \downarrow \Delta\Omega$ into a small solid angle $\Delta\Omega$ about θ_s.

Collectively particles of all sizes will establish a mean photo current which will determine the mean shot noise. The particles will contribute a differential cross section per unit volume (power scattered · Solid Angle^{-1} · volume^{-1} · intensity^{-1}) of

$$\frac{d\beta}{d\Omega}(\theta_s) = \int_{r_L}^{r_u} \frac{d\sigma}{d\Omega}(\theta_s)\,\frac{dN}{dr}\,dr = \int_{r_L}^{r_u} i(\theta_s)\left(\frac{\lambda}{2\pi}\right)^2 \frac{dN}{dr}\,dr \qquad (1)$$

where r_L and r_u are the lower and upper limits of the extent of the particle size distribution function dN/dr (see Fig. 1). For later reference note that $\frac{d\beta}{d\Omega}(\theta_s)$ can also be interpreted to be the differential scattering coefficient (power scattered · Solid angle^{-1} · length^{-1} · power illuminating^{-1}). Let it be assumed that a dual-scatter LDV collects backscattered light ($\theta_s \leq 180°$) only from the beam crossover region. Furthermore, assume that the radiation collection optics do not directly view a bright background and/or that very narrow (e.g. 2A°) bandwidth laser line filters are used to reject background radiation. Under such conditions the mean photocathode current, I_c, is determined cheifly on the collection of laser light scattered from within the probe volume,

$$I_c = \frac{d\beta}{d\Omega}(180°)\,P_L\left(\frac{\pi\theta_R^2}{4}\right)\left(\frac{2N_F\lambda}{\theta^2}\right)\frac{\eta e\lambda}{hc} \qquad (2)$$

All parameters in Eq. 2 are defined in Appendix I; the exp(-2) length of the probe volume is $2N_F\,\lambda/\theta^2$, the solid collection angle is $\pi\theta_R^2/4$, and $\eta e\lambda/hc$ converts watts to

cathode amps. I_c of Eq. 2 is the time average D.C. (photo) cathode current due to scatter centers of all sizes. The total D.C. shift due to the known presence of a particular particle size is

$$I_{total} \cong i_c + I_c$$

where i_c is contributed by the known particle and I_c is due to background. The signal to noise ratio is then

$$SNR \cong \frac{\frac{1}{2} i_c^2}{2e(i_c + I_c) f_e} \tag{3}$$

Assuming the electronic bandwidth f_e is adjusted to be

$$f_e = f_D = v\theta/\lambda$$

then Eq. (3) becomes

$$SNR \cong \frac{\lambda}{4ev\theta} \cdot \frac{i_c^2}{(i_c + I_c)} \tag{4}$$

A knowledge of the fringe intensity distribution together with the previous inputs allows one to predict the data rate, $\mathring{N}$, versus either the SNR or the epf rate of a dual scatter, back scatter LDV. These are given by

$$\dot{N}_{(SNR>SNR^*)} = \frac{\pi v}{\theta}\left(\frac{N_F \lambda}{2\theta}\right)^2 F(i_o^*) \tag{5}$$

$$\dot{N}(epf > epf^*) = \frac{\pi v}{\theta}\left(\frac{N_f \lambda}{2\theta}\right)^2 F(j_o^*) \tag{6}$$

where

$$F(x) = \int_{y=x}^{y=\infty} \frac{N(i>y)}{y}\, dy\,, \tag{7}$$

$$i_o^* = \frac{4\pi^2 hc N_F^2 SNR^* v}{\eta \lambda^2 \theta_R^2 \theta P_L}\left(1 + \sqrt{1 + \frac{\pi \lambda^3 \sigma P_L \theta_R^2 N_F \eta}{2hc\, \theta^3 v\, SNR^*}}\right), \tag{8}$$

and

$$j_o^* = \frac{2\pi^2 hc N_F^2 epf^* v}{\eta \lambda^2 \theta_R^2 \theta P_L} \tag{9}$$

$F(i_o^*)$ is most easily evaluated numerically with a computer. $N(i>y)$ was obtained by computing on both dN/dr (Fig. 1) and i(180°), where numerical values for the latter were obtained from appendix II of reference 5.

Figure 2 plots Eq. (5) and (6) in a generalized manner where $\mathring{N}/\upsilon$ is plotted against $SNR^* \upsilon / \eta P_L \theta_R^2$. Note that because $d F(x)/dx > 0$ (a plot of F(x) would reveal this to be the case) then

$$\frac{SNR^* \upsilon}{\eta P_L \theta_R^2} \leq \frac{(epf^*/2)\upsilon}{\eta P_L \theta_R^2},$$

and the abscissa arguments SNR^* and $epf^*/2$ can be interchanged provided

$$\frac{SNR^* \upsilon}{\eta P_L \theta_R^2} < \frac{\pi \lambda^3 \frac{d\beta}{d\Omega}(180°) N_F}{2 h c \theta^3}.$$

APPENDIX I: Identification of Symbols

Symbol	Identification	Units
c	Speed of light	$m \cdot sec^{-1}$
e	Electronic charge	coulomb
enf	Electrons per fringe generated at the photocathode by an individual particle in moving a distance of one fringe.	-
f_D	Doppler frequency	sec^{-1}
f_e	Electronic bandwidth	sec^{-1}
h	Planck's constant	joule · sec
$i(\theta_s)$	Mie intensity function of an individual particle; $i(\theta_s) = (2\pi/\lambda)^2 \, d\sigma(\theta_s)/d\Omega$	-
$\mathcal{I}$	Intensity	$watt \cdot m^{-2}$
i_c	The A.C. or D.C. photocathode current amplitude near y = 0 due to a single particle. (Ideally the A.C. and D.C. parts are equal.)	amp
I_c	The long time average D.C. photocathode current due to many particles.	amp
L	Denotes "laser" or "lower"	-
LDV	Laser Doppler Velocimeter	-
n	Index of refraction of particle.	-
$N(i \geq y)$	The number of particles per unit volume with a Mie intensity function (i) equal to or greater than a prescribed value (y).	m^{-3}
$\dot{N}$	Number per second data rate.	sec^{-1}
N_F	Number of fringes in the probe volume.	-

Symbol	Identification	Units
dN/dr	Particle size distribution function.	m^{-4}
P_L	Power of laser	watt
r	Particle radius	m
r_L	lower limit of r	m
r_u	Upper limit of r	m
SNR	Signal to noise (power) ratio	-
θ	Angle between the illuminating beams as defined in Fig. 2	-
θ_R	Angle of the cone of the received scattered radiation as defined in Fig. 2.	-
θ_s	Angle of scattering as defined in Fig. 2.	-
λ	Wavelength	m
Ω	Solid angle	-
$\Delta\Omega$	Solid angle of collected light; $\Delta\Omega \cong (\pi/4)(\theta_R)^2$ for small θ_R.	-
$\propto$	Particle size parameter; $\propto = 2\pi r/\lambda$	-
η	Quantum efficiency	electrons/photon
*	Superscript denoting "of sufficient value"	-
$d\beta(\theta_s)/d\Omega$	Either the differential cross section per unit volume (power scattered · solid angle^{-1} · intensity^{-1} · volume^{-1}) or the differential attenuation coefficient (power scattered · solid angle^{-1} · length^{-1} · power illuminating^{-1})	m^{-1}
$d\sigma(\theta_s)/d\Omega$	Differential cross section of a particle (power scattered · solid angle^{-1} · intensity^{-1}); $d\sigma(\theta_s)/d\Omega = (\lambda/2\pi)^2 i(\theta_s)$ ·	m^2

REFERENCES

1. C. E. Junge,
Vertical Profiles of Condensation Nuclei in the Stratosphere
J. Meteor. 18, 501 (1961)

2. K. Bullrich
Scattered Radiation in the Atmosphere and the Natural Aerosol.
Advances in Geophysics No. 10, Academic Press, New York, 99 (1964)

3. Handbook of Gcophysics and Space Environments, U.S.A.F. Cambridge Research Laboratories, McGraw Hill Inc., N. Y., N. Y., (1965)

4. G. Mie
Beiträge zur Optik trüber Medien, speziell kolloidaler Metallösunger.
Ann. Physik 25, 377 (1908)

5. McCormick, M. P., "Laser Backscatter Measurements in the Lower Atmosphere", PhD Thesis, Dept. of Physics, The College of William and Mary, Virginia, (1967)

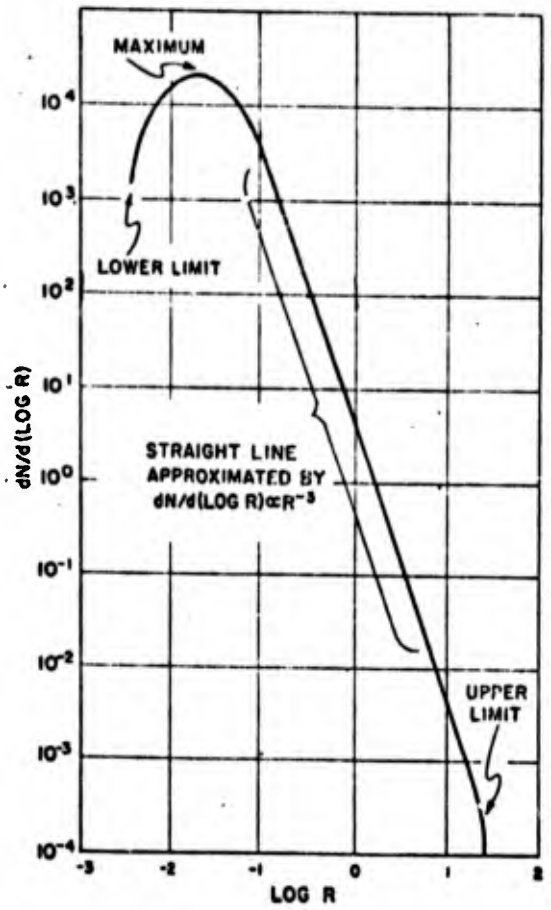

Figure 1. Particle Size Distribution Function

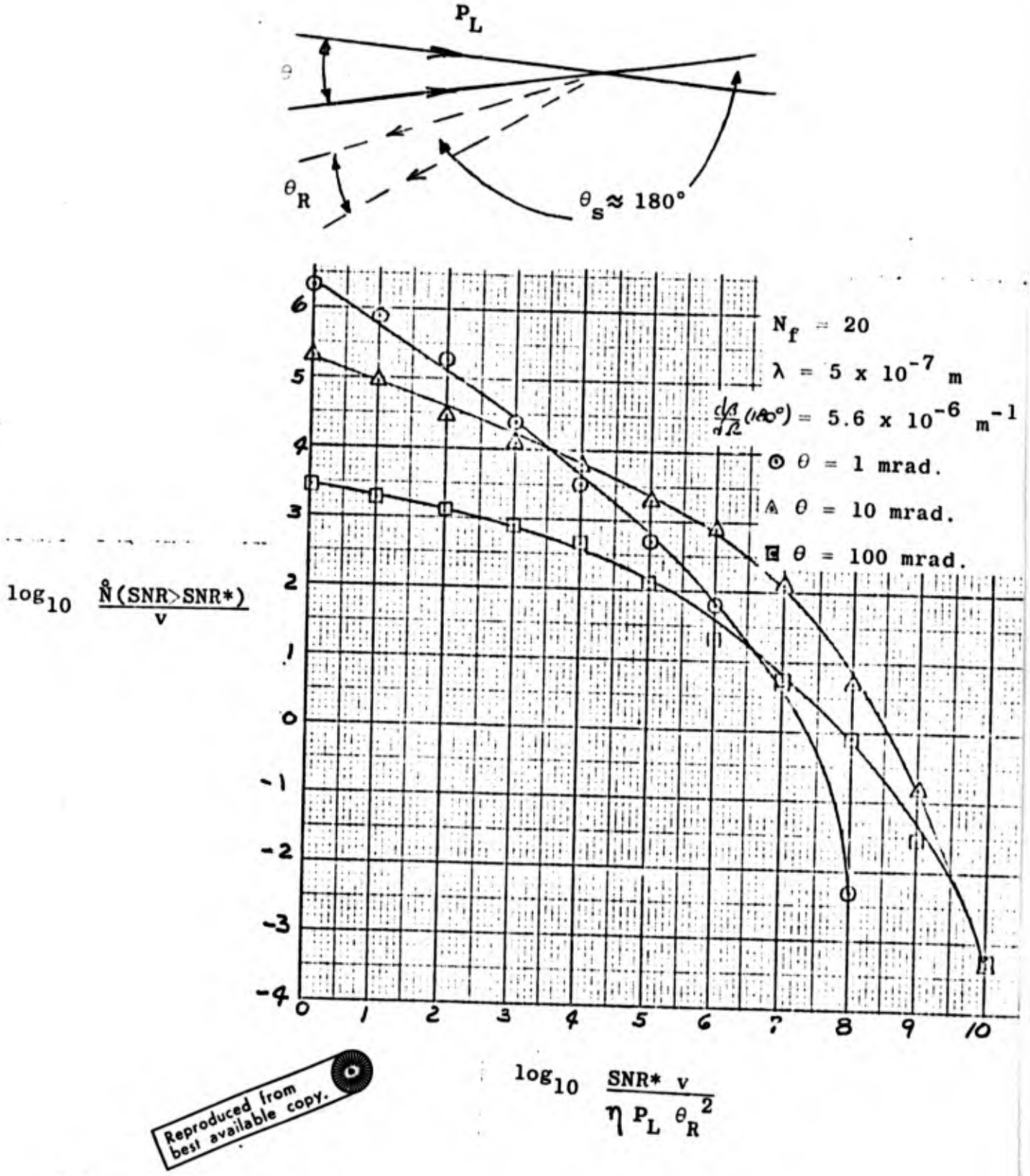

Figure 2. Back Scatter Data Rate ($\mathring{N}$) vs. Minimum Signal to Noise Power Ratio (SNR*) and other parameters. MKS units must be chosen for the plots to be correct.

SCHIFF: Do you have any information or know of any reference that gives the aerosol sizes as a function of wind velocity?

BRAYTON: I've seen data only over the sea, not over land. Those data are from Bullrich, Advances in Geophysics, No. 10, Academic Press (1964). Over the ground it would depend upon the terrain, what you're blowing off the ground, and so on. I doubt if such a plot would be available.

ASHER: You showed a burst and then took a lower level threshold off that burst. Is that before going through a low pass filter so that you don't have the zero crossing?

BRAYTON: Yes. I don't really see that it makes any difference.

ASHER: Well if you had a DC level that would be changing (this is very possible when your seeding rate changes) then you wouldn't want to be taking your low threshold off a burst which has not been low pass filtered to get rid of that changing DC.

BRAYTON: Typically we take it before it's low pass filtered. We take it right out of the photomultiplier tube. In wind tunnel work, the DC shift is almost unmeasurable. In atmospheric work there is a very measurable DC shift, but it's surprisingly steady. It's really due to all the particles in the detection volume and we verify that experimentally. We can get just above that and get reasonably high data rates. It's not jumping around.

ASHER: You do eventually low pass filter, that's the point. I'm just wondering why you don't do it at that point.

WHITELAW: It doesn't matter with the type of doppler signal processing which they used.

ASHER: Well, it's the same as we are using and it does matter.

WHITELAW: But they are checking a four count against an eight count.

ASHER: Well, the point is he has something that goes up and down and what he wants to do when he gets the signal in there is to determine the lower threshold. In other words, be in absolute terms

above a certain level of voltage.

WHITELAW: But the system would reject any bad values, would it not, on the basis of this double count.

ASHER: He is admitting another error. You don't want to lose things in dropout. The point is that you want to have the highest rate possible. This is just an added error thrown in. It's unnecessary.

BRAYTON: I'll put it this way. I've done most of my work in wind tunnels. Right now they are doing atmospheric work. I'm not directly involved with the experimental phase of it. It is filtered. The data I see does not have the DC shift on it. Is that what you are asking?

ASHER: Yes.

WILD CARD SESSION

Session Chairman: R. Goulard

515 B

BLACKBOARD DISCUSSION ON

FREQUENCY BROADENING IN DOPPLER SYSTEMS

During the Workshop a question was raised concerning the relative merits of velocity determination by period counting (as in a "doppler burst" signal processor) versus frequency domain processing with, e.g., a spectrum analyzer. The essence of the discussion is summarized here.

PIKE: The problem seems to be that the association of a broadening with a frequency analysis technique is confused with an indeterminancy. There should be no such confusion. If one has a piece of signal which is a single burst and one takes its Fourier transform then there is exact correspondence between the Fourier transform of that and what you get in time space. You can transfer it back and forth as many times as you like and you never lose any information. The frequency spectrum will have a breadth which is inversely proportional to that length of time (of the burst). It's a parameter that you've got in either system. If you want to know it, you can measure it from either record. One is just the reciprocal of the other. If you want to know the time it takes to go between zero crossings, then you look for the mean value of the frequency plot. All the information you want is in either form and there is nothing lost either way.

ASHER: What about the phase ambiguity that can be generated because the next burst coming through does not necessarily have to be in phase with the first?

PIKE: I have just spoken here about one particle. I haven't put another one in. If you want to work upwards, we can put another burst in there and then you look at this time. I will have a unique Fourier transform. Whatever signal you put up in real time on your oscilloscope trace will have a Fourier transform.

ASHER: How will that work when you have a highly turbulent flow? The dispersion of your distribution - of your Fourier analyzed signal - is going to be increased.

PIKE: That's no problem because whatever it is, it's just a Fourier transform of what it was in time space. If you want to go from one to the other you can. You don't lose anything.

ASHER: Are you saying you don't have an ambiguity at all?

PIKE: Perhaps I shouldn't have coined the word. It's only an ambiguity in the presence of noise. I haven't put noise into it. When you put noise into it, then of course you get into deep water because you want to know how do I get rid of the noise on either a trace like that or its Fourier transform when I don't know what the noise is.

GEORGE: I don't like the way you're backing up on the word ambiguity. It's always on ambiguity when you want to know something else.

PIKE: There is no ambiguity in the absence of noise. Everything is known. The interesting problems come when you put unknown noise on them and then you want to know the probability of the signal looking like that or slightly different from that in the presence of noise.

GEORGE: How about the turbulence ambiguity?

PIKE: That's not noise. Turbulence is the real physical signal and that's what you're trying to find.

The preceding discussion may be clarified by considering an idealized situation in which no velocity gradients exist and noise is negligible. A single particle passing through the probe volume generates the signal on the left below. The Fourier transform of this signal is shown on the right. Under these conditions an <u>exact</u> determination of

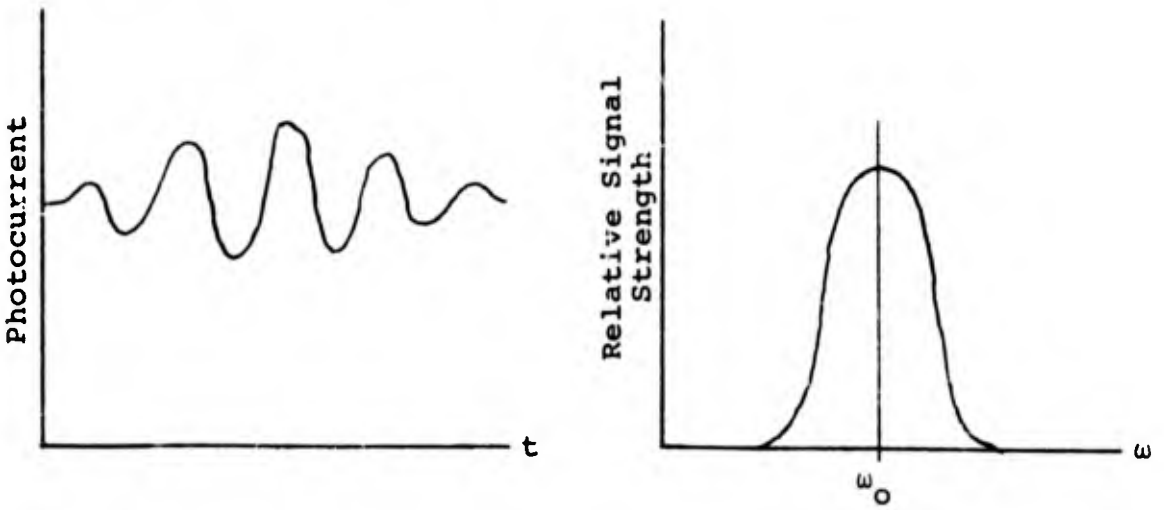

the velocity can be made either by measuring the period of the basic signal or by determining the center frequency of the Fourier transform. This is true regardless of the transit time broadening.

ATMOSPHERIC TURBULENCE MEASUREMENTS

E. R. Pike
Royal Radar Establishments
Malvem, England

We've been very interested in constructing a system at RRE for measuring the lower atmosphere in connection with problems of terminal approach at airports. The subject has a very interesting and somewhat controversial history which I can't go into. Basically a number of people some years ago were trying to work out which was the best way to do this. We ourselves were waiting for a long time for a laser to come along that would allow one to do radar-type applications. First the Argon laser appeared which could be put into single mode. Then the CO_2 laser appeared. Both of these at last, after all these years, offer good prospects for real laser-type radar applications. So there was a lot of toing and froing both in England and in the States comparing the merits of Argon systems and CO_2 systems for this type of laser doppler work.

Basically there were two camps in both countries. Both have gone ahead in spite of the paper studies. The real points of issue are rather difficult to quantify. One can say without a doubt that the visible system deteriorates as the range is increased, whereas the CO_2 system, being a true heterodyne laser radar, is better in this respect. One can say that powerful Argon lasers are unlikely to be used in real applications near airports because of their hazard. One can also say a few things on the other side. The upshot was that at RRE we decided to go ahead with the infrared system, and Huffaker's group at NASA went ahead with the infrared system. The Harwell people in England and ARO at Tullahoma went with the Argon laser system. Now the crunch is coming because the results obtained with these systems are becoming available. I don't have any brief to speak for Harwell's results, but they do have results. I'll just content myself

with showing you some slides indicating the results of our work.

Our system employs a nitrogen cooled lead-tin-telluride photovoltaic diode detector which has been developed under a contract with Plessey in England. The cooler is a nitrogen Leidenfrost-type system developed at RRE. The pre-amplifier which is necessary for low noise performance has been built around an FET which has again been developed under contract for RRE by Texas Instruments, and the frequency tracking system has been developed in my own group at RRE. The frequency tracker has some points of difference between the other ones that have been discussed during this conference. I will just say that the frequency lock loop is controlled digitally rather than by an analog-type system and the system essentially achieves the theoretical maximum tracking rates.

The laser is a nominal five watt single frequency CO_2 laser normally run in the two to four watt region. We comfortably achieve the theoretical heterodyne noise performance of the system. The whole system (Figure 1) is now on field trials at the Royal Aircraft Establishment at Bedford. Figure 2 is a comparison from these field trials of the velocity versus time of natural atmospheric movements compared with the output of a Gill-type vane anemometer. The two records have been put through a low frequency filter to correspond to the Gill response time which is very slow.

As Huffaker pointed out frequency response of the laser system is much faster, but this is not really very beneficial in the system as we described it, the coaxial system, because the laser averages over spatial volume much the same as the Gill-type anemometer. However, you can see from this piece of record that the laser anemometer is essentially giving you exactly the same information as the conventional anemometer and is a perfectly feasible instrument for short range remote wind velocity measurement.

There are several ways we intend to move forward. First of all we don't like the low spatial resolution at long range for this system although our signal/noise doesn't fall off very quickly with range. This is only because the sample of atmosphere that you are taking gets bigger and therefore you are getting some sort of average wind velocity over a big volume of space. We are working on a bi-static type system which will improve the performance of the instrument in this respect. As far as the commercial or military future is concerned this is still under deliberation. We are planning a users' meeting of possible civil air authorities who might be interested in the scheme. We are going to

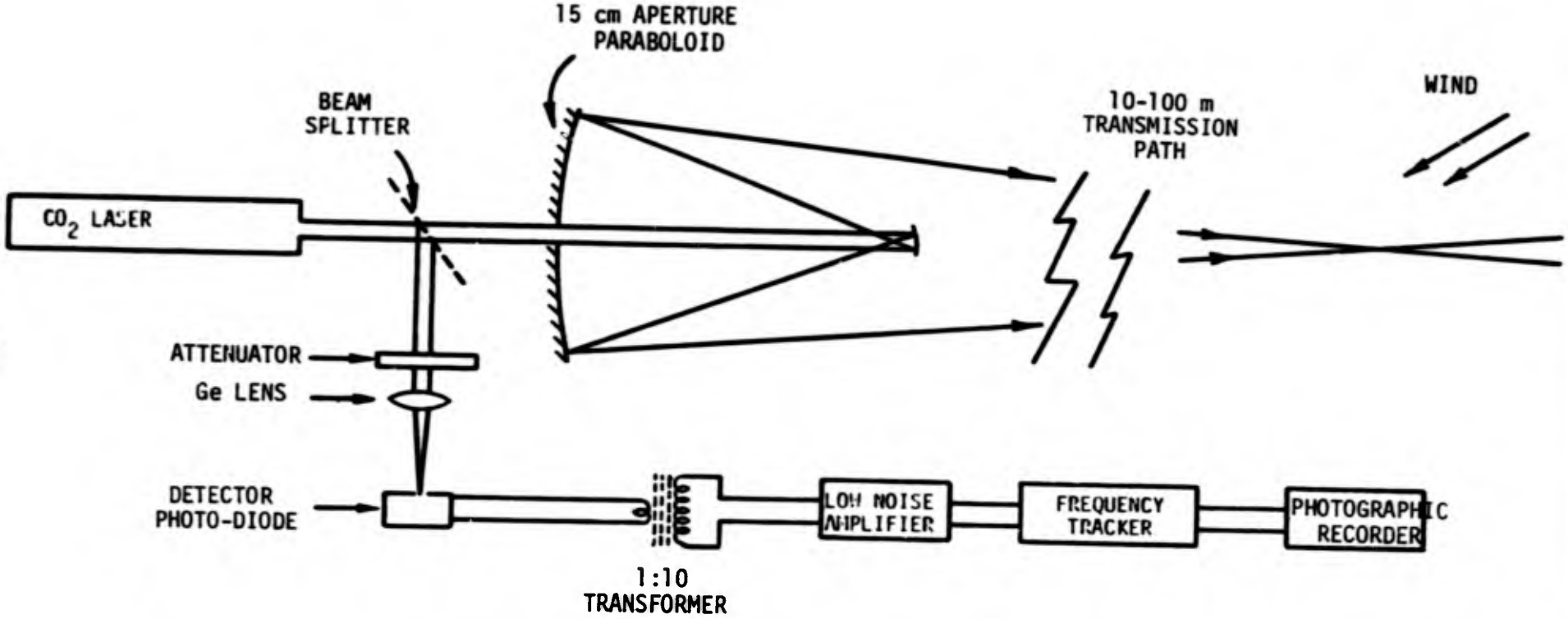

Fig. 1 Block diagram of the CO_2 laser anemometer system

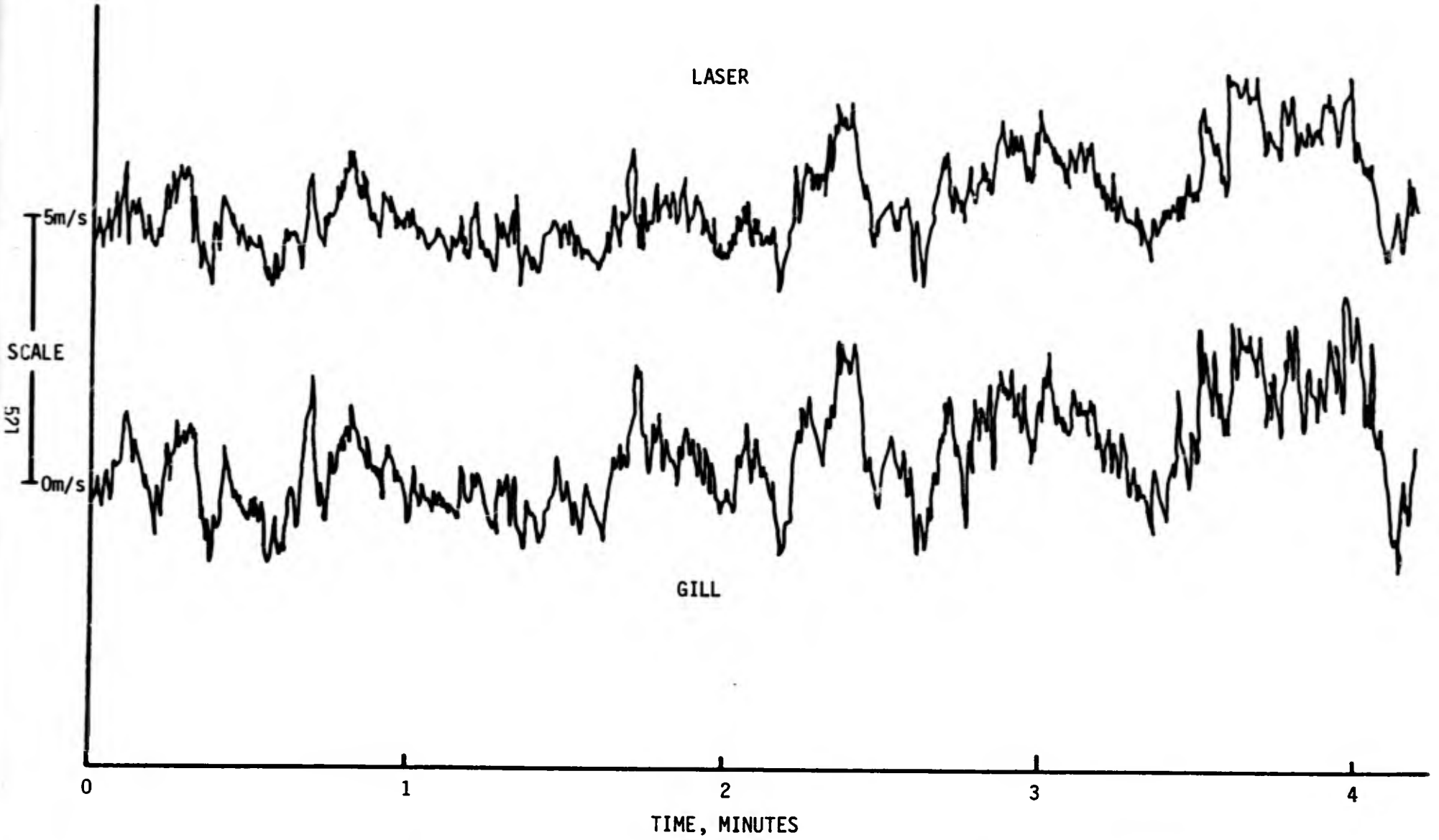

Fig. 2 Simultaneous records of velocity versus time from CO_2 laser anemometer (upper trace) and Gill vane anemometer (lower trace).

give a presentation on this to see how many people are really interested in taking the system further.

DISCUSSION

HAUER: Are there any plans to incorporate photon correlation techniques in the near future?

PIKE: Well, the advantage of photon correlation techniques lie where the "weight" of the photon is sufficiently heavy. Unfortunately at CO_2 frequencies the photon is just about room temperature and so it's not advantageous to use photon counting - in fact, it's not practical to use photon counting. I would certainly say as I mentioned after Mr. Lennert's presentation that it seems to me that photon correlation would be a better way of going about processing these signal bursts from both wind tunnel and atmospheric visible laser systems.

LAWRENCE: Have you investigated the possibility of combining an FM/CW radar to improve spatial resolution - imposing a triangular frequency?

PIKE: I didn't really want to go into this, but since you've raised the point the whole system can be operated as an FM/CW radar - yes. We have operated it in such a mode. There is a very interesting point. Following from my discussion of optimum ways of frequency signal processing the correlator system is equivalent to a parallel bank of filters and you couldn't do any better. The frequency tracker is equivalent to a single channel filter but it gets the advantage of the multiple channel system because it jumps around to follow the frequency. Naturally you can't get entirely the performance of a parallel bank in this way, but you can get somewhere towards it. Now there is a very interesting possibility of combining the correlator system in the middle of a frequency tracker so that you just use your frequency tracker to define instead of the one low pass bandwidth that we have at the moment, maybe ten of them. Inside that, since our frequency tracker is digital anyway, you just plug into a correlator. We are working on this idea. It should give you the best of all worlds.

WELCH: Could I get back to ambiguity for a minute? Can I make one more statement in review. It appears to me that this is a simple case of a true blue sample system. If you run one particle through at a time the Fourier transform of each burst as you say is unique. Now if we get the frequency information out for that burst each time and if we list that particular center frequency then what will come out

of this listing is a unique transform. It will be a sampled system. From a theoretical standpoint, if our rate of sampling is twice or more the rate of change of frequency we should be able to recover all information with no loss and no ambiguity even for turbuience.

FLOW SEEDING WITH AMMONIA - SO_2 REACTION

Allan Hauer

Pratt and Whitney Aircraft

E. Hartford, Conn.

It was felt by Doyle that I had gone through as much consternation as most in trying to arrive at a proper seeding system, so I thought I would just mention a few things that might be of value to you. I think that we have gone through at least twenty different types of seeding methods. I'm sure I would duplicate what Bill Yanta has said as far as particle flow following and so on, but basically there is also the question of compatibility with various types of flow systems. This is one thing I focused attention on recently. Jeff Asher was saying that he's used aluminum oxide. One thing that I would like to mention in that case is that you have to watch very closely the abrasive action of any particle as hard as aluminum oxide. When we levitated it the same way he did (with the levitation of powder) and injected this into a very high speed air flow we found after three days that it had eaten a hole through one of the feed tubes into the air flow rig and it was harming many of the valuable rig parts. Also aluminum oxide tends to agglomerate. You can get around that, but it is extremely difficult to do. We tried many different types of liquids. Liquids have the possibility of coating observation windows. They can't be used in hot flows and condensation is an old story to many of you.

The system that we came across very recently is a gas phase reaction which has proved to be advantageous in many types of flow. This is a reaction between anhydrous ammonia and anhydrous SO_2. This occurs in the air flow. You can change the mixing rate just by the valves on the system to change the seeding level and also particle size. It's been a very nice system for uniform and controllable seeding levels. The one disadvantage is that improper mixing does lead to a toxic flow but it's perhaps not as bad as many other systems in this regard.

Figure 1 is an electron photomicrograph of the particles. I found that impactometers and other ways for characterizing particle size distribution have been extremely unreliable. For a sample in the flow, in the situation that we are talking about, a photomicrograph is a very good technique for particle size characterization. These are ammonium sulphate particles produced in the reaction. They were somewhat larger than I expected - on the order of 1.5 micron average diameter. My conclusion is that when I ran this experiment I didn't have a proper mixing ratio because that's higher than I expected on the basis of some calculations made by an aerosol expert.

The question of whether to seed or not to seed is definitely a very pertinent one but we decided, as Dr. Pike said, that all readout methods are basically equivalent to some type of counting mechanism so that you can divide your data into two separate parts. You have mean velocity and turbulence intensity on one side and all higher order information - turbulence spectra and so on that require high sampling rates on the other. In other words you think of it purely from the basis of the sampling theorem. You may have more stringent requirements than that, but you're never able to do better than sampling at a rate at which you can characterize the mean value of the signal. So if you talk about forgetting seeding entirely perhaps you can do a lot of things, but I am quite skeptical.

Table I outlines some of the experiences we've had with various seeding systems.

I think I will just say one other thing that might be of value to some people. Those of us who are occasionally humble enough to only be desirous of mean velocity information sometimes will come up with some nifty little gimicks. This is one of ours that might be helpful to you. We have one flow measuring situation where we are trying to characterize a flow in the cooling passages of turbine blades and other very small devices similar to the fluidic device that Dr. Shih was describing this morning. One way of getting large amounts of mean velocity information we've found was to display the LDV signal on a cathode ray tube - in this case it was a television. The television had a 10 MHz response. Little trains of dots are the intensity being modulated by the LDV signal so that they are actually being spaced out as the intensity of the raster trace of the television is being modulated by the LDV signal. What we end up with is one photograph of a single scan 1/30 of a second and the intensity distribution on this particular piece of film is thus determined by the LDV signal. So we take this

TABLE I

Seeding material	Advantages	Disadvantages
1 Oil vapor smoke	Proper particle size Good scattering produced excellent LDV signals	Condensation clogged flow passages and caused nonuniform seeding at high flow rates. Caused coating of observation windows. Cannot be used for high temperature investigation.
2 Solid powder system		
a) $Ti_2 Cl_4$ + Air	----------	HCl produced as by product
b) Burning Mg	----------	Combustion hard to sustain at high airflow rates.
c) Al_1O_3 (powder injected directly	Standard size easily available Very high melting point	Abrasive action on rig parts. Uniform seeding hard to maintain. Powder tends to agglomerate.
d) Lampblack	Same as Al_2O_3 and simulates combustion by products	Same as Al_2O_3
3 Gas phase reactions NH_3 - SO_2	Very uniform controllable seeding level	Improper mixing leads to toxic exhaust

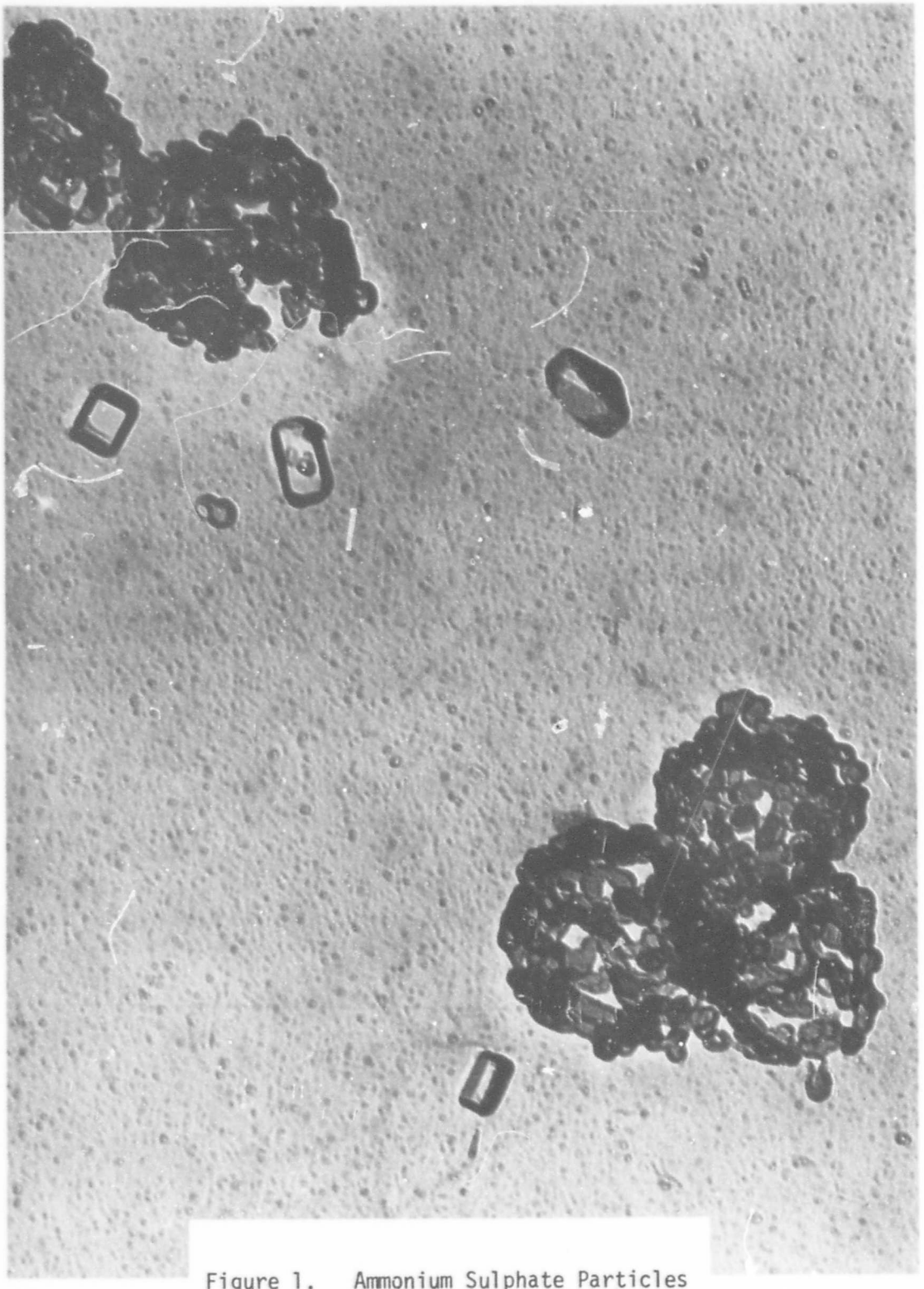

Figure 1. Ammonium Sulphate Particles
Magnification 42000x

transparency of a photograph of one trace and put it into an optical Fourier transformation system as shown in Figure 2 and come up with the Fourier transform. What we are actually doing is computing the frequency spectrum optically very fast. We can get what corresponds to reams of data just taking photographs of the television face and very easily obtain mean velocity data. This is just a very rough diagram of how the diffraction pattern of one particular transparency appears.* The streaks actually are of finite width which in this case corresponds to the instrumental broadening. The streaks can be measured very accurately to get mean velocity data. This system proved very convenient for us when we wanted large numbers of samples of mean velocity instead of taking thousands of spectrum analyzer tracers and photographing them.

DISCUSSION

FELLER: I think ammonium sulphate sometimes decomposes and blows railroad cars and ships apart. Have you had any problems with it breaking down in the air?

HAUER: No. Another thing is that one of the substances mentioned - titanium tetrachloride, which is beautiful for making lots of smoke - produces hydrochloric acid as a byproduct. Not being a chemist I shouldn't open my mouth further, but I am familiar with the situation you mentioned and it's never been a problem with us. The only problem we have had of any kind with this gas phase reaction has been improper mixing.

FELLER: How do you ever get the safety people to let you pour ammonia into the tunnel, let alone sulphur dioxide?

HAUER: You mean depending on where the exit is?

FELLER: Yes, I mean the safety people go crazy.

HAUER: That's true, you must be very persuasive.

*Editors note: Figure not available.

transparency of a photograph of one trace and put it into an optical Fourier transformation system as shown in Figure 2 and come up with the Fourier transform. What we are actually doing is computing the frequency spectrum optically very fast. We can get what corresponds to reams of data just taking photographs of the television face and very easily obtain mean velocity data. This is just a very rough diagram of how the diffraction pattern of one particular transparency appears.* The streaks actually are of finite width which in this case corresponds to the instrumental broadening. The streaks can be measured very accurately to get mean velocity data. This system proved very convenient for us when we wanted large numbers of samples of mean velocity instead of taking thousands of spectrum analyzer tracers and photographing them.

DISCUSSION

FELLER: I think ammonium sulphate sometimes decomposes and blows railroad cars and ships apart. Have you had any problems with it breaking down in the air?

HAUER: No. Another thing is that one of the substances mentioned - titanium tetrachloride, which is beautiful for making lots of smoke - produces hydrochloric acid as a byproduct. Not being a chemist I shouldn't open my mouth further, but I am familiar with the situation you mentioned and it's never been a problem with us. The only problem we have had of any kind with this gas phase reaction has been improper mixing.

FELLER: How do you ever get the safety people to let you pour ammonia into the tunnel, let alone sulphur dioxide?

HAUER: You mean depending on where the exit is?

FELLER: Yes, I mean the safety people go crazy.

HAUER: That's true, you must be very persuasive.

*Editors note: Figure not available.

OPTICAL READOUT OF LASER VELOCIMETER SIGNALS

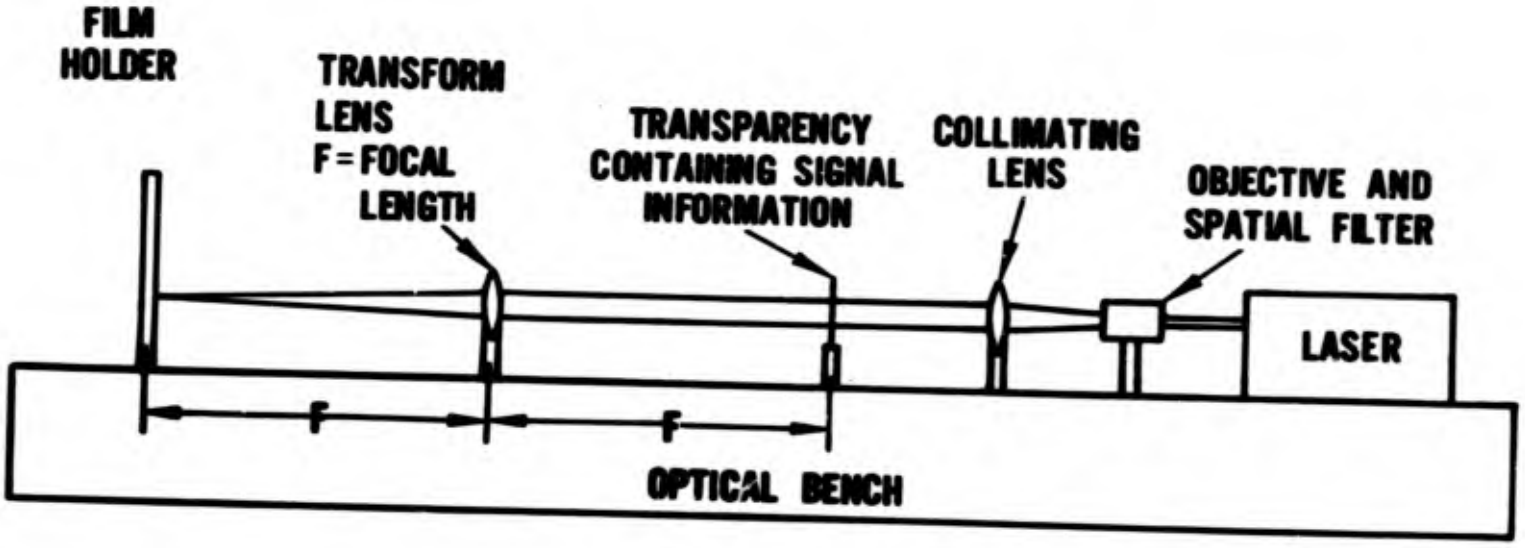

ANALYZING THE
L.D.V. SIGNAL

Figure 2

PARTICLE FLUCTUATIONS IN TURBULENT FLOWS

Neil S. Berman
Arizona State University

Nobody really has talked about the problem of measuring the turbulence intensity and the velocity difference that the particles would have from the fluid flow. Vic Goldschmidt said something about this and the fact that they had found that when you include some of the other terms you can get an increase. That is the particles in fact start going faster than the flow in some cases. Calculations that we did also confirm this. If you write down the equations of motion for the particle in addition to the ones we have seen before you find that there are three nonlinear terms and then a second derivative term in space that comes in. All four of these terms are normally neglected in making any of the analyses. If you do a fast calculation on what happens in most of your flow conditions you find that a few of these are more significant than the other terms that you normally keep.

The equations of motion for a particle in a fluid have been formulated by Soo (1) among others. If these are linearized a solution of the form shown below can be obtained for the relative error in velocity fluctuations in turbulent flow:

$$\frac{\overline{V_r^2}}{\overline{U^2}} = \int_0^\infty \frac{\Omega_R^{(1)}}{\Omega^{(2)}} f(\omega)d\omega \qquad (1)$$

where $V_r = U-V$

U = Fluid velocity fluctuations

V = Particle velocity fluctuations

$f(\omega)$ = Power spectral density of the turbulence

ω = frequency

$$\Omega_R = \left(\frac{1-\delta}{\delta}\right)^2 \left(\frac{\omega}{\Omega}\right)^2$$

$$\Omega^{(2)} = \frac{1}{\delta^2}\left(\frac{\alpha}{\omega}\right)^2 + \frac{\sqrt{6}}{\delta}\left(\frac{\alpha}{\omega}\right)^{3/2} + 3\left(\frac{\alpha}{\omega}\right) + \sqrt{6}\left(\frac{\alpha}{\omega}\right)^{1/2} + 1$$

$$\alpha = \frac{3\mu}{\rho r^2} \quad , \quad \delta = \frac{3\rho}{2\rho_p + \rho}$$

μ = fluid viscosity, ρ = fluid density,

r = particle radius, ρ_p = particle density.

If a power spectral density, PSD, is approximated as flat to a cut off frequency fu and then decaying as ω^{-2} up to another cut off at which the PSD drops to zero, the results shown in Figure 1 are obtained for particles from 0.15 microns to 2.5 microns as a function of fu and density when the fluid is air. Errors are quite large for particles greater than 0.5 microns in diameter.

The actual equation of motion contains non-linear terms. If these are assumed proportional to the velocity difference between particle and fluid with a proportionally constant $\alpha\delta K$, equation (1) is changed only by a slight modification of $\Omega^{(2)}$. The last two terms are replaced by

$$\sqrt{6}\ K\left(\frac{\alpha}{\omega}\right)^{1/2} + K^2$$

Now if $K>0$ or under some conditions regardless of the magnitude of K the relative error decreases. The ratio of $\overline{V^2}$ to $\overline{U^2}$ can similarly be obtained. Details are in a NASA contractors report by N. S. Berman (2).

1. Soo, S. L., "Fluid Dynamics of Multiphase Systems" Blaisdell Publishing Co., Waltham, Mass., 1967.

2. Berman, N. S., "Particle Fluid Interaction Corrections for Flow Measurements with a Laser Doppler Flowmeter" NASA-21397 Final Report.

DISCUSSION

JISHKE: Is this in air?

BERMAN: Yes. The density of the particles is one and the fluid is air. This is the linear case and will improve actually if I put

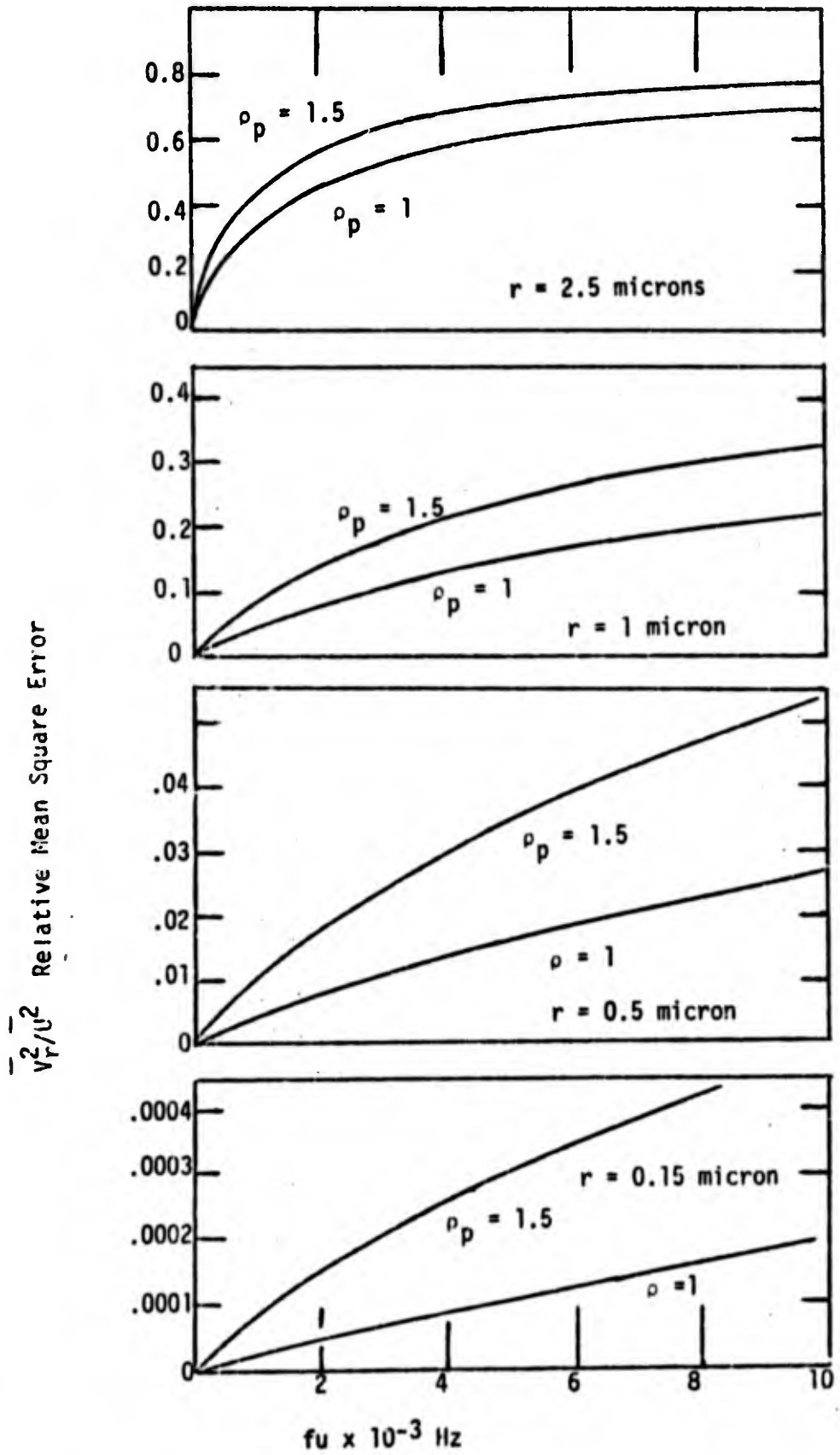

Figure 1. Particle Density Effect on Velocity Lag.

in the nonlinear terms. In fact, as pointed out, it could even go the other way which will bring it back up again. These are velocity lags I show here. We did some similar calculations using actual power density spectra but they give essentially the same results.

QUESTION: You refer to the linear case. Are you referring to Stoke's law - is that what you mean by linear?

BERMAN: No, in the equation of motion I've removed all the nonlinear terms and I assume here that the relative Reynolds number is low enough so that we do use Stoke's law.

QUESTION: What are the physical origins of these nonlinear terms you are referring to?

BERMAN: Let me refer you to some references on this. The equation is derived by Hinze in his book and also by Soo in his book and in Brockee's book on fluid flow. I think also in terms of the way I've done it probably Soo in his fluid dynamics of multiphase systems does a very similar analysis. It's quite a common equation found in the literature.

RELAXATION TIME OF SMALL PARTICLES

H. Pfeifer

Institute Franco-Allemand

I will give you only very briefly some experimental results we have obtained on the time relaxation of small particles. There are mainly two different methods to determine particle relaxation with respect to very high gaseous flow accelerations. One of them is to use stationary shock waves in a supersonic wind tunnel. In th's case the initial velocity is supersonic and the final velocity may be supersonic or subsonic and the velocity variation of the shock front may be from zero (a normal sound wave) to hundreds of meters per second. The other methods we have used in a traveling shock wave in a shock tube. In this case the velocity in front of the shock wave is zero and the velocity behind the shock wave can be chosen by the shock strength from zero (also a normal sound wave) to some hundreds of meters per second. For example, at a shock Mach number of 1.4 under normal conditions in the low pressure chamber the velocity behind the shock front is on the order of 200 meters per second. In any case the velocity variation occurs within a few mean free paths of the molecules and, under normal conditions, this means within a fraction of a micron.

Figure 1 shows the experimental setup. The helium-neon laser served as a triggering source only. One photomultiplier served for timing the passage of the shock front through the observation volume. We get our signal from this other photomultiplier. Now first of all the particle's diameter has to be determined. This is done by our chemical department. Figure 2, curve a is the size distribution of dust particles. These measurements are made with an electron microscope. Curve b is the size distribution of smoke particles in this shock tube. You see that they do not differ in order of magnitude.

Figure 3 shows a record of the signal. The upper part represents the signal from the photomultiplier which gives us the time of passage of the shock front through the fringe system. The lower part is the doppler signal. We obtained an accuracy of 5 percent for the velocity of the

particles behind the shock front. Figure 4 shows the result. You see here the result for Mach 1.4. The calculated velocity behind the shock front is 200 meters per second. You see here some uncertainty in the beginning of the passage of the shock front through our fringe system in the order of 2 microseconds. The total time of relaxation is in every case less than four microseconds for the particles shown in Figure 2.

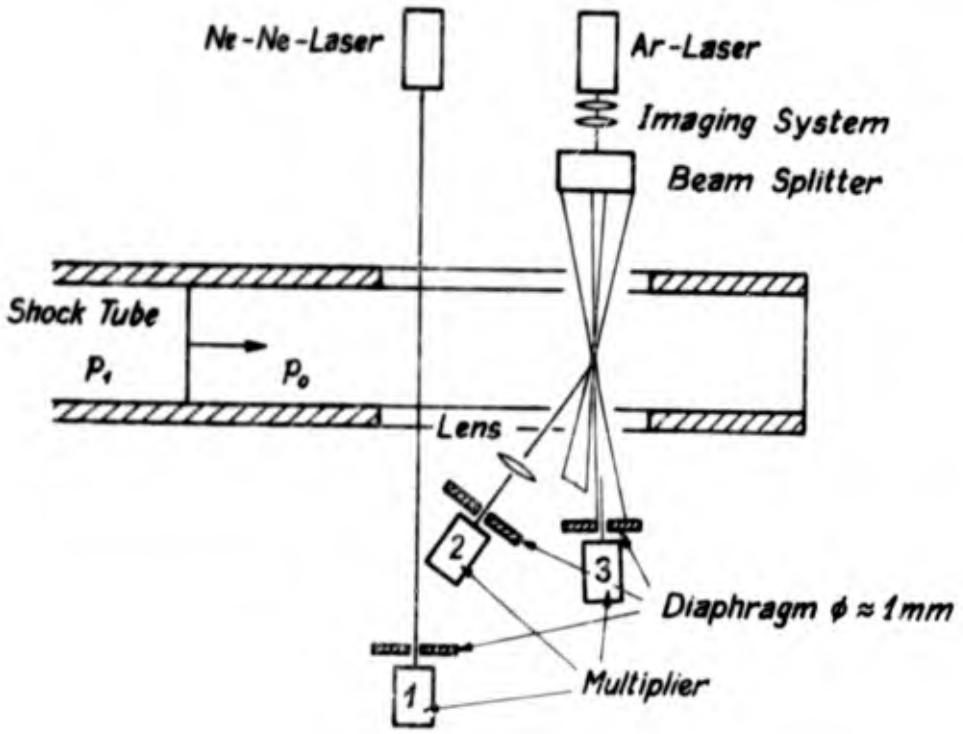

Figure 1

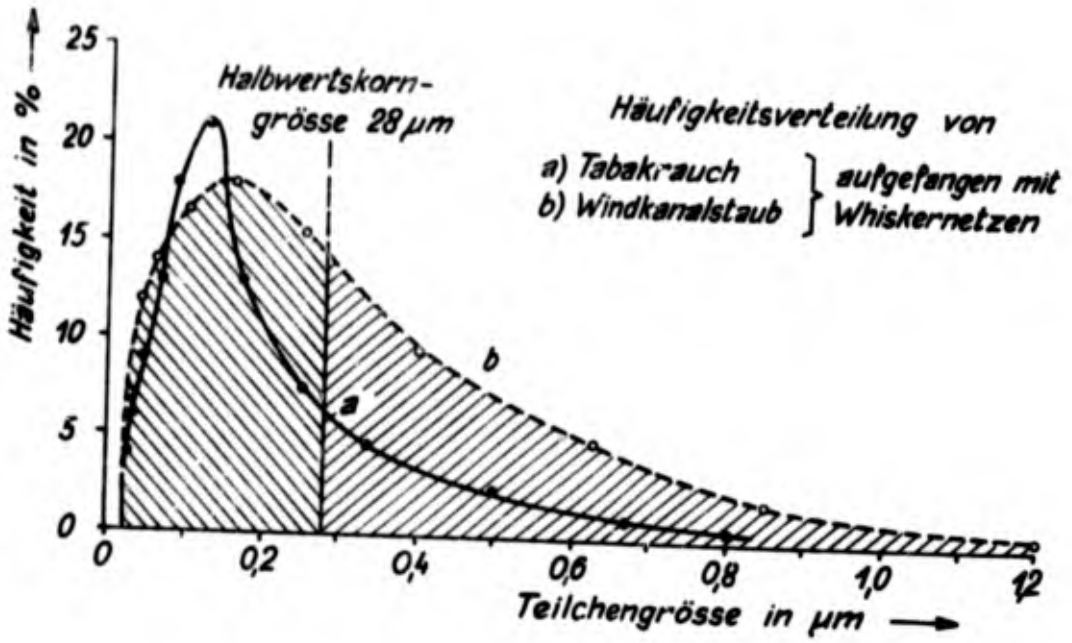

Figure 2

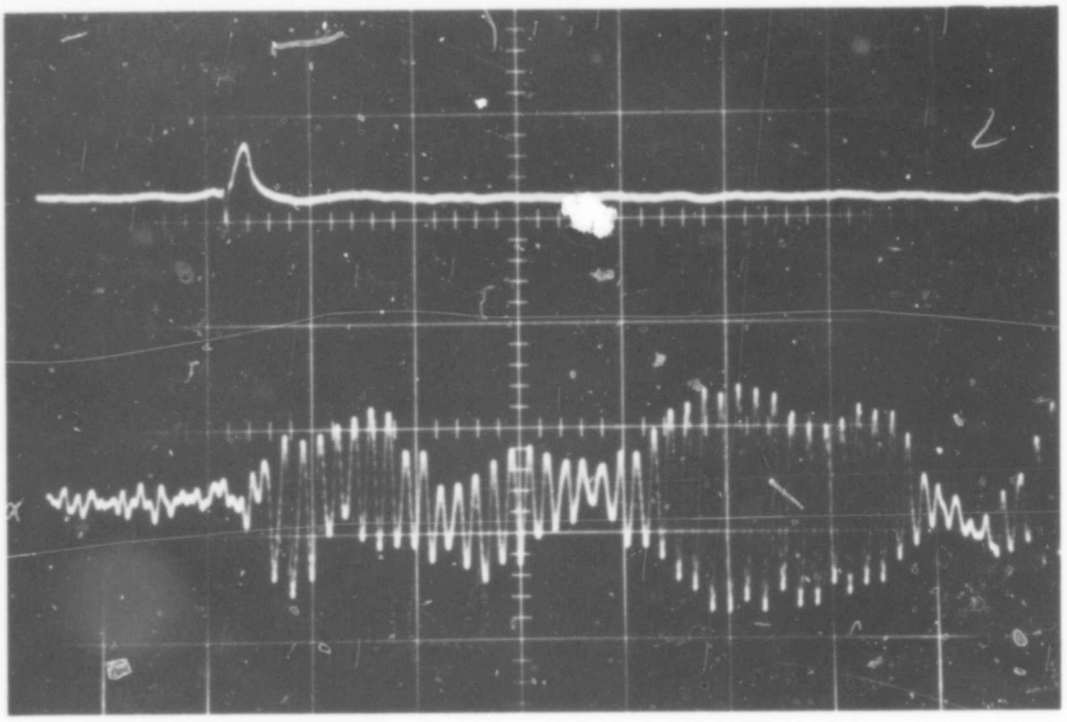

Figure 3

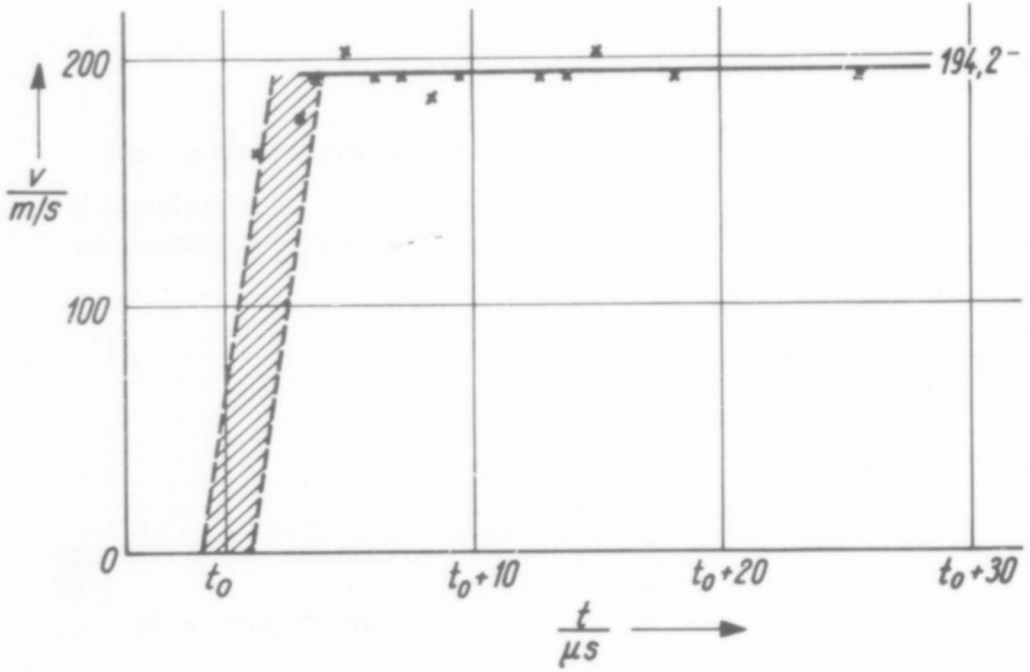

Figure 4

GENERAL COMMENTS ON PARTICLES AND SEEDING

J. H. Whitelaw
Imperial College of Science and Technology
London

I want to say something about particles and really what I want to say is to spread further the moderate feeling of gloom which we all have when we look at the particle situation. I can say first that our terms of reference relate largely to work in laboratories of the type where I suspect most operators of laser anemoneters will work. The people in industry with high-speed wind tunnels of large size are in a different ball park. If you look at the particle problem in detail, you find that you are faced with all sorts of problems which you can't really analyze. You have coagulation, your size changes, you have electrostatic forces, you have thermal phoresis. We have taken all these possible forces on the particles we could find and tried to do appropriate sums. In general, for the kind of flow in which we are interested, we don't come out too worried. We also go back to flow situations where hot wires taught us the answers five or ten years ago and make sure we measure the same answers with LDV.

Now if I can comment very briefly on the flow situations in which we tend to work. In water I don't believe there is any problem. We don't know accurately what the size distribution of the particles is. We do know it's polydispersed with the mean somewhere about a micron, perhaps a little less - at least in the water we work in. If you add latex or milk it doesn't seem to do anything to the signal. If you measure fully developed flow in a two-dimensional channel, for instance, and add latex particles of the right size so that you drown out the particles which are already in the flow, it doesn't do anything to the turbulence intensity or the range of turbulence i censity which is measured. The same can be said for milk. So in water I am really quite happy and normally we don't add anything. We just work with the dirt which we have in the available water.

In air the situation is a little bit worse if you work with what's in the atmosphere. Fortunately London, since the Clean Air Act of 15 years ago, is relatively clean. There are few particles around and what we have again suggests that they are polydispersed with a mean of about one micron. We don't work in the unseeded case - it takes too long for us to get answers. Either we burn tobacco smoke (and with this

we can reproduce two-dimensional, turbulent channel flow results) or we use silicone oil. We prefer silicone oil because we have much better control over the rate at which the silicone oil is produced. If we check again, the low turbulence situation of the two-dimensional channel is O.K. and the high turbulence situation in a turbulent jet flow also seems to be satisfactory (as satisfactory as you can tell because of the nonlinearity of the hotwire anemometer which you use to check the measurements).

I would make two comments regarding combustion systems. We tried some work with an industrial burner and with methane and air 5 percent above stochiometric with efficient mixing then you have a duty cycle which is less than 0.1 percent. In other words you have precious few particles around and you have to wait a long time to make a meaningful measurement. Again we seed the gas flow with silicone oil. The silicone oil particles will exist in the flame at least until the flame becomes very hot. They go quite a ways downstream before they disappear. We don't find that they clog windows nor do we find any great problems with condensation, but we recognize that you can't go all the way downstream in a flame with silicone oil. It does evaporate. We've been trying to generate magnesium oxide particles and I'll be interested to know if anyone else has tried it.

The last situation is in blood. In blood we have scattered off red cells which are about 8 microns in diameter. It's a laminar flow, so there are not many problems here. We think that we might be able to scatter off platelets which are about two microns in diameter and use a fringe system which will cut out signals from the 8 micron red cells. We hope to be able to do this.

I'll make three more points. Regarding the frequency response for silicone oil in air we work to a rule of thumb that if we have a one-micron particle it will follow somewhere up to around 10 KHz with an accuracy of 1 percent. If it jumps up to ten microns then we follow something like 700 Hz to one percent. Secondly health - this is something that does worry me. The long term effects of inhaling small particles which don't evaporate and stick in the lungs are unknown. You can use masks but they are not particularly effective. If you can get away without seeding it's much better.

The last thing I am going to say is that much of our work on particles was written up by Adrian Melling, one of our students, and there is a report available from Imperial College on that topic. Also he gave two lectures at a course we gave on optical anemometry last January and that also is available if anyone wants to have it.

DISCUSSION:

HAUER: We have tried magnesium oxide also. I'm not sure whether or not we pursued it far enough. One of the big problems we had is that the combustion is extremely hard to maintain accurately. When it

burns it looks energetic, but it's actually a fairly feeble type of combustion and it's very hard to maintain a very uniform seeding. In addition to that, a great amount of agglomeration takes place which you would not expect.

LENNERT: There is one point I would like to make. We ran some experiments with the LDV system and then took some shots with a double pulse holography setup. We noticed that the particles were rotating, and they were not spherical. I hope that when you start thinking about these particles you take into consideration the fact that the drag coefficients might not be what you think they are because the irregularity of the materials.